IDENTIFICATION OF GENES ASSOCIATED WITH ENDOCRINE RESISTANCE IN BREAST CANCER

Rajpal Singh Burmi

Tenovus Centre for Cancer Research
Welsh School of Pharmacy
Cardiff University, Cardiff, UK

September 2006

UMI Number: U584099

UMI U584099

Summary

Resistance to tamoxifen, Faslodex and oestrogen-deprivation represents a major hurdle in breast cancer management, and determining the underlying factors driving resistant growth may improve treatment and prognosis. Expression microarrays (Atlas Plastic Human 12K Microarrays; GeneSifter software) were used to identify genes altered in breast cancer models with acquired resistance to tamoxifen (TamR) or Faslodex (FasR) versus their parental MCF-7 cell line through cluster analysis, t-testing and ontological examination. Selected genes were verified by PCR, Western blotting and immunocytochemistry. Alongside known breast cancer-related genes (PEA3, vitronectin), two novel genes increased in resistance were the securin/cell-cycle regulator Pituitary Tumour-Transforming Gene-1 (PTTG1) (p=0.013 and p=0.013 in TamR and FasR cells respectively), and GDNF receptor-α3 (GFRα3) (p=0.014 in TamR cells) that promotes cell survival signalling via its coreceptor RET. Increased levels of PTTG1, GFRα3, or their family members were observed in further endocrine resistant states, including an additional faslodex-resistant model that has progressed to a highly-aggressive state (FasR-Lt) and cells resistant to oestrogen-deprivation (X-MCF-7). PTTG1 and GFRα3 induction in response to an anti-EGFR agent in the resistant models implicated these genes in limiting its growth inhibitory effect, and GFRα3 ligand (artemin) was shown to overcome anti-EGFR response (78% growth recovery). mRNA studies in clinical disease revealed a significant association of PTTG1 with lymph node spread (p=0.001), high tumour grade (p=0.001) and proliferation (p<0.001), while GFRα3 was enriched in ER-negative tumours (p=0.01), showing loss of tubular differentiation (p=0.04) and expressing EGFR (p=0.013), profiles implying roles in clinical resistance and aggressive tumour behaviour. Promisingly, PTTG1 or GFRα3 siRNA significantly reduced cell growth (by 72%;p=0.003 and 81%;p=0.004 respectively), proliferative capacity (by 23%;p<0.001 and 32%;p<0.001 respectively) and induced apoptosis (by 43%;p=0.05 and 103%;p=0.05 respectively) in resistant models. Cumulatively, these data indicate PTTG1 and GFRα3 may provide useful biomarkers and perhaps new therapeutic targets for multiple resistant states.

Acknowledgments

Declaration

This work has not previously been accepted in substance for any degree and is not concurrently submitted in candidature for any degree.

Signed.. (candidate)   Date...20/3/07
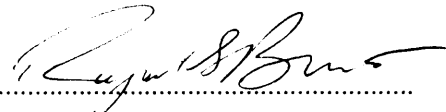
Statement 1

This thesis is being submitted in partial fulfilment of the requirements for the degree of PhD.

Signed.. (candidate)   Date...20/3/07
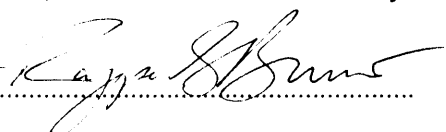
Statement 2

This thesis is the result of my own independent work/investigation, except where otherwise stated. Other sources are acknowledged by explicit references.

Signed.. (candidate)   Date...20/3/07

Statement 3

I hereby give consent for my thesis, if accepted, to be available for photocopying and for inter-library loan, and for the title and summary to be made available to outside organisations.

Signed.. (candidate)   Date...20/3/07

Contents

Chapter 1: Introduction

Chapter 2: Materials and Methods

Chapter 4: Detailed Study of Genes: PTTG1

Chapter 6: Discussion

Abbreviations

4-OHT	4-hydroxytamoxifen
AF	activation function
AI	aromatase inhibitor
AIB1	amplified in breast cancer 1
ANOVA	analysis of variance
APS	ammonium persulphate
ATCC	American Tissue Culture Collection
ATM	ataxia telangiectasia mutated
BCAR	breast cancer anti-oestrogen resistance
BRCA	breast cancer susceptibility protein
BSA	bovine serum albumin
C/EBPβ	CAAT/ enhancer-binding protein beta
CaCl$_2$	calcium chloride
CBP	CREB binding protein
CDK	cyclin dependant kinase
cDNA	complimentary DNA
CK2	casein kinase 2
CO$_2$	carbon dioxide
CREB	cyclic AMP response element binding
csf	colony stimulating factor
csFCS	charcoal-stripped foetal calf serum
DAB	diaminobenzidine
DAPI	4',6-Diamidino-2-phenylindole
DBD	DNA-binding domain
DNA	deoxyribose nucleic acid
DNase	doexyribonuclease
dNTP	deoxynucleoside triphosphate
DTT	dithiothreitol
E2	17-β oestradiol
EDTA	ethylene diamine tetraacetate
EGF	epidermal growth factor
EGFR	epidermal growth factor receptor
EMT	endothelial-mesenchymal transition

ER	oestrogen receptor
ERα	oestrogen receptor alpha
ERβ	oestrogen receptor beta
ERE	oestrogen response element
ERF-1	oestrogen receptor factor-1
ERα	oestrogen receptor alpha
EST	expressed sequence tag
FCS	foetal calf serum
FSH	follicle stimulating hormone
GDNF	Glial cell-derived neurotrophic factor
GFRα3	GDNF receptor alpha 3
H_2O_2	hydrogen peroxide
HAT	histone acetyl transferase
HCA	hierarchical cluster analysis
HCl	hydrochloric acid
HER2	human epidermal growth factor receptor type 2
HRP	horse radish peroxidase
HSP	heat shock protein
IGF	insulin-like growth factor
IGF-1R	insulin-like growth factor receptor type 1
K_2HPO_4	potassium hydrogen orthophosphate
KH_2PO_4	potassium di-hydrogen orthophosphate
LBD	ligand-binding domain
LH	luteinising hormone
LHRH	luteinising hormone releasing hormone
LTED	long term oestrogen deprived
MAPK	mitogen activated protein kinase
$MgCl_2$	magnesium chloride
MMLV	moloney monkey leukaemia virus
Na_2CO_3	sodium carbonate
Na_2MoO_4	sodium molybdate
Na_3VO_4	sodium orthovanadate
NaCl	sodium chloride
NaF	sodium fluoride
NaOAc	sodium acetate
NaOH	sodium hydroxide
NF-IL6	nuclear factor for interleukin 6

NFκB	nuclear factor kappa beta
NLS	nuclear localisation signal
PAGE	polyacrylamide gel electrophoresis
PAM	partitioning around medoids
PAO	phenylarsine oxide
PBS	phosphate buffered saline
PCR	polymerase chain reaction
PDGF	platelet-derived growth factor
PEA3	polyomavirus enhancer A binding protein-3
PgR	progesterone receptor
PI3K	phosphatidylinositol 3-kinase
PKA	protein kinase A
PKC	protein kinase C
PMSF	phenylmethylsulphonylfluoride
PTEN	phosphatase and tensin homolog
PTTG1	pituitary tumour transforming gene 1
RNA	ribonucleic acid
RNase	ribonuclease
RPMI	Roswell Park Memorial Institute
RT-PCR	reverse transcriptase PCR
SD	standard deviation
SDS	sodium dodecyl/ lauryl sulphate
SEM	standard error of the mean
ser	serine
SERDS	selective oestrogen receptor downregulator
SERM	selective oestrogen receptor modulator
siRNA	small interfering RNA
SNP	single nucleotide polymorphism
SSC	salt sodium citrate
STI	signal transduction inhibitor
TAE	tris-acetate-EDTA
TCCR	Tenovus Centre for Cancer Research
TEMED	tetramethylethylenediamine
TGF	transforming growth factor
TKI	tyrosine kinase inhibitor
tyr	tyrosine

Chapter 1

INTRODUCTION

INTRODUCTION

1.1 Breast Cancer

Breast cancer constitutes 15% of all reported cancer cases within the UK and is the most common tumour type in women, accounting for about one in three of female cancers (Cancer.Research.UK, 2004). It is estimated that 1 in 9 women will be affected by breast cancer and each year in the UK over 40,000 women are diagnosed with the disease (Cancer.Research.UK, 2004; Kelsey and Berkowitz, 1988) . While mortality rates for breast cancer showed a peak in the late 1980s, since 1990 there has been a steady fall, most likely attributable to a combination of factors, such as earlier diagnosis and more effective endocrine and cytotoxic treatments. For example, 14,620 women died from breast cancer in 1993,compared to 12,840 in 2002 (Cancer.Research.UK, 2004). However, despite this important decrease in mortality, it is clear that many people still die of this disease and moreover the incidence rate, particularly in the developed countries is increasing with a 46% increase reported over a 20 year period (Cancer.Research.UK, 2004). Thus, there is a need to understand the development of breast cancer and to develop more effective treatments to continue to improve patient survival.

The incidence of breast cancer increases with age, doubling about every 10 years until the menopause, after which the rate of increase is lower, but nevertheless still increasing (McPherson et al., 2000). The incidence in European and North American women, for example, is about 2.7% by the age of 55, around 5% by 65 and 7.7% by the age of 75 (Key et al., 2001). Rates of mortality and incidence are also higher in developed countries, exemplified by the four-fold increased incidence rate of North America over India, Africa and China (McPherson et al., 2000). Moreover, studies have also shown an elevation in the rate of breast cancer within a migrant population to the adoptive high-risk country within two generations (Key et al., 2001).

Factors which influence the risk of breast cancer include obesity and lifestyle factors such as diet. For example, there may be a protective effect provided by the consumption of vegetables, and phytooestrogens, which are found in high concentrations in foods such as soya (Key et al., 2001). The consumption of alcohol has also been associated with a moderate increased risk of breast cancer (Cancer.Research.UK, 2004; Key et al., 2001).

Another risk factor which can influence breast cancer is mutations in certain genes. These identified germline mutations include mutations in BRCA1, BRCA2, p53, PTEN, and ATM, where BRCA1 and BRCA2 gene mutations account for 5-10% of breast cancer (Casey, 1997; Easton, 1999). A predominant factor for increased breast cancer risk is lifetime exposure

to steroid hormones and risk factors linked to hormones. For example early age at menarche and late age at menopause increases the risk of developing breast cancer (Key et al., 2001).

Similarly, nulliparity and late-age at full term pregnancy are associated with increased risk of breast cancer. Women giving birth after the age of 30 have twice the risk of developing the disease compared to women who have their first child before the age of 20. (Kelsey et al., 1993; Key et al., 2001; McPherson et al., 2000). The use of oestrogen/ progesterone hormone-replacement therapy has also been linked to breast cancer (Beral, 2003).

Cancers which occur in the breast are generally described by their localisation within the breast and their ability to invade surrounding tissues. For example, ductal or lobular carcinoma describes the origin of the tumour as occurring within the milk ducts or the lobule respectively. These tumours can either be confined inside a basement membrane (in-situ) or exhibit spread (invasive) into the surrounding tissues (van de Vijver, 2005). They are also described as early disease (primary), where the tumour is confined to the breast/ lymph nodes and may be excised, or more advanced disease, where the tumour has spread to other life-threatening regions of the body and is inoperable. Breast cancer, like other types of malignancies, demonstrates a number of key features that confer a distinct advantage for growth expansion. Several critical factors have been identified including uncontrolled cellular proliferation, insensitivity to negative growth regulation, evasion of apoptosis, invasion and metastasis, angiogenesis and genomic instability (Hanahan and Weinberg, 2000; Sledge and Miller, 2003).

As stated above, numerous reproductive characteristics have been described that are associated with an increased risk of developing breast cancer. These data, together with *in-vitro* and *in-vivo* findings strongly suggest the etiological involvement of endogenous steroid hormones (Key and Pike, 1988). Of most interest in this regard is the female hormone oestrogen.

1.2   Oestrogens and Breast Cancer

The link between oestrogen and breast cancer was first suggested when Beatson in 1896 demonstrated a dramatic regression in locally advanced disease with improved prognosis as a consequence of oophorectomy (Beatson, 1896). His studies were based on earlier observations which suggested that tumour size altered with the phase of the menstrual cycle.

In 1958, Lerner and colleagues published the pharmacological properties of the first compound developed to inhibit the oestrogen mitogenic pathway, a non-steroidal antioestrogen, MER-25 (Lerner et al., 1958). This was followed in 1960 by Jensen and Jacobson who identified the oestrogen receptor (ER) as the mediator of the cellular actions of oestrogens (Jensen and Jacobson, 1962). The subsequent isolation (Toft and Gorski, 1966) and cloning of

the oestrogen receptor (Green et al., 1986) has led to the advancement in understanding of the classical mechanism of oestrogen signalling and its activity as a transcription factor in breast cancer cells. These findings were translated directly to the clinic when in 1971 a test for the ER was shown to predict the likelihood of patient response to surgical endocrine ablation (oophorectomy in premenopausal patients and adrenalectomy in postmenopausal patients) (Jensen et al., 1971), where patients with tumours exhibiting ER positivity showed a considerably higher response to endocrine strategies than those with ER negative disease (McGuire, 1975). Endocrine strategies have subsequently been developed to encompass several classes of agents which act as (i) selective oestrogen receptor modulators (SERMS) exemplified by the antihormone tamoxifen, (ii) selective oestrogen receptor downregulators (SERDS) such as Faslodex, and (iii) agents which target oestrogen biosynthesis, such as aromatase inhibitors (AIs) and luteinising hormone releasing hormone (LHRH) agonists. The ER and its signalling today still remains a major target for continued drug discovery for the treatment and prevention of breast cancer, and its cellular actions remain an intensely researched area of increasing complexity.

1.2.1   The Oestrogen Receptor

The ER is a member of the nuclear hormone superfamily whose members are capable of enhancing transcription of genes which contain the appropriate target hormone responsive element. The first and most predominant ER in breast cancer (and so more highly characterised) is ER alpha (ERα) (MacGregor and Jordan, 1998). The human ERα is located on chromosome 6q25.1 which encodes a protein of 595 amino acids with an approximate mass of 66kDa (Green et al., 1986). It is expressed in the female reproductive organs, the skeletal and cardiovascular system, and some regions of the brain (MacGregor and Jordan, 1998). It is also estimated that 15-20% of epithelial cells are ER-positive in the normal resting breast, with this figure fluctuating with the menstrual cycle. In addition to this, the receptor is overexpressed in breast cancer (Ali and Coombes, 2002)

More recently, the ER beta (ER-β) subtype has been isolated (Kuiper et al., 1996). The gene for the ERβ is found on chromosome 14q23-24 and encodes a 530 amino acid protein with a mass of 60 kDa (Enmark et al., 1997). The ERβ shows differences in tissue distribution compared to ERα. Although it is expressed in the ovaries, its expression is lower in other female reproductive tissues. It is however, highly expressed in several male organs and also in parts of the central nervous system (MacGregor and Jordan, 1998). ERβ, together with its subtypes are also found in breast cancer cells, and, the receptor has been suggested to have some

significance in the clinical response to anti-oestrogens (Murphy and Watson, 2006; Speirs et al., 2004)

The transcriptional regulation of the ERα gene can be initiated from two promoters, P0 and P1. P1 is the principal site, although this is tissue and cell-dependant. Its regulation is complex with a number of trans-acting factors shown to be involved in the transcriptional regulation of the ERα gene (Nicholson et al., 2002). For example, ERF-1 (oestrogen receptor factor-1) is a member of the AP-2 transcription factor family which has been shown to bind elements in the 5' non-coding region of the ERα gene (McPherson et al., 2000). The regulation of the ER protein is also complex and is again both tissue- and species-specific. Hormones are significantly involved in the regulation of ERα, and in-vitro models have shown variable ERα responses to oestrogens and progesterone (MacGregor and Jordan, 1998). A further factor involved in the regulation of ERα is phosphorylation of the ER protein which can impact on protein stability (Lannigan, 2003).

The ERα protein is a modular protein consisting of six functional domains, A to F which cumulatively enable nuclear localisation of the receptor, oestrogen binding, receptor dimerisation, association with DNA response elements, and subsequent transcriptional activation (Fig. 1) (Kumar et al., 1987).

The N terminal A/B region contains a hormone independent transactivation function, Activation Function (AF)-1, whereas a further transactivation function, AF-2 is located in the E region but is ligand dependant (Nicholson et al., 2002) (Fig. 1). In most cases these elements function synergistically to allow optimal ER activity, although their activity varies in different cellular contexts. In addition, optimal activation of AF-1 is thought to require phosphorylation of its key serine residues, including the Serine (ser-) residue at the 118 position of the ERα through the mitogen activated protein kinase (MAPK) signalling pathway (Joel et al., 1998; Kato et al., 1995) and also CDK9/TFIIH. Ser-104 and Ser-106 are targets for cyclin A2-CDK2 (Rogatsky et al., 1999), and AKT, rsk and casein kinase (CK) -2 respectively (Lannigan, 2003).

The C region of ERα houses the DNA-binding domain (DBD) (Fig. 1). It is configured as two zinc-stabilised DNA-binding fingers which are involved in DNA sequence recognition of the oestrogen response element (ERE) localised upstream of the oestrogen-responsive genes (MacGregor and Jordan, 1998). Additional amino acid residues in this region are thought to be also involved in nuclear localisation, receptor dimerisation, and heat shock protein (HSP) binding (Umesono and Evans, 1989), and where ser-167 and ser-236 may be subject to activation by protein kinase A (PKA) (Lannigan, 2003). The D domain appears to function as a hinge region between the DNA-binding domain and the Ligand-binding domain (LBD) and is thought to also be involved in nuclear localisation (Picard et al., 1990) although nuclear
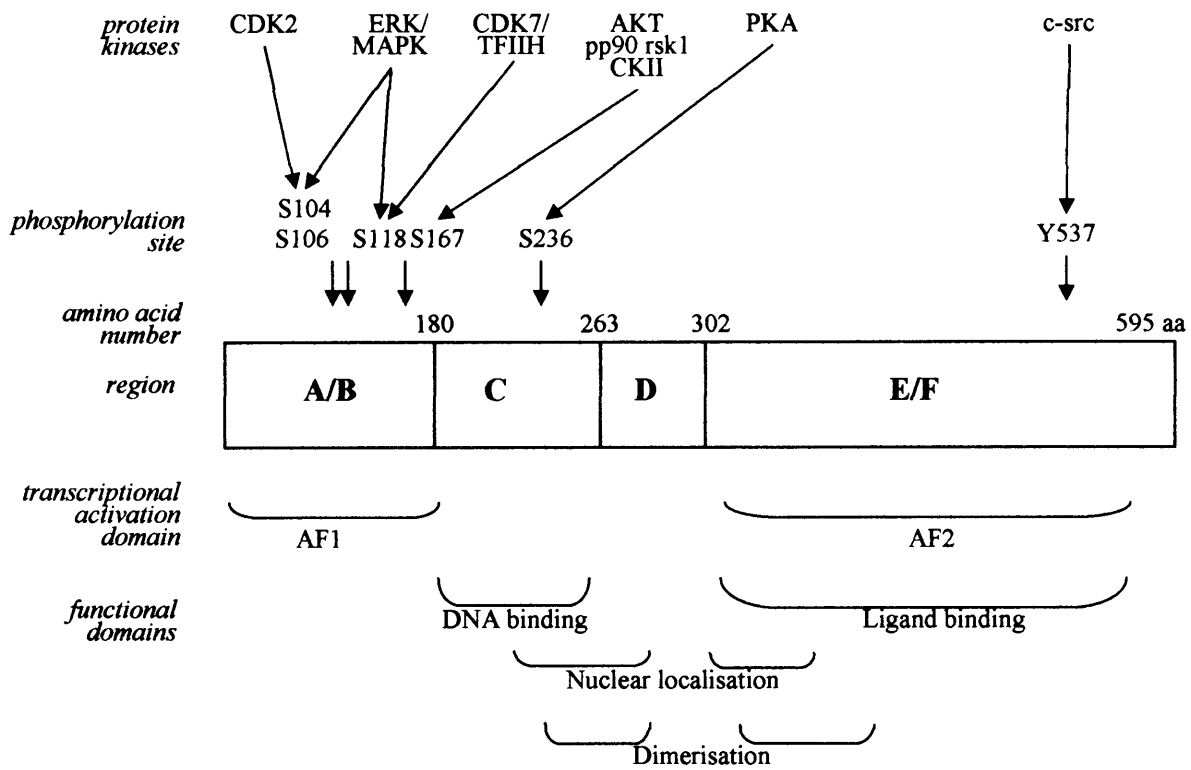
Figure 1. Structural and Functional Domains of the Human ER alpha Receptor. The receptor consists of six functional domains (A-F). Sites of potential phosphorylation are also shown together with the possible protein kinase capable of eliciting the event.

localisation signals (NLS) have also been reported in the LBD (MacGregor and Jordan, 1998) (Fig. 1).

The hydrophobic E region contains the LBD necessary for the binding of oestrogen to the receptor (Ponglikitmongkol et al., 1988) (Fig. 1). Crystallographic resolution of oestrogen and antagonist binding to the LBD reveals a pocket that sequesters ligand, comprising of 12 α-helices, a common motif in steroid receptors. The E region also houses the ligand-dependant transactivation function, AF-2 (Auchus and Fuqua, 1994). The ER dimerisation domain also resides in the C terminus of the E domain (Fawell et al., 1990) where phosphorylation of tyrosine 537 (possibly by c-src (Arnold et al., 1995a)) is thought to be an important factor in ERα dimer formation. Upon oestrogen binding, a number of important elements, such as coregulatory proteins are recruited to the LBD to modulate AF-2 activity (Berry et al., 1990). The E region is also important in binding chaperone proteins such as HSP90 and HSP70. These proteins exist as a complex with the receptor in the absence of the ligand and prevent receptor dimerisation, thus inhibiting DNA binding and ER-mediated gene transcription (Bohen et al., 1995). Also finally, the F region lies at the C terminal and may be involved in the transcriptional activity of oestrogen-antagonist regulated genes, and also responsible for the cell-specific behaviour of the receptor (Montano et al., 1995).

A number of functional domains of the ERα and ERβ show a high degree of homology, such as the DBD and LBD at 97% and 60% respectively. However, more divergence is observed at the N terminus of the proteins which share only 18% homology. The homologous characteristics of these proteins at the DBD and LBD suggest an interaction with identical DNA response elements with similar binding affinities for ligands (Hall, 2001).

1.2.2 Oestrogen Receptor Signalling

Oestrogens are steroid hormones which function via the ER to regulate cell growth. These hormones function in a wide range of target tissues including reproductive tract, mammary gland, and the skeletal, as well as the cardiovascular system (MacGregor and Jordan, 1998). Although other oestrogens are present, the most potent and dominant oestrogen in humans is 17 β-oestradiol (E2) (MacGregor and Jordan, 1998). With oestrogens demonstrating a wide range of physiological effects on target tissues, a complex mechanism of action is implied. Since identification of the ER in the 1960s, many laboratories have attempted to dissect E2/ER signalling. Cumulatively, a number of fundamental mechanisms of ER signalling have been recognised alongside the classical ligand-dependant nuclear ER signalling, notably ligand-independent nuclear ER signalling (ER-transcription factor cross-talk), and the non-genomic/ membrane ER signalling mechanisms (Hall et al., 2001) (see Fig.2).

1.2.2.1 Classical Mechanism of Nuclear ER Signalling

The classical mechanism of oestrogen signalling assumes the unstimulated receptor is in a state of inhibition localised within the nucleus as a multiprotein complex, bound to elements such as the HSP90/ HSP70 chaperonin, which are thought to stabilise the protein. The receptor may also be bound by co-repressors such as SMRT or NCoR in this state (Pratt and Toft, 1997).

Oestrogens are thought to freely diffuse through the cell membrane and bind to the ER (Guiochon-Mantel et al., 1996). All steroid receptors, including ERα have been shown to have enhanced phosphorylation after ligand binding (Weigel and Zhang, 1998), and ERα is phosphorylated at multiple sites (Lannigan, 2003), with a 3-4-fold increase in ERα phosphorylation following oestradiol exposure (Le Goff et al., 1994). This may be an important factor in dimer formation, enhancing nuclear translocation or increasing affinity for the target ERE and subsequent transcriptional activity. Although the ERα is thought to be phosphorylated at multiple seine residues, reports have also shown the activation of a tyrosine residue in the presence of E2 (Lannigan, 2003; Nicholson et al., 2002) (Fig.1).

E2 binds into a hydrophobic pocket in the LBD, and structural analysis of this domain reveals a compact configuration consisting of 12 α-helices (Shiau et al., 1998). On ligand binding, the conformation of the structure is altered such that helix-12 seals in the ligand. A subsequent conformational change in the receptor permits the dissociation of the receptor-associated proteins such as HSP90 and HSP70, and provides a surface onto which coregulatory proteins may interact (Shiau et al., 1998). The positioning of diverse ligands within this pocket is thought to result in different contact sites such that there is altered positioning of helix-12, and thereby altered coregulator recruitment. Thus, the binding of the natural ligand E2 to the ER allows recruitment of co-activator proteins and thus AF-2 activity, whereas the SERM tamoxifen or Raloxifene binding results in altered positioning of the 12-helix which inhibits this process (Brzozowski et al., 1997).

The dissociation of the HSP permits the receptor dimerisation. It is worth noting that where both ERα and ERβ are expressed, in-vitro studies have suggested a preferential heterodimerisation takes place, indicating the ratio of the two receptor types may be of some importance to oestrogen responsiveness (Hall and McDonnell, 1999). Following dimerisation, and subsequently localisation to the nucleus (Webb et al., 1998) interaction with the DNA double helix of the DBD occurs with the ER, subsequently mediated through the presence of two zinc finger motifs in the ER structure. The ER dimer binds with high affinity to a target region within the promoter of responsive genes, the oestrogen response element, which consists of a three nucleotide sequence flanked by a four sequenced palindromic inverted repeat that can vary from gene to gene. The extreme flanking sequences of this palindrome in E2-regulated genes are thought to be important in determining the ERα affinity for the ERE (Anolik et al.,
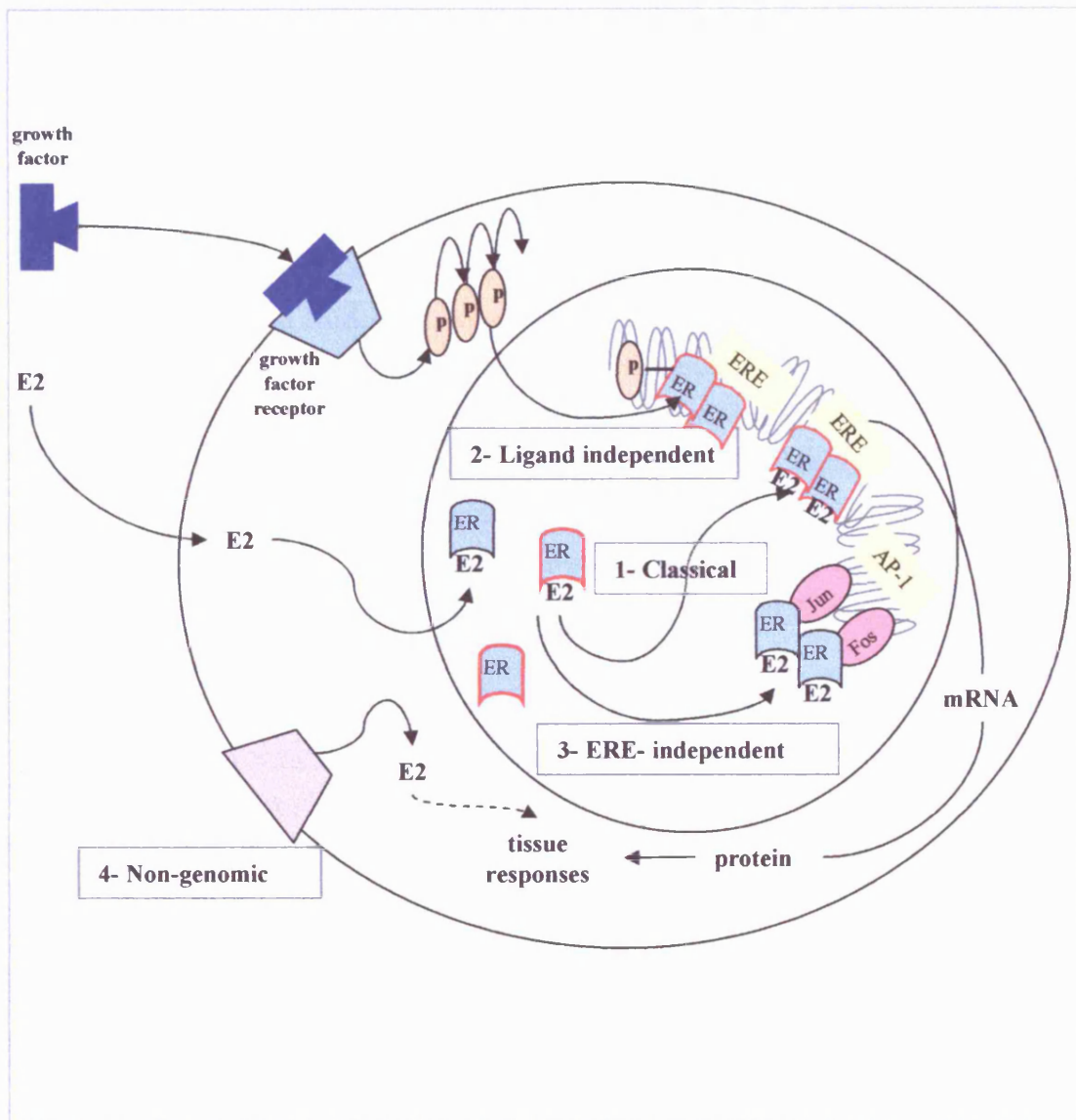
Figure 2. Mechanism of Oestrogen Receptor Signalling. Oestrogen (E2) elicits its biological effects through: (1) the classical pathway of ligand-dependent, E2-ER complex binding to EREs in target promoters leading to alterations in gene transcription with subsequent tissue responses; (2) The ligand-independent pathway, where agents such as Growth factors activate intracellular kinase pathways, leading to phosphorylation (P)/ activation of ER at ERE-containing promoters in a ligand-independent manner; (3) ERE-independent, nuclear-ER complexes alter transcription of genes containing alternative response elements such as AP-1 through association with other DNA-bound transcription factors (Fos/Jun), which alter gene expression by binding ER to DNA; (4) Non-genomic/ membrane signalling, where rapid tissue responses are generated through the activation of intracellular kinase signalling components by E2 (adapted from Hall et al,. 2001).

1995). Genes whose promoters contain functional EREs include those encoding for the human pS2 and progesterone receptor (PgR) (Jeltsch et al., 1987; Kraus et al., 1994).

Interaction with the ER results in a conformational change in the DNA, which is thought important for allowing interactions with multiprotein complexes. Interaction with these co-activator proteins serves to enhance ER-mediated transcription. Many co-activators, such as SRC-1, SRC-2, SRC-3, p300, cAMP-response-element-binding (CREB)-binding protein (CBP) exhibit histone acetyl transferase (HAT) activity to facilitate chromatin remodelling and thus gene transcription (Lonard and O'Malley, 2005). Gene transcription following the activation of the ER by E2 is initiated through a process involving numerous factors being assembled at the gene promoter, including the interaction with basal transcription factors and the involvement of the co-activators to form the transcription initiation complex, for the eventual recruitment of RNA polymerase II for initiation of transcription. Gene targets of oestrogen action (some via classical ERE) include a number of genes involved in proliferative signalling and cell cycle progression, such as cyclin D1, c-fos, c-jun, c-myc, c-myb, and transforming growth factor (TGF)-α (Foster et al., 2001; Loose-Mitchell et al., 1988; May and Westley, 1995; Weisz and Bresciani, 1993).

1.2.2.2 Ligand-Independent Activation of Nuclear ER

The ER can be phosphorylated at a number of key sites, either as a consequence of ligand, or in a ligand-independent manner. Ser-118 and ser-167 were demonstrated to be major sites of phosphorylation in the presence of E2 (Joel et al., 1995). However, these are also the predominant sites of ligand-independent activation following stimulation of MAPK or phosphoinositide-3 kinase (PI3K/AKT) signalling respectively (Campbell et al., 2001; Joel et al., 1995) (see also section1.5.1). In turn, cyclin A/ cdk2 can activate ser-104 and ser-106 in a ligand independent manner (Rogatsky et al., 1999). Ser-167 has also been shown to be phosphorylated in-vitro by CK2 (Arnold et al., 1995a), and ser-236 may be phosphorylated by PKA (Chen et al., 1999). In contrast to the above serine phosphorylation sites clustered around AF-1, the ERα is also reported to be phosphorylated at tyrosine (tyr)- 537 (Arnold et al., 1997). This site has been reported to be phosphorylated by c-src tyrosine kinase (Arnold et al., 1995b).

Ligand independent ER phosphorylation can occur where there are elevated levels of growth factor kinase signalling within the cells. For example, MCF-7 cells which have acquired resistance to antioestrogens exhibit increased levels of Epidermal Growth Factor Receptor (EGFR)/ HER2 and MAPK (Knowlden et al., 1997; McClelland et al., 2001). Studies have shown that the co-activators such as p68 RNA helicase and SRC-1 can be recruited in a ligand independent manner to enhance the activity of AF-1 in response to phosphorylation of ERα at ser-118 (Endoh et al., 1999), notably driven by MAPK (Britton et al., 2006). The impact of

ligand-independent growth factor-mediated activation of the ER will be fully discussed in the context of the development of resistance to antioestrogens (see section 1.5)

1.2.2.3 ER/ Nuclear Transcription Factor Cross Talk

There is a growing body of evidence demonstrating the ability of oestrogen-ER to affect gene expression through non-classical mechanisms by protein/protein interaction of nuclear ER with other transcription factors, including AP-1, SP-1 or nuclear factor kappa beta (NFκB). In this mechanism, the activities of the various transcription factors are modulated by the ER through the stabilisation of their DNA binding or through the enhanced recruitment of co-activators to the complex. ER/AP-1 for example is capable of transducing multiple mitogenic growth signals triggered from growth factors like the insulin-like growth factor (IGF), HER2 and epidermal growth factor (EGF) (DeNardo et al., 2005; Johnson et al., 2000; Kushner et al., 2000; Webb et al., 1995). Recent studies have also shown triggering of c-myc and cyclin D1 expression via ER-transcription factor interaction to promote cell cycle progression (Butt et al., 2005).

1.2.2.4 Non-genomic (membrane) ER Signalling

The observed rapid biological effects instigated via signalling by oestrogen occurring in the bone, breast, vasculature, and nervous system suggest that non-genomic signalling may be occurring at the plasma membrane. Indeed, although, the classical genomic mechanism of oestrogen action seems to be the dominant mechanism of ER action, several tyrosine kinase signal transduction proteins have been demonstrated to be rapidly triggered by E2, and have been identified in a number of cell lines, including MCF-7 breast cancer cells (Pedram et al., 2006). For example E2 causes the rapid induction (in minutes) of MAPK activity in breast cancer cells (Li et al., 2006) which is blocked by the MAPK inhibitor PD98059, and also inhibited by the antioestrogen Faslodex, confirming the role of the ER. The proliferative/ anti-apoptotic effects of E2 action through rapid triggering of MAPK have also been observed in osteoblasts (Kousteni et al., 2001), and E2 has been also shown to initiate rapid signalling through PI3-K and calcium calmodulin-dependent kinase IV in breast cancer cells (Duan et al., 2002; Qin et al., 2002).

Importantly, several transcription factors have been shown to be activated by oestrogens through non-genomic pathways resulting in the induction of a number of genes in ZR-75 and MCF-7 breast cancer cells. For example, when rapidly E2 activated the PI3K/AKT pathway (Castoria et al., 2001), leads to downstream modulation of the activity of transcription factors, such as Elk-1, CCAAT/enhancer-binding protein-beta (C/EBPβ), nuclear factor for interleukin-6 (NF-IL6), CREB and c-Fos/c-Jun (Kousteni et al., 2003), where such actions can promote cell entry into S-phase (Castoria et al., 2001).

1.3 Antihormone Therapies for Breast Cancer

On disease presentation, treatment for the breast cancer patient with early disease is principally surgical removal of the tumour, coupled to the use of a systemic adjuvant therapy for the prevention/ treatment of micrometastatic deposits. Such treatments have a curative aim. In patients with metastatic disease, systemic therapy is often the principal treatment, and is largely palliative (Cristofanilli, 2006). The choice of adjuvant treatment, i.e. endocrine or chemotherapeutic, is substantially dictated by the steroid hormone receptor status of the patient, where receptor-positive patients principally benefit from endocrine therapy. Such endocrine therapy is believed to be effective in more than 50% of ER (and/or PgR) positive patients, a contrast to only 11% of patients responding who are negative for both receptors (Buzdar, 2001; Osborne et al., 1980). Various endocrine therapies have been developed which aim to inhibit the production of oestrogens or prevent the action of oestrogens through blockade of the ER

In premenopausal women, the synthesis of oestrogens (circulating mainly as 17β-oestradiol) from androgen precursors using the aromatase enzyme, usually occurs in the ovaries and is regulated by the pituitary gonadotrophins, follicle-stimulating hormone (FSH) and luteinising hormone (LH). Lower levels of oestrogens are also synthesised by aromatase in the adipose tissue, skin, bone, a number of vascular regions, and the brain (Simpson and Davis, 2001). However, with the onset of menopause, such non-ovarian sources of oestrogen production become dominant sites of production of oestrogens. In addition, breast cancer cells are also capable of synthesising oestrogens from androgen precursors, and the intratumoural content of oestrogen has been suggested to be many fold higher than that detected in the plasma of postmenopausal women, (Castagnetta et al., 1996). Ablative treatment through the surgical removal of the ovaries in premenopausal women or, more recently, medical ablation by use of LHRH agonists, such as Zoladex, can be used to reduce oestrogen levels predominantly made by the ovaries (Cheer et al., 2005), and are used in combination with tamoxifen (see below). In postmenopausal women, however, when ovarian function ceases, aromatase inhibitors must be used to selectively target aromatase enzyme in peripheral tissues and tumour, thereby depleting E2 levels.

Modern AIs largely evolved from aminoglutethimide, a cytochrome P450 (CYP) inhibitor that demonstrated benefits in advanced breast cancer by the inhibition of the aromatase enzyme. AIs are classified according to their structure, being either steroidal, as derivatives of androstenedione that bind irreversibly to aromatase, or non-steroidal AIs that are competitive inhibitors which also block the heme moiety of aromatase (Berry, 2005). While agents such as aminoglutethimide show non-selectivity, and the second generation AIs, such as formestane,

exhibit relatively low effectiveness, the third-generation AIs, such as anastrozole, exemestane, and letrozole are now demonstrating highly efficient inhibition of aromatase (Dixon, 2004).

The improved third-generation AIs have relatively recently been the subject of a number of phase III trials showing favourable outcomes in the management of breast cancer, and the agents are currently being used as first-line therapy in patients with hormone receptor positive disease and are of increasing importance in the adjuvant (early) setting in postmenopausal women (Goss, 1999; Sainsbury, 2004).

Since the first reported assessment of the antioestrogen tamoxifen (Nolvadex; Astra Zeneca) in 1971 (Cole et al., 1971) in breast cancer many antioestrogens have been evaluated that all competitively inhibit oestrogen binding to the ER to bring about ER blockade (Howell et al., 2004). However, tamoxifen still represents the gold standard antioestrogen, and lies in a class of non-steroidal antioestrogens termed SERMs which exhibit mixed oestrogenic/ antioestrogenic activities (Osborne, 1998). More recently, steroidal antioestrogens have been developed that are devoid of any agonist activity. These are exemplified by the pure ER antagonist, (Selective Oestrogen Receptor-Downregulator; [SERD]) fulvestrant (Faslodex; ICI 182,780), which was licensed in the UK in 2004 for the treatment for advanced breast cancer as second-line therapy after antioestrogen (tamoxifen) failure (Howell et al., 2000). Both tamoxifen and Faslodex, and their mechanisms of action will be discussed in detail below.

1.3.1 Tamoxifen (a Selective Oestrogen Receptor Modulator; SERM)

Tamoxifen, first synthesised in the 1960s, was approved by the US Food and Drug Administration in 1977, and is currently the standard adjuvant treatment for ER positive breast cancer. It has been demonstrated to improve survival as an adjuvant therapy in early breast cancer, and is beneficial in the advanced setting. Tamoxifen has also been shown to reduce the incidence of breast cancer in healthy women at risk of developing the disease (1998; Cole et al., 1971; Fisher et al., 1998). Large-scale randomised trials have shown that tamoxifen administration after surgery for early-stage ER-positive breast cancer reduces mortality by 28% (Johnston and Dowsett, 2003), and it is estimated that many breast cancer patients in the developed countries have received, or are receiving tamoxifen. The reduction in mortality rates from breast cancer in the UK over the last 12 years is thought to be due, in part, to the use of tamoxifen in early-stage disease (Johnston and Dowsett, 2003).

Tamoxifen, a non-steroidal triphenylethylene based antioestrogen (Fig.3), belongs to a group of anti hormonal therapies termed SERMs. The structure of its metabolite 4-hydroxytamoxifen (4-OHT), has formed the basis for chemical modification of the drug, leading to further compound development, including alteration of the side chain to produce torimifene (Howell et al., 2004). However the majority of these compounds are inferior or, at best

---

10
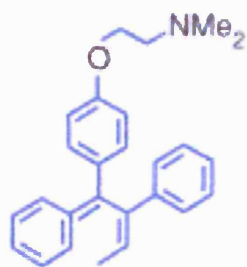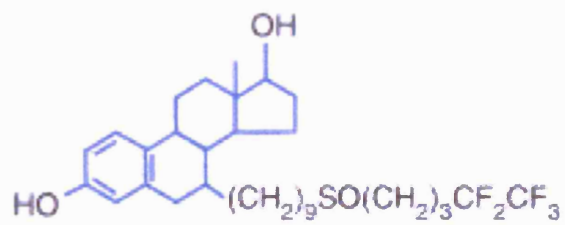
Figure 3. The structure of tamoxifen and Faslodex
(from Howell *et al.*, (2004))

equivalent to tamoxifen in terms of response and toxicity (Howell et al., 2004). As the name suggests, SERMs exhibit mixed oestrogenic/ antioestrogenic activity in a tissue-selective manner. Thus, tamoxifen gives rise to favourable oestrogen-like effects on bone and serum lipid concentrations, while in breast tissue acts antioestrogenically to inhibit tumour growth (Osborne et al., 2000). Some of the undesirable effects of tamoxifen include antioestrogen responses in the central nervous system (manifest as 'hot flushes'), thromboembolytic events, and oestrogenic actions on the endometrium leading to an increase in the risk of endometrial cancer (Osborne et al., 1995). However, the undesirable properties are outweighed by the considerable benefits tamoxifen has provided in breast cancer.

The mode of action of tamoxifen is, in some aspects similar to oestradiol, with diffusion through the plasma and nuclear membrane where interaction with the ER results in the binding of the antioestrogen to the LBD, promoting dissociation of receptor associated proteins. However, the conformation of the tamoxifen–ER complex is different to the E2 bound receptor and results in an altered helix-12 configuration due to the bulky side chain of tamoxifen (Levenson and Jordan, 1999; Shiau et al., 1998). Thus, although dimerisation of the receptor still occurs, tamoxifen binding alters the AF-2 conformation, preventing co-activator recruitment and maintaining corepressor binding (eg. NCOR/SMRT) (Clarke et al., 2001a; Klinge, 2000). In contrast, although the activity of AF-2 is attenuated, AF-1 activity remains, which is thought to provide the partial agonistic activities exhibited by tamoxifen. The latter activity, however, is dependent on cellular context and associated co-activator/ AF-1 kinase availability (Berry et al., 1990; McInerney and Katzenellenbogen, 1996).

1.3.2   Faslodex (a Selective Oestrogen Receptor Downregulator; SERD)

Although the standard endocrine agent of choice for the past 30 years has been tamoxifen in ER-positive breast cancer, considerable effort has been made to reduce its oestrogen-like properties, and thus, eliminate some of the unwanted side effects of antioestrogens. This, coupled with the phenomenon of resistance to tamoxifen treatment (see section 1.5) which may also be linked to its oestrogen-like properties, prompted the development of several steroidal agents devoid of oestrogenicity. One such compound is fulvestrant (Faslodex, ICI182,780, Astra Zeneca) which, unlike tamoxifen exhibits no agonist activity and is currently being used clinically in advanced breast cancer disease when patients relapse on tamoxifen (Dukes et al., 1993; Wakeling and Bowler, 1992). Recent reports from two phase III trials have shown that Faslodex is at least as effective as the third generation aromatase inhibitor anastrazole in postmenopausal women with advanced breast cancer following tamoxifen, thus demonstrating its potential for use in second-line therapeutic regimes. Additionally, Faslodex has shown some potential following AI failure (Howell, 2006).

Faslodex is a steroidal 7α-alkylsulfinyl analogue of oestradiol which exhibits a markedly higher affinity for the ER compared with tamoxifen (Wakeling et al., 1991). However, owing to the bulky side chain (Fig.3) steric hindrance prevents dimerisation of the receptor (Howell et al., 2004). Reports from *in-vitro* and *in-vivo* studies have also shown increased ER turnover, with a disruption in nuclear localisation and a concomitant reduction in the ER protein within the cell. As a consequence, decreased DNA binding occurs, and also, coupled with an inactivation of both AF-1 and AF-2, a substantial blockade of E2-regulated genes ensues (Howell et al., 2004).

Importantly, Faslodex treatment does not promote oestrogenic effects on the uterus, and has a superior inhibitory effect on breast cancer models, both *in-vitro*, and *in-vivo* (Howell et al., 2000). It is also able to block any stimulatory effects of oestrogen or tamoxifen (Dukes et al., 1993; Wakeling and Bowler, 1992). This pure antioestrogenic action of Faslodex is particularly important with regards to treating tamoxifen resistance (discussed later). *In-vitro* studies report tamoxifen-resistant cell lines remain ER-positive and responsive to Faslodex (Brunner et al., 1993; Coopman et al., 1994; Hu et al., 1993). In addition, studies in nude mice demonstrate the growth suppression of MCF-7 xenografts by Faslodex is twice the duration of that of tamoxifen (Osborne et al., 1995). A number of clinical studies have also demonstrated a therapeutic potential of Faslodex, where its potent ER downregulating capability is seen alongside its ability to profoundly decrease the levels of the E2-regulated gene, PgR and deplete proliferation markers (McClelland et al., 1996).

1.4 Antihormone Resistance in Breast Cancer

Antihormone therapies, as well as being relatively well tolerated, have proved to be invaluable approaches in the improvement of breast cancer patient survival. SERMS such as tamoxifen have remained the primary choice for therapy in ER-positive disease for several decades, although newer antihormone treatments are now emerging, notably, the pure antioestrogen Faslodex, and a number of third generation aromatase inhibitors exemplified by Anastrazole that may supersede tamoxifen in the clinic (Berry, 2005; Howell, 2006). However, for both tamoxifen and these newer therapies, the development of resistance remains a pervading problem.

1.4.1 Development of Endocrine Resistance

Clinical observations, together with cell tumour models are uncovering some of the elements that may be responsible for the development of resistance to tamoxifen, Faslodex, and oestrogen deprivation. A vast knowledge acquired in breast cancer research is in part due to the

in-vitro and *in-vivo* studies performed with breast cancer cell lines. As an unlimited source of relatively homogenous cells, they can be grown easily in most laboratories. Following the first cancer cell line in 1958 (Lasfargues and Ozzello, 1958) continued work has now established around 100 breast cancer cell lines. A number of attempts have been made to culture cells from primary breast cancers (Amadori et al., 1993; Gazdar et al., 1998), however, relatively low success rates are generally achieved due to technical difficulties. Thus, cell line models still remain a well established source of material for study. Although the usefulness of cell lines has been debated (Burdall et al., 2003) their careful application within a well structured study design, including the monitoring of phenotypic and genotypic characteristics, can be invaluable.

Many of the well known and exclusively used breast cancer cell line models, including ER-positive MCF-7 and T47D, and ER-negative MDA-MB-231 cells, were established in the late 1970s. One of the most popular ER-positive models, MCF-7 was derived from a metastatic, invasive ductal carcinoma, from the pleural effusion (Engel and Young, 1978; Soule et al., 1973). A recent study extensively comparing a large number of breast cancer cell lines concluded that although a wide range of genetic and phenotypic characteristics existed from one model to another, the MCF-7 breast cancer cell line was reflective of the ER-positive tumours *in-vivo* (Lacroix and Leclercq, 2004). A further property of MCF-7 cells which makes them attractive for study is that they demonstrate endocrine responsiveness. The MCF-7 cells, being ER-positive, are subject to the mitogenic effects of oestradiol, and are thus affected by the inhibitory actions of antihormones. This cell line has also been used to develop *de novo* resistance to tamoxifen by transfection of growth factor receptors (eg. HER2) and can acquire resistance by continuous culture *in-vitro* in the presence of inhibitory doses of antihormones (Knowlden et al., 2003; Shou et al., 2004). The characteristics of some of these models will be discussed in the proceeding sections in parallel with clinical observations.

1.4.1.1 Tamoxifen Resistance

While 70-80% of breast cancers are positive for ER, only around 40% of tumours respond to endocrine therapy, i.e. ~50% of ER positive breast cancers are innately resistant to tamoxifen treatment (*de novo* resistance). Inherent tamoxifen resistance is also observed in all ER-negative tumours. Also, those tumours that are initially responsive to tamoxifen acquire resistance and ultimately regrow resulting in disease relapse. Resistance associated cellular features include increased aggressive tumour behaviour, metastatic spread, and thereby poorer patient outlook (Cheung et al., 1997; Osborne and Fuqua, 1994). It is therefore of fundamental importance to uncover the mechanisms that allow tumour cells to circumvent tamoxifen response and a number of mechanisms have been proposed.

1.4.1.1.1 Loss of ERα Expression/ Function, ERβ and Variant Forms

While the level of expression of the ER is an important predictor for the initial responsiveness to tamoxifen therapy, *de novo* resistant disease is frequently ER-negative/ PgR-negative (Nicholson et al., 2002). This may occur through CpG island hypermethylation (Ottaviano et al., 1994), although ER expression can be lost on acquisition of resistance to tamoxifen, the majority of patients continue to express the receptor, and can, in some instances, respond to aromatase inhibitors or Faslodex, indicating that the ER is still functional in these patients (Howell et al., 2002; Osborne et al., 2002). In other patients however, dysfunctional forms of the ER have also been proposed to explain tamoxifen resistance, although mutational studies have rarely found mutant ER in the clinic (Karnik et al., 1994), and data linking ERα splice variants to endocrine resistance is, at best, inconclusive (Nicholson et al., 2002).

As described previously, the ERβ is highly homologous to the ERα in the DBD and LBD and has a similar affinity for oestrogen (MacGregor and Jordan, 1998). Although the predominant receptor type in breast cancer is ERα, heterodimers with ERβ are also found, and the ratio of ERα/ERβ may have some significance on the development of resistance. Indeed, increased expression of ERβ in more aggressive disease has been found (Clarke et al., 2001b). Significantly, an ERβ variant, ERβcx has also been described, and was found expressed in half of the breast cancer samples (Palmieri et al., 2004). This variant receptor can also heterodimerise with wild type ERα and may affect endocrine sensitivity (Speirs et al., 2004).

1.4.1.1.2 Growth Factor Pathways

In comparison to ER-positive states, the expression of EGFR, HER2 and TGFα are observed to be markedly elevated in ER-negative disease (Nicholson et al., 2004a), and may even promote ER loss through the hyperactivation of growth factor signalling pathways. Thus, in MCF-7 cells, EGF, IGF-1, TGFβ reduced ER levels *in-vitro*, with elevated signalling through PI3K/AKT, PKA and NFκB, believed to be integral to such responses (Normanno et al., 1994). Additionally however, at lower levels, activation of growth factor signalling is also thought to be an important mechanism for the *de novo* and acquired failure of endocrine therapies in ER-positive cells, with a number of growth factors reported to be overexpressed in such breast cancer cells, notably the EGF and IGF family receptors and ligands, and downstream signalling elements (Nicholson et al., 2005).

1.4.1.1.2.1 EGF Family

One of the dominant pathways which has been implicated in the development of tamoxifen resistance involves the EGF family of ligands and receptors. These comprise the receptors erbB1 (EGFR), erbB2 (HER2), erbB3 (HER3) and erbB4 (HER4), and ligands EGF, TGFα, and heregulins, and these receptors have been shown to share a high sequence homology, notably within the tyrosine kinase domain (Mosesson and Yarden, 2004). The HER2 receptor, described as an orphan receptor, is distinct from the other family members as it has no natural ligand although it is recognised as an effective heterodimerisation partner for other family members (Earp et al., 1995; Menard et al., 2000).

The successful clinical introduction of the humanised antibody to HER2, trastuzumab (Herceptin) in 1998 has highlighted the importance of this signalling network in breast cancer (Brand et al., 2006). Indeed, clinical reports have shown an association between poor prognosis for breast cancer and overexpression of HER2 and EGFR (Nicholson et al., 1994a). These receptors have been related to resistance *de novo* to tamoxifen, in both ER-positive and ER-negative states (Nicholson et al., 2004a). EGF-related ligands such as TGF-α have also been shown to be associated with endocrine non-responsiveness in ER-positive breast cancer specimens (Nicholson et al., 1994b), and the coexpression of ligands with EGFR (eg. amphiregulin, TGFα) has been reported in *in-vitro* models of acquired tamoxifen-resistance (Nicholson et al., 1999). Furthermore, in clinical disease, there can be increases in HER2 and EGFR in some patients on tamoxifen relapse (Gee et al., 2005).

A number of laboratories have developed models of ER-positive resistance to tamoxifen, either de novo or acquired. In our own laboratory, an ER-positive acquired tamoxifen-resistant cell line (TamR) was developed by the continual exposure of parental wild-type MCF-7 cells to 10^{-7} M 4-hydroxytamoxifen. After regular medium replacement and passaging for 3 months, growth rates increased subsequent to the initial responsive phase. The emergent cells had thus acquired resistance to tamoxifen (Knowlden et al., 2003). Studies in our laboratory have shown that EGFR and HER2 protein and mRNA are upregulated in the resistant cell line ,with increased levels of active EGFR/HER2 hererodimers versus the parental MCF-7 cells.

The dependency on such growth factor signalling is reiterated in the model of Osborne which is based on the MCF-7 cell line which has been engineered to overexpress HER2 through a HER2 expression vector (MCF-7/HER2-18) (Shou et al., 2004). MAPK activation is also demonstrated in MCF-7/HER2-18 cells. This downstream phosphorylation event observed in MCF-7 /HER2-18 cells is also in accordance with observations using the ER-positive and tamoxifen-resistant BT434 cell line, which exhibits HER2 gene amplification (Anzick et al., 1997; Lin et al., 1990). In our own ER-positive tamoxifen resistant cell models, alongside

EGFR upregulation, EGFR signalling through MAPK and AKT signalling is also observed, (Knowlden et al., 2003).

The importance of the erbB family of receptors/ligands in these various resistant cells is highlighted by the actions of the EGFR-specific tyrosine kinase inhibitor (TKI), Gefitinib, or the HER2 inhibitor Herceptin which promotes efficient growth inhibition of both acquired or de novo ER-positive models of tamoxifen resistant breast cancer (Knowlden et al., 2003; Shou et al., 2004).

Other models of resistance, such as those from Meijer and coworkers derived by genetic manipulation of ZR-75-1 cell lines to select for cell line colonies with acquired resistance to tamoxifen, again suggested that EGFR may be a mechanism for antioestrogen-resistant growth, as determined through gene expression microarray studies. However, further genes were revealed as involved in resistance, such as platelet-derived growth factor (PDGF) -α and -β, colony stimulating factor (csf) 1-R, neuregulin, and fibroblast growth factor (FGF) 17 (Meijer et al., 2006). This laboratory also identified a number of breast cancer antioestrogen resistance (BCAR) genes such as BCAR4 (Meijer et al., 2006) and BCAR1 (Dorssers et al., 2005). Indeed, BCAR1 or 4 has been strongly linked to the endocrine resistant phenotype (Dorssers et al., 2005).

14.1.1.2.2 IGF family

Components of the IGF signalling pathway have also been shown to be involved in driving antioestrogen resistant breast cancer cells, and may positively cross-talk with EGFR signalling (Gee et al., 2005; Knowlden et al., 2003). Indeed, overexpression and activation of IGF-1R and associated downstream proteins have been reported in breast cancer, and linked to disease progression and increased resistance to radiotherapy (Rocha et al., 1997).

The IGF growth factor system comprises three ligands, IGF-I, IGF-II and insulin, capable of interacting with the IGF-1R receptor, and a number of IGF- binding proteins exist to regulate IGF action, in part, through sequestering the IGF-1R ligands (Clemmons, 1998). The IGF-1R receptor is a transmembrane tyrosine kinase that is highly related to insulin receptor (IR). The type II IGF receptor (IGF-IIR) has high affinity for IGF-II, but unlike the other family members is thought to transmit no intracellular signal and has been characterized as a regulatory 'sink' for IGF-II (Clemmons, 1998). IGF signalling is initiated through the coupling of the receptor to adaptor proteins, Insulin Receptor Substrates (IRS) (Whitehead et al., 2000), which activate downstream signalling molecules such as MAPK and PI3K/AKT signalling (Sachdev and Yee, 2001; Whitehead et al., 2000). IGF-1R signalling is contributory to the growth of hormone responsive cells with MCF-7 cells demonstrating high levels of IGF-1R which can be readily blocked by IGFR-specific inhibitors (such as AG1024) to promote growth inhibition (Nicholson et al., 2004a). Importantly, the IGF-1R pathway impinges on ER

signalling, which in turn can induce aspects of IGF-1R signalling, to facilitate the mitogenic effects of oestrogens (Hamelers and Steenbergh, 2003). This is also consistent with the observations that IGF-1R levels are high in ER-positive clinical disease (Happerfield et al., 1997) and increased IGF-1R is generally found in hormone responsive tumours (Gee et al., 2005).

Significantly however, the IGF-1R pathway has recently been shown to interact with EGFR signalling in tamoxifen-resistant breast cancer cells in-vitro (Knowlden et al., 2005), and the pathway is active in tamoxifen-resistant clinical disease (Gee et al., 2005). Indeed, in the tamoxifen resistant cells developed in our own laboratories, both IGF-1R and EGFR activity could be induced by exposure to IGF-II (Knowlden et al., 2005), where IGF-1R enhanced EGFR pathway by a src-dependant phosphorylation of EGFR on tyr845. Such altered growth factor signalling has also been demonstrated in-vitro to contribute to changes in cellular morphology which resemble epithelial mesenchymal transition (EMT), with an observed higher growth rate, motile behaviour, and increased invasiveness in the acquired TamR cells. This is reflective of the clinical scenario on progression (Hiscox et al., 2004; Nicholson et al., 2005), where resistance can be associated with metastasis to unfavourable sites and poorer prognosis..

It is noteworthy that although erbB pathways appear dominant mechanisms in models derived from our laboratories, studies from other centres have shown tamoxifen or Faslodex resistance can develop in cells which maintain extremely low levels of EGFR expression, and which show no change in HER2 and no response to Herceptin (Briand and Lykkesfeldt, 1984); (Frogne et al., 2005). Although, these cells demonstrate minimal involvement of IGF-1R signalling, both tamoxifen and Faslodex resistant growth appears to involve the phosphorylation of AKT (Frogne et al., 2005).

1.4.1.1.3 ER Signalling as a Target for Growth Factor Pathway Cross-Talk

There is compelling evidence suggesting the existence of multiple regulatory interactions between the ER, growth factor, and kinase signalling networks that may contribute to tamoxifen failure. As eluded to earlier, peptide growth factors, including EGF, TGFα, IGF and heregulin, or their receptors can trigger ligand independent phosphorylation of the ER at multiple sites (see Fig. 1), which are capable of increasing transcriptional activity of ER and ER-mediated gene expression in the presence of tamoxifen (Le Goff et al., 1994). These phosphorylation events are mediated via growth factor-driven kinase signalling, such as MAPK pathways, which can, for example phosphorylate the ER at Ser118 position within the AF-1 region of the receptor (Nicholson et al., 1999), as frequently observed in in-vitro models of acquired tamoxifen resistance (Britton et al., 2006; Knowlden et al., 2003; McClelland et al., 2001). Interestingly, hyperexpression of MAPK signalling components have been reported in breast cancer tumours (Sivaraman et al., 1997), and this is also seen in the clinic where

increased ERK1/2 MAPK activity has been associated with poorer quality, shorter duration, and decreased survival in response to endocrine therapies (Gee et al., 2001). Our laboratory has also observed increases in ERK1/2/MAPK activity on clinical relapse with tamoxifen in the clinic, and hyperactivated growth factor signalling components are also present in acquired tamoxifen resistance models (Gee et al., 2001; Knowlden et al., 2003).

Additionally, studies have reported that the ER can be phosphorylated by other signalling components, such as Casein Kinase II, AKT, pp90rsk1, PKCδ, cyclinA/CDK2, and c-src (Lannigan, 2003). Links have also been suggested for the p38 MAPK pathway, which, interestingly also is elevated in tamoxifen resistance samples (Gutierrez et al., 2005). The PI3K/AKT pathway is of particular interest and has also been equated with tamoxifen resistance (Jordan et al., 2004; Kirkegaard et al., 2005). Indeed, increased phosphorylation of AKT, as well as MAPK signalling was observed downstream in our TamR model, with EGFR/ kinase signalling driving ser-118 and ser-167 phosphorylation of the ERα gene in the presence of tamoxifen (Britton et al., 2006). The phosphorylation of ERα and ERα-induced transcription was elevated in response to EGF-type ligands and was blocked by gefitinib showing the importance of upstream EGFR regulation of the kinases in this cross-talk. Moreover, increased phosphorylation of the ERα resulted in the synthesis of increased TGFα and amphiregulin, which was shown to sustain an EGFR/HER2 autocrine mitogenesis loop (Hutcheson et al., 2003).

In addition to impacting on ER phosphorylation, such kinases may crosstalk with ER signalling via increased promotion of expression or activation of co-activators in the presence of tamoxifen. HER2-positive tamoxifen resistant MCF-7 cells have been shown to have increased co-activator complex formation, involving ER, AIB1, CBP and p300. Studies have also reported that elevated levels of AIB1 may reduce the antagonist effect of tamoxifen, and recent clinical data suggest that the coexpression of AIB1 with HER2 predicted for a worse outcome in patients receiving tamoxifen after surgery (Johnston, 2006).

1.4.1.2 Faslodex Resistance

The introduction of the pure antioestrogen Faslodex into the clinic for the treatment of ER-positive breast cancer demonstrates a number of advantages over other antioestrogens such as tamoxifen, notably its ability to fully antagonise the ER and the reduction in unwanted oestrogen-like side-effects Clinical data are accumulating which suggest that Faslodex may be effective as second or third-line therapy after relapse on tamoxifen or AIs (Howell, 2006).

Unfortunately, resistance to therapy is again an inevitable consequence of the use of this drug. This is demonstrated *in-vitro* by our own model of Faslodex resistance. These cells were established as having acquired resistance to the pure antioestrogen Faslodex (McClelland et al., 2001), where this was achieved by the continuous exposure of parental wild-type MCF-7 cells

to 10^{-7}M Faslodex. Addition of the antioestrogen initially caused the growth rate to substantially decrease, but after 3 months of exposure, an increased growth rate again indicated the establishment of resistance (FasR). As with TamR cells, characterisation of these early FasR cells revealed upregulated EGFR protein and mRNA, and activation of MAPK signalling, with low levels of ER and its phosphorylation also potentially contributing to resistance. The importance of EGFR was demonstrated by gefitinib responses in such cells and ER signalling was fully recovered upon removal of Faslodex. Although the clinical phenotype of Faslodex resistant disease remains to be explored, second-line responses to further antihormone remain apparent in some FasR tumours, suggesting ER may indeed remain functional, as in tamoxifen-resistant disease (Howell, 2005).

Interestingly, FasR cells at a much later passage number (FasR-Lt) demonstrated a more severe phenotype with a less rounded de-differentiated morphology and substantially increased invasive behaviour. Additionally, these cells demonstrate a higher growth rate compared to early passage FasR cells (Nicholson et al., 2005). The transition from the early to a late/ advanced Faslodex-resistant model is also accompanied by the complete loss of ER protein and mRNA expression, phosphorylation, and transcriptional activity. Although studied with gefitinib suggest that there may be some role for EGFR signalling in FasR-Lt cells, growth inhibition is incomplete, and thus, other elements must be involved. The observation of ER loss is noteworthy since ER-negative patients often display a more aggressive and proliferative disease type (Nicholson et al., 1993).

In this regard, it is worth noting that other cell models of resistance to Faslodex, such as those developed by Sommer/ Lichtner derived from MCF-7, ZR-75-1, and T47D cells, similarly demonstrate a significant increase in EGFR protein expression (Sommer et al., 2003). The MCF-7 derived Faslodex-resistant LCC9 model from the laboratory of Clarke suggest that factors other than EGFR signalling may be of importance. For example, microarray analysis showed that the loss of expression of the putative tumour suppressor interferon regulatory factor-1 (IRF1) may be of significance (Bouker et al., 2004). More recently, the authors implicated NFκB in Faslodex resistance, whereby they demonstrated a synergistic role for both Faslodex and the NFκB- small molecule inhibitor, parthenolide, in reducing cell growth (Riggins et al., 2005).

1.4.1.3 Resistance to Oestrogen-Deprivation/ Aromatase Inhibitors

The observed benefits of AIs in the clinic have led to their increased use as a first line therapy for ER-positive advanced breast cancer, with emerging importance in the adjuvant setting (Goss, 1999; Sainsbury, 2004), however, resistance to oestrogen-deprivation strategies remains a pervading problem during treatment (Dowsett et al., 2005).

A number of cell models resistant to oestrogen deprivation have been developed which generally exhibit hypersensitivity to low E2 levels, elevated growth factor/ kinase signalling, as well as the retention of a functional ER (which may be inhibited by Faslodex). Additionally, some models also show evidence of growth factor- ER cross-talk, either in a non-genomic (membrane ER) or genomic (via increased ER phosphorylation) manner.

Reports have suggested that acquisition of resistance to oestrogen-deprivation may be as a consequence of breast cancer cells gaining hypersensitivity to low levels of E2, where such cells retain sensitivity to further E2/ER blockade (Santen et al., 2005). For example, the log-term oestrogen-deprived (LTED) model of Santen shows growth stimulation of tumour cells at 10^{-13}M E2 (Masamura et al., 1995). These cells also show markedly increased levels of growth factor signalling with an increased association of membrane ERα with IGF-1R (Song et al., 2005) and enhanced downstream activation of MAPK (Song et al., 2005), and AKT/PI3K signalling (Yue et al., 2003). Another model of LTED from Dowsett's group similarly exhibits oestrogen hypersensitivity where the cells show elevated levels of ERα expression and increased IGF-IR /HER2 with growth factor interplaying primarily within the nucleus (Chan et al., 2002; Martin et al., 2003; Martin et al., 2005).

Acquired resistance to oestrogen deprivation has also been investigated by Brodie and colleagues by stably transfecting the aromatase gene into MCF-7 cells, the resultant cells being termed MCF-7Ca. Subsequently culturing these cells in oestrogen deprived conditions eventually resulted in cells capable of overcoming the growth inhibitory effects of E2 withdrawal (Sabnis et al., 2005). These cells, UMB-1Ca, resistant to oestrogen deprivation, were demonstrated to have elevated ERα, increased expression of HER2 and increased activation of AKT phosphorylation.

The establishment of cells resistant to oestrogen deprivation has been similarly conducted in our laboratories by the continuous exposure of MCF-7 cells to extreme oestrogen-deprived condition achieved by growing in charcoal-stripped, heat-inactivated serum (Nicholson et al., 2004b; Staka et al., 2005). Continuous culture in this severely depleted medium initially caused the growth rate to decrease. However, after 6 months of exposure, an increased growth rate indicated establishment of an acquired resistant cell line (X-MCF-7). These X-MCF-7 cells demonstrate a functional nuclear ERα, the expression of which was elevated relative to the parental MCF-7 cell line. The ERα also demonstrated some increase in ser-118 phosphorylation compared to MCF-7 cells. However, unlike other models of LTED, the X-MCF-7 cell does not display hypersensitivity to oestrogen. The continued importance of ERα in X-MCF-7 cells was demonstrated by the reduction of cell growth by the use of Faslodex. There was no evidence of classical growth factor receptor signalling, such as EGFR, HER2 or IGF-1R. However, AKT was again deemed an important contributing pathway, cross-talking with ser-167 ER to promote cell growth (Staka et al., 2005).

1.5 Response and Resistance to Anti-Growth Factor Inhibitors

Given that resistance to anithormonal treatments is, in part, thought to be mediated by growth factor/ intracellular signalling, there is interest in targeting these proteins. As described earlier, EGFR and IGF-1R, as well as associated signalling networks, have been shown to contribute to endocrine failure, and small molecule signal transduction inhibitors (STIs) designed against these pathways are currently being evaluated clinically/ preclinically. Based on model system observations of significant growth inhibition of cells such as TamR, there is much promise for such agents.

The erbB signalling pathway has been a focus in this respect, exemplified by the introduction of the humanised monoclonal antibody trastuzumab (Herceptin) which aims to target the extracellular domain of HER2 (Brand et al., 2006). A number of other erbB STIs have entered clinical trials and are at various stages of development and evaluation, including EGFR inhibitors Gefitinib (Iressa), Erlotnib (Tarceva) and EKB-569, all of which have been evaluated at least at phase III, II and II respectively; the EGFR/HER2 agents Lapatinib (GW572016) and AEE-788 which are in phase I/III studies; and the pan erbB inhibitor canertinib (CI-1033) which is in phase II development (Johnston, 2005).

Gefitinib (Iressa; Astra Zeneca) is an orally active synthetic anilinoquinazoline (4-(3-chloro-4-fluroanilino)-7-methoxy-6-(3-morpholinopropoxy) quinazoline) that, as a competitive inhibitor of ATP binding, selectively inhibits the tyrosine kinase activity of EGFR but is also effects HER2 with a higher activity (Camirand et al., 2005). *In-vitro* studies demonstrate some effectiveness as an inhibitor in human breast cancer cells, including tamoxifen resistant cells, either alone or in combination with other therapeutic agents. While phase II trials in advanced breast cancer patients showed partial response in fewer than 10% of patients (Camirand et al., 2005), interestingly, a much higher response rate was observed in ER-positive acquired tamoxifen resistant patients (>60%), thus mimicking the TamR model (Agrawal et al., 2005).

Previous *in-vitro* studies performed on MCF-7 cells with acquired resistance to tamoxifen showed that both gefitinib and trastuzumab as single agents significantly reduced several downstream signal transduction cascades and cell growth (Knowlden et al., 2003). Similar results have been demonstrated with de novo tamoxifen resistant HER2-transfected MCF-7 cells treated with trastuzumab and the HER2 tyrosine kinase inhibitor AG1478, and by inhibiting downstream MAPK signalling with the MEK inhibitor UO126 (Kurokawa et al., 2000). Gefitinib also inhibited the resistant phenotype of the HER2 overexpressing MCF-7 model subverting ER/HER2/AIB1 interactions (Shou et al., 2004). However, despite initial response, resistance to such agents develops in models and in the clinic.

Importantly however, clinical evaluation of TKIs has in general showed relatively disappointing results with, for example, the evaluation of gefitinib through three phase II trials (Johnston, 2005) showing low clinical response rates and short times to disease progression. Indeed, in many instances, disease stabilisation was noted rather than objective responses (Agrawal et al., 2005).

In model system studies, the establishment of TamR cells that have gained further resistance to the EGFR TKI gefitinib (TamR/TKI-R) have been developed in our laboratories (Jones et al., 2004). This was achieved by the continuous exposure of TamR cells to 1μM gefitinib. Addition of the agent caused the growth rate to initially significantly decrease. However, after 6 months of treatment, gefitinib-resistant cells emerged (TamR/TKI-R) demonstrated by an increased growth rate in the presence of the EGFR inhibitor. In parallel with increased growth there was also an increase in invasive capacity of the cells versus the TamR cells. Characterisation of TamR/TKI-R cells revealed elevated levels of activated IGF-1R, HER2, AKT and PKCδ signalling. As such, these cells were growth sensitive to the IGR-1R inhibitor AG1024, which also reduced their migratory capacity. Taken together, these results suggest that on blockade of the EGFR pathway other growth factor-driven networks become recruited to reinitiate tumour cell growth.

Recent preclinical work has also shown that the IGF-1R is an appropriate cotarget with the EGFR in primary human glioblastoma cells, and furthermore with HER2 in breast cancer cells, since IGF-1R signalling is increased in Herceptin resistance (Camirand et al., 2005).

Although development of newer targeted therapies, such as for the IGF hold some promise, other factors may hinder this progress. These include, for example, the ubiquitous expression of growth factor receptors throughout the body, the non-selectivity of growth factor receptor inhibitors (Ibrahim and Yee, 2005; Yee, 2006), and the acquisition of resistance to the inhibitory agents targeting the receptors (Vasilcanu et al., 2006). Clearly much remains to be learnt about the development of both antihormones and anti growth factor resistance, and it is hoped that the introduction of newer technologies, such as microarray gene discovery will provide valuable additional information.

1.6   Microarray Analysis

The sequencing of the entire human genome expanded genetic information and added impetus to further research into the expression of every gene in the human body. The simultaneous analysis of more than 30,000 genes can now be achieved by microarray technology, which evolved in the 90's, and is now in 2006 a standard tool in genomics laboratories. The microarray technique allows the broad profiling and comparative analysis of genes in one experiment, generating a plethora of expression data. (Eisen and Brown, 1999; King and Sinha, 2001)

Microarray technology provides a global analysis of gene expression at the transcriptional level. This is highly significant as genetic and epigenetic alterations are fundamental to neoplastic transformation, cardiovascular disease, and other pathogeneses and therapeutic responses. Previous to the advent of microarray technology, molecular biology was performed sequentially and linearly with research being conducted on a single candidate gene with techniques such as Northern Blotting. Thus, the translation of discoveries regarding gene profiling into clinical medicine remained relatively slow. Microarrays however, by permitting the analysis of tens of thousands of genes simultaneously, are now quickening the identification of clinical biomarkers and potential (Leung and Cavalieri, 2003).

The application of microarrays to clinical samples was initially directed towards the transcriptional profiling of tumours, with studies being conducted in a number of cancer types. Array technology is particularly significant in cancer research since malignancy may be derived from the altered expression of cancer-causing genes. These abnormalities can promote the basic traits of cancer, namely: proliferation and self-sufficiency; insensitivity to growth inhibitory signals; apoptosis evasion; potential of unlimited replication; angiogenic induction and metastasis (Hanahan and Weinberg, 2000).

1.6.1   Microarray Principle

Microarrays can be defined as miniaturised ordered arrangements of nucleic acid fragments from specific genes localised on a solid support, the application of which permits an assessment of the expression level from particular cells, tissues or organs. The principal concept and methodology of the microarray is that RNA extracted from cells or tissue is reverse transcribed, and is labelled, either fluorescently or radioactively (Fig. 7). After denaturing, the labelled probe is then hybridised to the array, which comprises single stranded DNA sequences corresponding to individual genes. The base pairing between the target and probe provides a quantitative measure of the abundance of a particular gene sequence, by the signal detected after

capturing the image of the array (Leung and Cavalieri, 2003). Hybridisation signal patterns are then compared from one sample to another to reveal genes which may be upregulated or downregulated, and thus perhaps posses some significance in physiological processes and warrant further study.

Much research is focussing on the data associated for microarray experiment, with an ever expanding range of analysis tools. Indeed, the quality of the results will ultimately be reflective, not only of the microarray platform performance, but also the dada processing, where procedures such as array image scanning and normalising can affect the final gene outcome. Diverse analysis procedures such as hierarchical clustering, which groups genes according to their similarities of gene expression, alongside other statistical analysis are available (Eisen et al., 1998).

1.6.1.1 cDNA Microarrays

The cDNA microarray utilises cloned probe molecules. These gene sequences, usually from a PCR product derived from cDNA and expressed sequence tag (EST) clones, range from 100 to 2000 bases in size. These are assembled on a matrix of glass or nylon to form the microarray. The first arrays comprised cDNA clones spotted onto nylon membranes and radioactively labelled cDNAs were used for comparative hybridisation (Desai et al., 2002). cDNA arrays are manufactured by the application of double stranded cDNA onto the membrane through robotic means. The sample total RNA is radioactively labelled (^{33}P-cATP or ^{32}P-cATP) by reverse transcription prior to hybridisation. However, although the array is relatively inexpensive and no specialist equipment is required for label detection cDNA arrays have demonstrated issues with regards to sensitivity of gene detection (Draghici et al., 2006). The first glass slides for printing cDNA clones were introduced by Schena in 1995 (Desai et al., 2002). These types of arrays are produced by the robotic application of usually cDNA or genomic clones onto the glass surface (Cooper, 2001). The advantage of this technology is that the probes are covalently attached to the appropriately coated slide, which itself is extremely durable and non-permeable. These properties mean that efficient access for the labelled RNA to the cDNA probes, and washing steps can be performed. Additionally, the glass confers a non-flexible medium which improves spot quality. For these glass slides, total RNA from test and reference sample is extracted which are then differentially labelled with fluorescent cyanine dyes (Cy3-dUTPor Cy5-dUTP) by reverse transcription. The fluorescently labelled samples are then hybridised to a single array. After image acquisition, the ratio of the two dyes is calculated to compare expression of each gene from one sample to the next. However, large sample preparations may be required for hybridisations using glass arrays (Cooper, 2001) and dye-swapping experiments may be essential.

1.6.1.2 Oligonucleotide Microarrays

The oligonucleotide array comprises synthetic probe sequences, which are based on gene database information (Gershon, 2002). These can be assembled in a number of formats including glass, nylon, and, as used in this study, a plastic format, which was new at the time of instigation of this project. Oligonucleotide arrays have been designed to perform well in terms of specificity to the target gene as the sequences can be designed with precision. Specific sequences are produced by several methods including chemical synthesis directly onto the glass slide using photolithographic technology (as the Affymetrix microarrays) (Fodor et al., 1993), or by inkjet printing technologies through the direct building of the oligonucleotide on to the platform (eg. Agilent technology) (Hughes et al., 2001). The direct spotting of the oligonucleotides (up to 70 bases long) can also be performed, and the deposition of the oligonucleotide onto a gel matrix applied onto the slide has also been used (Amersham-Codelink microarrays) (Ramakrishnan et al., 2002). As in other array formats, these arrays utilise RNA from a sample which is reverse transcribed, whereby ultimately a fluorescent label is incorporated into the sample RNA. Alternatively, the RNA may be labelled radioactively, as in the Atlas Plastic arrays

1.6.1.2.1 Atlas Plastic 12k Microarray

The Atlas Plastic Human 12K Microarray, as utilised in this project, comprises approximately 12,000 oligonucleotides immobilised onto a rigid, translucent, plastic support by UV radiation. It is non-porous, as with glass microarrays, a feature which is thought to enhance hybridisation kinetics, minimise washing, and reduce background. As for Nylon arrays, the plastic format is used with radioactively labelled cDNA from the test sample and the image subsequently detected by phosphorimaging. However (unlike Nylon arrays) due to the high spot density of genes the plastic format uses a radioactive ^{33}P-labelled probe, which improves resolution compared to Nylon arrays. In addition, this format this format is reported to be able to be stripped and reused, unlike glass array platforms (Clontech_BD-Biosciences:Atlas_pdf, 2006).

The genes present on these plastic arrays are represented by single-stranded long oligonucleotides which are on average 80 bases in length. The property of the long oligonucleotide is believed to provide a compromise between the hybridisation efficiency of cDNA arrays, and discriminatory ability due to its relatively shorter length (compared to cDNAs). Due to their novelty, there are as yet few publications employing smaller 5k or 8k arrays in this plastic array area (Franscini et al., 2004; Sarkijarvi et al., 2006; Tasheva et al., 2004; Tsuchiya et al., 2005) . Long oligonucleotides are deemed superior to very long cDNA or arrays with extremely short oligonucleotide arrays (Barrett and Kawasaki, 2003; Zhu et al., 2005). However at the start of this project, the Atlas Plastic arrays were selected for gene

analysis tools as they provided a ten-fold increase over gene numbers analysed compared to the previously used Nylon format. The Plastic oligonucleotide format also provided a high proportion of genes which were relatively well characterised, compared to other technologies such as Affymetrix, which also contain many uncharacterised probe sequences. In addition, there were no other array technologies available to the TCCR, and with being relatively inexpensive, the Plastic array format showed ease of handling with no requirement for specialist equipment.

1.6.2   Microarray Applications to Breast Cancer Research

Gene expression profiling by microarrays has considerable potential in cancer research, and a number of array-based studies have been performed both in model systems and clinical disease which demonstrate the prognostic and predictive potential of array analysis, as well as providing a means to explore transcriptional events underlying cancer biology, including E2 action. In the pioneering study by Perou in 2000, array analysis was successfully used to classify breast cancers according to their expression profiles (Perou et al., 2000). In this study 456 cDNA clones were employed to phenotypically classify tumours into four major sub-groups before and after treatment with doxorubicin chemotherapy: (i) basal-like, expressing keratin 5/6 and 7, B4 and laminin, with low ER; (ii) HER2-positive cluster, expressing elevated levels of HER2 with no ER; (iii) characteristically normal breast-like; and (iv) luminal cell-like, with high ER, expressing ER regulated genes, such as LIV-1, GATA-binding protein 3, and prolactin receptor. Gene patterns pre- and post-treatment with chemotherapy demonstrated similar trends. Interestingly, a proportion of the samples showed a 'normal' gene profile post-treatment suggesting therapy had been effective. In an extension to this study, Sorlie performed array analysis to determine the correlation between array-based tumour classification and clinical outcome (Perou et al., 2000). Initial classifications derived by Perou were further dissected to reveal a sub-set of tumours predicted to relapse after treatment. This subset of tumours was derived from the luminal sub-type and was further divided into two major groups, A (with high GATA3 binding protein and ERα expression) and B/C (with genes of no coordinated function). Using an alternative expression array platform, van't Veer identified a 70-gene prognostic signature in a cohort of 78 breast cancer patients with axillary lymph node negative disease, which was found to comprise a number of genes involved in cell-cycle regulation, angiogenesis, invasion and metastatic development, and was indicative of poor prognosis (van 't Veer et al., 2002). This disease signature predicted adverse and good outcome with a sensitivity of 85% and 81% respectively.

Gene expression profiling has more recently identified markers that may be used to predict response to hormonal and neoadjuvant therapy (Jansen et al., 2005). This study used

gene expression profiling on a cohort of ER-positive primary breast carcinomas from patients with advanced disease. Response to tamoxifen was measured by tumour size and time to progression (progression-free survival), with the predictive signature permitting discrimination of responders versus patients with progressive disease. Eighty-one genes were identified as being involved in oestrogen action, immune response, apoptosis, and extracellular matrix formation

Array technology has also been used to identify genes responsive to oestrogen challenge and altered in response to antioestrogens using antihormone responsive breast cancer models. For example a study identified genes regulated by oestrogen, tamoxifen , and Faslodex which may provide makers for prediction for response to treatments (Inoue et al., 2002). Tamoxifen was shown using arrays, to function as a molecular agonist, inducing a number of cell cycle-associated genes, including fos, myc, myb, cyclins E and A2, with a kinetics similar to E2 treatment in MCF-7 cells (Hodges et al., 2003). . In another study, a number of genes including 14-3-3z were found to correlate with disease recurrence following tamoxifen treatment in patients with ER-positive cancers, thus possibly providing markers for poor prognosis (Frasor et al., 2006). Gene expression signatures were also analysed in MCF-7 cells in response to oestrogen, tamoxifen, raloxifene, and Faslodex with robust differential gene expression profiles that showed fundamental differences among of SERMs and SERDs and may provide insights into their distinct biological effects in breast cancer (Frasor et al., 2004).

Antihormones were again evaluated in a recent gene expression microarray study which explored the aromatase inhibitors, Letrozole and Anastrazole, and the antioestrogen tamoxifen, together with the hormones E2 and testosterone in aromatase-transfected MCF-7 cells (Itoh et al., 2005). Using Affymetrix genechips 104 and 109 genes were up- and down-regulated by hormones respectively, which were effectively reversed by the antihormones. Both aromatase inhibitors showed similar profiling to each other that was differential compared to tamoxifen, demonstrating the unique capabilities and gene signatures associated with different classes of antihormonal agents diverse agents. Additionally, although there are still few gene expression microarray studies with cells resistant to oestrogen-deprivation, in Santens model of LTED a number of genes, which were altered in response to oestradiol, were found to be those not linked to the growth factor signalling, demonstrating that alternative elements may be responsible for E2 response within this model (Santen et al., 2005). Recently, Kristensen investigated the effects of AI (anastrazole) administration on a tumour samples, albeit from 12 patients with locally advanced tumours, before and after 15 weeks of treatment (Kristensen et al., 2005). Tumours with no or low ER expression clustered together and were characterized by a strong basal-like signature including the overexpression of keratins 5/17, cadherin 3, frizzled and apolipoprotein D. The luminal epithelial tumour cluster, highly expressed genes such as ER, GATA binding protein 3 and N-acetyl transferase. In addition to this, a HER2 cluster was found

due to the marked over-expression of the HER2 gene, with GRB7 and PPAR binding protein in this patient material.

In cell lines developed with resistance to antihormones, the application of microarray technology can be revealing. In an E2-independant, Faslodex-resistant model (LCC9 cells), array analysis revealed a role for NFκB signalling (Shibata et al., 2002).

It is anticipated that following further research, the application of microarray analysis as prognosticators will be useful, as well as in revealing new targets for novel therapies which will have major impact in the field of breast cancer. However, resistance to antihormones is still a pervading problem, and there is much to be learned in this area if new elements are to be studied that can be targeted to subvert resistance.

AIMS AND OBJECTIVES

Antihormone treatments, notably tamoxifen, and more recently, Faslodex and aromatase inhibitors are valuable approaches in combating breast cancer in ER-positive patients. However, despite the relative success of these treatments, clinical resistance to such antihormones has been observed, commonly resulting in a more aggressive disease, thus demonstrating the need to uncover mechanisms which may be contributing to this phenomenon. Through applying gene expression microarray analysis to human breast cancer models previously developed at the TCCR, which have acquired resistance to tamoxifen or Faslodex *in-vitro*, the project aims to reveal previously unrecognised genes in the context of antihormone resistance that may provide new potential therapeutic targets or biomarkers in this state.

The project aims in detail are to:

- Optimise methodologies for use with the Atlas Plastic Human 12k microarray, specifically RNA extraction and purification, as well as hybridisation protocols.

- Reveal differentially expressed genes in TamR and FasR resistant cells relative to the parental MCF-7 cell line using Atlas/ GeneSifter softwares, and prioritise genes through ontological examination of significantly altered genes.

- Verify up to 30 genes for expression in resistant cells through RT-PCR analysis, with the subsequent selection of two high priority genes induced in both forms of resistance for study in detail.

- Explore the high priority genes (PTTG1 and GFRα3) and their associated family receptors and ligands in antioestrogen resistant cells and also in cells resistant to oestrogen deprivation using RT-PCR analysis.

- Examine PTTG1 and GFRα3 protein expression in resistant cells using Western immunoblotting and also immunocytochemistry.

- Study the impact of therapies known to target candidate pathway signalling, notably the EGFR inhibitor gefitinib and also ER blockade with Faslodex, on PTTG1 and GFRα3 gene and protein expression in the resistant cells.

- Study the prevalence of PTTG1 and GFRα3 in clinical breast cancer by examining mRNA expression by RT-PCR, and determine any associations with key clinicopathological and biological markers. In addition, to see if the proteins are also expressed in archival clinical samples using immunocytochemistry.

- Using siRNA gene knockdown, study the impact of PTTG1 and GFRα3 in antioestrogen resistant cells on endpoints such as cell growth, proliferation and apoptosis and thus establish any targeting potential.

Chapter 2

MATERIALS
&
METHODS

MATERIALS AND METHODS

2.1   Materials, Reagents and Equipment

2.1.1   Cell culture

Materials and Reagents: The human breast cancer cell line MCF-7 was obtained from the American Tissue Culture Collection (ATCC) (Virginia, USA). Roswell Park Memorial Institute (RPMI) 1640 medium and phenol red-free RPMI medium, foetal calf serum (FCS), penicillin/streptomycin, fungizone, L-glutamine and Dulbecco's phosphate buffered saline (PBS; as supplied containing calcium chloride and magnesium chloride ($CaCl_2$ and $MgCl_2$)) were purchased from Invitrogen Life Technologies (Paisley UK). Bovine trypsin was from Lorne Laboratories (Reading, UK). 17-β-oestradiol and 4-hydroxytamoxifen (4-OHT; experimentally referred to as tamoxifen) were purchased from Sigma (Dorset, UK). Faslodex (fulvestrant, ICI182,780) and Gefitinib (Iressa, ZD1839) were obtained as gifts from Astra Zeneca Pharmaceuticals (Cheshire, UK).

Equipment and Plasticware: All tissue culture was performed in a MDH intermed vertical circulating class II biological safety cabinet (Bioquell, Hampshire, UK), and cells maintained in a BB16 Function Line cell incubator (Heraeus Instruments, Cheshire, UK). Cells in culture were observed using a Nikon eclipse TE200 phase-contrast microscope and photographed using a Nikon 35mm F70 SLR camera (Nikon, UK). Cells were counted using a Beckman Coulter Counter Multisizer II (High Wycombe, UK) and centrifuged in a Jouan-c312 centrifuge supplied by Thermo Electron Corporation (Berkshire, UK). Plasticware, disposable pipettes, 50ml falcon tubes, and Coulter Counter receptacles were all supplied by Sarstedt (Germany). All other tissue culture plasticware was from Nalgene Nunc International (Roskilde, Denmark).

2.1.2   Optimisation of RNA Extraction for Plastic Microarray Hybridisation

Materials and Reagents: Chloroform, isopropanol, sodium chloride (NaCl) and ethanol were purchased from Fisher Scientific (Loughborough, UK). MMLV Reverse Transcriptase enzyme (all RT-PCR reagents were molecular biology grade), PBS (as supplied with calcium $CaCl_2/MgCl_2$) and dithiothreitol (DTT) were obtained from Invitrogen Life Technologies (Paisley UK). Tri Reagent, DNase/RNase free water, sodium dodecyl sulphate (SDS), ethylene diamine tetraacetate (EDTA), Tris-HCl, glass wool, dimethylchlorosaline, sodium acetate (NaOAc), sodium hydroxide (NaOH), saturated phenol, ethidium bromide, β-mercaptoethanol

and other PCR reagents not listed (molecular biology grade) were from Sigma (Dorset, UK). RNEasy mini Kit [contents include: RNEasy mini spin columns, Buffer RLT, Buffer RPE, and 2ml collection tubes] was from Qiagen (Crawley, UK). Oligo(dT)cellulose was purchased from New England Biolabs (Hertfordshire, UK). Clontech Nucleotrap mRNA purification kit [kit components: NucleoTrap mRNA suspension, buffer RM1 (binding buffer), buffer 2xRM1 (binding buffer), buffer RM2 (wash buffer I), buffer RM3 (wash buffer II), NucleoSpin microfilters] was from Clontech/ BD Biosciences, (Hampshire, UK). Atlas Pure Total RNA Labelling System Kit [Kit components: denaturing solution, saturation buffer for phenol, 2M NaOAc; pH4.5, 10x Termination mix, Streptavidin magnetic beads, 1x Binding buffer, 2x Binding buffer, 1x Reaction buffer, 1x Wash buffer, DNase (1unit/µl), 10x DNase1 buffer, Biotinylated oligoDT, MMLV Reverse transcriptase] was also from BD Biosciences/ Clontech. Polyallomer centrifuge tubes were from Beckman (CA, USA). Polypropylene copolymer tubes, 2ml syringes, cell scrapers and other plasticware were provided by Nalgene Nunc International (Roskilde, Denmark). Agarose for gel preparation (multipurpose) and 1kb ladder (Hyperladder I) were from Bioline (London, UK).

Equipment: RNA extractions/ purifications were performed in an APMG vertical biological safety cabinet/ fume hood (Manchester, UK). Centrifugations for large volume RNA extraction (>15ml) using polypropylene tubes were performed in a Sorvall IC5B Plus centrifuge, whereas smaller volumes using 1.5ml tubes (<1.5ml) were using an IEC Micromax RF microcentrifuge (Thermo Electron Corporation, Berkshire, UK) or a Haraeus Labofuge Functionline 400R centrifuge (Cheshire, UK). Ultracentrifugation was performed in polyallomer tubes within a Beckman L-80 ultracentrifuge, both supplied by Beckman (Buckinghamshire, UK). Vortexing was performed using a Fisons Whirlmaster vortex (Fisons Scientific Equipment, Leicestershire, UK). Sample preparations in 1.5ml tubes were heated using a Techne-DB2A Dri-block heater (Cambridge, UK), and larger volumes (>1.5ml) were heated in a Grant W14 waterbath (Grant Instruments Ltd, Cambridge, UK). Magnetic particle separator was provided by Promega (Southampton, UK). The UV Spectrophotometer (Cecil CE2041) and quartz cuvettes employed were from Cecil Instruments (Cambridge, UK). BioRad supplied the horizontal gel apparatus and associated powerpacks, and densitometric analysis was performed using a BioRad GS690 densitometer. Agarose gels were visualised using a UV illuminator supplied by Fotodyne Inc (Wisconsin, USA) and photographed using a GelCam camera, supplied by Polariod (Bedfordshire, UK).

2.1.3 PCR Assessment of Genomic Contamination/ Cell Line Verification and PCR Gene Verification

Materials and Reagents: Taq DNA polymerase (5u/µl), agarose for gel preparation (multipurpose), and 100bp ladder (Hyperladder IV) were from Bioline (London, UK). MgCl$_2$, dNTP of each nucleotide and Random Hexamers were purchased from Pharmacia (Milton Keynes, UK). DTT and RNase-inhibitor was from Promega (Southampton, UK). DNase/ RNase-free water and all other PCR reagents not listed were molecular biology grade, and purchased from Sigma (Dorset, UK). All purchased primers were stored at -20°C at a stock concentration of 100pmol/µl made in DNase/ RNase-free water, with a 1:5 dilution for a working concentration. For assessment of genomic contamination, and cell line verification primers were from MWG Biotech (Ebersberg, Germany). For genomic contamination determination IGF1 forward primer sequence was 5'TGC TCT TCA GTT CGT GTG TG 3' and IGF1 reverse primer was 5'TGG CAT GTC ACT CTT CAC TC 3'. Genomic standards were Human Genomic DNA (G304A) from Promega (Southampton, UK). For cell line confirmation, the following primers were used: β-Actin (204bp) forward sequence was: 5'-GGA GCA ATG ATC TTG ATC TT-3' and reverse sequence was: 5'-CCT TCC TGG GCA TGG AGT CCT-3'; for pS2 (Trefoil factor1; 336bp) forward sequence was: 5'-CAT GGA GAA CAA GGT GAT CTG-3' and reverse was: 5'-CAG AAG CGT GTC TGA GGT GTC-3'; for EGFR (636bp) the forward sequence was: 5'-CAA CAT CTC CGA AAG CCA-3' and reverse was: 5'-CGG AAC TTT GGG CGA CTA T-3'. Where coamplification with β-actin (204bp) was not possible due to similar size of the gene to be coamplified, β-actin (385bp) was used, and vice-versa, where the forward sequence was: 5'-CTA CGT CGC CCT GGA CCT CGA GC-3' and reverse sequence was: 5'-GAT GGA GCC GCC GAT CCA CAC GG-3'. All other primer sequences used in this project for gene verification are listed in table 1 and were purchased from Invitrogen Life Technologies (Paisley UK).

Equipment: RT-PCR for assessment of contamination and cell line verification were performed in a BioRad i-cycler supplied by BioRad (Hertfordshire, UK). All other subsequent RT-PCR for gene verification studies were using a PTC-100 Thermal cycler supplied by MJ Research/ BioRad (Hertfordshire, UK).

2.1.4 Microarray Hybridisation, Detection and Data Analysis

Materials and Reagents: The following reagents, provided by Clontech/ BD Biosciences (Hampshire, UK) comprised the Atlas Plastic Trial/ 12k Microarray kit: Clontech Atlas Plastic Human Trial or 12k Microarrays, 10x dNTP mix (5mM each dCTP, dGTP, dTTP), BD Powerscript Reverse Transcriptase, 5x BD Powerscript Reaction Buffer, Random Primer mix (with or without synthesis control), synthesis control cDNA, and for array hybridisation, BD PlasticHyb Hybridisation solution. Also provided in the kit for column chromatography/ probe purification were BD Atlas NucleoSpin Extraction kit [consists of: NucleoSpin Extraction spin columns, 2ml collection tubes, Buffer NT2, Buffer NT3, Buffer NE]. Radioactivity: [α-^{33}P]dATP at 10μCi/μl; >2500 Ci/mmol was provided by Amersham (Buckinghamshire, UK). DTT was from Invitrogen Life Technologies (Paisley, UK). For microarray stripping, NaOH, SDS, sodium carbonate (Na_2CO_3) were all from Sigma (Dorset, UK)

Equipment: All microarray experiments, including hybridisations, washes, probe preparation, were performed in an authorised designated area for radioactive study, and all radioactivity was handled behind a safety β-cabinet enclosure from Scotlab (Coatbridge, UK). A Biometra UNO Thermal cycler was used for radioactive probes preparation (Gottingen, Germany), and probes were centrifuged in a MSE Microcentaur centrifuge supplied by MSE (UK). Probe radioactivity was determined using a Tri-Carb 2900 TR Scintillation counter from Packard Bioscience (UK). Array hybridisations were performed initially in rollerbottle system (hybridiser HB-1D) supplied by Techne (UK) but subsequently and preferentially in plastic hybridisation boxes supplied by BD Biosciences/ Clontech (Hampshire, UK), in a hybridisation oven/ rocker (si20h) supplied by Stuart Scientific (UK). Array signal radioactivity was detected using a phosphorscreen, supplied by Amersham (Buckinghamshire, UK), or by means of a Kodak autoradiograph film from GRI (Rayne, UK) placed within the phosphorscreen cassette. Array signal on phosphorscreen was captured using a Typhoon Model 8600 Phosphorimager from Molecular Dynamics (UK).

For Microarray Data Analysis, minimum computer requirements were: For AtlasImage, Windows 95, Pentium II processor, 64+MB of RAM, 17-inch colour monitor, video card with support for 16-bit colour at 800x600 resolution, CD-ROM or DVD-ROM drive; AtlasNavigator, Windows 95, Pentium II processor, 128+MB of RAM, 17-inch colour monitor, video card with support for 16-bit colour at 1024x786 resolution, Approximately 50MB hard disk space for expression data. CD-ROM or DVD-ROM drive; GeneSifter, Windows, Mac OS, Linux or Unix environments, which is connected to the internet and is capable of running a modern browser, such as Firefox, Internet Explorer 5.5 or, or Netscape: 6.1. For softwares, Array signal intensity

Table 1. Primers used for PCR analysis for selected genes and associated genes used in this study.

Gene Ref	Gene Name	Gene Name (full)	Forward Primer 5' to 3'	Reverse Primer 5' to 3'	Fwd size (bp)	Rev size (bp)	Product size (bp)	Source Designed (d) or CD-ROM (cd)
NM_000713	Biliverdin Reductase B	Biliverdin reductase B	TGC ACA AGG TGC TGC GGG AAT CAG	CTG TGT CCG TCG TAC TCA TCG GTG	24	24	190	cd
M59040	CD44	CD44 (hyaluronan receptor)	AGA TAA AGA CCA TCC AAC AAC TTC TAC TC	CTC CTG ATA AGG AAC GAT TGA CAT TAG A	29	28	206	cd
NM_006869	Centa-1	Alpha Centaurin	TAC ACT CTG GGC GTC TTC ATC	GTC AGC ACA AAC TTC CGG CTC	21	21	361	d
X51688	CyclinA2	Cyclin A2	GGC ACT GCT GCT ATG CTG TTA GCC TC	TTG TCC CGT GAC TGT GTA GAG TGC TAA A	26	28	342	cd
NM_016594	FKBP-11	FK506 binding protein precursor	GAA CGA GGG TCC TAG CTG CC	ATG TCG AGA AGA CTC TGC TC	20	20	379	d
NM_001496	GFRα3	GDNF family receptor alpha 3	CAT CTA TTG GAC CGT TCA CC	CCT TCT CGA AGA AAG TGA GC	20	20	275	d
D55696	LGMN	Legumain	CAG TGA TCG TGG CAG GTT CAA ATG G	TCG GGA CTC CCT GAT AGA CAT CTG	25	24	210	cd
NM_000900	Matrix GLA	Matrix Gla protein	CCG CCT TAG CGG TAG TAA CTT TGT G	CCA TAA ACC ATG GCG TAG CGT TCG	25	24	229	cd
NM_002539	ODC	Ornithine decarboxylase 1	AGA TCA CCG GCG TAA TCA ACC CAG	TAC ATA AAG GTC TGC TCA CTC GAC TC	24	26	199	cd
L48513	PON2	Paraoxonase 2	ACT TGA GCT GGA TAC ACT GG	CAC AAT ACA AGG CTC TGT GG	20	20	274	d

Table 1 continued

Gene Ref	Gene Name	Gene Name (full)	Forward Primer 5' to 3'	Reverse Primer 5' to 3'	Fwd size (bp)	Rev size (bp)	Product size (bp)	Source Designed (d) or CD-ROM (cd)
NM_006238	PPAR-δ	Peroxisome proliferative activated receptor, delta	CAG GAG CGG GAG AAT TCT GC	GAA GTG CAT GCT GTG GTC CC	20	20	458	d
NM_005037	PPAR-γ	Peroxisome proliferative activated receptor, gamma	CAA GAC AAC CTG CTA CAA GC	CCT CAG AAT AGT GCA ACT GG	20	20	264	d
NM_004219	PTTG1	Pituitary tumor-transforming 1	ATG CGG CTG TTA AGA CCT GC	CTG GAT AGG CAT CAT CTG AGG	20	21	348	d
NM_006627	POP4	POP4 (processing of precursor , S. cerevisiae) homolog	GCA GAG ATA CAG CCT TTT CC	GAA CAC GCA GTT TAG CTT GG	20	20	274	d
NM_006423	RabAc1	Rab acceptor 1 (prenylated)	AGA AGG ACC AGC AGA AAG ATG C	CAG GAA CAC GAA CAC ATA GTT G	22	23	239	d
AB004903	STAT-i2	STAT induced STAT inhibitor-2	AGC TGG ACC AAC TAA TCT TCG AAT CG	GGT GAG CCT ACA GAG ATG CTG CAG	26	24	244	cd
NM_013351	T-Box21	T-Box21	AGC TAT GAG GCT GAG TTT CG	AAT CTC AGT CCA CAC CAA GG	20	20	261	d
NM_004804	WD40 protein Ciao1	WD40 protein Ciao1	TGC CAG CTT TGA TGC TAC CAC TTG C	AAC ACT GAC ACA TTC ATA CTC ATC CTC	25	27	202	cd
NM_001145	Angiogenin	Angiogenin	TGG CCT AAT TTG GTG ATG CTG TTC TTG	TGC CAG CTT TGA TGC TAC CAC TTG C	27	24	310	cd
J02853	CK2	Casein Kinase II, alpha 1 polypeptide	GGC CTT GGA TTT CCT GGA CAA ACT G	AAT CAC TGG TGA GCC TGC CAG AGG	25	24	232	cd

Table 1 continued

Gene Ref	Gene Name	Gene Name (full)	Forward Primer 5' to 3'	Reverse Primer 5' to 3'	Fwd size (bp)	Rev size (bp)	Product size (bp)	Source Designed (d) or CD-ROM (cd)
NM_005451	Enigma	Enigma (LIM domain protein)	TGT CAG ATC AAC CTG GAA GG	CAG GTT TAT TGT GGC ACT GG	20	20	322	cd
NM_004839	Homer2	Homer, neuronal immediate early gene, 2	TCG GAT CAT CAG TGT GGA CG	TGG TCA GCC GTG CAT TGC TC	20	20	428	d
NM_006855	KDEL-3	KDEL 3	GAC AGT GAG AAT GAC ACA TTC C	CTG AAG GTC CTC AGA TTG GC	22	20	397	cd
U18018	PEA3	Ets variant 4 (PEA3)	TGA GCT GCT CAC CGG AGT CAT GG	CCT GCC AGT ATG AAG TTG GGA AGC	24	24	217	cd
NM_000638	Vitronectin	Vitronectin	CAT GGC TGG CCG CAT CTA CAT CTC AG	GAG CGA TGG AGC GTG GGT AGG GAG	26	24	353	cd
NM_005264	GFRα1	GDNF family receptor alpha 1	AAC ATC CCT AAC GAG CAT CCG	AGC TCA GCA TGC AGC GAT	21	18	420	d
NM_003881	WISP2	WNT1 inducible signaling pathway protein 2	GGT CTG TCT GGA CGA GTA TGG	GGA CTG CTT GTC CCA TCT CTT GCC	21	24	191	cd
NM_003976	Artemin	Artemin	TTC ATG GAC GTC AAC AGC	AGG CAC TTT CAA CCA AGC	18	18	478	d
NM_001495	GFRα2	GDNF family receptor alpha 2	AAG CTA CGC AGA CAA GAA CAG C	AGG GTC CAG AGA GAA AAA CAC C	22	22	279	d
NM_022139	GFRα4	GDNF family receptor alpha 4	GGC ATC TTG GTT GTA AGT CC	GCT ACA ATG GTG GGT AAT GC	20	20	264	d
NM_006607	PTTG2	Pituitary tumor-transforming 2	TGT GAA AAT GCC CTC TCC	GAC ATA TCC CCA AAG AGT ACG G	18	22	291	d

Table 1 continued

Gene Ref	Gene Name	Gene Name (full)	Forward Primer 5' to 3'	Reverse Primer 5' to 3'	Fwd size (bp)	Rev size (bp)	Product size (bp)	Source Designed (d) or CD-ROM (cd)
NM_021000	PTTG3	Pituitary tumor-transforming 3	AAA CGA AGA ACC AGG CAT CC	CAG GTC AAA ACT CTC GAA GC	20	20	361	d
NM_004339	PBF	Pituitary tumor-transforming 1–binding/ interacting factor	CTC TTC TCA GTT TGT GAA ACG CTA A	CTG CCC TGG GAG AAT GAC A	25	19	108	d
BC004257	RET	RET proto-oncogene	AGA GGG CTC ACA AGA CAC ATT TGT GCC	AGG TGT AGC AGT CCT TGG TCA TTG TCA T	27	28	346	cd

Table 2. Optimised PCR conditions for selected genes and associated genes used in study.

Gene	Accession number	Annealing temperature / °C	Cycle number	ß-Actin coAmplification in PCR
Biliverdin reductase B	NM_000713	55	23	Y
CD44	M59040	55	35	N
centaurin, alpha 1	NM_006869	55	26	Y
Cyclin A2	X51688	55	27	Y
FK506 binding protein precursor	NM_016594	55	27	Y
GDNF family receptor alpha 3	NM_001496	62	27	Y
Legumain	D55696	55	27	Y
Matrix Gla protein	NM_000900	55	29	N
Ornithine decarboxylase 1	NM_002539	55	27	Y
Paraoxonase 2	L48513	55	30	N
Peroxisome proliferative activated receptor, delta	NM_006238	65	29	N
Peroxisome proliferative activated receptor, gamma	NM_005037	55	29	Y
Pituitary tumor-transforming 1	NM_004219	55	26	Y
POP4	NM_006627	55	33	N
Rab acceptor 1	NM_006423	60	26	N
STAT induced STAT inhibitor-2	AB004903	63	30	N
T-box21	NM_013351	55	35	N
WD40 protein Ciao1	NM_004804	62	26	N
Angiogenin	NM_001145	63	36	N
Casein kinase 2	J02853	55	27	Y
Enigma	NM_005451	55	25	Y
Homer2	NM_004839	55	26	Y
KDEL	NM_006855	55	26	Y
PEA3	U18018	58	35	N
GDNF family receptor alpha 1	NM_005264	55	28	Y
WISP2	NM_003881	60	28	N
Artemin	NM_003976	57	34	Y
GDNF family receptor alpha 2	NM_001495	64	32*	N
GDNF family receptor alpha 4	NM_022139	55	35*	N
Pituitary tumor-transforming 2	NM_006607	59	40	N
Pituitary tumor-transforming 3	NM_021000 (AF095289)	63	34*	N
Pituitary tumor-transforming 1 – binding factor/ interacting factor	NM_004339	55	26	Y
RET proto-oncogene	BC004257	55	30	N

* PCR reaction performed in 15% glycerol to enhance specific gene product.

reports were generated using AtlasImage software, version 2.7, and reports were normalised using AtlasNavigator version 2.0, from BD Biosciences/ Clontech (Hampshire, UK), and Gene analysis was performed using online software GeneSifter (GeneSifter.url, 2006) from VizX Labs (Washington, USA).

2.1.5 SDS PAGE/ Immunoblotting

Materials and Reagents: Rainbow marker (range 10-250kDa) was purchased from Amersham (Buckinghamshire, UK). Bromophenol blue was supplied by BDH Chemicals Ltd (Poole, UK). NaCl, Methanol and acetic acid were from Fisher Scientific (Loughborough, UK). Kodak Autoradiography film was supplied by GRI (Rayne, UK). PBS and DTT were from Invitrogen (Paisley, UK). Signal detection using Perbio Chemiluminescent Super Signal West Pico/ Dura/ Femto was supplied from Pierce and Warner (Cheshire, UK). Primary antibodies were diluted in a solution of Western Blocking reagent as supplied by Roche Diagnostics (Mannheim, Germany). Aprotinin, leupeptin, phenylmethylsulphonylfluoride (PMSF), phenylarsine oxide (PAO) , sodium orthovanadate (Na_3VO_4), sodium fluoride (NaF), sodium molybdate (Na_2MoO_4), acrylamide/ bisacrylamide 30%v/v, ammonium persulphate (APS), tetramethylethylenediamine (TEMED), Tris-HCL, EDTA, NaCl, SDS, glycerol, glycine, Trizma base, Trizma-HCL, Tween-20, bovine serum albumin (BSA) and Ponceau S were from Sigma (Dorset, UK). BioRad protein assay kit (DC) [kit contents: reagent A, reagent B, substrate S] was supplied by BioRad Laboratories (Hertfordshire, UK). Skimmed milk powder was obtained as commercially available Marvel. The mouse anti-human monoclonal antibody to pituitary tumour-transforming gene 1 (PTTG1) (ncl-securin) was from Novo Castra (Newcastle upon Tyne, UK) (stock concentration 1mg/ml stored at -20°C). The mouse anti-human monoclonal antibody to Glial cell-derived neurotrophic factor (GDNF) receptor alpha 3 (GFRα3) (mab6701) was from R&D Systems (Abingdon, UK) (stock concentration 1mg/ml stored at -20°C). The mouse anti-human monoclonal antibody for RET proto-oncogene (ref: ab1840) (supplied as tissue culture supernatant and stored at -20°C). The mouse anti-human monoclonal antibody to PEA3 (sc-113) was from Santa Cruz (CA, USA) (supplied as 0.2mg/ml concentration and stored at 4°C).

Equipment: Stuart Scientific STR6 platform rocker used was from Bibby Sterilin (UK). Centrifugation was performed using an IEC Micromax RF microcentrifuge supplied by Thermo Electron Corporation (Berkshire, UK). The Spectrophotometer (CE2041) was from Cecil (Cambridge, UK). The autoradiograph developer/ fixer was from XO-Graph Imaging System (Tetbury, UK). Autoradiography cassettes (Hypercassette) were obtained from Amersham Biosciences (Buckinghamshire, UK). Nitrocellulose transfer membrane (Protran 0.2µM) and filter paper (grade 3) were supplied by Whatman (Maidstone, UK). All tissue culture and cell

lysis was performed in a MDH intermed vertical circulating class II biological safety cabinet (Bioquell, Hampshire, UK). Electrophoresis and Western blotting equipment, and the BioRad GS-700 scanner system were supplied by BioRad (Hertfordshire, UK). Tissue culture plasticware was as listed in 2.1 otherwise supplied by Nalgene Nunc International (Roskilde, Denmark).

2.1.6 Immunocytochemistry

Materials and Reagents: Diaminobenzidine (DAB) substrate chromagen system (K3468; DAB+ chromagen system (containing 3,3'-diaminobenzidine chromagen solution)) and its substrate buffer solution hydrogen peroxide (H_2O_2) (pH7.5], mouse/ rabbit Envision horse radish peroxidase (HRP) DAB secondary system, were supplied by DAKO Cytomation (Cambridgeshire, UK). Xylene, Ethanol, H_2O_2 (30%), NaCl, di-potassium hydrogen orthophosphate (K_2HPO_4; anhydrous), and potassium di-hydrogen orthophosphate (KH_2PO_4) were purchased from Fisher Scientific (Loughborough, UK). Sodium citrate, methyl green, Tween-20, Protease (from *Streptomyces griseus*; P6911), and DPX mountant medium (Fluka) were from Sigma (Dorset, UK). The rabbit anti-human polyclonal antibody for PTTG1 (34-1500) was from Zymed Laboratories (San Francisco, USA) (stock concentration 0.25mg/ml stored at 4°C). The rabbit anti-human polyclonal antibody for GFRα3 (ab8028) (stock solution 0.5mg/ml stored at 4°C) and the mouse anti-human monoclonal antibody to Vitronectin (ab13413; VN58-1) (stock at 1mg/ml stored at -20°C) was from Abcam (Cambridge, UK). The mouse anti-human monoclonal antibody to PEA3 (sc-113) was from Santa Cruz (CA, USA). All other antibodies used are listed in 2.1.5.

Equipment: The BH2 Research Microscope and DP12 digital camera were from Olympus (London, UK). Incubation ovens were from Heraeus (Cheshire, UK). Commercially available Microwave (950W) was from Proline and pressure cooker from Prestige (UK). Coated and plain glass slides, and also coverslips were from Fisher Scientific (Loughborough, UK). Snowcoat extra adhesive slides were from Surgipath (Peterborough, UK). The Hallandal jars & other immunocytochemical glassware were supplied by RA Lamb (Eastbourne, UK). Vertical biological safety cabinet/ fume hood was from APMG (Manchester, UK). The PAP pen was supplied by DAKO Cytomation (Cambridgeshire, UK).

2.1.7 Gene Knockdown Studies Using siRNA

Materials and Reagents: Phenol red-free DCCM media (without glutamine) was supplied by Biological Industries (Staffordshire, UK). DharmaFect1 transfection reagent (T-2001-01), siGlo RISC-Free siRNA (D-001600-01-05), siControl Lamin A/C siRNA (human/ mouse/ rat; D-001050-01-05), Missense siRNA siControl Non-targeting siRNA#1, PTTG1 (siGENOME SMARTpool) siRNA (M-004308-01), GFRα3 (siGENOME SMARTpool) siRNA (M-007915-01), and 5x siRNA buffer were supplied by Dharmacon (Denver, USA). RNase/DNase-free water, sucrose and glycerol were from Sigma (Dorset, UK). Vectashield mountant medium for fluorescence (H1300) containing 4'-6-Diamidino-2-phenylindole (DAPI) was from Vector Laboratories Inc. (CA, USA). Clear nail-varnish (containing lycra) manufactured by Rimmel was commercially available. Ki67 (Mib1 clone; M7240) antibody was supplied by DAKO Cytomation (Cambridgeshire, UK). Xylene, Ethanol, NaCl and Formaldehyde (37%) were from Fisher Scientific (Loughborough, UK). Apoalert Mitochondrial Membrane Sensor Kit was supplied by Clontech/ BD Biosciences (UK). All antibodies used for PTTG1 and GFRα3 are as listed in section 2.1.6 and other reagents not listed are as 2.1.1-2.1.6.

Equipment: All tissue culture/ siRNA transfections were performed in a MDH intermed vertical circulating class II biological safety cabinet (Bioquell, Hampshire, UK), and cells maintained in a BB16 Function Line cell incubator (Haraeus, Cheshire, UK). Cells in culture were observed using a Nikon eclipse TE200 phase-contrast microscope and photographed using a Nikon 35mm F70 SLR camera (Nikon, London, UK). Apoptosis assay fluorescence was observed using an Olympus BX51 research fluorescence microscope (London, UK). Cells stained with siGlo/ DAPI for evaluation of the siGlo assay were observed/ photographed using a Leica DMIRE2 Inverted Research fluorescent microscope with Improvision digital image capture software. All other equipment not listed are as in 2.1.1-2.1.6.

2.2 Methods

2.2.1 Cell Culture

2.2.1.1 Routine Maintenance of MCF-7 cells

The MCF-7 cell line was routinely passaged (as with all cell culture procedures) within a class II biological safety cabinet, and maintained in T75 flasks in RPMI 1640 medium supplemented with 5 % FCS, (10 iU/ml–100 µg/ml penicillin–streptomycin, and 2.5 µg/ml fungizone. Cells were grown as monolayers in T75 cell culture flasks at 37°C in a humidified atmosphere with 5 % CO_2 Cell culture medium was changed at approximately 3 days, and cells were routinely passaged by trypsinisation after reaching approximately 70 % confluency with trypsin/EDTA (0.05 % (v/v)/ 0.02 % (v/v)). Trypsinisation was performed by the replacement of cell culture media with 10ml trypsin solution (0.2g/l EDTA, 0.5g/l bovine trypsin in PBS) followed by 5 minutes incubation at 37°C to allow cell detachment. An equal volume of media was then added to the trypsinised cells and the cell suspension was centrifuged at 1350g for 5 minutes at room temperature. The pellet was then resuspended in 10ml medium ensuring homogenous suspension, and the cells were seeded into new T75 flasks at 1:10 dilution for a total volume of 15ml.

2.2.1.2 MCF-7 cells: experimental studies

For experimental studies, MCF-7 cell monolayers were harvested by trypsinising as 2.2.1.1. The cell suspension washed with PBS, and resuspended into media as above, with the exception of using phenol red-free RPMI and 5% charcoal-stripped steroid-depleted FCS [csFCS]; see Appendix 1). Prior to seeding, cells were counted using a Coulter Counter (see 2.2.1.8). Cells were seeded at a density of approximately 1×10^6 cells/ dish into 150mm plastic dishes in such medium. Cell culture medium was changed at day 4 of seeding, and the cells harvested at approximately 70% confluency at day 7. Where MCF-7 cells were treated with 17-β-oestradiol, cells were seeded and grown as above, but with the inclusion of 10^{-9}M 17-β-oestradiol (see Appendix for preparation of tissue culture solutions) at day 4 of seeding, for a total of 3 days of treatment. Where MCF-7 cells were treated with Gefitinib, cells were seeded and grown as above with the inclusion of 10^{-6}M of the inhibitor at day 1 of seeding, for a total of 4 or 7 days of treatment.

2.2.1.3 TamR Cells

Cells with acquired resistance to tamoxifen were generated for study at the TCCR as described previously by Knowlden et al., (2003). Briefly, parental MCF-7 cells were cultured in phenol red-free RPMI supplemented with 5% csFCS, in the presence of (10^{-7}M) 4-OHT until around 3 months. At this point, following a growth inhibitory phase, the growth rate increased in the presence of the antioestrogen, where upon the cells were deemed to be resistant to the inhibitor. Cells were stored at -80°C until required. The cells were then seeded and grown under experimental conditions as parental MCF-7 cells, but in the continual presence of 10^{-7}M 4-OHT (see Appendix I for preparation of tissue culture solutions). Cells were again grown to ~70% confluency, cell culture medium changed at day 4, again including 4-OHT.

TamR cells were verified as resistant to inhibition by tamoxifen through cell growth assays, and shown to be comparable to cells at the time of derivation (Knowlden etal., 2003). TamR cells at equivalent passage number to those used within this study were cultured in T75 flasks as described in 2.2.1.3 to approximately 70% confluency before being harvested, trypsinised (see 2.2.1.1) and counted (see 2.2.1.8). Cells were then seeded into 24 well plates at a density of 20,000 cells/well in phenol red-free RPMI, supplemented as described in section 2.2.1.3, either in the absence or presence of the antioestrogen for up to 16 days (performed by Tissue Culture Unit at TCCR).

Where TamR cells were treated with Gefitinib, cells were seeded and grown as above with the inclusion of 10^{-6}M of the inhibitor at day 1 of seeding, for a total of 4 or 7 days of treatment.

2.2.1.4 FasR Cells

Cells with acquired resistance to Faslodex were generated for study at the TCCR as described previously by McClelland et al. (2001). Briefly, parental MCF-7 cells were cultured in phenol red-free RPMI supplemented with %5csFCS, in the presence of 10^{-7}M Faslodex until around 3 months when the initial growth inhibitory effect of the agent was overcome, where upon the cells were considered resistant to the inhibitor. These were stored at −80°C until required. Cells were seeded and grown for experiments as MCF-7 cells, but in the presence of 10^{-7}M Faslodex (see Appendix I for preparation of stock solutions). Cells were again grown to ~70% confluency, cell culture medium changed at day 4, again including Faslodex.

FasR cells were verified as resistant to inhibition to Faslodex through cell growth assays, and shown to be comparable to cells at the time of derivation (McClelland etal., 2001). FasR cells at equivalent passage number to those used within this study were cultured in T75 flasks as described in 2.2.1.4 to approximately 70% confluency before being harvested, trypsinised (see 2.2.1.1) and counted (see 2.2.1.8). Cells were then seeded into 24 well plates

at a density of 20,000 cells/well in phenol red-free RPMI, supplemented as described in section 2.2.1.4, either in the absence or presence of the antioestrogen for up to 12 days (performed by Tissue Culture Unit at TCCR).

Where FasR cells were treated with Gefitinib, cells were seeded and grown as above with the inclusion of 10^{-6}M of the inhibitor at day 1 of seeding, for a total of 4 or 7 days of treatment.

2.2.1.5 FasR-Lt Cells

A further Faslodex-resistant model, FasR long-term (FasR-Lt) was generated for study at the TCCR as described previously by Nicholson etal., (2005) from the continuous culture of FasR cells (section 2.2.1.4) for a further 30 passages when stable phenotypic/ morphological changes were noted (eg. gain of fibroblastic morphology, loss of ER) (Nicholson etal., 2005). These were stored at −80°C until required. Cells were seeded and grown for experiments as FasR cells (2.2.1.4). Cells were again grown to ~70% confluency, cell culture medium changed at day 4, again including Faslodex.

2.2.1.6 X-MCF-7 cells

Cells with acquired resistance to stringent oestrogen deprivation conditions were generated at the TCCR as described previously (Nicholson et al., 2004; Staka et al., 2005). Briefly, for the generation of X-MCF-7 cells, parental MCF-7 cells were cultured in phenol red-free RPMI medium containing 5% charcoal-stripped, heat-inactivated FCS (termed 'X-medium' medium; see Appendix I for X-medium preparation), which is believed to severely deplete oestrogens and also exogenous growth factors. X-MCF-7 cells were generated by continual culture of MCF-7 cells in x-medium when around 4 months, the initial marked growth inhibitory effects of deprivation were overcome, and growth rate returned to that of parental cells prior to treatment. Cells were stored at −80°C until required. Cells were grown to ~70% confluency for experimental work, with cell culture X-medium changed at day 4.

2.2.1.7 TamR/TKI-R cells

The cell line with acquired resistance to tamoxifen and the EGFR-TKI gefitinib was developed at the TCCR as described previously by Jones et al. (2004). Briefly, this was achieved by the continual exposure of TamR cells (section 2.2.1.3) to the presence of 10^{-7}M 4-OHT and 10^{-6}M gefitinib for 6 months, in phenol red-free RPMI supplemented with 5% csFCS. Following the inhibitory phase, cell growth returned to that before treatment. Cells were stored at −80°C until required. For experiments, cells were seeded and maintained in culture

conditions as listed for MCF-7 cells but in the presence of $10^{-7}M$ tamoxifen and $10^{-6}M$ Gefitinib. Cells grown to ~70% confluency (for 7 days), with media changing at day 4.

2.2.1.8 Cell Counting

Subsequent experimental work on all cell lines using 6, 12 or 24 well plates involved cell counting prior to seeding. After trypsinisation (see 2.2.1.1) a volume of cell suspension was drawn into a 5ml syringe with a 25gauge needle. A homogeneous suspension was achieved by the expelling and drawing in of the suspension through the needle. A volume of 4ml was added to the Coulter Counter receptacle containing 6ml of isoton solution (see Appendix I for constituents of solution), with subsequent counting until a constant cell number value was achieved, using a Beckman Coulter Counter. An average cell count from 2 counts per sample was determined.

Note: all experiments were performed on cells within a window of approximately 20 passages to ensure the characteristics of the cell lines remained consistent.

2.2.2   Optimisation of RNA Extraction for Plastic Microarray Hybridisation

In order to maximise yield of RNA and to obtain microarrays with low background and high signal strength, a number of RNA extraction procedures were evaluated. In methods where RNA yield and quality was deemed to be sufficient for subsequent DNase treatment and array hybridisation, the resultant RNA was used to hybridise to Atlas Plastic Human Trial Microarrays in the first instance (see 2.2.9 and Fig.4). Initial hybridisations studies were performed on these arrays until an optimised extraction method (a combination of Tri Reagent extraction, DNase treatment, Qiagen column clean-up, poly A+ RNA selection) that showed suitable signal/ background intensity on the arrays was obtained, after which the larger Atlas Plastic Human 12K test microarrays were utilised routinely (see Fig.5).

2.2.2.1 Tri Reagent Extraction

Tri Reagent is based on the single-step total RNA isolation reagent developed by (Chomczynski and Sacchi, 1987), which in turn is a modification of the Guanidinium Thiocyanate method for isolating intact RNA from Chirgwan et al. (Chirgwin et al., 1979). The Tri Reagent RNA isolation method is reported to allow quick, economical, and efficient isolation of total RNA.

Cell lines were grown in 150mm dishes under experimental conditions as described in 2.2.1.1 to 70% confluency. For harvesting, cells were processed in batches of 4 dishes in a fume hood. The medium was aspirated and cells washed twice with 10ml of prewarmed (37°C) PBS.

This was then removed and immediately replaced with 1.5ml of Tri Reagent per dish. After ensuring complete coverage of the dish with the reagent, cells were scraped into a 50ml Falcon tube and placed on ice. This was repeated until cells from a total of 6 to 8 dishes were collected in a tube. The Tri Reagent/cell suspension were either stored at -80°C or processed immediately for RNA extraction.

The cell suspension was vortexed, transferred to a 35ml polypropylene tube, followed by the addition of 0.2ml of chloroform per ml Tri Reagent. This was briefly vortexed and placed on ice for 10 minutes. The resulting mixture was centrifuged at 11000g for 15 minutes at 4°C in a Sorvall IC5B centrifuge. The subsequent aqueous layer was transferred into a clean polypropylene tube and 0.5ml of isopropanol added per ml of Tri Reagent. This was mixed by gentle inversion and stored at -20°C for at least 20 minutes. After centrifuging as above, the supernatant was carefully removed and discarded. The pellet was washed by the addition of about 4ml of 75% ethanol and centrifuged as above. The pellet was then air dried after removal of supernatant. The pellet was subsequently solubilised in 30 to 50µl of DNase/RNase-free water and the RNA concentration determined (see 2.2.3), followed by visual evaluation of the RNA quality by agarose gel electrophoresis (see 2.2.4). The RNA was then subject to DNase treatment (see 2.2.5) and Qiagen RNA clean-up (see 2.2.6) (see also Fig.6)

2.2.2.2 Clontech Nucleotrap mRNA Purification

This method is reported to allow the improved purification of nucleic acid through binding to silica beads in a chaotrophic salt solution (Clontech_Nucleotrap, 2006). Following binding of the RNA to the beads (in this instance previously extracted by Tri Reagent, see 2.2.2.1), the beads are washed in the spin column, and the RNA subsequently eluted (see also Fig.6).

The procedure was performed according to the Clontech Nucleotrap mRNA purification kit protocol. An equal volume of 2xRM1 buffer was added to 150 to 200µg of total RNA from Tri Reagent extraction, at 1µg/ul dilution. NucleoTrap mRNA suspension beads were resuspended by vortexing and added to the RNA at 15 µl per 100 µg of RNA. After mixing, the suspension was heated at 68°C and incubated at room temperature for 10 minutes with tube inversion every 2 minutes. The tubes were centrifuged at 5000 rpm for 15 seconds, and then centrifuged at 14000rpm for 5 minutes. The supernatant was discarded and the resultant pellet dissolved in 0.6ml of buffer RM2. The suspension was transferred to a NucleoSpin microfilter column and centrifuged at 5000rpm for 15 seconds, then 14000rpm for 2 minutes. After discarding the flow through, 0.5ml of buffer RM3 was added to the filter within the column and beads were resuspended by pipetting. The NucleoSpin column was centrifuged at 14000rpm for 2 minutes and the flow through discarded. The above wash step was repeated by the addition of
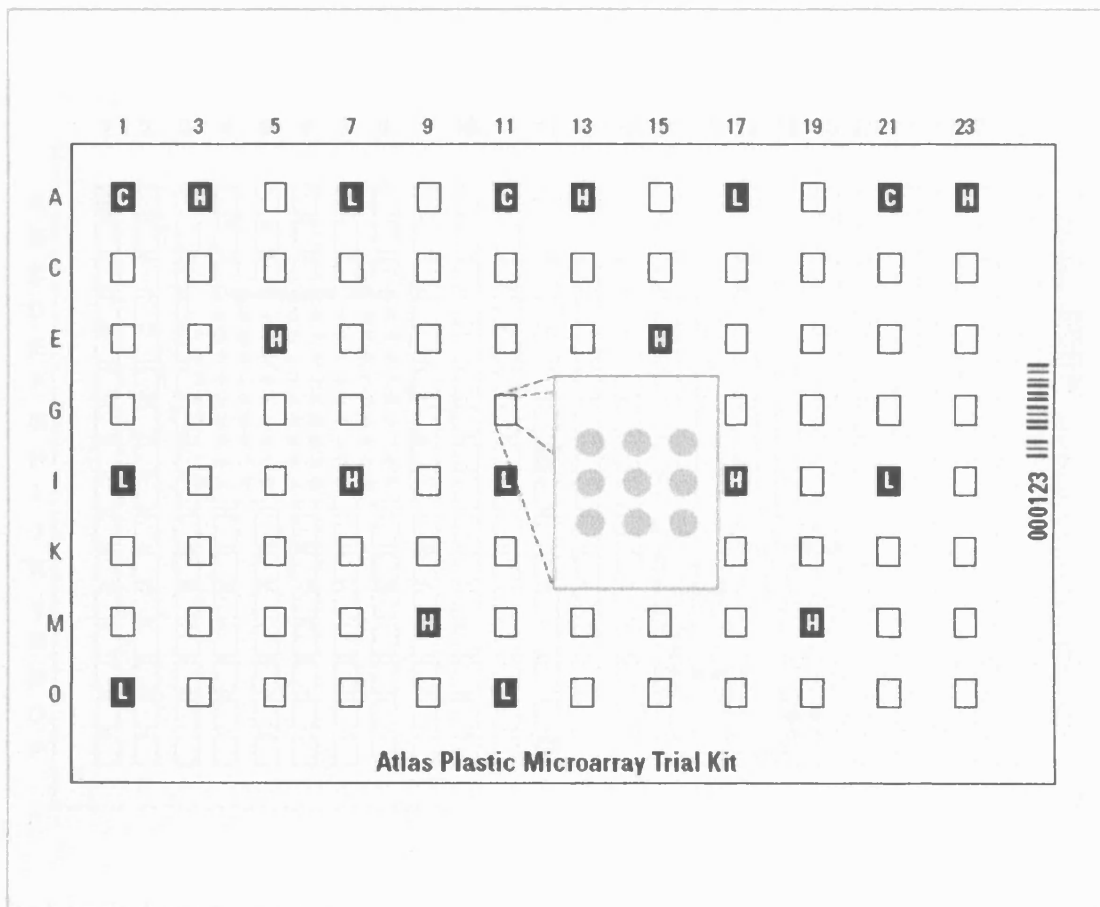
Figure 4. Atlas Plastic 12K Trial Microarray Layout. The layout of the Atlas Plastic Trial Microarray is a repeating block of 9 spots as shown in the enlarged inset. Each of the 9 spots in a block contain the same oligonucleotide. This block pattern is repeated 96 times (labelled A–O by 1–23). Blocks labelled "C" contain spots corresponding to the cDNA Synthesis Control Blocks labelled "H" contain housekeeping genes. Each block labelled "L" contains a different phage λDNA sequence and serves as a negative control. From (from www.clontech.com).
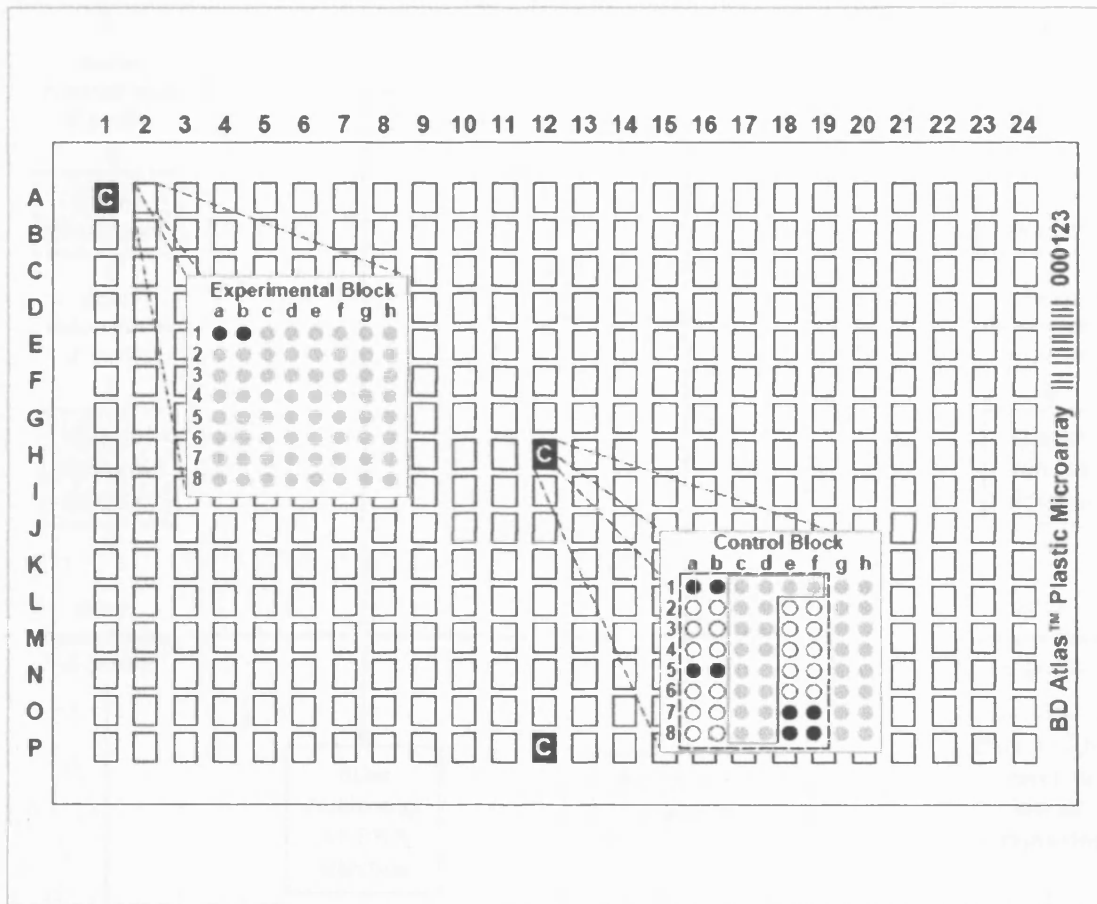
Figure 5. Atlas Plastic 12K Trial Microarray Layout. The layout of the Atlas Plastic 12K Microarray is a repeating block of 64 spots (labelled a–h by 1–8). This block pattern is repeated 384 times (labelled A–P by 1–24). Blocks labelled "C" consist of identical sets of control spots (enclosed in a dotted box) plus experimental genes (columns g & h). The enlarged inset diagrams show a sample experimental block (A2) and a sample control block (H12). Each long oligonucleotide is printed in duplicate side-by-side spots. Black spots at positions a1 & b1 of each experimental block (and at positions a1/b1/a5/b5/e7/f7/e8/f8 of the control blocks) correspond to the cDNA Synthesis Control. The white circles in the control block correspond to negative controls (various phage λsequences). The housekeeping genes are outlined with a solid line in the control block. (from www.clontech.com)
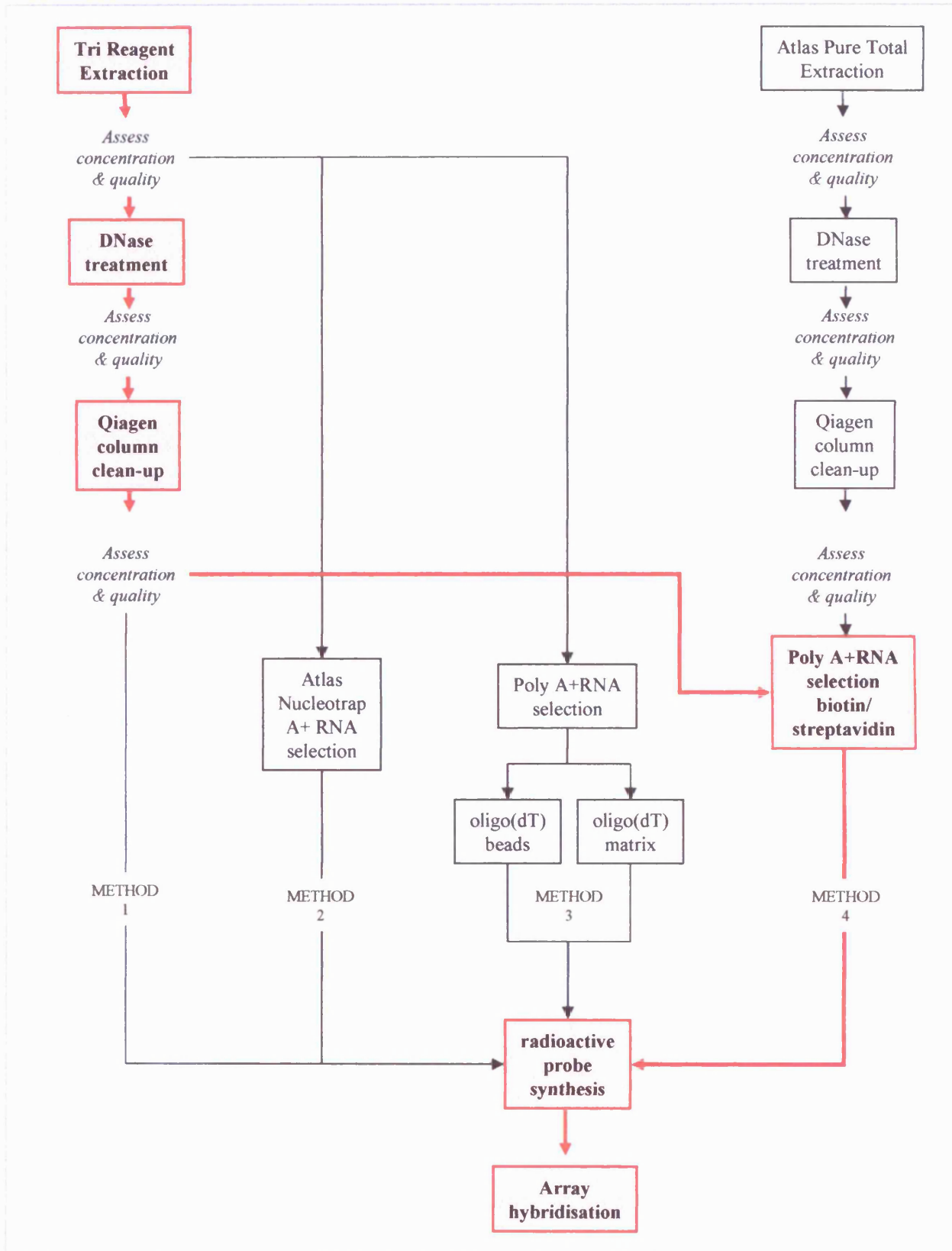
Figure 6. Strategy for RNA Extraction.
(Optimised method is highlighted in red).

0.5ml buffer RM3, bead resuspension and centrifugation. After discarding the flow through, the column was centrifuged at 14000rpm for 1 minute to remove the wash buffer. To elute RNA, 60μl of prewarmed (68°C) RNase-free water was added to the column, and the beads resuspended. The column was incubated at 68°C for 7 minutes, and then centrifuged at 14000rpm for 1minute. RNA concentration was determined from the eluate (see 2.2.3).

2.2.2.3. Poly A+ mRNA Selection

Two methods were also used to extract poly A+/ mRNA from total, Tri Reagent extracted RNA in an attempt to obtain high hybridisation signal intensity with low background (Fig.6).

2.2.2.3.1 Poly A+ RNA Selection using oligo(dT) Cellulose Beads

This method of polyadenylated (PolyA+) RNA extraction was based on that described by Aviv and Leder (1972).Oligo (dT)-cellulose is an affinity matrix used for the isolation of polyadenylated mRNA. The matrix consists of oligo (dT)25 covalently coupled to a cross-linked cellulose bead. The large porous surface area of the beads permits a high density of RNA binding (Gilham and Rosenberg, 1971). The protocol uses a lysis buffer, a high salt wash buffer, and a low salt elution buffer. Two variations, method A or method B, of this protocol were attempted using the solutions as listed in table 3.

Table 3. buffers for poly A+ RNA selection using oligonucleotide(dT) beads.

	Lysis buffer	High salt wash buffer	Low salt elution buffer
Method A	0.5M NaCl, 0.2% SDS, 0.1M EDTA, 10mM TrisHCL pH7.6	0.5M NaCl, 0.1M SDS, 0.1M EDTA	10mM TrisHCL; pH7.6
Method B	0.02%SDS, 0.1M EDTA, 10mM TrisHCl	0.5M NaCl, 0.02%SDS, 5mM EDTA, 10mM TrisHCl	5mM EDTA, 10mM TrisHCl

In a 15ml tube, 10ml of lysis buffer A or B was added to 200μg of RNA, previously extracted using Tri Reagent (see 2.2.2.1). This was incubated at 65°C for 12minutes followed by the addition of 50mg of oligo(dT)cellulose which was mixed by inversion, and further incubated at 65°C for 15 minutes. The tube was centrifuged at 2500rpm for 10minutes at room temperature. After removing the supernatant, 10ml of high salt wash buffer A or B was added to the resultant pellet and mixed by inversion. The tube was centrifuged and this wash step repeated. After discarding the supernatant, 1.4ml of low salt (elution) buffer was added to the

pellet and the mixture transferred to a sterile 1.5ml tube. The tube was centrifuged at 1000rpm for 3minutes, the supernatant discarded, and 140µl (1/10th volume) sodium acetate, pH5.2, and 3.5ml (2.5x volume) 100% ethanol was added to the pellet, which was subsequently stored overnight at -20°C. After transferring to a polyallomer centrifuge tube, the mixture was centrifuged at 40,000rpm for 40 minutes at 4°C. After removing the supernatant, 1ml of 75 % ethanol was added, and the pellet washed and transferred to a 1.5 ml tube. This was centrifuged at 14000 rpm for 10 minutes at 4°C followed by the addition of 200µl of TE buffer (10mM TrisHCL pH7.4, 1mM EDTA pH8) to the resultant pellet, and stored overnight at -20°C.

Ethanol precipitation was then performed to further concentrate the RNA. A volume of 20µl (1/10th volume) sodium acetate and 500µl (2.5x volume) 100% ethanol was added to the tube, and centrifuged at 14,000rpm for 10minutes at 4°C. After removing the supernatant, 60µl of 100% ethanol was added and the tube centrifuged as above. The supernatant was removed and the resultant pellet briefly air-dried and solubilised in 10µl DNase/RNase-free water.

2.2.2.3.2 Poly A+ RNA Selection using oligo(dT) Cellulose Matrix

This method is based on the protocol as described in Sambrook et al., (1989) which utilises Oligo(dT)cellulose matrix packed effectively as a column for the purification of mRNA from total RNA. Glass wool and all glassware and plasticware were silanised by treatment with dimethyldichlorosaline in the fume hood, which involved brief soaking in the reagent, draining and air drying, followed by rinsing with deionised water before use.

An oligo(dT)cellulose column was prepared by packing a sterile 2ml syringe with a 1cm bed volume of glass wool, followed by the addition of oligo(dT)cellulose, which had been prepared by adding 100mg of oligo(dT)cellulose to 5ml of 0.1M NaOH. The column was prepared by the addition of 5 column volumes of buffer1 (0.1M NaOH, 5mM EDTA), followed by 10 column volumes buffer2 (10mM TrisHCl, 1mM EDTA). The column was washed with 1x column loading buffer (20mM TrisHCl (pH7.6), 0.5M NaCl, 1mM EDTA (pH8), 0.1%SDS) until the pH of the effluent was less than 8.0.

1mg of total RNA was heated to 65°C for 5 minutes, then rapidly cooled in ice. An equal volume of 2x column loading buffer (40mM TrisHCl (pH7.6), 1M NaCl, 2mM EDTA (pH8), 0.2%SDS) was added and the RNA solution applied to the prepared column. The flow-through was collected in 0.5ml fractions in 1.5ml tubes. When all the RNA had entered the column, 1 column volume of 1x column-loading buffer was added to the column and the flow-through was collected.

When all the solution had eluted, the eluate was heated to 65°C for 5min, reapplied to the top of the column, and the eluate collected. The column was washed with 5 column volumes of 1x column-loading buffer, followed by collection of 1ml eluate fractions. PolyA+RNA was

eluted from the oligoDT-cellulose column by the addition of 3ml of elution buffer (10mM TrisHCl pH7.6, 1mM EDTA pH8, 0.05% SDS). The eluate was collected in 1ml fractions and a preliminary concentration of RNA determined (2.2.3).

The eluted PolyA+RNA was mixed with 3M sodium acetate (pH 5.2) to a final concentration of 0.3M followed by 2.5 volumes of 100% ethanol and mixed well. This was stored on ice for 30 min and the polyA+RNA recovered by centrifugation at 10,000rpm for 15min at 4°C. After carefully discarding the supernatant, the pellet was washed with 0.2ml of 70% ethanol and centrifuged as above. The supernatant was removed and the pellet was air dried, dissolved in 20µl of DNase/RNase-free water, and the final RNA concentration determined.

2.2.2.4 Atlas Pure Total RNA Labelling System;

This method permits the purification of total RNA, PolyA+RNA enrichment. The RNA, after isolation, is incubated with biotinylated Oligo(dT), which binds the poly A+ RNA fraction. Then, once the Streptavidin Magnetic Beads (with affinity for biotin) are added, the polyA+ fraction can be collected by magnetic separation. The resultant complex can be used directly in any Atlas Microarray probe labelling protocols (see also Fig.6).

2.2.2.4.1 Cell Lysis and Total RNA Extraction:

Cell lines were grown in 150mm dishes as described in 2.2.1. For harvesting, cells were processed in batches of 4 dishes in a fume hood. The medium was removed and cells washed with about 10ml of PBS. After removing the PBS, 6ml of denaturing solution (as supplied by Clontech/ BD Biosciences) was added uniformly across one dish and cells scraped into the next dish until the batch was processed. The cell lysates were stored on ice in a 50ml Falcon tube.

The cell suspension was vortexed and stored on ice for 10 minutes. Tubes were centrifuged at 11,000rpm for 5 minutes to remove cell debris, after which the supernatant was transferred to polypropylene tubes. A volume of 12ml of saturated phenol was added to the lysate with subsequent vortexing for 1 minute and incubation on ice for 5 minutes. After the addition of 3.6ml chloroform the sample was vortexed for 2 minutes and incubated on ice for 5 minutes. The homogenate was centrifuged at 11,000rpm for 10minutes at 4°C, after which the upper layer was transferred to a new polypropylene tube. A second round of phenol/chloroform extraction was performed as above using 9.6ml phenol and 3.6ml chloroform. After centrifugation the upper layer was transferred to a new polypropylene tube and 12ml isopropanol added slowly. This was mixed, incubated on ice for 10minutes, and then centrifuged at 11,000rpm for 15minutes at 4°C. After discarding the supernatant, 6ml of 80% ethanol was added to the pellet and the tube centrifuged at 11,000rpm for 5minutes at 4°C. The

supernatant was removed, and the pellet air dried and resuspended in 0.5ml DNase/ RNase-free water. The RNA concentration was determined (see 2.2.3), followed by visual inspection of the RNA by agarose gel electrophoresis (see 2.2.4). The RNA was then subject to DNase treatment (see 2.2.5) and Qiagen RNA clean-up (see 2.2.6).

2.2.2.4.2 PolyA+RNA Enrichment Prior to Array Hybridisation

Streptavidin Magnetic Bead Preparation was performed according to the manufacturers instructions. Briefly the magnetic beads were resuspended and 15µl aliquotted into a 0.2ml tube per reaction. The beads were separated on a magnetic particle separator and the supernatant removed. The beads were washed with 150µl of 1x binding buffer and mixed by pipetting. The beads were separated as before and the supernatant discarded. This procedure was repeated three times as above. The beads were finally resuspended in 15µl of 1x binding buffer per reaction.

Poly A+RNA Enrichment was achieved by firstly diluting 50µg of total RNA to a volume of 45µl in a 0.2ml tube. After adding 1µl of Biotinylated Oligo(dT), the contents of the tube were mixed and incubated at 70°C for 2 minutes in a preheated thermal cycler. The tube was removed and cooled at room temperature for 10 minutes, followed by the addition of 45µl of 2x binding buffer, and the tube mixed. The resuspended, washed beads from the first step were added to the above RNA mixture. The tube was thoroughly mixed by vortexing for 25 minutes at room temperature. The beads were separated on the magnetic separator and the supernatant discarded. The beads were then resuspended in 50µl of 1x wash buffer, separated as above, and the supernatant discarded. This was repeated followed by a final resuspension in 50µl of 1x reaction buffer. The beads were then separated, supernatant discarded, and the beads resuspended in 3µl of DNase/RNase-free water (where the random primer mix was supplied without cDNA synthesis control, subsequently in the probe synthesis step, the beads were resuspended in 2µl of water).

2.2.3 Determination of RNA Concentration

Extracted RNA concentration was determined by UV spectrophotometry. An aliquot of 4µl of RNA was diluted in 996µl of buffer 1x TNE buffer and the optical density measured at 260nm and 280nm (see Appendix II for TNE recipe). The RNA concentration (in µg/ml) can be ascertained by multiplying the optical density at 260nm, the dilution factor, and the extinction coefficient (which in the case of RNA is 40). In addition the ratio of the readings at 260nm and 280nm provides an indication of the purity of the sample (where a ratio of 1.7 to 2.0 is deemed suitable).

2.2.4 Agarose Gel Electrophoresis

The integrity of the extracted RNA was assessed by resolving a quantity of it through an agarose gel with ethidium bromide staining. Agarose gel was prepared by the heating of 2% w/v agarose in TAE buffer in a 950W microwave at full power for about 1 minute with periodic agitation (see Appendix II for TAE recipe). Upon cooling, 10ng/ml ethidium bromide was added and mixed. The gel was set in a horizontal tray with the comb in place. The gel was assembled in the electrophoresis apparatus with 1xTAE running buffer, and 1μg of total RNA in a total loading buffer volume of 5-10μl was loaded into the gel and a constant current of approximately 80-100mA was applied to separate the RNA (see Appendix II for 6x gel loading buffer recipe). This was visualised by UV illumination after ethidium bromide staining, and photographed. RNA quality was assessed by observation of ribosomal 18S and 28S bands, where adequate quality RNA was indicated by no observable degradation seen as low molecular weight products, and with the 28S band at approximately 1.5-2x the intensity of the 18S band (Sambrook et al., 1989).

2.2.5 DNase Treatment of RNA

A protocol using Sigma DNase kit ensured no genomic DNA contamination was present in the extracted RNA which may interfere with subsequent studies. For each 0.5ml of total RNA at a concentration of 1mg/ml, the following reagents were added to give a total volume of 1ml: 100μl 10x DNase buffer, 50μl DNase I, 350μl deionised water. The solution was mixed well by pipetting, incubated at 37°C for 30min in a heating block, and the reaction then terminated with 100μl of termination mix. The solution was stored on ice.

2.2.6 Qiagen RNA Clean-up

The Qiagen RNeasy kit allows RNA isolation based on the selective binding of the membrane. High quality RNA of >200 nucleotides are then eluted from the spin columns. This is particularly relevant in this project, where low molecular weight nucleic acids are required to be excluded, as well as the clean-up and removal of all reagents from previous procedures, notably DNase-treatment. Total RNA clean-up was performed according to the Qiagen RNeasy mini kit protocol. Assuming that the binding capacity of the column is 100μg of RNA, and that losses will have occurred through DNase treatment, approximately 150μg of RNA was initially processed from DNase treatment to Qiagen clean-up. After transferring the appropriate volume

of total RNA to a sterile 5 ml tube, , 350ul of buffer RLT was added to each 100μl of total RNA (in a fume hood) and mixed thoroughly (β-Mercaptoethanol was added to buffer RLT before use at 10μl/ml of buffer RLT). To each 100μl of initial RNA volume, 250μl 100% ethanol was then added. This was mixed thoroughly by pipetting and added in 0.7ml volumes to an RNeasy mini column placed in a 2ml collection tube. The tube was centrifuged at 10,000rpm for 15 seconds and the flow through discarded. After transferring the column to a new 2ml collection tube, 0.5ml buffer RPE was pipetted onto the column and centrifuged as above. The flow through was discarded and another 0.5ml of Buffer RPE was added to the column and centrifuged at 10,000rpm for 2 minutes. To dry the silica gel and to ensure no ethanol was carried over during elution, the columns were transferred to new collection tubes and centrifuged at 14,000rpm for 1 minute. To elute the RNA, the RNeasy column was transferred to a new sterile 1.5ml collection tube and 30 to 50ul of RNase-free water was directly added to the silica membrane. The tubes were allowed to stand for 2 to 3min after which they were centrifuged at 10,000rpm for 1 minute. RNA concentration was determined (see 2.2.3), followed by visual inspection of the RNA by agarose gel electrophoresis (see 2.2.4). To ensure no genomic DNA was carried over from RNA processing, PCR was performed using the RNA directly in the reaction (see 2.2.7).

2.2.7   PCR Assessment of DNA Contamination of RNA

Further estimation of the purity of RNA was provided by the polymerase chain reaction (PCR) where the purified RNA was used directly as a template using primers for well characterised genes, in this instance, insulin-like growth factor 1 (IGF1). Using a primer for the gene sequence, containing a long intron region, it will amplify any genomic DNA fragment present corresponding to the IGF1 gene.

For the detection of genomic DNA contamination 2μl of 10x Buffer (containing a final $MgCl_2$ concentration of 1.6mM) 10.9mM dNTP, 2.5u Taq polymerase, 0.2μl of both forward and reverse IGF1 primers were added to a PCR tube to a total volume of 4.5μl per reaction (sequences in materials and reagents). This was added to total reaction volume of 18.4μl, to amplify either 0.5μg of total RNA sample or of up to 1μg genomic standard. The following protocol was run in a BioRad thermal cycler: denaturation at 94°C for 2min, followed by 35 cycles of (92°C for 30s, 50°C for 30s, 75°C for 90s), with a final extension at 75°C for 5min. The products were visualised on a 1.5% agarose gel with ethidium bromide staining, as described in 2.2.4. The PCR reaction should produce no product at 35 cycles as visualised on an ethidium bromide gel.

2.2.8 Validation of Cell Lines by PCR

To ensure RNA preparations obtained for microarray studies were representative of each cell line, prior to array studies they were monitored for known gene expression changes across the various model systems (Knowlden et al., 1997; Knowlden et al., 2003; McClelland et al., 1996). Total RNA extracted from cells was subject to DNase treatment and Qiagen clean-up as described previously. cDNA generated from RT-PCR was then subject to PCR using the primers as described below.

2.2.8.1 RT-PCR

For initial reverse transcription where complimentary DNA (cDNA) was generated from RNA, $1\mu g$ of extracted total RNA is added to a mastermix, comprising: $2\mu l$ of 10x Buffer (containing a final $MgCl_2$ concentration of 1.6mM), 2.5mM dNTP, 0.1M DTT and $100\mu M$ of random hexamers, to give a volume of $18.5\mu l$. The solution was mixed, denatured at 95°C for 5 min in a BioRad thermal cycler, and rapidly cooled on ice. After adding $1\mu l$ of MMLV reverse transcriptase and $0.5\mu l$ of RNase inhibitor, the tube was mixed and briefly spun. The tube was returned to the thermal cycler for the RNA to be reverse transcribed according to the following protocol: annealing at 22°C for 10min, extension at 42°C for 42 min, and denaturation at 95°C for 5min.

2.2.8.2 PCR Reaction

$2.5\ \mu l$ of 10x Buffer (containing a final $MgCl_2$ concentration of 1.5mM), 2.5 mM dNTP, 0.63ul (0.5mM) of both forward and reverse primers and 1unit Taq polymerase were added to a PCR tube, together with $0.5\mu l$ of cDNA (as generated from the RT-PCR protocol) to a total volume of $25\mu l$ per reaction with DNase/RNase-free water. The following protocol was run in a BioRad thermal cycler: for β-Actin (204bp) and pS2: denaturation at 95°C for 2 minutes, then 55°C for 1 minute and 72°C for 2 minutes, followed by 26 cycles of (94°C for 30s, 55°C for 30s, 72°C for 60s), with a final step at 94°C for 1 minute and 60°C for 5 minutes; for EGFR: denaturation at 95°C for 2 minutes, then 55°C for 1 minutes and 75°C for 2 minutes, followed by 30 cycles of (94°C for 30s, 55°C for 30s, 72°C for 60s), with a final step at 94°C for 1 minute and 60°C for 5 minutes. (Sequences listed in materials and reagents). The products were visualised on a 1.5%-2% agarose gel with ethidium bromide staining, and photographed as described in 2.2.4.

2.2.8.3 Densitometric Analysis

Following scanning of the photograph of the fluorescent gel image using a BioRad GS-700 scanner system, densitometric analysis was performed using the Molecular Analyst software, and values were recorded for each band present from the photographed gel (with background subtraction for each band from an average of 6 background readings across the image). Band intensities were normalised against those of β-actin which served as a housekeeping gene prior to graphical display of data.

2.2.9 Microarray Methodology

The BD Atlas Plastic Human 12K Microarrays employed, consist of ~12,000 of long oligonucleotides , of approximately 28 bases, which are immobilised onto a plastic support (Fig.5). However, initial optimisation studies involved using TRIAL Atlas Plastic Human Microarrays (Fig.4), bearing 100 well-characterized human genes printed in nine replicates.

2.2.9.1 Probe Preparation

Optimisation of array protocols initially involved comparing probes prepared from Tri Reagent extracted total RNA from responsive or resistant cells, which had been DNase-treated and subject to RNA clean-up using a Qiagen column, or probes prepared from RNA prepared as above, with polyA+RNA separation (the latter ultimately according to the Atlas Pure Total RNA Labelling System protocol).

2.2.9.1.1 cDNA Probe Synthesis from Total RNA

The Atlas Plastic Microarray handbook protocol was used for probe preparation from Tri Reagent extracted total RNA (2.2.2.1) which had been DNase-treated and had undergone Qiagen clean-up. The following components were mixed in a 0.2ml tube to form the mastermix at room temperature: 5μl of 5x BD PowerScript Reaction Buffer, 2.5μl of 5μl of 10x dNTP mix, 1.5μl DTT and 7μl of [α-^{33}P]dATP, for a total volume of 16μl per reaction. The following were combined in a separate reaction tube: 5μg extracted total RNA (of 1μg/μl), 1μl diluted (1:200) cDNA synthesis control, 1μl of 10x random primer mix. The mixture was incubated at 65°C in a preheated thermal cycler for 2 minutes, then 42°C for 2 minutes. During this incubation, 2μl of BD PowerScript reverse transcriptase was added for each reaction to the master mix and mixed. After 2 minutes incubation at 42°C, 18μl of the mastermix, was added to each reaction tube, and the tubes returned to the thermal cycler to incubate at 42°C for 30 minutes. After the incubation, 2μl of 10x termination mix was added to each reaction. Column chromatography was then performed to purify the probe (see 2.2.9.2).

2.2.9.1.2 cDNA Probe Synthesis following PolyA+RNA Enrichment

The protocol was followed according to the Atlas Pure Total RNA Labelling System handbook for probe preparation from RNA which had been extracted using the Atlas Pure Total RNA Labelling System, with polyA+ RNA enrichment (section 2.2.2.4). The following components in a 0.2ml tube formed a reaction mastermix at room temperature: 4µl of 5x BD PowerScript Reaction Buffer, 2µl of 5x 10x dNTP mix, 0.5µl DTT and 5µl of [α-^{33}P]dATP, for a total volume of 11.5µl per reaction. To the resuspended beads from the polyA+ enrichment step (2.2.2.4.2), 4µl of random primer mix were added and the tube mixed (for a no cDNA synthesis control, 1µl of the diluted control was added). The bead/primer mix was incubated at 65°C in a preheated thermal cycler for 3 minutes, then 42°C for 2 minutes. During this incubation 2µl of BD PowerScript reverse transcriptase was added for each reaction to the master mix and mixed. After the 2 minute incubation at 42°C, 13.5µl from the mastermix was added to the bead/primer mix per reaction and the tubes returned to the thermal cycler to incubate at 42°C for 30 minutes. After the incubation 2µl of 10x termination mix was added to each reaction. Column chromatography was then performed to purify the probe (see 2.2.9.2).

2.2.9.2 Column Chromatography

Column chromatography was performed on all probes regardless of RNA extraction/ purification procedure, in order to remove unincorporated components from previous labelling procedures.

cDNA probe synthesis was conducted as above with probe purification subsequently performed according to the Atlas Plastic Microarray method. This purification procedure aimed to separate labelled cDNA from unincorporated ^{33}P-labelled nucleotides and small cDNA fragments. 180µl of Buffer NT2 was added to each probe generated and mixed. This was then pipetted into a NucleoSpin Extraction spin column, which was placed in a 2ml collection tube, and centrifuged at 13,000rpm for 1 minute. The collection tube and flow through were discarded. The column was inserted into a new collection tube and 400µl of buffer NT3 was added and centrifuged as above. This step was repeated twice. After transferring the spin column to a new 1.5ml collection tube, 100µl of Buffer NE was added to the column and allowed to soak for 2 minute. This was then centrifuged as above to elute the purified probe. Probe specific activity was subsequently determined by retaining 1µl volume for scintillation counting. The amount of radioactivity incorporated into the probe was determined as counts per minute using a Tri-Carb 2900 TR Scintillation counter in order to assess the approximate equivalence of radioactive labelling in samples. Counts were deemed to be satisfactory ranging from approximately 20,000- 30,000 counts per minute.

2.2.9.3 Microarray Hybridisation and Phosphorimage Detection

The microarrays were rinsed with 15ml of prewarmed BD PlasticHyb Hybridisation Solution at 60°C for 30min. This was achieved with the microarrays facing-up in a rollerbottle hybridisation chamber (and later, BD Atlas Hybridisation Box, in a heated rocking oven). The synthesised probes were denatured by incubating in a boiling water bath for 10 minutes followed by cooling in ice for at least 10 minutes. The probe was combined with 15ml of hybridisation solution used for microarray rinsing, added to the arrays, and left overnight to incubate at 60°C with continuous rocking.

The hybridisation solution was then discarded and replaced with 45ml of prewarmed High Salt Wash Solution (2xSSC, 0.1%SDS) with further rocking at 58°C for 5 minutes (see Appendix III for 20x SSC recipe). This wash was repeated, and then the wash solution was replaced with 45ml of prewarmed Low Salt Wash Solution 1 (0.1xSSC, 0.1%SDS) and washed as above twice at 58°C. This solution was then replaced with 50ml of room-temperature Low Salt Wash Solution 2 (0.1%SSC) and rocked at 30°C for 5 minutes. The microarray was then removed from the Hybridisation Box, transferred to a beaker containing room temperature Low Salt Wash Solution 2, rinsed and air dried. The printed surface of the array was subsequently exposed to a phosphorimage screen for 7 to 10 days. Signals present on the phosphorscreen were then detected using a Typhoon 8600 phosphorimager and the image scanned at a resolution of 50µM. This was stored either in a .tif or .gel file format for subsequent gene analysis (see 2.2.10).

2.2.9.4 Stripping cDNA probes from the Microarrays:

In order to reuse the arrays, the cDNA was stripped from them using low salt buffer. However, the standard stripping procedure from BD Biosciences/Clontech proved inadequate for removing all signal from the microarrays, with 10-20% signal remaining (see Appendix III for standard Atlas array stripping protocols). Thus, as subsequently recommended by Clontech/ BD Bioscience (*personal communication*), microarrays were placed face up in a BD Atlas Hybridisation Box and incubated with 40ml of prewarmed strip solution (0.2M NaOH, 0.1%SDS) on a rocking platform at 37°C for 10 minutes. The solution was then replaced with new prewarmed strip solution and the incubation repeated. The arrays were then rinsed twice in a beaker of room temperature water, air dried, then exposed to autoradiograph for at least 7 days to assess the degree of stripping. Array was deemed adequately stripped when negligible/ no signal remained after this period.

2.2.9.5 Optimised Protocol for RNA extraction and

Ongoing RNA extractions together with microarray optimisations allowed the following protocols to be generated. This has demonstrated to provide high yield of RNA, and adequate signal strength on the arrays with low background. The protocol is described in Results.

2.2.10 Microarray Data Analysis

A number of factors dictate the success of a microarray study, not only the RNA quality, and efficiency of array hybridisation, but also data acquisition, preprocessing, and analysis/ gene selection techniques (Leung and Cavalieri, 2003). With increasingly complex methods of data analysis available, we have approached this task with a clear biological question to reveal genes altered in resistance using integrated statistics, clustering, and ontological methodologies. With a multitude of softwares available on the market for all the various steps, the study used software supplied/ recommended for acquisition and preprocessing with the specific array, AtlasImage and AtlasNavigator, as well as complex gene analysis and gene selection being performed using established web-based GeneSifter (GeneSifter.url, 2006), and ontological database resources such as GeneCard (Genecards.url, 2006) and Medline.

Figure 7 shows the schematic for the array data analysis approach here adopted for gene selection. Using Atlas Plastic 12k Human Microarrays, after hybridisation image acquisition was performed on quadruplicate arrays using phosphorimaging, which was subsequently aligned and intensity data generated for the reference sample (parental MCF-7 line) and resistant test sample (TamR, FasR) using AtlasImage software. Following signal intensity report generation, data was normalised in AtlasNavigator software. In order to subsequently select genes for verification and further analysis, a number of analytical tools available within GeneSifter software were then used, together with a biological intuitive approach for gene examination.

The analysis methods adopted within this project were statistical testing Hierarchical Cluster Analysis (HCA), Partitioning Around Medoids (PAM), and Ontolological Examination of the gene (Fig.7 right panel). The aim was to end up with a manageable list of new genes with interesting signalling ontology that may contribute to resistant growth/ associated features of progression for the eventual verification by PCR and selection for protein studies. Genes which were increased in both TamR and FasR were deemed high priority as these may provide generic targets which are fundamental to resistance. The proceeding sections will now describe the methods for grid alignment, normalisation, analysis and gene selection in detail.

2.2.10.1 AtlasImage

AtlasImage software (BD Biosciences/Clontech) allows the phosphorimage of the array to be processed for the generation of gene signal intensity reports. In summary, firstly, the process of 'gridding' is performed, ie. coordinates are assigned to each of the spots which correspond to a gene; then segmentation differentiates image pixels as foreground or background; and intensity extraction produces the final intensity value for each spot on the array, the foreground intensities, background intensities. As gridding is performed manually, it allows poor quality spots to be flagged for removal (see also BD AtlasImage 2.7 User Manual).

2.2.10.1.1 Grid Alignment

Atlas arrays were analysed firstly by opening and aligning the saved array image to the AtlasImage Grid Template (Fig.8a). This is achieved by the alignment of orientation spots (located at each opposite corners of the array) and allows AtlasImage to determine the location of all the genes on the array. This was followed by aligning sub-areas within the array (Fig.8b)

Fine-tuning re-alignment is normally required to compensate for errors from the previous alignment step resulting from signal spots which may be problematic (Fig.8c and Fig.8d). Such signals may cause incorrect spot alignment due to, interfering signal (signal bleed) from neighbouring spots, background interference, or spot printing errors. The template alignment window will show coloured circles superimposed at or near each spot, the colour representing the signal characterisation, black: signal at or near background; green: signal above background; red: error, where there is significant variation between left and right duplicate spots, or olive: where the user had excluded the spot from analysis). AtlasImage allows settings for signal thresholds to be varied.

2.2.10.1.2 Error Correction

Errors may finally be compensated for by relocating one or both superimposed circles on the incorrectly spotted signal (Fig.8c and Fig.8d). Where signal bleeding may be causing errors in duplicate spots, the aberrant signal can be excluded from subsequent analysis. Where even signal bleeding is caused by two spots interfering onto two neighbouring spots, the spots may be excluded from the analysis if the spots are greatly affected. Alternatively, AtlasImage allows local background correction to be used for calculations for any genes which may be affected by bleeding. In this case, the local background immediately surrounding the spot may be used for background calculations, as opposed to the default setting for background correction which is set at the median intensity of the blank space between the different panels within the array.
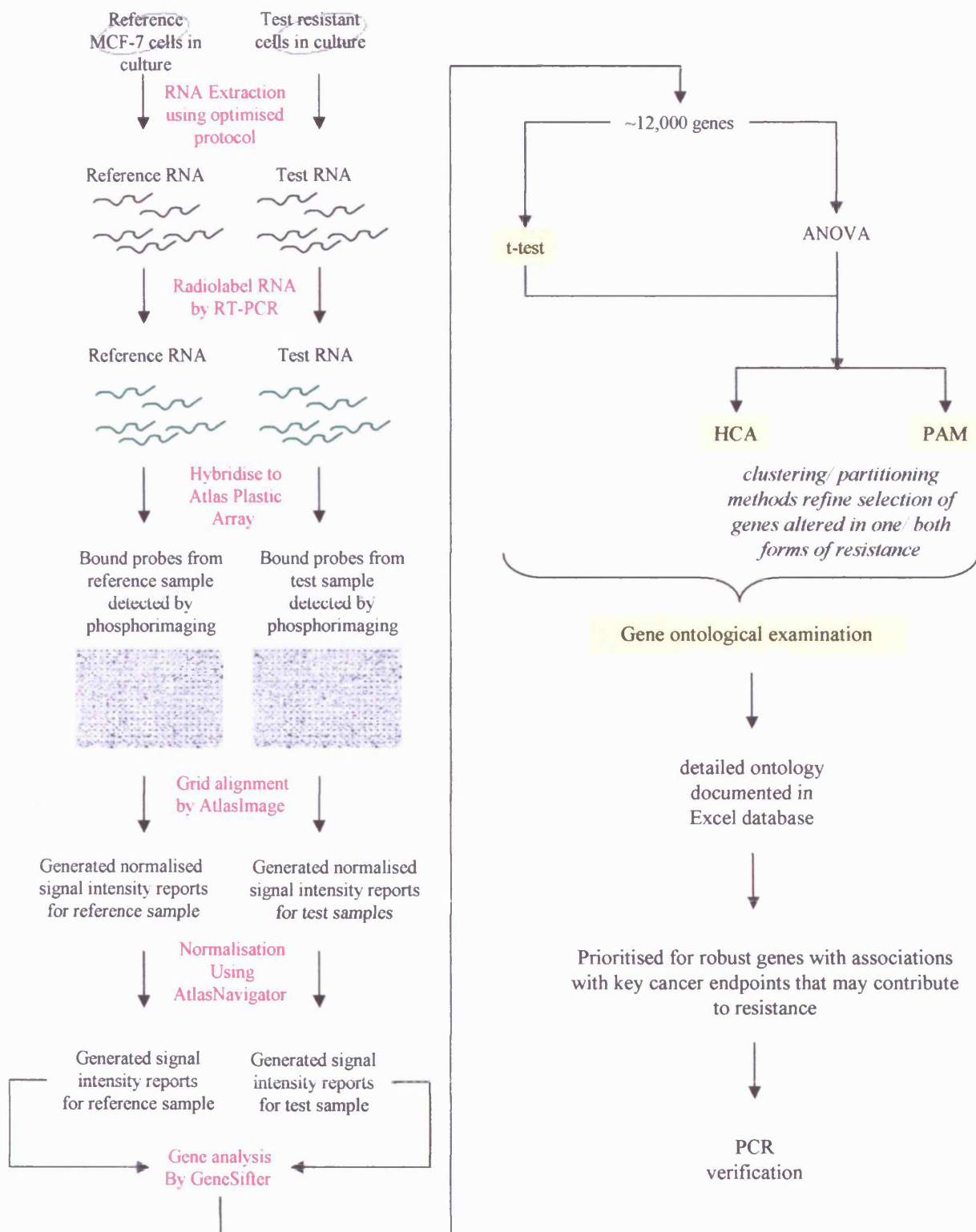
Figure 7. Schematic of microarray procedure and analysis. RNA optimally extracted from test resistant cells and reference endocrine responsive MCF-7 cells were radioactively labelled and hybridised to Atlas Plastic Human 12k Microarrays in 4 replicates. Following phosphorimaging, signal intensity reports generated and normalised using Atlas associated software and imported into GeneSifter for selection of altered genes. Significant genes using ANOVA/ t-test were then processed for selection of target genes using a number of selection criteria. Hierarchical Cluster Analysis (HCA) and Partitioning Around Medoids (PAM) was used to reveal the breadth of genes altered in shared/ individual forms of resistance. GeneSifter pairwise analysis (t-tests) was used to identify genes altered in one or both forms of resistance versus control MCF-7 cells. Detailed ontological examination of genes was subsequently performed through literature searches with the establishment of an Excel database for the t-test list. Data from all selection criteria were considered for the final gene list for PCR validation.

Figure 8. Atlas Image Grid Alignment and Fine tuning for Array Signal Intensity Report File Generation.
Plastic Plastic Human 12k Microarray phosphorimages were imported into AtlasImage for gridding and fine tuning. Images were (a) aligned to the whole grid area, (b) aligned to individual sectors within, and (c) re-aligned for misaligned individual spots, and (d) corrected for local background when necessary. This is repeated for a total of 4x replicates for each test sample (MCF-7, MCF-7+E2, TamR, FasR).

(a) Autoalign total array area
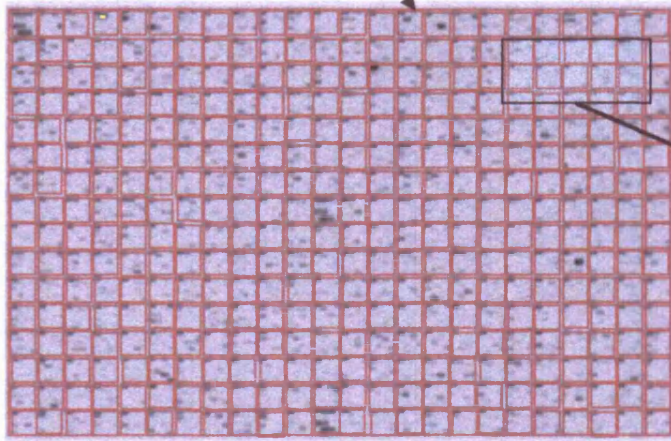
(b) Align sub-areas in array
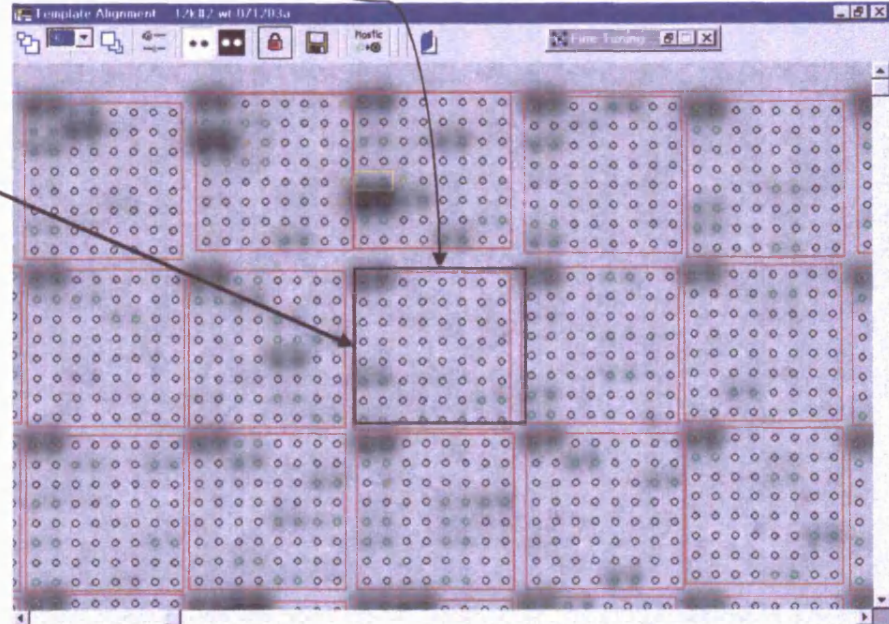
(c) Re-align individual signal spots
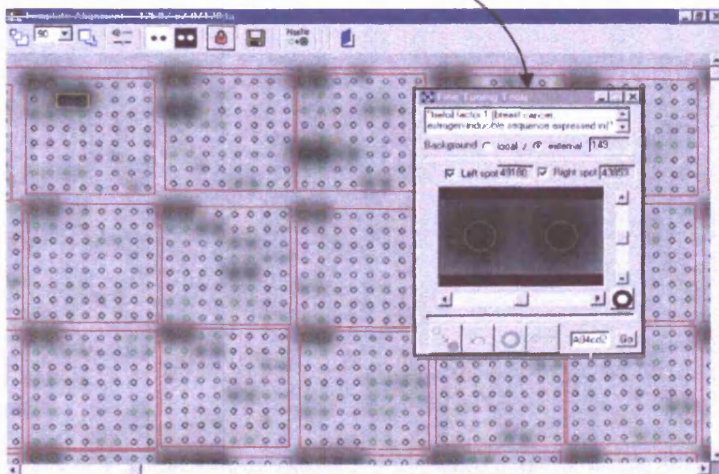
(d) Correct for local background where signal bleed (in this instance from lower spots) may interfere with neighbouring gene
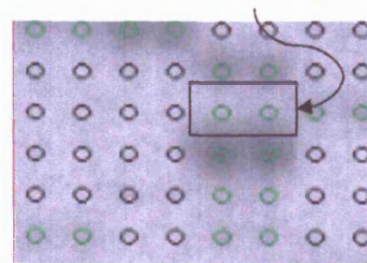
2.2.10.1.3 Signal Intensity Report File Generation

Once alignment of the arrays was complete, a report of signal intensities was generated by opening the pair of arrays (reference control MCF-7 versus resistant cell line) to be analysed through the "compare two arrays" menu of AtlasImage. The array with overlaid grid may be observed with a close-up of the selected gene, together with its intensity (average from duplicate spots), the calculated background value, adjusted intensity (average minus background), ratio of one array to another, and the difference.

2.2.10.2 Atlas Navigator

AtlasNavigator software (BD Biosciences/Clontech) allows the analysis and visualisation of complex gene expression generated with AtlasImage generated reports above. Although the software also permits only very basic data analysis, it will only be utilised for normalising AtlasImage signal intensity report. The process of Normalisation aims to remove systemic errors inherent in the data (Knudsen, 2002). These scaling adjustments allow the standardisation of the ratio distribution across replicate experiments to prevent any experiment becoming incorrectly biased, confusing downstream analysis.

2.2.10.2.1 Loading AtlasImage Files onto AtlasNavigator

Intensity data as Atlas Image reports were firstly saved into the relevant Atlas Navigator folder ready for loading. After opening the software main window, the files were imported using the 'Autoloader' option, which permits AtlasImage files to be directly imported. Upon recognition of the report files as AtlasImage files, the appropriate array was selected from the menu and consecutive onscreen dialogue boxes were correctly chosen for: a 'one colour experiment', and then more files were added when prompted.

2.2.10.2.2 Normalisation

AtlasNavigator permits a number of normalisation options to control for differing signal intensities, many of which can be used in any combination. The first normalisation method, 'Each sample to itself', was used to compensate for any array which may be underperforming, for example, when overall signal intensity is low. In this case, normalisation will standardise one array to another by taking into account the overall median signal intensity of the array. Secondarily, 'Each gene to itself' normalisations are performed, which permits the standardisation of the median for each gene on each of the different arrays. It intends to remove differing intensity scales and binding rates from multiple experimental readings. Each gene is normalised to itself, so the median of the measurements taken for that gene is one. In this way, a similar set of genes across arrays may be graphically on the same scale, rather than demonstrating the same pattern of changes on widely differing scales. Once Normalisation is

achieved, the resultant intensity report files are exported as Excel (.xls) or tab-delimited (.txt) files prior to uploading and full Data Analysis using GeneSifter software.

2.2.10.3 GeneSifter

Following data pre-processing and normalisation, data analysis was performed using the online software program GeneSifter (GeneSifter.url, 2006). Through inputting data from replicate arrays a number of analysis tools were available including statistical tools such as students t-test (see 2.2.10.3.2) and Analysis of Variance (ANOVA; see 2.2.10.3.3), as well as hierarchical cluster analysis (HCA;) and partitioning tools such as Partitioning Around Medoids (PAM) (see 2.2.10.4). Data can also subsequently be exported for further examination of the genes (see Ontological Exanimation of genes; 2.2.10.3.5). However, prior to uploading data for this GeneSifter Gene Analysis, some further processing was necessary, as outlined below.

2.2.10.3.1 Formatting Data Files and Uploading into GeneSifter

The oligonucleotide composition of the Atlas Plastic Human 12k Arrays renders them highly specific for the individual genes being studied. However, other properties of the array format, which will be discussed later, may contribute to a lower proportion of detectable signal present on this platform, resulting in a higher proportion of 'zero' values. This was problematic as GeneSifter, at the commencement of the project, converted these zero values to '1', with the inability of the software to compensate such magnitude of zero values. Such a default for zero replacement may produce misleading results, particularly when low signals (<1) were detected. For example, an intensity value of 0.4 from a zero baseline, is regarded as upregulation, however replacement of zero with a value of 1, will render this a downregulated gene.

One method for compensating for this, is for the replacement of zero values with an arbitrarily very low value, ie., 0.0001, as recommended by GeneSifter and confirmed by P. Lewis (personal communication). This alternative zero substitution was thus undertaken for all replicate datasets in Excel before GeneSifter data import. Although this method of data processing will not permit absolute fold change to be obtained, it will however allow those genes which are highly expressed in reference to control data to be acknowledged (many of which were subsequently verified using PCR and a more recent array platform, Affymetrix genechip analysis (see section 2.2.12).

Tab-delimited text files (.txt) files were prepared in a format which could be accepted by GeneSifter. Data spreadsheets from AtlasNavigator were opened in MSExcel and edited to contain the following columns: (i) Gene Accession Number, (ii) Gene Identifier (eg. Full name of gene), (iii) Signal Intensity Value: ARRAY 1 MCF-7, (iv) Signal Intensity Value: ARRAY 1 MCF-7 +E2, (v) Signal Intensity Value: ARRAY 1 TamR, (vii) Signal Intensity Value:

ARRAY 1 FasR. Similarly, the remainder columns contained MCF-7, MCF-7 +E2, TamR, and FasR data for ARRAY 2-4.

Once formatted, files were loaded into GeneSifter using the 'Batch Upload' menu as a '*txt.*' file format. The loaded data could to create Projects (analysis of gene expression patterns across all cell lines) or be used to make comparisons between two samples/cell lines.

2.2.10.3.2 T-Test Analysis between Two Groups in GeneSifter (Pairwise Analysis)

Pairwise analysis allows two groups of data to be analysed for genes which may be differentially expressed between the two groups. A two-sample t-test was applied through GeneSifter software, using GeneSifter to generate genelists for significantly altered genes ($p \leq$ 0.05) in TamR or FasR cells relative to MCF-7.

To achieve this, in the main window, the 'Pairwise' option and the specific arrays were selected. Selecting the 'Analyse' icon results in a list of experimental arms (eg. MCF-7, TamR and FasR) displayed. Group 1 experiments (control set) were selected as MCF-7 1 to 4 (corresponding to arrays 1-4), and Group 2 experiments were selected as, for example, TamR replicates 1-4. Further settings were adjusted for optimum analysis of the two groups of data. From the pull-down menu, Statistical analysis included was the t-test (two-tailed, Student), threshold (either upregulated or downregulated) was set to ≥ 1.5. In addition, the data was log-transformed. Finally selecting the 'Analyse' option produced a list of differentially expressed genes ranked in order of ratio, with the most differentially expressed at the top of the list. This list can also be ranked by p-value, and the data can be exported as an Excel file format if required.

The user friendly 'One-click gene summary' feature of GeneSifter allows the expression profile plot of the individual gene to be displayed, together with a brief gene summary, including GeneSifter ontology, and various other useful internet links, such as to Genecards or Medline.

Although genes with positive Ontologies (such as associations with cancer, signalling), which were significantly altered in both TamR and FasR cells using t-test analysis were deemed as high priority for further study, also worthy of consideration for study were genes which were statistically altered in one resistant state only, but showed a profile which could be considered as "borderline" shared. The breadth of these could be revealed by HCA and PAM. Statistically significantly altered genes from t-test analysis together with those from ANOVA (across MCF-7, TamR, FasR arrays; 2.2.10.3.3) were compiled as a genelist to be studied for gene-grouping using HCA and PAM.

2.2.10.3.3 ANOVA Selection in GeneSifter (Project Analysis)

ANOVA analysis allows data to be analysed for genes which may be differentially expressed across a number of groups (Peck et al., 2000). Analysis was applied across the quadruplicate arrays for MCF-7, TamR, and FasR, using GeneSifter to generate genelists for significantly altered genes ($p \leq 0.05$). As GeneSifter software at the commencement of this study did not permit complex analysis such as clustering on large datasets as obtained with 12k arrays across multiple replicates/ experimental arms, ANOVA also served to filter and reduce the data to amore manageable set for HCA/PAM analysis.

ANOVA testing and subsequent HCA/PAM required the creation of a "project" in GeneSifter. A project is a user-defined set of experimental arms grouped by condition or by user-defined categories. Setting up a project allowed gene expression analysis across all the groups, ie. MCF-7, TamR and FasR. A new project was set up by selecting 'create a new project' from the main menu. After giving a title and description to the new project, the appropriate array and set of experimental arms were selected (MCF-7, TamR and FasR). Statistically significantly altered genes from ANOVA analysis, together with those from t-test analysis (2.2.10.3.2) were compiled as a genelist to be further studied for clustering using HCA and PAM.

All individual gene profiles generated through GeneSifter (through t-test, ANOVA) were displayed as log-intensity plots showing standard errors (SEM) alongside. Heatmaps were also displayed that showed gene expression relative to control (MCF-7) as downregulated (green) or upregulated (red).

2.2.10.3.4 Hierarchical Cluster Analysis (HCA) and Partitioning Around Medoids (PAM) using GeneSifter

Genes which have been selected as significantly altered using t-test (MCF-7 versus TamR or FasR) and ANOVA (across all models were defined as a separate sub-group within GeneSifter, and then this group was subject to HCA or PAM.

Cluster-analysis programs run on algorithms which group objects on the basis of their similarities and within this project the genes were clustered according to their similarities in gene expression patterns across the responsive/ resistant cell lines. Data clustering algorithms may be classified as either hierarchical (eg. HCA) or partitional (eg. PAM).

Results of such HCA can be represented by a dendrogram tree (see Fig.19; in results), the branches of the tree linking the genes together which are similar in profile. Then other branches (or gene clusters) can refine this group further down the tree. HCA produces a readily interpretable figure which can be used for prediction of patterns of gene expression across multiple groups, particularly when new hypotheses are being formulated. Partitioning algorithms, on the other hand, begin by having a predefined number of clusters, to which genes

are added according to their similarity to that profile (Kaufman and Rousseeuw, 2005). This study utilised GeneSifter-based HCA , where the degree of gene similarity allows the creation of groups. For this we have selected the Euclidean distance within GeneSifter, a commonly used factor, which treats each gene as a point in multidimensional space, the axes representing levels of gene expression (Butte, 2002). The clustering method uses a distance measure of average linkage, which is the average distance between two objects of different clusters. HCA was used in his study to identify genes which demonstrated gene expression profiles that were robustly increased in both TamR and FasR cells, as well as those genes which were elevated significantly in one resistant cell line, but showed a trend of increase in the other with a favourable cluster placement in the dendrograms.

PAM is a method of data analysis which partitions the dataset into pre-specified number of K groups (Kaufman and Rousseeuw, 2005). The programme operates on a distance (Euclidean) matrix which, for a predefined number of clusters, searches for the K representative objects (medoids) among the objects to be clustered. After medoids have been identified, each observation is assigned to the nearest medoid. PAM also permits the generation of silhouette plots which graphically represent the average profile of the cluster. The average silhouette width (zero to one) also gives an indication of the overall strength of clustering within the group, a value of 1 being a perfect cluster. The number of clusters chosen for PAM analysis using GeneSifter software was determined empirically where a compromise was made between mean silhouette width and number of manageable clusters. In addition, as HCA had been performed on the dataset, the dendrogram and heatmap profiling conditions MCF-7, TamR and FasR indicated the approximate number of clusters to be tested in PAM. PAM analysis was used in his study, like HCA, to find genes, not only which were significantly altered in both resistant cells lines, but also to help select for those genes that may suggest an increase in both owing to their favourable cluster placement.

2.2.10.3.5 Ontological Examination of Genes

Further gene selection for verification was performed manually by prioritising the entire t-test significant gene list (up- and down-regulated genes for both TamR and FasR relative to MCF-7) in particular, highlighting those which have previously been associated with cancer, specifically with links to therapeutic and clinical outcomes in breast tumours, signal transduction pathways, or in influencing key endpoints of cancer, such as proliferation, cell survival, invasion and angiogenesis. The extensive research of genes identified in this study using literature searching, according to Medline, GeneCard (Genecards.url, 2006) and GeneSifter (GeneSifter.url, 2006) information, was incorporated into an Excel database, listing all t-test significant genes by names/ ID according to such categories in sheets clearly (see examples in tables 6-9 and refer to attached CD-ROM).

2.2.11   PCR Verification of Selected Genes

In order to confirm gene changes in the cell preparations, PCR assessment was performed, initially on RNA which was used to hybridise to the array that had been extracted using the optimised protocol (section 2.2.9.5). RNA samples available for RT-PCR were those used for hybridisation to Arrays 2 to 4, for all samples MCF-7, MCF-7+E2, TamR and FasR.. Additional RNA preparations from cells subsequent to the original RNA set were also used to further confirm gene expression in some selected genes. This set also contained the X-MCF-7 cell line RNA preparation, which was not available for array analysis at the start of this project. PCR primers for the genes of interest were either selected from the primer oligonucleotide list available from Clontech CD-ROM or designed using the nucleotide sequence. In both instances, primer sequences were verified using NCBI Blast software. Primer sequences and final optimised PCR conditions are listed in tables 1 and 2 respectively.

2.2.11.1   PCR Primer Design

2.2.11.1.1   Generation of Primer Sequences using Primer3 Software

Primers were constructed from the sequence of the gene. The accession number or other gene identifier was used to generate the sequence from Pubmed nucleotide (http://www.ncbi.nlm.nih.gov/entrez/query.fcgi?db=Nucleotide). Gene sequence was then pasted into the Primer3 software program (Rozen and Skaletsky, 2000) (http://frodo.wi.mit.edu/cgi-bin/primer3/primer3_www.cgi) and the 'left' and 'right' primer criteria were selected. Product sizes were selected as 275 to 375 bp. This was in order to allow co-amplification with the ß-actin primers (where possible), which were used as internal standards and were either 204bp or 385 bp. Primer sizes were selected as ranging from 20 to 23 bp. The melting temperature (Tm) ranged from 55°C to 60°C. The GC content of the primers (Minimum and Maximum percentage of Gs and Cs in any primer) was selected to range from 48% to 52%. The GC clamp (specified number of consecutive Gs and Cs at the 3' end of both the left and right primer) was set to 2. The Primer Design software subsequently produced a list of possible primer sets which may be used in the PCR reaction to amplify the specific gene.

2.2.11.1.2   Determining the Fidelity of the Primer Sequence using NCBI BLAST

It is imperative to determine the reliability of the primer set in order to amplify the correct gene sequence, and avoid amplifying sequences which are wholly unrelated to the required gene, therefore falsifying PCR results.

NCBI BLAST (http://www.ncbi.nlm.nih.gov/blast/) permits the confirmation of the primer for its specificity for the gene. It is used for comparing the sequence of a particular gene or protein

with all other sequences from a variety of organisms. The primer sequence was pasted into the BLAST page and searched. This was repeated for both forward and reverse primer. Results were graphically displayed and also descriptions of statistically-significant alignments, the upper description being the most closely matched. For example 21 hits produced for a sequence, may produce a number of matches for non-human related genes (which may for our purposes be ignored). In addition, matches may be produced for other human genes, which may be problematic, but only if the equivalent match is found in the second primer of the pair. As alternative names and aliases of genes exist, it was important not to disregard the primer set if human gene sequence matches were produced in a primer pair. The GeneCard website was thus also accessed in order to clarify alternative names for the required gene. Primer forward and reverse oligonucleotide sequences were subsequently made from a commercial source as listed in materials and reagents.

2.2.11.1.3 Pre-designed Primer Sets by Clontech

A number of reliable primer sets were also available where sequences were supplied in a CD-ROM format from BD Biosciences/ Clontech. However, these sequences were also checked for possible non-specific hybridisations to other known human sequences using NCBI-Blast as described previously, prior to use for primer synthesis as described above.

2.2.11.2 RT-PCR

Materials and Reagents, and Methods for RT-PCR can be found as listed in section 2.1.3. All concentrations for reagents were similar, but with the reaction volume made to a total of 20µl and RT-PCR performed in a BioRad PTC-100 thermal cycler.

2.2.11.3 PCR Reaction

For gene detection, 2.5 µl of 10x Buffer (containing a final $MgCl_2$ concentration of 1.5mM), 2.5 mM dNTP, 0.63µl (0.5mM) of both forward and reverse primers and 1u Taq polymerase were added to a PCR tube, together with 0.5µl of cDNA (as generated from the RT-PCR protocol using RNA preparations from endocrine resistant and responsive cells) to a final volume of 25µl per reaction. In addition, primers for β-actin were included for coamplification (where possible, thus adjusting final volume accordingly), at a volume of 0.16µl each primer. Where coamplification of β-actin together with the selected gene primer could not be performed, β-actin was amplified separately (at 58°C/27 cycles). A negative control was also included in all PCR reactions containing no cDNA.

The following general protocol was run in a thermal cycler for each primer set, where the annealing temperature (T) and cycle numbers (N) may differ. Optimised protocols for each

set of gene primers are shown in Table 2. The table additionally also shows related genes that were subsequently explored (ie. PTTG1 or GFRα3- related genes, by PCR). The PCR protocol commenced with denaturation at 95°C for 2 minutes, then 55°C for 1 minute and 72°C for 2 minutes, followed by N cycles of (94°C for 30s, T°C for 30s, 72°C for 60s), with a final step at 94°C for 1 minute and 60°C for 5 minutes. The products were visualised on a 2 % agarose gel with ethidium bromide staining, photographed, and subject to densitometric analysis (section 2.2.4 and 2.2.8.3).

2.2.12 TCCR Affymetrix UG133A Genechip confirmation of Selected Genes

At a later stage in the project, in addition to Atlas Plastic Human 12k Microarrays, an Affymetrix HG-U133A (25k) genechip database for the various cell lines recently generated through the TCCR research programme was accessed to further confirm profiles (alongside PCR) for genes selected through the Atlas Plastic arrays. Access to the Affymetrix database also allowed closely-related genes/ gene family-members for the genes taken forward to be profiled, where not present on the Atlas Plastic arrays.

In brief, RNA extraction for the eventual analysis using Affymetrix genechip had been performed as described in 2.2.2.1. The DNase-treated, 'Qiagen column-cleaned' RNA extracted was then sent to University of Wales College of Medicine (UWCM), Central Biotechnology Services (M. Musson, UWCM, Cardiff University, Heath Park, Cardiff) in triplicate, to be hybridised to Affymetrix genechip, and genechip expression data was provided as raw data through the use of Affymetrix Microarray Suite software (MAS). The provided raw data was analysed at the TCCR using GeneSifter as described previously, for the genes of interest. These were analysed using t-test and displayed as log-intensity plots with SEM and Heatmaps as described previously.

2.2.13 PCR Examination in Clinical Material of Selected Genes

See section 2.1.3 for Materials and Reagents. PTTG1 and GFRα3 PCR primers are listed in Table 2. All clinical primary breast cancer RNA specimens (n=78; extracted as described by Knowlden et al., 2003) were stored at the TCCR and accessible for this study. These had clinical pathological and biological marker data available for association with test gene expression, such as ER-status, lymph node spread, tumour grade, tumour nuclear pleomorphism, mitotic activity, tubular differentiation, proliferative capacity (Ki67 staining), EGFR protein staining, and Fos staining. Specimens had been sourced from a larger historical frozen clinical breast cancer series obtained through external collaboration with Nottingham City Hospital (covered under an approved ethics application from Dr. Ian Ellis on behalf of

Nottingham City Hospital to Nottingham Research Ethics committee 2: "Development of a molecular genetic classification of breast cancer" R&D ref: 03H101; Ethics Committee no. C1080301, April 2003-April 2008).

RT-PCR was performed as described in 2.2.8.1 on the RNA samples previous to the commencement of the project and was provided as cDNA format. PCR was performed on samples using the primers for PTTG1 or GFRα3.

For detection of PTTG1 and GFRα3 gene in clinical samples, the following were added into a PCR tube: 2.5 μl of 10x Buffer (containing a final $MgCl_2$ concentration of 1.5mM), 2.5 mM dNTP, 0.63μl (0.5mM) of both forward and reverse PTTG1 or GFRα3 primers, and 1u Taq polymerase were added, together with 0.5μl of cDNA (as generated from the RT-PCR protocol on clinical samples) to a final volume of 25μl per reaction. For PTTG1, β-actin was co-amplified, and 0.16μl (0.0125mM) of both forward and reverse β-actin (204bp) primers was added to the reaction mix, and the volume adjusted, again for a total 25μl per reaction.

The PCR protocol commenced with denaturation at 95°C for 2 minutes, then 55°C for 1 minute and 72°C for 2 minutes, followed by N cycles of (94°C for 30s, T°C for 30s, 72°C for 60s), with a final step at 94°C for 1 minute and 60°C for 5 minutes. For PTTG1, N=27 and T=62°C; for GFRα3, N=27, T=58°C. In the case of GFRα3, β-actin was amplified separately, where N=27' T=58°C. The products were visualised on a 2 % agarose gel with ethidium bromide staining, (as described in section 2.2.4), photographed, and subject to densitometric analysis (section 2.2.8.3).

2.2.14 SDS PAGE/ Western Blotting for Protein Expression of Selected Genes

Genes verified at the PCR level selected for further study, PTTG1 and GFRα3, were subsequently analysed at the protein level within cell lines using SDS polyacrylamide gel electrophoresis (PAGE) and Western blotting.

2.2.14.1 Cell Culture and Lysis

MCF-7, TamR and FasR-Lt cells, either grown under basal conditions as for microarrays, or in the presence/ absence of $10^{-6}M$ Gefitinib were seeded into 100mm dishes as described in section 2.2. Untreated cell lines were grown to ~70% confluency/ log-phase of growth for 7 days before being harvested. For the experiment in the presence/ absence of gefitinib, treated cells were harvested at this time also. In this experiment, an additional set of cells were also harvested at day 4 of treatment.

Cell were subsequently harvested for Western blotting by firstly gently washing twice in warm (37°C) sterile PBS (2x5ml) After ensuring all PBS was removed, 150μl ice-cold lysis

buffer (50nM Tris-HCL, 5mM EDTA, 150mMol NaCl, 1% Triton X-100 (v/v), pH 7.5 in distilled water, supplemented with protease/ phosphatase inhibitors: 2mM Na$_3$VO$_4$, 20nMol NaF, 1mM PMSF, 10μg/ml leupeptin, 20mM phenylarsine oxide, 10μg/ml aprotinin, and 10mM sodium molybdate) was added to each dish and immediately placed on ice for 5min,. Cells were then removed from the dish surface using a cell scraper, after which the lysate was transferred to a 1.5ml tube and stored on ice for at least 5 minutes. The lysate was then cleared by centrifugation at 14,000g for 15 minutes at 4°C and the supernatant stored in aliquots at -20°C.

2.2.14.2 Protein Assay

The protein concentration of the cell lysate was initially determined using the BioRad (DC) protein assay, based on the method of Lowry (Lowry et al., 1951) using BSA as the standard protein against which samples were measured. In order to construct a standard curve, a range of BSA standards (0-1μg/μl) were diluted in duplicate in 50μl of lysis buffer. 250μl of premixed reagent S and reagent A (20μl reagent S/ml reagent A) followed by 2ml of reagent B, was added to this volume of standard or cell lysate. Each sample was mixed briefly, ensuring no air bubbles were generated. After 5 minutes of colour-development, the absorbance was read at 750nm in a Cecil-CE2041 spectrophotometer. The cell lysate protein concentration was determined from the BSA standard curve and corrected for dilutions.

2.2.14.3 SDS-PAGE

For the majority of proteins examined in this study a 7.5% resolving gel was used, which was overlaid with a 4% stacking gel. For the lower molecular weight protein, PTTG1 (~28kDa) a 15% gel was employed for improved resolution. An aliquot of each lysate, equivalent to 50μg of protein, was added to an equal volume of 2x Laemmli buffer (Laemmli, 1970) (comprising of 4%SDS (w/v), 20% glycerol (v/v), 120mM Tris-HCl (pH6.8), 0.1% bromophenol blue (w/v), and DTT -which was added just prior to sample preparation). Proteins were denatured by heating the mixture to 100°C for 10 minutes on a heating block, and then centrifuging briefly. Samples were loaded onto the gel and subject to electrophoresis using a BioRad mini protean II electrophoresis unit with Tris-glycine running buffer (250mM trizma base, 2M glycine, 40mM SDS; pH8.3). Gels were run on a constant voltage of 150v for ~1hour, or until the blue dye front was at the base of the gel. A 5μl volume of Rainbow prestained molecular weight marker was also loaded, which not only indicated apparent molecular mass of the protein of interest, but also demonstrated successful protein transfer onto the nitrocellulose membrane after subsequent Western blotting. Gel compositions for SDS-PAGE for proteins used in this study can be found in Appendix IV.

2.2.14.4 Western Blotting

Proteins separated by SDS-PAGE were transferred onto a nitrocellulose membrane (pore size 0.2μM) by Western blotting using the BioRad mini transblot apparatus. All components for Western blotting were soaked in Transfer buffer (0.2M glycine, 25mM Trizma base, 20% methanol (v/v), in distilled water; pH8.3) for at least 20 minutes prior to protein transfer. The gel, along with a series of filter pads were prewetted with transfer buffer and assembled within the gel-holder cassette. Ensuring all components were submerged in transfer buffer, two Whatman 3MM filters were layered on top of the thin fibre pad, followed by the gel. Then ensuring no bubbles were introduced, the nitrocellulose membrane was carefully placed on the gel, followed by further 2x Whatman filters, and a fibre pad. The gel-holder cassette was closed and placed in the transfer tank with the membrane nearest to the anode. An ice block was placed in the tank of transfer buffer to prevent overheating during transfer and even temperatures were maintained by using a magnetic stirrer. Transfer of proteins was completed with a constant voltage of 100v for 1 hour. Successful transfer was indicated by transfer of the Rainbow marker onto the membrane.

After a brief rinse in 1x TBS-Tween (10mM Tris, 0.1M NaCl, 0.05% (v/v) Tween20; pH 7.5), the membrane was stained with Ponceau S (0.1% in 5% acetic acid) in order to initially determine acceptable protein loading. Ponceau S was then removed by washes in TBS-Tween (2x 3minutes). Potential non-specific antibody binding sites on the membrane were then blocked on the membrane by incubation with 5% skimmed milk powder in TBS-Tween (w/v) for at least 1hour on a slowly rocking platform. After three brief rinses in TBS-Tween, the membrane was incubated with the appropriate primary antibody. All primary antibodies were diluted in TBS-Tween containing 5% Western Blocking Reagent, and 10mM sodium azide (as a preservative). Sodium azide was omitted from the secondary antibody preparation as it inhibits the chemiluminescence reaction. The dilutions and incubation conditions for each antibody were optimised and are summarised in Table 4. All incubations were performed on a slowly-rocking platform.

Table 4. Antibodies and conditions used in Immunodetection.

Antibody	Species	Dilution	Incubation
PTTG1	Mouse monoclonal	1:1000	Overnight/ 4°C
GFRα3	Mouse monoclonal	1:1000	2 hours/ room temp
RET	Mouse monoclonal	1:500	Overnight/ 4°C
PEA3	Mouse monoclonal	1:1000	Overnight/ 4°C

Following incubation with primary antibody, the membranes were washed vigorously with ~40ml TBS-Tween (2x5minutes) on a rocking platform, after which they were incubated for 1 hour on a slow rocking platform with 20ml sheep anti-mouse horse radish peroxidase (HRP)- (for monoclonals) or goat anti-rabbit HRP (for polyclonals)- conjugated secondary antibody prepared at 1:10,000 dilution. After incubation with the secondary antibody, the membranes were washed 5 times in ~40ml TBS-Tween for 5 minutes with vigorous agitation on a rocking platform. Proteins of interest were detected by even application of Super Signal Dura chemiluminescent substrate (detects high femtograms of protein), to the membrane for 5 minutes. After removing the excess substrate, the membrane was placed between two plastic sheets inside an autoradiograph cassette, and exposed in the dark to autoradiographic film for 2-3 minutes before developing using an X0-Graph developer. This process was repeated with varying exposure times if necessary until a satisfactory level of signal intensity was achieved. Alternatively, Super Signal Femto chemiluminescent substrate (detects low femtogram amounts of protein) was used if no/weak signal was observed. Autoradiographs were subject to densitometric analysis using a BioRad GS-700 scanner system (Molecular Analyst software). Following satisfactory detection of the protein of interest, the membrane was washed (3x 5 minutes) and reprobed for the housekeeping protein β-actin (1:10,000 dilution) for 2 hours in order to confirm equal protein loading. This was subsequent to the same detection protocol as above, and densitometric analysis then performed for normalisation purposes.

2.2.15 Immunocytochemistry for PTTG1 and GFRα3

2.2.15.1 Immunocytochemical Assay Development for PTTG1 and GFRα3 Proteins

Immunocytochemical staining for a specific protein is highly dependant on a number of factors, including the antibody dilution/ titer. Other significant factors that may influence quality of staining in fixed paraffin embedded material is the choice of antigen retrieval needed for optimal unmasking of antigenic sites due to formalin-fixation (Boenisch, 2006; Key, 2006). Thus, a number of methods for antigen retrieval were attempted in this project with various antibody concentrations for both poly- and monoclonal PTTG1 and GFRα3. PTTG1 antibody concentrations tested ranged from 1:50 to 1:500 for the polyclonal, and 1:15 to 1:180 for the monoclonal. For GFRα3, the range of antibody concentrations investigated were 1:150 to 1:2000 for the polyclonal and 1:750 to 1:2000 for the monoclonal. These concentrations were used alongside various antigen retrieval methods, namely, (i) no retrieval, (ii) 0.01M citric acid; pH6, heat (microwave) retrieval; (iii) 0.01 M EDTA; pH8, heat (microwave) retrieval; (iv) 0.01M sodium citrate; pH6, heat (pressure cooker) retrieval; 0.01M EDTA; pH8, heat (pressure cooker) retrieval; (v) 0.02% enzymatic (protease) retrieval. Methods for these retrievals not detailed below are described in Appendix IV. Optimisation was performed on cell pellets

(single or in composite array format, bearing the various endocrine responsive and resistant cell lines. These had been formalin-fixed, and paraffin embedded, and sectioned at 5μm as described in Appendix IV, previously performed by M. James at the TCCR.

The optimised immunocytochemical method which were used with these cell preparations are subsequently described:

2.2.15.2 Optimised Immunocytochemical Assay for PTTG1 Protein

Paraffin embedded cell pellets for PTTG1 studies were in a composite pellet array format comprising of various ER-positive cell lines including: MCF-7, TamR, FasR, X-MCF-7, and also an ER-negative breast cancer cell line, MDA-231. Dewaxing and rehydration of 5μm sections was performed in the fume hood by immersion of the slide in a metal slide-holder to xylene for 2x 7minutes, followed by immersion in graded ethanol for 2 minutes each through 2x 100%, 2x 90%, and 2x 70%. Sections were finally immersed in distilled water for 5 minutes. As endogenous peroxidases may interfere with subsequent signal detection, these were subsequently eliminated by application of 3% aqueous solution of hydrogen peroxide (H_2O_2) to each section for 5 minutes, followed by rinsing with distilled water for 5 minutes in a Hellendahl jar. The optimised method for antigen retrieval PTTG1 was heat by pressure cooking sections housed in the metal slide-holder in 2L of 0.01M sodium citrate buffer (pH6) for 2 minutes at full pressure. After heat treatment, sections were cooled in running tap water within the open pressure cooker for 10 minutes and then immersed for 5 minutes in PBS (145.4mM NaCl, 8.2mM K_2HPO_4, 1.84 mM KH_2PO_4). Sections were then outlined on the slide using a waterproof PAP pen to ensure subsequent applications of antibodies/ reagents were confined to the section area. After sections were washed in PBS-Tween (0.02%) for 5 minutes in a Hellendahl jar, 50μl of a 1:15 dilution (made in PBS) of the PTTG1 monoclonal mouse anti-human was applied to the section and incubated overnight at 23°C in an humidified chamber. Assay controls comprised of the omission of the primary antibody from the slides and were also performed. Sections were then washed briefly in PBS for 3 minutes, followed by 2x 5 minute washes with PBS-Tween. After removing excess buffer from each slide, 1 drop of Envision labelled polymer-HRP anti-mouse secondary antibody was applied to each sections, followed by incubation for 2 hours at 23°C in a humidified chamber. Sections were again briefly washed for 3 minutes in PBS, followed by 2x 5 minute washes in PBS-Tween. Envision DAB+ chromagen/ substrate buffer solution was made according to the DAKO manufacturers instructions (1 drop DAB/ml substrate solution) and ~60μl was applied to the drained section for 10 minutes. After draining excess DAB solution, the sections were thoroughly rinsed in distilled water Enhancement of the resultant signals was performed using 0.5% copper sulphate (aq) for 20 minutes. Following 3 washes in distilled water for 1 minute, an aqueous solution of

0.5% methyl green was applied to counterstain the nuclei in each section for up to 5 minutes and the sections thoroughly rinsed with distilled water. The slides were then air dried before being mounted with glass coverslips in a fume hood. Coverslips were initially cleaned with 100% ethanol and dried. Following the application of 1 drop of DPX mountant, the slide was carefully lowered onto the coverslip ensuring no air bubbles were generated. The coverslip was then positioned, and where necessary, air bubbles were pushed out. Slides were then dried overnight before assessment and photographing using an Olympus BH2 microscope with a DP12 digital camera. The number of PTTG1-positive cells (nuclear and cytoplasmic) were assessed for each slide by consensus agreement of two observers (RSB and P.Finlay) (n=6; two counts from each three replicates).

2.2.15.3 Optimised Immunocytochemical Assay for GFRα3 Protein

Staining was performed using MCF-7, TamR and FasR cells as formalin-fixed, as separate (3-6 replicates/slide) paraffin embedded pellets per cell line per section/ slide, rather than composite pellet arrays. Dewaxing and rehydration, and Elimination of endogenous peroxidases was as described for PTTG1. In this instance, the optimised method for antigen retrieval for the monoclonal mouse anti-human GFRα3 antibody was enzymatic (protease) treatment of sections. Prior to performing antigen retrieval, all PBS were briefly warmed to 37°C. The slides containing pellet sections were placed into 37°C PBS to warm for 10 minutes before commencement of protease antigen retrieval. During this time, 0.02g of protease (supplied as 4.8u/mg solid) was weighed using a microbalance. The enzyme was then added to a Hellendahl jar, followed by addition of 100ml of warm PBS, and the enzyme dissolved by mixing. Sections were incubated within this enzyme solution for 5 minutes at 37°C, after which the reaction was stopped with running tap water for 5 minutes. Sections were then immersed in PBS for 5 minutes and outlined on the slide using the waterproof PAP pen After sections were washed in PBS-Tween (0.02%) for 5 minutes in a Hellendahl jar, 50μl of a 1:750 dilution (made in PBS) of the GFRα3 monoclonal mouse anti-human antibody was applied to the section and incubated overnight at 23°C in a humidified chamber. Subsequent Envision secondary antibody and chromagen steps were as performed for PTTG1. Counterstaining with methyl green (0.5%, aq) was performed in this instance for 2 minutes, with no subsequent signal enhancement. Slides were mounted as in 2.2.15.2, and again viewed and photographed as described for PTTG1. The number of GFRα3-positive cells were assessed monitoring cytoplasmic and plasma membrane staining by consensus agreement of two observers (RSB and P.Finlay) (n=6; two counts from each three replicates).

2.2.16 Gene Knockdown Studies using siRNA

The project assessed mRNA and protein knockdown by optimising gene-specific siRNA for both PTTG1 and GFRα3. As PTTG1 and GFRα3 were elevated maximally in FasR-Lt and TamR cells respectively, these cell lines were used for inhibition studies with these specific siRNA. In parallel with mRNA and protein effects, the effects of gene knockdown were determined on the cellular endpoints, of growth (phase contrast microscopy), proliferation by Ki67 immunostaining and apoptosis, determined by the Apoalert apoptosis assay.

2.2.16.1 Preparation of siRNA

The siRNA sequences used were Smartpool as supplied by Dharmacon (actual sequences not supplied). These duplexes are believed to minimise any effect from altered target gene sequences (such as single nucleotide polymorphisms (SNP)) by being derived from four highly functional sequences designed to target different regions of the open reading frame of the gene (Dharmacon.smartpool.url).

A 20μM stock solution of each (5nmol as supplied) siRNA was prepared by the addition of 250μl of 1x siRNA buffer (50μl 5x siRNA buffer and 200μl RNase/ DNase-free sterile water). Stocks were aliquotted for storage at -20°C to minimise freeze-thaw cycles (as recommended by manufacturer).

2.2.16.2 Cell culture and Transfection using 6 and 12 well Plates

TamR or FasR cells were grown in T75 flasks as described in 2.2.1. Cells were trypsinised and seeded into 6 well or 12 well plates in the appropriate TamR or FasR RPMI medium. For initial experiments for the assessment of RNA and protein effects of gene knockdown at 24hours and 48hours transfection respectively, cells were seeded at a high density overnight prior to transfection. These were approximately 500,000 for 6 well plates and 250,000 cells for 12 well plates. For incubations with siRNA reagents for longer durations, ie. 4 or 7 days, cells were seeded at approximately 250,000 or 125,000 cells per well for a 6 or 12 well plate respectively.

Transfections were performed in either 6 well plates (for RNA and protein), or 12 well plates (for growth assessment by phase contrast microscopy, Ki67 staining and Apoptosis Assay). siRNA treatment was undertaken using phenol red-free DCCM media (supplemented with 4mM L-glutamine) since it was recognised that transfection medium should be devoid of serum, antibiotics/ fungizone to minimise interference in this process (where this medium used for transfections is subsequently referred to as "siRNA media").

The following protocol was used for 6 well plates with a total volume of 2ml per well, while 12 well plates, volumes were calculated as half with a total 1ml volume per well. For each well, the following were prepared in separate 1.5ml or 5ml sterilin tubes, and the volumes adjusted according to the number of replicates used within an experiment (generally 2-3): Tube A: 10μl of test siRNA [of 20μl stock] plus 190μl of siRNA media, and Tube B: 5μl DharmaFect -1 plus 195μl siRNA media. The contents of tubes A and B were mixed by gentle pipetting followed by incubation for 20 minutes at room temperature. Media was removed by aspiration from all 6 or 12 well plates containing cells (except well containing RPMI media) and cells were gently washed twice with warm (37°C) sterile PBS. Cells were then gently overlaid with 1.6ml siRNA media per well, and 400μl of the appropriate siRNA/ control was gently added. Alongside "test" siRNA for PTTG1 and GFRα3, controls included in each plate were : (i) RPMI medium (phenol red-free, 5%csFCS RPMI: TamR- or FasR-specific medium); (ii) siRNA medium only; (iii) DharmaFect transfection reagent only; (iv) Missense (non-targeting) siRNA; (v) siControl Lamin A/C siRNA; (vi) siGlo RISC-Free siRNA. Wells (iii) – (iv) were prepared in siRNA media for 6 or 12 well plates (and also contain DharmaFect with the appropriate targeting agent). The plate was gently agitated to mix the contents of the well, and incubated for 24hours, 48hours, 4days, or 7days at 37°C/ 5%CO$_2$. For 4-7 days incubations, cells were regularly observed using a Nikon eclipse phase contrast microscope for cell growth as well as to check for absence of bacterial/ yeast contamination.

TamR or FasR cells were harvested from T75 flasks and seeded into 6 well plates day 4 or 7 for harvesting as described above. Cells were visualised/photographed using a Nikon eclipse TE200 phase contrast microscope/ Nikon 35mm SLR camera at x10 magnification 1-3 hours prior to harvesting. Cells were subsequently counted from four fields per photograph for each control/ siRNA treatment for an estimation of cell growth.

2.2.16.3 mRNA Knockdown Assessment

TamR or FasR cells were harvested from 6 well plates as described 2.2.2.1, at either 24 or 48 hours, or 4 or 7 days, with controls as described, with subsequent processing performed in 1.5ml tubes. Cells were then harvested for total RNA extraction according to the Tri Reagent method (Chomczynski and Sacchi, 1987) as described in 2.2.2.1 with a 200μl volume of Tri Reagent, and subsequent steps performed with 40μl chloroform, 100μl isopropanol, with the RNA pellet being resuspended in 10μl DNase/RNase-free water. RNA estimation was performed as described in 2.2.3 using a reduced volume quartz cuvette. The extracted RNA was subject to RT-PCR as described in 2.2.8.1, using 1μg total RNA. PCR was performed according to the method as in 2.2.8.2 using the primers for Lamin A/C, PTTG1 and GFRα3 as appropriate. Primer sequences for PTTG1 and GFRα3 are as listed in table 1, while Lamin A/C was as

follows : forward sequence 5'-CCT CTC ACT CAT CCC AGA CAC AGG-3' and reverse sequence: ATG TGC CAA TTG CCC ATG GAC TGG-3'.

The general protocol as described in 2.2.8.2 with β-actin coamplification for all primers, was run in a thermal cycler for each primer set, commencing with denaturation at 95°C for 2 minutes, then 55°C for 1 minute and 72°C for 2 minutes, followed by N cycles of (94°C for 30s, T°C for 30s, 72°C for 60s), with a final step at 94°C for 1 minute and 60°C for 5 minutes. For Lamin A/C, N=27 and T=55; for PTTG1, N=26 and T=54; and for GFRα3, N=27 and T=55. The products were separated on a 2% agarose gel and visualised by UV illumination after ethidium bromide staining, (as described in section 2.2.4), photographed, and subject to densitometric analysis and normalisation to β-actin (section 2.2.8.3).

2.2.16.4 Protein Knockdown Assessment

Again, subsequent to section 2.2.16.2, TamR or FasR cells were harvested for protein following gene knockdown with appropriate controls, using the method as described in 2.2.14.1 with a 150µl volume of lysis buffer. Protein assay, SDS-PAGE, and Western blotting using monoclonal antibodies to either PTTG1 or GFRα3 were performed as described in 2.2.14. Membranes were subsequently probed for β-actin for indication of equal loading and normalisation.

2.2.16.5 Transfection Efficiency Assessment using siGlo and coverslip preparation

TamR or FasR cells were harvested from T75 flasks and seeded into 2x 35mm dishes containing TESPA-coated coverslips (see Appendix IV), according to reagent volumes relevant to 12 well plates (volumes half of as described in 2.2.16.2), with the inclusion of siGlo RISC-Free siRNA in one dish. All reagents containing siGlo, and transfections with siGlo were foil-covered, while all transfection with siGlo were incubated at 37°C/ 5%CO$_2$ overnight again covered with foil. Cells on coverslips were then immediately fixed by placing the coverslips in a 3.7% formaldehyde solution (in PBS) for 15 minutes at room temperature in the dark. After 2x 5 minute PBS washes, the excess was drained off and, again under foil, 1x drop of Vectashield (containing DAPI) was added to each coverslip. The coverslip was inverted on a clean slide, and after removing excess VectaShield, the coverslip was sealed onto the slide using clear nail-varnish. Slides were air-dried in the dark before viewing. Fluorescence was viewed and photographed using a Leica DMIRE2 Inverted Research fluorescent microscope at x20 or x40 magnification, with Improvision software, where siGlo fluorescence was evaluated using the red imaging filter at 594nm wavelength, and DAPI stained nuclei were observed at 488-615nm wavelength. Images obtained for both wavelengths were superimposed in order to determine percentage efficiency of transfection in each cell sample (n=3).

2.2.16.6 Knockdown Effects on Proliferation using coverslips (Ki67/Mib1 staining)

Cells were seeded at the appropriate cell densities as described in 2.2.16.2 onto TESPA-coated coverslips (Appendix IV) and transfected with the test siRNA and appropriate controls. Coverslips within 12 well plates containing the transfected cells were then removed and immediately fixed in 3.7% formal saline solution (comprising 0.9% NaCl (w/v), 3.7% formal saline (v/v) in water) for 10 minutes. Coverslips were then immersed in 100% ethanol for 5 minutes followed by a brief wash in fresh 100% ethanol. Coverslips were then immersed in PBS for 5 minutes and briefly washed again in fresh PBS before storage in cold sucrose/glycerol storage medium at -20°C prior to assay. For Ki67 assay, sucrose storage medium was removed from the coverslips by rinsing with PBS, and the excess drained before application of the primary antibody. The DAKO Ki67 (Mib1 clone; MT240) antibody was applied to the coverslip in a 35mm dish at a 1:125 dilution and left to incubate at 23°C in a humidified chamber for 1 hour. Coverslips were then washed in PBS for 3 minutes, followed by 2x 5 minute washes in PBS-Tween. After removing excess buffer reagent from each slide, 1 drop of Dako Envision labelled polymer-HRP anti-mouse secondary antibody was applied to each coverslip, followed by incubation for 75 minutes at 23°C in a humidified chamber. Coverslips were briefly washed for 3 minutes in PBS, followed by 2x 5 minute washes in PBS-Tween. 60µl of fresh Dako DAB+ chromagen/ substrate buffer solution was applied to the drained section for 10 minutes and counterstained as previously described (section 2.2.15.1) prior to mounting. Coverslips were viewed and photographed using an Olympus BH2 Research Microscope/ DP12 digital camera at x40 and the percentage of Ki67 positive cells were assessed by a consensus of 2 viewers for 6 fields.

2.2.16.7 Knockdown Effects on Apoptosis using ApoAlert Assay

The Apoalert Mitochondrial Membrane Sensor Kit was used to detect apoptotic cells. It permits the detection of altered permeability in the mitochondrial membranes as an indication of early apoptosis (Green and Reed, 1998) and has been used in our laboratory previously (Gee et al., 2003). Red fluorescent mitochondrial aggregates are formed in live cells, but on early apoptotic cells, where membrane permeability is compromised, the MitoSensor dye is displayed as a fluorescent green.

Prior to performing the assay on transfected cells, an assay positive control was prepared by irradiating MCF-7 cells with UV in the tissue culture cabinet for 20 minutes. These cells were then returned to the 37°C/ 5% CO_2 incubator for ~4 hours to allow apoptosis to commence. An equivalent set of untreated MCF-7 cells were also included as a baseline control. MitoSensor solution was made immediately prior to use as 5µ/ml (1µl MitoSensor added to 1ml

incubation buffer, included in the kit), and vortexed to ensure complete mixing. Cells grown on round TESPA coated coverslips (Appendix IV) within 12 well plates with transfected siRNA and appropriate controls, and the MCF-7 assay controls were washed in 1ml of prewarmed (37°C) serum free media (DCCM1; phenol red-free). A volume of 1ml of MitoSensor solution was added to each coverslip and incubated at 37°C/ 5%CO_2 in a tissue culture incubator for 20 minutes, protecting from light with foil. MitoSensor solution was removed and the coverslips were gently rinsed with 1ml of prewarmed (37°C) DCCM1, with ~1ml freshly added in order to keep the coverslip wet. Coverslips were immediately inverted onto a glass slide and viewed using an Olympus BX51 research fluorescence microscope. Red/ green cells were counted immediately and photographed within 5 minutes of fluorescence detection from a total of 6 fields.

2.2.17 Statistical Analysis

For analysis of PCR gene expression results for PTTG1 or GFRα3 using clinical material, independent groups were compared using a Mann-Whitney U test, while the correlation of biological markers was carried out using a Spearman Rank Correlation. Both these analyses were performed with statistical package SPSS 12.0.

All other statistical analyses were performed using Microsoft Excel using a 2-tailed independent samples Students t-test. All tests were performed using a 5% significance level.

Chapter 3

RESULTS

RESULTS

3.1 Microarray Studies: Sample Optimisation & Verification

Confirmation of Antioestrogen-Resistant Cell Lines

3.1.1 Cell Growth Analysis of Antioestrogen-Resistant Cells

As an important factor in any microarray study is the initial starting material, TamR and FasR cells were verified as resistant to tamoxifen or Faslodex respectively. Resistant cells of equivalent passage number to those used within this study were cultured in the presence of their respective antioestrogen up to 16 days and compared to the growth kinetics of these cells when originally derived (Knowlden et al., 2003, McClelland et al., 1996). Both TamR and FasR cells were shown to grow at equivalent rates in the absence or presence of their antioestrogen confirming resistance (Fig. 9).

Optimisation of RNA Extraction and Hybridisation for Plastic Microarray Platform

The array approach was designed to be able to detect differences between responsive MCF-7 versus the acquired resistant TamR or FasR cells, and in turn to reveal genes altered in both forms of resistance as potential future markers or therapeutic targets. As a compromise between the preferred larger number of arrays used against the cost of performing an array experiment, each cell line was analysed with quadruplicate replicate set of Atlas Plastic Human 12k Arrays using independently extracted RNA preparations. An additional was provided by oestradiol-treated MCF-7 cells (MCF-7+E2), not only to check RNA quality/ array performance through the examination of known oestradiol-responsive marker genes, but also to ultimately monitor regulation in the presence of the hormone for selected genes.

A significant factor in array hybridisation and eventual successful gene selection procedure is the yield and quality of the RNA used to synthesise the probes used for array hybridisation. Initial experiments were thus performed to optimise RNA extraction for subsequent adequate array hybridisation to the plastic array platform. These studies employed Atlas Plastic Human TRIAL microarrays. These arrays differ from the Atlas Plastic 12k microarrays in that they are composed of 96 genes which are present in blocks of 9 on the array with known housekeeping genes, such as β-actin, at regular localisations (see also Fig.4). These optimised procedures were then applied to the Atlas Plastic Human 12k Microarrays which were used for selection of genes increased in antioestrogen resistant cell lines prior to PCR validation and ontological deciphering (see also Fig.5).

The methods for initial optimisation principally involved evaluating a succession of RNA extraction protocols that gave varying degrees of success regarding resultant RNA yield/

quality or array hybridisation performance. These procedures and their outcomes are summarised in Table.5 and described in detail hereafter.

Table 5. Summary of RNA extraction methods and resultant RNA yield, quality and array hybridisation performance during optimisation of RNA and array protocols.

Method for RNA Extraction	Resultant RNA yield & quality	Resultant Array Performance
[1] Tri Reagent total RNA extraction with Qiagen clean-up.	High yield, Adequate quality.	High background, low signal strength
[2] Clontech Nucleotrap mRNA purification	Variable, Low yield. Low quality.	*Insufficient RNA for hybridisation*
[3] mRNA / polyA+ RNA isolations	No detectable yield.	*Insufficient RNA for hybridisation*
[4] Atlas Pure Total RNA extraction kit with Qiagen clean-up and polyA+ separation).	High yield, Inadequate quality (low molecular weight species)	Low background, but low signal strength.
[5] OPTIMISED METHOD • Tri Reagent total RNA extraction (from [1]) • with Qiagen clean-up. • Poly A+ RNA separation (from [4]).	**High yield, Good quality**	**Low background, Good signal strength.**

3.1.2 Tri Reagent Extraction and Trial Human Plastic Microarrays

The Tri Reagent method (see section 2.2.2.1) of extraction can result in high yields of total RNA and can even detect rare gene events using RT-PCR from small quantities of starting material compared to other commercially available RNA extraction procedures (Chadderton et al., 1997). In this project, from a typical extraction the expected yield was from 0.5mg to 1.2mg, depending on the cell preparation (where MCF-7+E2 > TamR > MCF-7 > FasR cells) from 8-10x 150mm dishes (at 50-70% confluency). Typical yields after processing total RNA with DNase and Qiagen clean-up show intact 28S and 18S RNA bands (an approximate indication of total RNA integrity; (Sambrook et al., 1989) (Fig.10a) with around 80% recovery. There was importantly no genomic contamination (Fig.10b) as determined by PCR using primers for IGF1 (section 2.2.7).

Total RNA extracted using Tri Reagent was considered to be of adequate quality for microarray studies. Thus, as well as the appearance of clear and intact ribosomal 18S and 28S bands, a ratio of 28S/18S around 2 was also obtained indicating an RNA purity (Sambrook et al., 1989). RNA samples prepared using this method was subsequently used to produce probes for hybridisation to Atlas Plastic Trial Microarrays (section 2.2.9).
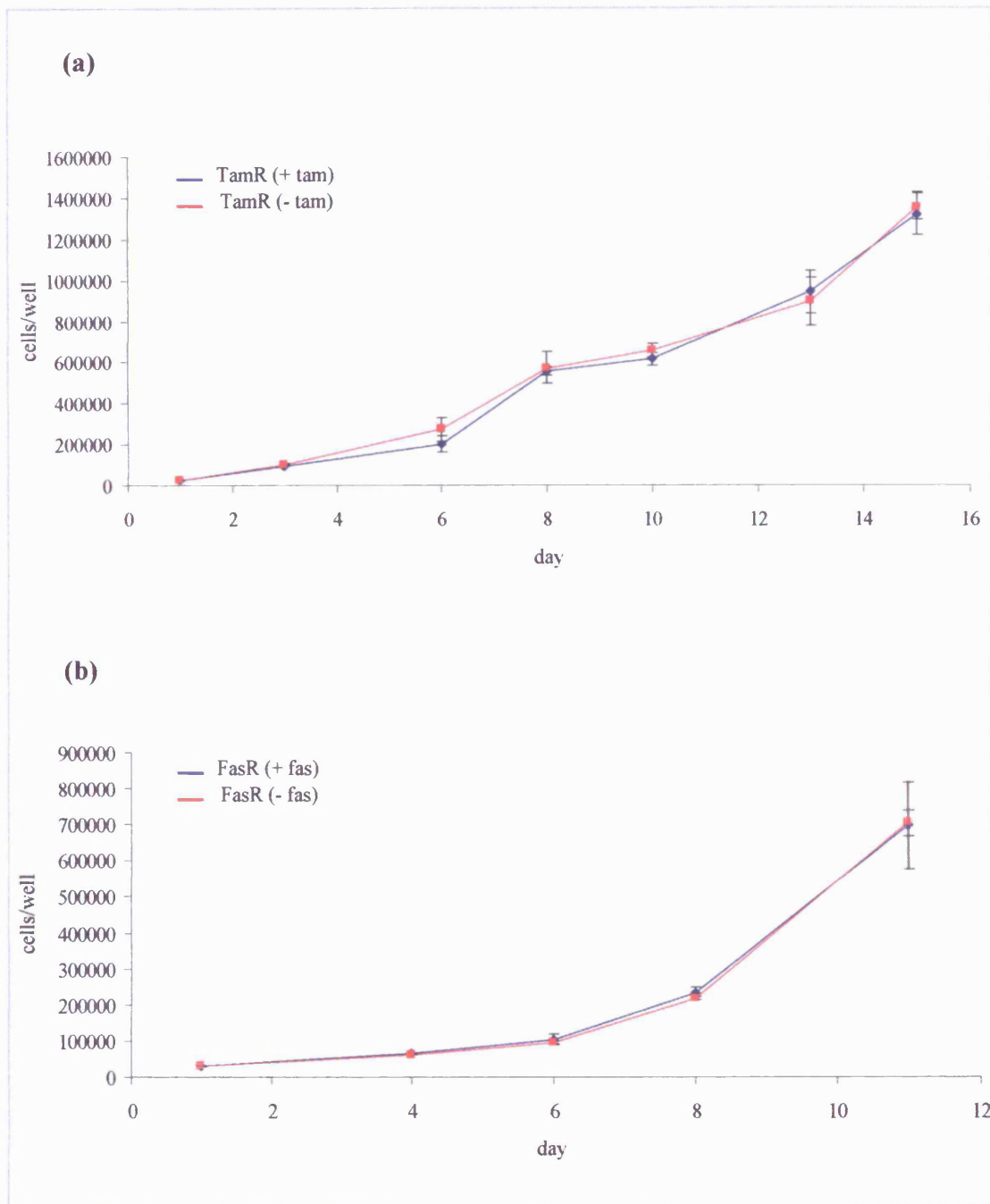
Figure 9. TamR and FasR cell growth in the presence and absence of tamoxifen or Faslodex. TamR or FasR cells of equivalent passage status to those used in this study for microarray studies were seeded into 24 well plates in the absence or presence of their respective antioestrogens and cells counted for up to 16 days (standard deviations are shown for triplicate experiments).
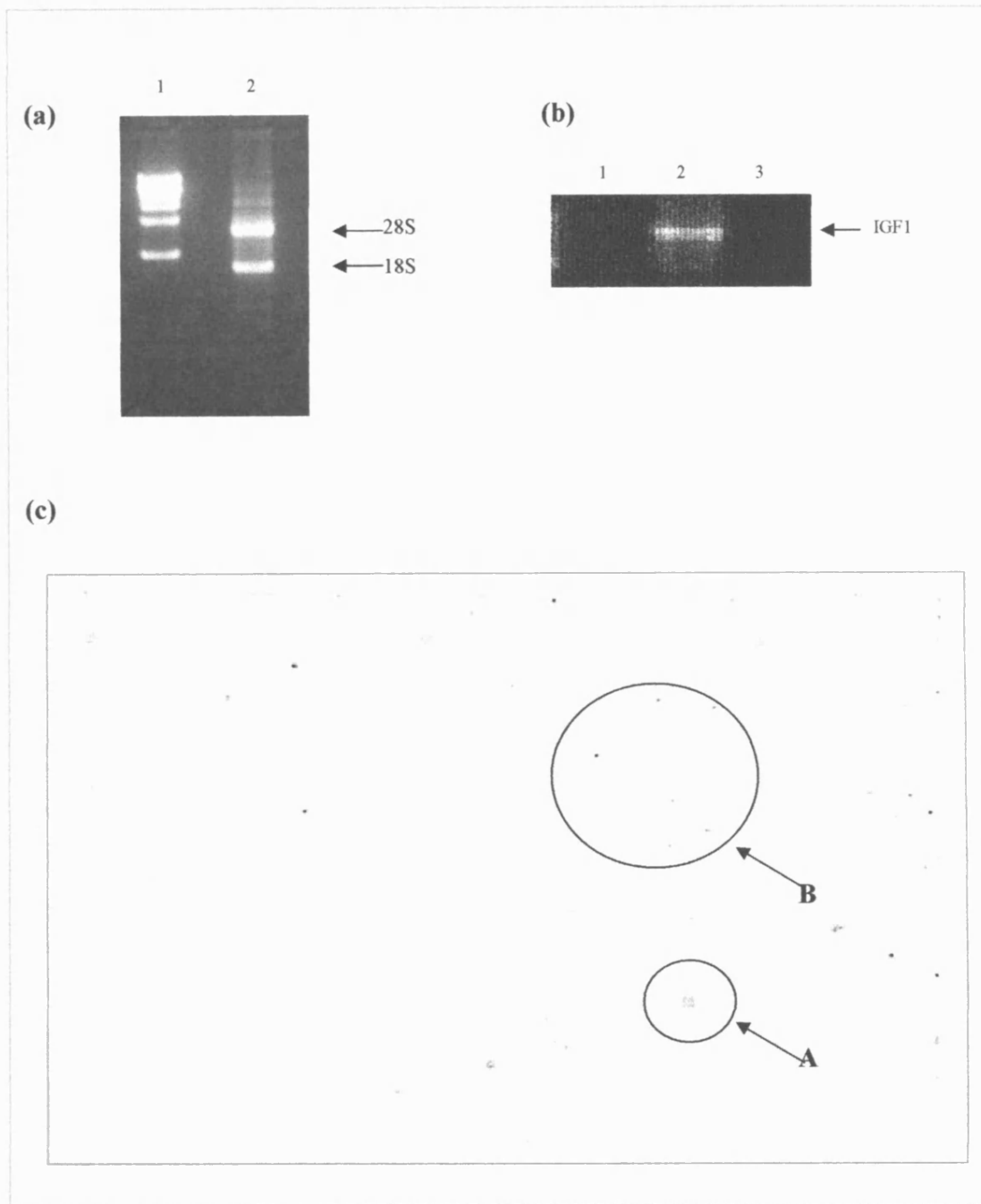
Figure 10. RNA Extraction Using Tri Reagent and hybridisation to Atlas Plastic Trial Arrays. (a) Total RNA was extracted using Tri Reagent was subsequently DNase-treated and subject to Qiagen clean-up. *A volume of 1 µl was separated on a 1.2 % agarose gel and visualised by ethidium bromide staining.* Lane 2 shows total RNA extracted from MCF-7 cells (lane 1 is the 1kb ladder). (b) Tri Reagent Extracted RNA was checked for genomic contamination. RNA extracted using Tri Reagent was DNase-treated and subject to Qiagen clean-up. PCR was performed using exon-spanning primers for IGF1 for the detection of genomic contamination. The absence of PCR product (lane 1) indicates no genomic contamination using *0.5ug extracted RNA. Positive control was 50 ng of genomic DNA standards (lane 2) and PCR negative* control (lane 3). (c) Tri Reagent extracted total RNA from MCF-7+E2 sample, which was DNase-treated and Qiagen cleaned, was used for hybridisation to Atlas Plastic Trial Microarrays. Arrays were exposed to phosphoscreen for 3 days before being processed. Circled gene A represents the housekeeping gene β-Actin, and circled area B highlights non-specific background.

However, although RNA extraction procedures with Tri Reagent resulted in high yields and, apparently adequate quality, initial studies using Atlas Plastic TRIAL Microarrays showed the predominance of high background (non-gene specific signal on the array), also with unacceptably low signal strength (Fig.10c; see example of MCF-7+E2 treated cells). Thus, the only genes which may be observed subsequent to hybridisation represent housekeeping genes such as β-Actin, probably since these are found in high abundance.

Several attempts were made to address the issue of increased array background with this approach. As the plastic microarray platform is a relatively recent format, publications which can help in optimising this technology are limited and hence the array manufacturer (BD Biosciences; Clontech) was approached for suggestions to improve this protocol. Emphasis was placed on the use of Atlas Hybridisation Boxes. However, although a slight reduction of background on the arrays was observed and array handling was improved, the introduction of the hybridisation box failed to completely remove background problems or address low signal strength. It was therefore concluded from these results that the sole use of the Tri Reagent extraction procedure for RNA extraction was inadequate for microarray hybridisation.

3.1.3 Clontech Nucleotrap mRNA purification kit.

A subsequent protocol was followed according to the Clontech Nucleotrap mRNA method (2.2.2.2) as this was highly recommended by the manufacturer for use with the plastic arrays (*personal communication from Clontech and see Ref: (Clontech-Nucleotrap-website, 2006)*) to purify mRNA in order to improve array hybridisation performance . The purification of mRNA was attempted using the Clontech Nucleotrap mRNA purification kit on total RNA initially extracted using Tri Reagent (Methods 2.2.2.1). However, considerable inconsistencies with the resultant extracted mRNA yield were repeatedly found. This is exemplified in Figure 11, where two relatively similar RNA starting preparations ([lane2] 207µg and [lane3] 176µg) were purified using this protocol simultaneously, but resulted in substantially different yields (4.2µg and 0.01 µg respectively). A volume of 5µl from each sample was subsequently separated on a 1.2 % ethidium bromide stained agarose gel to check integrity and quality of the mRNA (Fig.11).

Although visual inspection of the RNA product separated on agarose gel indicated the presence of mRNA (seen as a smear, more clearly in lane 2 than 3 in Fig.11), a proportion of contaminating 18S and 28S ribosomal RNA species can also be observed in the extracted product. This may account for a proportion of the RNA concentration value obtained, and also illustrates the inefficiency of the method for extracting pure mRNA species from total RNA. This method was thus deemed unsuitable for any array work as unacceptable yields, inconsistencies, and poor quality of mRNA was revealed.

3.1.4 Poly A+RNA Extraction Protocols

In light of the array background problems encountered with using Tri Reagent-based extractions alone, attempts were made to subsequently extract polyadenylated (PolyA+) RNA as this protocol may remove impurities from the sample and improve array hybridisation results. Polyadenylated RNA was extracted (method 2.2.2.3) from Tri-Reagent-extracted, DNase-treated, Qiagen 'cleaned' RNA. This procedure, involving the use of Oligo(dT)cellulose, takes advantage of the fact that mRNA molecules, which posses a 3'poly A tail, can bind Oligo(dT) which is linked to cellulose beads, and following washing, the PolyA+RNA is eluted (Sambrook et al., 1989). However, these methodological variations of the principal of mRNA extraction produced no detectable yield of RNA, shown by the absence of ethidium bromide staining on a 1.2% agarose gel (not illustrated).

3.1.5 Atlas Pure Total RNA Extraction

Relatively high yields of RNA, comparable to Tri Reagent RNA extractions were obtained with the Atlas Pure Total RNA Labelling System extraction procedure. This allows the extraction of total RNA using a denaturing solution with PolyA+RNA selection and probe labelling for array hybridisation. Typical yields of an experiment using the Atlas Pure Total extraction method, from 6-10x 150mm dishes (at 50-70% confluency) were around 1.0mg, depending on the cell preparation (where MCF-7+E2 > TamR > MCF-7 > FasR cells). After processing total RNA with DNase and Qiagen clean-up show clear and intact 28S and 18S bands on an ethidium bromide stained gel across multiple samples (Fig.12a) with around 60% recovery, and with no genomic contamination, as determined by IGF1 PCR (Fig.12b).

RNA extracted using this method appeared initially to be both the quality and yield which could be used for microarray studies. The resultant sample RNA was used to produce probes for hybridisation to the Trial Arrays to monitor signal strength and levels of background.

RNA extracted using Atlas Pure Total RNA Labelling System produced arrays which demonstrated low background (Fig.13a). However, although control spots (seen as a regular grid on the array, used for orientation during analysis) were strikingly apparent, there was the obvious absence of a high proportion of gene-specific signals and thus low array signal strength (Fig.13b).

Using the complete protocol, including RNA extraction with the denaturing solution as supplied with the kit may have contributed to selection for low molecular weight RNA species (or the procedure may have contributed to the degradation of RNA), observed in Fig.12a as a low molecular weight, abundant band. This may in turn have contributed to incorrect estimation of RNA content during quantitation, low probe synthesis, and hence arrays with weak signals.
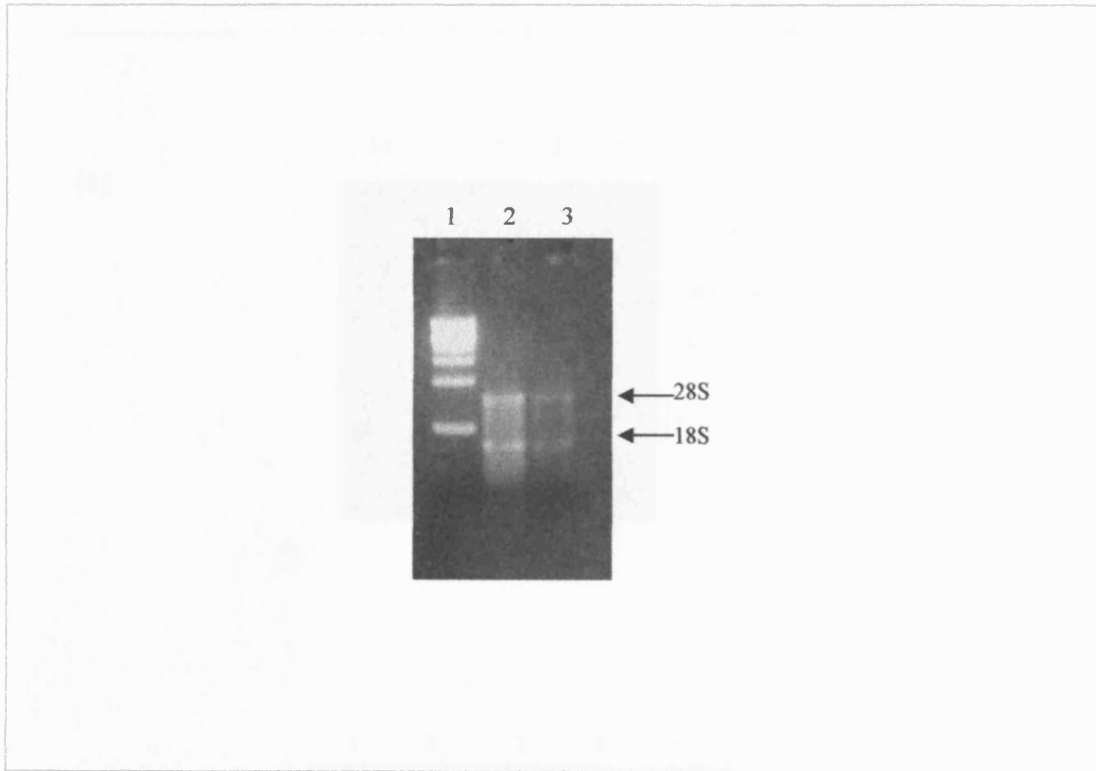
Figure 11. mRNA Extraction Using Clontech Nucleotrap. Total RNA from samples 2 and 3 were extracted using Tri Reagent, followed by DNase-treatment and Qiagen clean-up. Total RNA of 207µg (2) and 176µg (3) was then purified for mRNA using Clontech Nucleotrap mRNA Purification Kit. A volume of 5µl was then separated on a 1.2% agarose gel and visualised by ethidium bromide staining. Figure shows 28s and 18s RNA bands weakly visible (lane 1 shows the 1 kb ladder).
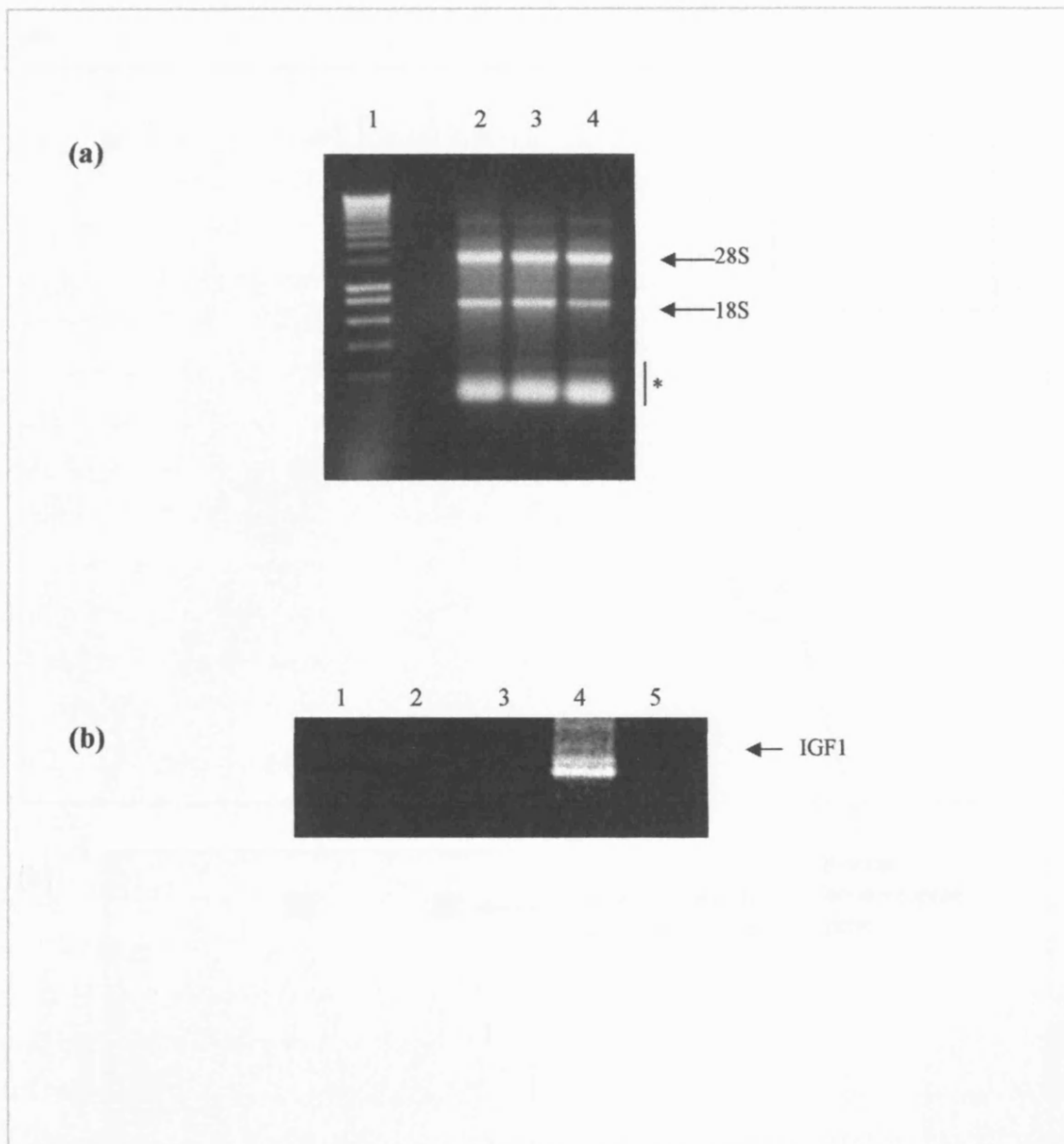
Figure 12. Total RNA Extraction Using Atlas Pure Total System. (a) RNA extracted using Atlas Pure Total RNA Labelling System was subsequently DNase-treated and subject to Qiagen clean-up. RNA of 1µg was separated on a 1.2% agarose gel and visualised by ethidium bromide staining. (Shown are RNA from (2) MCF-7, (3) MCF-7+E2 and (4) TamR cells. Lane 1 shows 1kb ladder and asterisk marks localisation of unwanted low molecular weight constituents. (b) RNA extracted using Atlas Pure Total System was DNase-treated and subject to Qiagen clean-up. The absence of PCR product for IGF1 indicates no genomic contamination. The following RNA were present in the PCR reaction: Lanes 1-3: MCF-7, MCF-7+E2 and TamR respectively, all at 0.5ug RNA; Lane 4: 50ng DNA standard. Lane 5 shows negative control.

(a)

(b)

control signals for
array orientation

β-actin
housekeeping
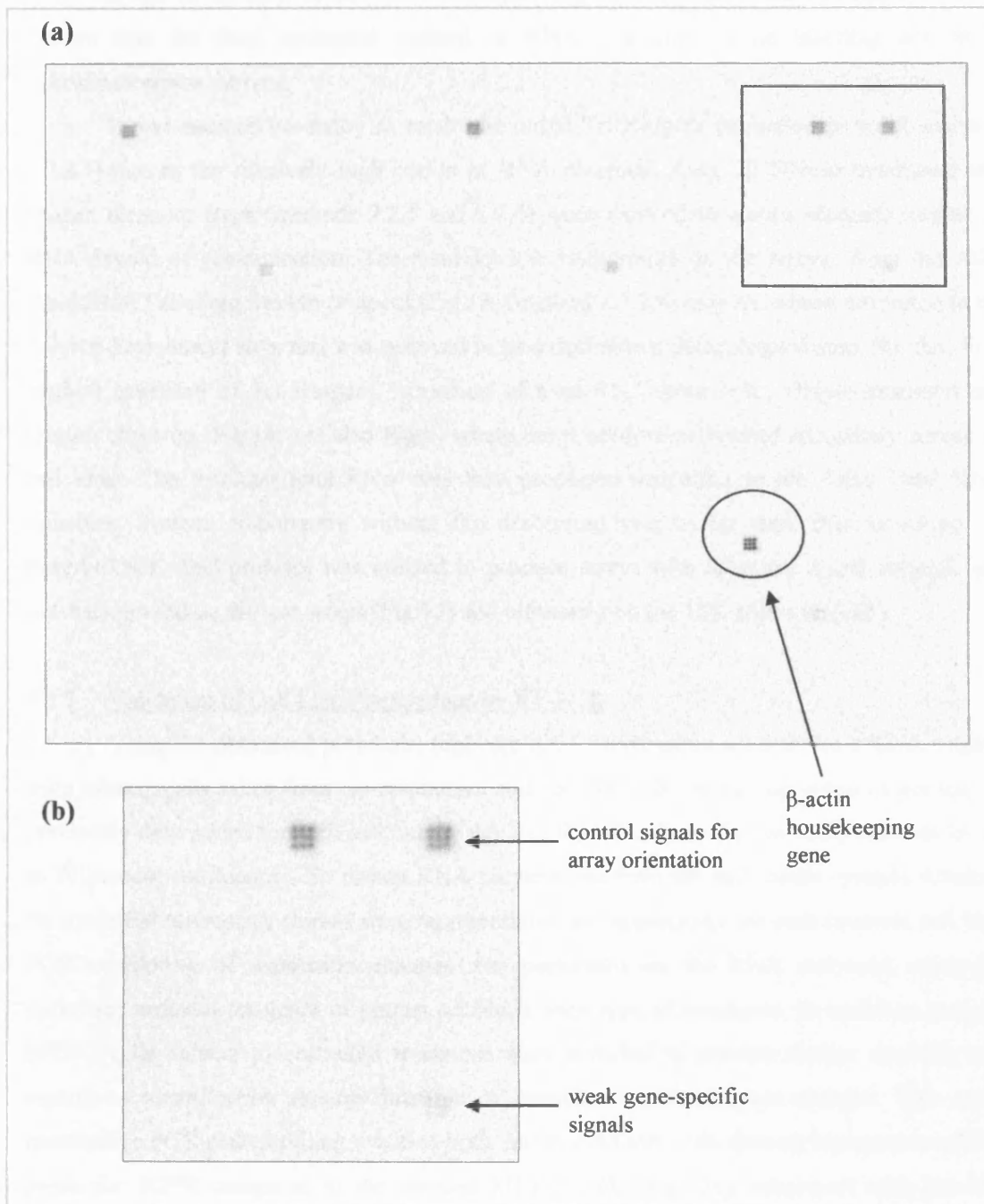gene

weak gene-specific
signals

Figure 13. Atlas Pure Total System Extracted RNA Hybridisation to Atlas Plastic Trial Arrays.
(a) RNA extracted using Atlas Pure Total RNA Labelling System was DNase-treated and subject to
Qiagen clean-up. Resultant PolyA+ RNA was hybridised to Atlas Plastic Trial Microarrays. Arrays
were then exposed to phosphoscreen for 7 days before detection. (b) Magnified area of array from Fig A
shows the predominance of control specific signals with low gene-specific signals.

3.1.6 RNA Extraction: Optimised Protocol

It was on the basis of the results obtained using the Tri Reagent and the Atlas Pure Total System that the final optimised method of RNA extraction, probe labelling and array hybridisation was derived.

It was deemed necessary to retain the initial Tri Reagent extraction protocol (method 2.2.2.1) due to the relatively high yields of RNA obtained. Also, all DNase treatments and Qiagen clean-up steps (methods 2.2.5 and 2.2.6) were retained to ensure adequate quality of RNA devoid of contamination. The resultant low background on the arrays from the Atlas Total RNA Labelling System protocol (Fig.13) (method 2.2.2.4) may have been attributed to the PolyA+ Enrichment step, and was believed to be a desirable methodological step. So, the final method consisted of Tri Reagent Extraction of total RNA from cells, DNase-treatment and Qiagen clean-up (Fig.14; see also Fig.6) where the procedure performed adequately across all cell lines. The resultant total RNA was then processed according to the Atlas Total RNA Labelling System, importantly without the denaturing/lysis buffer step, thus enriching for PolyA+RNA. This protocol was utilised to produce arrays with adequate signal strength and low background on the test arrays (Fig.15) and ultimately on the 12K arrays (Fig.16).

3.1.7 Validation of Cell Line Preparations by RT-PCR

Using the optimised protocols, triplicate RNA preparations used for microarray studies were subsequently taken from the responsive and resistant cell lines in log phase of growth (as previously determined for each cell line by the TCCR Cell Culture Unit as being cultured for up to 70 percent confluency). To ensure RNA preparations from the cell model systems obtained for the initial microarray studies were representative and appropriate for each resistant cell line, PCR monitoring of expression changes was performed on the RNA extracted using the optimised protocol for genes of known profile in each type of resistance. In addition, parental MCF-7 cells subject to oestradiol treatment were included to provide further controls with regards to identification and confirmation of oestradiol regulated gene changes. This semi-quantitative PCR gene profiling revealed both TamR and FasR cells showed increases in mRNA levels for EGFR compared to the parental MCF-7 cells (Fig.17a), consistent with previous observations (Knowlden et al., 2003, McClelland et al., 2001). In addition, mRNA levels for the ER regulated gene pS2 were also shown appropriately regulated (Gee et al., 1995, Knowlden et al., 1997), with decreases in this gene in the resistant cells and obvious E2 induction in the parental cell line (Fig.17b). The gene for β-actin was also amplified for each cell line for normalisation of pS2 and EGFR, and shows equivalent PCR reaction conditions.
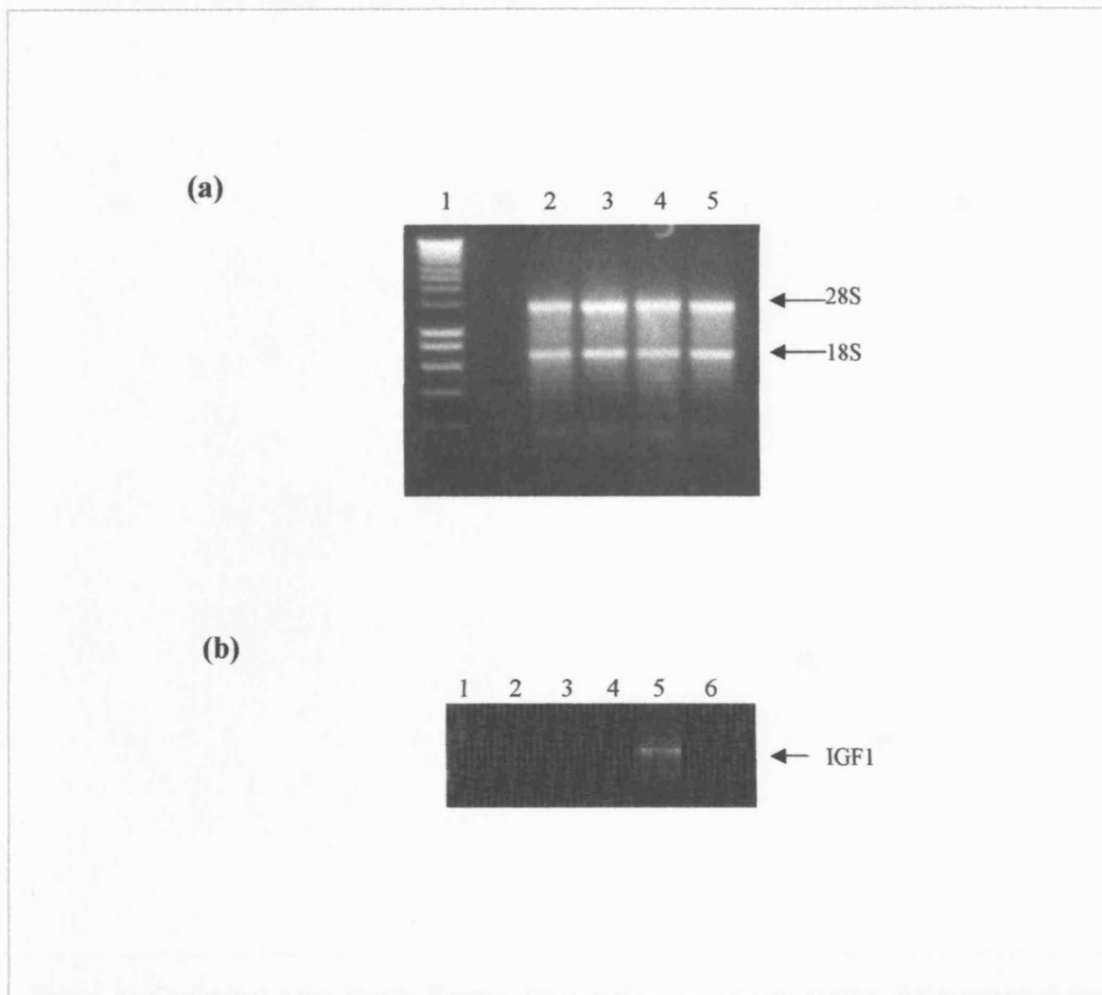
Figure 14. RNA Extraction Using Tri Reagent prior to using the Optimised Protocol. (a) Total RNA was extracted from cell lines using Tri Reagent followed by DNase-treatment and Qiagen clean-up (lanes 2-5 from MCF-7, MCF-7+E2, TamR and FasR respectively). A total volume of 1µg was separated on a *1.5% agarose gel and visualised by ethidium bromide staining. Lane 1 shows 1kb ladder. (b) Tri Reagent* Extracted RNA- Check for Genomic Contamination. RNA extracted using Tri Reagent was DNase-treated and subject to Qiagen clean-up. The absence of PCR product for IGF1 indicates no genomic contamination. The following were present in the PCR reaction: Lanes 1-4: MCF-7, MCF-7+E2, Tam-R and FasR respectively; all at 0.5ug RNA; Lane 5: 50ng DNA standard. Lane 6 shows negative control.
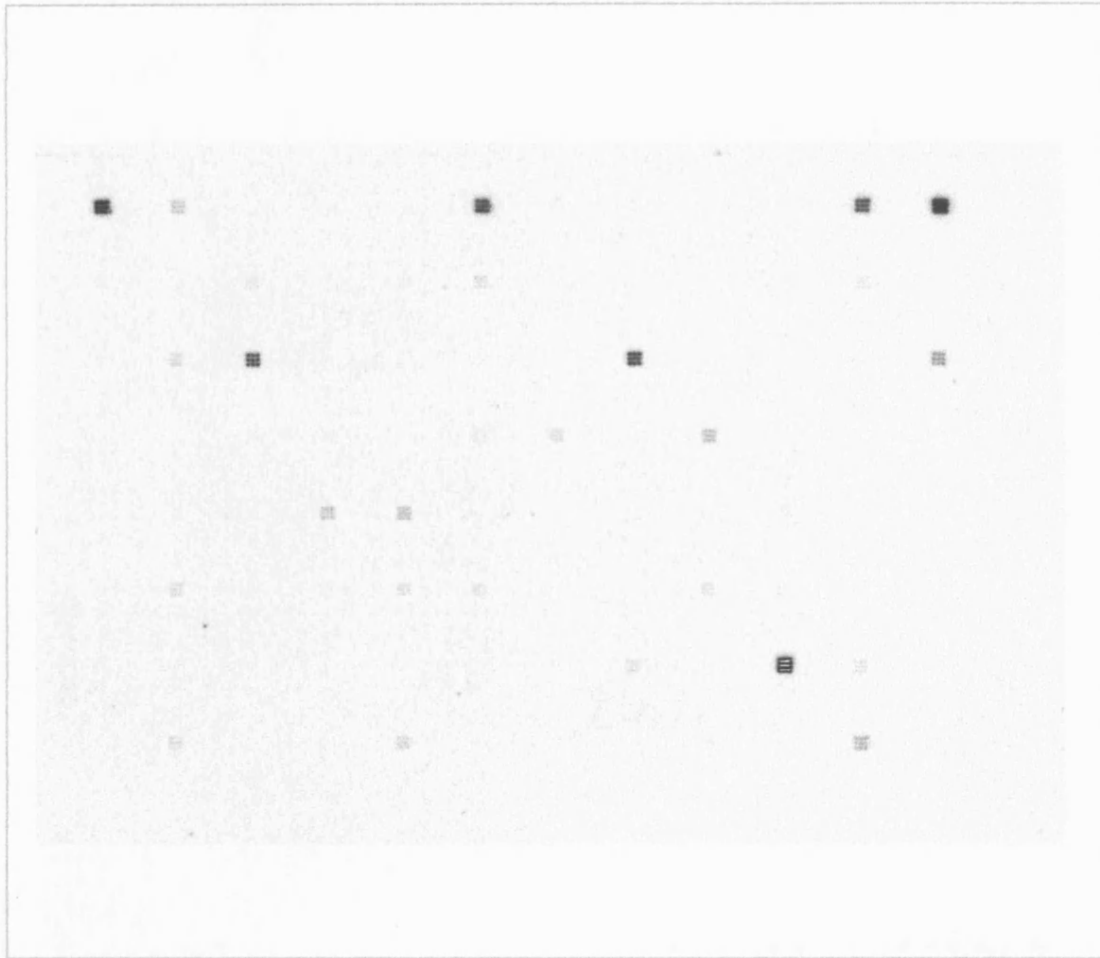
Figure 15. Optimised Atlas Plastic Human Trial Microarray signal quality. RNA extracted from endocrine responsive/ resistant cells were processed according to the final 'Optimised' protocol, labelled and hybridised to Atlas Plastic Human 12k Microarrays. Example is shown with image generated using phosphorimaging exposed for 7 days, from array hybridised with radiolabelled TamR RNA
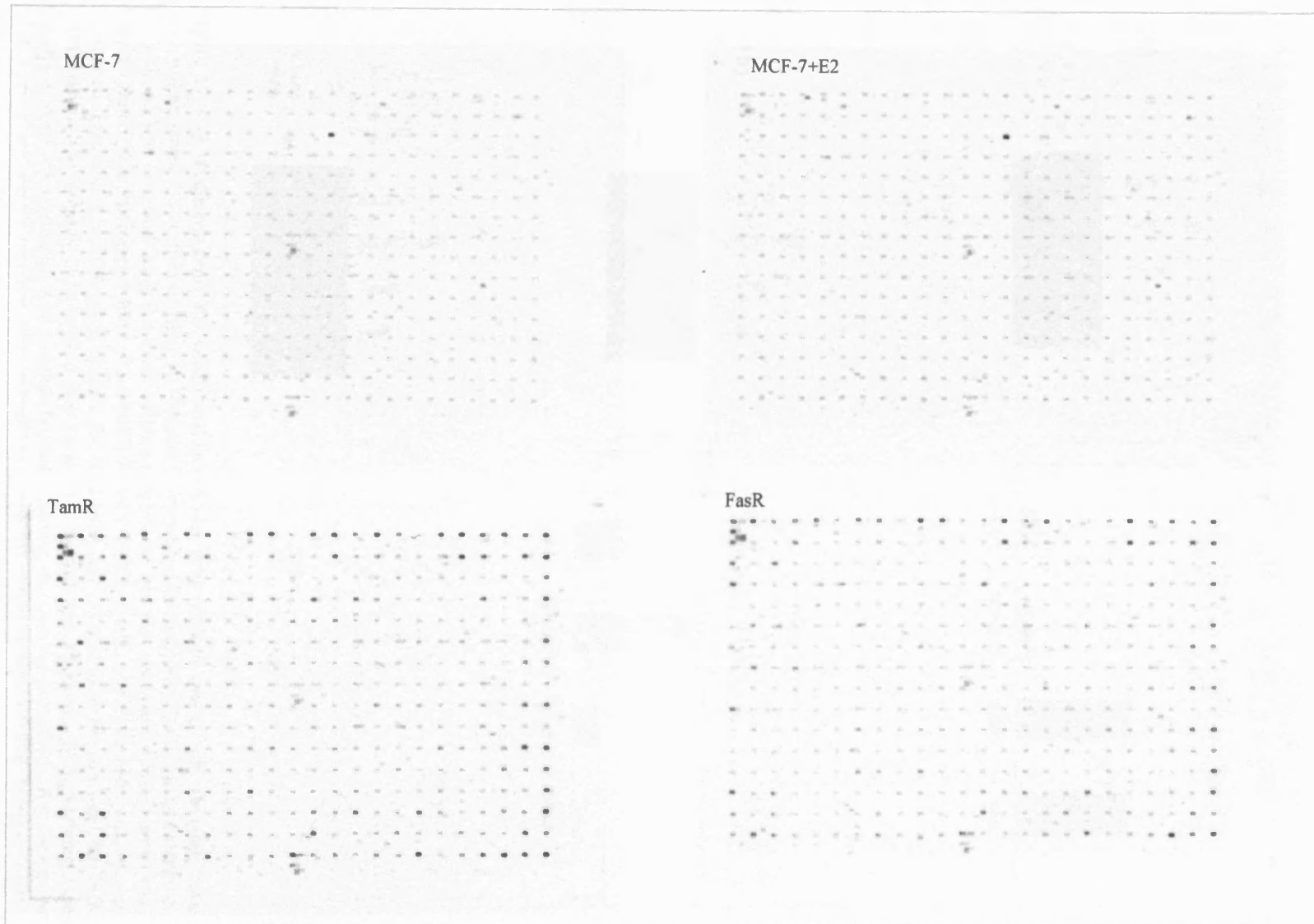
Figure 16. Optimised Atlas Plastic Human 12k Microarray Performance for cell preparations. RNA extracted from MCF-7, MCF-7+E2, TamR and FasR cells were processed according to the final' Optimised' protocol, labelled and hybridised to Atlas Plastic Human 12k Microarrays. Figure shows image generated by phosphorimaging using radiolabelled array exposed for 7 days.
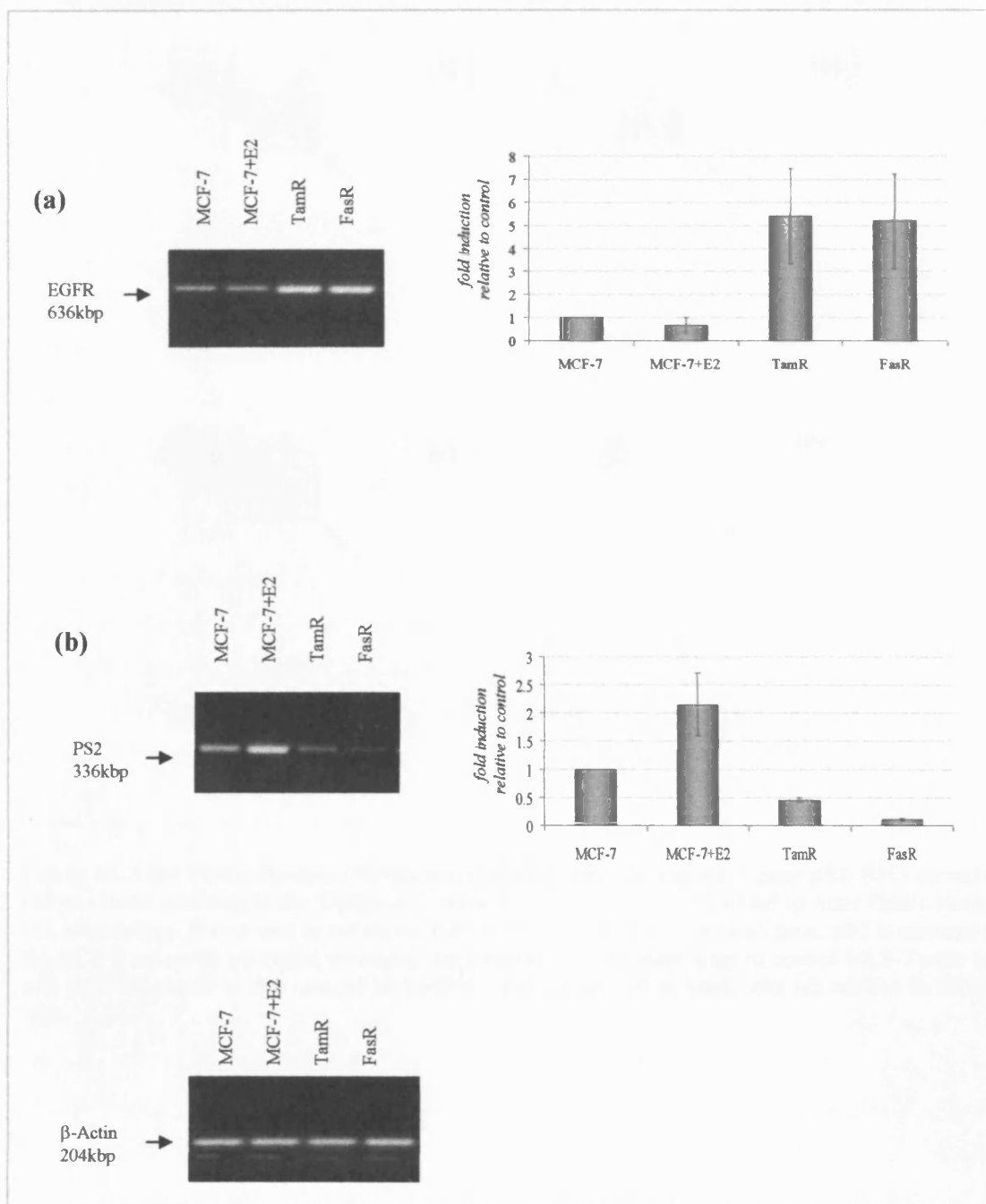
Figure 17. Key landmark genes are confirmed in cell line preparations using PCR analysis. Total RNA was extracted from cell lines using Tri Reagent followed by DNase-treatment and Qiagen clean-up. RNA shown was extracted using the final 'optimised' protocol and was subsequently used with Atlas Plastic Human 12K Microarray. RNA from MCF-7, MCF-7+E2, TamR and FasR cells was reverse transcribed then subject to PCR using primers for (a) EGFR and (b) pS2. β-Actin was used for PCR normalisation. The intensity of each band was normalised against that of β-actin. PCR products were visualised on a 1.5% agarose gel with ethidium bromide staining, as described in methods. Representative PCR profiles are shown together with normalised graphical representation of fold increase across replicate samples (n=3) with standard error.
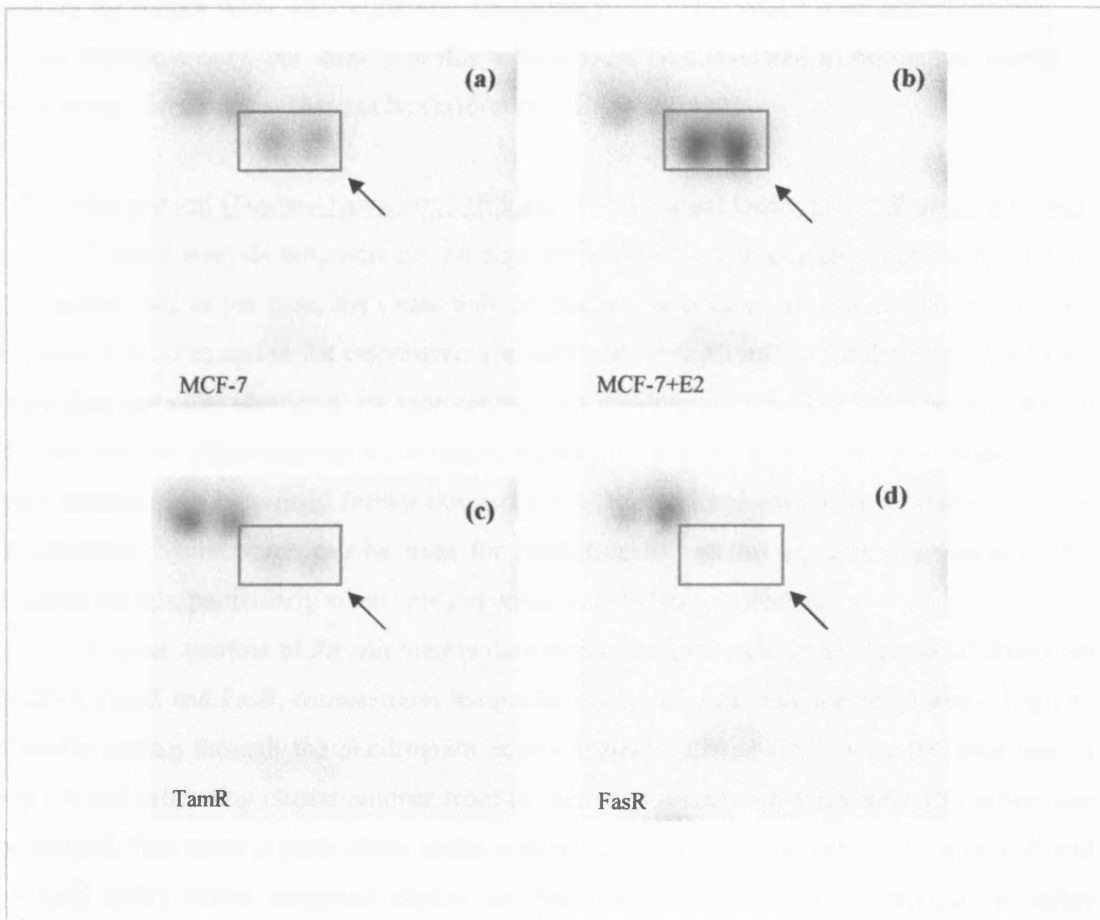
Figure 18. Atlas Plastic Human 12k Microarrays demonstrate landmark gene pS2. RNA extracted and processed according to the 'Optimised' protocol was labelled and hybridised to Atlas Plastic Human 12k Microarrays. Boxed area in red shows mRNA for the oestradiol-regulated gene, pS2 is elevated in (b) MCF-7 cells with oestradiol treatment, compared to the equivalent gene in control MCF-7 cells (a). pS2 gene expression is also reduced in TamR (c) and further still in FasR cells (d) relative to MCF-7 cells.

FasR cells using t-test analysis (n=28 upregulated; n=4 downregulated) were deemed as high priority for further study, also worthy of consideration are genes which were statistically altered in one condition only, but show a profile which could be considered as borderline altered in both forms of resistance. This can be verified by HCA and PAM.

3.2.2 Hierarchical Cluster Analysis of Differentially Expressed Genes in TamR and FasR cells

Cluster-analysis programs run on algorithms which group objects on the basis of their similarities, and in our case, the genes will be clustered according to their similarities in gene expression profiles across the responsive/ resistant cell lines. Results of such GeneSifter-based (Euclidian distance) clustering are represented by a dendrogram tree (Fig.19). The branches of the tree link the genes together according to similarities in expression. Then other branches (or gene clusters) can be refined further down the tree. Hierarchical clustering produces a readily interpretable figure which can be used for prediction of patterns of gene expression across multiple groups, particularly when new hypotheses are being formulated.

Cluster analysis of the microarray data derived from the quadruplicate set of arrays for MCF-7, TamR and FasR, demonstrates the predominance of clear and distinct clusters (Fig 19). Visually cutting through the dendrogram approximately halfway (shown by the blue line in Fig.19) and estimating cluster number from the heatmap reveals approximately 15 clusters can be formed. This value is particularly useful with partitioning methods such as PAM (which will be used later) where estimated cluster number from HCA will be a prerequisite before partitioning the data.

Detailed pattern analysis of a number of critical clusters generated by HCA have clearly demonstrated the breadth genes which are, for example, downregulated in one (cluster 1 and 6) or both forms of resistance (cluster 2; Fig.20 [eg, GFRα3, WISP2]). Clusters are also resolved where genes are upregulated in TamR (cluster 3; Fig.21 [eg. Homer2, PEA3 (ets variant 4), casein kinase 2, KDEL], and also cluster 5 [eg. Enigma], cluster 7, cluster 11 [eg. Angiogenin]), or FasR (cluster 13; Fig.22 [eg. Vitronectin] and also cluster 15). Genes upregulated in both forms of resistance may be exemplified by cluster 14 (eg. paroxonase2, CD44, PTTG1, cyclin A2, PPAR-δ, alpha centaurin; Fig.23), but also found in cluster 4 (see below), cluster 8 (eg, Rab acceptor 1, Legumain, Matrix Gla protein), and other weaker clusters such as cluster 12 (eg, POP4, WD40 ciao) and occasionally within cluster 10 (biliverdin reductase, ODC). Although some TamR and FasR induced clusters contain genes which are also significantly induced in both TamR and FasR cells by t-test analysis, for example T-Box21 (cluster 4; Fig.24), a number of genes which are significantly altered in only one resistant cell line, but with a trend in the other resistant cell line, are also included in the cluster, such as GFRα3 and FK506bp, PPAR-γ and STAT-i2. Such co-clustering supports the choice of such singly t-test induced genes as borderline shared in both resistant cell lines.
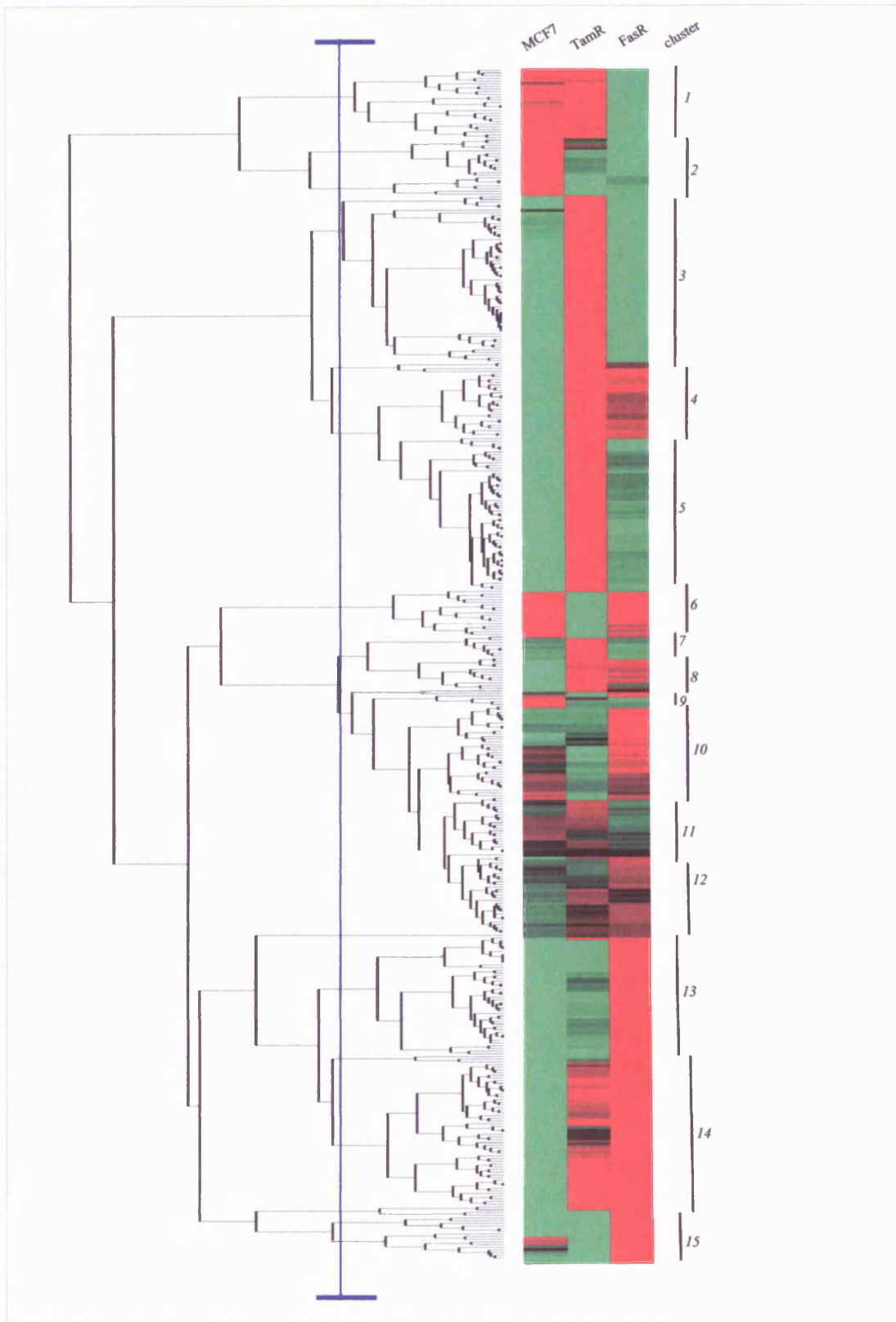
Figure 19. Hierarchical Cluster Analysis. Significantly altered genes in TamR and FasR relative to MCF-7 determined by project analysis through GeneSifter software in quadruplicate samples of MCF7, TamR and FasR cells were subject to hierarchical cluster analysis (Euclidian distance, average linkage) using GeneSifter. Dendrogram is shown left of the heatmap. Estimated clusters are also identified to the right of the heatmap. Position of blue line bisecting dendrogram was used to estimate number of partitions for PAM analysis.

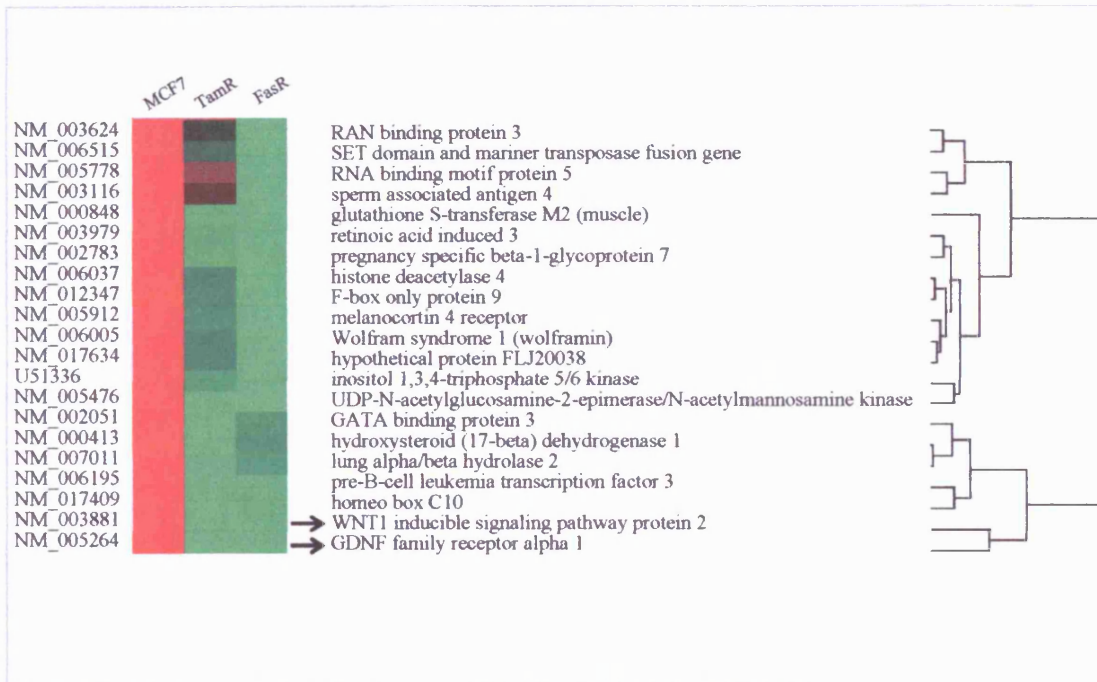|	MCF7	TamR	FasR	
NM_003624				RAN binding protein 3
NM_006515				SET domain and mariner transposase fusion gene
NM_005778				RNA binding motif protein 5
NM_003116				sperm associated antigen 4
NM_000848				glutathione S-transferase M2 (muscle)
NM_003979				retinoic acid induced 3
NM_002783				pregnancy specific beta-1-glycoprotein 7
NM_006037				histone deacetylase 4
NM_012347				F-box only protein 9
NM_005912				melanocortin 4 receptor
NM_006005				Wolfram syndrome 1 (wolframin)
NM_017634				hypothetical protein FLJ20038
U51336				inositol 1,3,4-triphosphate 5/6 kinase
NM_005476				UDP-N-acetylglucosamine-2-epimerase/N-acetylmannosamine kinase
NM_002051				GATA binding protein 3
NM_000413				hydroxysteroid (17-beta) dehydrogenase 1
NM_007011				lung alpha/beta hydrolase 2
NM_006195				pre-B-cell leukemia transcription factor 3
NM_017409				homeo box C10
NM_003881				→ WNT1 inducible signaling pathway protein 2
NM_005264				→ GDNF family receptor alpha 1

Figure 20. Hierarchical Cluster Analysis: Detail of Cluster 2 showing genes at lower levels in both resistance cell lines relative to MCF-7. Dendrogram together with gene name and accession numbers are shown alongside the heatmap. Genes of interest are highlighted with arrow.
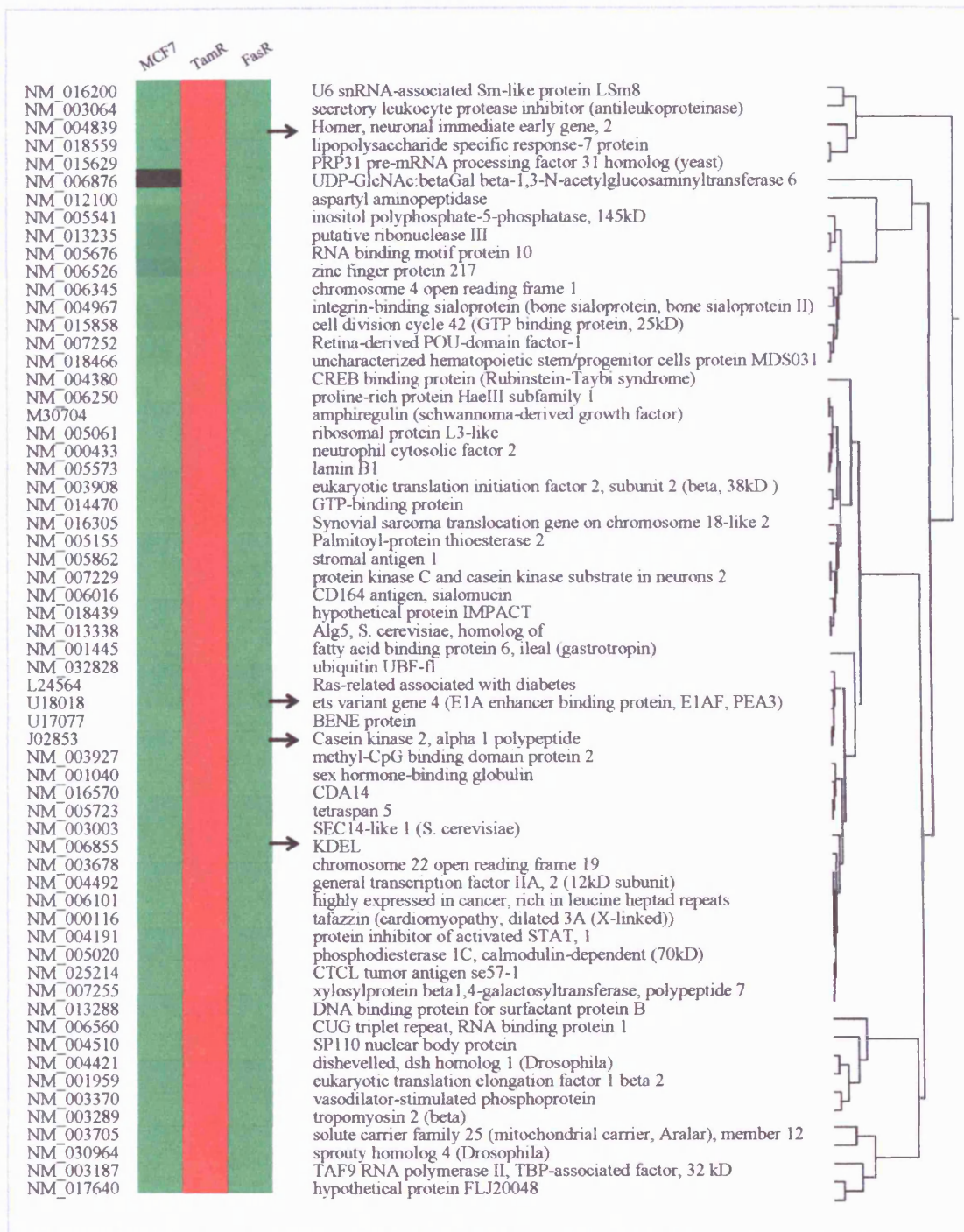
Figure 21. Hierarchical Cluster Analysis: Detail of Cluster 3 showing genes at higher level in TamR cell line only. Dendrogram together with gene name and accession numbers are shown alongside the heatmap. Genes of interest are highlighted with arrow.
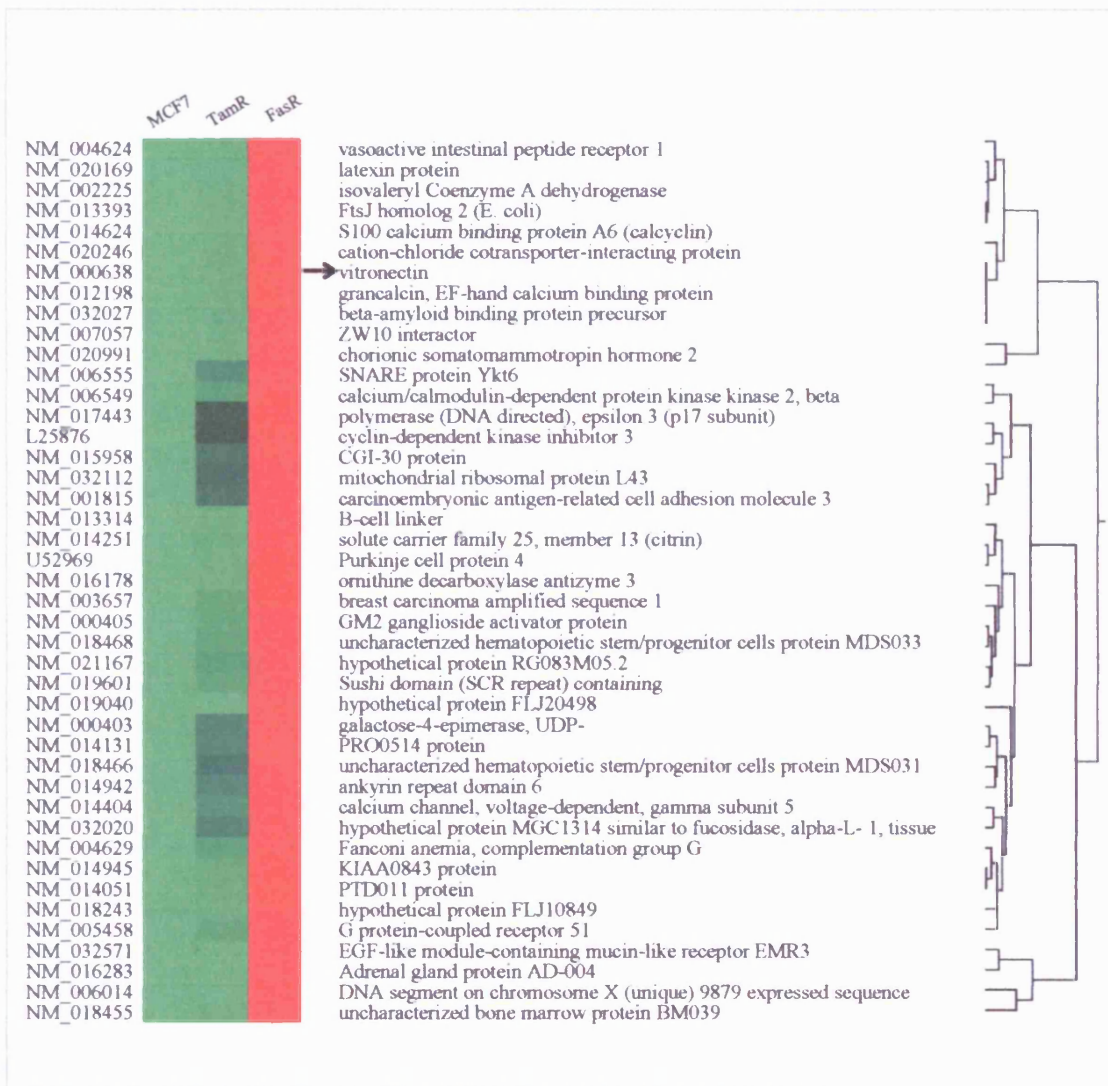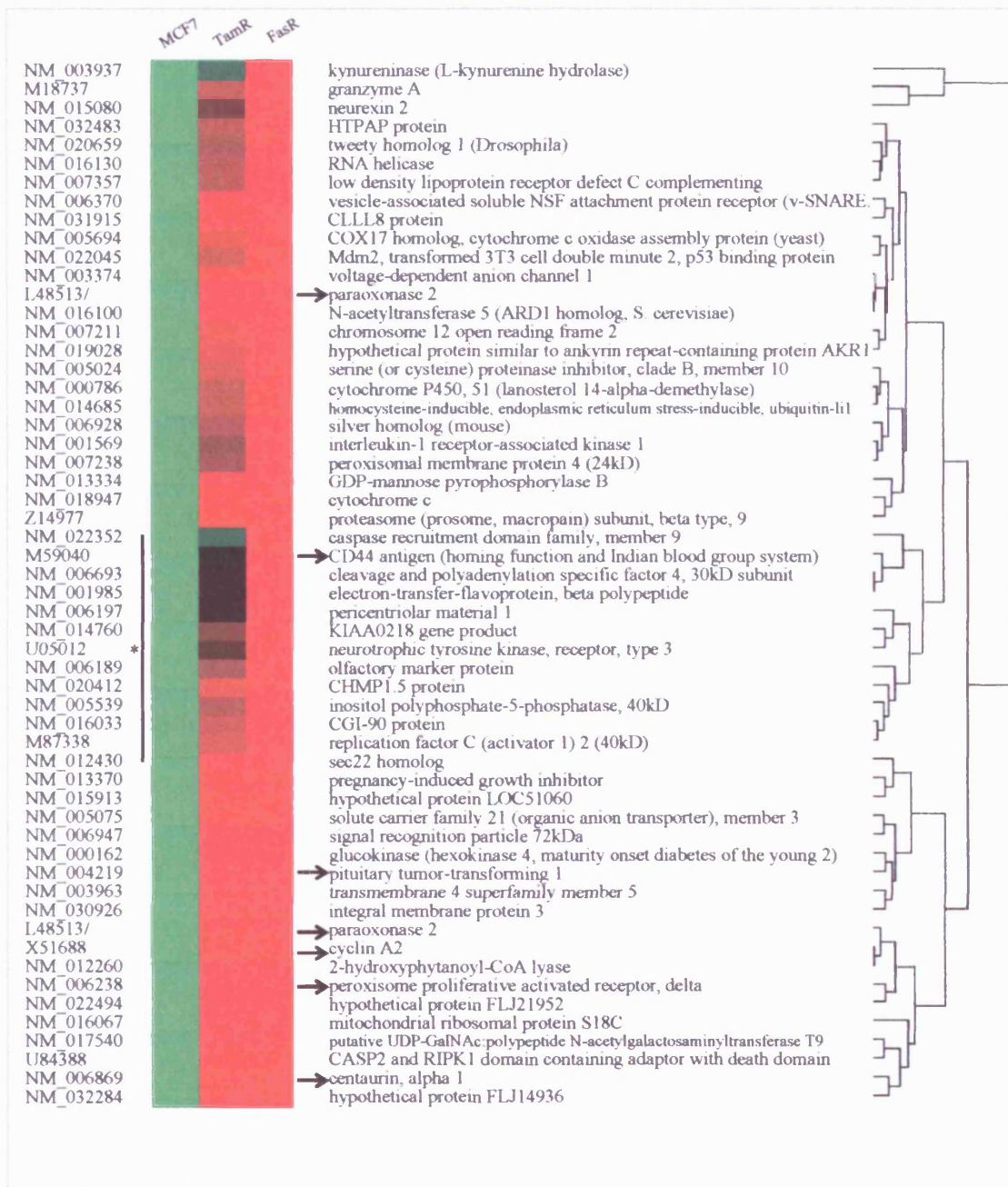
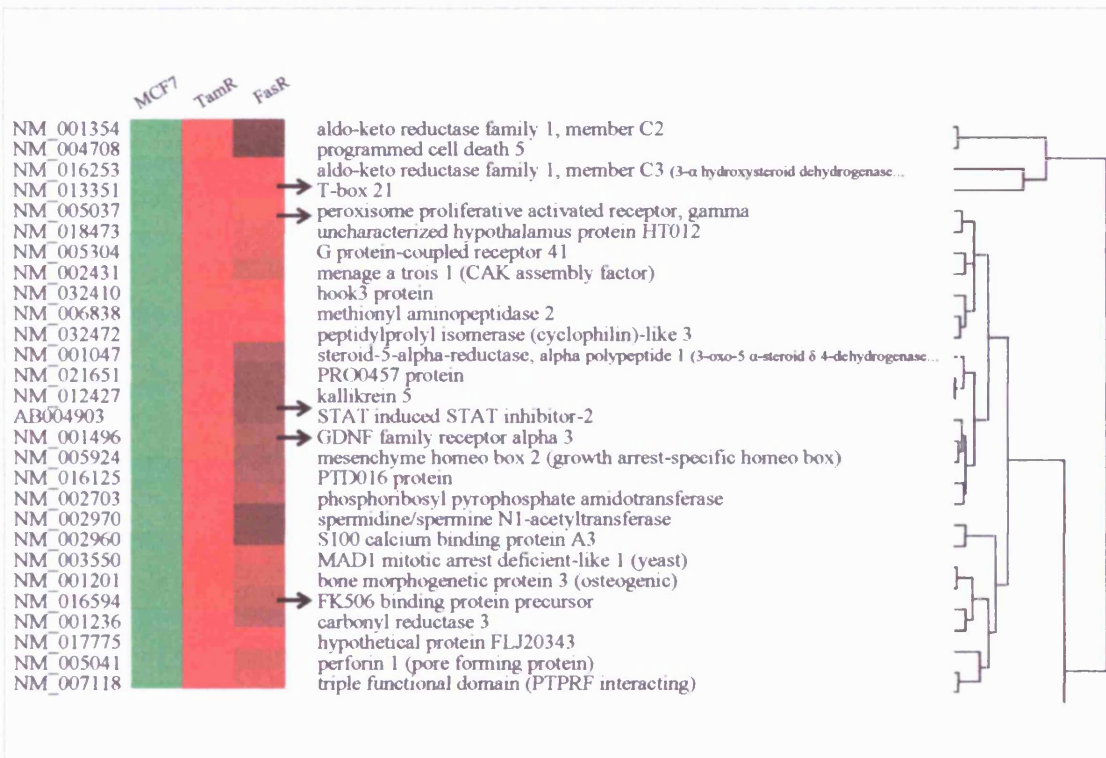|	MCF7	TamR	FasR	
NM_004624				vasoactive intestinal peptide receptor 1
NM_020169				latexin protein
NM_002225				isovaleryl Coenzyme A dehydrogenase
NM_013393				FtsJ homolog 2 (E. coli)
NM_014624				S100 calcium binding protein A6 (calcyclin)
NM_020246				cation-chloride cotransporter-interacting protein
NM_000638				vitronectin
NM_012198				grancalcin, EF-hand calcium binding protein
NM_032027				beta-amyloid binding protein precursor
NM_007057				ZW10 interactor
NM_020991				chorionic somatomammotropin hormone 2
NM_006555				SNARE protein Ykt6
NM_006549				calcium/calmodulin-dependent protein kinase kinase 2, beta
NM_017443				polymerase (DNA directed), epsilon 3 (p17 subunit)
L25876				cyclin-dependent kinase inhibitor 3
NM_015958				CGI-30 protein
NM_032112				mitochondrial ribosomal protein L43
NM_001815				carcinoembryonic antigen-related cell adhesion molecule 3
NM_013314				B-cell linker
NM_014251				solute carrier family 25, member 13 (citrin)
U52969				Purkinje cell protein 4
NM_016178				ornithine decarboxylase antizyme 3
NM_003657				breast carcinoma amplified sequence 1
NM_000405				GM2 ganglioside activator protein
NM_018468				uncharacterized hematopoietic stem/progenitor cells protein MDS033
NM_021167				hypothetical protein RG083M05.2
NM_019601				Sushi domain (SCR repeat) containing
NM_019040				hypothetical protein FLJ20498
NM_000403				galactose-4-epimerase, UDP-
NM_014131				PRO0514 protein
NM_018466				uncharacterized hematopoietic stem/progenitor cells protein MDS031
NM_014942				ankyrin repeat domain 6
NM_014404				calcium channel, voltage-dependent, gamma subunit 5
NM_032020				hypothetical protein MGC1314 similar to fucosidase, alpha-L- 1, tissue
NM_004629				Fanconi anemia, complementation group G
NM_014945				KIAA0843 protein
NM_014051				PTD011 protein
NM_018243				hypothetical protein FLJ10849
NM_005458				G protein-coupled receptor 51
NM_032571				EGF-like module-containing mucin-like receptor EMR3
NM_016283				Adrenal gland protein AD-004
NM_006014				DNA segment on chromosome X (unique) 9879 expressed sequence
NM_018455				uncharacterized bone marrow protein BM039

Figure 22. Hierarchical Cluster Analysis: Detail of cluster 13 showing genes at high levels in FasR cell line. Dendrogram together with gene name and accession numbers are shown alongside the heatmap. Genes of interest are highlighted with arrow.

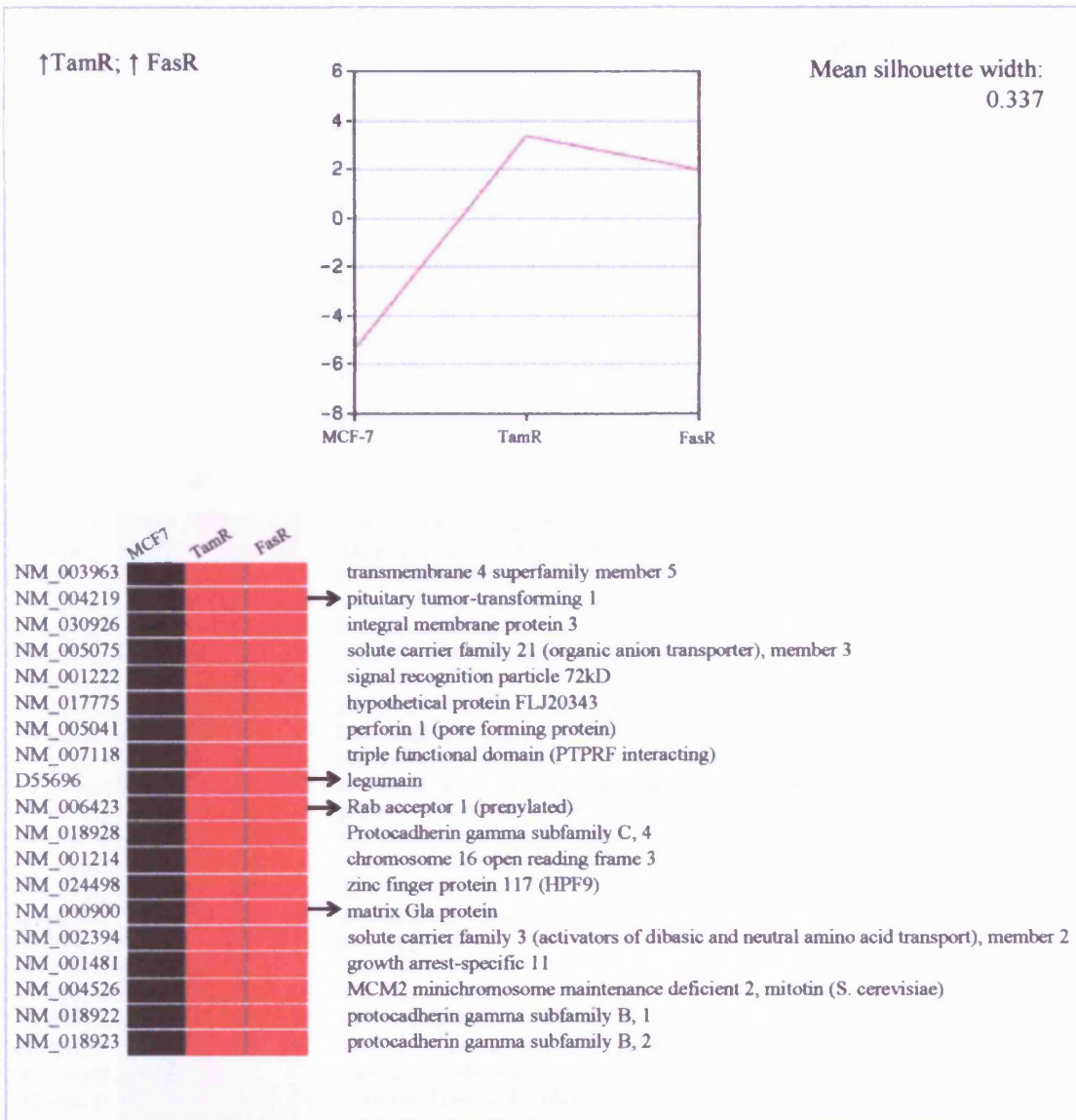|	MCF7	TamR	FasR	
NM_003937				kynureninase (L-kynurenine hydrolase)
M18737				granzyme A
NM_015080				neurexin 2
NM_032483				HTPAP protein
NM_020659				tweety homolog 1 (Drosophila)
NM_016130				RNA helicase
NM_007357				low density lipoprotein receptor defect C complementing
NM_006370				vesicle-associated soluble NSF attachment protein receptor (v-SNARE)
NM_031915				CLLL8 protein
NM_005694				COX17 homolog, cytochrome c oxidase assembly protein (yeast)
NM_022045				Mdm2, transformed 3T3 cell double minute 2, p53 binding protein
NM_003374				voltage-dependent anion channel 1
L48513/				→ paraoxonase 2
NM_016100				N-acetyltransferase 5 (ARD1 homolog, S. cerevisiae)
NM_007211				chromosome 12 open reading frame 2
NM_019028				hypothetical protein similar to ankyrin repeat-containing protein AKR1
NM_005024				serine (or cysteine) proteinase inhibitor, clade B, member 10
NM_000786				cytochrome P450, 51 (lanosterol 14-alpha-demethylase)
NM_014685				homocysteine-inducible, endoplasmic reticulum stress-inducible, ubiquitin-lil
NM_006928				silver homolog (mouse)
NM_001569				interleukin-1 receptor-associated kinase 1
NM_007238				peroxisomal membrane protein 4 (24kD)
NM_013334				GDP-mannose pyrophosphorylase B
NM_018947				cytochrome c
Z14977				proteasome (prosome, macropain) subunit, beta type, 9
NM_022352				caspase recruitment domain family, member 9
M59040				→ CD44 antigen (homing function and Indian blood group system)
NM_006693				cleavage and polyadenylation specific factor 4, 30kD subunit
NM_001985				electron-transfer-flavoprotein, beta polypeptide
NM_006197				pericentriolar material 1
NM_014760				KIAA0218 gene product
U05012 *				neurotrophic tyrosine kinase, receptor, type 3
NM_006189				olfactory marker protein
NM_020412				CHMP1.5 protein
NM_005539				inositol polyphosphate-5-phosphatase, 40kD
NM_016033				CGI-90 protein
M87338				replication factor C (activator 1) 2 (40kD)
NM_012430				sec22 homolog
NM_013370				pregnancy-induced growth inhibitor
NM_015913				hypothetical protein LOC51060
NM_005075				solute carrier family 21 (organic anion transporter), member 3
NM_006947				signal recognition particle 72kDa
NM_000162				glucokinase (hexokinase 4, maturity onset diabetes of the young 2)
NM_004219				→ pituitary tumor-transforming 1
NM_003963				transmembrane 4 superfamily member 5
NM_030926				integral membrane protein 3
L48513/				→ paraoxonase 2
X51688				→ cyclin A2
NM_012260				2-hydroxyphytanoyl-CoA lyase
NM_006238				→ peroxisome proliferative activated receptor, delta
NM_022494				hypothetical protein FLJ21952
NM_016067				mitochondrial ribosomal protein S18C
NM_017540				putative UDP-GalNAc:polypeptide N-acetylgalactosaminyltransferase T9
U84388				CASP2 and RIPK1 domain containing adaptor with death domain
NM_006869				→ centaurin, alpha 1
NM_032284				hypothetical protein FLJ14936

Figure 23. Hierarchical Cluster Analysis: Detail of Cluster 14 showing genes increased in both TamR and FasR relative to MCF-7. Dendrogram together with gene name and accession numbers are shown alongside the heatmap. Genes of interest are highlighted with arrow. (*subcluster is also marked).
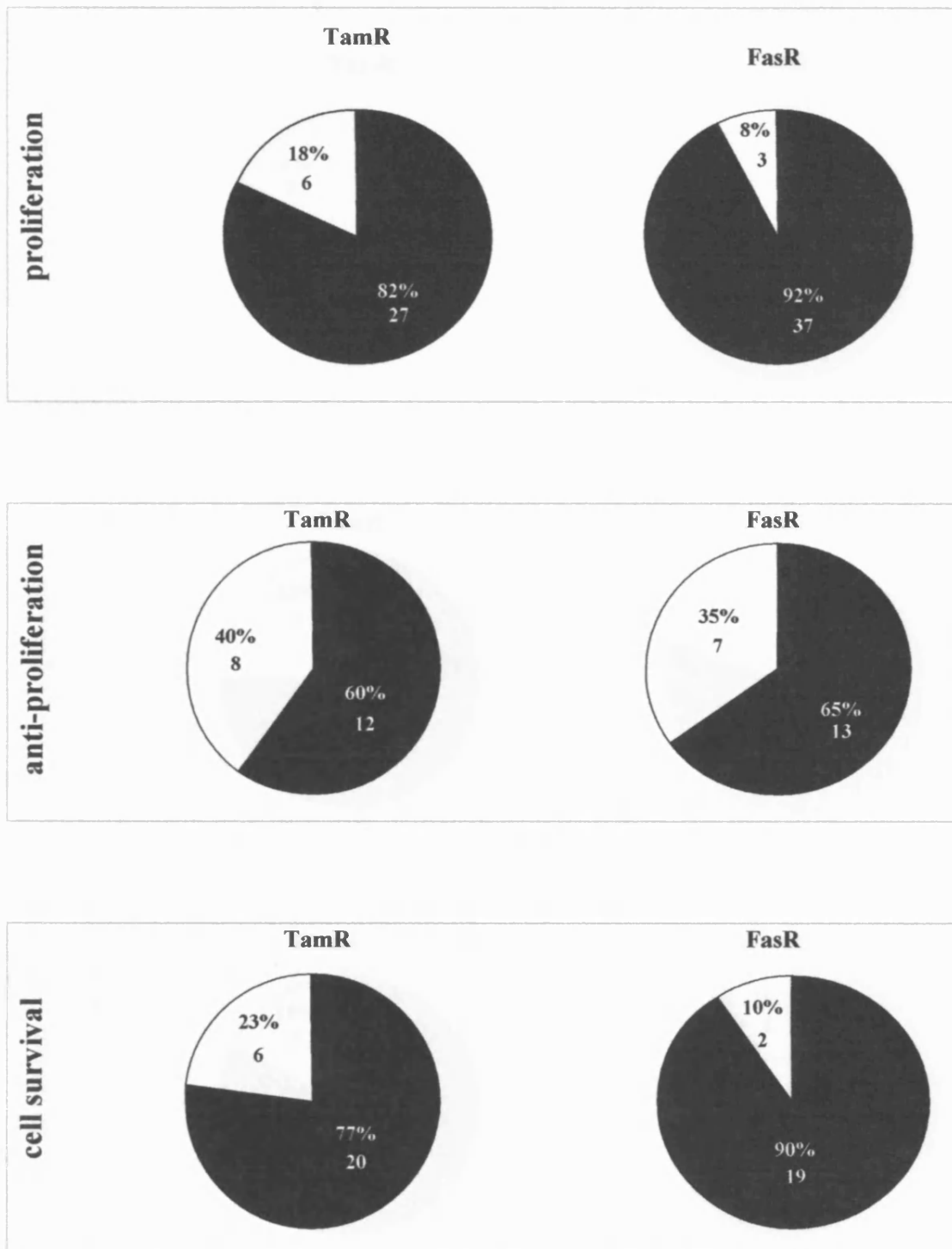
NM_001354		aldo-keto reductase family 1, member C2
NM_004708		programmed cell death 5
NM_016253		aldo-keto reductase family 1, member C3 (3-α hydroxysteroid dehydrogenase...
NM_013351	→	T-box 21
NM_005037	→	peroxisome proliferative activated receptor, gamma
NM_018473		uncharacterized hypothalamus protein HT012
NM_005304		G protein-coupled receptor 41
NM_002431		menage a trois 1 (CAK assembly factor)
NM_032410		hook3 protein
NM_006838		methionyl aminopeptidase 2
NM_032472		peptidylprolyl isomerase (cyclophilin)-like 3
NM_001047		steroid-5-alpha-reductase, alpha polypeptide 1 (3-oxo-5 α-steroid δ 4-dehydrogenase...
NM_021651		PRO0457 protein
NM_012427		kallikrein 5
AB004903	→	STAT induced STAT inhibitor-2
NM_001496	→	GDNF family receptor alpha 3
NM_005924		mesenchyme homeo box 2 (growth arrest-specific homeo box)
NM_016125		PTD016 protein
NM_002703		phosphoribosyl pyrophosphate amidotransferase
NM_002970		spermidine/spermine N1-acetyltransferase
NM_002960		S100 calcium binding protein A3
NM_003550		MAD1 mitotic arrest deficient-like 1 (yeast)
NM_001201		bone morphogenetic protein 3 (osteogenic)
NM_016594	→	FK506 binding protein precursor
NM_001236		carbonyl reductase 3
NM_017775		hypothetical protein FLJ20343
NM_005041		perforin 1 (pore forming protein)
NM_007118		triple functional domain (PTPRF interacting)

Figure 24. Hierarchical Cluster Analysis : Detail of Cluster 4 showing shared genes increased in both TamR and FasR relative to MCF-7. Dendrogram together with gene name and accession numbers are shown alongside the heatmap. Genes of interest are highlighted with arrow.
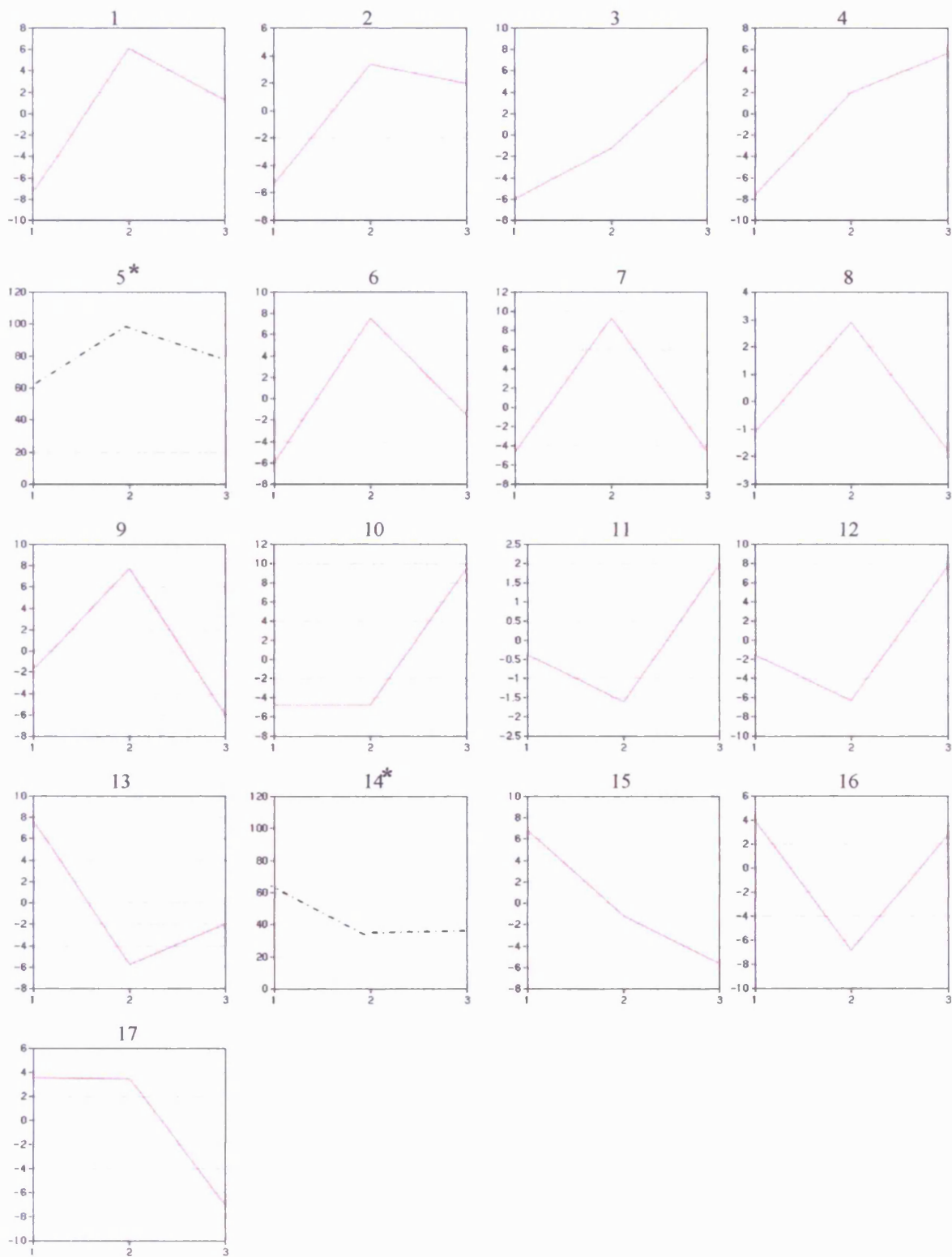
Figure 25. Partitioning (PAM) Cluster Analysis of Genes. Significantly altered genes in TamR and FasR relative to MCF7 were subject to PAM cluster analysis (Euclidian distance, row mean centred, for 16 clusters) using GeneSifter. Silhouette plots are shown for the cluster (MCF-7, TamR and FasR are represented by 1, 2 and 3 on the x-axis respectively). *(note: cluster 5 was manually bisected into clusters 5 and 14).

↑TamR; ↑ FasR

Mean silhouette width: 0.428

	MCF7	TamR	FasR	
NM_016253				aldo-keto reductase family 1, member C3
NM_001354				aldo-keto reductase family 1, member C2
NM_004708				programmed cell death 5
NM_013351				→ T-box 21
NM_005037				→ peroxisome proliferative activated receptor, gamma
NM_018473				uncharacterized hypothalamus protein HT012
NM_006838				methionyl aminopeptidase 2
NM_032472				peptidylprolyl isomerase (cyclophilin)-like 3
NM_001047				steroid-5-alpha-reductase, alpha polypeptide 1 (3-oxo-5 alpha-steroid delta 4-dehydrogenase...
NM_005304				G protein-coupled receptor 41
NM_032410				hook3 protein
NM_021651				PRO0457 protein
NM_012427				kallikrein 5
NM_016125				PTD016 protein
NM_002703				phosphoribosyl pyrophosphate amidotransferase
NM_002431				menage a trois 1 (CAK assembly factor)
NM_001496				→ GDNF family receptor alpha 3
NM_005924				mesenchyme homeo box 2 (growth arrest-specific homeo box)
NM_003550				MAD1 mitotic arrest deficient-like 1 (yeast)
AB004903				→ STAT induced STAT inhibitor-2
NM_001201				bone morphogenetic protein 3 (osteogenic)
NM_016594				→ FK506 binding protein precursor
NM_001236				carbonyl reductase 3
NM_002970				spermidine/spermine N1-acetyltransferase
NM_014624				S100 calcium binding protein A6 (calcyclin)

Figure 26. Partitioning (PAM) Cluster Analysis of Genes: Detail of Cluster 1 showing genes increased in TamR and FasR versus MCF-7. The silhouette plot is shown together with a value for the average silhouette for the cluster. Gene names and accession numbers are shown alongside the heatmap. Genes of interest are highlighted with arrow.

↑TamR; ↑ FasR

Mean silhouette width:
0.337

Accession	Gene
NM_003963	transmembrane 4 superfamily member 5
NM_004219	→ pituitary tumor-transforming 1
NM_030926	integral membrane protein 3
NM_005075	solute carrier family 21 (organic anion transporter), member 3
NM_001222	signal recognition particle 72kD
NM_017775	hypothetical protein FLJ20343
NM_005041	perforin 1 (pore forming protein)
NM_007118	triple functional domain (PTPRF interacting)
D55696	→ legumain
NM_006423	→ Rab acceptor 1 (prenylated)
NM_018928	Protocadherin gamma subfamily C, 4
NM_001214	chromosome 16 open reading frame 3
NM_024498	zinc finger protein 117 (HPF9)
NM_000900	→ matrix Gla protein
NM_002394	solute carrier family 3 (activators of dibasic and neutral amino acid transport), member 2
NM_001481	growth arrest-specific 11
NM_004526	MCM2 minichromosome maintenance deficient 2, mitotin (S. cerevisiae)
NM_018922	protocadherin gamma subfamily B, 1
NM_018923	protocadherin gamma subfamily B, 2

Figure 27. Partitioning (PAM) Cluster Analysis of Genes: Detail of Cluster 2 showing genes increased in TamR and FasR versus MCF-7. The silhouette plot is shown together with a value for the average silhouette for the cluster. Gene names and accession numbers are shown alongside the heatmap. Genes of interest are highlighted with arrow.
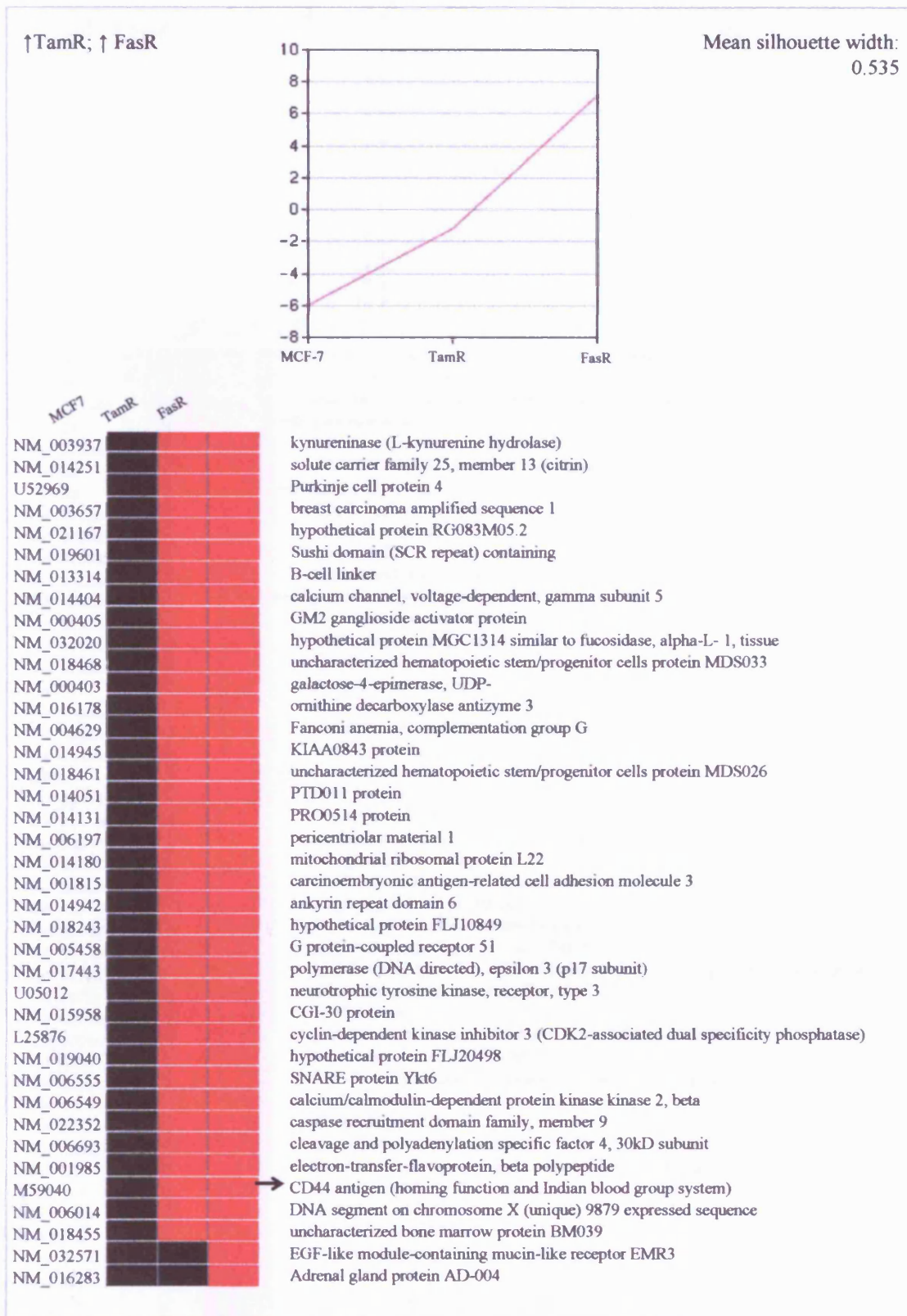
Figure 28. Partitioning (PAM) Cluster Analysis of Genes: Detail of Cluster 3 showing genes increased in TamR and FasR versus MCF-7. The silhouette plot is shown together with a value for the average silhouette for the cluster. Gene names and accession numbers are shown alongside the heatmap. Genes of interest are highlighted with arrow.
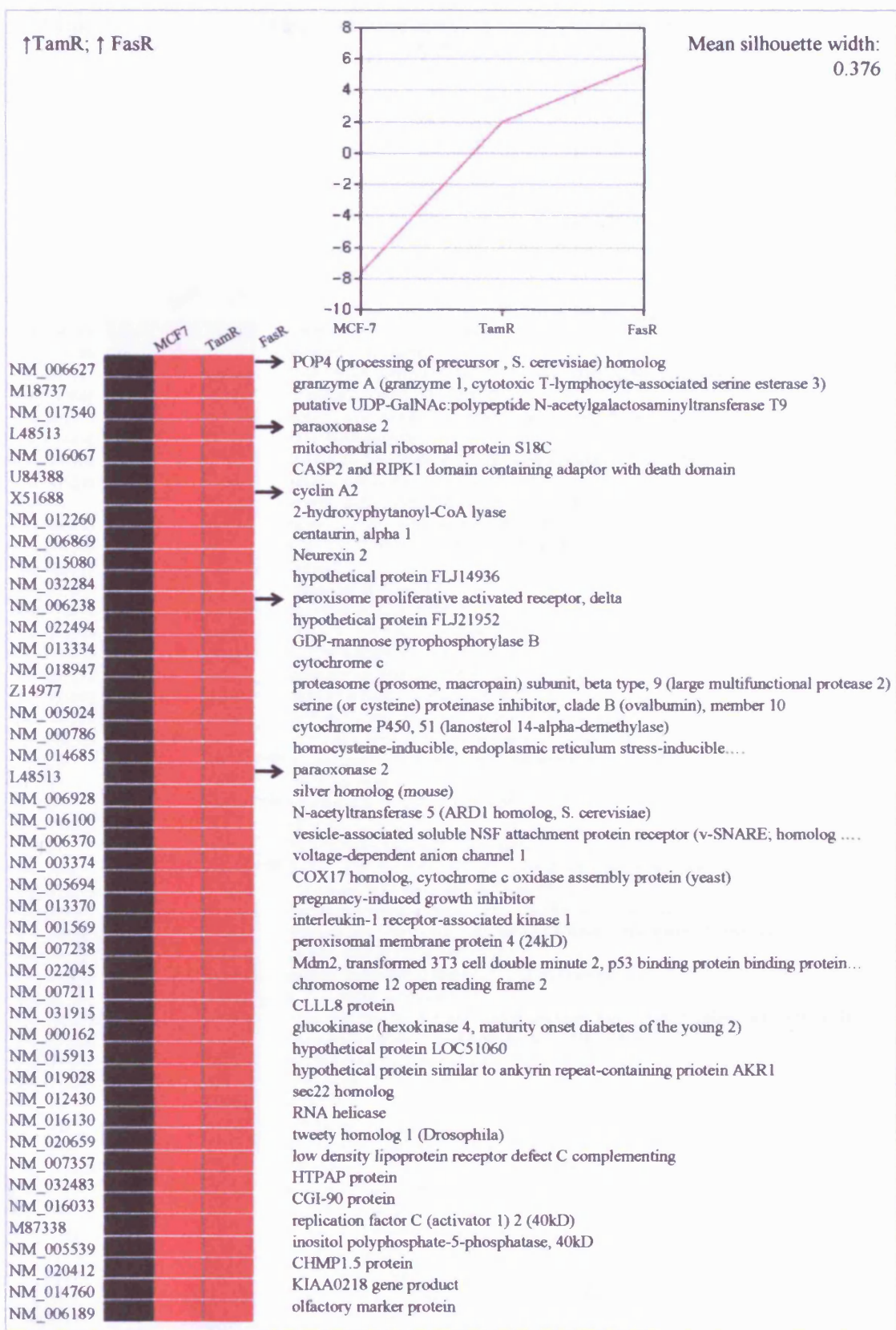
Figure 29. Partitioning (PAM) Cluster Analysis of Genes: Detail of Cluster 4 showing genes increased in TamR and FasR versus MCF-7. The silhouette plot is shown together with a value for *the average silhouette for the cluster. Gene names and accession numbers are shown alongside the* heatmap. Genes of interest are highlighted with arrow.
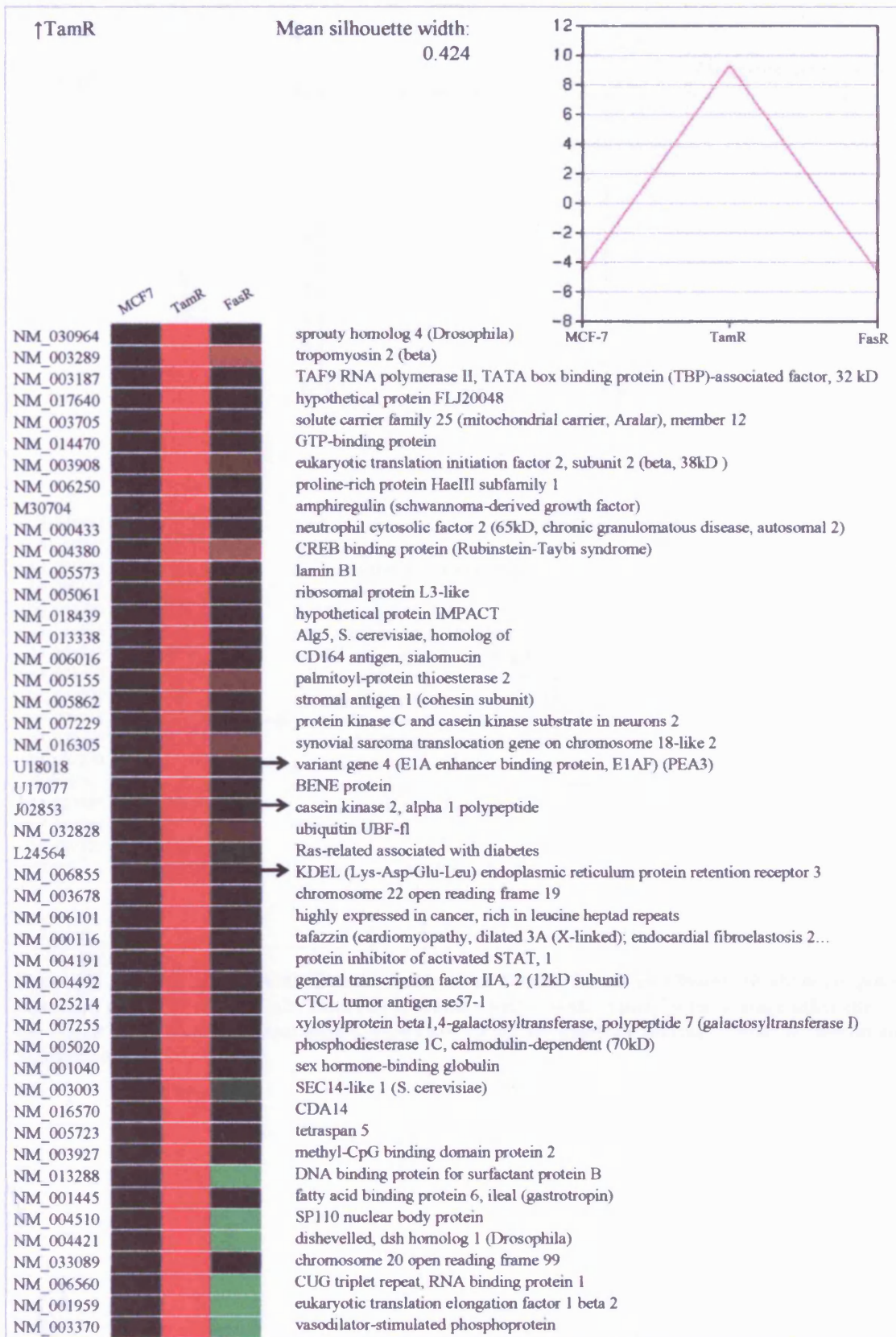
Figure 30. Partitioning (PAM) Cluster Analysis of Genes: Detail of Cluster 7 showing genes largely increased in TamR only. The silhouette plot is shown together with a value for the average silhouette for the cluster. Gene names and accession numbers are shown alongside the heatmap. Genes of interest are highlighted with arrow.
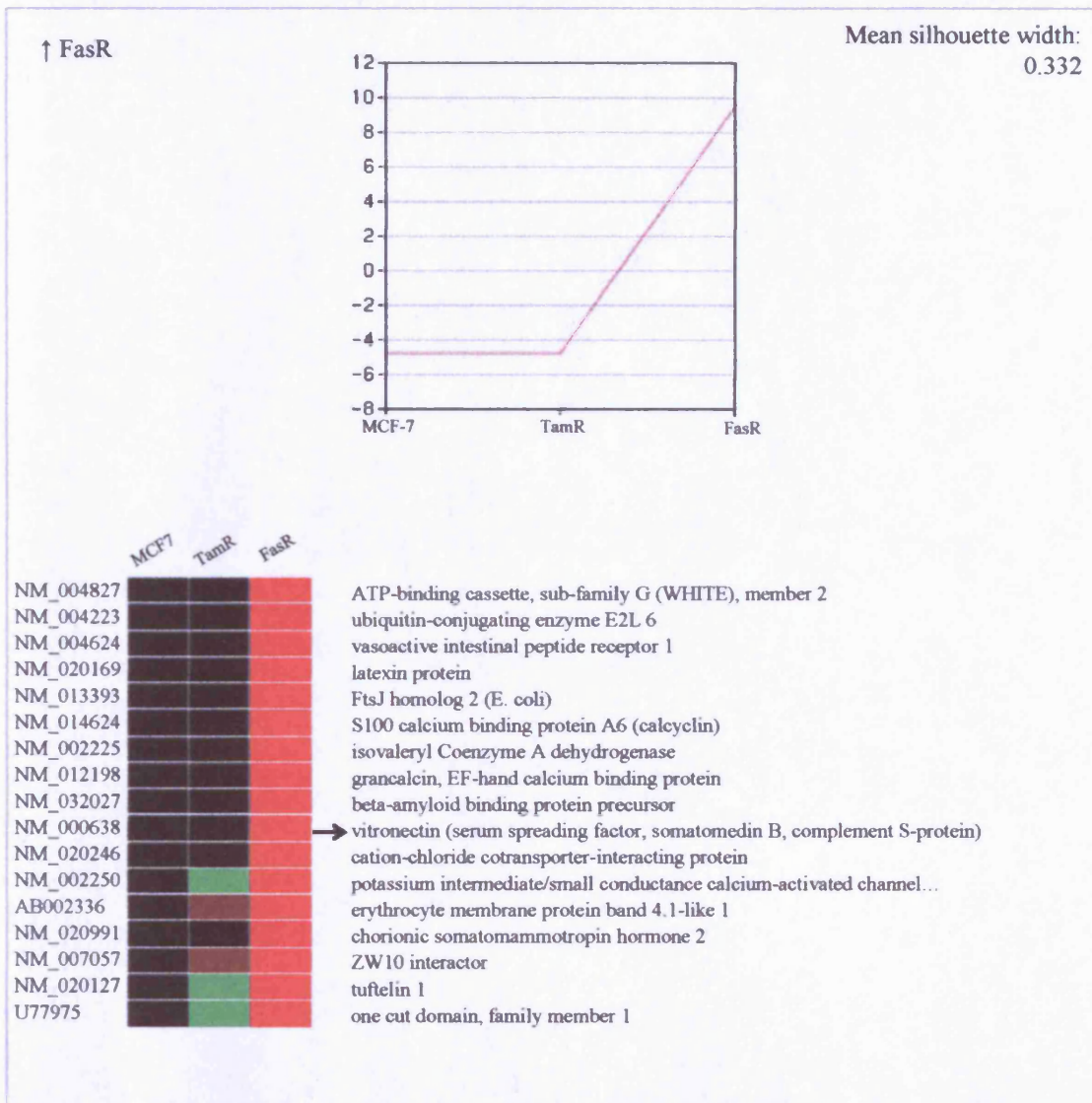
Figure 31. Partitioning (PAM) Cluster Analysis of Genes: Detail of Cluster 10 showing genes increased in FasR only. The silhouette plot is shown together with a value for the average silhouette for the cluster. Gene names and accession numbers are shown alongside the heatmap. Genes of interest are highlighted with arrow.
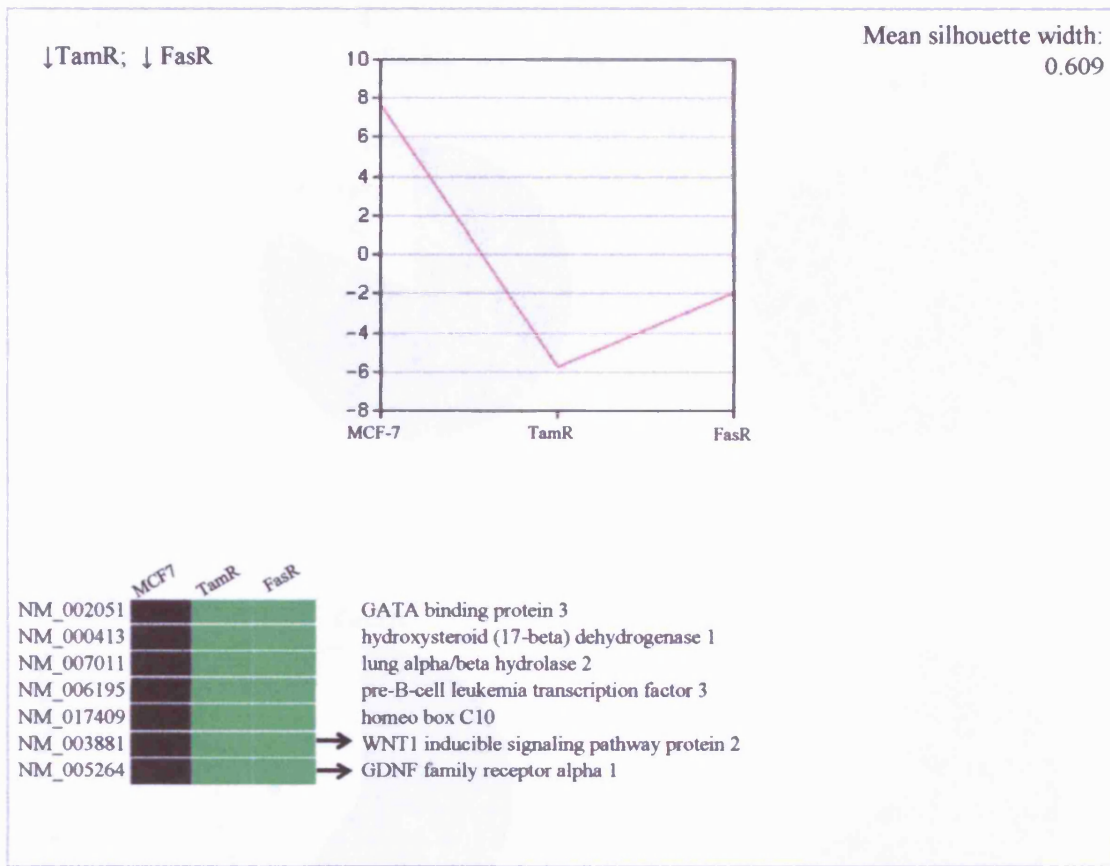
Figure 32. Partitioning (PAM) Cluster Analysis of Genes: Detail of Cluster 13 showing genes at lower expression in TamR and FasR versus MCF-7 cells. The silhouette plot is shown together with a value for the average silhouette for the cluster. Gene names and accession numbers are shown alongside the heatmap. Genes of interest are highlighted with arrow.

proliferation

TamR

18%
6

82%
27

FasR

8%
3

92%
37

anti-proliferation

TamR

40%
8

60%
12

FasR

35%
7

65%
13

cell survival

TamR

23%
6

77%
20

FasR

10%
2

90%
19

Fig 33. Selected Cancer Ontologies for altered genes in TamR and FasR cells. Genes significantly upregulated (■) or downregulated (□) using t-test analysis in either TamR or FasR cells were classified according to their associations to key endpoints of cancer (proliferation, anti-proliferation, cell survival, *apoptosis, angiogenesis, invasion*) *as recorded in Excel-based database. The number of altered genes are* shown within the selected ontology group, with its representation as a percentage of the set.
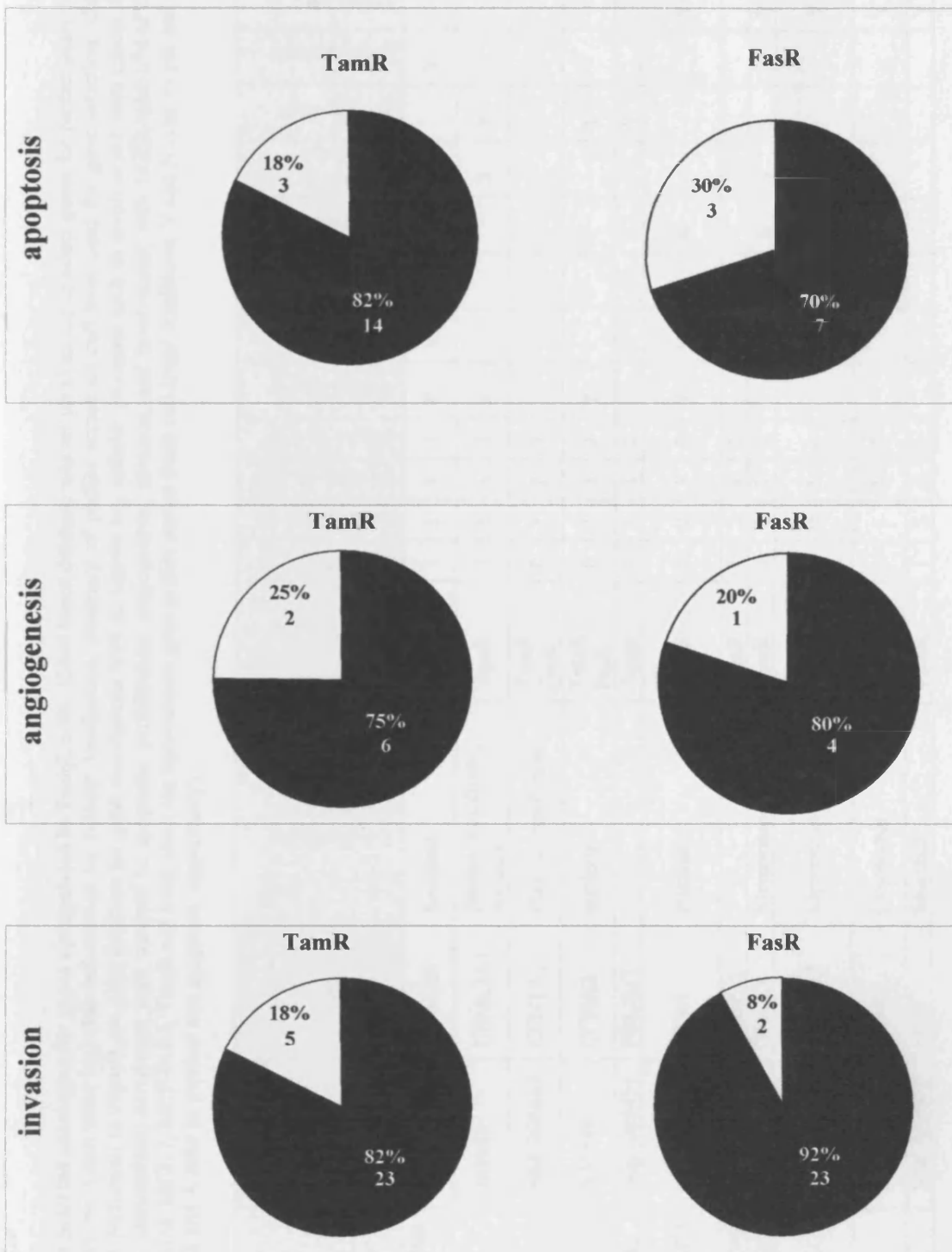
Figure 34. Selected Key Cancer Ontologies for altered genes in TamR and FasR cells. Genes significantly upregulated (■) or downregulated (□) using t-test analysis in either TamR or FasR cells were classified according to their associations to key endpoints of cancer (proliferation, anti-proliferation, cell survival, apoptosis, angiogenesis, invasion) as recorded in Excel-based database. The number of altered genes are shown within the selected ontology group, with its representation as a percentage of the set.

Table 6. Ontology database: Selected ontologies for genes upregulated in TamR cells. Excel based database was set up as an aid to select genes for further analysis, and to manage genelists for reference. Gene table included information on cellular localisation, summary of profile across all cell lines used for gene selection. Detailed examination of literature was performed to expand the gene database for gene associations with its known key cellular processes such as involvement with cancer, breast cancer or resistance, clinical associations, correlation with survival or apoptosis, proliferation, angiogenesis, invasion, and involvement with EGFR/erbB2/MAPK/Ras. (Numbers under columns headed: MCF-7, MCF-7+E2, TamR and FasR show the approximate gene profile across these cell lines/ conditions; Y and N refer to yes and no; G and B refer to good and bad; S and A refer to survival and apoptosis respectively).

Full name	Gene ID	GC ID	Localisation-Cellular/sub cellular	Induced	MCF-7	MCF-7+E2	TamR	FasR	Breast cancer	Cancer	Resistance	Prognosis	Survival/apoptosis	Proliferation	Angiogenesis	Invasion	EGFR/HER2/MAPK/Ras
angiogenin, ribonuclease, RNase A family, 5	NM_001145	RNASE4	Secreted	TamR	1	1	3	1	Y	Y					Y		
casein kinase 2, alpha 1 polypeptide	J02853	CSNK2A1	plasma membrane, nucleus.	TamR	1	1	3	1	Y				S	Y			
centaurin, alpha 1	NM_006869	CENTA1	Plasma membrane	TamR/FasR	0	1	2	3									
cyclin A2	X51688	CCNA2	nucleus	TamR/FasR	0	2	3	3	Y					Y			Y
enigma (LIM domain protein)	NM_005451	PDLIM7		TamR	0	1	3	1						Y			
ets variant gene 4 (E1A enhancer binding protein, E1AF) (PEA3)	U18018	ETV4	Nuclear.	TamR	0	0	3	0	Y	Y		B				Y	Y
FK506 binding protein precursor	NM_016594	FKBP11		TamR	1	2	3	2									Y
GDNF family receptor alpha 3	NM_001496	GFRA3	Membrane	TamR	1	1	3	2		Y	Y	B	S			Y	Y
KDEL (Lys-Asp-Glu-Leu) endoplasmic reticulum protein retention receptor 3	NM_006855	KDELR3	Membrane	TamR	0	0	3	0								Y	Y
legumain	D55696	LGMN	Lysosomal	TamR/FasR	1	1	3	3								Y	Y
matrix Gla protein	NM_000900	MGP	Secreted.	TamR	1	3	3	3								Y	

Table 6 continued

Full name	Gene ID	GC ID	Localisation-Cellular/subcellular	Induced	MCF-7	MCF-7+E2	TamR	FasR	Breast cancer	Cancer	Resistance	Prognosis	Survival/apoptosis	Proliferation	Angiogenesis	Invasion	EGFR/HER2/MAPK/Ras
Neurexin 2	NM_015080	NRXN2	Type I membrane protein	TamR/FasR	0	1	2	3									
paraoxonase 2	L48513	PON2	Membrane	TamR/FasR	0	1	3	3					S				
peroxisome proliferative activated receptor, delta	NM_006238	PPARD	Nuclear	TamR/FasR	0	0	3	3	Y	Y				Y			Y
peroxisome proliferative activated receptor, gamma	NM_005037	PPARG	Nuclear	TamR	0	2	3	2	Y			G	A	Y		Y	
pituitary tumor-transforming 1	NM_004219	PTTG1	Cytoplasmic (some Nuclear)	TamR/FasR	1	2	3	3	Y	Y	Y	B	S	Y	Y	Y	Y
POP4 (processing of precursor , S. cerevisiae) homolog	NM_006627	POP4	Nuclear	TamR/FasR	0	0	3	3						Y			
Rab acceptor 1 (prenylated)	NM_006423	RABAC1		TamR	1	1	3	2					A				
STAT induced STAT inhibitor-2	AB004903	SOCS2	Cytoplasm	TamR	1	1	3	3			Y		S	N			
T-box 21	NM_013351	TBX21	Nuclear	TamR/FasR	0	2	3	2					S			N	
WD40 protein Ciao1	NM_004804	CIAO1	Nuclear	TamR/FasR	1	2	3	2						Y			

Table 7. Ontology database: Selected ontologies for genes upregulated in FasR cells. Excel based database was set up as an aid to select genes for further analysis, and to manage genelists for reference. Gene table included information on cellular localisation, summary of profile across all cell lines used for gene selection. Detailed examination of literature was performed to expand the gene database for gene associations with its known key cellular processes such as involvement with cancer, breast cancer or resistance, clinical associations, correlation with survival or apoptosis, proliferation, angiogenesis, invasion, and involvement with EGFR/erbB2/MAPK/Ras. (Numbers under columns headed: MCF-7, MCF-7+E2, TamR and FasR show the approximate gene profile across these cell lines/ conditions; Y and N refer to yes and no; G and B refer to good and bad; S and A refer to survival and apoptosis respectively).

Full name	Gene ID	GC ID	Localisation-Cellular/sub cellular	Induced	MCF-7	MCF-7+E2	TamR	FasR	Breast cancer	Cancer	Resistance	Prognosis	Survival/ apoptosis	Proliferation	Angiogenesis	Invasion	EGFR/ erbB2 /MAPK /Ras
biliverdin reductase B	NM_000713	BLVRB	Cytoplasmic	FasR	1	1	2	3					S				
CD44	M59040	CD44	Type I membrane protein.	FasR	1	2	2	3	Y			G				Y	
centaurin, alpha 1	NM_006869	CENTA1	Membrane	FasR/ TamR	0	1	2	3									
cyclin A2	X51688	CCNA2	nucleus	FasR/ TamR	0	2	3	3	y					Y			
ornithine decarboxylase 1	NM_002539	ODC1		FasR	1	1	2	3		Y	Y	B		Y		Y	Y
paraoxonase 2	L48513/ NM_000305	PON2	Membrane	FasR/ TamR	0	1	3	3					S				
peroxisome proliferative activated receptor, delta	NM_006238	PPARD	Nuclear	FasR/ TamR	0	0	3	3	Y	Y				Y			Y
pituitary tumor-transforming 1	NM_004219	PTTG1	Cytoplasmic (some Nuclear)	FasR/ TamR	1	2	3	3	Y	Y	Y	B	S	Y	Y	Y	Y
pituitary tumor-transforming 3	NM_021000	PTTG3	cytoplasm; nucleus	FasR	1	3	2	3		Y			S	Y			Y
POP4 (processing of precursor, S. cerevisiae) homolog	NM_006627	POP4	Nuclear	FasR/ TamR	0	0	3	3						Y			
T-box 21	NM_013351	TBX21	Nuclear	FasR/ TamR	0	2	3	2					S			N	

Table 7. continued

Full name	Gene ID	GC ID	Localisation-Cellular/sub cellular	Induced	MCF-7	MCF-7+E2	TamR	FasR	Breast cancer	Cancer	Resistance	Prognosis	Survival/ apoptosis	Proliferation	Angiogenesis	Invasion	EGFR/ erbB2 /MAPK /Ras
vitronectin (serum spreading factor, somatomedin B, complement S-protein)	NM_000638	VTN	Extracellular.	FasR	0	0	0	3							Y	Y	
WD40 protein Ciao1	NM_004804	CIAO1	Nuclear	FasR/ TamR	1	2	3	2						Y			

Table 8. Ontology database: Selected ontologies for genes downregulated in TamR cells. Excel based database was set up to select genes for further analysis, and manage genelists for reference. Gene table included information on cellular localisation, summary of profile across all cell lines used for gene selection. Detailed examination of literature was performed to expand the gene database for gene associations with its known key cellular processes such as involvement with cancer, breast cancer or resistance, clinical associations, correlation with survival or apoptosis, proliferation, angiogenesis, invasion, and involvement with EGFR/erbB2/MAPK/Ras. (Numbers under columns headed: MCF-7, MCF-7+E2, TamR and FasR show the approximate gene profile across these cell lines/ conditions; Y and N refer to yes and no; G and B refer to good and bad; S and A refer to survival and apoptosis respectively).

Full name	Gene ID	GC ID	Localisation-Cellular/sub cellular	Suppressed	MCF-7	MCF-7+E2	TamR	FasR	Breast cancer	Cancer	Resistance	Prognosis	Survival/ apoptosis	Proliferation	Angiogenesis	Invasion	EGFR/ erbB2 /MAPK /Ras
GDNF family receptor alpha 1	NM_005264	GFRA1	Attached to membrane by GPI-anchor	TamR/ FasR	1	1	3	3		Y			S	Y			
WNT1 inducible signaling pathway protein 2	NM_003881	WISP2	Secreted	TamR/ FasR	1	1	3	3	Y	Y							

Table 9. Ontology database: Selected ontologies for genes downregulated in FasR cells. Excel based database was set up to aid to select genes for further analysis, and manage genelists for reference. Gene table included information on cellular localisation, summary of profile across all cell lines used for gene selection. Detailed examination of literature was performed to expand the gene database for gene associations with its known key cellular processes such as involvement with cancer, breast cancer or resistance, clinical associations, correlation with survival or apoptosis, proliferation, angiogenesis, invasion, and involvement with EGFR/erbB2/MAPK/Ras. (Numbers under columns headed: MCF-7, MCF-7+E2, TamR and FasR show the approximate gene profile across these cell lines/ conditions; Y and N refer to yes and no; G and B refer to good and bad; S and A refer to survival and apoptosis respectively).

Full name	Gene ID	GC ID	Localisation-Cellular/sub cellular	Suppressed	MCF-7	MCF-7+E2	TamR	FasR	Breast cancer	Cancer	Resistance	Prognosis	Survival/ apoptosis	Proliferation	Angiogenesis	Invasion	EGFR/ erbB2 /MAPK /Ras
GDNF family receptor alpha 1	NM_005264	GFRA1	Attached to membrane by GPI-anchor	TamR/ FasR	1	1	3	3		Y			S	Y			
WNT1 inducible signaling pathway protein 2	NM_003881	WISP2	Secreted	TamR/ FasR	1	1	3	3	Y	Y							

3.2.3 Partitioning (PAM) Analysis of Differentially Expressed Genes in TamR and FasR cells

The number of clusters chosen for PAM analysis in GeneSifter software was determined empirically where a compromise was made between mean silhouette width and number of manageable clusters. In addition, as hierarchical cluster analysis had been performed on the dataset, the dendrogram and heatmap profiling conditions MCF-7, TamR and FasR indicates 12-16 clusters were ultimately tested in PAM.

Following testing this cluster range, PAM analysis selecting for 16 clusters produced a range of silhouette plots (Fig.25). For ease of interpretation, these have been ranked manually in order of similarities. One cluster (5) was subsequently poorly resolved so was manually divided into two clusters 5 and 14, giving a total of 17 clusters. Akin to HCA, in general, PAM analysis produced clear and distinct clusters, although there appeared to exist some degree of profile similarities. These dominant clusters include genes which are upregulated in both TamR and FasR (clusters 1-4; Figs.26-29 [containing T-box21, PPAR-γ, GFRα3, STAT-i2, FK506-bp, PTTG1, Legumain, Rab acceptor, Matrix Gla protein, CD44, POP4, paroxonase2, cyclin A2, alpha centaurin, PPAR-δ]), in only TamR (clusters 5-9 [containing Angiogenin, Homer2, Enigma, PEA3, casein kinase 2, KDEL] eg. Fig.30) or only FasR (clusters 10-12 [containing Vitronectin]; eg. Fig.31), or decreased in both forms of resistance (clusters 13-15 [containing GFRα1, WISP2]; eg. Fig.32) or individual forms of resistance (clusters 16-17). Again PAM revealed alongside the significant genes induced in both forms of resistance a considerable breadth of further genes with similar expression profiles (clusters 1-4).

3.2.4 Gene Ontological Examination

Further gene selection was performed manually to prioritise the entire t-test significant gene list for those which have previously been associated with cancer, in particular any relationship in breast tumour progression or therapeutic response, if available, role in signal transduction pathways (eg. EGFR, MAPK), or in influencing key endpoints of cancer, such as proliferation, cell survival, invasion and angiogenesis (see also Fig.33- Fig.34). The extensive research of genes identified in this study using online literature database searching, according to sources including Medline, GeneCard and GeneSifter information, has resulted in the establishment of an Excel database listing genes by names and ID according to such categories. An example of the database with selected columns has been reproduced in tables 6-9 and is also currently located as a shared resource at the TCCR. Additional information indicates whether genes were significantly induced using t-test and cellular localisation.

Broad analysis of the t-test significant (n=348) genes within the database, according to known ontology, revealed that 33 and 40 proliferation-related genes were altered in TamR and

FasR cells respectively versus MCF-7 cells. Interestingly, in both resistant states, the majority of genes were upregulated, with a possible higher proportion of these induced genes in FasR cells. In contrast, a lower number of antiproliferative genes were altered in the resistant states. Examination of genes related positively to cell survival showed 26 altered in TamR and 21 in FasR. Again the majority were upregulated with possibly a greater proportion of these induced in FasR cells. Examination of genes associated to tumour cell invasion revealed 28 altered in TamR and 25 in FasR cells, again with the majority upregulated in FasR, and again, a higher proportion of these in FasR cells. However, lower number of gene changes were observed from the examination of apoptotic and angiogenesis-related genes, although the majority of these genes were upregulated in the resistant models.

3.2.5   t-test, HCA and PAM are Complimentary Methods of Data Analysis

By the use of T-test, HCA and PAM Data analysis, together with detailed ontological examination, genes were subsequently selected for PCR analysis (highlighted in Tables 6-9 and listed in the database [see CD-ROM]).

Genes which were shared by t-test significance as both forms of resistance, were highlighted as priority, provided a favourable ontology with regards to adverse cancer cell endpoints was found. However, genes which demonstrated reasonable ontologies in terms of relevance to cancer endpoints (or favourable targeting localisation) were also taken into account, if a favourable expression profile was demonstrated within a suitable cluster using HCA and/or PAM analysis. Both HCA and PAM demonstrate distinct clusters of genes (Fig.19 and Fig.25). On closer inspection, many of the strong clusters, such as those exhibiting upregulation in both TamR and FasR cells using HCA (Fig.22 and Fig.23) and PAM (Fig.26-29) house potential candidates for further exploration, alongside genes significant by t-test with interesting ontology. HCA and PAM analysis revealed the true breadth of "shared" induced genes in TamR and FasR cells. Within HCA there were two substantial clusters of genes which demonstrated increased expression in both TamR and FasR cells relative to MCF-7. Although generally, upregulated in both resistant states, the first noticeable difference between HCA clusters 4 and 14 (Fig.24 and Fig.23) is that visually there exists a subtle predominance of high expression in one cell line over the other for many genes. Where cluster 4 demonstrates higher expression in TamR cells, there is a tendency for genes in cluster 14 to be more highly expressed in FasR over TamR according to HCA. This profile across MCF-7, TamR and FasR is mirrored using PAM analysis (Fig.26-29), where, for example, PAM cluster 1 (Fig.26) has a predominance of TamR expression over FasR in the silhouette plot. Exploration of HCA cluster 4 and PAM cluster 1 revealed (Fig.24 and Fig.26) a number of signalling genes with interesting ontologies common to both these clusters, such as GFRα3, PPAR-γ, STAT-i2 and FK506bp, all

significantly induced in TamR with a trend for increase in FasR, alongside the t-test significant shared gene, T-Box21.

In contrast to PAM cluster 1, PAM cluster 2 silhouette plot shows a slight increase in FasR relative to TamR expression compared to PAM cluster 1, and PAM clusters 3 and 4 a higher still expression in FasR cells, such that this exceeds the TamR level (Fig.27-29). These clusters house a number of t-tested significant genes which have been taken into consideration for further analysis, based on ontology and cancer endpoints, such as PTTG1, PPAR-δ, cyclin A2, paraoxonase 2, alpha centaurin, legumain. Some of these genes are also present in HCA cluster 14 (Fig.23). It is also worth noting that within HCA cluster 14, a sub-cluster of genes which, although it exhibits higher expression in both resistant cells versus MCF-7, has an unusually higher expression in FasR cells, exemplified by the gene for CD44. This sub-cluster has been resolved into the silhouette plot using PAM analysis into cluster 3 (Fig.28).

Genes which have an increased expression in TamR cells only have been identified in groups including cluster 3 using HCA (Fig.21). Among these, particularly ontologically appealing genes that are robustly increased using t-testing (table 6-7) fall into a distinct, cluster 7 using PAM analysis (Fig.30) which is markedly TamR induced from very low expression. These are exemplified by PEA3, KDEL and casein kinase 2. Similarly, genes which are increased in FasR cells only (eg. Vitronectin) can be identified, not only using t-test analysis (table 7), but as those genes which are grouped using HCA (cluster 13; Fig.23) and sharing a similar profile using PAM analysis (cluster 10; Fig.31). Genes which are downregulated in TamR and FasR genes distinctly fall into HCA cluster 2 (Fig.20) and a small amount in cluster 9. It is worth noting that as well as robust selection through t-test analysis (table 8-9) a number of these are also represented within PAM cluster 13 (Fig.32), such as WISP2 and GFRα1.

3.3   Ontological Examination & RT-PCR for Selected Genes

As described above, genes for verification were initially selected according to their array expression profile across TamR and FasR cells according to t-test and HCA/PAM relative to MCF-7 cells, and basic ontology (exemplified in tables 6-9), focussing predominantly on genes with increased expression. However, a full ontological examination of these selected genes was subsequently also a major contributing factor in the final choice of gene selection (see also CD-ROM included in thesis). These genes of interest were then subject to PCR verification of the induced profile.

RT-PCR assessment was performed initially on the RNA samples from the various cell lines which were used to hybridise to the array, previously extracted using the optimised protocol (section 3.1.6). Specific primers for each gene were either designed using Primer3 software or predesigned by Clontech (BD Biosciences) coamplifying with β-actin for normalisation, where

possible. The genes analysed and primer sequences are displayed in Tables 1 and 2 in the methods section, alongside their optimised PCR conditions (cycle number, annealing temperature, etc). There were 25 induced genes and 2 suppressed genes evaluated, as in table 1.

The very recent introduction of the Affymetrix HGUA-133 genechip microarray system in TCCR allowed further profile verification in equivalent MCF-7, MCF-7+E2, TamR and FasR samples, and has been included alongside Atlas Plastic 12K Microarray and/or RT-PCR profiles for the purposes of further confirming the final genelist.

3.3.1 Genes Upregulated in TamR and FasR Cells

3.3.1.1 Pituitary Tumour Transforming 1 (PTTG1)
Detailed Ontological Results

Pituitary tumour transforming gene (PTTG1, or securin) is reported to encode a protein which is localised within the cytoplasm as well as partially in the nucleus (Chien and Pei, 2000), and was originally identified from rat pituitary tumour cells (Pei and Melmed, 1997); (Chen et al., 2000) have also reported two PTTG1 homologues, PTTG2 and PTTG3 with around a 90% sequence homology at the protein level.

In normal human tissues, the expression of PTTG is restricted in a tissue-specific manner, with high levels in the testis, but low levels detectable in other tissues, such as the thymus, colon, and small intestine. In contrast, PTTG is expressed at high levels in a variety of human primary tumours, as well as tumour cell lines, including carcinomas of the ovary, lung, testis, kidney, colon, thyroid, pituitary, liver, adrenal, breast, prostate, melanoma, leukaemia, and lymphoma (Kakar, 1998, Zhang et al., 1999, Dominguez et al., 1998, Wang et al., 2001, Puri et al., 2001, Yu et al., 2000b, Heaney et al., 2001, Heaney et al., 2000). In a recent study investigating the expression of PTTG1 in breast cancers, a direct correlation was found between expression levels and lymph node infiltration and higher degree of tumour recurrence (Solbach et al., 2004), but no reports have mentioned this gene in relation to endocrine response or acquisition of resistance.

The level of PTTG expression is reported to be increased in rapidly proliferating cells and is regulated in a cell cycle-dependent manner, peaking at G2/M phase (Ramos-Morales et al., 2000). PTTG1, by virtue of its function as a securin, ensures that there is no premature separation of sister chromatids in normal cells through the inhibition of separin (Nasmyth, 2005).

Consistent with its role as a cell cycle regulatory protein, PTTG1 overexpression was observed to disrupt sister chromatid separation leading to aneuploidy, (Christopoulou et al., 2003, Yu et al., 2003). Aneuploidy (an abnormal number of chromosomes) is characterised by the emergence of macro/micro/multiple nuclei in tumour cells and is common in tumours

including breast cancer (Kops et al., 2005). Overexpression of PTTG1 increases cell proliferation, induces cellular transformation *in vitro*, and promotes tumour formation *in-vivo* (Kakar and Jennes, 1999), suggesting an oncogenic role for the PTTG1 gene (Schwab et al., 1985, Land et al., 1983). In addition to its tumour forming capabilities, PTTG1 has also been demonstrated to prime gene expression. It was shown to stimulate fibroblast growth factor (FGF-2)- mediated angiogenesis and in pituitary tumours upregulated VEGF expression (McCabe et al., 2002). In thyroid cancer, this angiogenic capabilities of PTTG1 were demonstrated when it was reported to have regulated angiogenic and apoptotic-associated genes (Kim et al., 2006). Additionally, the expression of c-myc can also be regulated by PTTG1 (Pei, 2001).

With regards to the regulation of PTTG1, at a protein and mRNA level, in a glioma cell line, EGF, TGF-alpha, and MAPK signalling were demonstrated to upregulate PTTG1 (Tfelt-Hansen et al., 2004), and also insulin/IGF-1 via PI3K/AKT (Chamaon et al., 2005, Thompson and Kakar, 2005). PTTG also houses a SP1 and NF-Y binding promoter (Clem et al., 2003), as well as an insulin response element (IRE), and AP1/ AP2 binding sequences , suggesting growth factor regulation (Kakar and Jennes, 1999). It is also MAPK activation, as well as interaction with a PTTG binding factor (PBF) which may facilitate the nuclear translocation of PTTG1 (Pei, 2000) and hence its function. More recently, the p53 tumour suppressor gene has been demonstrated to directly bind to the promoter of PTTG1, thus suppressing its tumour-forming capabilities (Kho et al., 2004). However, p53-dependant apoptosis can involve PTTG1, but where there is an absence/failure of functional p53, PTTG1 can promote aneuploidy (Yu et al., 2000a).

RT-PCR Verification Results

This study demonstrates the significant upregulation of PTTG1 in both TamR and FasR cell lines, in both array (p=0.013 and 0.014 respectively) and by subsequent PCR studies (p=0.0888 and p=0.0057 respectively in Fig.35) versus MCF-7. These results also show a small induction by oestradiol in MCF-7 (which is in accordance with other reports; (Tfelt-Hansen et al., 2004). The profile is also verified using Affymetrix analysis where the gene is readily detectable. The "shared" induced gene was considered as high priority for further studies involving protein analysis based both on ontology, profile and verification. .
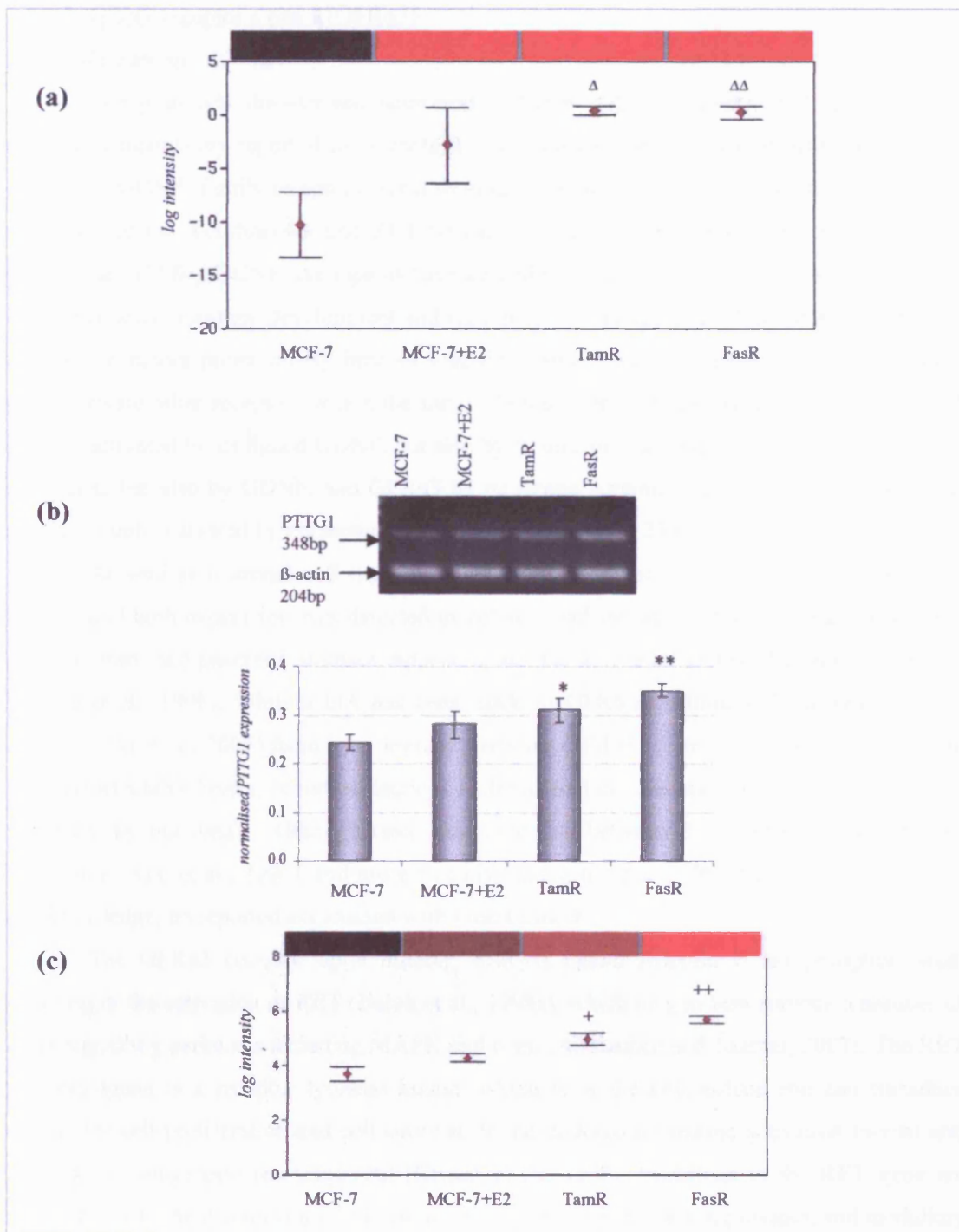
Figure 35. PTTG1 gene is expression profile in MCF-7, TamR, FasR cell lines. PTTG1 mRNA was monitored as (a) using Atlas Plastic Human 12k Microarrays. Log intensity graphical output and heatmap are shown. (b) by PCR analysis using primers for PTTG1 co-amplified with β-actin (normalisation purposes). PCR products separated on an agarose gel were visualised by ethidium bromide staining. Representative PCR profile is shown from triplicate experiments. PCR signals were then subject to densitometric analysis and normalised data plotted (plot shows standard error). (c) using Affymetrix HG-U133A gene chips. (Identical RNA preparations were used for all studies of mRNA expression). Additional controls were provided by MCF-7 cells subject to oestradiol treatment. (Δp=0.013 and ΔΔp=0.014 respectively for TamR and FasR relative to MCF-7; *p=0.0888 and **p=0.0057 respectively for TamR and FasR relative to MCF-7; +p=0.0166 and ++p=0.002 respectively for TamR and FasR relative to MCF-7 [Students t-test]).

3.3.1.2 GDNF receptor alpha 3 (GFRα3)

Detailed Ontological Results

The glial cell line-derived neurotrophic factor (GDNF) family of 4 receptors and associated ligands are reported to promote the survival and maintenance of different neuronal cell types. GDNF family receptors signal through a complex composed of a GDNF family co-receptor and the membrane-bound RET tyrosine-kinase receptor (Sariola and Saarma, 2003, Baloh et al., 1998a). GDNF-like ligands have several roles outside the nervous system, such as a morphogenesis in kidney development and regulating spermatogonial differentiation. Although the four receptors preferentially bind to specific ligands, some of these ligands can weakly cross activate other receptors within the family (Airaksinen and Saarma, 2002). Thus, GFRα1 may be activated by its ligand GDNF, but also by Neurturin, and Artemin; GFRα2 by its ligand Neurturin, but also by GDNF; and GFRα3 by its ligand Artemin, but also by GDNF whereas GFRα4 is only activated by Persephin (Airaksinen and Saarma, 2002).

As well as neuronal cell types, GFRα3 has been found to be expressed in peripheral tissues, and high expression was detected in colon, small intestine, pancreas, heart, testis, and prostate, testis and pancreas, stomach, appendix, and the urogenital system (Baloh et al., 1998b, Masure et al., 1998). While a link has been made to GFRα signalling and pancreatic cancer invasion (Ito et al., 2005) there is no literature relating GFRα3 in breast cancers to date, it may be in undetectable levels, or indeed induced under altered cellular states (such as resistance, as suggested by our data). Although there exists the link between RET and medullary thyroid carcinoma (Asai et al., 2006), and more recently pancreatic cancer (Ito et al., 2005), there is to our knowledge, no reported association with breast cancer.

The GFRα3 receptor upon binding with its ligand Artemin is autophosphorylated, resulting in the activation of RET (Baloh et al., 1998a), which may in turn activate a number of other signalling pathways including MAPK and c-src (Airaksinen and Saarma, 2002). The RET protooncogene is a receptor tyrosine kinase, which is at the cell-surface and can transduce signals for cell proliferation and cell survival. It can undergo oncogenic activation *in-vivo* and *in-vitro* by cytogenetic rearrangement (Grieco et al., 1990). Mutations in the RET gene are associated with the disorders multiple endocrine neoplasia, Hirschsprung disease, and medullary thyroid carcinoma (Asai et al., 2006), and more recently, as mentioned, linked to pancreatic cancer (Ito et al., 2005). However, there is, to our knowledge, no reports between RET and breast cancer, other than a study which induced overexpression of RET/PTC fusion protein (a frequently observed chimeric gene in papillary thyroid cancer) was able to induce mammary tumours in mice (Portella et al., 1996).
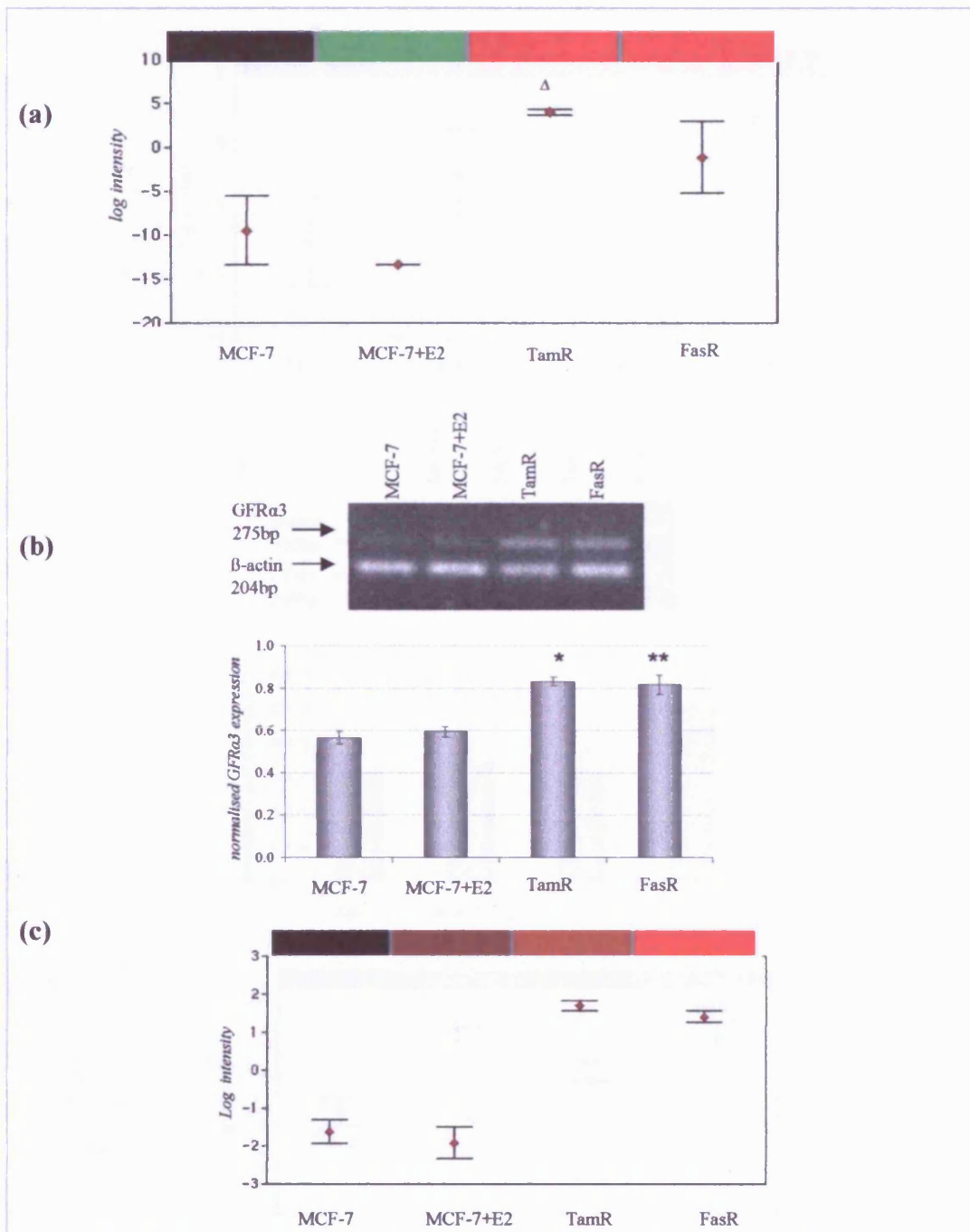
Figure 36. GFRα3 gene is expression profile in MCF-7 TamR and FasR cell lines. GFRα3 (glial cell-derived neurotrophic factor [GDNF] receptor alpha 3) mRNA was monitored as (a) using Atlas Plastic Human 12k Microarrays. Log intensity graphical output and heatmap are shown. (b) by PCR analysis using primers for GFRα3 co-amplified with β-actin (normalisation purposes). PCR products separated on an agarose gel were visualised by ethidium bromide staining. Representative PCR profile is shown from triplicate experiments. PCR signals were then subject to densitometric analysis and normalised data plotted (plot shows standard error). (c) using Affymetrix HG-U133A gene chips. (Identical RNA preparations were used for all studies of mRNA expression). Additional controls were provided by MCF-7 cells subject to oestradiol treatment. (Δp=0.0136 for TamR relative to MCF-7; *p=0.0035 and **0.0131 respectively for TamR and FasR relative to MCF-7; +p<0.001 and ++p=*0.001 respectively for TamR and FasR relative to MCF-7 [statistical analysis performed using students t-test]).
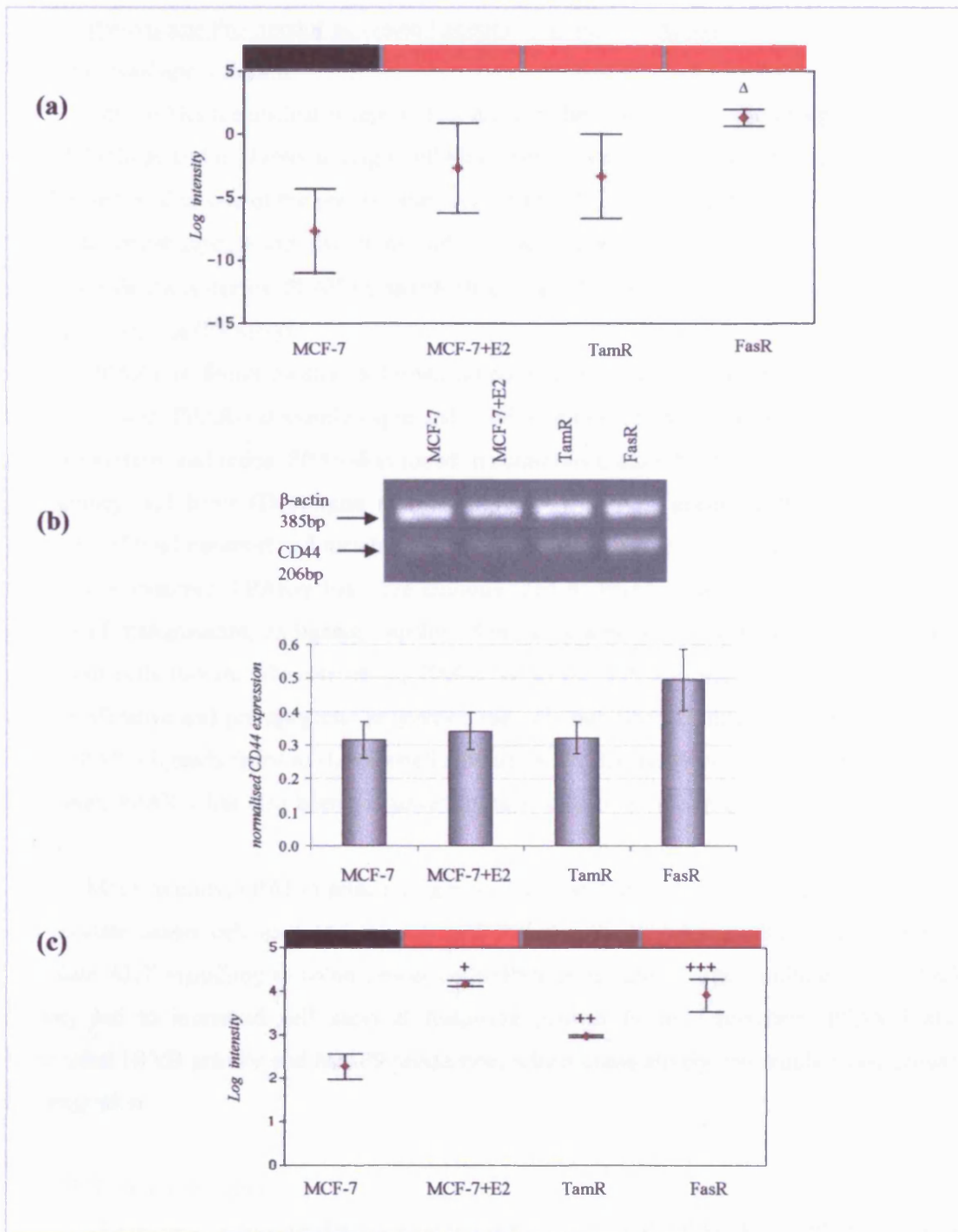
Figure 37. CD44 gene in resistant cells. CD44 antigen mRNA was monitored as (A) using Atlas Plastic Human 12k Microarrays. Log intensity graphical output and heatmap are shown. (B) by PCR analysis using primers for CD44. β-actin was also amplified (normalisation purposes). PCR products separated on an agarose gel were visualised by ethidium bromide staining. Representative PCR profile is shown from triplicate experiments. PCR signals were then subject to densitometric analysis and normalised data plotted (plot shows standard error). (C) using Affymetrix HG-U133A gene chips. (Identical RNA preparations were used for all studies of mRNA expression). Additional controls were provided by MCF-7 cells subject to oestradiol treatment. (Δp=0.038 for FasR relative to MCF-7; +p=0.0016, ++p=*0.0306 and p=0.0235 respectively for MCF-7+E2, TamR and FasR relative to MCF-7 [students t-test];

RT-PCR Verification Results

Microarray profiles obtained in this study indicate that in both TamR and FasR cells there is an increased level of GFRα3 gene from a state of no detectable gene expression in parental cells, this being significant in TamR cells (p=0.0136), by t-test (Fig.36). There was no gene induction with oestradiol treatment of MCF-7 cells. The profile of induction in both resistant cell lines was confirmed by PCR studies, where both TamR and FasR cells showed significant induction over control cells (p<0.0035 and 0.0131 respectively), and the induction was further confirmed by Affymetrix analysis. This gene was considered as high priority for future studies based on its ontology, microarray profile and RT-PCR verification.

3.3.1.3 CD44

Detailed Ontological Results

Cell surface adhesion receptors, such as CD44, act as cell anchors, regulate cell mobility, and allows cooperation between cells and the surrounding environment. CD44 is a broadly distributed transmembrane glycoprotein that plays a critical role in a variety of cellular behaviours, including adhesion, migration, invasion, and survival (Marhaba and Zoller, 2004). CD44 mediates cell–cell and cell–matrix interactions in a large part through its affinity for hyaluronan (HA), a glycosaminoglycan constituent of extracellular matrices, but also potentially through its affinity for other ligands such as osteopontin, collagens, and matrix metalloproteinases (MMPs). The CD44 family of transmembrane glycoproteins, and CD44 variants, that also have been implicated in mammary tumour progression (Cichy and Pure, 2003). Indeed, in our own tamoxifen resistant TamR cells, which display a more aggressive phenotype, and have demonstrated increased EGFR signalling (Knowlden et al., 2003), an association of this pathway and CD44 via β-catenin activity was suggested, where β-catenin is implicated with invasive capacity in these cells (Hiscox et al., 2006).

RT-PCR Verification Results

Microarray study revealed CD44 as significantly upregulated in FasR cells (p=0.038) by t-test with a trend in TamR cells, as further indicated by HCA/PAM relative to MCF-7 cells, a pattern also suggested by the PCR profile (Fig.37) and Affymetrix arrays, although in both instances FasR induction predominated. An upregulation of CD44 protein in TamR and Tam-R cells has previously been shown within our laboratory, and there is an ongoing interest for study of its role in resistance using siRNA with examination of key CD44 variants (*M. Harper, unpublished data*).

3.3.1.4 Peroxisome Proliferator-activated Receptor-Delta; (PPAR-δ) *and*

Peroxisome Proliferator-activated Receptor-Gamma; (PPAR-γ)

Detailed Ontological Results

The PPARs are nuclear receptors that mediate the effects of diverse group of chemicals of both biologic and nonbiologic origin. PPARs heterodimerise with 9-cis retinoic acid receptor (RXR), and bind to one of the peroxisome proliferator (PP) response elements (PPRE) residing within the target gene to stimulate transcription. (Desvergne and Wahli, 1999). Three separate genes encode the isoforms: PPAR alpha (PPAR-α), PPAR beta (PPAR-β) (also named delta -δ), and PPAR gamma (PPAR-γ).

PPARα is found mostly in brown adipose tissue and liver, then kidney, heart and skeletal muscle. PPAR-γ is mainly expressed in adipose tissue and, to a lesser extent, the colon, immune system, and retina. PPAR-δ is found in numerous tissues, but to a greater degree in the gut, kidney and heart (Desvergne and Wahli, 1999). PPARs generally function to effect pathways of lipid transport and metabolism, but have shown both a positive and negative role in cancer. For example, PPAR-γ has been demonstrated to have an antiproliferative effect in a number of malignancies, its ligands capable of inducing terminal differentiation and apoptosis of tumour cells *in-vitro* (Demetri et al., 1999). However PPAR-γ ligands in cells may show anti-proliferative and pro-apoptotic properties, the only published clinical trial in breast cancer using PPAR-γ ligands failed to show benefits in metastatic disease (Fenner and Elstner, 2005). Moreover, PPAR-γ has also been suggested to have a positive role in colon cancer (He et al., 1999).

More recently, PPAR-δ selective agonists have been shown to increase growth in breast and prostate cancer cell lines and primary endothelial cells. PPAR-δ has also been shown to modulate AKT signalling in colon cancer cells (Park et al., 2001). The resulting higher AKT activity led to increased cell survival following growth factor deprivation. PPAR-δ also potentiated NFκB activity and MMP9 production, which cumulatively can regulate cell growth and migration.

RT-PCR Verification Results

The microarray results demonstrate the induction of both PPAR-δ and PPAR-γ (Fig.38 and Fig.39) in TamR cells (p=0.025 for both). FasR cells also showed an induction in both PPAR types, apparent from HCA/PAM analysis, although this was significant only for PPAR-δ by t-test (p=0.026). However, following PCR, PPAR-δ showed a modest increase in FasR cells, a profile mirrored by Affymetrix profiling. PPAR-γ was significantly increased in TamR cells by PCR (p=0.0016), with some induction also in FasR, confirmed by Affymetrix analysis. In total, there was some indication of a shared profile for PPARγ, although ontology was

controversial, and there was a less convincing profile for PPARδ, despite an interesting ontology. In total, these genes were not deemed high priority.

3.3.1.5 α-Centaurin (p42IP4)

Detailed Ontological Results

The centaurin family of proteins contain a pleckstrin homology domain, a module which mediates phosphoinositide binding in numerous proteins, hence a signalling role (Leevers et al., 1999). In addition they are regulatory proteins for ARFS, GTP binding proteins functioning in vesicular trafficking and cytoskeletal regulation (Chavrier and Goud, 1999). A nuclear and cytoplasmic protein, alpha centaurin is recruited to the plasma membrane upon EGF-dependent activation of phosphatidylinositol 4,5-diphosphate (PtdInsP2) 3-kinase (Sedehizade et al., 2005). It has also been reported to associate with phosphorylated PKC (Zemlickova et al., 2003) and casein kinase 1 (Zemlickova et al., 2003).

RT-PCR Verification Results

Our microarray data revealed that there is a significant induction in α-centaurin in both resistant TamR and FasR cells (p=0.031 and 0.024) (Fig.40), also indicated with HCA/PAM. However, PCR data demonstrated only a modest induction in FasR cells alone. This more obvious FasR effect was also suggested by Affymetrix analysis. While there was an increase with oestradiol on the arrays, this did not persist at the PCR level. In total, this was not a high priority gene since PCR profile does not confirm α-centaurin as a shared gene.

3.3.1.6 POP4 (rpp29)

Detailed Ontological Results

POP4 is a constituent of ribonuclease P, a protein complex that generates mature tRNA molecules by cleaving their 5'ends. It may function with RPP38 to coordinate the nuclear targeting and/or assembly of RNase P (Jarrous et al., 1999). Although a direct link between POP4 and malignancy has not directly been confirmed, the increased processivity of RNA due to RNase P action may be of some significance in resistant growth.

RT-PCR Verification Results

Microarray analysis in our study reveals a significant induction of POP4 in both resistant cell lines (p<0.001 for both). Although this is suggested with HCA/PAM, this effect is only weakly suggested in FasR cells using PCR confirmation (Fig.41), with a predominant effect only in these cells by Affymetrix analysis. There was also no obvious oestradiol regulation observed. In total, due to lack of confirmation as a shared gene, the gene was considered low priority.

Figure 38. PPAR-δ gene in resistant cells. PPAR-δ mRNA was monitored as (a) using Atlas Plastic Human 12k Microarrays. Log intensity graphical output and heatmap are shown. (b) by PCR analysis using primers for PPAR-δ. β-actin was also amplified (normalisation purposes). PCR products separated on an agarose gel were visualised by ethidium bromide staining. Representative PCR profile is shown from triplicate experiments. PCR signals were then subject to densitometric analysis and normalised data plotted (plot shows standard error). (c) using Affymetrix HG-U133A gene chips. (Identical RNA preparations were used for all studies of mRNA expression). Additional controls were provided by MCF-7 cells subject to oestradiol treatment. (Δp=0.025 and $\Delta\Delta$p=*0.026 respectively for TamR and FasR relative to MCF-7 [students t-test].

(a)

(b)

β-actin
385bp →

PPAR-γ
264bp →

(c)

Figure 39. PPAR-γ gene in resistant cells. PPAR-γ mRNA was monitored as (a) using Atlas Plastic Human 12k Microarrays. Log intensity graphical output and heatmap are shown. (b) by PCR analysis using primers for PPAR-γ co-amplified with β-actin (normalisation purposes). PCR products separated on an agarose gel were visualised by ethidium bromide staining. Representative PCR profile is shown from triplicate experiments. PCR signals were then subject to densitometric analysis and normalised data plotted (plot shows standard error). (c) using Affymetrix HG-U133A gene chips. (Identical RNA preparations were used for all studies of mRNA expression). Additional controls were provided by MCF-7 cells subject to oestradiol treatment. (Δp=0.025 for TamR relative to MCF-7.*p=0.0016 for TamR relative to MCF-7 cells; +p=0.004, and ++p=0.0151 respectively for TamR and FasR relative to MCF-7 [students t-test]).
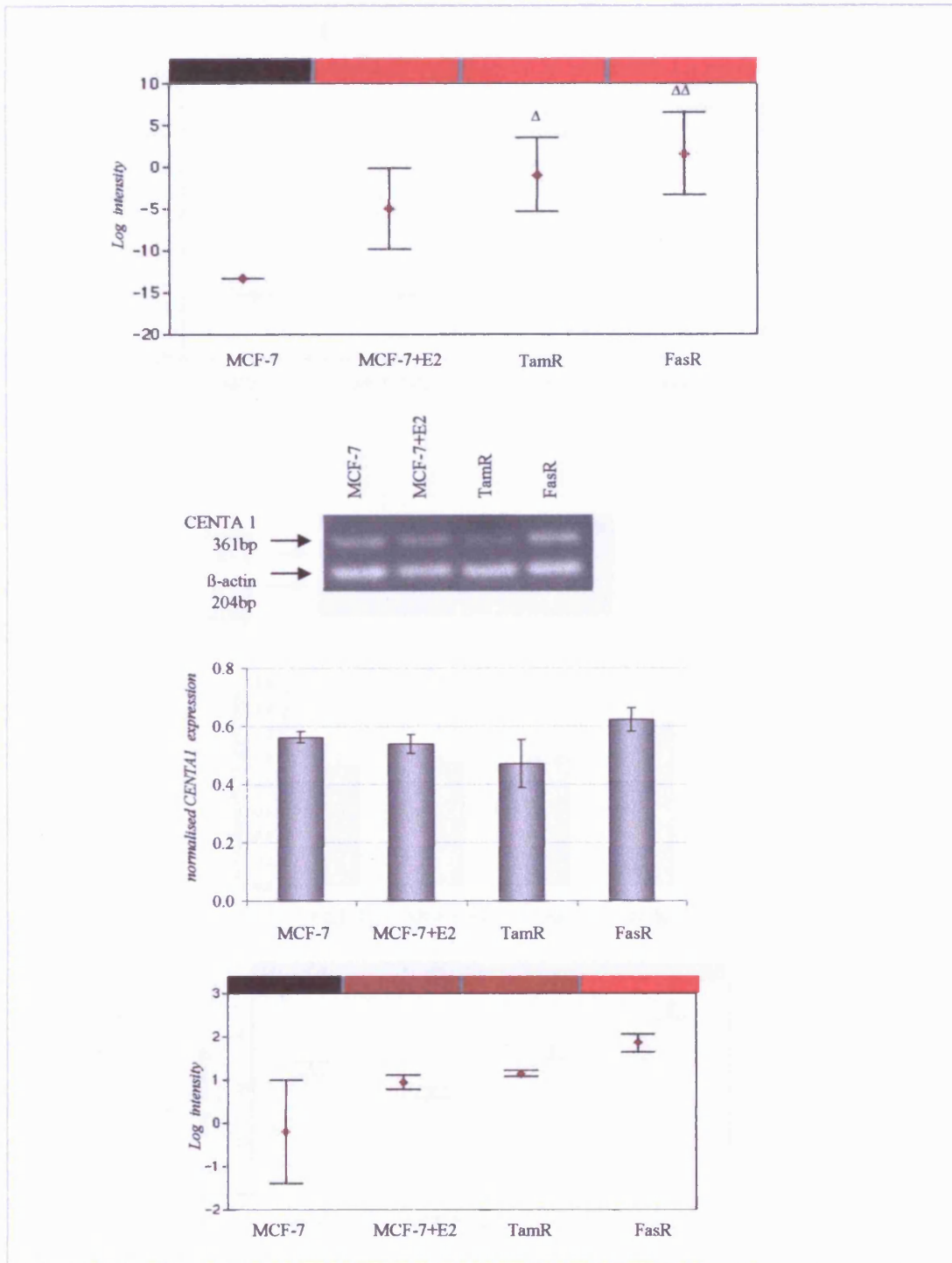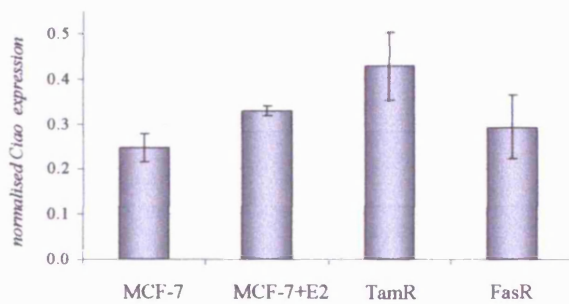
Figure 40. Alpha Centaurin gene in resistant cells. CENTA1 mRNA was monitored as (A) using Atlas Plastic Human 12k Microarrays. Log intensity graphical output and heatmap are shown. (B) by PCR analysis using primers for alpha centaurin co-amplified with β-actin (normalisation purposes). PCR products separated on an agarose gel were visualised by ethidium bromide staining. Representative PCR profile is shown from triplicate experiments. PCR signals were then subject to densitometric analysis and normalised data plotted (plot shows standard error). (C) using Affymetrix HG-U133A gene chips. (Identical RNA preparations were used for all studies of mRNA expression). Additional controls were provided by MCF-7 cells subject to oestradiol treatment. (Δp=0.031 and ΔΔp=*0.024 respectively for TamR and FasR relative to MCF-7 [students t-test].
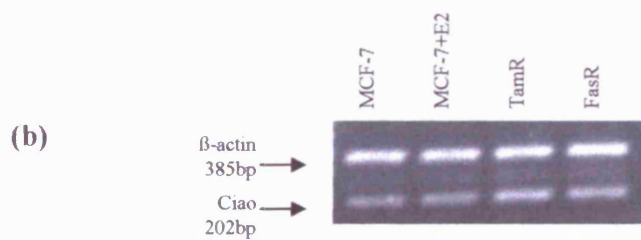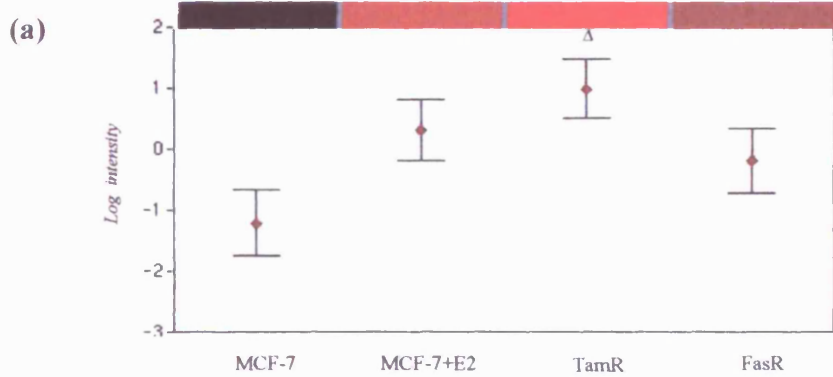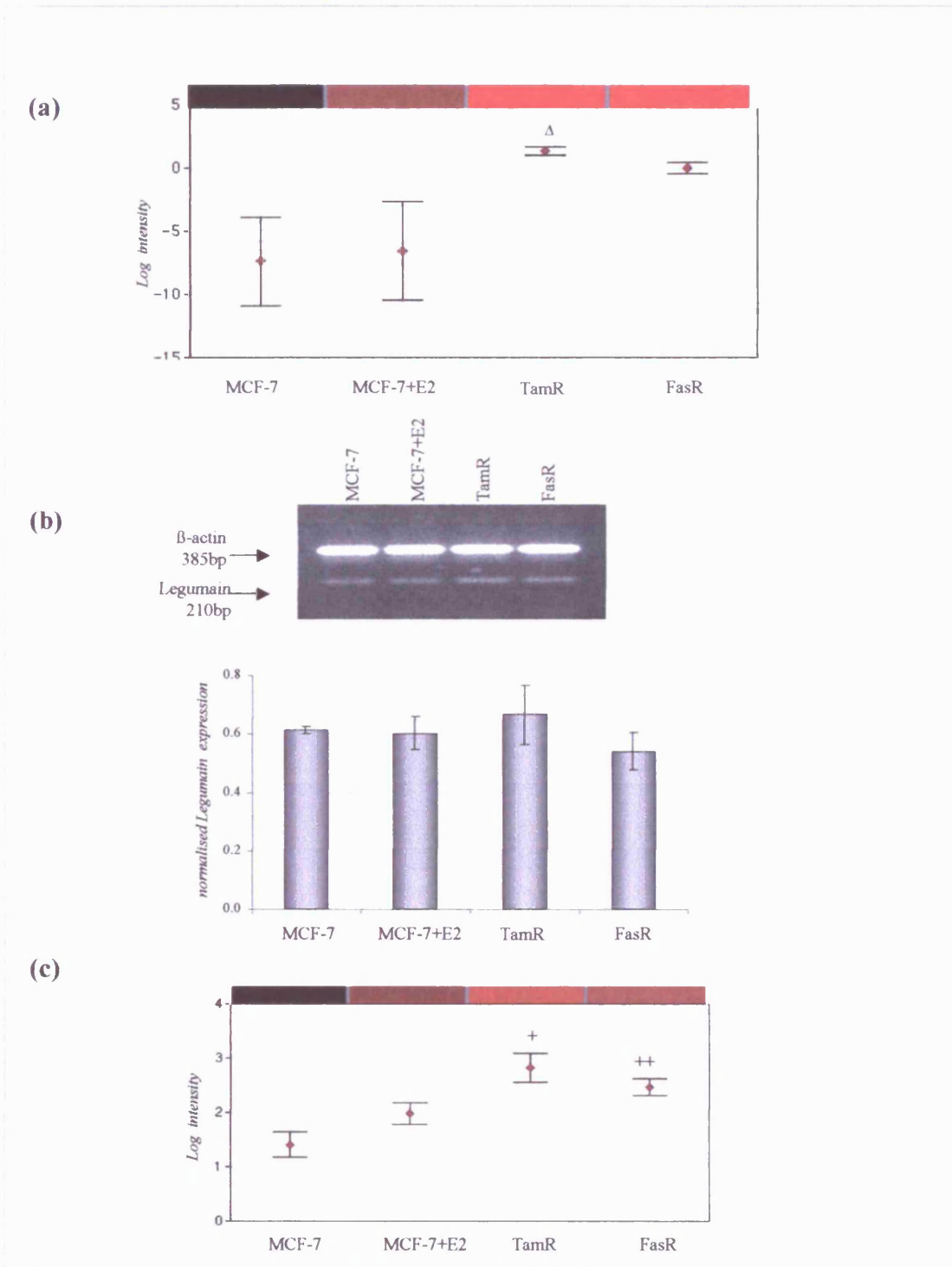
(a)

(b)

β-actin
385bp

POP4
274bp

(c)
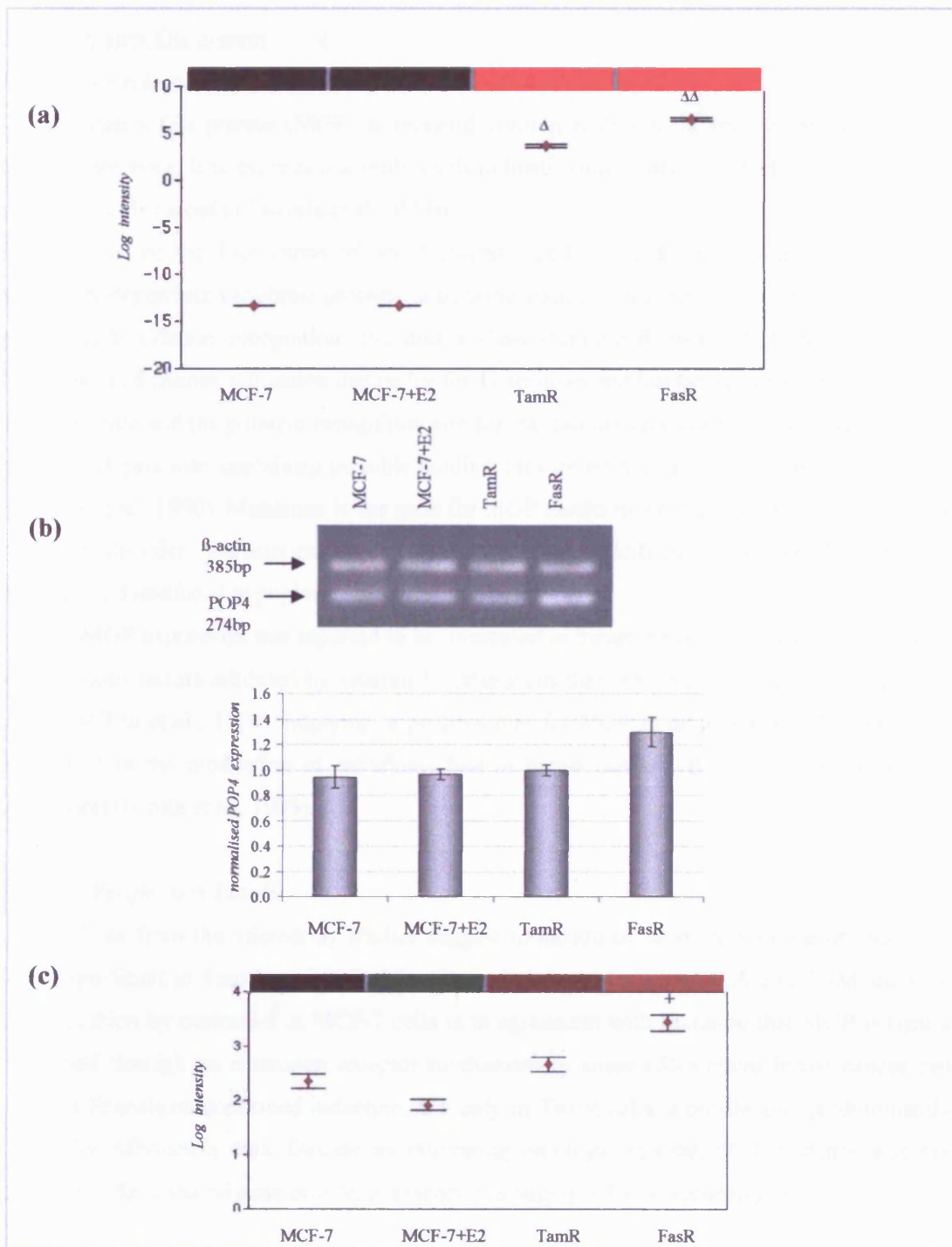
Figure 41. POP4 gene in resistant cells. POP4 mRNA was monitored as (a) using Atlas Plastic Human 12k Microarrays. Log intensity graphical output and heatmap are shown. (b) by PCR analysis using primers for POP4. β-actin was also amplified (normalisation purposes). PCR products separated on an *agarose gel were visualised by ethidium bromide staining. Representative PCR profile is shown from* triplicate experiments. PCR signals were then subject to densitometric analysis and normalised data plotted (plot shows standard error). (c) using Affymetrix HG-U133A gene chips. (Identical RNA preparations were used for all studies of mRNA expression). Additional controls were provided by MCF-7 cells subject to oestradiol treatment. (Δand ΔΔp<0.001 for both TamR and FasR relative to MCF-7; +p=0.005 for FasR *relative to MCF-7* [students [students t-test].

3.3.1.7 Matrix Gla protein

Detailed Ontological Results

Matrix Gla protein (MGP) is secreted vitamin K-dependent protein initially isolated from bovine bone. It is expressed at high levels in heart, kidney, and lung and is upregulated by vitamin D in bone cells (Cancela et al., 1990).

Each of the four exons of MGP corresponded to the domains found in all known vitamin K-dependent vertebrate proteins: a transmembrane signal peptide, followed by putative gamma-carboxylation recognition site, and a Gla-containing domain. MGP also contains a fourth exon of unknown function that codes for 11 residues and lies between the transmembrane signal peptide and the putative recognition site for the gamma-carboxylase. There are 2 regions of the MGP promoter containing possible binding sites for retinoic acid and vitamin D receptors (Cancela et al., 1990). Mutations in the gene for MGP results in Keutel syndrome, an autosomal recessive disorder characterized by abnormal cartilage calcification, peripheral pulmonary stenosis, and midfacial hypoplasia (Munroe et al., 1999).

MGP expression was reported to be increased in breast cancer cells, and MGP may be among those factors inhibited by vitamin K antagonists that reduce metastases in experimental models (Chen et al., 1990), implying a positive role for MGP in progression. It has also been implicated in the production of calcifying foci in breast cancers (the deposition of calcium phosphate) (Hirota et al., 1995).

RT-PCR Verification Results

Data from the microarray studies suggest induction of MGP in both TamR and FasR cells (significant in TamR, p=0.027) (Fig.42), and also suggested in HCA and PAM analysis. The induction by oestradiol in MCF-7 cells is in agreement with literature that MGP is tightly controlled through an oestrogen receptor mechanism in some ER-positive breast cancer cell lines. PCR analysis confirmed induction, but only in TamR cells, a profile also predominantly shown by Affymetrix data. Despite an interesting ontology, in total, PCR evidence was not convincing for a shared gene profile, but rather it is largely a TamR induced gene.

3.3.1.8 Rab acceptor 1 (prenylated)

Detailed Ontological Results

Prenylated Rab acceptor-1 (or YIP1, PRA1, Prenylin) was isolated in 1999 (Bucci et al., 1999) encoding a 185-amino acid protein that interacted with all the active (GTP-bound) prenylated Rab proteins tested. Strongest expression was found in placenta, pituitary gland, kidney, and stomach. The protein was found equally distributed between cytosol and membranes. This integral membrane protein acts catalytically to dissociate complexes of
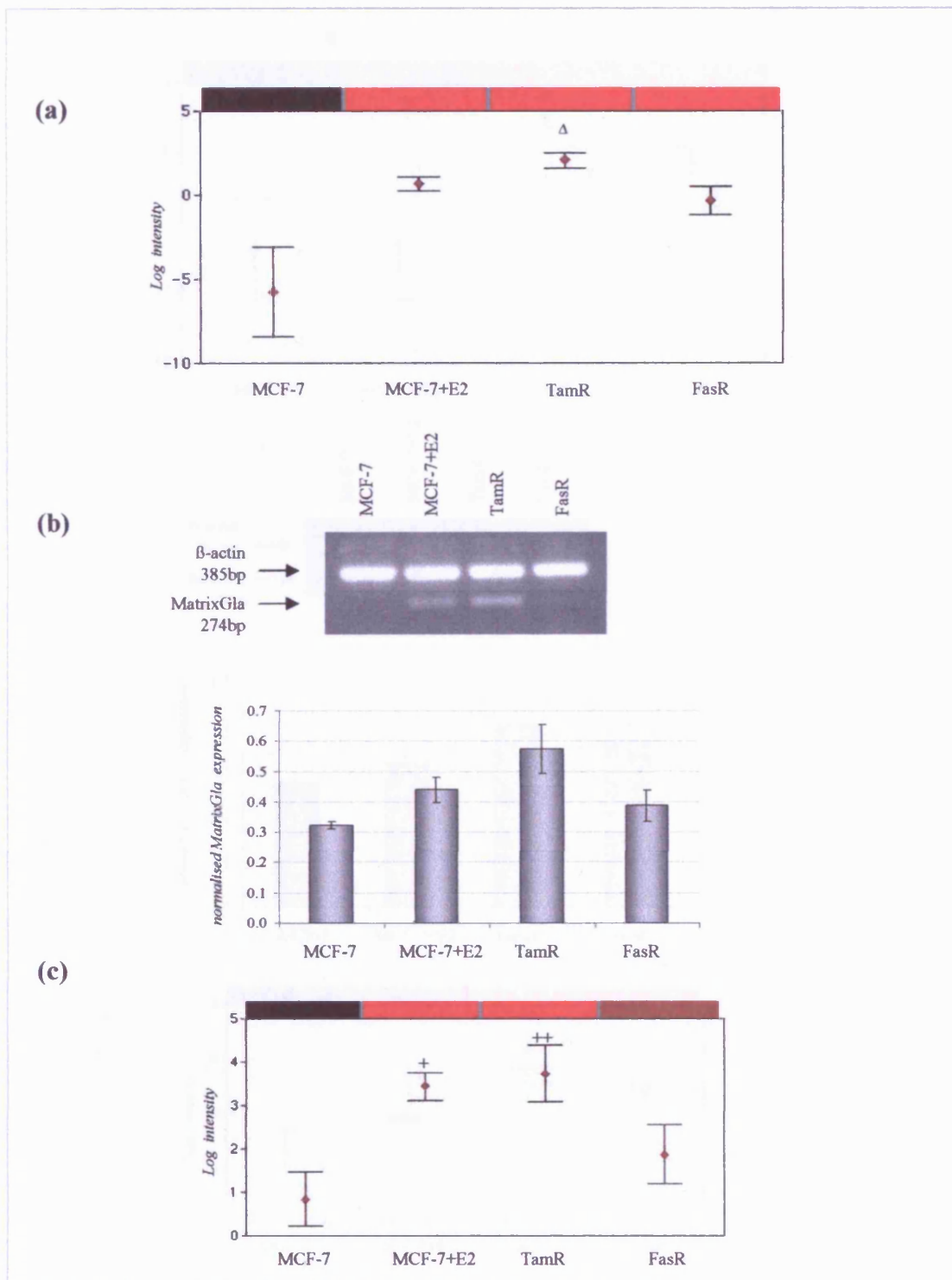
Figure 42. Matrix-GLA gene in resistant cells. Matrix Gla protein mRNA was identified as significantly upregulated in TamR and FasR cells using GeneSifter software in (a) Atlas Plastic Human 12k *Microarrays, and (b) profile was determined by PCR analysis. (c) Profiles using Affymetrix HG-* U133A gene chips. (P33-labelled RNA used for hybridisation to Affymetrix genechips were also previously used with Atlas Plastic 12k Microarrays) are also shown Graphical output and heatmap are shown for all outputs. Array plots show log mean intensity and standard errors. Additional controls were provided by parental MCF-7 cells subject to oestradiol treatment. (Δp=0.027 for TamR relative to MCF-7; +p=0.0205 and ++p=0.0332 *respectively for TamR and FasR relative to MCF-7 [students t-test]).*

endosomal Rabs bound to guanine nucleotide dissociation inhibitor (GDI), and to deliver them onto membranes (Sivars et al., 2003). The authors proposed that the conserved Yip proteins serve as GDI displacement factors for the targeting of Rab GTPases in eukaryotic cells. The Rab proteins with which Prenylated Rab acceptor-1 may interact are small GTPases of the Ras superfamily involved in the regulation of intracellular membrane trafficking in endosomal systems. RAB proteins have been postulated to regulate the targeting and fusion of membranous vesicles during organelle assembly and transport. RAB proteins undergo regulated exchange of GTP for GDP, and they slowly hydrolyze the bound GTP in a reaction that is thought to regulate the timing and unidirectional nature of these assembly events (Zahraoui et al., 1989). Although there is no direct link between Rab acceptor 1 and cancer, endosomal vesicles transport is fundamental in delivery of drugs and also contributes to growth factor signalling pathways (Ceresa, 2006).

RT-PCR Verification Results

Our data from microarray analysis suggested that there is gene induction of Rab acceptor 1 in both resistant cell lines, significantly in TamR cells (p=0.047) (Fig.43) and as indicated by HCA/PAM. The PCR profile correlated with this array profile, with an Affymetrix profile again indicating induction in both resistant states. Although there was a suitable profile, together with an interesting ontology, due to a lack of direct association with cancer, the gene was considered lower priority. However, it may be considered for future study.

3.3.1.9 WD40 protein (Ciao1)

Detailed Ontological Results

This WD40 protein Ciao 1, which is a member of a family of proteins that contain WD40 or -transducin repeats (Neer et al., 1994) has been shown specifically to interact with the Wilms Tumour (WT) tumour suppressor protein WT1 (Johnstone et al., 1998). WT1 is a zinc finger-containing transcription factor that is capable of activating or repressing transcription depending on cell type and promoter context (Johnstone et al., 1998). Consistent with a suppressor function, mutations within the gene for WT1 have been detected in ~10% of sporadic Wilms' tumours and reintroduction of wild type WT1 into Wilms tumour cell lines expressing aberrant WT1 results in growth suppression (Madden et al., 1991). Ciao 1 may affect the transcriptional activity of WT1 by either causing a conformation change of the WT1 protein that masks its activation function, or by negatively interfering with the communication between the activation domain of WT1 and the basal transcriptional machinery (Johnstone et al., 1998), and as such may contribute positively to proliferation.
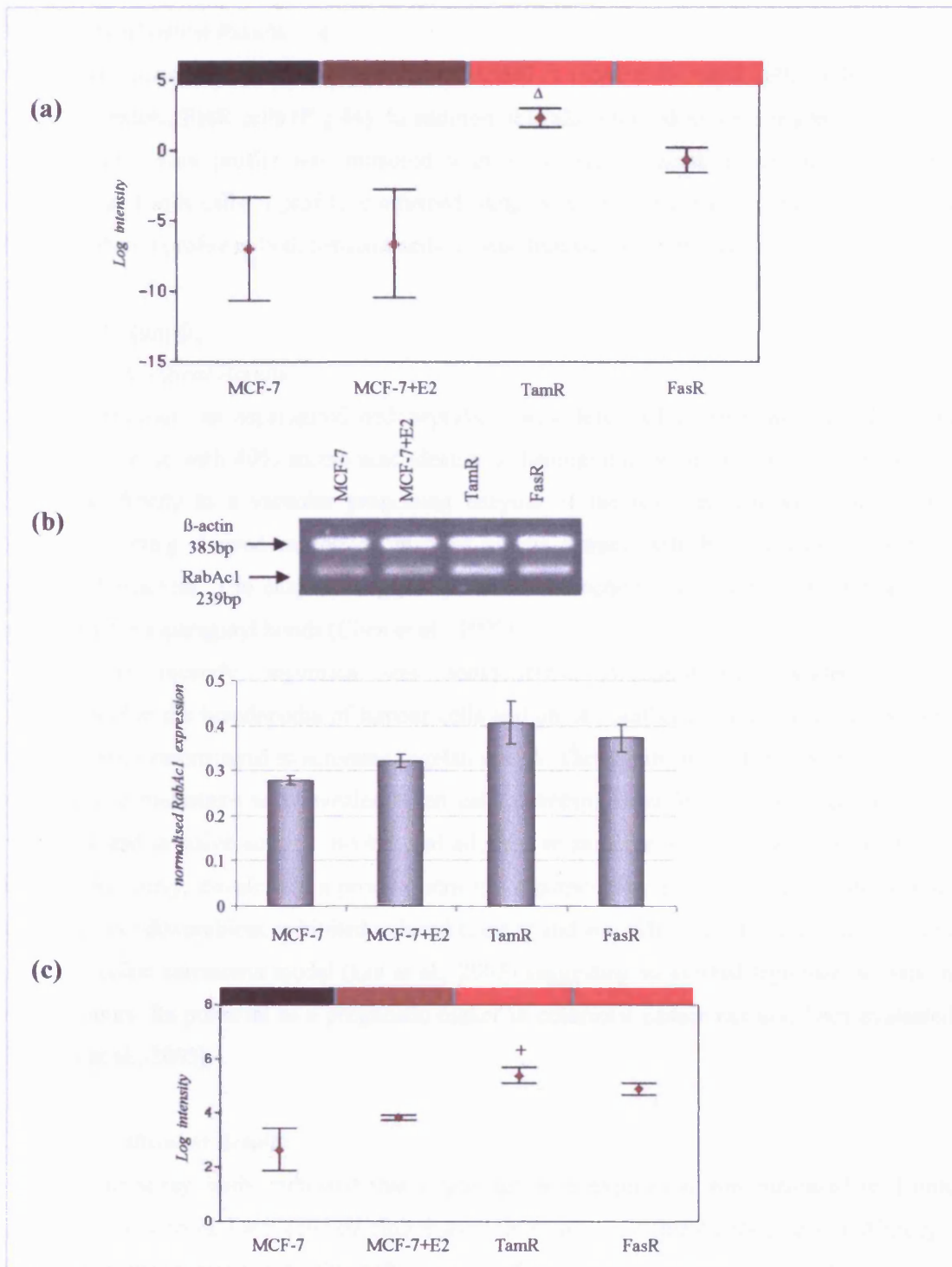
Figure 43. Rab acceptor 1 gene in resistant cells. mRNA was monitored as (a) using Atlas Plastic Human 12k Microarrays. Log intensity graphical output and heatmap are shown. (b) by PCR analysis using primers for Rab acceptor 1. β-actin was also amplified (normalisation purposes). PCR products separated on an agarose gel were visualised by ethidium bromide staining. Representative PCR profile is shown from triplicate experiments. PCR signals were then subject to densitometric analysis and normalised data plotted (plot shows standard error). (c) using Affymetrix HG-U133A gene chips. (Identical RNA preparations were used for all studies of mRNA expression). Additional controls were provided by MCF-7 cells subject to oestradiol treatment. (Δp=0.047 for TamR relative to MCF-7; +p=0.0302 for TamR and FasR relative to MCF-7 [students t-test]).

RT-PCR Verification Results

Microarray analysis demonstrated that Ciao1 is induced in TamR cells (p=0.022), and to a lesser extent, FasR cells (Fig.44). In addition, it is also induced to some degree in response to oestradiol. This profile was mirrored with PCR studies, again revealing predominant induction in TamR cells, a profile, confirmed using Affymetrix analysis. As this gene showed lack of a shared profile in both resistant cells, it was deemed a low priority.

3.3.1.10 Legumain

Detailed Ontological Results

Legumain, an asparaginyl endopeptidase, was described in 1996 as a novel human cysteine protease with 40% amino acid identity to hemoglobinase of the schistosome parasite and 36% identity to a vacuolar processing enzyme of the soybean (Tanaka et al., 1996). Northern blotting showed expression in most human tissues, with highest levels in kidney, heart, and placenta. The enzyme is glycosylated and functions as a cysteine peptidase with specificity for asparaginyl bonds (Chen et al., 1997).

More recently, legumain was demonstrated in membrane-associated vesicles concentrated at the invadopodia of tumour cells and on cell surfaces where it colocalised with integrins and demonstrated to activate progelatinase A. The significance of legumain in tumour invasion and metastasis was revealed when cells overexpressing legumain showed increased migratory and invasive activity *in-vitro* and adopted an invasive and metastatic phenotype *in-vivo*. Interestingly, developing a prodrug strategy incorporating a legumain-cleavable peptide substrate onto doxorubicin, exhibited reduced toxicity and was effectively tumoricidal *in-vivo* in a murine colon carcinoma model (Liu et al., 2003) suggesting substantial legumain activity in such tumours. Its potential as a prognostic maker in colorectal cancer has also been evaluated (Murthy et al., 2005).

RT-PCR Verification Results

Microarray study indicated that Legumain gene expression was increased in TamR (p=0.047) and also in, FasR cells by cluster analysis relative to control cells (Fig.45). Although this profile was confirmed by the Affymetrix profile, this observation was not duplicated in PCR studies, where expression was generally comparable across the models. This was not considered high priority for study, despite interesting ontology.

3.3.1.11 FK506 binding protein precursor

Detailed Ontological Results

FK506-binding proteins (FKBPs) are peptidyl-prolyl cis/trans isomerases (PPIases), cyclophilin-like molecules that bind the immunosuppressive drug FK506. Generally, PPIases occur in every compartment, both as free species and anchored to membranes. Diverse posttranslational modifications such as glycosylation, N-terminal modifications and phosphorylation constitute the additional functional features of PPIases. Folding, assembly and trafficking of proteins are regulated by PPIases. These enzymes accelerate the rate of *in-vitro* protein folding during protein synthesis and they have the ability to bind proteins and act as chaperones. Some PPIases are coregulatory subunits of molecular complexes including heat-shock proteins, glucocorticoid receptors and ion channels, and stabilise certain proteins including the oestrogen receptor to influence its signalling. Secreted forms of PPIases are inflammatory and chemotactic agents for monocytes, eosinophils and basophils (Galat, 1993).

RT-PCR Verification Results

The microarray studies revealed FK506 binding protein precursor (FKBP11) gene expression was induced in TamR (p=0.013) and FasR cells by cluster analysis (Fig.46). This profile was verified using Affymetrix analysis where 2 probed were available. However, PCR methods failed to confirm this gene profile, and so this gene was not deemed high priority for further study.

3.3.1.12 Paraoxonase 2

Detailed Ontological Results

Paraoxonase 2 (PON2) is a membrane associated protein which hydrolyses the toxic metabolites of a variety of organophosphorus insecticides and is capable of hydrolyzing a broad spectrum of organophosphate substrates and a number of aromatic carboxylic acid esters. PON2 has antioxidant activity and so may facilitate cell survival. More recently it has been shown to have antioxidant properties (Aviram et al., 2005).

RT-PCR Verification Results

The microarray studies revealed significant increase in PON2 gene expression in both TamR and FasR cells (p=0.026 and 0.025 respectively) (Fig.47), with the profile confirmed twice, since the gene was represented by two probe sets on the arrays, as well as by cluster analysis. The profile was also confirmed by Affymetrix analysis. However PCR failed to
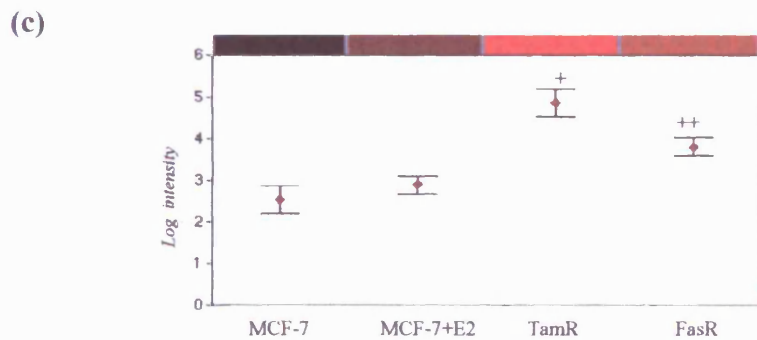
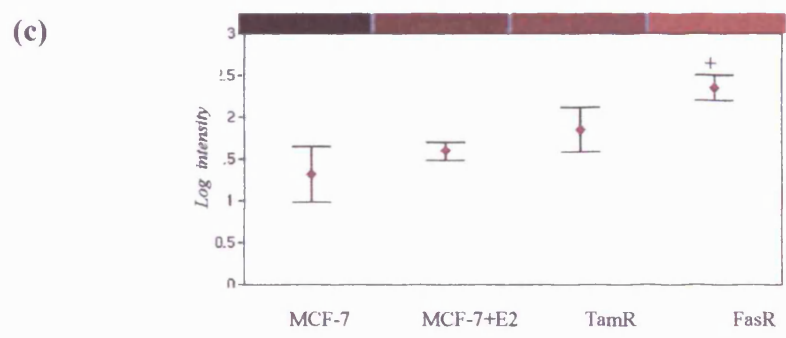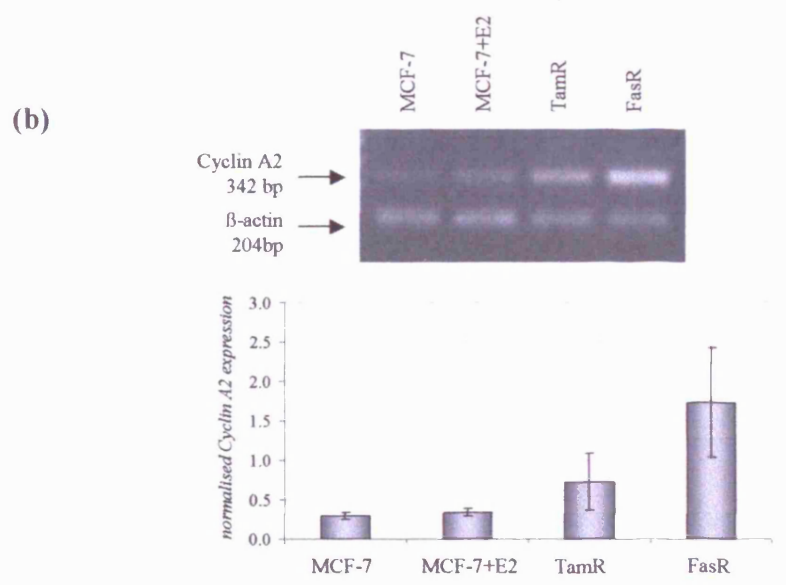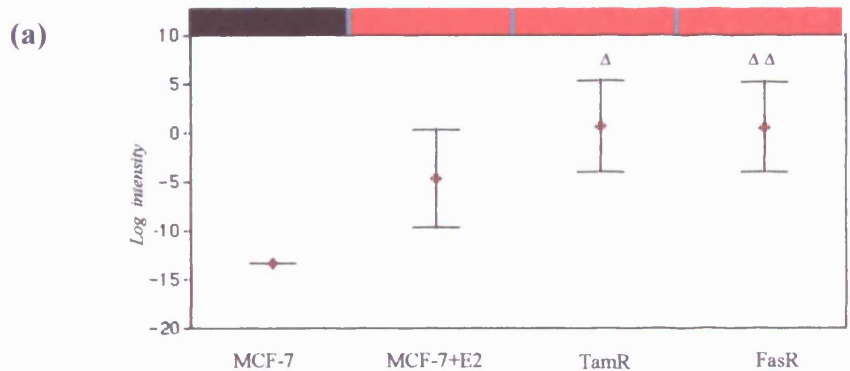Figure 44. Ciao 1 gene in resistant cells. WD40 protein Ciao1 mRNA was monitored as (a) using Atlas Plastic Human 12k Microarrays. Log intensity graphical output and heatmap are shown. (b) by PCR analysis using primers for Ciao1. β-actin was also amplified (normalisation purposes). PCR products separated on an agarose gel were visualised by ethidium bromide staining. Representative PCR profile is shown from triplicate experiments. PCR signals were then subject to densitometric analysis and normalised data plotted (plot shows standard error). (c) using Affymetrix HG-U133A gene chips. (Identical RNA preparations were used for all studies of mRNA expression). Additional controls were provided by MCF-7 cells subject to oestradiol treatment. (Δp=0.022 for TamR relative to MCF-7; +p=0.0079 and ++p=0.0325 respectively for TamR and FasR relative to MCF-7 [students t-test]).

(a)

(b)

β-actin
385bp →

Legumain →
210bp

(c)

Figure 45. Legumain gene in resistant cells. legumain mRNA was monitored as (a) using Atlas Plastic Human 12k Microarrays. Log intensity graphical output and heatmap are shown. (b) by PCR analysis using primers for Legumain co-amplified with β-actin (normalisation purposes). PCR products separated on an agarose gel were visualised by ethidium bromide staining. Representative PCR profile is shown from triplicate experiments. PCR signals were then subject to densitometric analysis and normalised data plotted (plot shows standard error). (c) using Affymetrix HG-U133A gene chips. (Identical RNA preparations were used for all studies of mRNA expression). Additional controls were provided by MCF-7 cells subject to oestradiol treatment. (Δp=0.047 for TamR relative to MCF-7; +p=0.0174 and ++p=0.0222 respectively for TamR and FasR relative to MCF-7 [students t-test]).
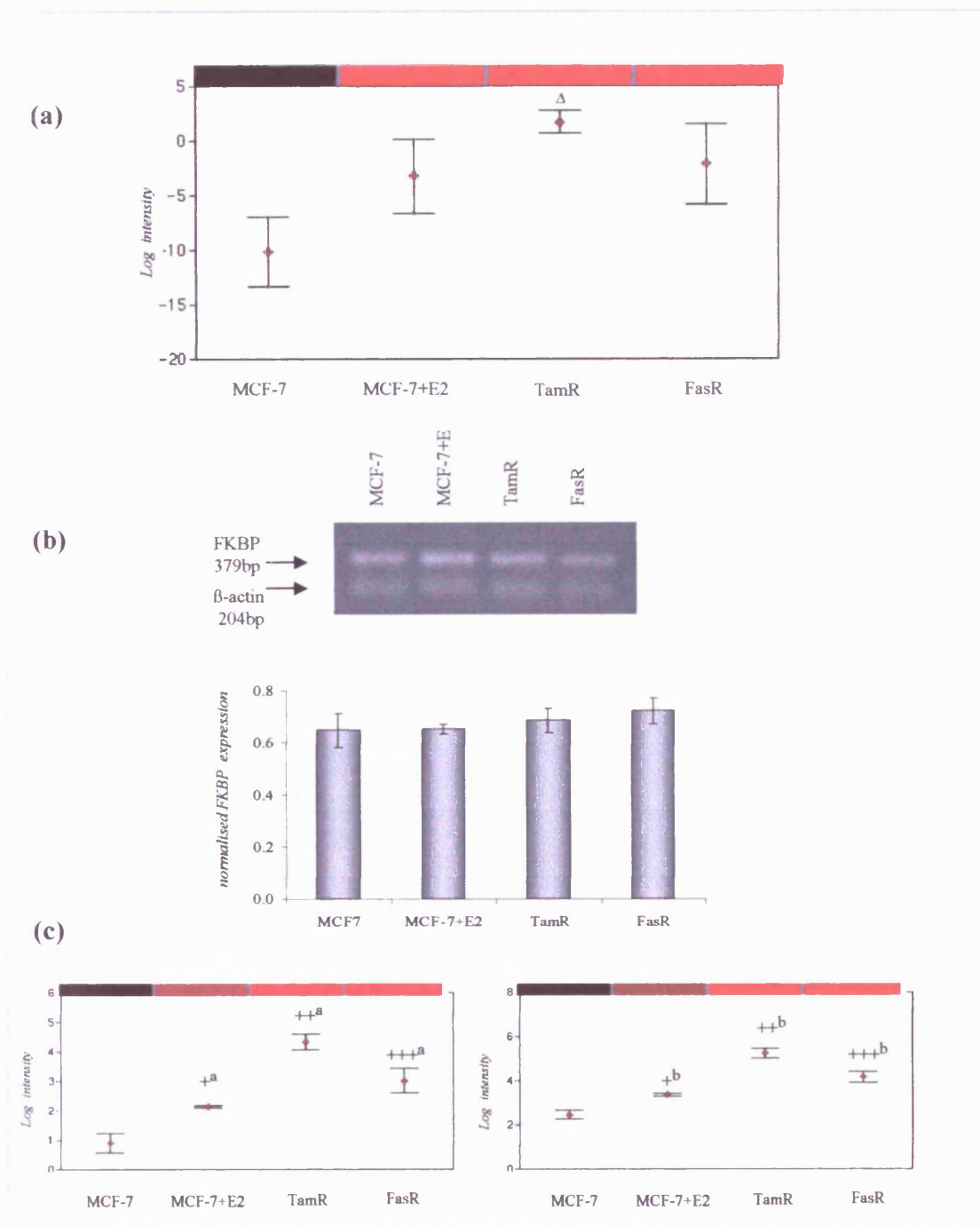
Figure 46. FK506 binding protein precursor gene in resistant cells. FK506 binding protein precursor mRNA was monitored as (a) using Atlas Plastic Human 12k Microarrays. Log intensity graphical output and heatmap are shown. (b) by PCR analysis using primers for FK506 binding protein precursor co-amplified with β-actin (normalisation purposes). PCR products separated on an agarose gel were visualised by ethidium bromide staining. Representative PCR profile is shown from triplicate experiments. PCR signals were then subject to densitometric analysis and normalised data plotted (plot shows standard error). (c) using Affymetrix HG-U133A gene chips, where FKBP gene was represented twice on the array. (Identical RNA preparations were used for all studies of mRNA expression). Additional controls were provided by MCF-7 cells subject to oestradiol treatment. (Δp=0.013 for TamR relative to MCF-7; +[a]p=0.0.0199, ++[a]p=0.0013 and +++[a]p=0.0159 respectively for MCF-7+E2, TamR and FasR relative to MCF-7; +[b]p=0.0124, ++[b]p=0.0007 and +++[b]p=0.0056 respectively for MCF-7+E2, TamR and FasR relative to MCF-7 [students t-test]).
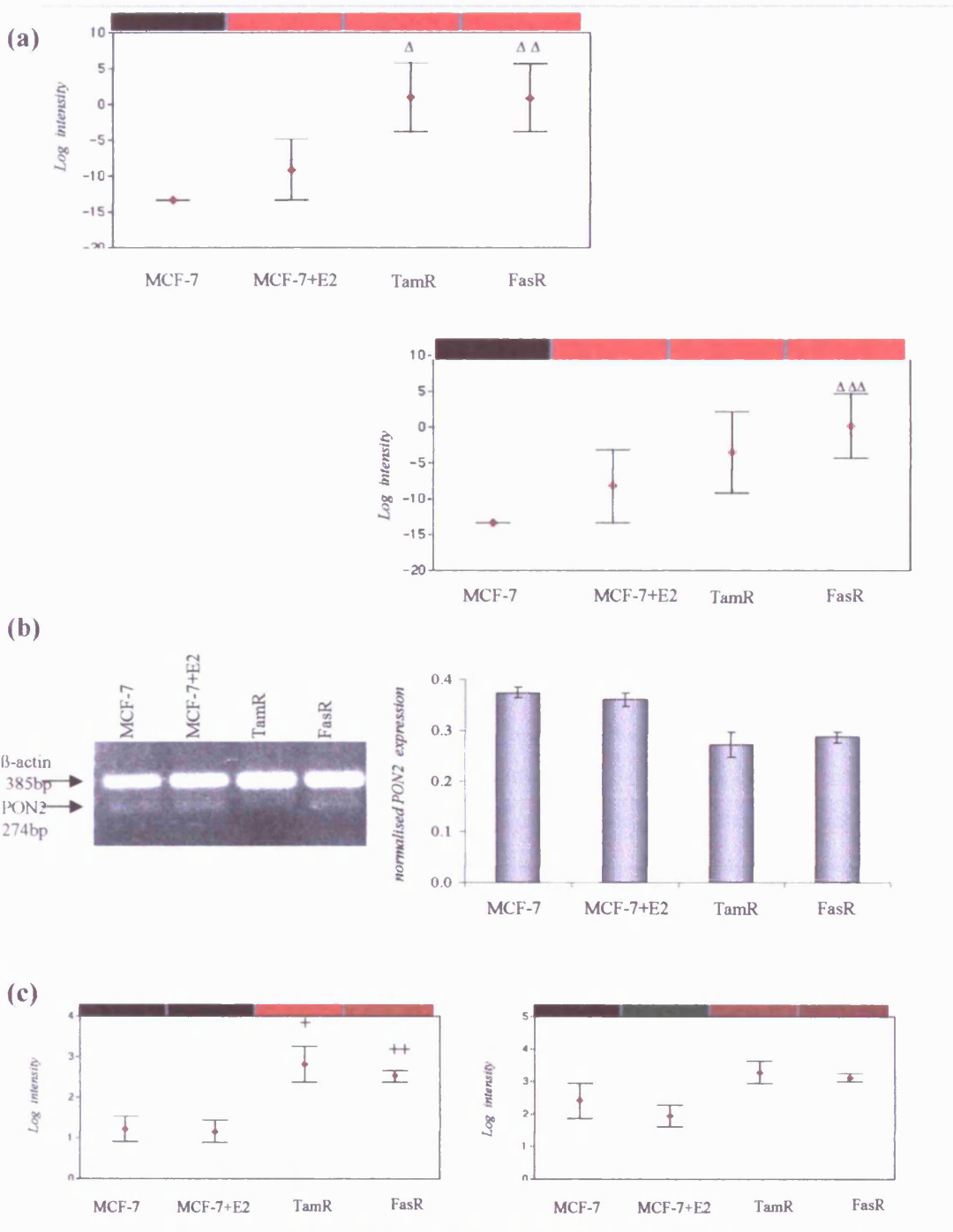
Figure 47. Paraoxonase2 gene in resistant cells. PON2 mRNA was monitored as (a) using Atlas Plastic Human 12k Microarrays. Log intensity graphical output and heatmap are shown for the gene which was represented twice on the array. (b) by PCR analysis using primers for PON2. β-actin was also amplified (normalisation purposes). PCR products separated on an agarose gel were visualised by ethidium bromide staining. Representative PCR profile is shown from triplicate experiments. PCR signals were then subject to densitometric analysis and normalised data plotted (plot shows standard error). (c) using Affymetrix HG-U133A gene chips. Gene was represented twice on the array (identical RNA preparations were used for all studies of mRNA expression). Additional controls were provided by MCF-7 cells subject to oestradiol treatment. ($^\Delta$p=0.026 and $^{\Delta\Delta}$p=0.025 for respectively for TamR and FasR relative to MCF-7; $^{\Delta\Delta\Delta}$p=0.025 for FasR relative to MCF-7; +p=0.0411 and ++p=0.0180 respectively for TamR and FasR relative to MCF-7 [students t-test].

confirm the profiles. There was no evidence of obvious oestradiol regulation. Owing to the lack of PCR verification, this gene was not considered high priority for further study.

3.3.1.13 Ornithine Decarboxylase

Detailed Ontological Results

Ornithine decarboxylase (ODC1) is the first enzyme in polyamine synthesis, a transcriptional target of MYC (Guo et al., 2000) and a modifier of APC -dependent tumourigenesis (Fultz and Gerner, 2002). Translation of ODC, a rate-limiting enzyme in the biosynthesis of polyamines, peaks twice during the cell cycle, at the G1/S transition and at G2/M. A cap-independent internal ribosome entry site (IRES) was identified in the ODC mRNA that functions exclusively at G2/M (Pyronnet, 2000), ensuring elevated levels of polyamines, which are implicated as having an important role in mitotic spindle formation and chromatin condensation.

Ornithine decarboxylase (ODC) expression was shown to be increased by growth factors and is obligatory for progression through the cell cycle in a wide variety of cell types. A recent study showed mRNA levels in human breast tumour cell lines and xenografts elevated about 3-fold in ER-negative tumours (MDA-MB-231) when compared with ER-positive (ER+) tumours (MCF-7) (Wright et al., 1995). With regards to breast cancer prognosis, ODC activity measured biochemically in breast cancers has been associated with increased risk for recurrence of disease and death, and shown as an *in-vitro* and *in-vivo* parameter in aggressive and metastatic behaviour by human breast cancer cells (Love et al., 2003, Manni et al., 2002). ODC has also been reported to be regulated by NFκB (Tacchini et al., 2004) as well as having transforming capabilities enhanced by EGFR signalling (Moshier et al., 1995).

RT-PCR Verification Results

Our data suggest that ODC gene expression was upregulated in FasR cells (p=0.005), and to a very much lesser degree in TamR cells by cluster analysis. There was no obvious impact on expression of oestradiol treatment in MCF-7 cells (Fig.48). The array profile shows a correlation with PCR data and also in the Affymetrix data. The most obvious increases were observed with FasR (p<0.001) and to a lesser extent in the TamR (p=0.0259). The gene ontology was interesting and there is some indication of a shared expression, and the gene could be considered for future studies, however, it was not selected for further work as it appeared to be a predominantly FasR induced gene.

3.3.1.14 Biliverdin Reductase B

Detailed Ontological Results

The enzyme heme oxygenase-1 (HO-1) catalyses the oxidative degradation of heme to form biliverdin, carbon monoxide (CO), and free iron. Biliverdin is subsequently reduced to bilirubin by biliverdin reductase. This mechanism is thought to be important in cytoprotection, also because the downstream products of biliverdin reductase are reported to have beneficial antioxidant properties (Kirkby and Adin, 2006). Biliverdin reductase has also been shown to function in a cell signalling capacity via insulin receptor/ MAPK signalling (Maines, 2005), and its overexpression has been found in renal cell carcinoma (Maines et al., 1999).

RT-PCR Verification Results

The gene for biliverdin reductase was found to be overexpressed in FasR cells using Atlas Plastic arrays (p=0.005) although a small increase was also observed in TamR cells by cluster analysis (Fig.49). This induction was also seen using Affymetrix analysis, and a significant increase was similarly confirmed in FasR cells using PCR analysis (p=0.0031) with a very small TamR increase. Although the gene had an interesting ontology, it was considered lower priority due to its predominantly FasR induction.

3.3.1.15 Cyclin A2

Detailed Ontological Results

Cyclins are elements which interact with cyclin-dependant kinase (CDK) and have an essential role in cell cycle regulation. The dysregulation of cyclins, including A1 and A2 can have a profound effect on the cell, and may lead to the genesis of cancers. It is because of this role that, not surprisingly, cyclins such as A2 associate closely with cellular proliferation and may be regarded as reliable prognosticators for a number of cancer types (Yasmeen et al., 2003).

RT-PCR Verification Results

Cyclin A2 gene was found to be significantly elevated in both TamR and FasR cells using Atlas Plastic arrays (p=0.024 and p=0.025 respectively), and by cluster analysis, and less profoundly in Affymetrix arrays (Fig.50). However, the PCR profile only confirmed the obvious elevation in FasR cells with a minor TamR effect. This gene was deemed low priority as its expression was mainly elevated in FasR cells.
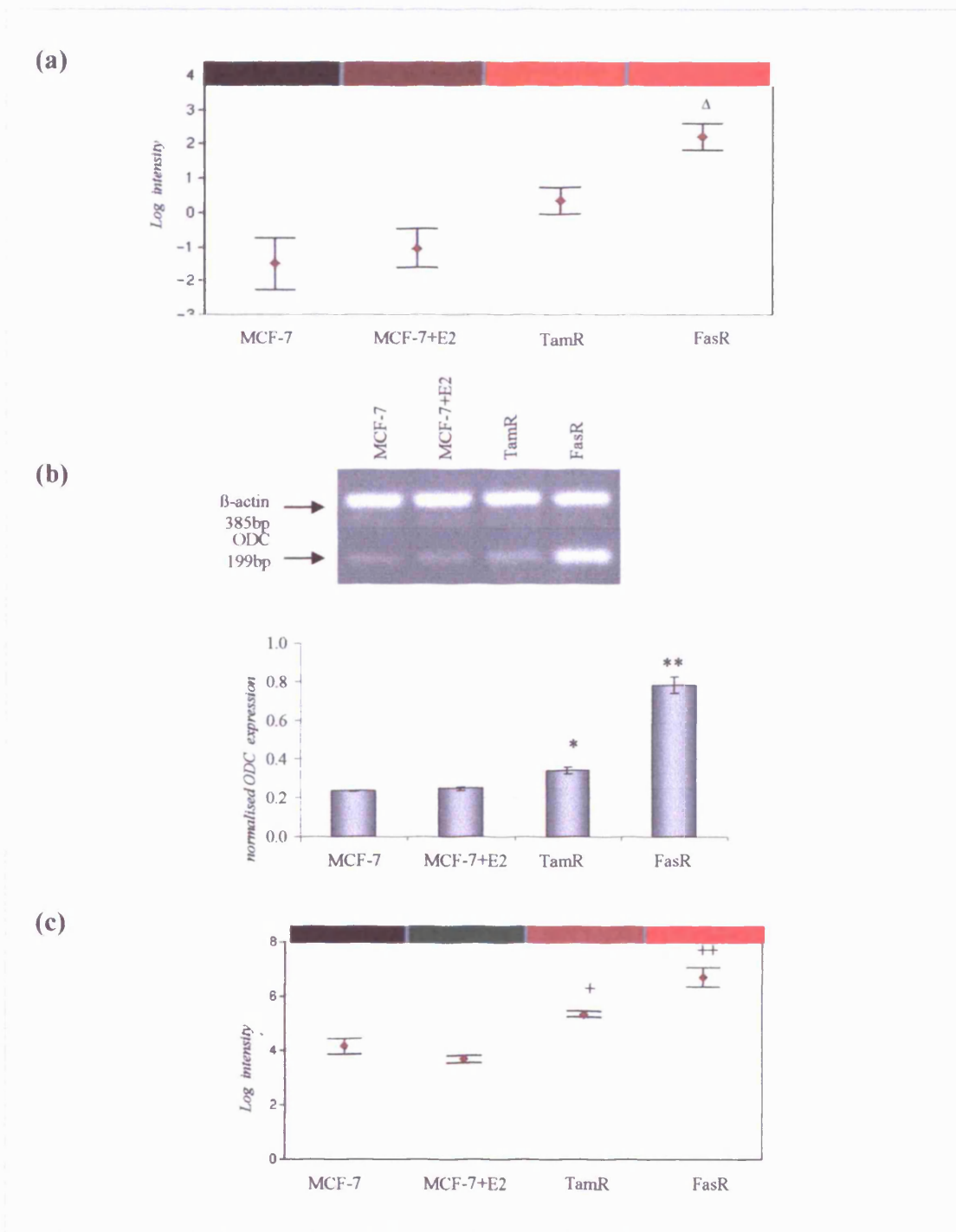
Figure 48. Ornithine Decarboxylase gene in resistant cells. ODC mRNA was monitored as (a) using Atlas Plastic Human 12k Microarrays. Log intensity graphical output and heatmap are shown. (b) by PCR analysis using primers for ODC co-amplified with β-actin (normalisation purposes). PCR products separated on an agarose gel were visualised by ethidium bromide staining. Representative PCR profile is shown from triplicate experiments. PCR signals were then subject to densitometric analysis and normalised data plotted (plot shows standard error). (c) using Affymetrix HG-U133A gene chips. (Identical RNA preparations were used for all studies of mRNA expression). Additional controls were provided by MCF-7 cells subject to oestradiol treatment. (plot shows standard errors). (Δp=0.005 for FasR relative to MCF-7; *p=0.0259 and **p<0.001 for TamR and FasR relative to MCF-7 cells; +p=0.0208 and ++p=0.005 respectively for TamR and FasR relative to MCF-7 [students t-test]).
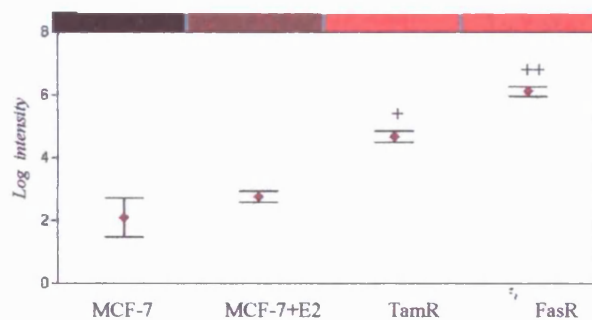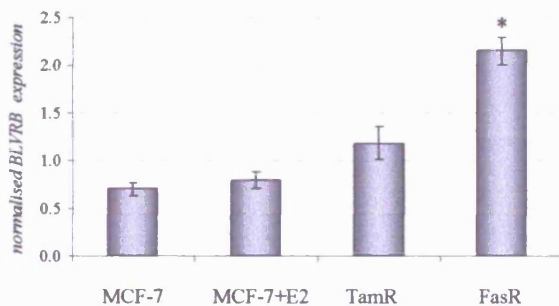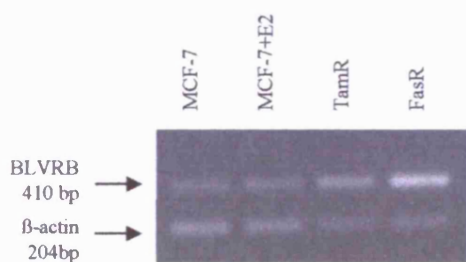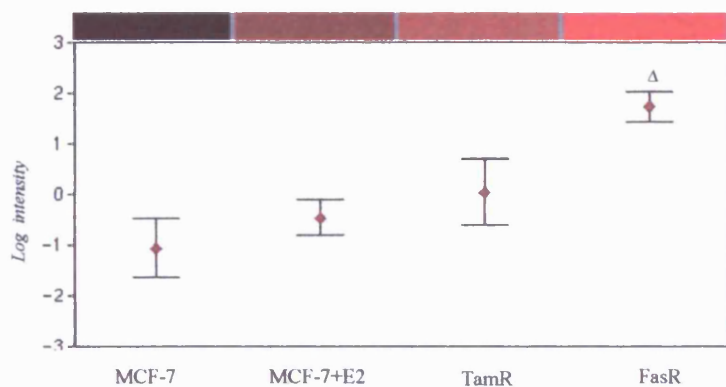
Figure 49. Biliverdin reductase B. Biliverdin reductase B mRNA was monitored as (a) using Atlas Plastic Human 12k Microarrays. Log intensity graphical output and heatmap are shown. (b) by PCR analysis using primers for Biliverdin reductase B co-amplified with β-actin (normalisation purposes). PCR products separated on an agarose gel were visualised by ethidium bromide staining. Representative PCR profile is shown from triplicate experiments. PCR signals were then subject to densitometric analysis and normalised data plotted (plot shows standard error). (c) using Affymetrix HG-U133A gene chips. (Identical RNA preparations were used for all studies of mRNA expression). Additional controls were provided by MCF-7 cells subject to oestradiol treatment. (plot shows standard errors) (Δp=0.005 for FasR relative to MCF-7; *p=0.0031 for FasR compared to MCF-7 cells; +p=0.0152 and ++p=0.0031 respectively for TamR and FasR relative to MCF-7 [student t-test]).

Figure 50. Cyclin A2. Cyclin A2 mRNA was monitored as (a) using Atlas Plastic Human 12k Microarrays. Log intensity graphical output and heatmap are shown. (b) by PCR analysis using primers for cyclin A2 co-amplified with β-actin (normalisation purposes). PCR products separated on an agarose gel were visualised by ethidium bromide staining. Representative PCR profile is shown from triplicate experiments. PCR signals were then subject to densitometric analysis and normalised data plotted (plot shows standard error). (c) using Affymetrix HG-U133A gene chips. (Identical RNA preparations were used for all studies of mRNA expression). Additional controls were provided by MCF-7 cells subject to oestradiol treatment. (plot shows standard errors). (Δp=0.024 and $\Delta\Delta$p=0.025 respectively for TamR and FasR relative to MCF-7; +p=0.0453 respectively for FasR relative to MCF-7 [students t-test]).

3.3.1.16 Stat-Induced Stat Inhibitor 2 (Suppressor of cytokine signalling2)

Detailed Ontological Results

Suppressor of cytokine signalling (SOCS) proteins have been shown to be negative regulators of cytokine receptor signalling through the Jak/Stat pathway, SOCS was also suggested to have a regulatory role in IGF1 signalling (Dey et al., 1998), where it preferentially interacted with activated IGF-1R in yeast 2-hybrid screen. However, it has also been correlated negatively to proliferation (Farabegoli et al., 2005), suggesting it has a tumour suppressive role, including in breast cancer (Marini et al., 2006).

RT-PCR Verification Results

Although the profile was interesting, showing an increase predominantly in TamR cells (Fig.51), owing to the controversial, tumour suppressive ontology of the gene, it was considered low priority.

3.3.2 TamR Induced Genes

While this study has focussed primarily on identifying and verifying genes induced in both forms of resistance, a small number of genes induced in individual resistant states were also explored.

3.3.2.1 PEA3 (ets variant gene 4; E1AF)

Detailed Ontological Results

The ETS family of genes encode a number of transcription factors and have been shown to be involved in tumourigenesis. Members of the PEA3 family can be activated by signalling components including MAPK (O'Hagan et al., 1996). PEA3 overexpression has been strongly associated with a number of malignancies including breast cancer, and increased transcription of PEA3 has been liked with HER2 positive tumours, as well as with individual pro-invasive factors such as MMPs, including MMP7 (Davidson et al., 2004, Lynch et al., 2004, Matsui et al., 2006). Tumours with high metastatic potential show increased PEA3 expression, and non-metastasising tumours with high PEA3 expression have also been shown to subsequently metastasise with the activation of factors such as MMPs and adhesion molecules such as I-CAM (de Launoit et al., 2000). PEA3 was also reported to interact with β-catenin-Lef-1 and c-Jun in regulation of osteopontin transcription, where osteopontin has been implicated in mammary development, neoplastic change, and metastasis (El-Tanani et al., 2004). In colorectal cancer cells nitric oxide, via β-catenin signalling, stimulated PEA3 to increase COX-2 activity (implicated in colorectal cancer).

Verification Results

PEA3 mRNA was found to be significantly elevated in TamR cells using GeneSifter analysis on Plastic 12k arrays, with no change in FasR cells and E2 treated MCF-7 cells (Fig 52). This profile was mirrored with PCR confirmation with induction in TamR cells (p=0.0116) but with a smallincrease in E2 treated MCF-7 cells versus control MCF-7 cells.

In addition to mRNA increases in TamR cells, PEA3 protein was also elevated in TamR cells using Western blotting (Fig.53a), and immunocytochemical staining for the protein also showed that TamR cells were highly stained in the nucleus compared to MCF-7 cells (Fig.53b).

3.3.2.2 KDEL 3

Detailed Ontological Results

KDEL3 ((Lys-Asp-Glu-Leu) endoplasmic reticulum protein retention receptor 3) is a seven transmembrane protein required for the retention of luminal endoplasmic reticulum proteins. It determines the specificity of the luminal ER protein retention system and is also required for normal vesicular traffic through the Golgi.

RT-PCR Verification Results

KDEL3 mRNA was found to be significantly elevated in TamR cells (p=0.027) only using GeneSifter analysis on Plastic 12k arrays, with no change in FasR cells or oestradiol-treated MCF-7 cells (Fig.54). This profile was again confirmed at the PCR and Affymetrix level.

3.3.2.3 Angiogenin

Detailed Ontological Results

Angiogenin is a 14.1-kDa protein with a high amino acid sequence identity with human pancreatic ribonuclease and displays ribonucleolytic activity. Capable of inducing angiogenesis, it is a potent inducer of neovascularisation within *in-vivo* models. Although normally present in the plasma, Angiogenin is overexpressed in cancer patients and it is also linked with hypoxia in breast cancer, with increased grade, and ER-positive disease, suggesting a role in progression (Campo et al., 2005), although relationship to prognosis is controversial.

RT-PCR Verification Results

Angiogenin expression was found to be significantly increased in TamR relative to MCF-7 cells using Atlas Plastic 12k arrays (p=0.0032), and was also apparent by Affymetrix. However, PCR analysis failed to confirm this elevation (Fig.55).

(a)

(b)

(c)
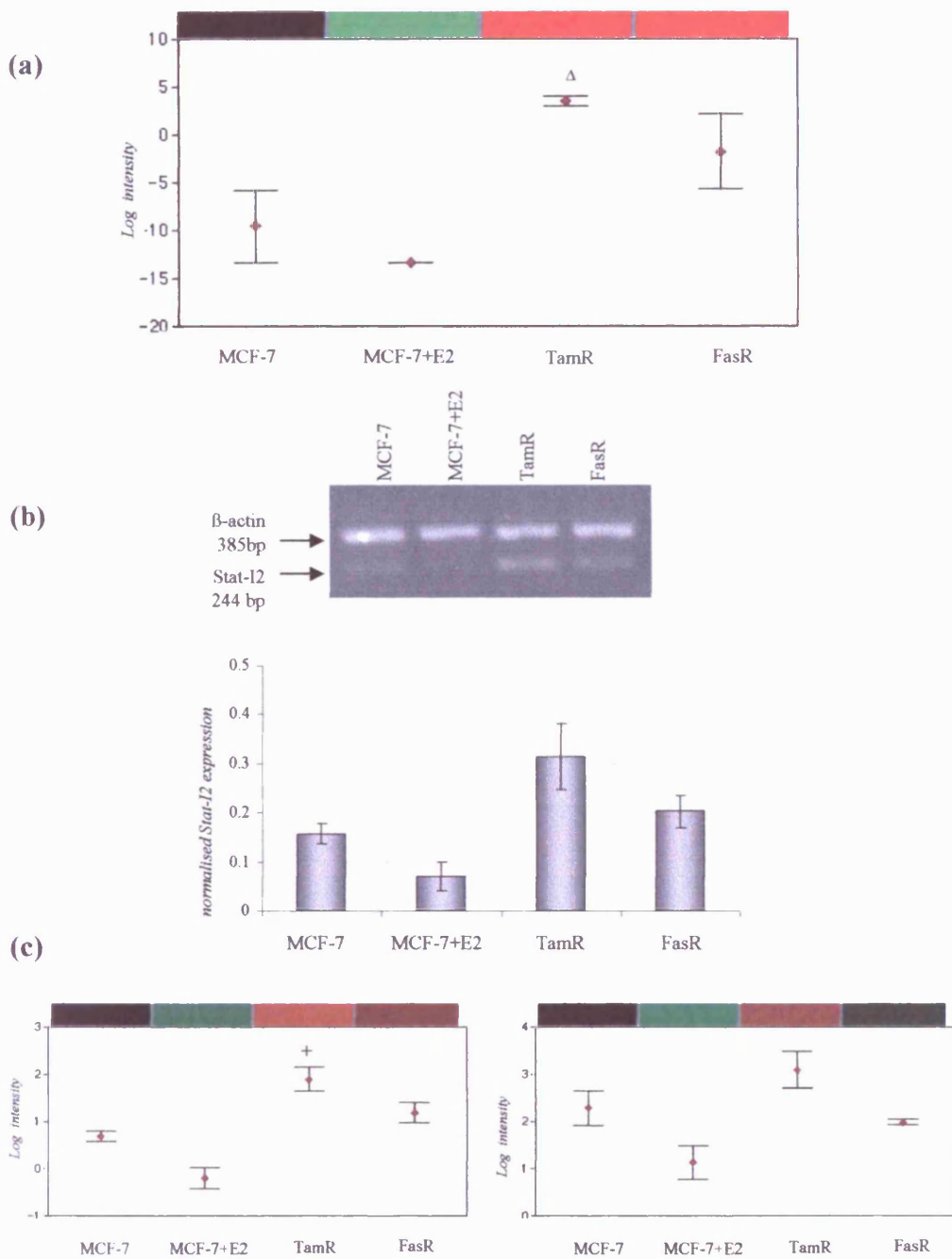
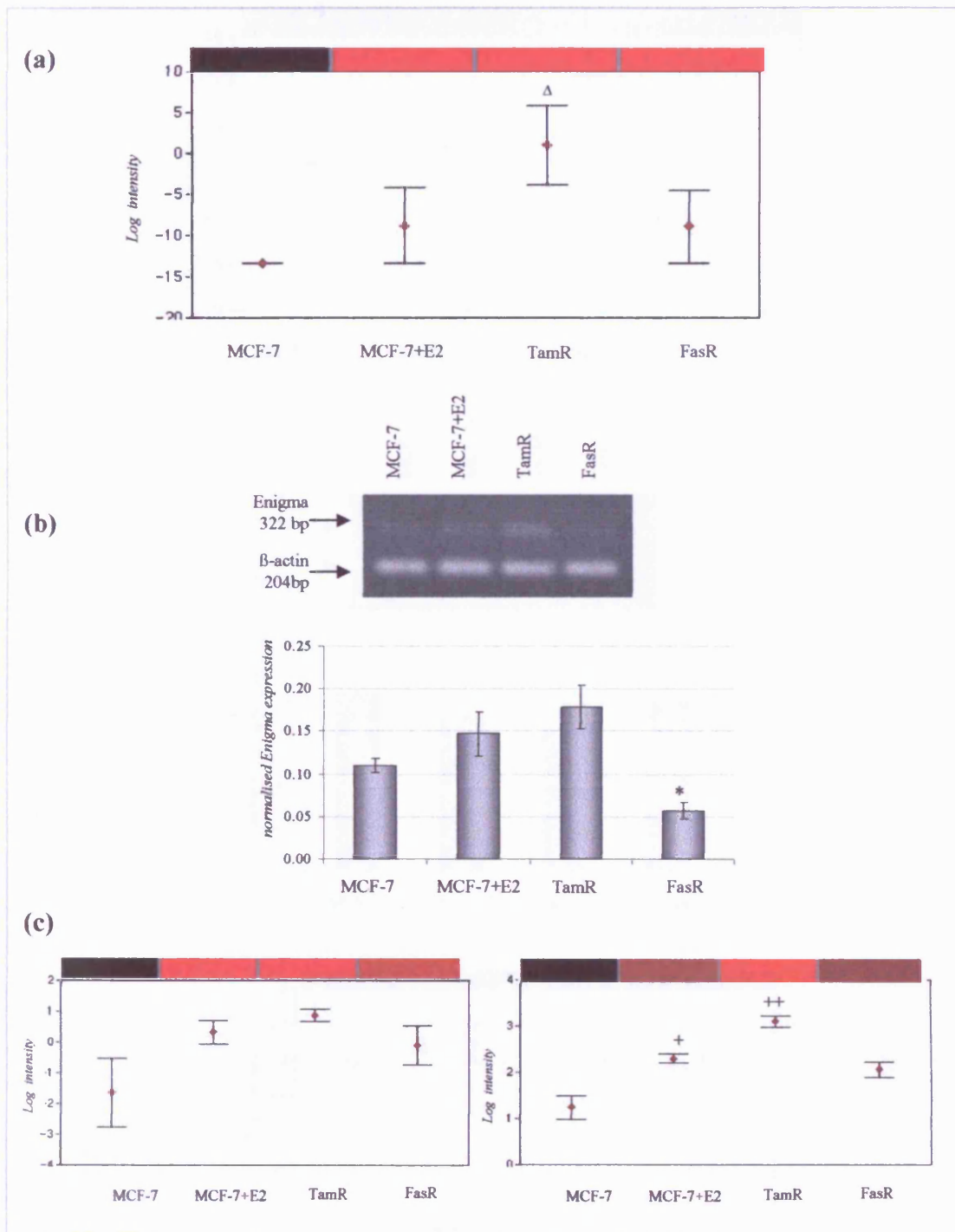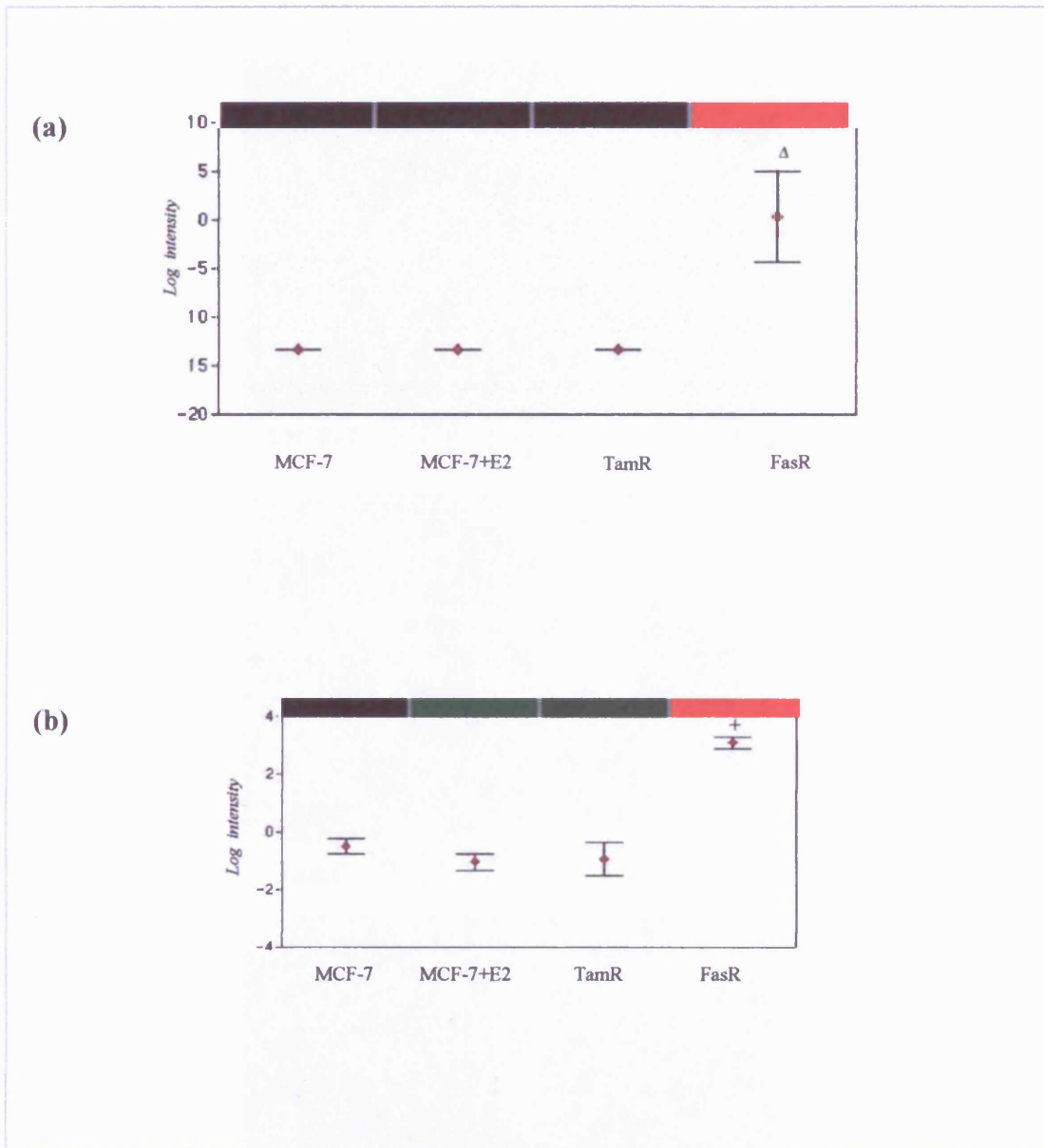**Figure 51. Stat-Induced Stat Inhibitor 2 gene expression profile in resistant cells.** Stat-I2 mRNA was monitored as (a) using Atlas Plastic Human 12k Microarrays. Log intensity graphical output and heatmap are shown. (b) by PCR analysis using primers for Stat-I2. β-actin was also amplified (normalisation purposes). PCR products separated on an agarose gel were visualised by ethidium bromide staining. Representative PCR profile is shown from triplicate experiments. PCR signals were then subject to densitometric analysis and normalised data plotted (plot shows standard error). (c) using Affymetrix HG-U133A gene chips. Gene was represented twice on the array. (Identical RNA preparations were used for all studies of mRNA expression). Additional controls were provided by MCF-7 cells subject to oestradiol treatment. (Δp=0.0013 for FasR relative to MCF-7; +p=0.0113 respectively for TamR relative to MCF-7 [student t-test]).
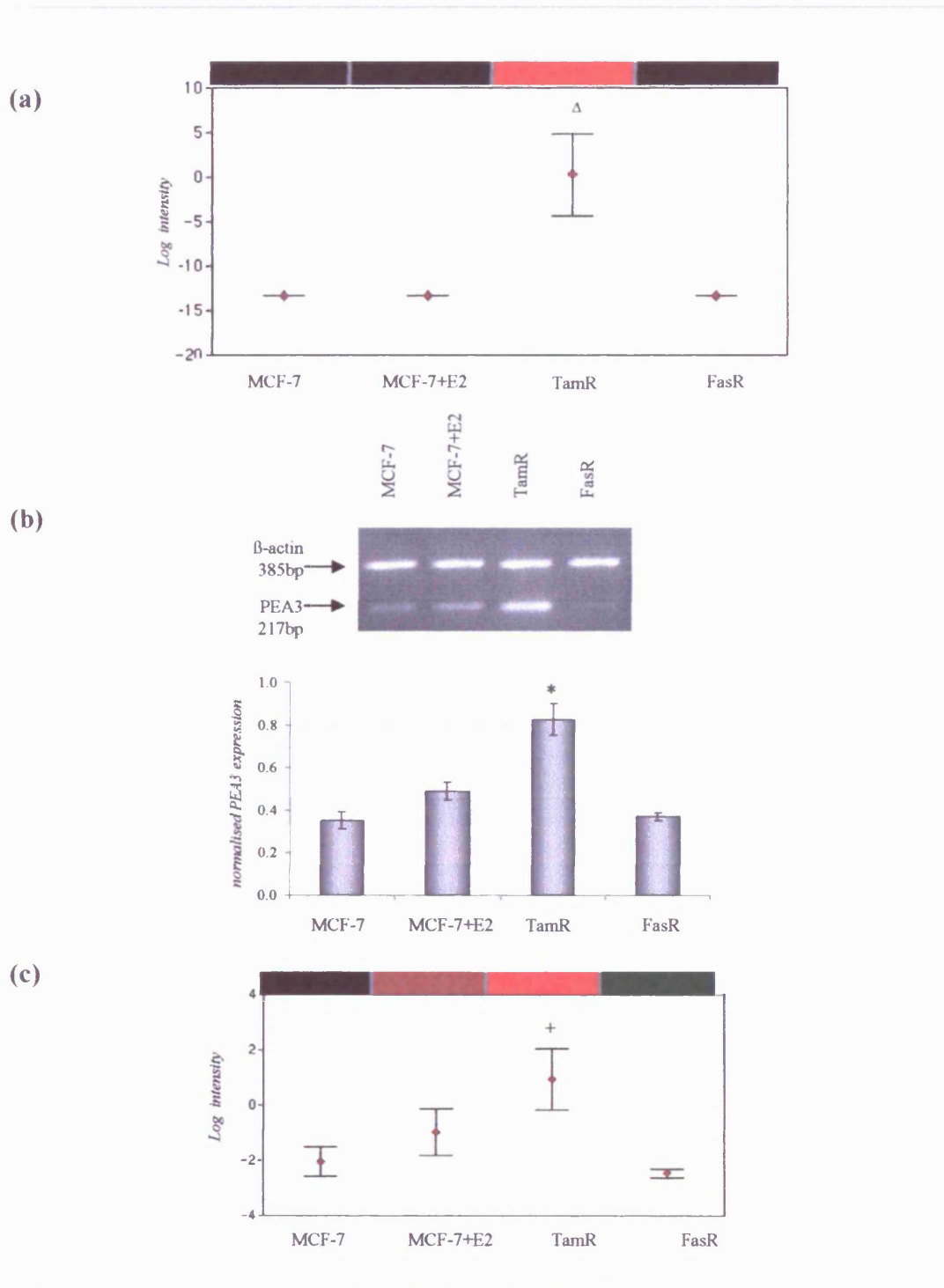
**Figure 52. PEA3 gene expression profile in resistant cells.** PEA3 mRNA was monitored as (a) using Atlas Plastic Human 12k Microarrays. Log intensity graphical output and heatmap are shown. (b) by PCR analysis using primers for PEA3. β-actin was also amplified (normalisation purposes). PCR products separated on an agarose gel were visualised by ethidium bromide staining. Representative PCR profile is shown from triplicate experiments. PCR signals were then subject to densitometric analysis and normalised data plotted (plot shows standard error). (c) using Affymetrix HG-U133A gene chips. (Identical RNA preparations were used for all studies of mRNA expression). Additional controls were provided by MCF-7 cells subject to oestradiol treatment. (Δp=0.024 for TamR relative to MCF-7; *p=0.0116 for TamR compared to MCF-7 cells; +p=0.003 for TamR relative to MCF-7 [student t-test]).

(a)   MCF-7   TamR   FasR

PEA3
66 kd →

(b)
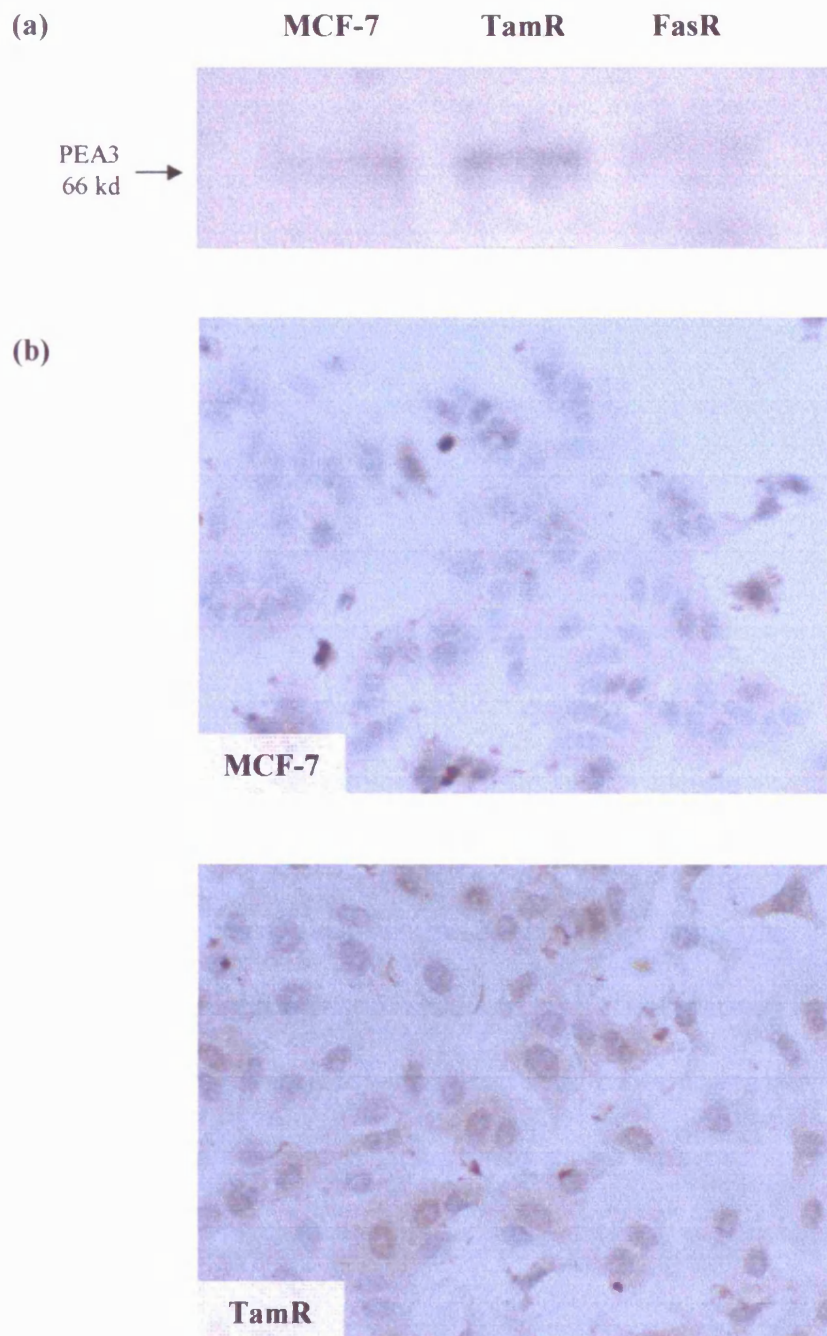
MCF-7

TamR

Figure 53. PEA3 protein in resistant cells. (a) Cells grown in 100m dishes were harvested and 50 μg subject SDS-PAGE/ Western blotting and probed using the monoclonal PEA3 antibody. (b) MCF-7 and TamR cells grown on coverslips were fixed and stained using the monoclonal antibody to PEA3. Images show x40 original magnification.
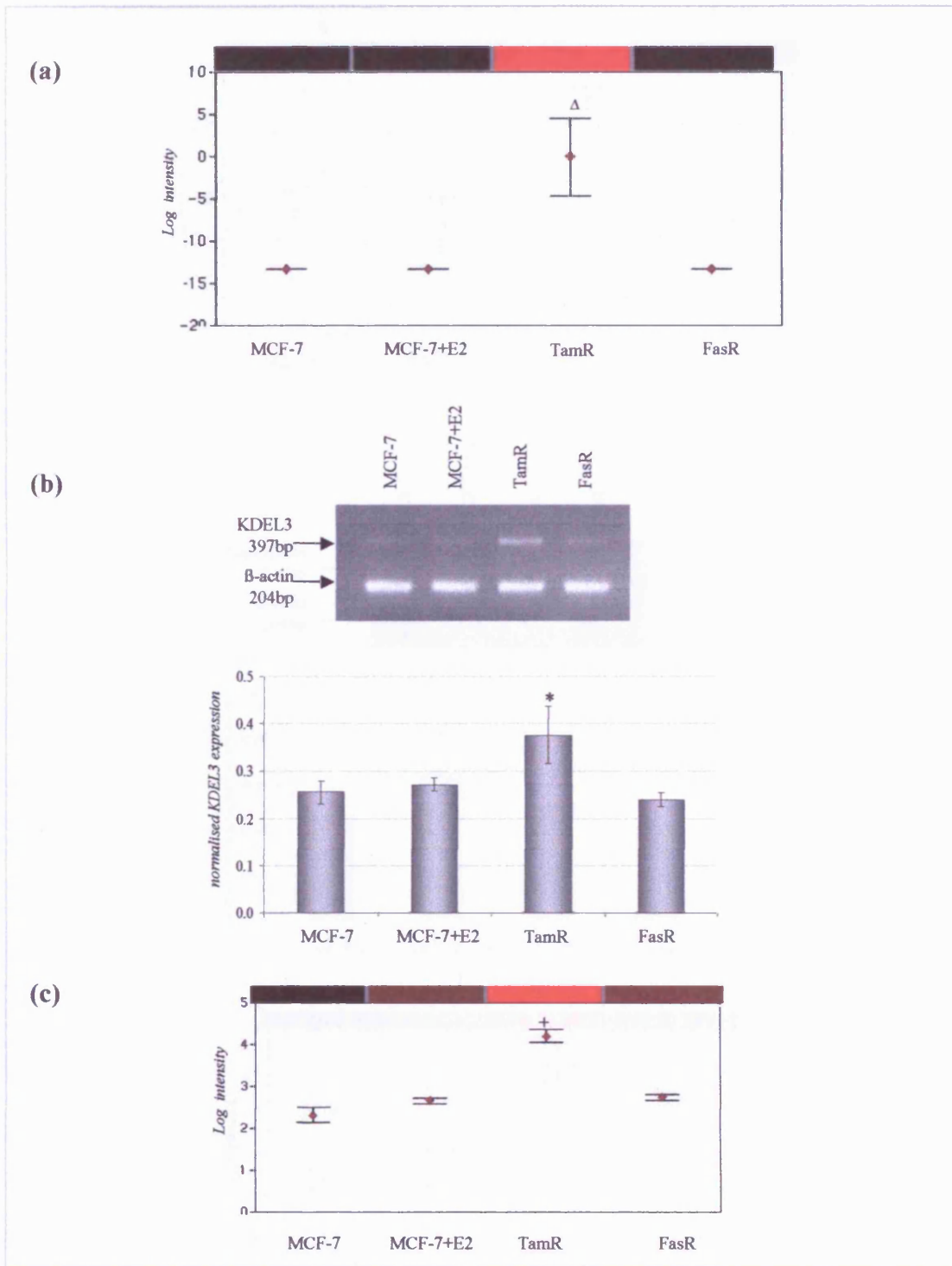
Figure 54. KDEL3 gene expression profile in resistant cells. KDEL3. mRNA was monitored as (a) using Atlas Plastic Human 12k Microarrays. Log intensity graphical output and heatmap are shown. (b) by PCR analysis using primers for KDEL co-amplified with β-actin (normalisation purposes). PCR products separated on an agarose gel were visualised by ethidium bromide staining. Representative PCR profile is shown from triplicate experiments. PCR signals were then subject to densitometric analysis and normalised data plotted (plot shows standard error). (c) using Affymetrix HG-U133A gene chips. (Identical RNA preparations were used for all studies of mRNA expression). Additional controls were provided by MCF-7 cells subject to oestradiol treatment. (Δp=0.027 for TamR relative to MCF-7; *p=0.0240 for TamR relative to MCF-7; +p=0.0185 for TamR relative to MCF-7 [student t-test]).
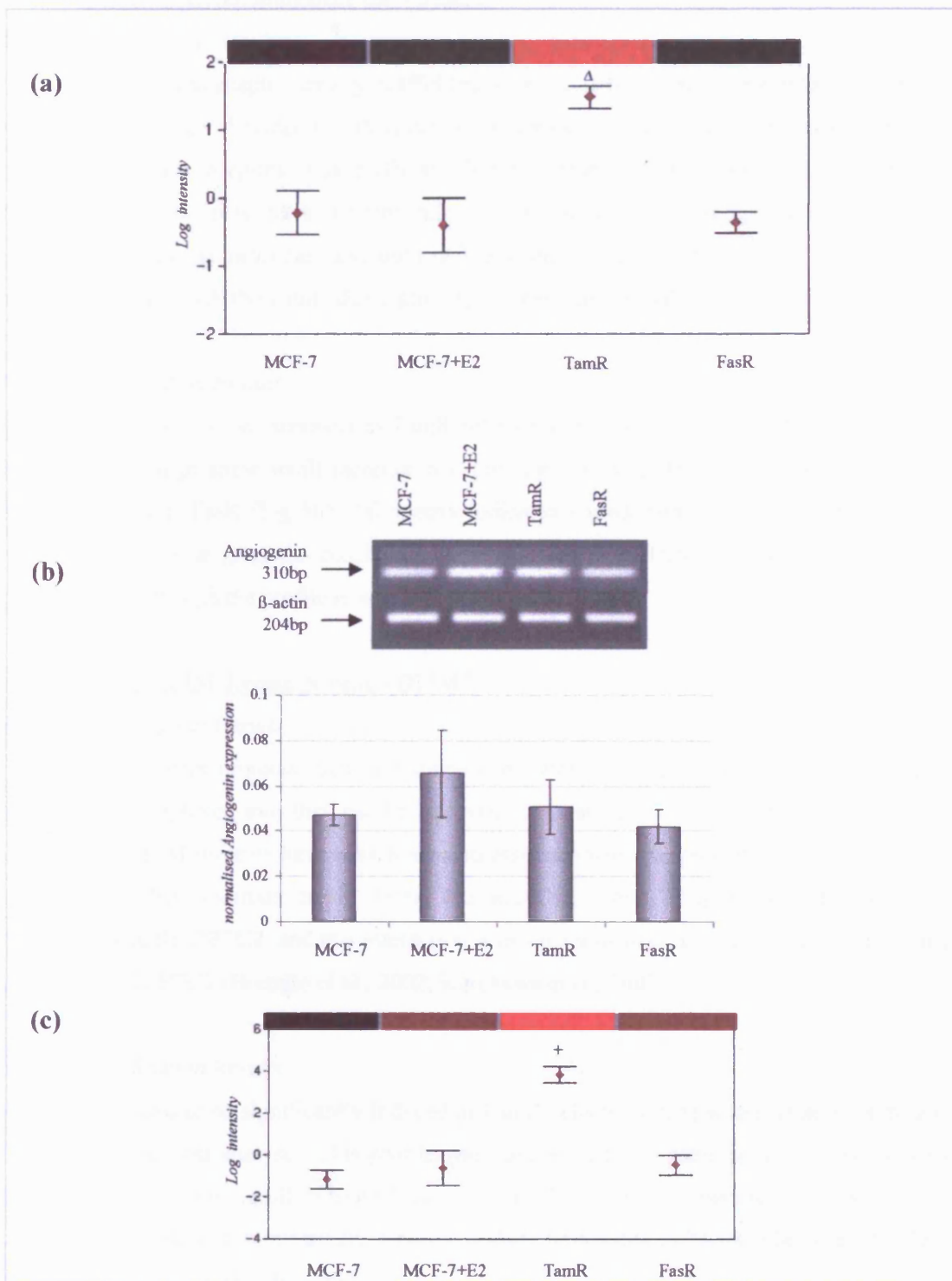
Figure 55. Angiogenin gene expression profile in resistant cells. Angiogenin mRNA was monitored as (A) using Atlas Plastic Human 12k Microarrays. Log intensity graphical output and heatmap are shown. (B) by PCR analysis using primers for Angiogenin. β-actin was also amplified (normalisation purposes). PCR products separated on an agarose gel were visualised by ethidium bromide staining. Representative PCR profile is shown from triplicate experiments. PCR signals were then subject to densitometric analysis and normalised data plotted (plot shows standard error). (C) using Affymetrix HG-U133A gene chips. (Identical RNA preparations were used for all studies of mRNA expression). Additional controls were provided by MCF-7 cells subject to oestradiol treatment. ($\Delta p=0.0032$ for TamR relative to MCF-7; $+p=0.0009$ for TamR relative to MCF-7 [student t-test]).

3.3.2.4 Homer, neuronal immediate early gene, 2

Detailed Ontological Results

'Homer 2' is a postsynaptic density scaffolding protein. It binds and cross-links cytoplasmic regions of a number of proteins with endoplasmic reticulum-associated receptors and aids the coupling of surface receptors to intracellular calcium release. Homer isoforms can be differently regulated and may play an important role in maintaining the plasticity at glutamatergic synapses, and during neuronal development has been shown to interact with brain derived neurotrophic factor (BDNF) and AKT signalling for neuronal growth (Schratt et al., 2004)

RT-PCR Verification Results

Homer2 was found to be increased in TamR relative to MCF-7 cells using Plastic 12k arrays (p<0.001), although some small increase in expression was also detected in oestradiol-treated MCF-7 as well as FasR (Fig 56). Affymetrix indicated a predominantly TamR induced gene. PCR analysis for angiogenin confirms a small increase in TamR across triplicate RNA preparations, although the profile is weak.

3.3.2.5 Enigma (LIM domain protein, PDLIM7)

Detailed Ontological Results

LIM domain proteins such as Enigma can function as scaffolds for the formation of multiprotein complexes, thus they can be involved in cytoskeletal organisation and oncogenesis (Bach, 2000). LIM proteins have been known to associate with components such as the insulin receptor and PKC (Kuroda et al., 1996, Wu and Gill, 1994). Enigma was also found to colocalise with RET/PTC2, and this interaction is in such a manner as to enhance the mitogenic activity of RET/PTC2 (Borrello et al., 2002, Kurokawa et al., 2003).

RT-PCR Verification Results

We found Enigma to be significantly induced in TamR cells (p=0.025) with a small induction in FasR cells by cluster analysis. This profile was confirmed twice using probes on Affymetrix arrays, but was mainly TamR induced (Fig.57). A small induction in oestradiol-treated MCF-7 cells was also observed. Interestingly, Enigma is also upregulated in TamR cells where GFRα3, a RET coreceptor, is also substantial.

3.3.2.6 Casein Kinase 2

Detailed Ontological Results

Casein Kinase 2 (CK2) is a protein serine/threonine signalling kinase which plays a role in cells growth and proliferation, but is also a potent suppressor of apoptosis, and has also been found to be dysregulated in a number of cancers. CK2 was found to be capable of inducing NFκB in

breast cancer cells (Eddy et al., 2005), is a positive regulator of WNT signalling (Seldin et al., 2005, Song et al., 2003), interacts with BRCA1 (O'Brien et al., 1999) and may phosphorylate the ER on ser167 (Arnold et al., 1995).

RT-PCR Verification Results

Although CK2 was found to be significantly elevated in TamR cells (p=0.03) using Atlas Plastic arrays, Affymetrix and PCR were not able to confirm any upregulation, and only a very small increase by PCR in FasR (Fig.58).

3.3.3 FasR Induced Genes

3.3.3.1 Vitronectin

Detailed Ontological Results

Vitronectin belongs to a group of structurally and functionally homologous adhesive proteins (fibrinogen, fibronectin, von Willebrand factor) essential in the procoagulant phase of the hemostatic system, interacting with platelets and the vessel wall. Vitronectin has also been reported to enhance the migration of breast cancer cells *in-vitro* (Bartsch et al., 2003, Campo McKnight et al., 2006).

Verification Results

On both Atlas Plastic and Affymetrix arrays, Vitronectin was significantly increased in FasR cells (p=0.026), and there was no consistent oestradiol regulation observed (Fig.59) Due to time constraints, PCR profiling of Vitronectin could not be performed. However, the protein is of interest in our laboratory, where studies have confirmed an obvious increase in Vitronectin staining in FasR models, as shown by immunocytochemistry (Fig.60; M. Harper *personal communication*).

3.3.4 Genes Downregulated in TamR and FasR Cells

3.3.4.1 GFRα1

Detailed Ontological Results

GFRα1 belongs to a family of receptors which include GFRα3 (see 3.3.2 for full description of the family receptor/ligands). GFRα1 is activated preferentially by its ligand GDNF, although it may also be activated also by Neurturin, and Artemin (Airaksinen and Saarma, 2002). The family receptors function to further activate their corrector, the RET protooncogene (Sariola and Saarma, 2003, Baloh et al., 1998a). Although RET has been implicated in a number of conditions such as medullary thyroid carcinoma (Asai et al., 2006),
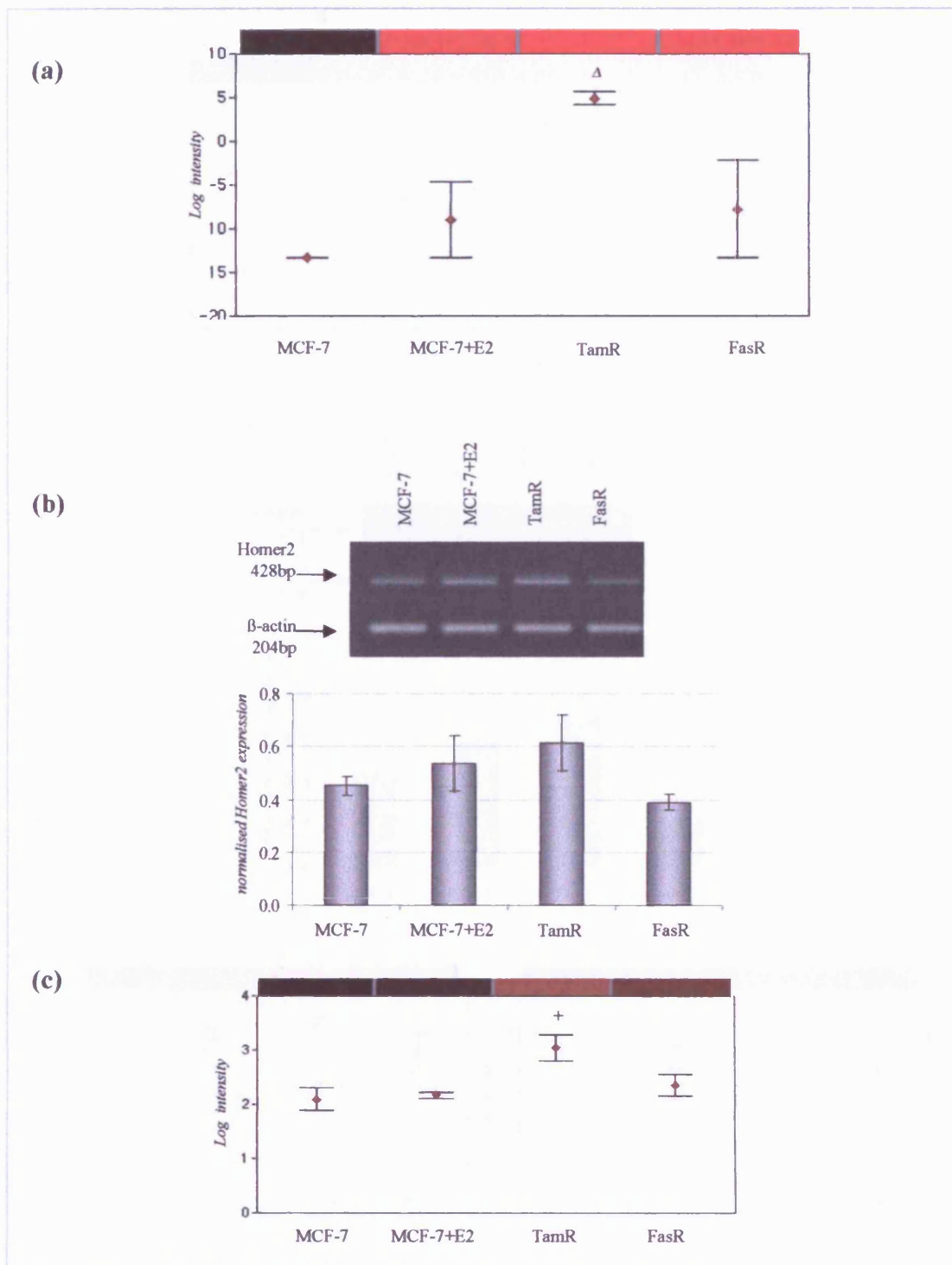
Figure 56. Homer2 gene expression profile in resistant cells. Homer2 mRNA was monitored as (a) using Atlas Plastic Human 12k Microarrays. Log intensity graphical output and heatmap are shown. (b) by PCR analysis using primers for Homer2 co-amplified with β-actin (normalisation purposes). PCR products separated on an agarose gel were visualised by ethidium bromide staining. Representative PCR profile is shown from triplicate experiments. PCR signals were then subject to densitometric analysis and normalised data plotted (plot shows standard error). (c) using Affymetrix HG-U133A gene chips. (Identical RNA preparations were used for all studies of mRNA expression). Additional controls were provided by MCF-7 cells subject to oestradiol treatment. (Δp<0.001 for TamR relative to MCF-7; +p=0.0436 for TamR relative to MCF-7 [student t-test]).

Figure 57. Enigma gene expression profile in resistant cells. Enigma mRNA was monitored as (a) using Atlas Plastic Human 12k Microarrays. Log intensity graphical output and heatmap are shown. (b) by PCR analysis using primers for Enigma co-amplified with β-actin (normalisation purposes). PCR products separated on an agarose gel were visualised by ethidium bromide staining. Representative PCR profile is shown from triplicate experiments. PCR signals were then subject to densitometric analysis and normalised data plotted (plot shows standard error). (c) using Affymetrix HG-U133A gene chips. Gene was represented twice on the array. (Identical RNA preparations were used for all studies of mRNA expression). Additional controls were provided by MCF-7 cells subject to oestradiol treatment. . (Δp=0.025 for TamR relative to MCF-7; *p=0.0144 for FasR compared to MCF-7 cells; +p=0.0192 and ++p=0.0030 respectively for MCF-7+E2 and TamR relative to MCF-7 [student t-test]).
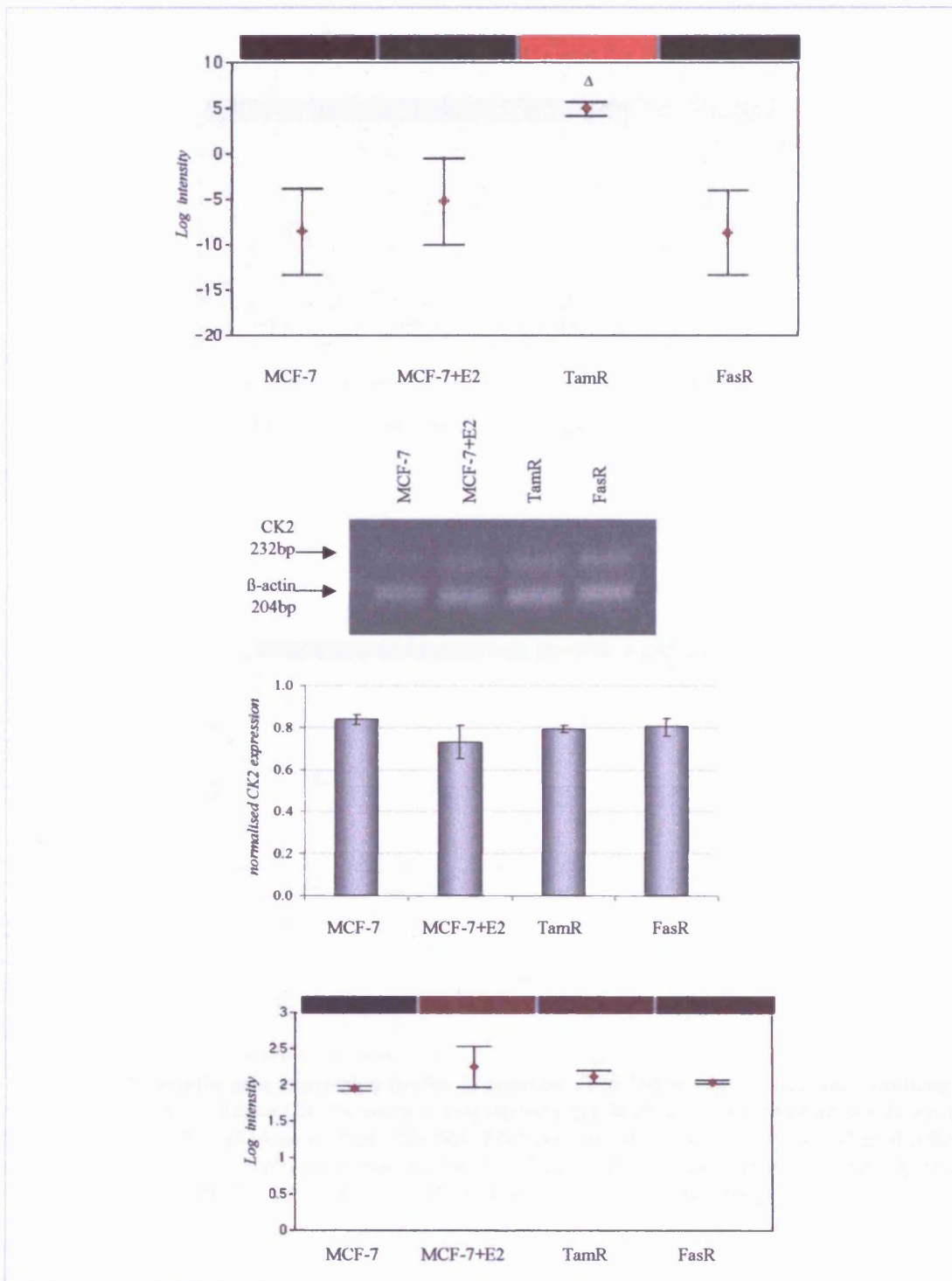
Figure 58. Casein Kinase II gene expression profile in resistant cells. Casein Kinase II alpha polypeptide mRNA was monitored as (a) using Atlas Plastic Human 12k Microarrays. Log intensity graphical output and heatmap are shown. (b) by PCR analysis using primers for CK2 co-amplified with β-actin (normalisation purposes). PCR products separated on an agarose gel were visualised by ethidium bromide staining. Representative PCR profile is shown from triplicate experiments. PCR signals were then subject to densitometric analysis and normalised data plotted (plot shows standard error). (c) using Affymetrix HG-U133A gene chips. (Identical RNA preparations were used for all studies of mRNA expression). Additional controls were provided by MCF-7 cells subject to oestradiol treatment. (Δp=0.03 for TamR relative to MCF-7 [student t-test]).

Figure 59. Vitronectin gene expression profile in resistant cells. Vitronectin mRNA was monitored as (a) using Atlas Plastic Human 12k Microarrays. Log intensity graphical output and heatmap are shown. (b) using Affymetrix HG-U133A gene chips. (Identical RNA preparations were used for all studies of mRNA expression). Additional controls were provided by MCF-7 cells subject to oestradiol treatment. (^p=0.026 for FasR relative to MCF-7; +p=0.0005 for FasR relative to MCF-7 [student t-test]).
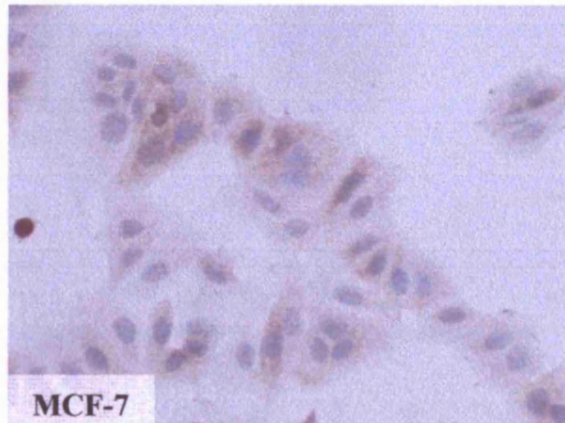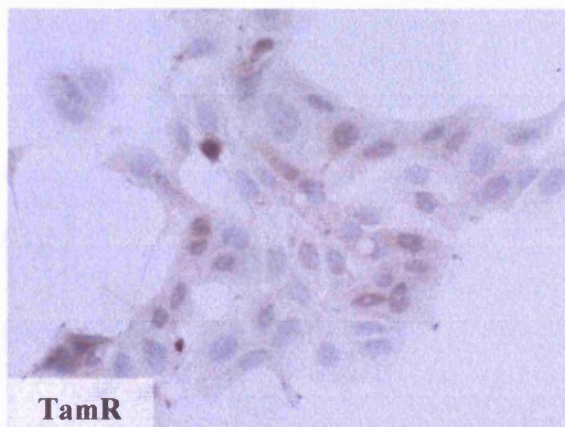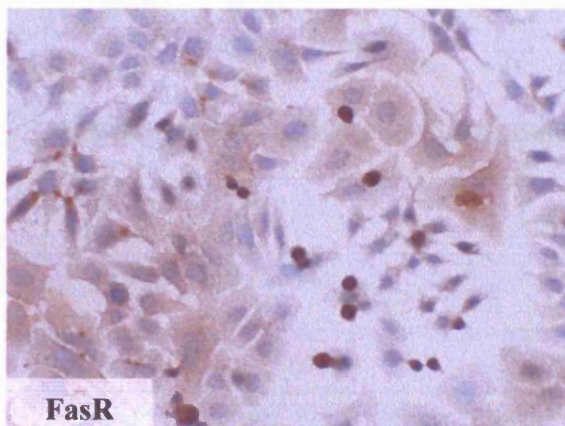
Figure 60. Vitronectin protein increase in resistant cells.MCF-7, TamR and FasR cells grown on coverslips were fixed and stained using the monoclonal antibody to Vitronectin. Images show x20 original magnification. *Courtesy of M. Harper & C. Smith.*
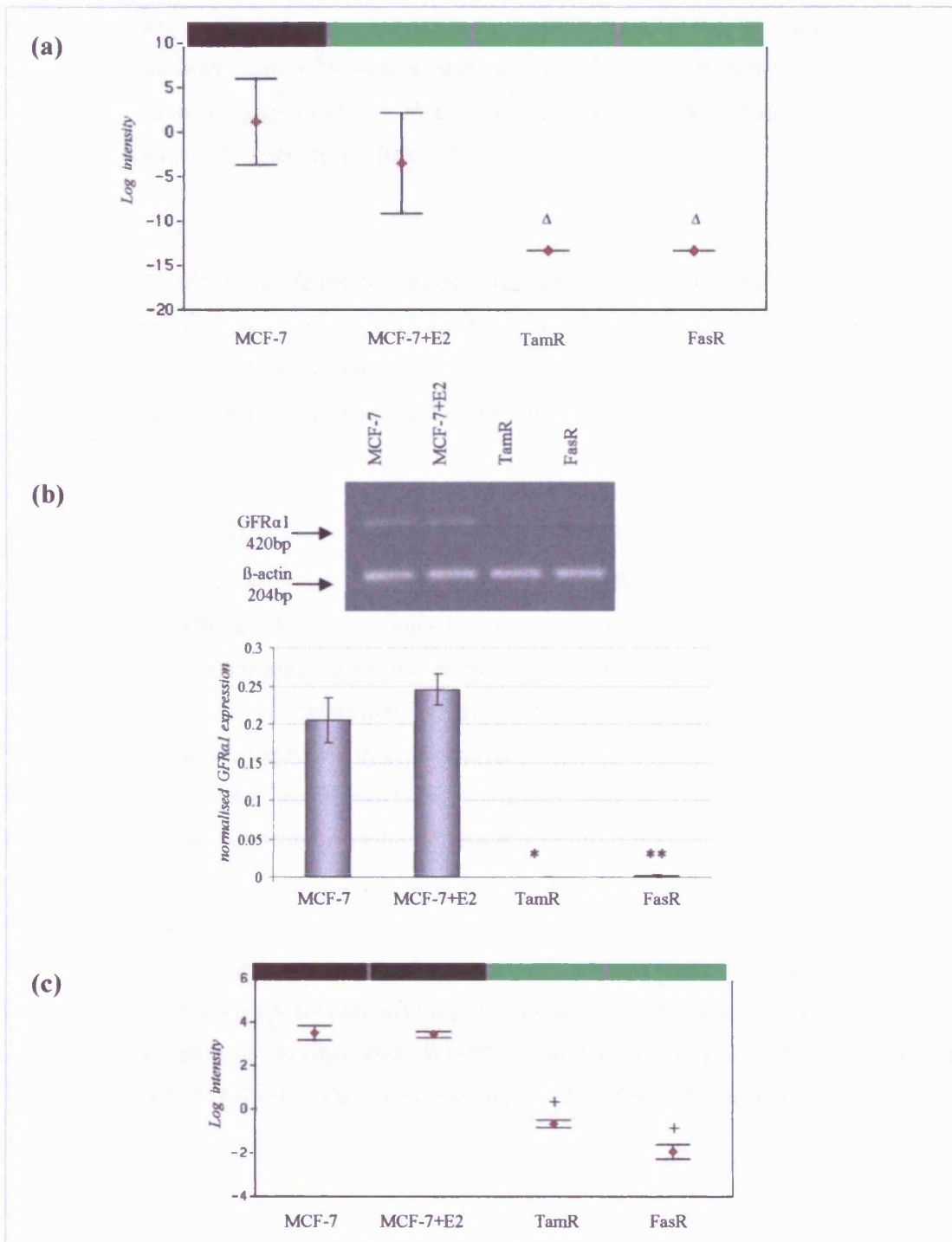
Figure 61. GFRα1 gene Downregulation in TamR and FasR cells. GFRα1 mRNA was identified as (a) downregulated in TamR and FasR cells using Atlas Plastic Human 12k Microarrays. Graphical output and heatmap are shown. (b) Verification of gene profile was performed by PCR analysis using primers for GFRα1 co-amplified with β-actin (normalisation control). PCR products separated on agarose gel was visualised by ethidium bromide staining. Representative PCR profile is shown from triplicate experiments. PCR profiles were then subject to densitometric analysis. (plot shows standard errors) (c) Profiles using Affymetrix HG-U133A gene chips are also shown. (RNA preparations used for Affymetrix genechips were identical to those used for Atlas Plastic arrays). Graphical output and heatmap are shown . Additional controls were provided by parental MCF-7 cells subject to oestradiol treatment. (Δp=0.0245 for both TamR and FasR relative to MCF-7; (*p<0.001 and **p=0.0024 respectively for TamR and FasR relative to MCF-7; (+p<0.001 for both TamR and FasR relative to MCF-7 [all statistical analysis performed using students t-test]).

and more recently pancreatic cancer (Ito et al., 2005), there is our knowledge, no direct association with breast cancer. However more recently GFRα1 been noted to be oestrogen regulated in hormone responsive ZR-75-1 cells and associated with also ER-positivity in clinical array studies (Dorssers et al., 2005).

Verification Results

GFRα1 mRNA was found significantly reduced in both TamR and FasR cells versus MCF-7 cells using Atlas Plastic arrays, which was confirmed by both PCR and Affymetrix analysis (Fig.61). A slight induction of GFRα3 is suggested in oestradiol-treated MCF-7 cells by PCR, although this is not significant, and is not confirmed by Atlas or Affymetrix arrays.

3.3.4.2 WISP2

Detailed Ontological Results

The wnt1-inducible signalling pathway protein (WISP) family have 3 members (Pennica et al., 1998) and have been linked to a number of cancer types. These proteins are thought to stimulate mitosis, apoptosis, extracellular matrix production and cell invasion (Brigstock, 2003). WISP1-3 expression was demonstrated to be differential when WISP1 and WISP3 were found overexpressed in colon cancers, whereas WISP2 was reduced (Pennica et al., 1998). WISP2 has also been shown to be regulated by oestrogen, which could be blocked by Faslodex, suggesting interaction with the ER (Banerjee et al., 2003).

Verification Results

WISP2 was found significantly decreased in TamR and FasR cells using Atlas Plastic arrays (Fig.62). This significant reduced mRNA expression was further confirmed using PCR and Affymetrix analysis. Furthermore, WISP2 showed a significant mRNA induction in oestradiol-treated MCF-7 cells, which was also suggested by Affymetrix analysis.
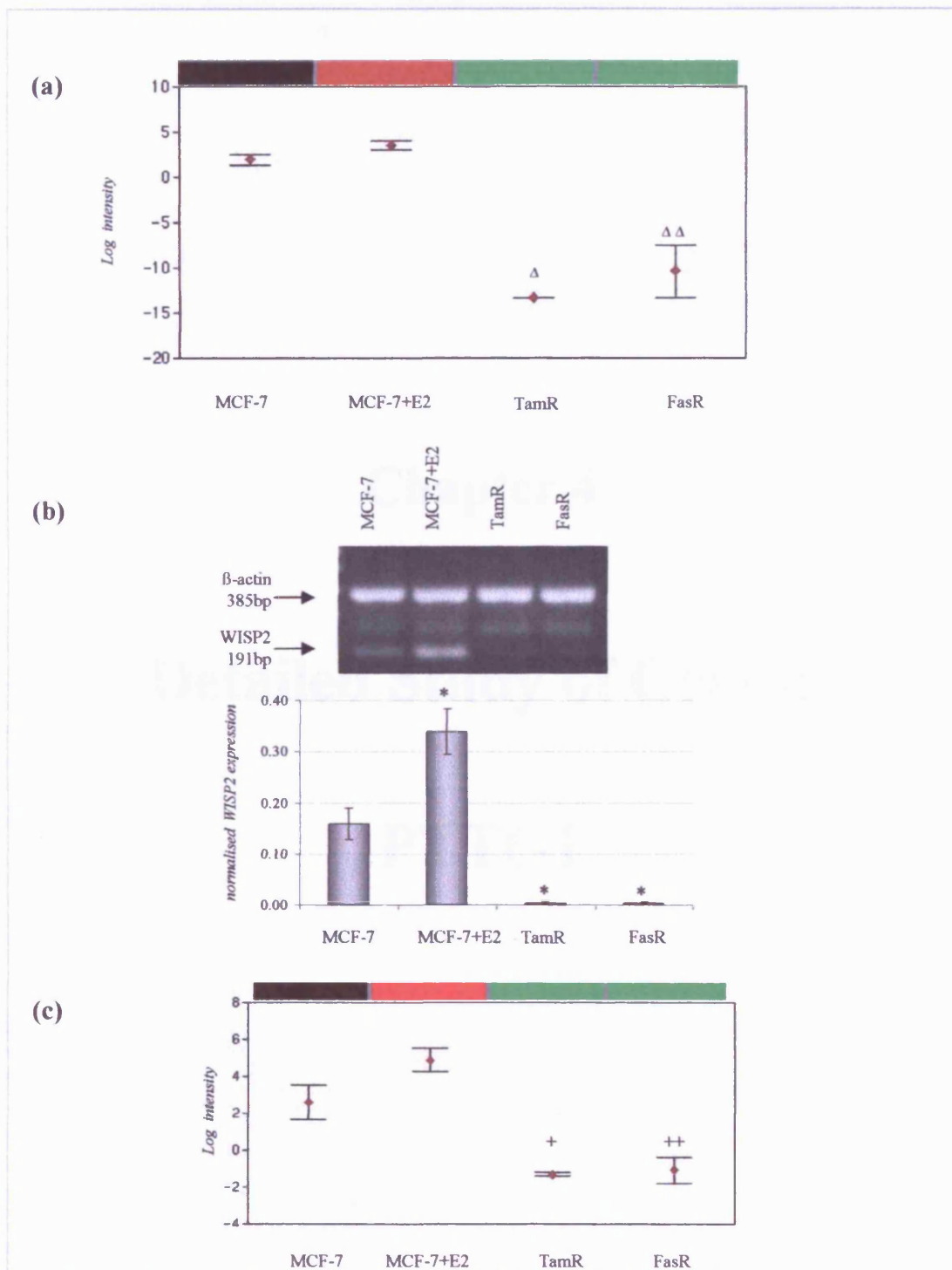
Figure 62. WISP2 downregulation in resistant cells. WISP2 mRNA was identified as significantly downregulated in TamR and FasR cells using GeneSifter software in (A) Atlas Plastic Human 12k Microarrays, and (B) profile was determined by PCR analysis. (C) Profiles using Affymetrix HG-U133A gene chips. (P33-labelled RNA used for hybridisation to Affymetrix genechips were also previously used with Atlas Plastic 12k Microarrays) are also shown Graphical output and heatmap are shown for all outputs. Additional controls were provided by parental MCF-7 cells subject to oestradiol treatment. ($^\Delta$p<0.001 and $\Delta\Delta$p=0.006 respectively for TamR and FasR relative to MCF-7 [students t-test]; *p<0.05 relative to MCF7; +p=0.0143 and ++p=0.0353 respectively for TamR and FasR relative to MCF-7 [students t-test]).

Chapter 4

Detailed Study of Genes:

PTTG1

4.1   PTTG1

Gene selection using Plastic 12k Human Microarrays revealed the gene for PTTG1 as significantly induced in both TamR and FasR cells, with some induction in oestradiol-treated MCF-7 cells, and this profile was confirmed using PCR analysis and Affymetrix analysis (see section 3.3.1 and Fig.35).

4.1.1   PTTG1 Gene Induction in Resistant Cells

In addition to the above PCR verification on the array sample set, PCR confirmation was also performed on additional sets of RNA samples extracted subsequent to the arrayed RNA set. Profiles for these endocrine responsive and resistant cell lines confirmed the above gene induction in FasR (p=0.05) as well as, to a lesser degree in TamR and oestradiol-treated MCF-7 cells (Fig.63).

Subsequent PCR analysis also demonstrated over a hundred-fold increase in PTTG1 mRNA in the further FasR model, FasR-Lt relative to parental MCF-7 cells (Fig.64a). FasR-Lt cell expression was also observed not only to be elevated relative to parental MCF-7 cells, but also approximately 7-fold increased compared to FasR cells. Although parallel Affymetrix analysis confirmed PTTG1 gene elevation in FasR and FasR-Lt compared to MCF-7 cells (p=0.002 and p=0.0025 respectively), the increase in FasR-Lt versus FasR was less pronounced (Fig.64b).

A cell model developed within the TCCR with acquired resistance to severe oestrogen deprivation was also studied to determine the levels of PTTG1 gene. These X-MCF-7 cells showed significantly increased levels of PTTG1 mRNA as determined by PCR analysis versus control MCF-7 (Fig.65a; p=0.008). This was further verified using Affymetrix data which similarly demonstrated a significant induction (Fig.65b; p=0.0044). The highest PTTG1 gene induction was observed in FasR-Lt cells, followed by X-MCF-7, FasR, TamR and MCF-7+E2 versus MCF-7 cells.

4.1.2   PTTG1 Protein Induction in Resistant Cells

4.1.2.1   Western Blotting Analysis of PTTG1 Protein

Use of a monoclonal antibody to the PTTG1 protein permitted the demonstration of the induction of PTTG1 in both TamR and FasR-Lt cell lines relative to control MCF-7 cells by Western blotting, thus confirming mRNA studies performed previously. This protein increase was more pronounced within the FasR-Lt cells (Fig.66) as noted in PCR studies.

4.1.2.2 Immunocytochemical Analysis of PTTG1 Protein

Immunocytochemical assay development allowed the localisation of PTTG1 protein within paraffin-embedded cell pellet blocks containing a replicate number of endocrine resistant and responsive cell lines including TamR, FasR-Lt, X-MCF-7 and MCF-7, as well as an ER-negative *de novo* tamoxifen-resistant mode; MDA-MB-231.

4.1.2.2.1 Development of Immunocytochemical Assay for PTTG1

The immunocytochemical method developed for the analysis of PTTG1 protein involved heat mediated (citrate buffer, pH 6) antigen retrieval and used a monoclonal PTTG1 antibody with DAKO Envision detection. However, owing to the relatively weak staining signal in paraffin embedded material, copper sulphate enhancement was also used to improve visualisation across the cell lines in the fully developed assay (see example staining in Fig.67).

4.1.2.2.2 Immunocytochemical Analysis Using Optimised ICC Assay for PTTG1

Paraffin cell pellet arrays bearing endocrine responsive and resistant cell lines in replicates of 6 pellets per cell line (2 from each 3 experimental replicates) were scored for positively staining cells as described previously. PTTG1 staining where present was localised as both cytoplasmic and nuclear, and was notably increased across all of the resistant cell lines compared to MCF-7 cells (Fig.67 and Fig.68). Following assessment of total PTTG1 expression, relative to parental cells, there was a significant 3.8 fold increase in total PTTG1 staining in TamR ($p<0.001$), and a 3.7 fold increase in FasR-Lt and X-MCF-7 cells ($p<0.001$ and $p=0.003$ respectively). However, the most apparent increase, of 5.2 fold, was observed in the oestrogen receptor-negative MDA-MB-231 cell line ($p<0.001$), which was also significantly increased over FasR-Lt ($p<0.05$) and other cell lines present on the cell array.

4.1.3 Further PTTG Family Members Induced in Resistant Cells

Recent reports have identified further PTTG genes which share a high sequence homology to PTTG1, notably PTTG2 and PTTG3 (Chen et al., 2000). In parallel with PTTG1 studies, PCR analysis using primers for these genes, and Affymetrix analysis, also revealed differential expression across the resistant cell lines used in this study. The PTTG2 gene was however, not present on the Atlas Plastic Human 12k Array platform for comparison.

PTTG2 mRNA was significantly increased in FasR cells ($p=0.0133$) compared to parental MCF-7 cells using PCR analysis (Fig.69a), which was further confirmed using Affymetrix arrays ($p=0.0478$; Fig.69b). While PCR data also suggested a small degree of repression in oestradiol-treated MCF-7 cells (Fig.69a), this was not verified using Affymetrix
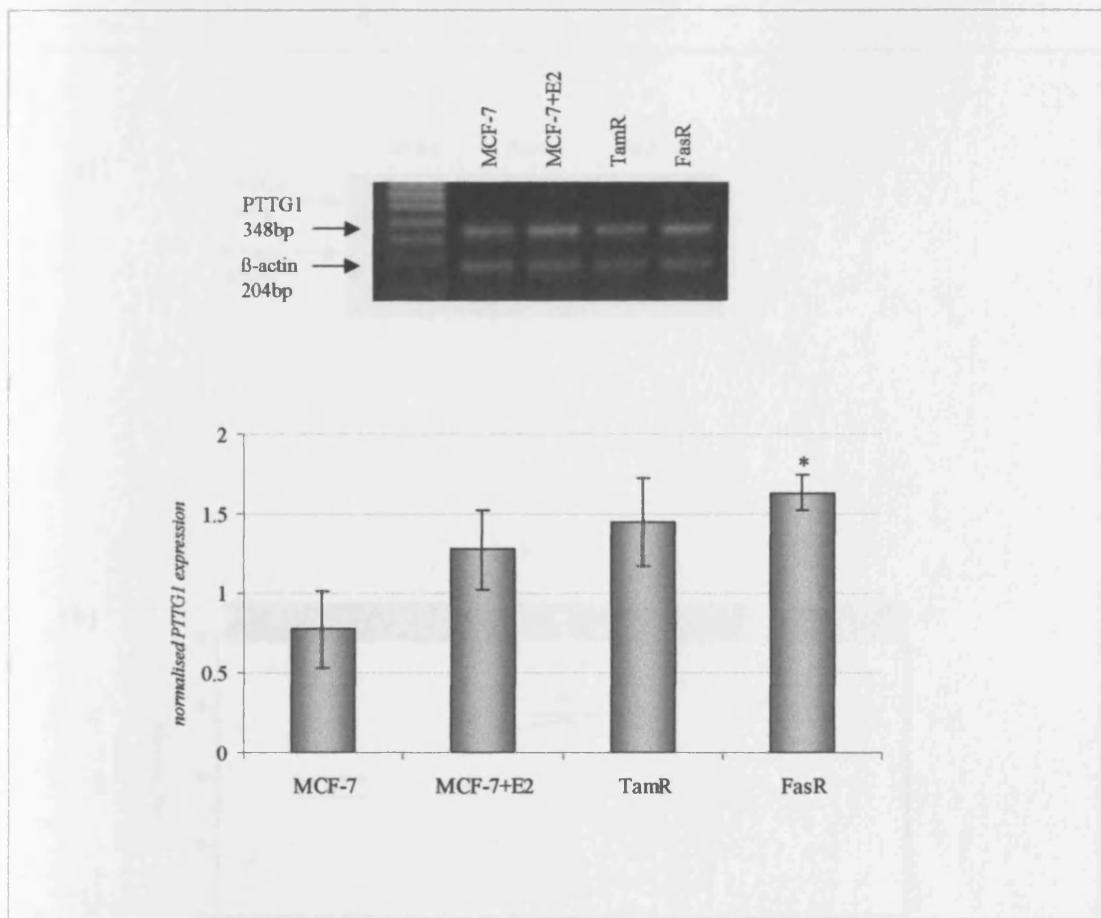
Figure 63. PTTG1 gene upregulation in resistant cells is further confirmed. PTTG1 mRNA was further confirmed as increased in resistant cells using RNA preparations extracted from an additional replicate experiment. This was achieved by PCR analysis using primers for PTTG1 co-amplified with β-actin (normalisation control). PCR products separated on agarose gel were visualised by ethidium bromide staining. A representative PCR profile is shown. PCR profiles were then subject to densitometric analysis and normalised before plotting. (Plot shows standard errors). (*p=0.05 FasR cells relative to MCF-7 cells [Students t-test]).
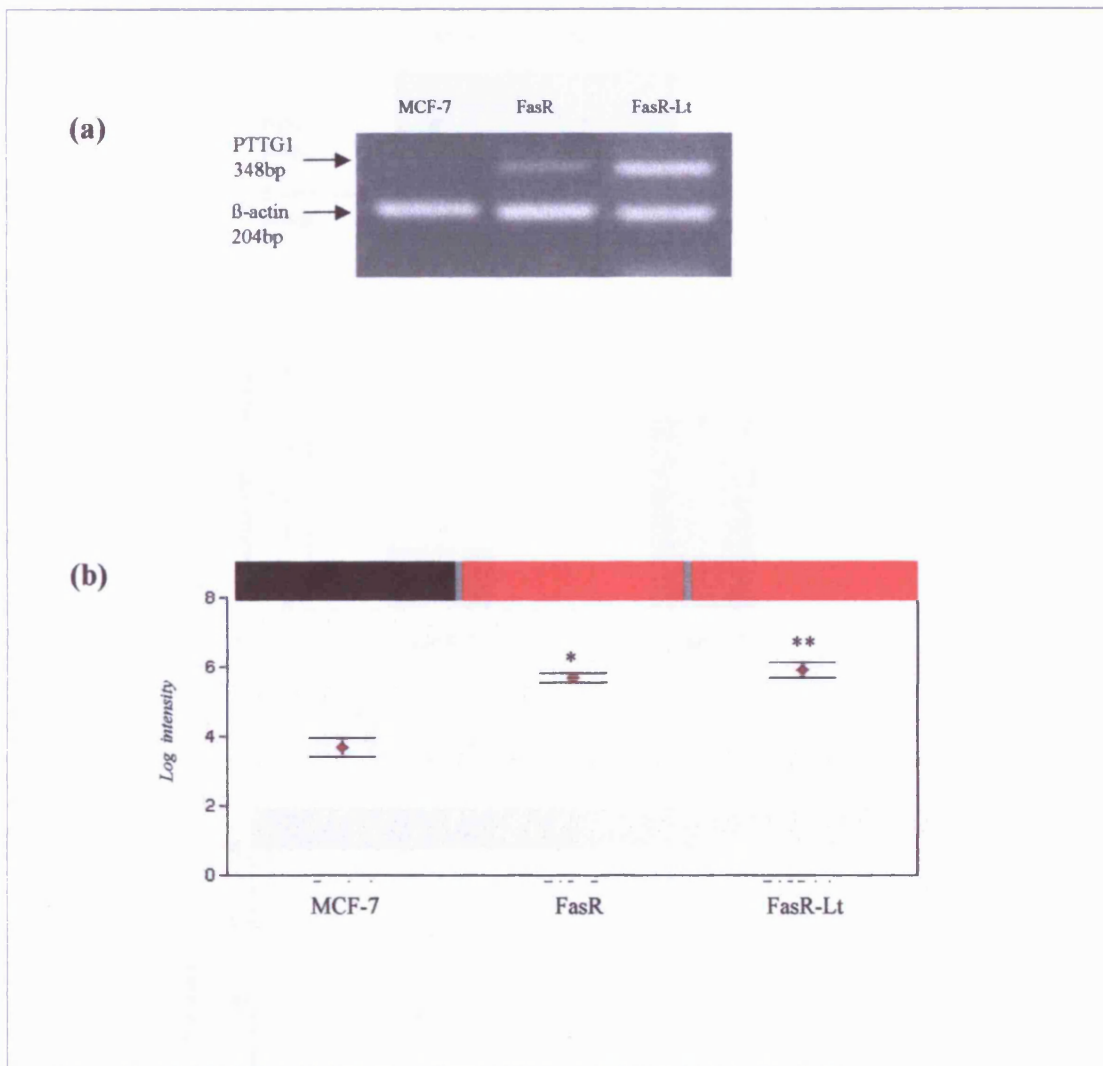
Figure 64. PTTG1 gene upregulation in FasR and FasR-Lt cells. (a) PTTG1 gene was shown to be elevated further to FasR cells, in the FasR-Lt cell line. PCR analysis was achieved using primers for PTTG1 co-amplified with β-actin (normalisation control). PCR products separated on agarose gel were visualised by ethidium bromide staining. Representative PCR profile is shown. (b) PTTG1 RNA was identified as significantly altered in FasR and FasR-Lt cells using GeneSifter software in Affymetrix HG-U133A gene chips. Graphical output and heatmap are shown. Plot shows log mean intensity and standard errors. (*p=0.002 and **p=0.0025 for FasR and FasR-Lt relative to MCF-7 [Students t-test]).

(a)

MCF-7   X-MCF-7

PTTG1
348bp

ß-actin
204bp

(b)
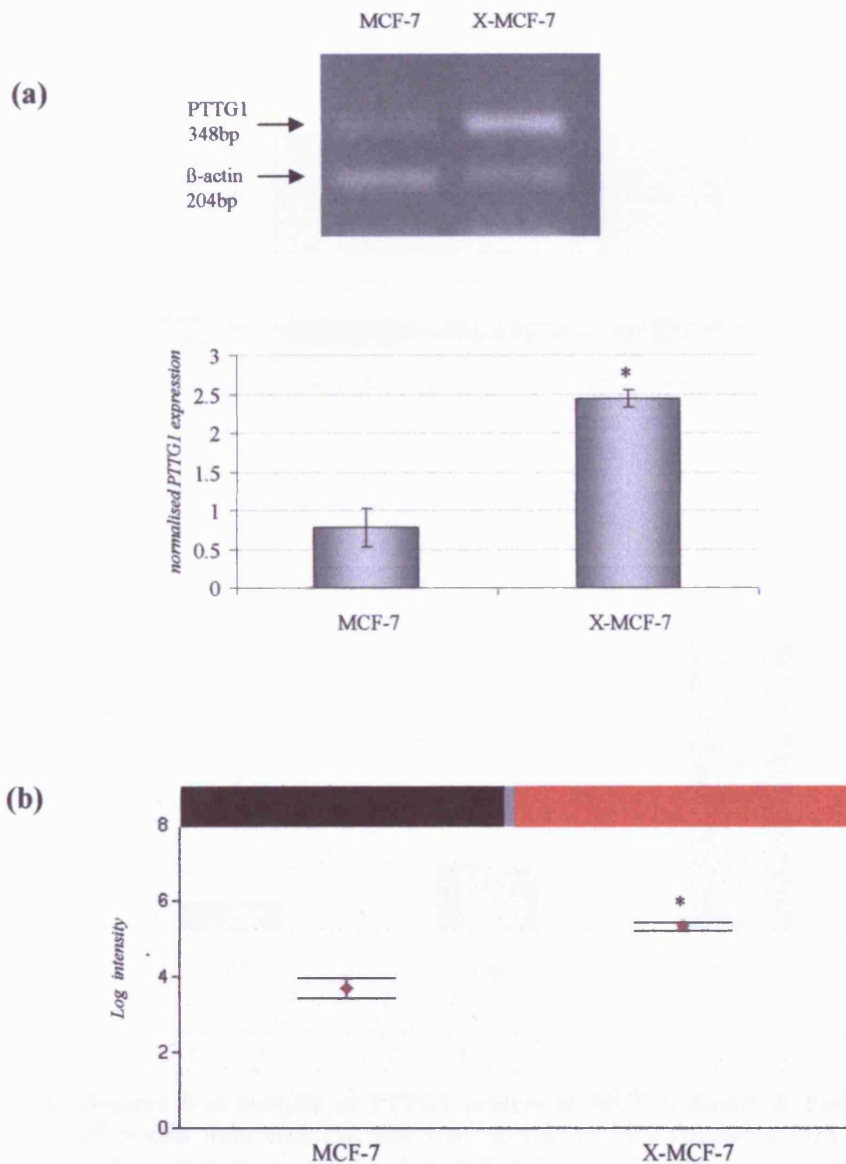
Figure 65. PTTG1 gene regulation in model resistant to oestrogen-depravation, X-MCF-7 cells. RNA was subject to RT-PCR using primers for PTTG1 and visualised by ethidium bromide staining. B-actin was coamplified and used as an internal control. Representative signal is shown for triplicate experiment. PCR profiles were then subject to densitometric analysis and normalisation before plotting. (*p=0.008 relative to MCF-7 [students t-test]). (b) PTTG1 mRNA was identified as in X-MCF-7 cells using GeneSifter software in Affymetrix HG-U133A gene chips. Graphical output and heatmap are shown for the gene. Plot shows log mean intensity and standard errors. (*p=0.0044 for X-MCF-7 relative to MCF-7 [student t-test]).
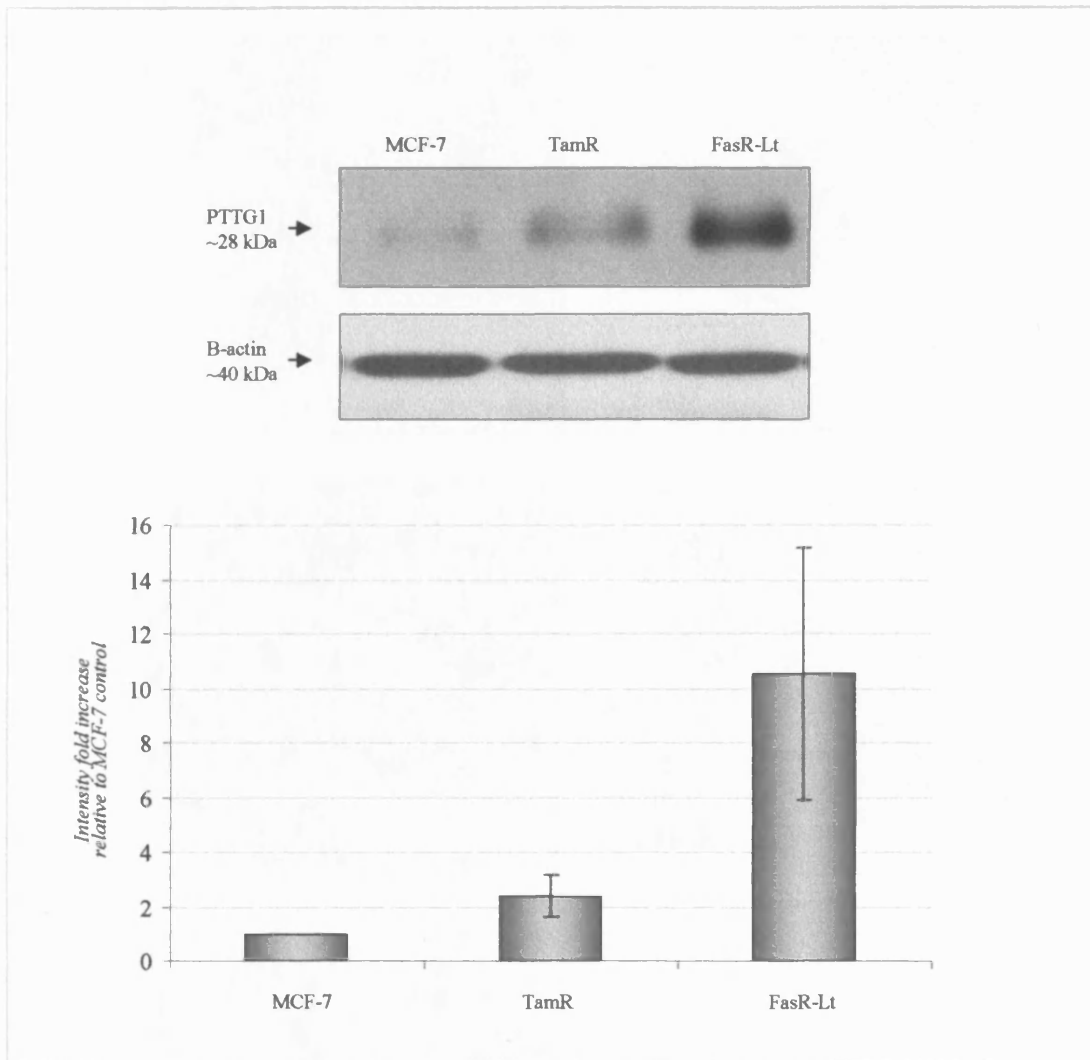
Figure 66. Western Blot analysis of PTTG1 protein in MCF-7, TamR & FasR-Lt cells. Fifty micrograms of protein from each cell line were subject to 15% denaturing SDS PAGE, Western blotting and probed using monoclonal anti-human PTTG1 antibody with chemiluminescence detection. (Plot shows fold increase in normalised expression relative to control MCF-7 cells with standard errors). Representative blot is shown from triplicate experiments.
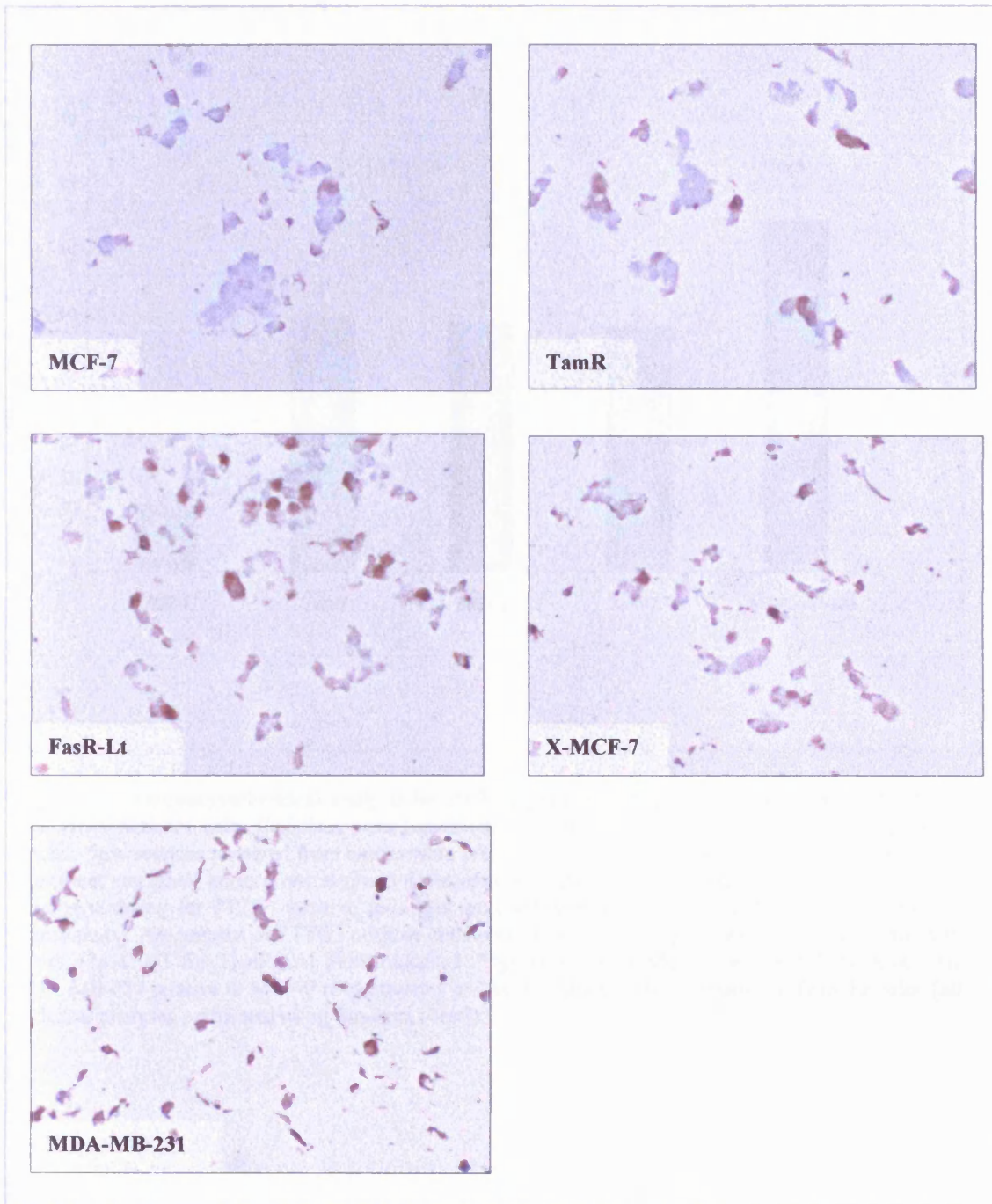
Figure 67. Immunocytochemical detection of PTTG1 protein in MCF-7, TamR & FasR-Lt. MCF-7, TamR & FasR-Lt, X-MCF-7 and MDA-MB-231 cells were harvested, formalin fixed, and pellets embedded in paraffin blocks. 5µm sections prepared from blocks were probed using monoclonal anti-human PTTG1 antibody (67µl/ml) after (heat mediated) antigen retrieval, with copper sulphate enhancement and detected using DAKO Envision detection system with DAB staining. Figures show x20 magnification.
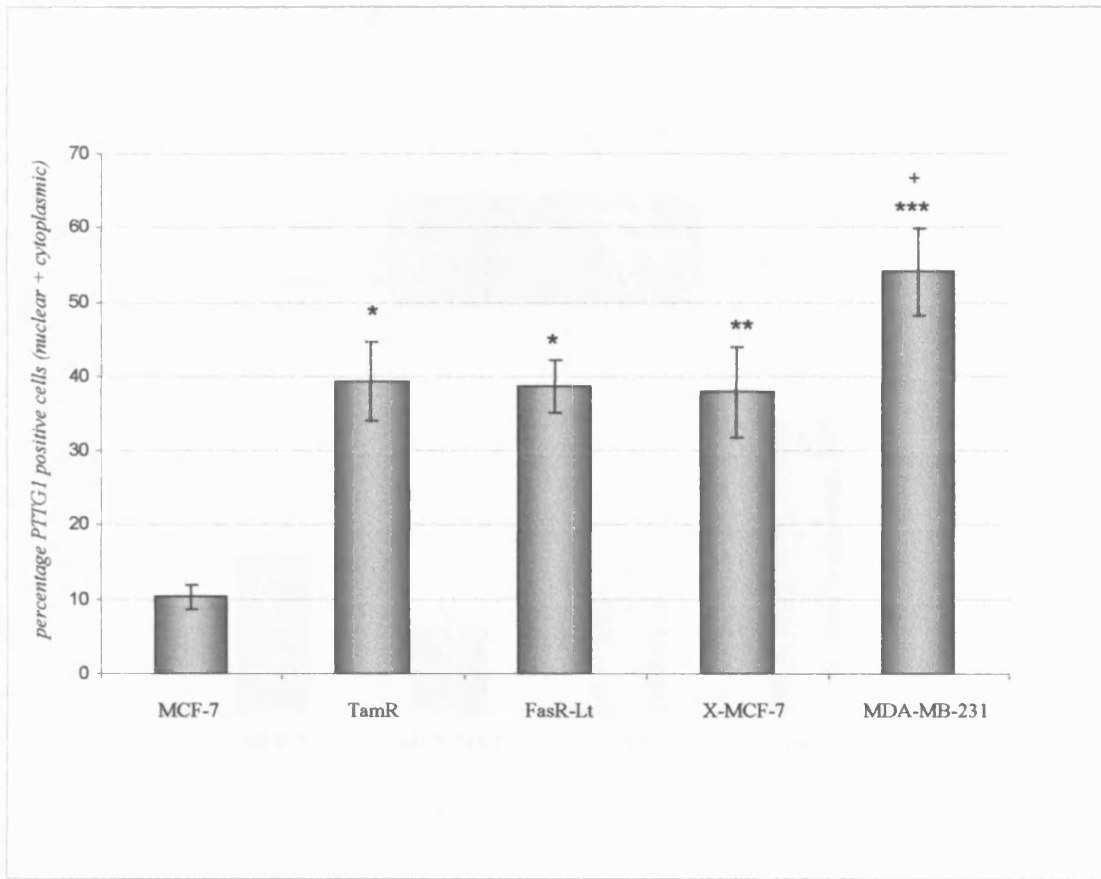
Figure 68. Immunocytochemical analysis for PTTG1 protein in MCF-7, TamR, FasR-Lt, X-MCF-7 & MDA-MB-231 cells. Cell lines were harvested, formalin fixed, and pellets embedded in paraffin blocks. 5μm sections prepared from blocks were probed using monoclonal anti-human PTTG1 antibody after (heat mediated) antigen retrieval and detected using DAKO Envision detection system with DAB staining. Staining for PTTG1 positive cells was recorded from six fields (2 fields from each triplicate experiments). Assessment of PTTG1 positive cells performed at x20 magnification. Plots show standard errors. (*p<0.001 for TamR and FasR-Lt cells, **p=0.003 for X-MCF-7 cells and ***p<0.001 for MDA-MB-231 relative to MCF-7 respectively; +p<0.05 for MDA-MB-231 relative to FasR-Lt cells [all statistical analyses performed using Students t-test]).
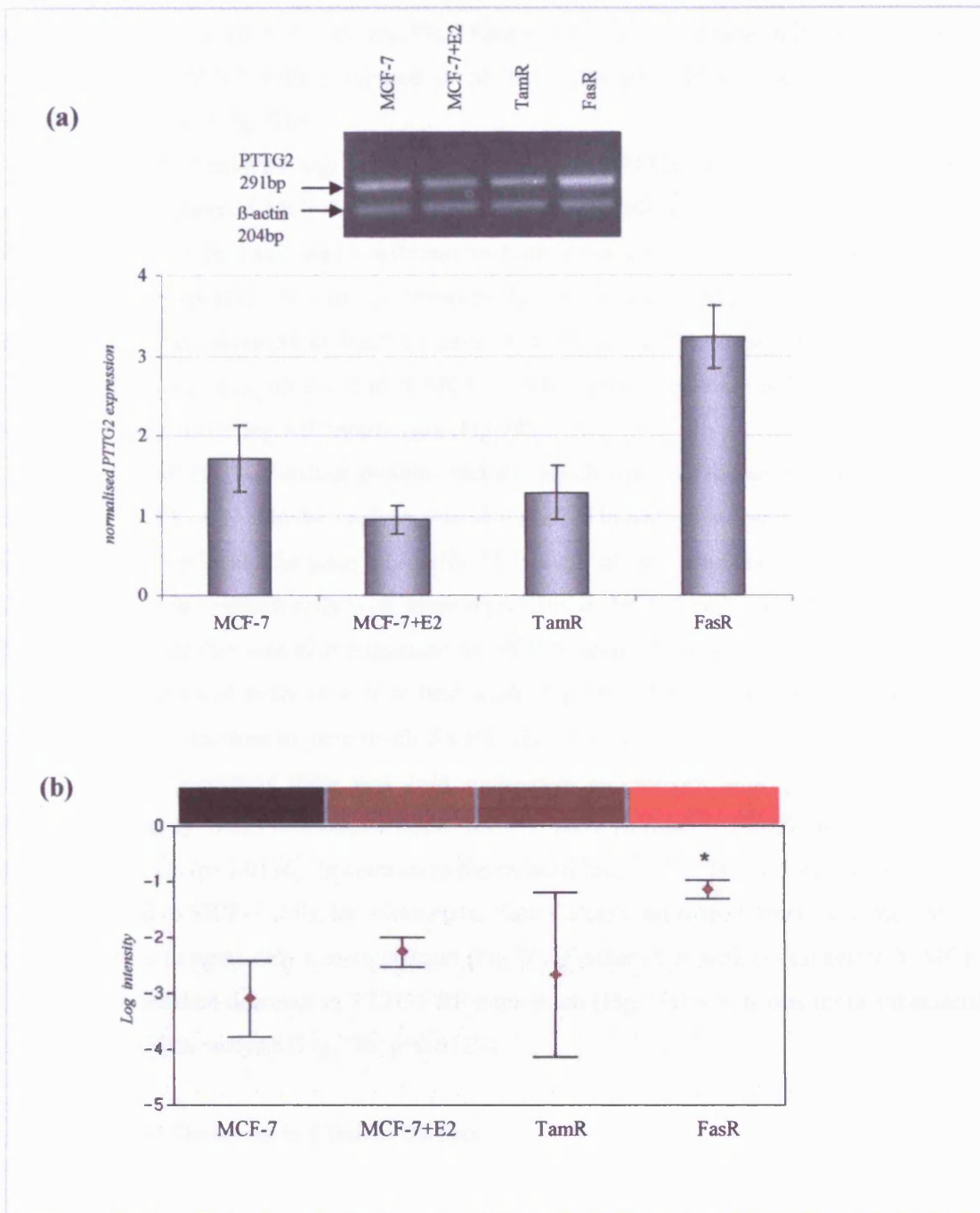
Figure 69. PTTG2 gene confirmation in resistant cells. (a) Verification of gene profile was performed by PCR analysis using primers for PTTG2 co-amplified with β-actin (normalisation control). PCR products separated on agarose gel were visualised by ethidium bromide staining. Representative PCR profile is shown. PCR profiles were then subject to densitometric analysis for normalised intensity plots (profile shows standard errors). (b) PTTG2 mRNA was identified as differentially expressed in TamR and FasR cells using GeneSifter software in Affymetrix HG-U133A gene chips. Graphical output and heatmap are shown for the gene. Plot shows log mean intensity and standard errors. Additional controls were provided by parental MCF-7 cells subject to oestradiol treatment. (*p=0.0478 for FasR relative to MCF-7 [students t-test]).

data (Fig.69b). Affymetrix analysis also suggested PTTG2 mRNA was induced in FasR-Lt compared to MCF-7 cells; however this increase was no more than the induction observed in FasR cells relative to MCF-7 cells (Fig.70). There was also some increase in PTTG2 gene level suggested in X-MCF-7 cells compared to MCF-7 cells using PCR (Fig.71a) and also by Affymetrix analysis (Fig.71b).

Using PCR analysis, significant gene induction for PTTG3 gene was observed in FasR cells relative to parental MCF-7 cells (p=0.05; Fig.72a), with no significant change in other cells. An increase in FasR was confirmed in both Atlas Plastic (p=0.083) and Affymetrix microarray analysis (Fig.72b and 72c respectively). As well as being induced in FasR cells, PTTG3 gene was increased in FasR-Lt cells (p=0.0464; Fig.73). A significant increase in PTTG3 mRNA was also observed in X-MCF- 7 cells using PCR analysis (p=0.0269; Fig.74) with an increase also using Affymetrix data (Fig.74b).

The PBF (PTTG-binding protein/ factor), which has been demonstrated to facilitate translocation of PTTG1 into the nucleus, was also studied in endocrine responsive/ resistant cell lines at the mRNA level. The gene profile for PTTG1-BP using Atlas Plastic arrays suggested a slight induction in resistant cells with some repression in MCF-7 cells treated with oestradiol (Fig.75a). This profile was also suggested by PCR analysis, however, overall gene changes using both methods of analysis were at best weak (Fig.75b). Affymetrix analysis on the other hand suggested a decrease in gene levels for PTTG1-BP in all resistant cells relative to MCF-7 cells (Fig.75c), suggesting there was little consistency in changes, although as in the Atlas Plastic microarray data, oestradiol-treated MCF-7 cells showed a significant reduction in PTTG1-BP levels (p=0.0136). In contrast to the reduced levels of PTTG1-BP suggested in FasR cells compared to MCF-7 cells, by Affymetrix, FasR-Lt cells indicated a small induction of the gene, but this was again only non-significant (Fig.76). Further PCR analysis suggested X-MCF-7 cells had a marked decrease in PTTG1-BP expression (Fig.77a) which was more substantial by Affymetrix data analysis (Fig.77b; p=0.0127).

4.1.4   PTTG1 Detection in Clinical Disease

4.1.4.1   PTTG1 Gene Expression Correlates to Key Endpoints in Clinical Disease

Differential expression was observed across primary clinical breast cancer series (see examples in Fig.78) for the PTTG1 gene using PCR analysis (n=78; median PTTG1 mRNA level by densitometry=0.167; range = 0-1.18; Fig.78b), with only 2 patients completely negative for expression of this gene. There proved to be a high degree of association of PTTG1 expression with a number of key clinicopathological features, including those reflective of tumour growth and increased metastatic potential: both before and after for subdivision by ER status.

To summarise table 10, Mann-Whitney analysis revealed that increased PTTG1 was associated with increased spread to the lymph nodes (Fig.79), increased tumour grade, with poorly-differentiated Grade 3 tumours (see also Fig.80), with increased nuclear pleomorphism (see also Fig.81), with elevated mitotic activity (see also Fig.82), and with proliferative capacity as measured by Ki67 immunostaining (see also Fig.83). These associations were retained after subdivision with ER-positive and ER-negative disease. There was a further linear association by Spearmann's analysis between PTTG1 and Ki67 level (Fig.84; p<0.001), and also in ER+ disease (p<0.001). In ER+ disease, PTTG1 also tended to be at increased levels in premenopausal patients (p=0.04).

Among the biomarkers we examined versus PTTG1, there was no obvious association with status of the HER2 or EGFR growth factor receptors. Similarly, there was no association with ER or PgR status in all patient groups, although there was a direct linear association between PTTG1 and these steroid hormone receptors within the ER+ patient cohort (Fig.85 and Fig.86; p=0.008 and p=0.027 for ER and PgR respectively). There was also a PTTG1 association in tumours showing high staining for Fos transcription factor (Fig.87; p=0.004).

Table 10. PTTG1 mRNA expression correlation with clinicopathalogical endpoints in clinical breast cancer.

Clinical Association	p-value (Mann-Whitney U test)		
	All patients	ER-positive only	ER-negative only
Increased lymph node spread (>4nodes)	0.001	0.006	0.065
Increased tumour grade (grade3)	0.001	0.019	0.006
Increased nuclear pleomorphism	0.002	0.05	0.023
Increased mitotic activity	<0.001	0.004	0.009
Elevated proliferative capacity (Ki67 staining; >30%)	<0.001	0.018	0.022

4.1.4.2 PTTG1 Protein Differentially Expressed in Clinical Breast Cancer Samples

In order to confirm the presence, and thus possibly a role for PTTG1 protein within clinical breast cancer, optimised PTTG1 immunostaining was applied to a pre-prepared formalin-fixed, paraffin embedded clinical breast cancer sections. After heat-mediated antigen retrieval, a primary antibody concentration of 67µg/ml (1:15 dilution) was used with copper sulphate enhancement, as described previously. Similar to cell pellet arrays, PTTG1 immunostaining within the clinical samples was observed as both nuclear and cytoplasmic, in the tumour epithelial cells (Fig.88a). Although the assay was only subsequently applied to a
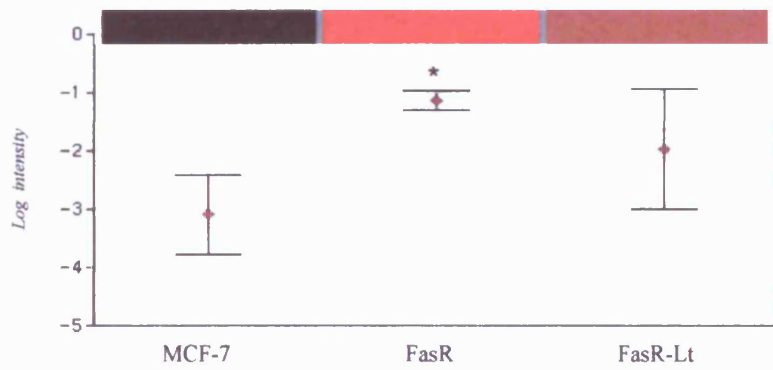
Figure 70. PTTG2 gene in FasR & FasR-Lt cells from a database constructed from Affymetrix data. PTTG2 mRNA was identified as increased in FasR and FasR-Lt cells using GeneSifter software in Affymetrix HG-U133A gene chips. Graphical output and heatmap are shown for the gene. Plot shows log mean intensity and standard errors (*p=0.0478 FasR relative to MCF-7 [students t-test]).
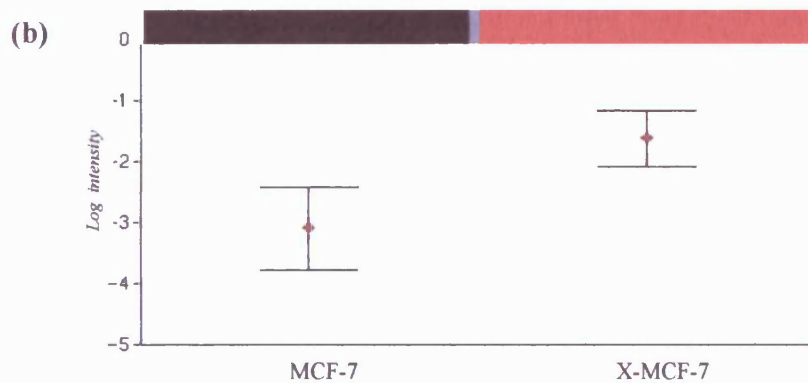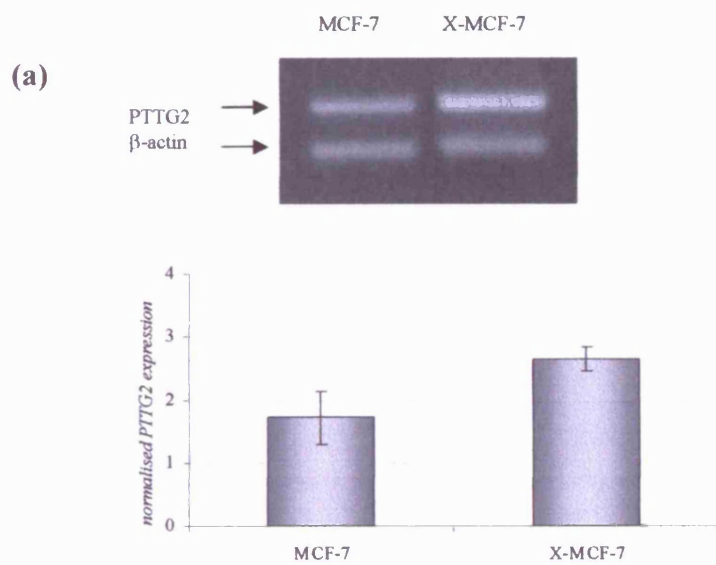
Figure 71. PTTG2 gene confirmation in X-MCF7 cells. (a) RNA was subject to RT-PCR using primers for PTTG2 co-amplified with β-actin. PCR products separated on agarose gel was visualised by ethidium bromide staining, densitometric analysis and subsequently normalised prior to plotting. Representative PCR profiles are shown. Plot shows standard errors. (b) PTTG2 mRNA was identified as increased in X-MCF-7 cells using GeneSifter software in Affymetrix HG-U133A gene chips. Graphical output with log mean intensity and standard errors, and heatmap are shown for the gene.
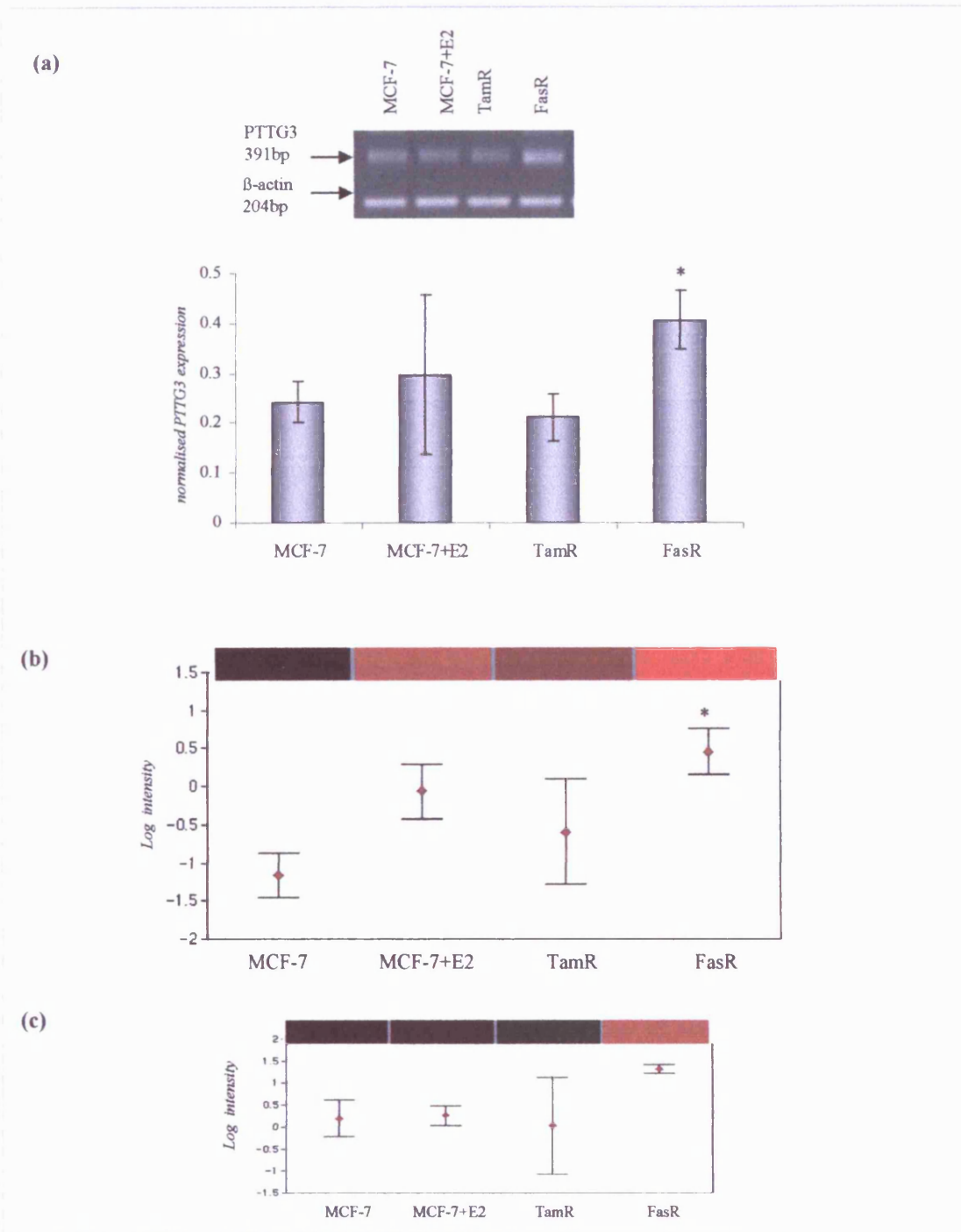
Figure 72. PTTG3 gene confirmation in resistant cells. (a) Verification of gene profile was performed by PCR analysis using primers for PTTG3. PCR for β-actin was also performed (normalisation control). PCR products separated on agarose gel were visualised by ethidium bromide staining. Representative PCR profile is shown for triplicate experiments. PCR profiles were then subject to densitometric analysis prior to normalised intensity plotting. Plot shows standard errors (*p=0.05 in FasR relative to MCF-7 [Students t-test]). (b) PTTG3 mRNA was identified as upregulated in FasR cells using Atlas Plastic Human 12k Microarrays and (c) Affymetrix HG-U133A gene chips. Identical RNA preparations were used for Atlas Plastic array and Affymetrix genechip. Graphical output and heatmap are shown for the gene. Plot shows log mean intensity and standard errors. Additional controls were provided by parental MCF-7 cells subject to oestradiol treatment. (*p=0.083 FasR relative to MCF-7 [Students t-test].
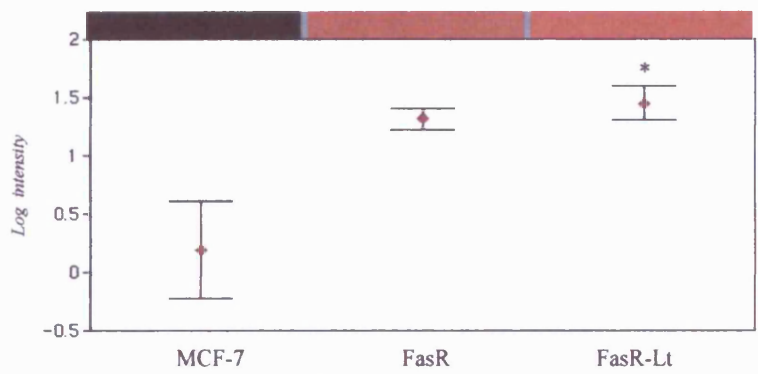
Figure 73. PTTG3 gene in FasR & FasR-Lt cells from a database constructed from Affymetrix data. PTTG3 was identified as increased in FasR and FasR-Lt cells using GeneSifter software in Affymetrix HG-U133A gene chips. Graphical output and heatmap are shown for the gene. Plot shows log mean intensity and standard errors. (*p=0.0464 for FasR-Lt relative to MCF-7 [Students t-test]).
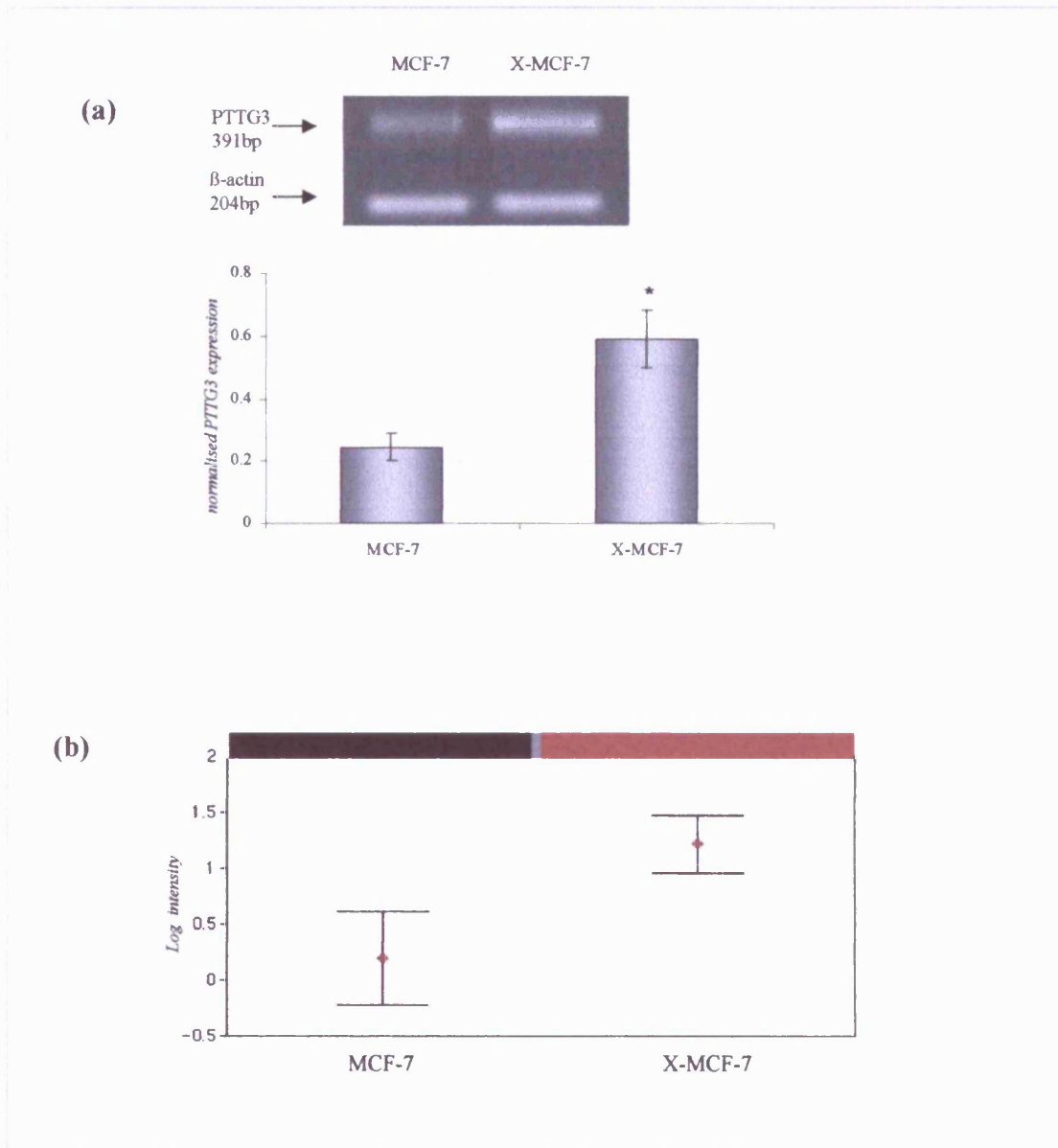
Figure 74. PTTG3 gene confirmation in X-MCF7 cells. (a) RNA was subject to RT-PCR using primers for PTTG2. β-actin was also amplified for normalisation. PCR products separated on *agarose gel was visualised by ethidium bromide staining, densitometric analysis and subsequently* normalised prior to plotting. Representative PCR profiles are shown. Plot shows standard errors.(p=0.0265 for PTTG3 relative to MCF-7 [Students t-test]). (b) PTTG3 mRNA was identified as increased in X-MCF-7 cells using GeneSifter software in Affymetrix HG-U133A gene chips. Graphical output with log mean intensity and standard errors, and heatmap are shown for the gene.
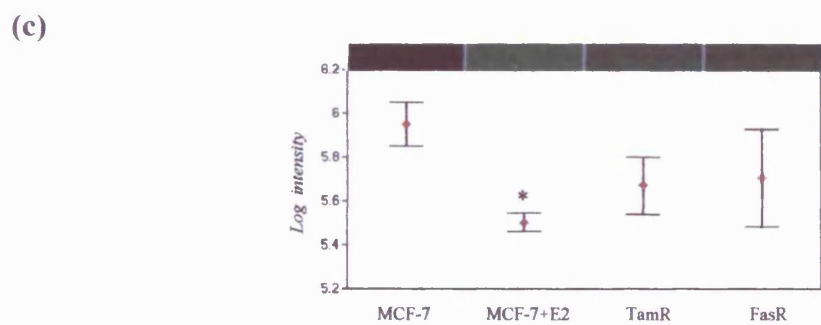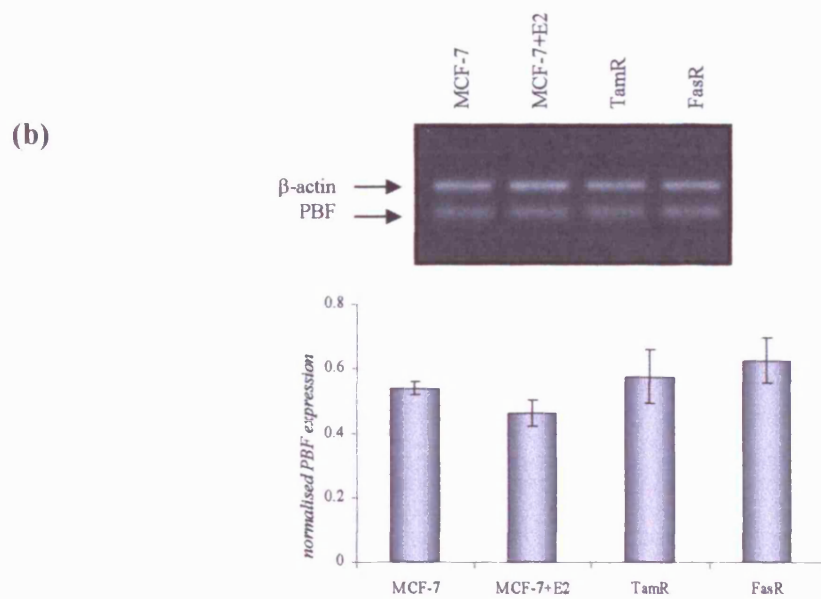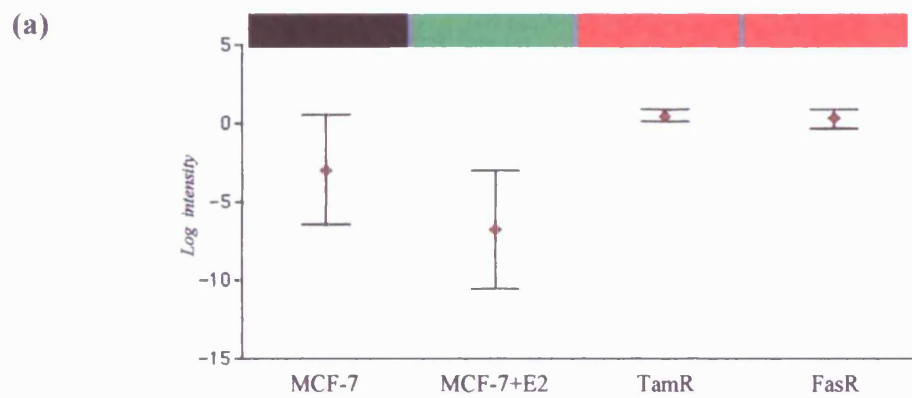
Figure 75. PBF gene regulation in resistant cells. PBF mRNA was identified as differentially expressed using (a) Atlas Plastic Human 12k Microarrays; Graphical output with log mean intensity and standard errors, and heatmap are shown for the gene. (b) Verification of gene profile was performed by PCR analysis using primers for PBF co-amplified with β-actin (normalisation control). PCR products separated on agarose gel were visualised by ethidium bromide staining and subject to densitometric analysis, prior to normalised intensity plotting. Representative PCR profile is shown from triplicate experiments. Plot shows standard errors. (c) Profiles using Affymetrix HG-U133A gene chips are also shown as graphical output with log mean intensity and standard errors, and heatmap is shown for the gene. Identical RNA preparations were used for Atlas Plastic array and Affymetrix genechip. Additional controls were provided by parental MCF-7 cells subject to oestradiol treatment. (*p=0.0134 for MCF-7+E2 relative to MCF-7 [students t-test]).
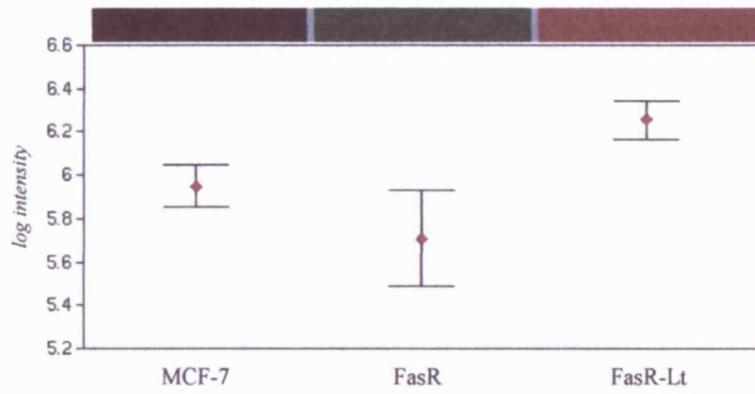
Figure 76. PBF gene in FasR & FasR-Lt cells from a database constructed from Affymetrix data. PBF mRNA was identified as differentially expressed in FasR and FasR-Lt cells using GeneSifter software in Affymetrix HG-U133A gene chips. Graphical output with log mean intensity and standard errors, and heatmap is shown for the gene.
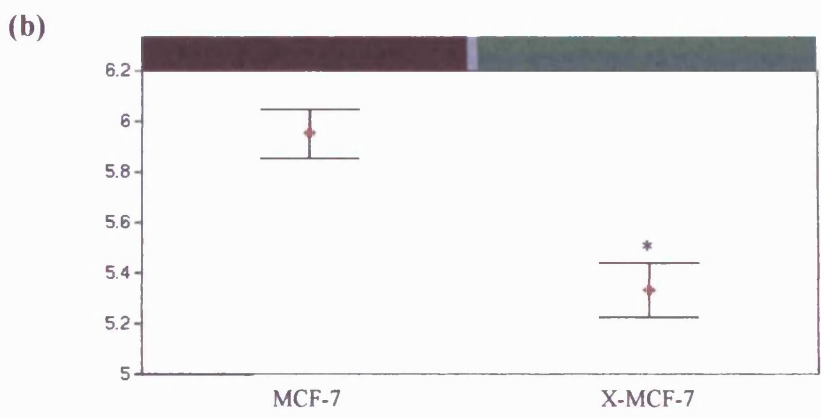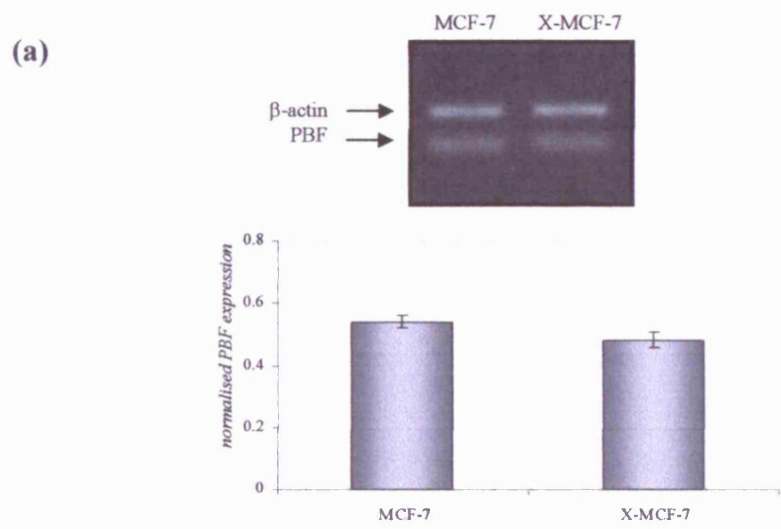
Figure 77. PBF gene regulation in the oestrogen-depravation model, X-MCF-7 cells. (a) RNA was subject to RT-PCR using primers for PBF and visualised by ethidium bromide staining. β-actin was coamplified and used as an internal control. Representative signal is shown for triplicate experiment. PCR products separated on agarose gel were visualised by ethidium bromide staining and subject to densitometric analysis, prior to normalised intensity plotting. (plot shows standard errors). (b) PTTG3 mRNA was identified as in X-MCF-7 cells using GeneSifter software in Affymetrix HG-U133A gene chips. Graphical output with log mean intensity and standard errors, and heatmap are shown for the gene. (*p=0.0127 for X-MCF- relative to MCF-7 [students t-test]).
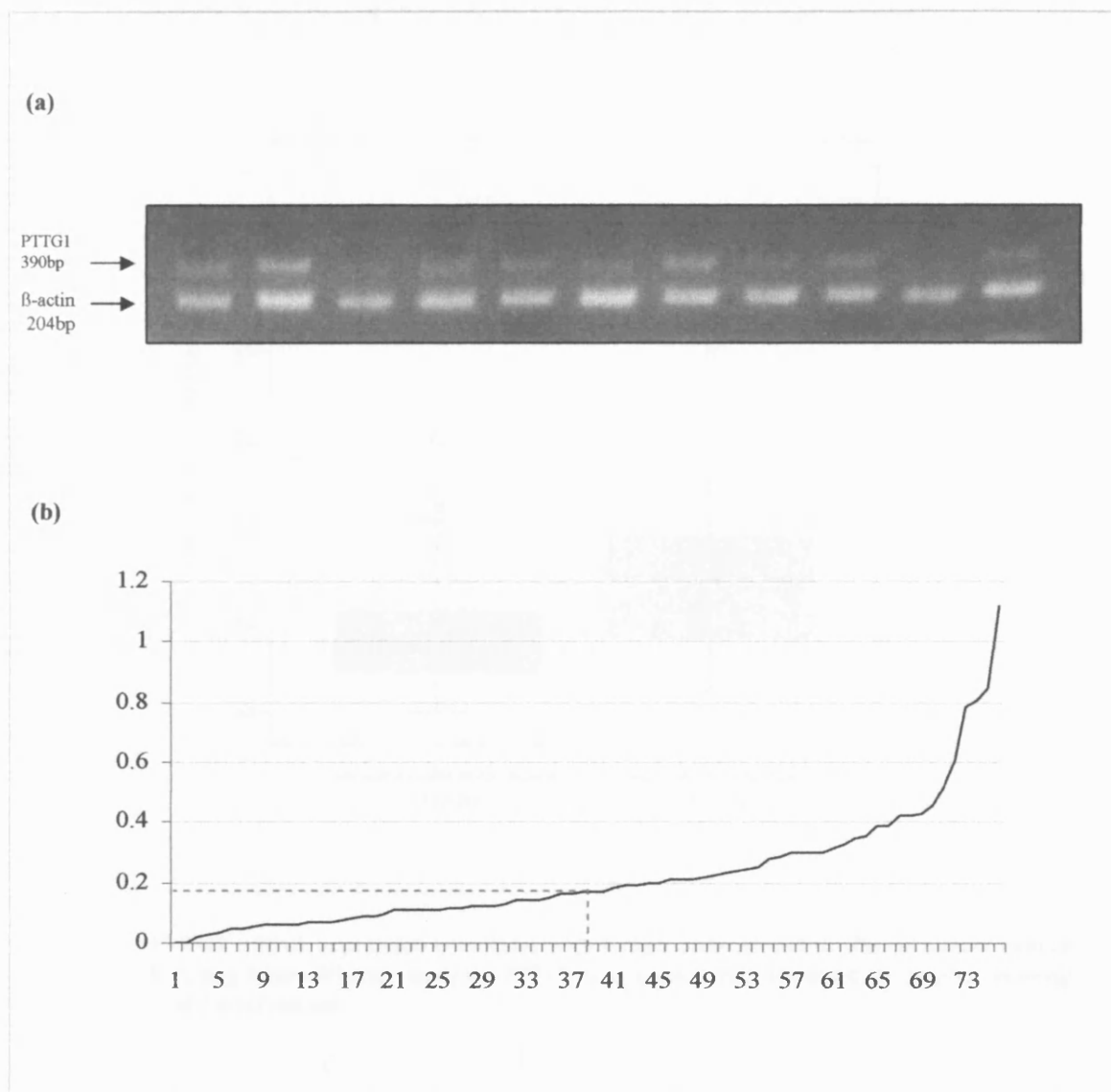
Figure 78. PCR analysis of PTTG1 gene in clinical breast cancer series. (a) Clinical breast cancer sample (n=78) RNA was subject to PCR using primers for PTTG1 co-amplified with β-actin for 28 cycles. PCR *products separated on agarose gel were visualised by ethidium bromide staining.* (b) *Frequency distribution* chart shows PCR densitometry signal intensity for n=78 samples encompassing a range 0 to 1.18, and median 0.167 (marked as dashed line).
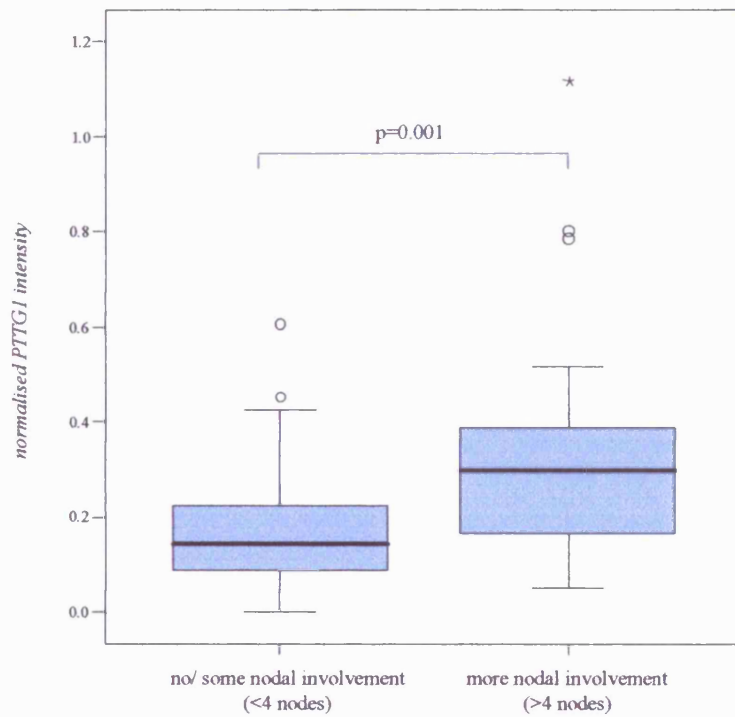
Figure 79. PTTG1 mRNA expression correlates with lymph node spread in clinical breast cancer series (n=78) Using Mann-Whitney analysis, PTTG1 was significantly increased in patients showing *more than 4 nodal involvement.*
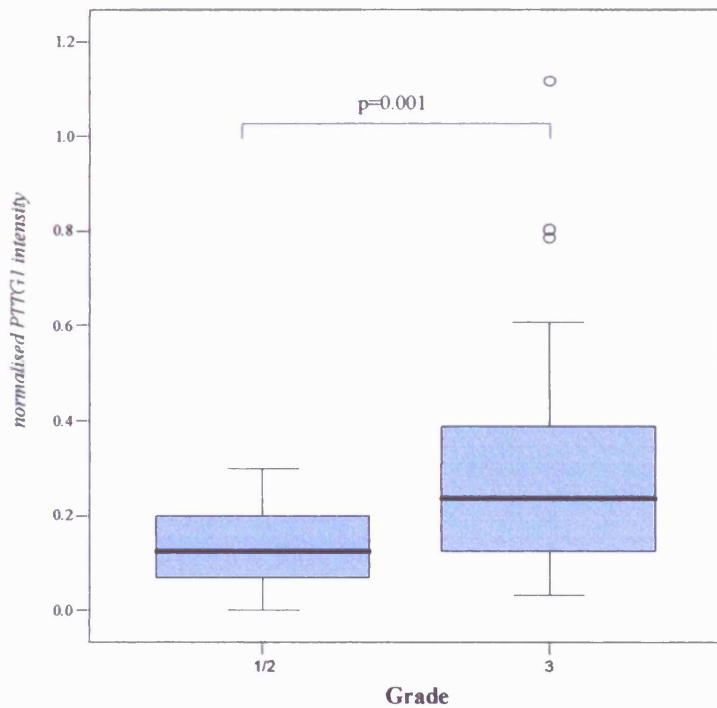
Figure 80. PTTG1 mRNA expression correlates with poorly differentiated tumours in clinical breast cancer series (n=78). Using Mann-Whitney analysis PTTG1 gene was significantly increased in tumours exhibiting grade 3 versus grade 1 or 2 tumours. This relationship was maintained after subdivision for ER positivity/ negativity.
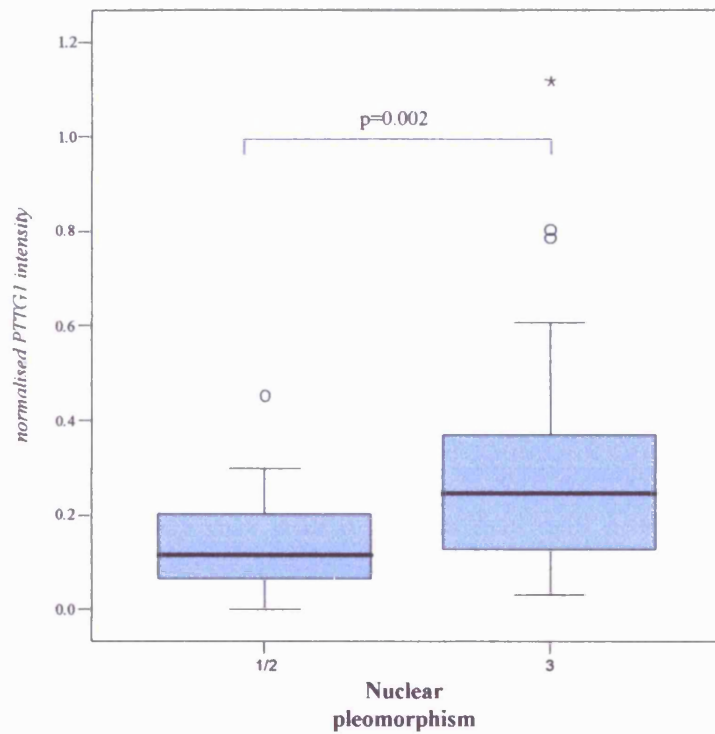
Figure 81. PTTG1 mRNA expression correlates with nuclear pleomorphism in clinical breast cancer series (n=78). Using Mann-Whitney analysis PTTG1 gene was significantly increased in tumours showing increased nuclear pleomorphism (3) versus low levels (1 or 2).
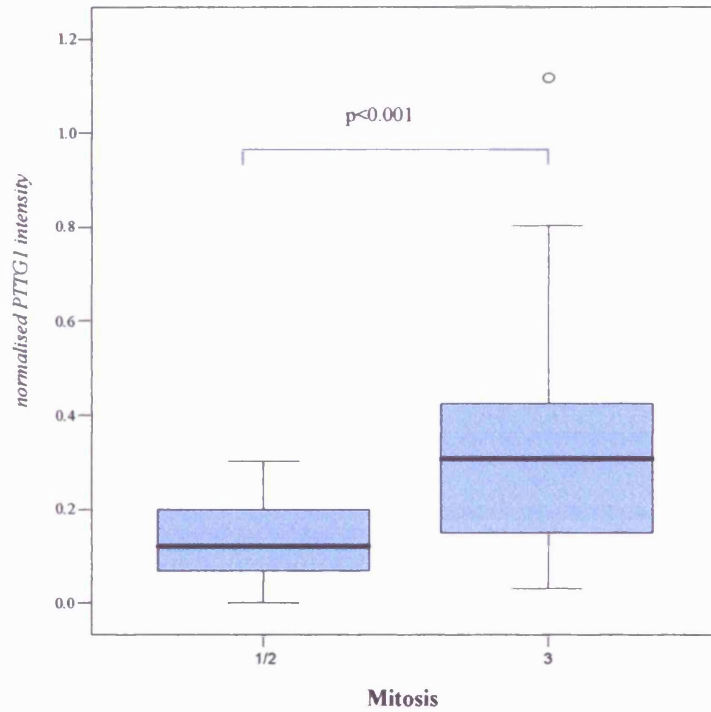
Figure 82. PTTG1 mRNA expression correlates with mitotic activity in clinical breast cancer series (n=78). Using Mann-Whitney analysis PTTG1 gene was significantly increased in tumours *exhibiting high mitotic activity (3) compared to low mitosis (1 or 2)*.
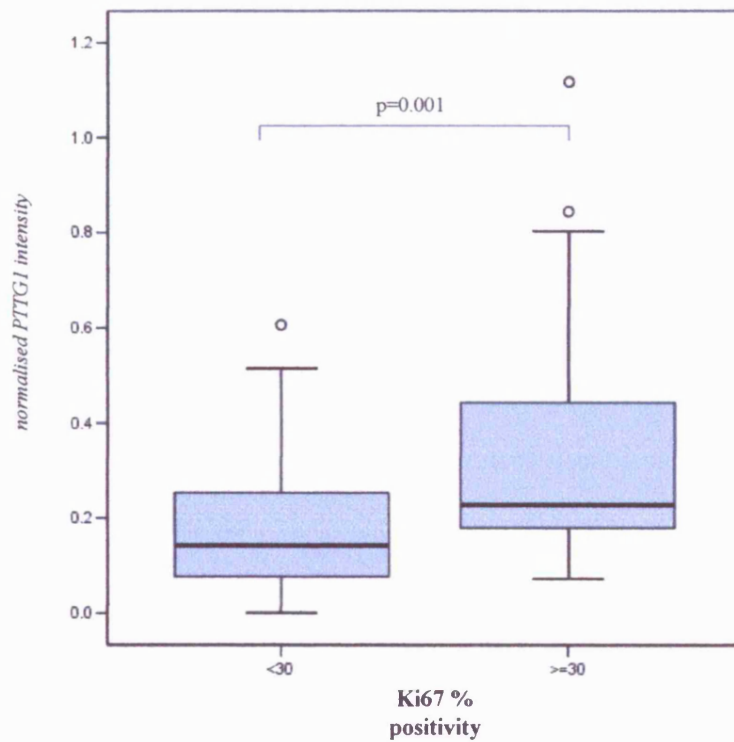
Figure 83. PTTG1 mRNA expression correlates with elevated proliferative capacity (ki67 staining) in clinical breast cancer series (n=78). Using Mann-Whitney analysis PTTG1 gene was significantly increased in tumours showing increased proliferation by ki67immunostaining.
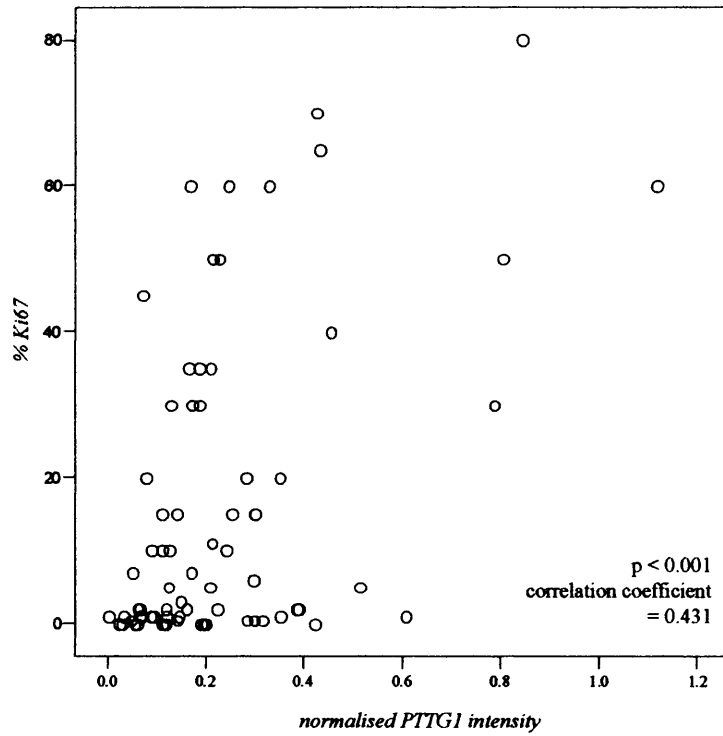
Figure 84. PTTG1 mRNA correlates with elevated proliferative capacity (ki67 staining) in clinical breast cancer series (n=78). Using Spearmann's analysis PTTG1 gene was directly associated with ki67immunostaining in all patients.
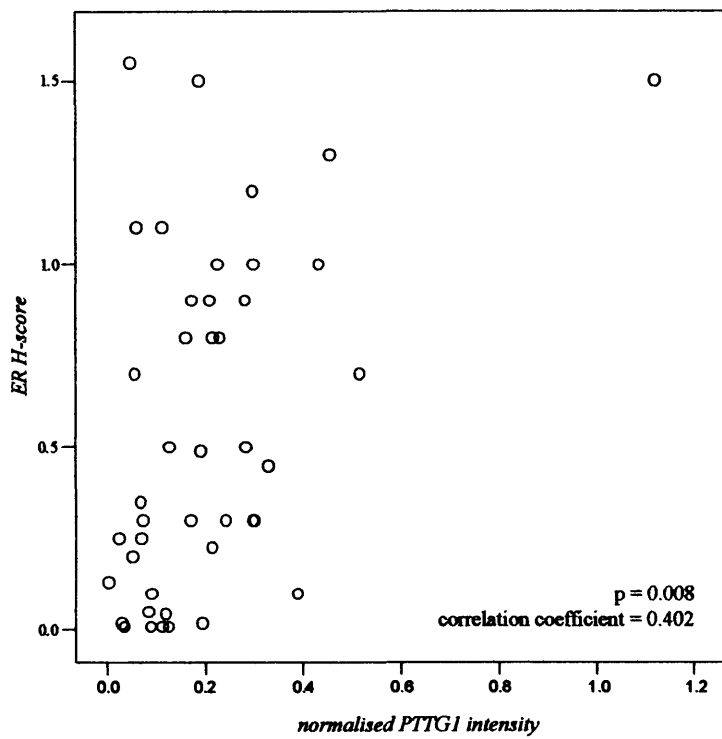
Figure 85. PTTG1 mRNA expression correlates with ER in ER-positive clinical breast cancers (n=43). Using Spearmann's analysis PTTG1 was directly associated in ER-positive tumours with ER..
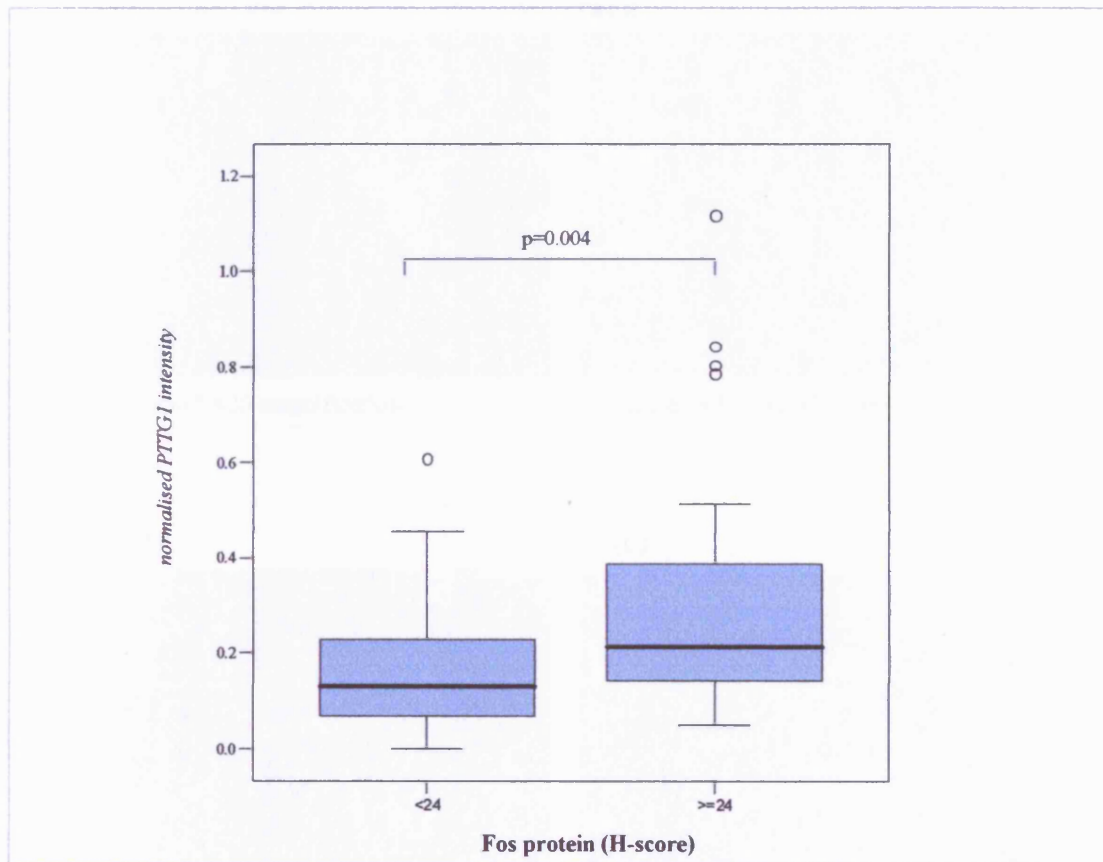
Figure 87. PTTG1 mRNA expression associates with Fos positivity (H-score status) (n=78).

(a) i
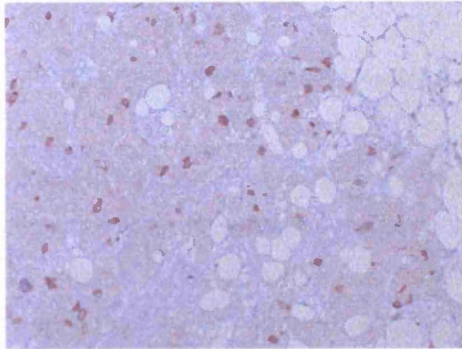
Sample1 x20 magnification

(a) ii
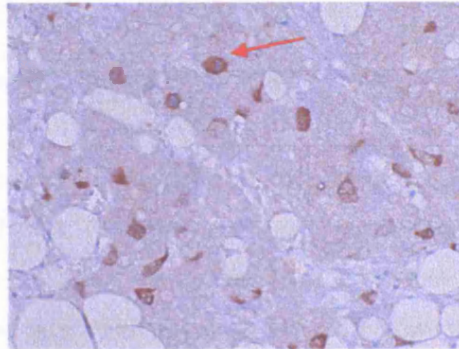
Sample1 x40 magnification

(b)
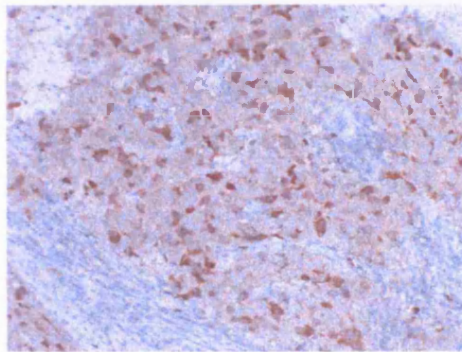
Sample2 x20 magnification

(c)
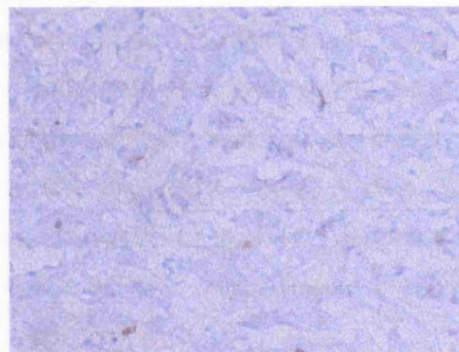
Sample3 x20 magnification

Figure 88. Immunocytochemical analysis for PTTG1 in primary clinical breast cancer samples. Breast cancer samples were formalin fixed, and embedded in paraffin blocks. 5μm sections prepared *from blocks were probed using monoclonal anti-human PTTG1 antibody after (heat mediated) antigen* retrieval with copper sulphate enhancement and detected using DAKO Envision detection system with DAB staining. Fig. a and b show samples 1 and 2 demonstrating significant staining, whereas Fig c shows almost negative PTTG1 immunostaining. Red arrow shows high PTTG1 immunostaining was frequently observed within highly mitotic cells.

small number of clinical samples (n=3) PTTG1 staining was nevertheless differential, varying from intensely staining (86b) to the very weakly staining (Fig.88c). In addition, intense PTTG1 staining was frequently observed within highly mitotic cells.

4.1.5 PTTG1 Gene Knockdown Studies using siRNA

Although the gene for PTTG1 was induced in all resistant cell lines using Atlas Plastic 12k Human Microarray and Affymetrix HG-U133A Genechip analysis, this elevation was observed as most highly significant in FasR-Lt cells, not only at the gene level, but also as protein expression through Western blotting and ICC. FasR-Lt cells were therefore used in PTTG1 gene knockdown studies to begin to address whether PTTG1 was contributory to growth of the acquired resistant phenotype.

4.1.5.1 Estimation of Transfection Efficiency using siGlo

A siGlo RISC-Free siRNA transfection control was included in the siRNA gene knockdown study to provide an estimation of transfection efficiency in the model. Additionally, as these stable, fluorescent compounds are chemically modified to impair any RISC- siRNA interactions, as well as uptake efficiency monitors, they form, negative assay controls. Successful overnight transfection with siGlo was determined by positively fluorescent siGlo signal nuclei. Within these cells a transfection rate of 74% was achieved (±18 standard deviation; Fig.89).

4.1.5.2 Estimation of Knockdown Efficiency Using Lamin siRNA

Positive silencing control siRNA directed against the reported housekeeping gene Lamin A/C in FasR-Lt cells provided some initial indication of gene knockdown that can generally be achieved using the Dharmacon siRNA system in these cells. RNA extracted one day post transfection showed a substantial 73% reduction in Lamin mRNA with Lamin-specific gene knockdown compared to missense/ scrambled control (or PTTG1 siRNA) as determined by PCR analysis (Fig.90). This considerable Lamin mRNA reduction provides evidence of the success of the siRNA protocol in the model system used.

4.1.5.3 PTTG1 Gene and Protein Expression Are Successfully Reduced by PTTG1 siRNA

Following the successful knockdown of Lamin A/C, siRNA directed towards the PTTG1 gene was applied according to the protocol used previously (seeding at 70-80% confluency). The gene for PTTG1 was reduced by 97% at 24 hours post transfection as shown by PCR studies (Fig.91a). Although minor variation was observed within the control set of

samples, the PTTG1 knockdown was substantial compared to all controls used in the experiment.

Owing to the 4-7 day timescale considered for subsequent proliferation, apoptosis, and growth experiments, cells were seeded at an initial density of 250,000 cells/ well instead of the 70-80% appropriate used for 24 hour timepoint analysis. Also included within subsequent knockdown experiments is a DharmaFect (DF; transfection reagent) only control. PCR analysis shows a reduction of PTTG1 gene with the specific siRNA at approximately 62% at day 4 post-transfection compared to missense control in FasR-Lt cells, and 74% versus DCCM control (Fig.91b). Following the re-application of PTTG1 siRNA at day 4, cells harvested subsequently at day 7 again showed a gene knockdown of around 79% compared to missense control, and 80% relative to DCCM control (Fig.91c). It is worth noting that the addition of DF either alone, or with Lamin/ missense siRNA to the culture medium (comparing media only controls to these controls) caused a partial and variable inhibitory effect on the cells in culture following extended time points.

FasR-Lt cells seeded at a high initial density were subject to PTTG1 knockdown and protein analysed using Western blotting analysis at 48 hours post-transfection (Fig.92a). PTTG1 protein (28kDa) was shown to be reduced to an undetectable level. Although a small reduction was observed in the Lamin control over other control samples, an unusual variation was demonstrated by the low PTTG1 protein level in cells grown in basal (home) medium (media control). This however was inconsistent and not noted in later timepoints and their replicates.

As with mRNA studies 4-7 day timescale of subsequent experiments, FasR-Lt cells were seeded at an initial density of 250,000 cells/ well. Again, a DF (transfection reagent) only control was included within this set of experiments. Western blotting showed a reduction of PTTG1 protein of 95% at day 4 post-transfection compared to missense control and 98% compared to DCCM control (Fig.92b). Following the re-application of PTTG1 siRNA at day 4, cells harvested at day 7 again showed a protein knockdown compared to missense control of around 97%, and 99% versus DCCM control (Fig.92c). However, PTTG1 protein was observed to be significantly affected by the inclusion of DF within the cell culture (although less marked at day 4), evidenced by the differences between media controls (media control and DCCM control) and DF control test samples (DF, Lamin siRNA, missense control).

4.1.5.4 PTTG1 Knockdown Effects on Cell Growth

The proliferative effects of using siRNA directed to the PTTG1 gene is evident from observation of cells in culture (Fig.93). Microscopic evaluation at day 4 of PTTG1 siRNA treatment viewed from four replicate fields revealed a 72% decrease in cell number compared to missense control (Fig.94; p=0.0031). Although a degree of reduction was also observed in the DF control and Lamin siRNA control, cell numbers within the PTTG1 siRNA-treated sample
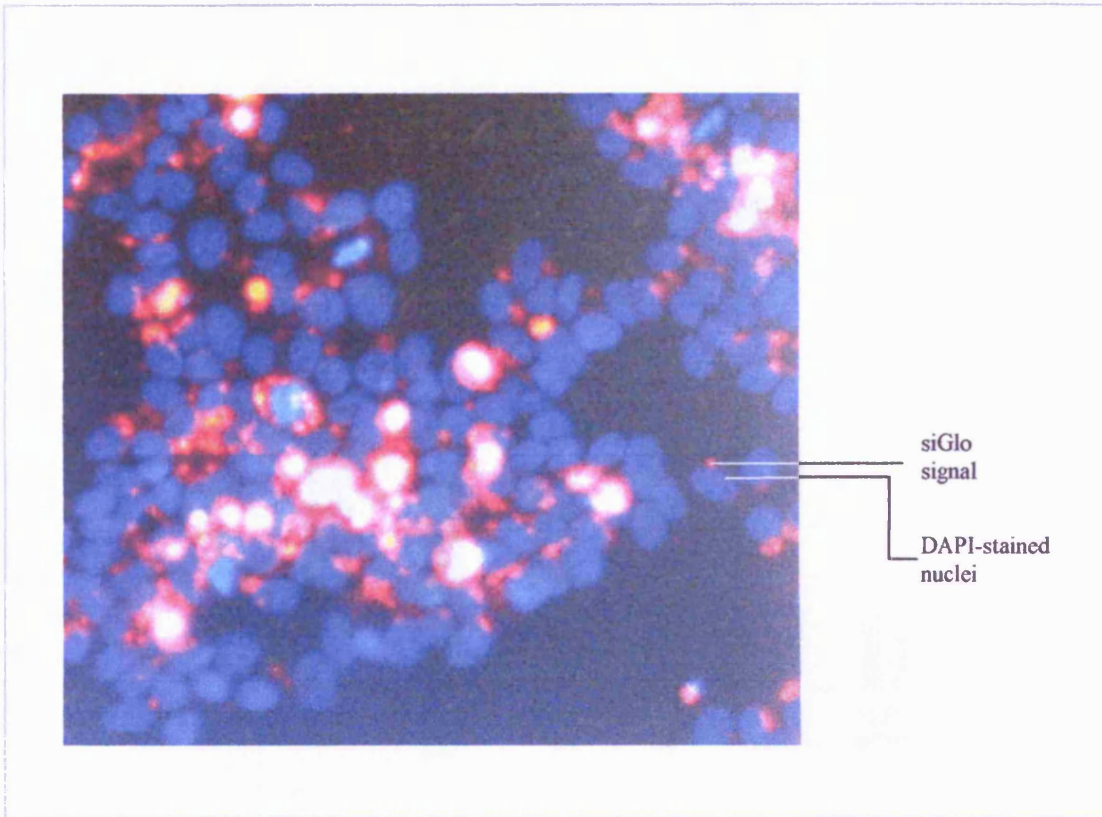
Figure 89. **Estimation of siRNA transfection efficiency using siGlo in FasR-Lt cells.** FasR-Lt cells transfected with 100nmol siGlo overnight (~12 hours) were fixed, mounted using Vectashield agent, and fluorescence detected. Photograph shows area of x40 magnification with DAPI-stained nuclei with siGlo transfection fluorescent (red) marker.
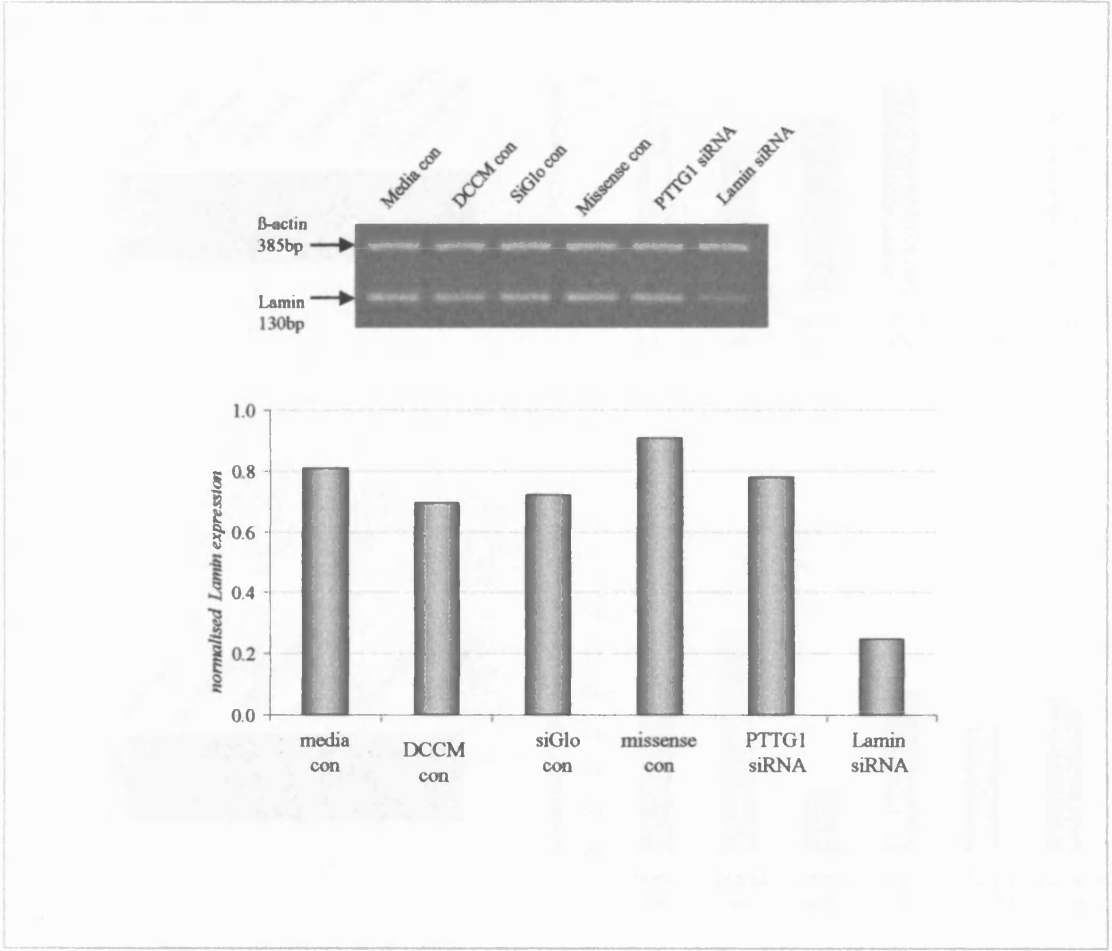
Figure 90. siRNA specific Lamin gene knockdown in FasR-Lt cells to confirm Dharmacon siRNA performance. Lamin gene knockdown was achieved in TamR cells using 100nmol Smartpool reagents according to the Dharmacon protocol. One microgram of RNA extracted from cells 24 hours post siRNA transfection was reverse transcribed and gene expression was determined using primers for Lamin (with β-actin co-amplification for normalisation). Controls included were irrelevant (PTTG1) siRNA, siGlo, missense, DCCM media, and media (phenol red-free RPMI/ 5% serum) control alongside the Lamin siRNA.
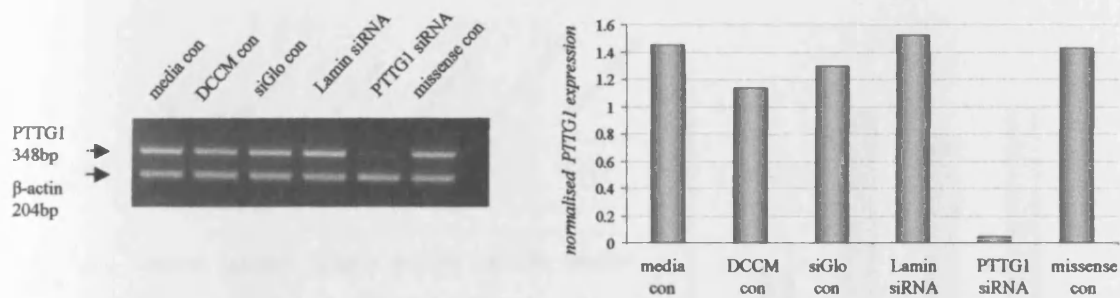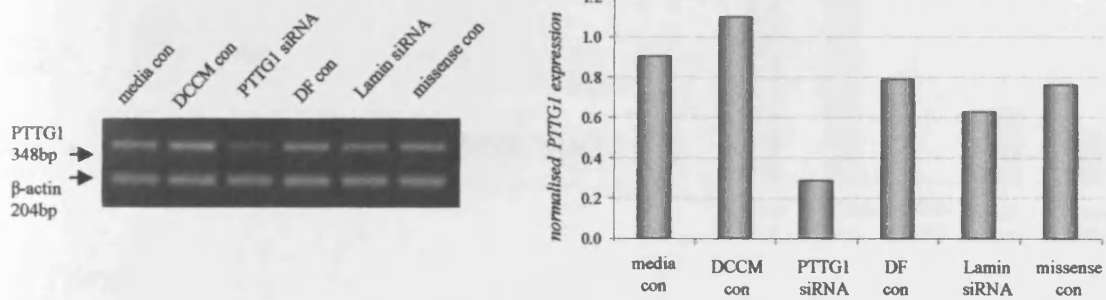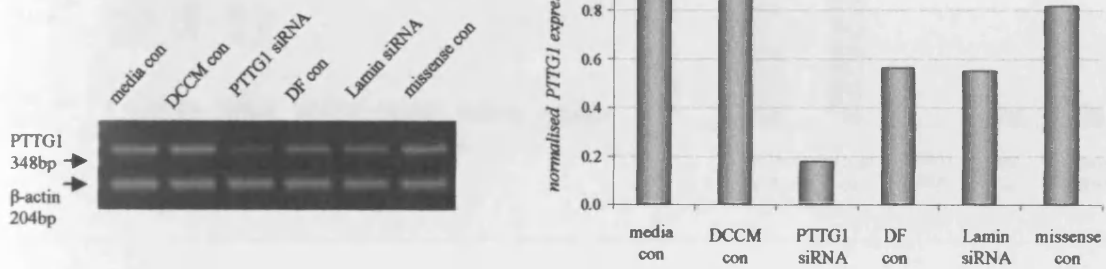
Figure 91. PTTG1 siRNA mediated gene knockdown in FasR cells. PTTG1 gene knockdown was achieved in FasR-Lt cells using 100nmol smartpool reagents according to the Dharmacon protocol. One microgram of RNA extracted from cells (a) 24 hours, (b) 4 days, and (c) 7 days siRNA transfection was reverse transcribed and gene expression was determined using primers for PTTG1 (with β-actin co-amplification for normalisation). Controls included were siGlo, missense, Lamin siRNA, DharmaFECT (DF) transfection reagent, DCCM media, and media (phenol red-free RPMI/ 5% serum) control versus PTTG1 test siRNA.

(a) 48 hours

(b) 4 days

(c) 7 days
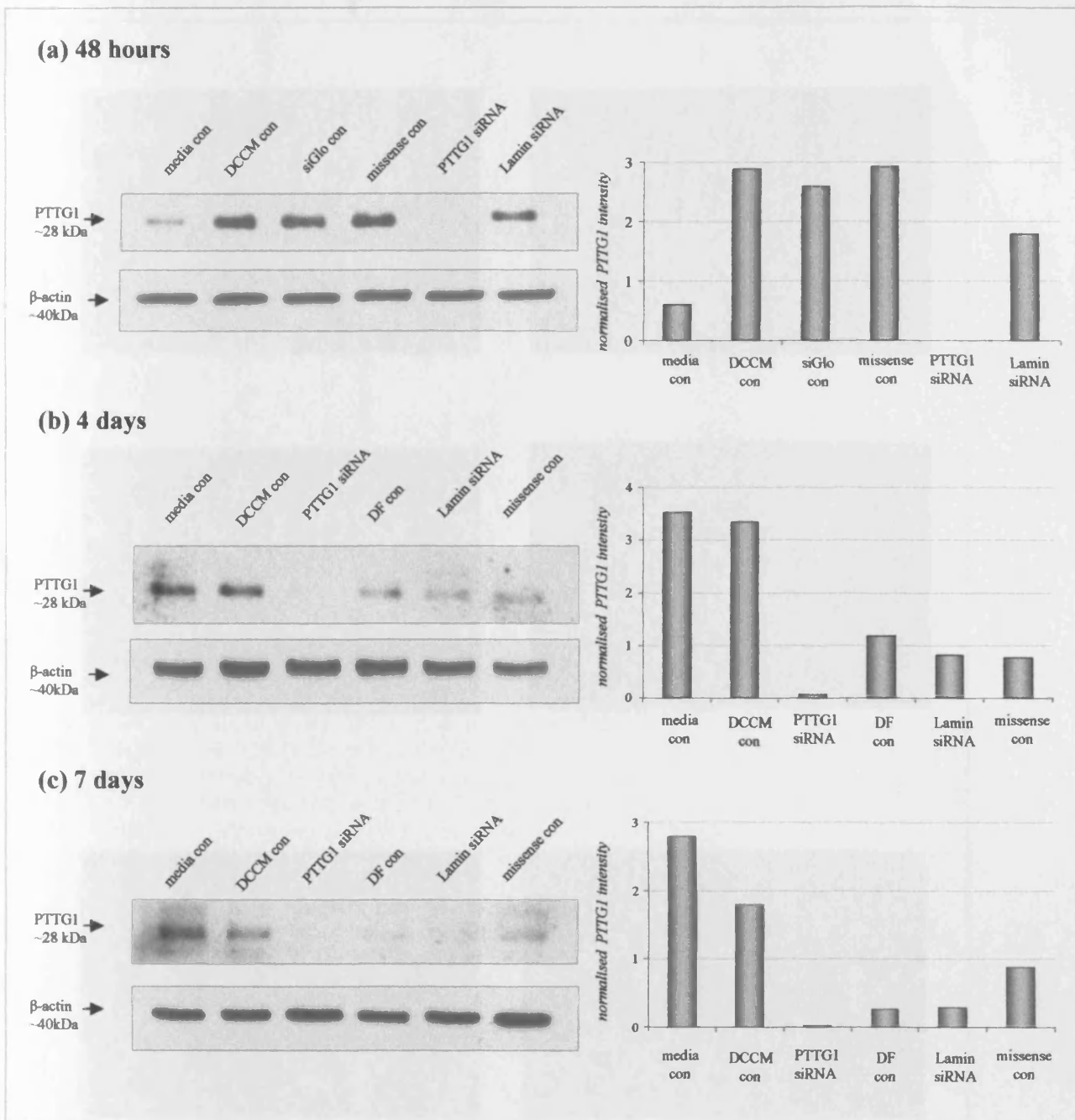
Figure 92. PTTG1 siRNA mediated protein knockdown in FasR-Lt cells. PTTG1 gene knockdown was achieved in FasR-Lt cells using 100nmol Smartpool reagents according to the Dharmacon protocol. PTTG1 protein knockdown was determined by subjecting 50ug protein from cells (a) 48 hours, (b) 4 days, and (c) 7 days siRNA transfection to 15% SDS PAGE and Western blotting. Proteins were probed with monoclonal anti-PTTG1 antibody with chemiluminescent detection. Equivalence of protein loading in Western blots was subsequently demonstrated by detection of β-actin on the same blot using monoclonal antibody to the protein. Controls included were siGlo, missense, Lamin siRNA, DharmaFECT (DF) transfection reagent, DCCM media, and media (phenol red-free RPMI/ 5% serum) control versus PTTG1 test siRNA.
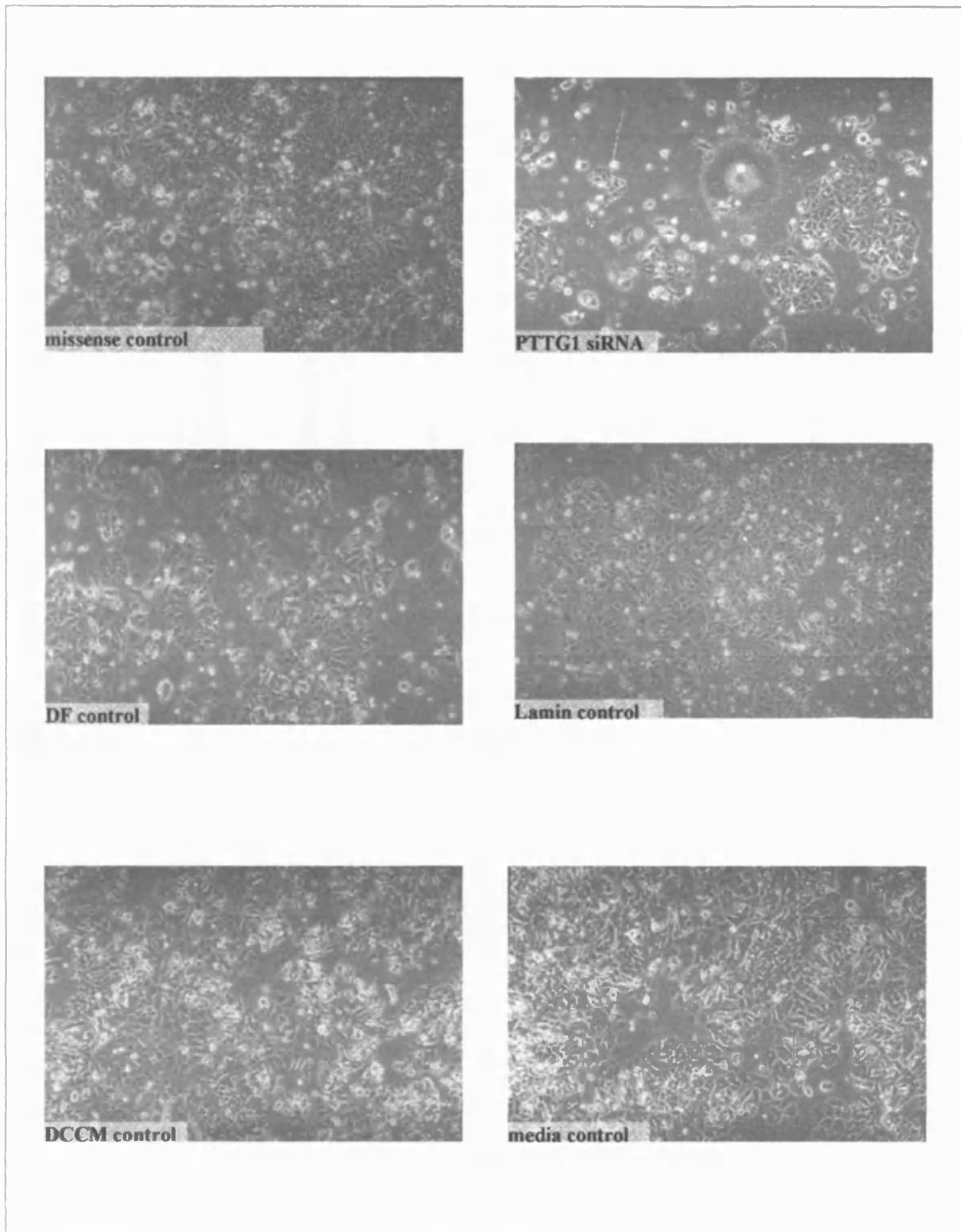
Figure 93. Phase contrast microscopy of FasR-Lt cells subject to PTTG1 siRNA knockdown at day 4. PTTG1 gene knockdown was achieved in FasR-Lt cells using 100nmol Smartpool reagents according to the Dharmacon protocol and as described in Methods. Control or test cells were counted from four fields photographed at 10x magnification. Controls included were missense, DharmaFECT (DF) transfection reagent, Lamin siRNA, DCCM media, and media (phenol red-free RPMI/ 5% serum) control, alongside PTTG1 test siRNA.
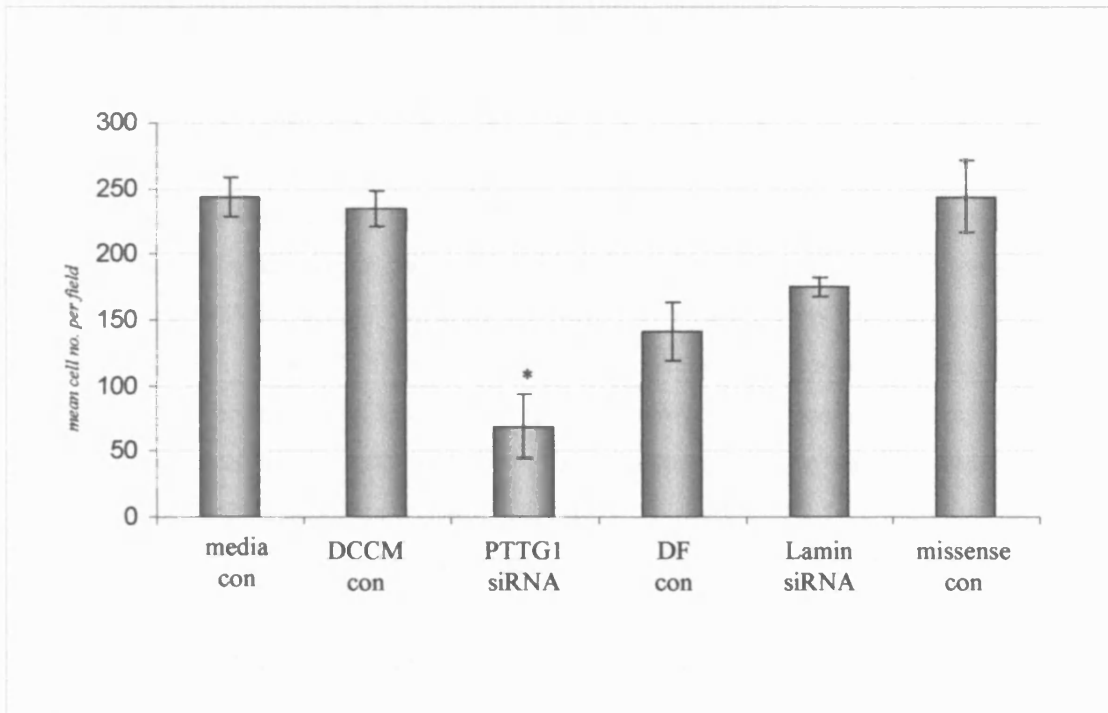
Figure 94. Phase contrast of FasR-Lt mean cell counts following PTTG1 siRNA knockdown at day 4. PTTG1 gene knockdown was achieved in FasR-Lt cells using 100nmol Smartpool reagents according to the Dharmacon protocol. Control or test cells were photographed at 10x magnification and evaluation of cells was performed counting for a total of 4 fields. Controls included were missense, DharmaFECT (DF) transfection reagent, Lamin siRNA, DCCM media, and media (phenol red-free RPMI/ 5% serum) control, versus PTTG1 test siRNA. Plot shows standard errors (*p=0.0031 for PTTG1 siRNA relative to missense control; p<0.02 for PTTG1siRNA relative to Med con, DCCM con and Lamin siRNA controls [Students t-test performed]).

also remained obviously lower than the DF control, Media control, DCCM control, and Lamin siRNA control (p<0.02 in the latter 3 controls relative to PTTG1 siRNA cell number count).

4.1.5.5 PTTG1 Knockdown Effects on Cell Proliferation- Ki67 (Mib1) Staining

In parallel to the above studies, the effects on proliferation of PTTG1 siRNA applied to FasR-Lt cells were determined by Ki67 (Mib1) immunostaining. After 4 days of transfection, cells were fixed and immunostained for Ki67 as described previously. The staining across the samples indicated a decrease in staining in Ki67 with PTTG1 siRNA compared to the missense control (Fig.95). Microscopic counting of Ki67 immunoreactivity revealed a significant reduction of 23% with PTTG1 siRNA treatment compared to missense control (p<0.001; Fig.96) and 34% relative to DCCM control (p<0.001). An obvious loss of cell number was also observed on the coverslips with PTTG1 siRNA-treatment with a smaller reduction in cell numbers in control preparations containing DF reagent (see also 4.1.5.4). Samples used within the Ki67 experiments showed less variability across the controls, although a non-significant reduction in Ki67 immunostaining was observed in the Lamin A/C sample (14% and 21% reduction compared to missense and DCCM control respectively; Fig.96).

4.1.5.6 PTTG1 Knockdown Effects on Apoptosis (ApoAlert Assay)

The effect of PTTG1 siRNA on apoptosis was determined in FasR-Lt cells 4 days post-transfection using the ApoAlert Apoptosis Mitochondrial Membrane Sensor Kit (BD Biosciences) according to the manufacturers instructions. Microscopic evaluation of the samples again showed an obvious reduction in the number of cells present on the slide following PTTG1 siRNA treatment (see also 4.1.5.4). Moreover, in the remaining cells, an obvious induction of apoptosis was demonstrated by the increase in green MMS staining (Fig.97). Evaluation of the dead cells (green) revealed a 43% further increase with PTTG1 siRNA-treated cells compared to missense control and a 88% increase versus DCCM control (p=0.05 and p<0.001 respectively; Fig.98). Generally, all samples showed slightly higher levels of dead cells relative to the media control, including some apoptotic effects observed within all samples containing siRNA for either Lamin or missense control (53% and 31% respectively versus DCCM control; Fig.98).

4.1.6 Impact of EGFR Inhibitor Gefitinib and Faslodex on PTTG1 Gene and Protein Expression in Resistant Cells

In order to determine if PTTG1 was EGFR regulated, PTTG1 gene expression was determined using PCR analysis in resistant cell lines which were subject to a growth inhibitory dosage of EGFR-TK inhibitor (TKI) Gefitinib ($10^{-6}M$) treatment for seven days. Treatment with the inhibitor resulted in a further induction of PTTG1 gene in both TamR and FasR-Lt cells at approximately a six-fold and two-fold increase respectively versus basal levels (Fig.99). Western blotting confirmed a substantial increase in PTTG1 protein in response to Gefitinib in TamR cells (Fig.100). This elevation in protein levels was observed at both 4 days and at 7 days of Gefitinib treatment. There was only a marginal increase with the agent in FasR-Lt cells, although basal levels were higher than TamR cells, as observed previously. Using PCR analysis, PTTG1 mRNA was also observed to be induced in TamR cells treated with ($10^{-7}M$) Faslodex by approximately two-fold (Fig.101), although Western blotting profile was not explored.
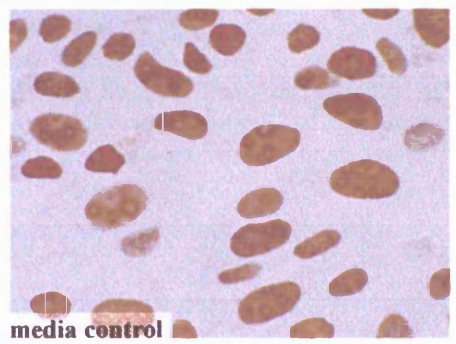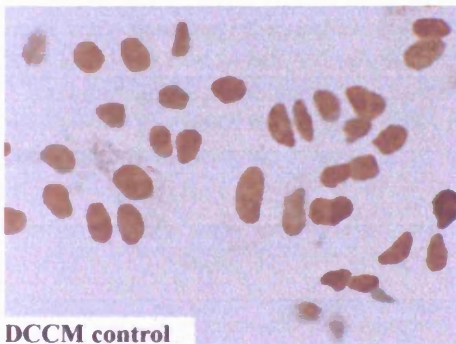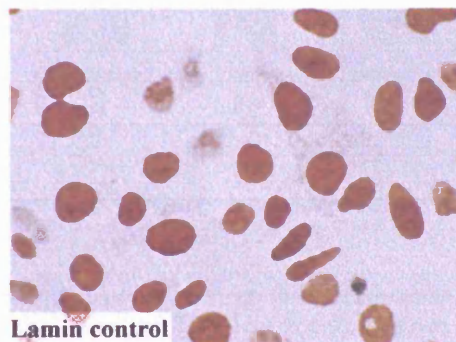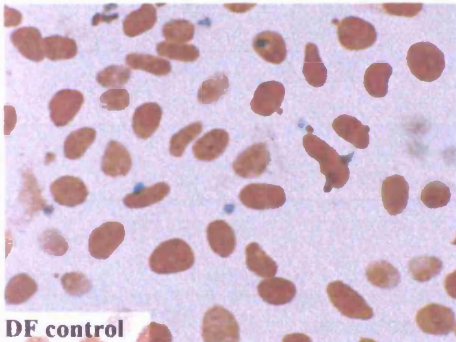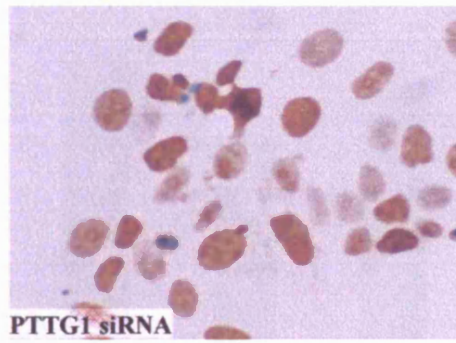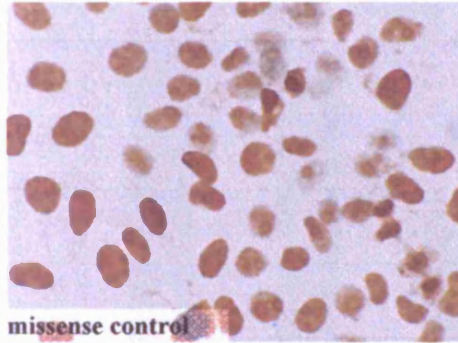
Figure 95. Effect on proliferation of PTTG1 siRNA knockout at day 4 as measured by Ki67 -Mib1) immunostaining in FasR-Lt cells. PTTG1 gene knockdown was achieved in FasR-Lt cells using 100nmol Smartpool reagents according to the Dharmacon protocol. Control or test cells were fixed in formaldehyde solution 4 days post transfection, probed using monoclonal anti-human antibody to mib1 and detected using DAKO Envision detection system with DAB staining. Controls included were missense, DharmaFECT (DF) transfection reagent, Lamin siRNA, DCCM media, and media (phenol red-free RPMI/ 5% serum) control, versus PTTG1 test siRNA (Photographs show immunostaining at x40 magnification).
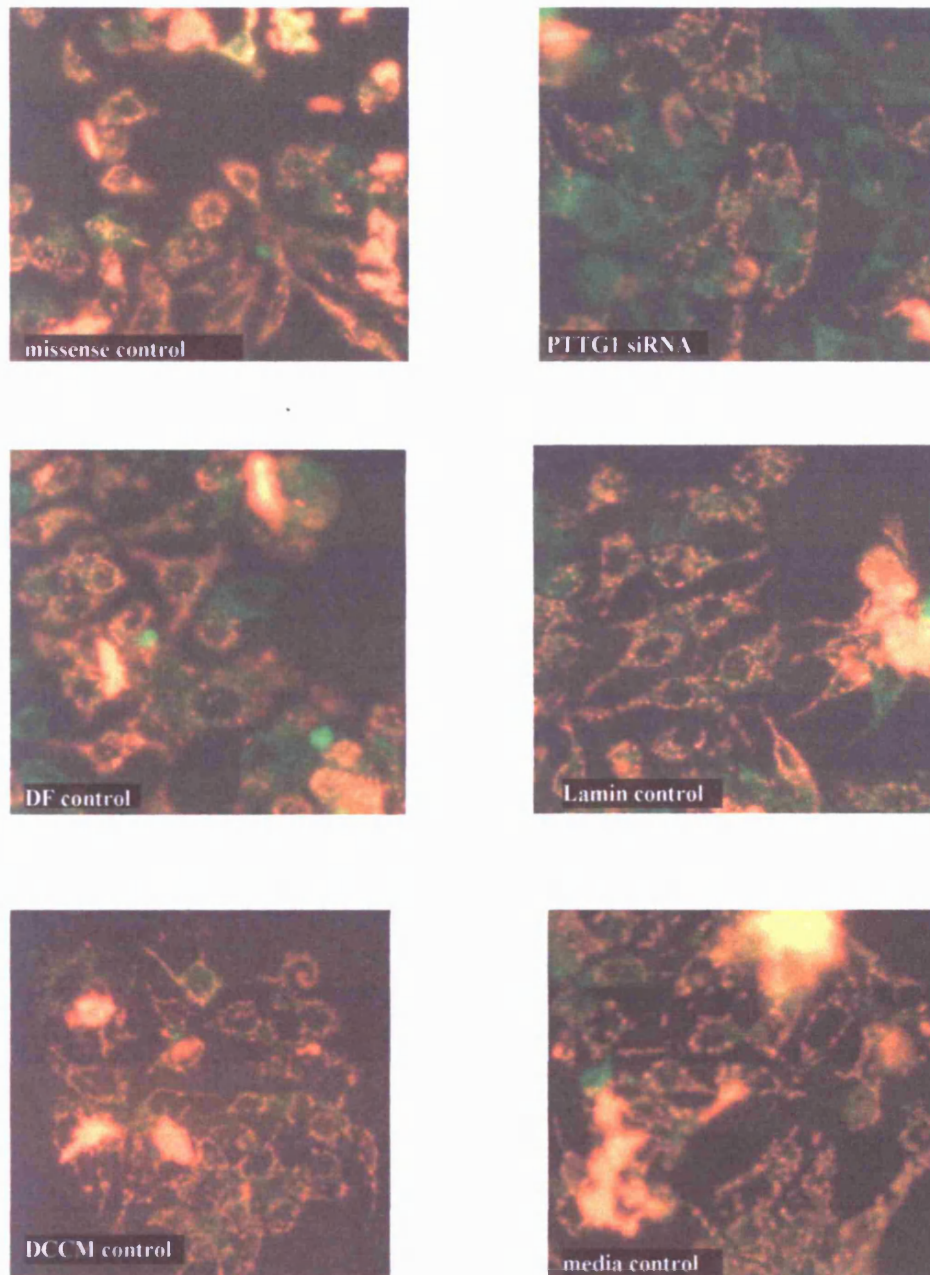
Figure 97. Apoptotic effects of PTTG1 siRNA knockout at day 4 as measured by Apoalert Apoptosis Mitochondrial Membrane Sensor kit in FasR-Lt cells. PTTG1 gene knockdown was achieved in FasR-Lt cells using 100nmol Smartpool reagents according to the Dharmacon protocol. Cells were processed for detection of apoptosis using the Apoalert Apoptosis Mitochondrial Membrane Sensor kit according to the manufacturers instructions. Controls included were missense, DharmaFECT (DF) transfection reagent, Lamin siRNA, DCCM media, and media (phenol red-free RPMI/ 5% serum) control, versus PTTG1 test siRNA. Live or apoptotic cells are represented by red or green fluorescence respectively (images show cells at x40 magnification).
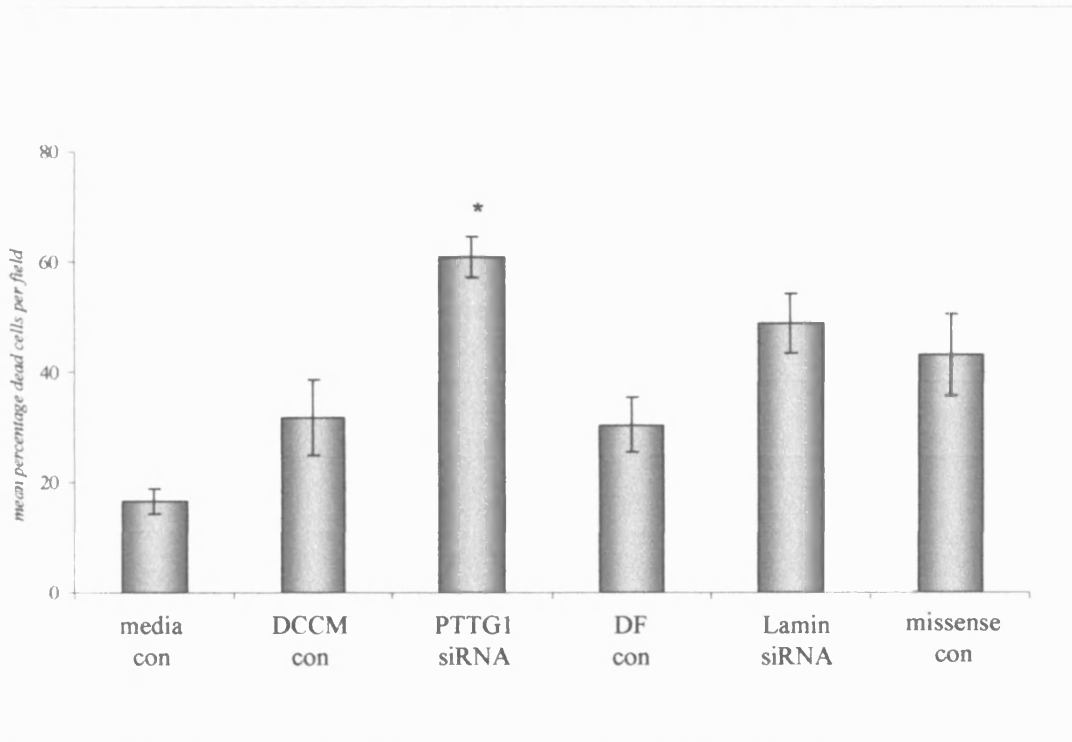
Figure 98. Microscopic Evaluation of the Apoptotic effects of PTTG1 siRNA knockout at day 4 as measured by Apoalert Apoptosis Mitochondrial Membrane Sensor kit in FasR-Lt cells. PTTG1 gene knockdown was achieved in FasR-Lt cells using 100nmol smartpool reagents according to the Dharmacon protocol and as described in Methods. Control or test cells were processed for detection of apoptosis using the Apoalert Apoptosis Mitochondrial Membrane Sensor kit according to the manufacturers instructions. Microscopic evaluation for apoptosis was performed at 40x magnification using red and green fluorescence detection and graded as red or green cell numbers from six fields per test slide. Controls included were missense 'scrambled', DharmaFECT (DF) transfection reagent, Lamin siRNA, DCCM media, and media (phenol red-free RPMI/ 5% serum) control. (plot shows standard errors) (*p=0.05 and p<0.001 for PTTG1 siRNA relative to missense and DCCM controls respectively, and p<0.001 compared to DF and Media controls).
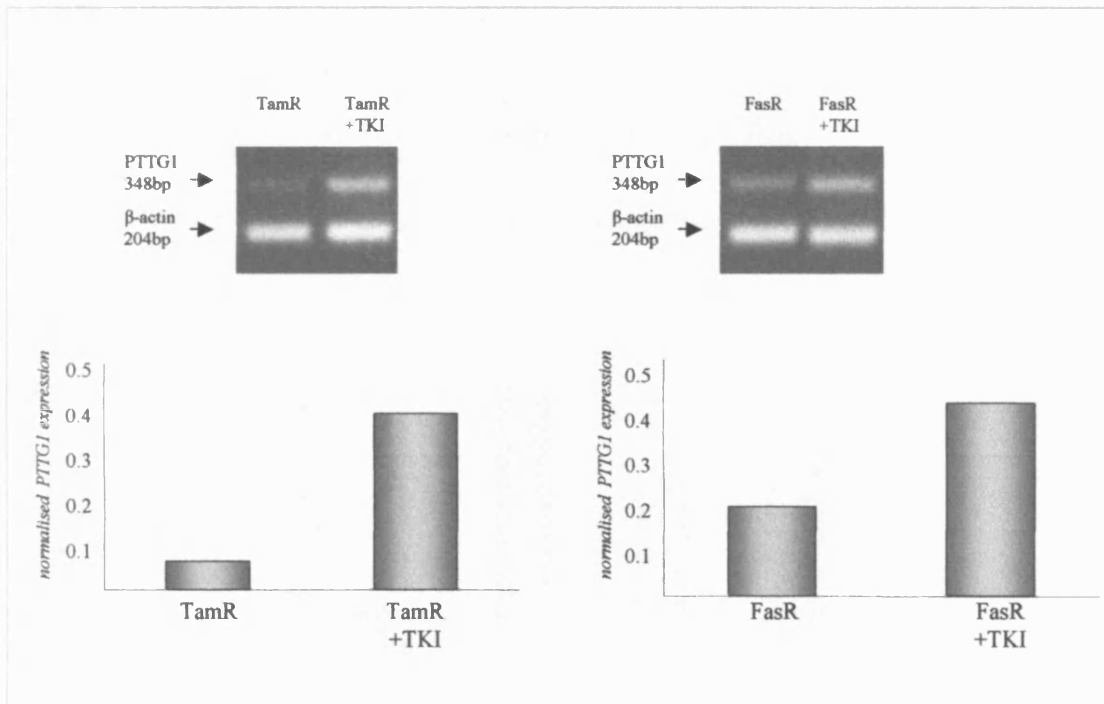
Figure 99. PTTG1 gene induction in TamR & FasR cells treated with Gefitinib. TamR and FasR cells were grown in 100mm dishes in the presence or absence of the EGFR-TKI Gefitinib (TKI; 10^{-6}M) for 7 days before harvesting according to the optimised Tri Reagent protocol. One microgram of RNA extracted from cells was reverse transcribed and gene expression was determined using primers for PTTG1 (with β-actin co-amplification for normalisation). Representative PCR profiles are shown which were subject to densitometric analysis and normalisation to β-actin before generation of plot.

(a) TKI at day4
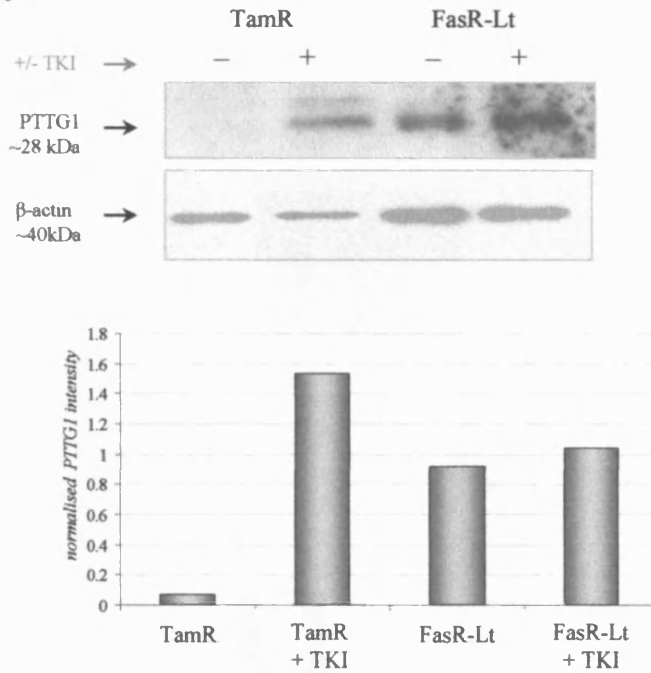
(b) TKI at day7
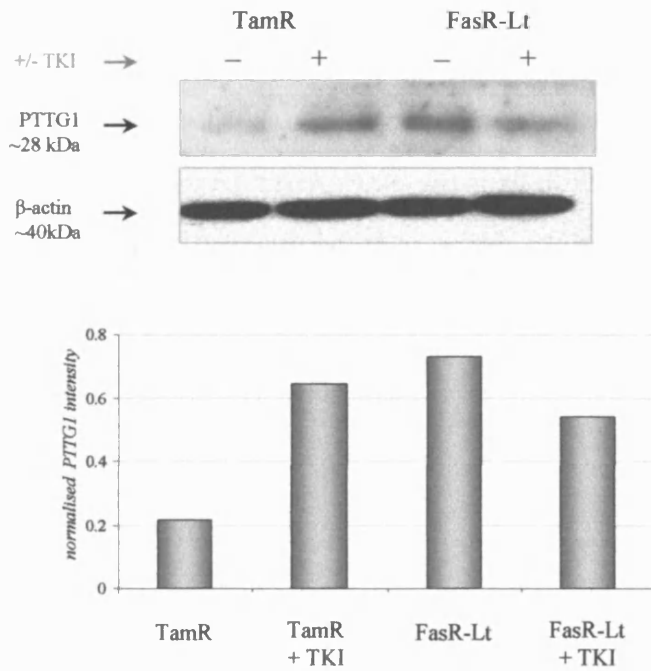
Figure 100. PTTG1 protein in TamR & FasR-Lt cells treated with EGFR-TKI Inhibitor Gefitinib.
TamR and FasR-Lt cells grown in 100nn dishes in the presence or absence of EGFR-TKI Gefitinib
(TKI; 10^{-6}M) for (a) 4 and (b) 7 days before harvested for protein. PTTG1 protein was determined by
subjecting 50ug protein from cells to 15% SDS PAGE and Western blotting. Proteins were probed with
monoclonal anti-PTTG1 antibody with chemiluminescent detection. Equivalence of protein loading in
Western blots was subsequently demonstrated by detection of β-actin on the same blot using monoclonal
antibody to the protein.
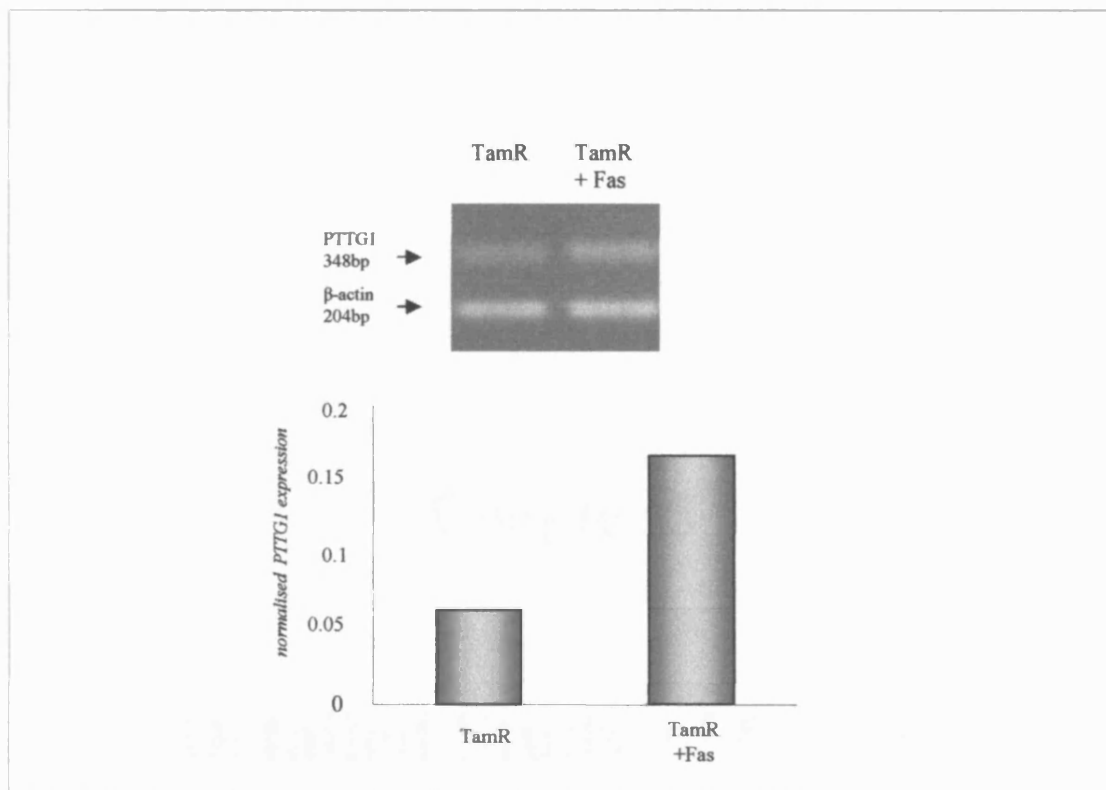
Figure 101. PTTG1 gene induction in TamR cells treated with 10^{-7}M Faslodex. TamR cells were grown in 100mm dishes in the presence or absence of Faslodex (10^{-7}M) for 7 days before harvesting according to the optimised TriReagent protocol. One microgram of RNA extracted from cells was reverse transcribed and gene expression was determined using primers for PTTG1 (with β-actin co-amplification for normalisation). Representative PCR profiles are shown which were subject to densitometric analysis and normalisation to β-actin prior to plotting.

Chapter 5

Detailed Study of Genes:

GFRα3

5.1 GFRα3

Atlas Plastic Microarrays and subsequent PCR analysis had revealed that the gene expression for GFRα3 was significantly induced in TamR cells and to a lesser extent in FasR cells compared to parental MCF-7 cells, a profile confirmed by Affymetrix genechip analysis (see also Fig.36).

5.1.1 GFRα3 Gene Induction in Resistant Cells

PCR verification was subsequently performed on further replicate experimental sets of RNA samples extracted after to the arrayed RNA set. Profiles for these resistant cell lines confirmed GFRα3 gene induction in FasR ($p<0.001$) as well as TamR ($p=0.0163$) with no change in oestradiol-treated MCF-7 cells (Fig.102).

The highly invasive FasR-Lt cells demonstrated by PCR analysis at least as high levels of GFRα3 mRNA as in the FasR cells (Fig.103a).Using Affymetrix gene analysis, GFRα3 mRNA levels were also suggested as induced in FasR-Lt cells relative to parental MCF-7 cells (-0.83 versus -1.63), although levels were not significantly elevated as FasR cells in this instance (1.40 versus -1.63) (Fig.103b).

Cell lines with acquired resistance to oestrogen deprivation developed at TCCR were also studied to determine the levels of GFRα3. Levels of the gene were low in both MCF-7 and X-MCF-7 cells, as measured by PCR (Fig.104a), with similarly no significant change observed using Affymetrix data (Fig.104b).

5.1.2 GFRα3 Protein Induction in Resistant Cells

5.1.2.1 Western Blotting Analysis of GFRα3 Protein

Using a monoclonal antibody to GFRα3 protein Western blotting confirmed induction of GFRα3 at the protein level (band at ~43kDa) in TamR and again to a lesser extent in FasR-Lt cell lines (3.3- and 1.6-fold respectively) relative to control MCF-7 cells (Fig.105).

5.1.2.2 Immunocytochemical Analysis of GFRα3 Protein

Immunocytochemical assay development allowed the detection of GFRα3 protein within formalin-fixed paraffin-embedded cell pellet blocks housing a replicate number of resistant and responsive cell lines including TamR, FasR-Lt and MCF-7.

A number of antibody concentrations, as well as antigen retrieval methods were used in order to initially optimise assays using polyclonal or monoclonal antibodies to GFRα3. The final immunocytochemical method adopted for the analysis of GFRα3 protein used the

monoclonal antibody at 1μg/ml and involved enzyme-mediated (pronase) antigen retrieval step (Fig.106).

Stained paraffin cell pellets bearing endocrine responsive and resistant cell lines in replicates of 6 pellets per cell line (2 from each of 3 experimental replicates) were subsequently scored for positively staining cells in cytoplasm and membrane as described previously. GFRα3 staining was localised predominantly within the cytoplasm and membrane, with no detectable nuclear staining (Fig.107). PCR profiles, as well as GFRα3 protein levels observed in Western blotting studies were paralleled using immunocytochemical analyses with increased staining in the resistant cells (Fig.106 and Fig.107). A marked elevation in staining for GFRα3 within the cytoplasm was observed in TamR cells (p<0.001) compared to MCF-7 cells, with a more modest but nevertheless obvious increase in FasR-Lt cells (p<0.001). GFRα3 membrane staining was also significantly increased in TamR cells and FasR cells.

5.1.3 Further GFRα Family Members and Ligands in Resistant Cells

5.1.3.1 Receptors

Alongside detailed study of GFRα3, PCR analysis using primers for the spectrum of GFRα receptors and their ligands, as well as genes associated with these proteins, have revealed differential expression across the resistant cell lines used in this study.

Affymetrix data for GFRα4 revealed a significant induction in TamR and FasR cells (Fig.108a; p=0.0087 and p=0.0372 respectively) versus MCF-7 cells. However, GFRα4 mRNA profiling by PCR analysis confirmed significant elevation only in FasR cells (p=0.0102) compared to MCF-7 cells (Fig.108b). Affymetrix analysis confirmed the increase in FasR cells, but this did not extend to FasR-Lt cells (Fig.109). There was also some increase in GFRα4 gene levels in X-MCF-7 cells compared to MCF-7 cells using PCR (Fig.110a) and also by Affymetrix analysis (Fig.110b).

Using Atlas Plastic microarray analysis, this project had observed GFRα1 gene to be significantly repressed in both TamR and FasR cells versus MCF-7, falling to a level not detectable (with no change in oestradiol-treated MCF-7 cells), thus considered a 'shared repressed gene' (see Fig.61a). This marked reduction in GFRα1 mRNA in resistant cells had also been confirmed at the PCR level and using Affymetrix analysis (see Fig.61b and Fig.61c respectively). Subsequent PCR verification was performed on additional sets of RNA samples. Resistant cell lines were again confirmed as having reduced GFRα1 gene levels relative to parental MCF-7 cells, with no significant change in oestradiol-treated MCF-7 (Fig.111). As well as being repressed in FasR cells, GFRα1 gene levels were also significantly reduced in the FasR-Lt cell line according to Affymetrix data analysis (Fig.112; p<0.001 relative to MCF-7).
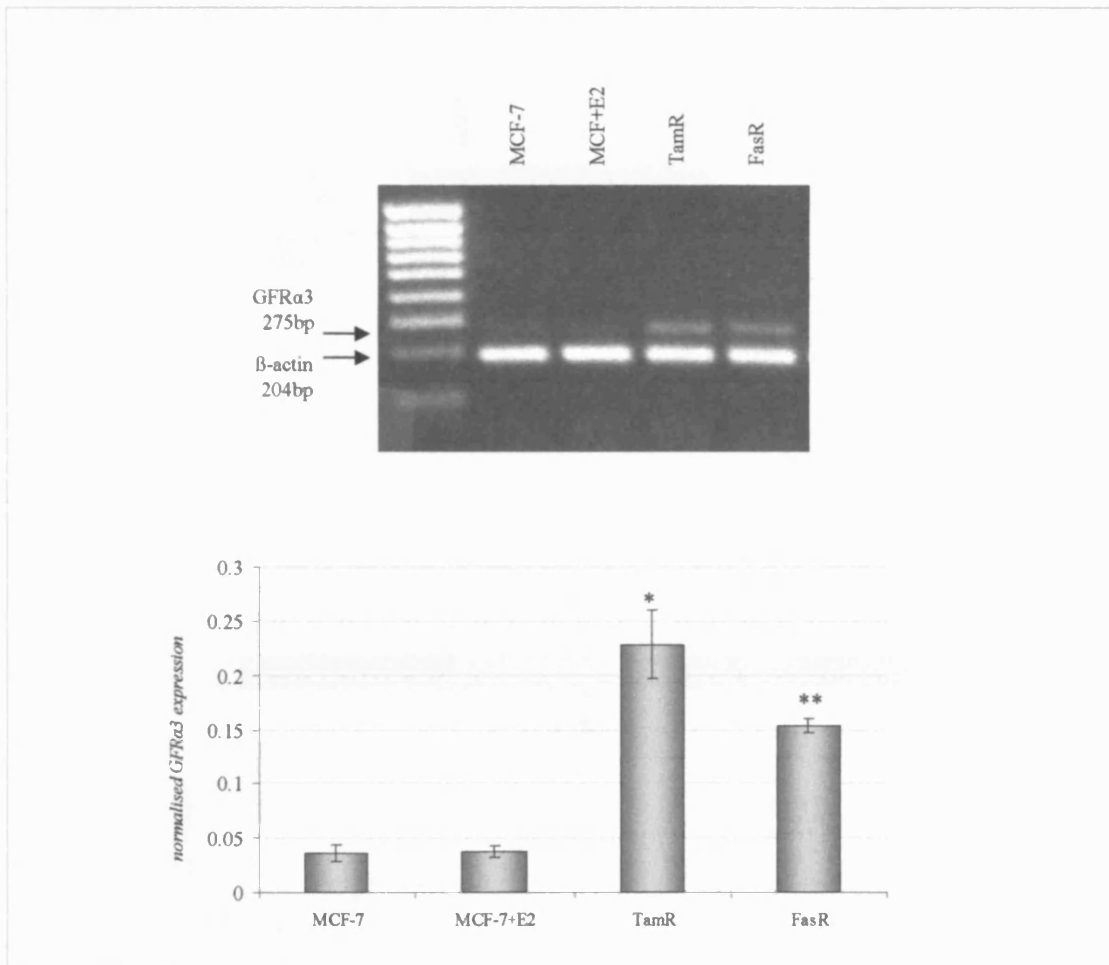
Figure 102. GFRα3 gene upregulation in TamR and FasR cells is further confirmed in replicate RNA preparations. This was achieved by PCR analysis using primers for GFRα3 co-amplified with β-actin for normalisation. PCR products separated on an agarose gel were visualised by ethidium bromide staining. A representative PCR profile is shown from triplicate experiments. PCR profiles were then subject to densitometric analysis (plot shows standard error). (*p=0.0163 and **<0.001 respectively for TamR and FasR relative to MCF-7 [Students t-test]).

(a)

GFRα3
275bp

ß-actin
204bp

(b)

Log intensity

MCF-7   FasR   FasR-Lt
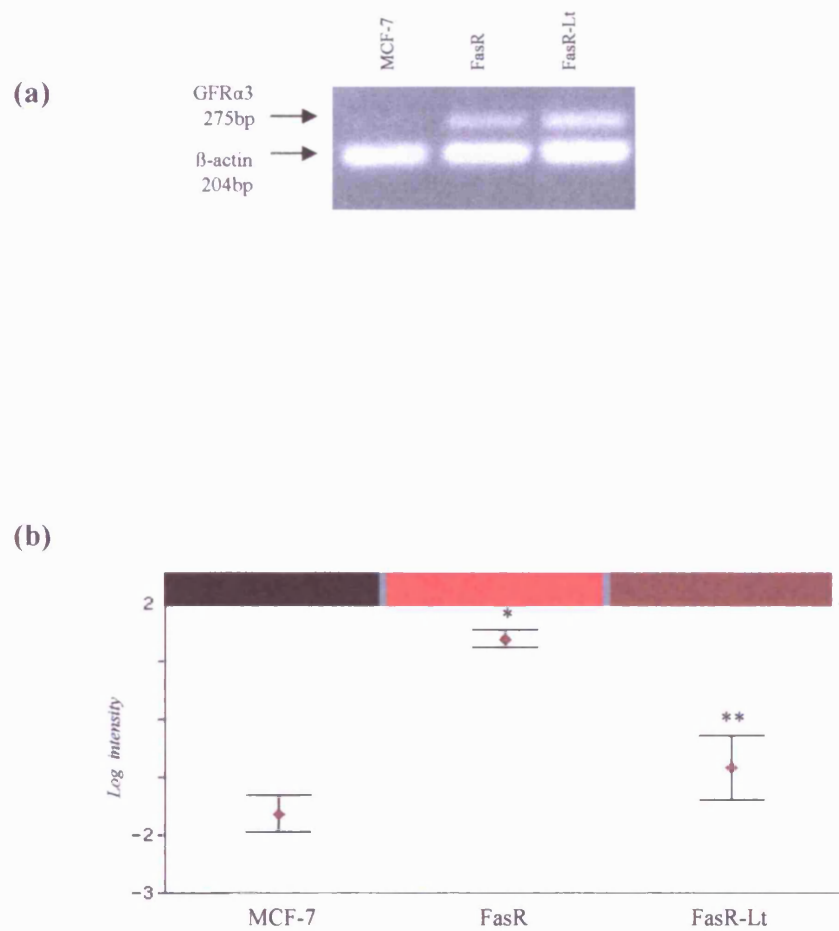
Figure 103. GFRα3 gene upregulation in FasR and FasR-Lt cells. (a) PCR analysis was performed using primers for GFRα3 co-amplified with β-actin for normalisation. PCR products were separated on an agarose gel and visualised by ethidium bromide staining. (b) GFRα3 mRNA was identified as differentially expressed using GeneSifter software applied to Affymetrix HG-U133A gene chip data. Log-intensity graphical output and heatmap are shown. (plot shows log-mean intensity with standard errors; *p=0.014 for FasR relative to MCF-7 and **p=0.0175 for FasR-Lt relative to FasR [Students t-test]).
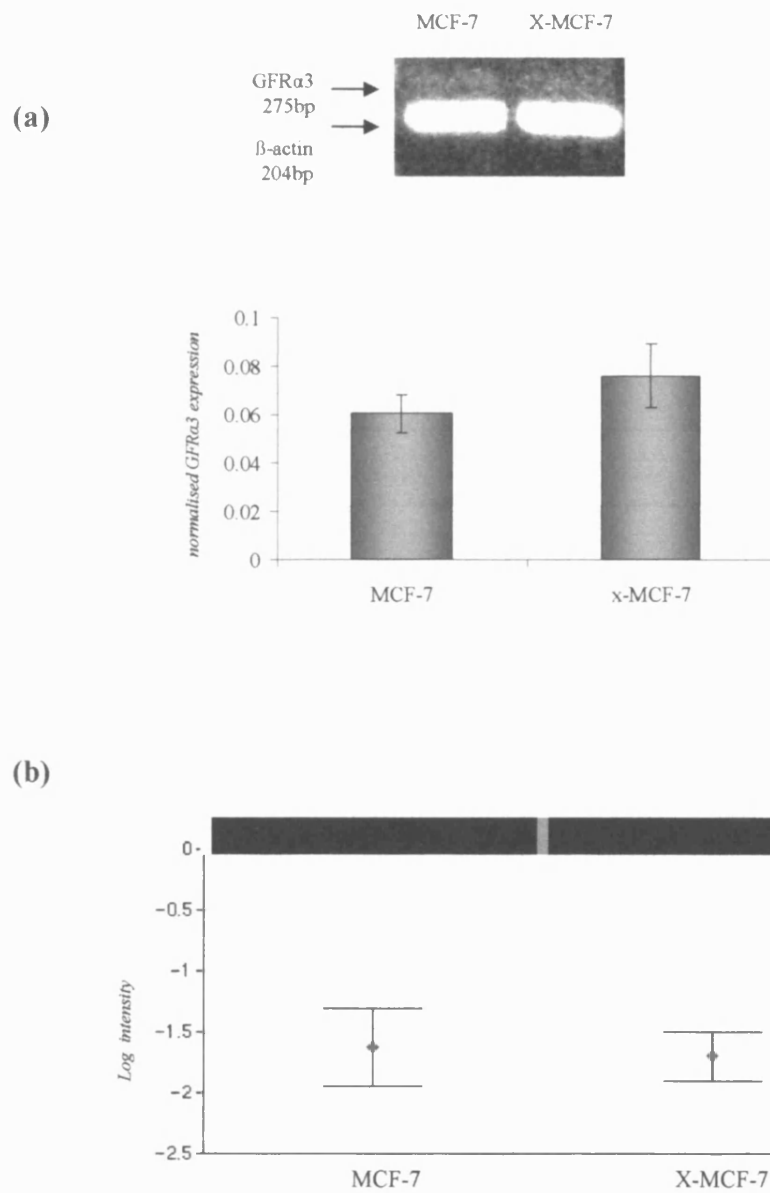
Figure 104. GFRα3 gene regulation in the resistance to oestrogen-deprivation model, X-MCF-7 cells. (a) PCR analysis was performed using primers for GFRα3 co-amplified with β-actin for normalisation. PCR products were separated on an agarose gel, visualised by ethidium bromide staining, and then subject to densitometric analysis. Representative signal is shown for triplicate experiment (plot shows standard errors). (b) GFRα3 mRNA was profiled using GeneSifter software applied to Affymetrix HG-U133A gene chip data. Log-intensity graphical output and heatmap are shown (plot shows mean intensity with standard errors
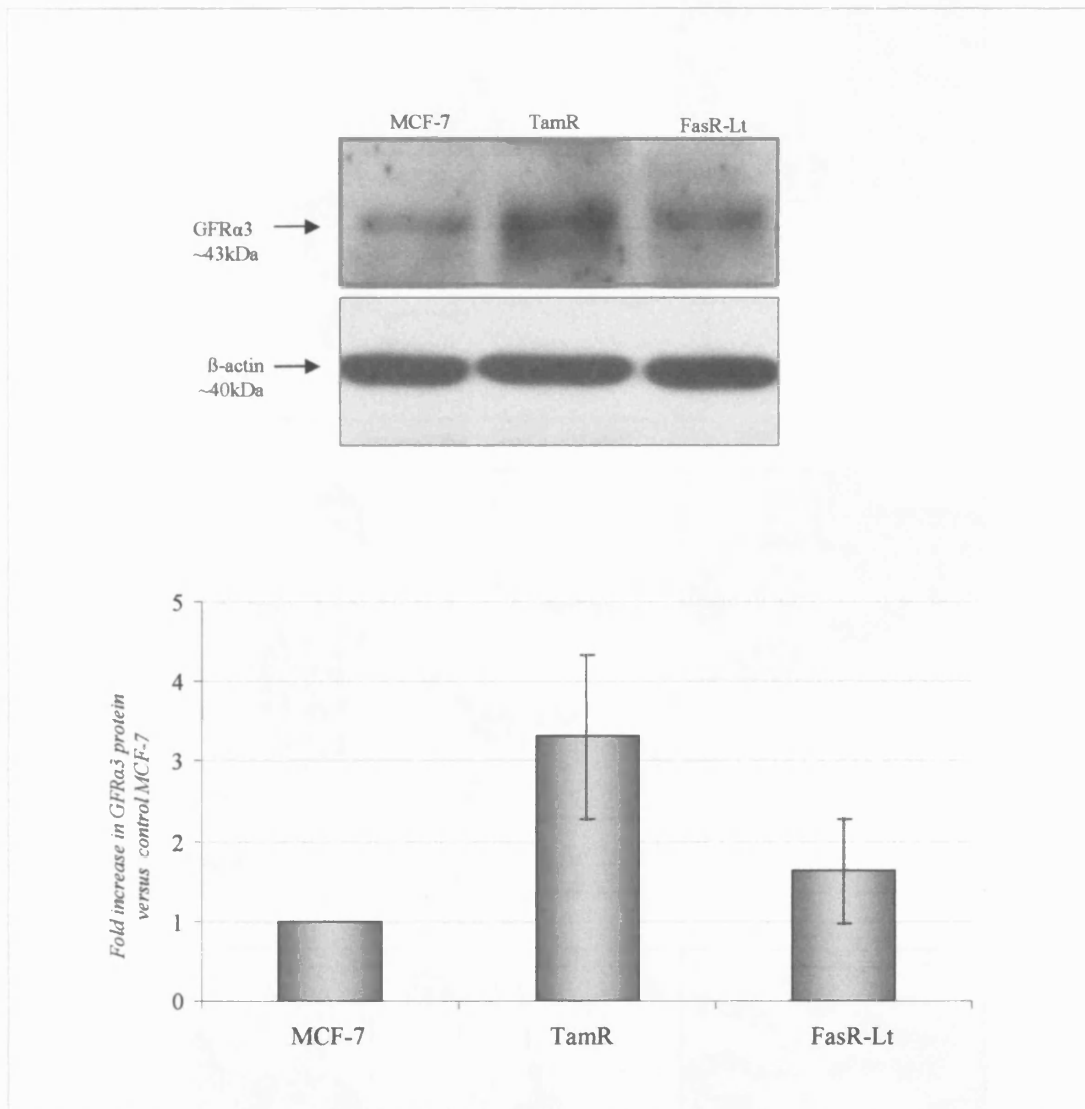
Figure 105. Western Blot analysis of GFRα3 protein in MCF-7, TamR & FasR-Lt cells. Fifty micrograms of protein from each cell line were subject to 7.5% denaturing SDS PAGE, Western blotting and probed using monoclonal anti-human GFRα3 antibody with chemiluminescence detection. Blots were subject to densitometric analysis and actin normalisation (plot shows fold increase in normalised expression relative to control MCF-7 cells with standard errors). Representative blot is shown from triplicate experiment.
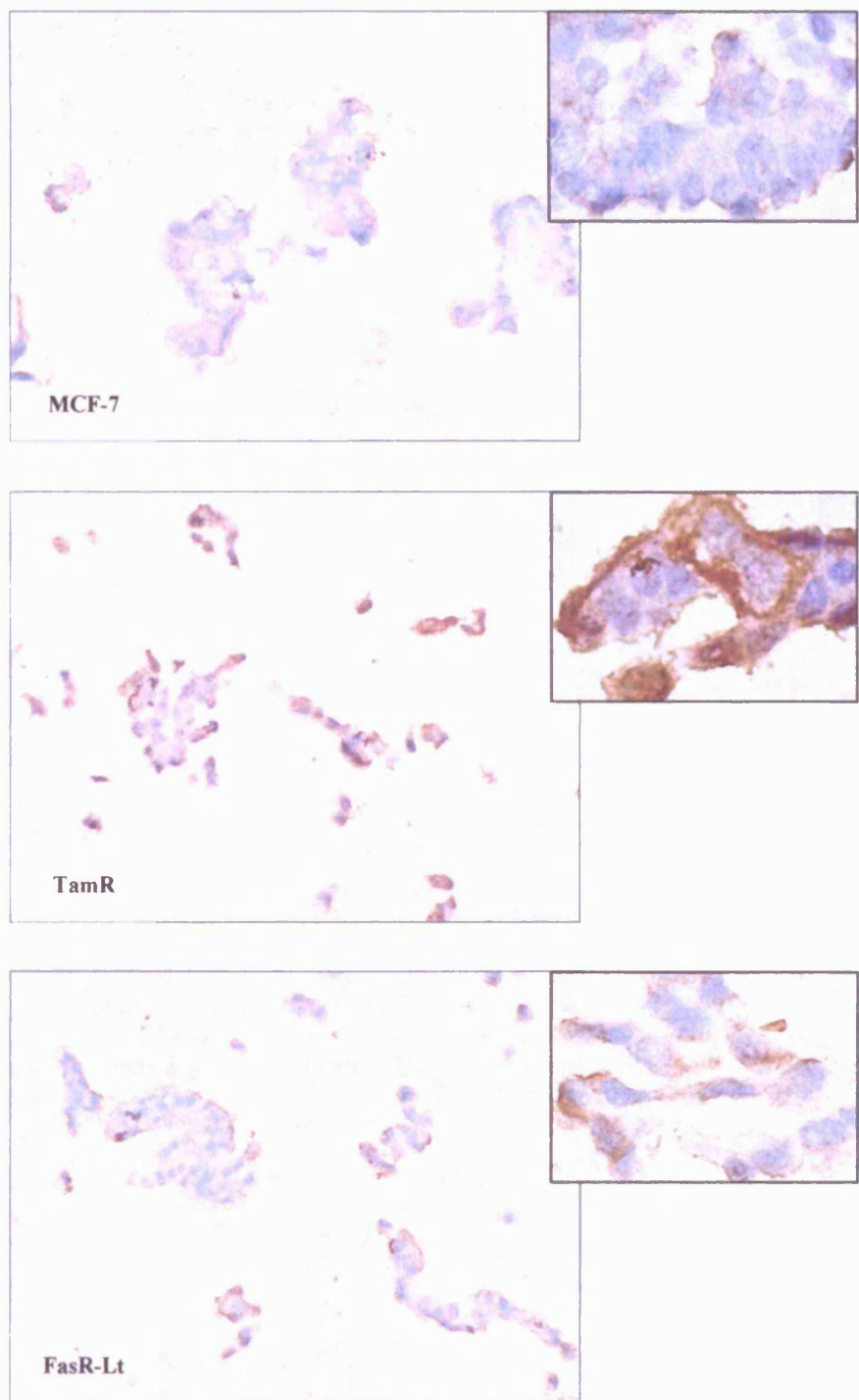
Figure 106. Immunocytochemical detection of GFRα3 protein in MCF-7, TamR & FasR-Lt Pellet arrays. MCF-7, TamR & FasR-Lt cells were harvested, formalin fixed, and pellets embedded in paraffin blocks. 5μm sections prepared from blocks were probed using monoclonal anti-human GFRα3 antibody after enzymatic antigen retrieval and detected using the DAKO Envision detection system with DAB staining, (photographs shown at x20 original magnification; inserts at x40).
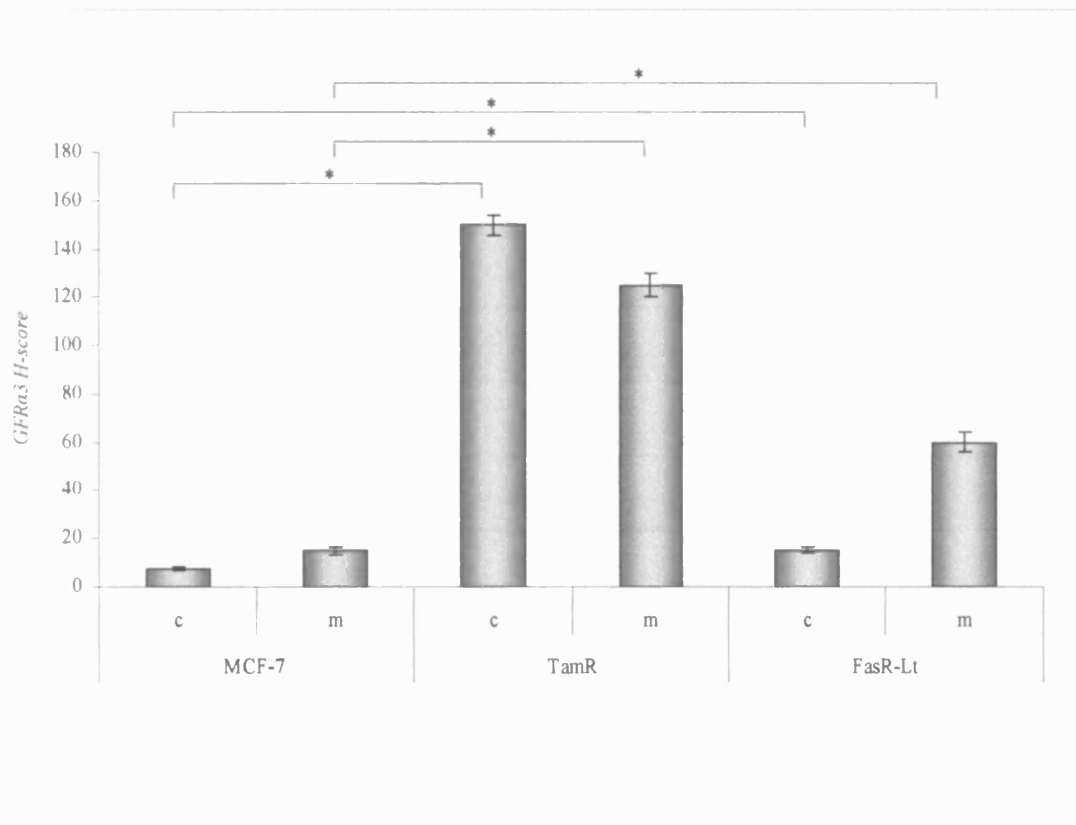
Figure 107. Immunocytochemical analysis of GFRα3 protein in MCF-7, TamR & FasR-Lt. MCF-7, TamR & FasR-Lt cells were harvested, formalin fixed, and pellets embedded in paraffin blocks. 5μm sections prepared from blocks were probed using monoclonal anti-human GFRα3 antibody after enzymatic antigen retrieval and detected using DAKO Envision detection system with DAB staining. Microscopic evaluation of H-score GFRα3 immunoreactivity in cytoplasm (c) and membrane (m) was graded from six fields per test slide, and plotted showing standard errors. (*p<0.001 for cytoplasmic or membrane staining for TamR or FasR compared to MCF-7 cells [Students t-test]).
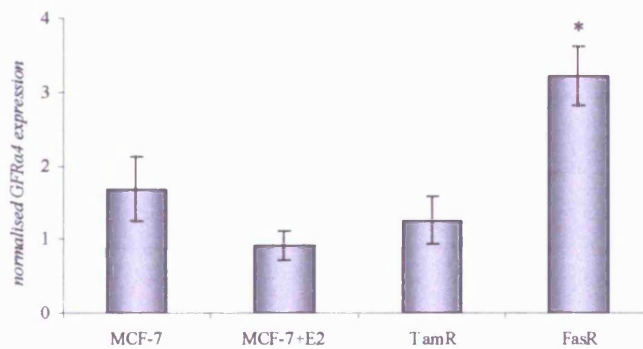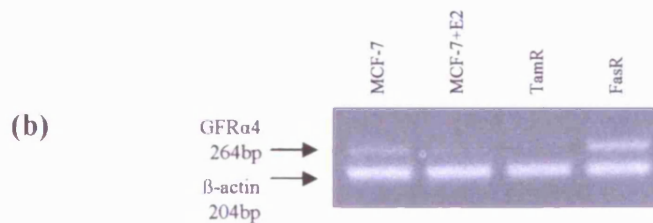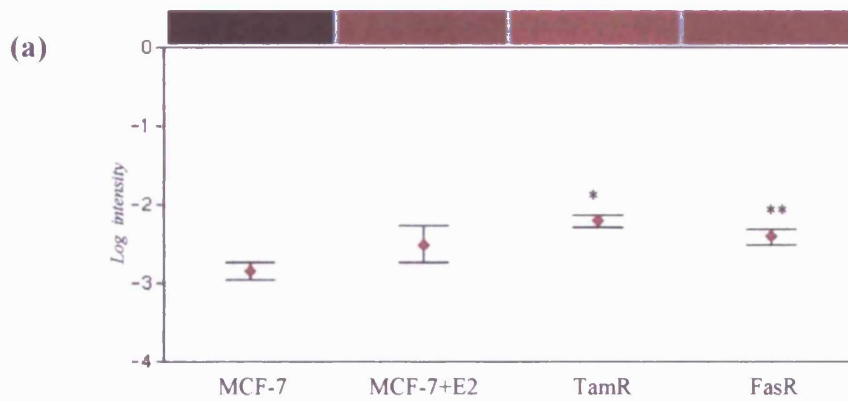
Figure 108. GFRα4 gene expression in TamR and FasR cells. (a) GFRα4 mRNA was identified as differentially expressed in TamR and FasR cells using GeneSifter software applied to Affymetrix HG-U133A gene chip data. Log-intensity graphical output and heatmap are shown. Additional controls were provided be parental MCF-7 cells subject to oestradiol treatment. (plot shows mean intensity with standard errors; *p=0.0087 and **p=0.0372 for TamR and FasR respectively, relative to MCF-7 [Students t-test]). (b) Verification of gene expression profile was performed by PCR analysis using primers for GFRα4 co-amplified with β-actin for normalisation. PCR products separated on agarose gel, visualised by ethidium bromide staining, and then subject to densitometric analysis, normalisation, and graphically displayed with standard errors. Representative PCR profile is shown from a triplicate experiment. (*p=0.0102 for FasR relative to MCF-7).
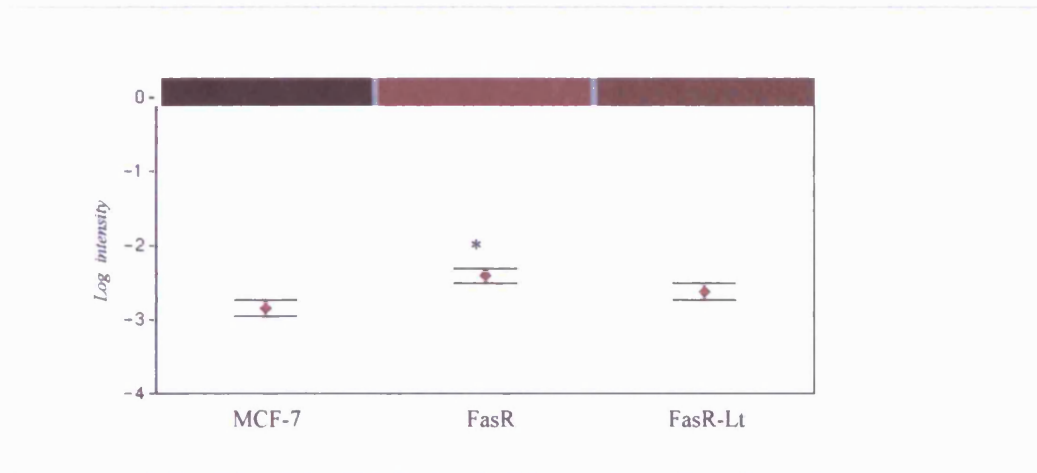
Figure 109. GFRα4 gene in FasR & FasR-Lt cells from a database constructed from Affymetrix data. GFRα4 mRNA was profiled in FasR and FasR-Lt cells using GeneSifter software applied to Affymetrix HG-U133A gene chip data. Log-intensity graphical output and heatmap are shown f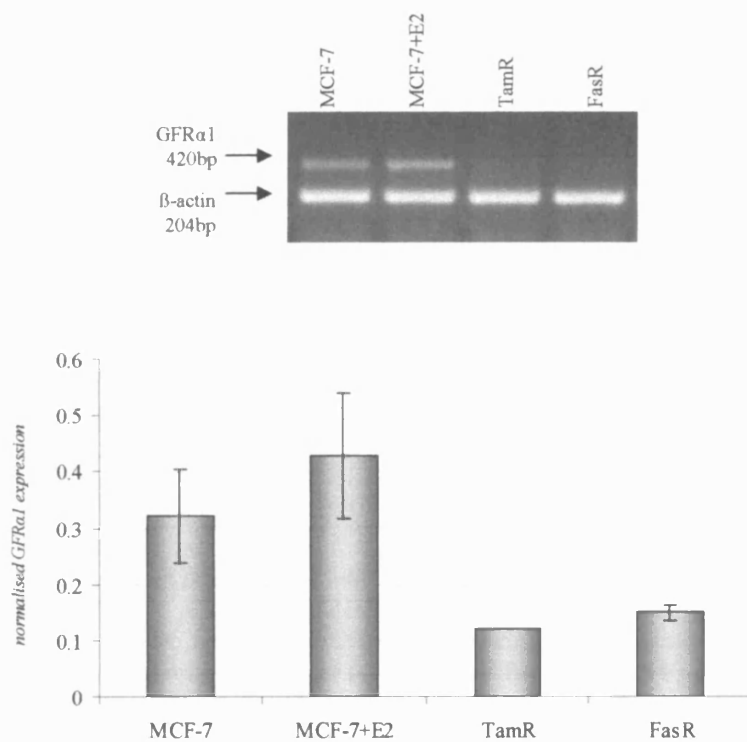or the gene. (plot shows mean intensity with standard errors; *p=0.0372 for FasR relative to MCF-7 control [Students t-test]).

Figure 110. GFRα4 gene expression in the resistance to oestrogen-deprivation model, X-MCF-7 cells. (a) PCR analysis was performed using primers for GFRα4 co-amplified with β-actin for normalisation. PCR products were separated on an agarose gel, visualised by ethidium bromide staining, subject to densitometric analysis, and normalised prior to plotting. Representative signal is shown for triplicate experiment (plot shows standard errors). (b) GFRα4 mRNA was profiled in X-MCF-7 cells versus MCF-7 control using GeneSifter software applied to Affymetrix HG-U133A gene chip data. Log-intensity graphical output and heatmap are shown (plot shows mean intensity with standard errors

Figure 111. GFRα1 gene downregulation in TamR and FasR cells. GFRα1 mRNA was confirmed as decreased in resistant cells using RNA extracted from experimental replicate preparations and PCR analysis using primers for GFRα1 co-amplified with β-actin as a normalisation control. PCR products were separated on agarose gel and visualised by ethidium bromide staining. Representative PCR profile is shown. PCR profiles were then subject to densitometric analysis with normalisation before plotting (plot shows standard errors).
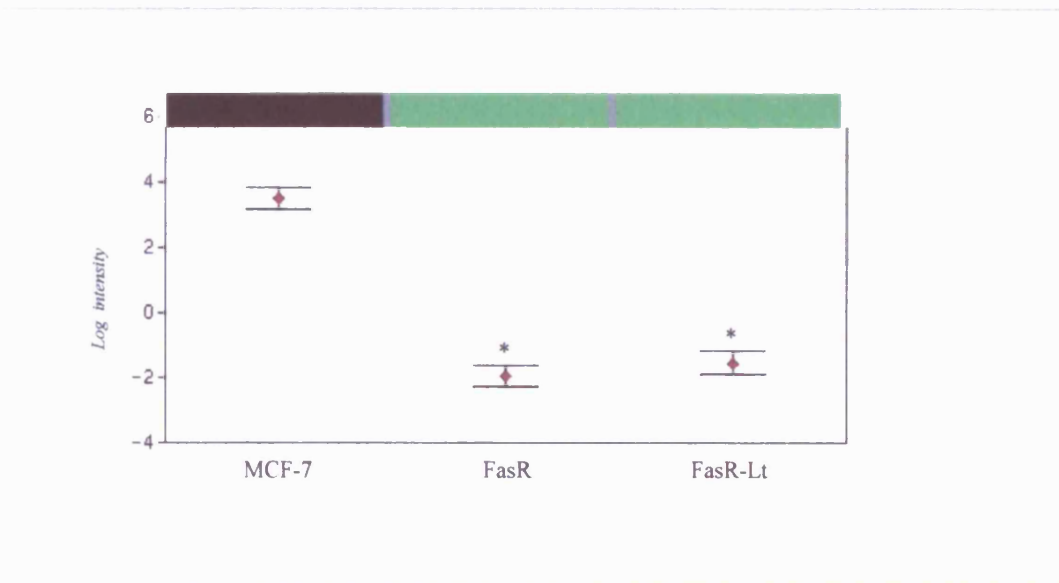
Figure 112. GFRα1 gene expression in FasR & FasR-Lt cells from a database constructed from Affymetrix data. GFRα1 mRNA was identified as decreased in FasR and FasR-Lt cells using GeneSifter software applied to Affymetrix HG-U133A gene chip data. Log-intensity graphical output and heatmap are shown for the gene. ($p < 0.001$ for both FasR and FasR-Lt relative to MCF-7 control [students t-test]).

GFRα3 mRNA were also reduced in X-MCF-7 cells compared to parental MCF-7 cells using PCR analysis (Fig.113a), which significance using Affymetrix data (Fig.113b; p=0.0151).

While GFRα2 gene levels were suggested as slightly increased in FasR cells relative to parental MCF-7 cells, this was non-significant also with no change in TamR cells as determined by PCR analysis (Fig.114a). A slight, but again non-significant induction in GFRα2 was also suggested in MCF-7 cells upon oestradiol treatment. Similarly, no significant changes were noted across all endocrine responsive/ resistant cells using Affymetrix analysis (Fig.114b). Levels of GFRα2 also remained unchanged across FasR-Lt cells compared to either MCF-7 or FasR cells (Fig.115). PCR studies showed some induction of GFRα2 in X-MCF-7 cells (Fig.116a), although this was unparalleled by Affymetrix data (Fig.116b).

The co-receptor for the GDNF family of receptors, the RET proto-oncogene, was expressed in all cell lines and differential at the mRNA level as determined by PCR studies (Fig.117a). A significant RET gene induction was observed in oestradiol-treated MCF-7 cells (p=0.0486) compared to parental MCF-7 cells, also with increased levels in TamR cells (p=0.0408). There was no change in (but still detectable levels) in FasR cells versus MCF-7. The significant increase in RET in MCF-7 cells with oestradiol treatment was confirmed by Affymetrix analysis (Fig.117b; p=0.0052), and while other increases did not reach significance, the gene was again readily detectable in all models. Affymetrix data also showed no overall change in RET gene levels across FasR-Lt compared to FasR or MCF-7 control (Fig.118). In contrast, the RET gene was significantly induced in X-MCF-7 cells compared to parental MCF-7 cells using PCR analysis (Fig.119a; p=0.0328), which was paralleled by Affymetrix profiling (Fig.119b; p=0.0037). Additionally, the RET receptor protein was detectable in all cell lines probed using Western blotting, with a slight increase suggested in TamR cells versus MCF-7 (Fig.120).

5.1.3.2 Ligands

The GFRα3 ligand Artemin was detectable in all endocrine responsive and resistant cell lines by PCR analysis (Fig.121a). However, an induction of Artemin was observed in MCF-7 cells treated with oestradiol compared to parental MCF-7 cells (p=0.004), while there was a significant decrease of expression in both TamR and FasR cells (p=0.013 and p=0.0205 respectively). Affymetrix profiling of the Artemin gene again revealed oestradiol induction (p=0.0331), although there was no suppression in TamR and FasR cells detectable by this method (Fig.121b). No change in expression was seen in FasR-Lt (Fig.122). As with PCR for TamR and FasR, a significant repression of the gene was seen in X-MCF-7 cells using PCR analysis (p=0.0204; Fig.123a). However, again this profile was not paralleled by an equivalent Affymetrix profile (Fig.123b).

The GFRα4 ligand Persephin explored only by Affymetrix showed some induction in TamR cells compared to parental MCF-7 cells, but there was no change suggested in FasR cells (Fig.124a), FasR-Lt (Fig.124b) or X-MCF-7 cells (Fig.124c). The GFRα1 ligand GDNF was suggested to be possibly induced to a small degree in FasR cells compared to control MCF-7 cells, but this was not significant. There was also no change in TamR or oestradiol-treated MCF-7 cells (Fig.125a), in FasR-Lt cells (Fig.125b), or X-MCF-7 cells (Fig.125c). Affymetrix analysis showed the GFRα2 ligand Neurturin gene to be significantly induced in MCF-7 cells upon oestradiol treatment compared to parental MCF-7 cells (Fig.126a; p=0.0356), with a much smaller, non-significant induction in TamR and FasR cells. Affymetrix analysis also suggested Neurturin mRNA was possibly slightly increased in FasR-Lt as in FasR cells (Fig.126b) and also in X-MCF-7 versus MCF-7 (Fig.126c), but these changes did not reach significance.

5.1.4 GFRα3 Detection in Clinical Disease

5.1.4.1 GFRα3 mRNA Expression in Clinical Disease

Gene expression for GFRα3 was observed at the mRNA level using RT-PCR in a series of clinical primary breast cancer samples (Fig.127, n=78). These clinical samples confirmed expression was markedly differential in breast cancer (median GFRα3 mRNA level by densitometry=0.227; range= 0-5.74), with 23 patients negative for GFRα3 expression. Mann-Whitney analysis subsequently revealed a significant inverse association between GFRα3 and ER receptor status, with this gene enriched in ER-negative disease (Fig.128; p=0.01) and lower levels in ER-positive patients. This relationship was further confirmed with Spearmann's analysis which showed a significant indirect correlation between levels of ER and GFRα3 (p=0.025). GFRα3 expression also directly associated with EGFR expression by Spearmann's analysis (Fig.129; p=0.013). GFRα3 expression also associated with decreased (category 3) tubular differentiation (Fig.130; p=0.04). There was also a significant linear (Spearmann's) association between GFRα3 and PTTG1 mRNA (Fig.131; p<0.001) that was maintained in ER-positive (p=0.007) and as a trend in ER-negative disease (p=0.084). An association was also observed in GFRα3 mRNA expression with the protein expression of the transcription factor Fos (Fig.132; p=0.004), which was maintained in ER-negative (p=0.038) and as a trend in ER-positive disease (p=0.057).

5.1.4.2 GFRa3 Protein Expression in Clinical Samples

Optimised GFRα3 immunostaining was applied to a small number of formalin-fixed, paraffin embedded clinical breast cancer sections to determine if protein expression can be detected in-vivo. After enzyme-mediated (pronase) antigen retrieval, a monoclonal primary antibody concentration of 1µg/ml was detected using the DAKO Envision detection system with
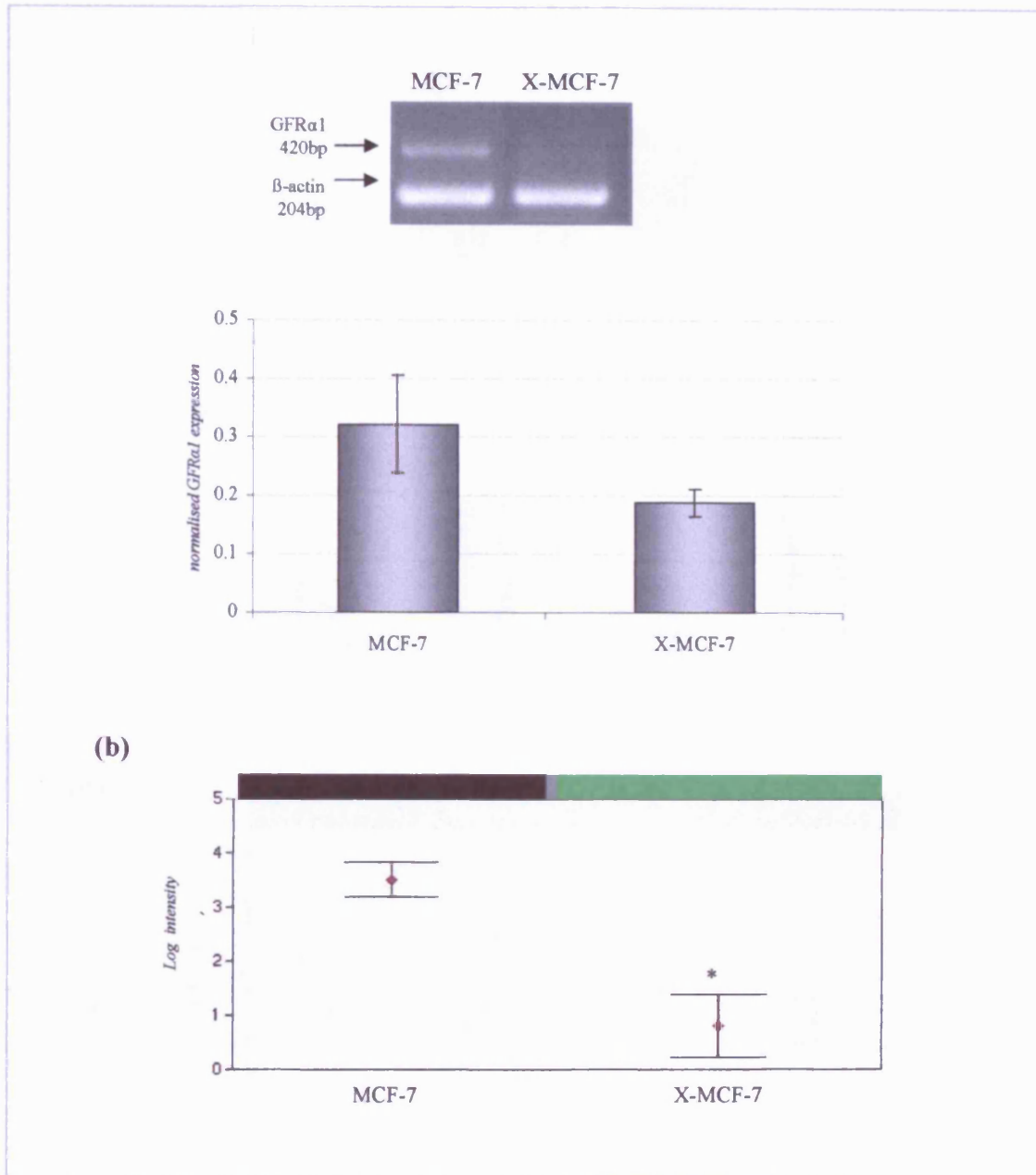
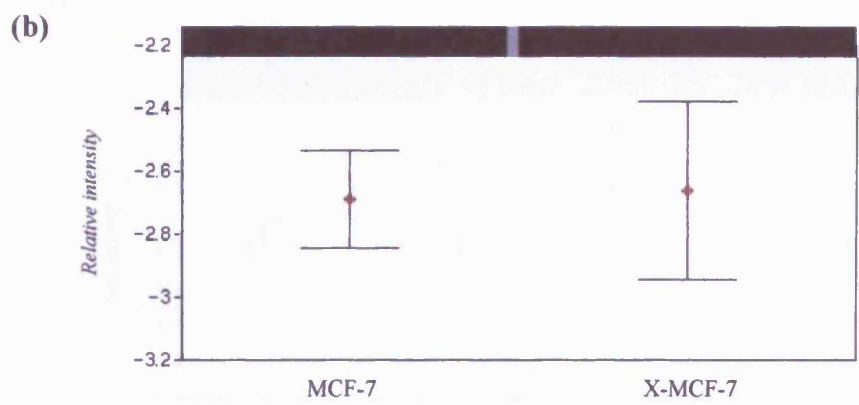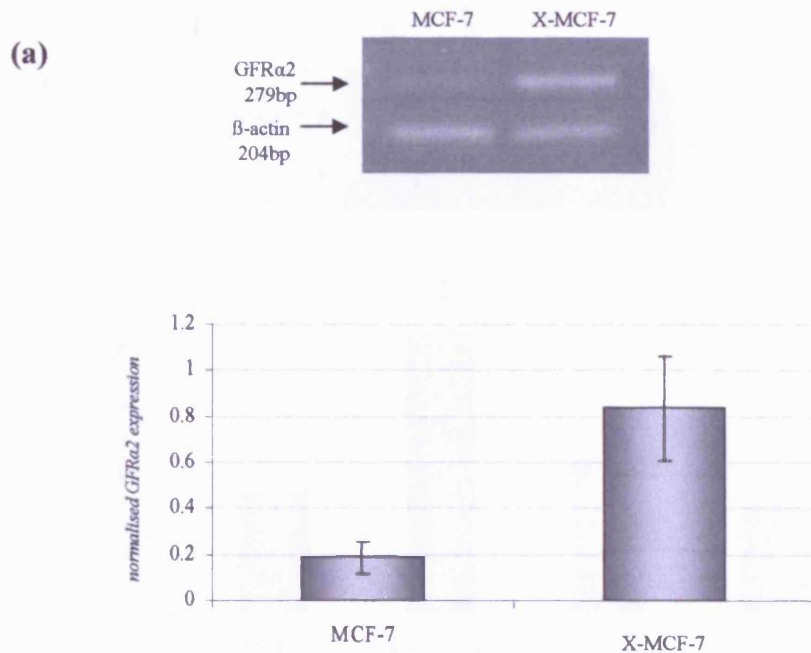Figure 113. GFRα1 gene expression in the resistance to oestrogen-deprivation model, X-MCF-7 cells. (a) PCR analysis was performed using primers for GFRα1 co-amplified with β-actin for normalisation. PCR products were separated on an agarose gel, visualised by ethidium bromide staining, subject to densitometric analysis, and normalised prior to plotting. Representative signal is shown for triplicate experiment (plot shows standard errors). (b) GFRα1 mRNA was profiled in X-MCF-7 cells versus MCF-7 control using GeneSifter software applied to Affymetrix HG-U133A gene chip data. Log-intensity graphical output and heatmap are shown (plot shows mean intensity with standard errors; *p=0.0151 for X-MCF-7 relative to MCF-7 [student t-test]).
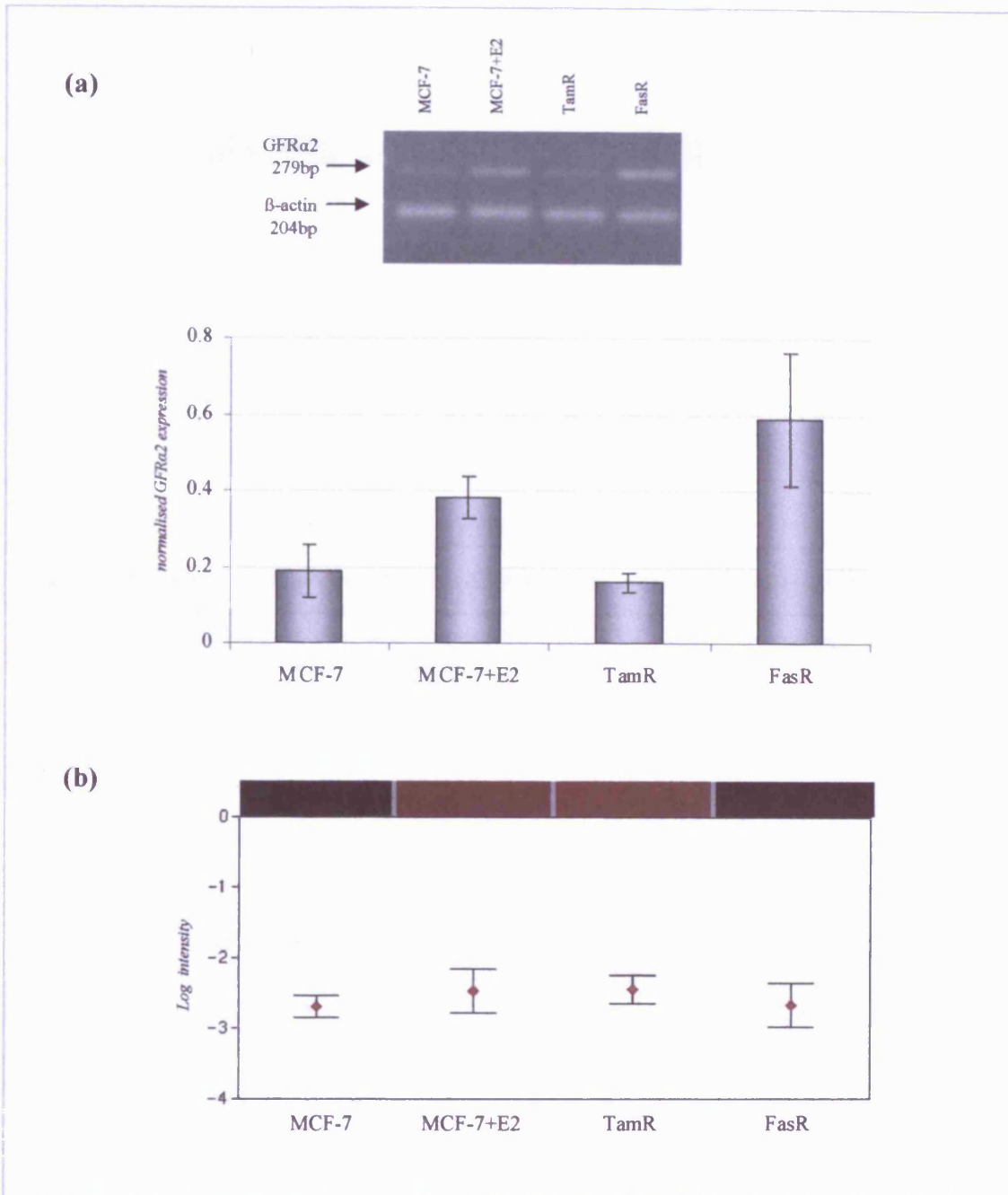
Figure 114. GFRα2 gene expression in TamR and FasR cells. (a) GFRα2 mRNA was analysed in resistant cells using RNA extracted from experimental replicate preparations and PCR analysis using primers for GFRα2. β-actin was also amplified as a normalisation control. PCR products were separated on agarose gel and visualised by ethidium bromide staining. Representative PCR profile is shown. PCR profiles were then subject to densitometric analysis with normalisation before plotting (plot shows standard errors). (b) GFRα4 mRNA was profiled in TamR and FasR cells using GeneSifter software applied to Affymetrix HG-U133A gene chip data. Log-intensity graphical output and heatmap are shown. Additional controls were provided be parental MCF-7 cells subject to oestradiol treatment. (plot shows mean intensity with standard errors).

Figure 115. GFRα2 gene in FasR & FasR-Lt cells from a database constructed from Affymetrix data. GFRα2 mRNA was profiled in FasR and FasR-Lt cells using GeneSifter software applied to Affymetrix HG-U133A gene chip data. Log-intensity graphical output and heatmap are shown for the gene (plot shows mean intensity with standard errors).

Figure 116. GFRα2 gene expression in the resistance to oestrogen-deprivation model, X-MCF-7 cells. (a) PCR analysis was performed using primers for GFRα2. β-actin was also amplified for the purpose of normalisation. PCR products were separated on an agarose gel, visualised by ethidium bromide staining, subject to densitometric analysis, and normalised prior to plotting. Representative signal is shown for triplicate experiment (plot shows standard errors). (b) GFRα2 mRNA was profiled in X-MCF-7 cells versus MCF-7 control using GeneSifter software applied to Affymetrix HG-U133A gene chip data. Log-intensity graphical output and heatmap are shown (plot shows mean intensity with standard errors
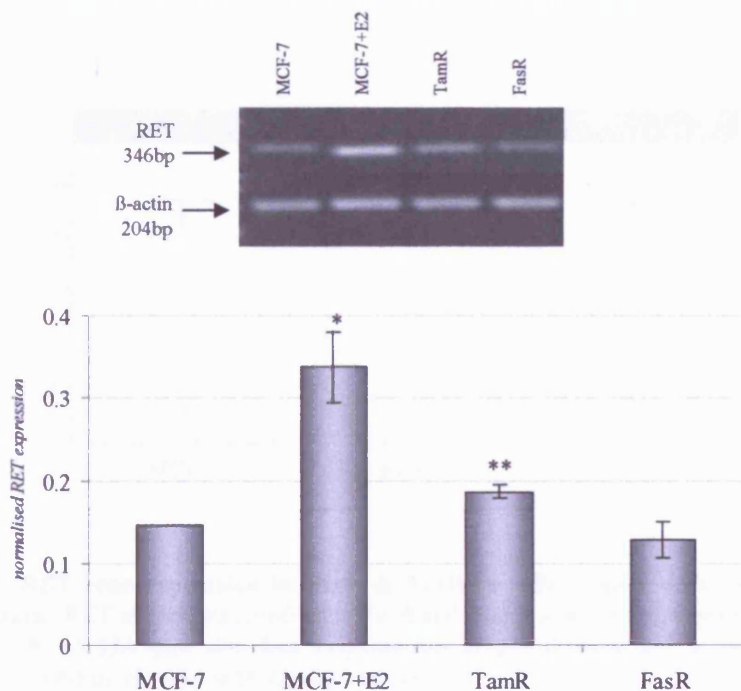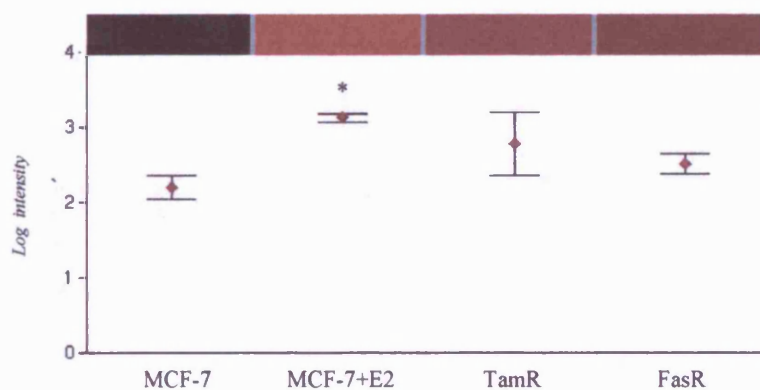
Figure 117. RET gene expression in TamR and FasR cells. Analysis of gene profile was performed by PCR analysis using primers for RET. β-actin was also amplified for the purposes of normalisation. PCR products were separated on an agarose gel and visualised by ethidium bromide staining. A representative PCR profile is shown from triplicate experiments. PCR profiles were then subject to densitometric analysis and plotting after normalisation (Plot shows standard errors). (*p=0.0486 and **p= 0.0408 respectively for MCF-7+E2 and TamR relative to MCF-7 [Students t-test]). (b) RET mRNA was profiled in TamR and FasR cells using GeneSifter software applied to Affymetrix HG-U133A gene chips. RNA preparations used for Affymetrix genechip data were identical to those used for Atlas Plastic arrays. Log-intensity output and heatmap are shown for the gene. Additional controls were provided be parental MCF-7 cells subject to oestradiol treatment (plot shows mean intensity with standard errors). (*p=0.0052 for MCF-7+E2 relative to MCF-7 [Students t-test]);
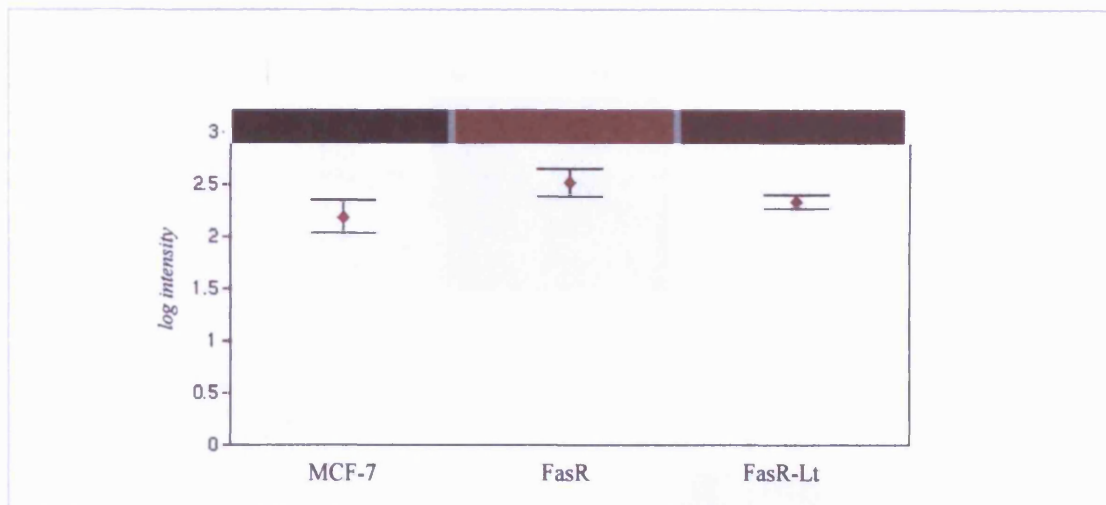
Figure 118. RET gene expression in FasR & FasR-Lt cells from a database constructed from Affymetrix data. RET mRNA was profiled in FasR and FasR-Lt cells using GeneSifter software applied to Affymetrix HG-U133A gene chip data. Log-intensity graphical output and heatmap are shown for the gene (plot shows mean intensity with standard errors).
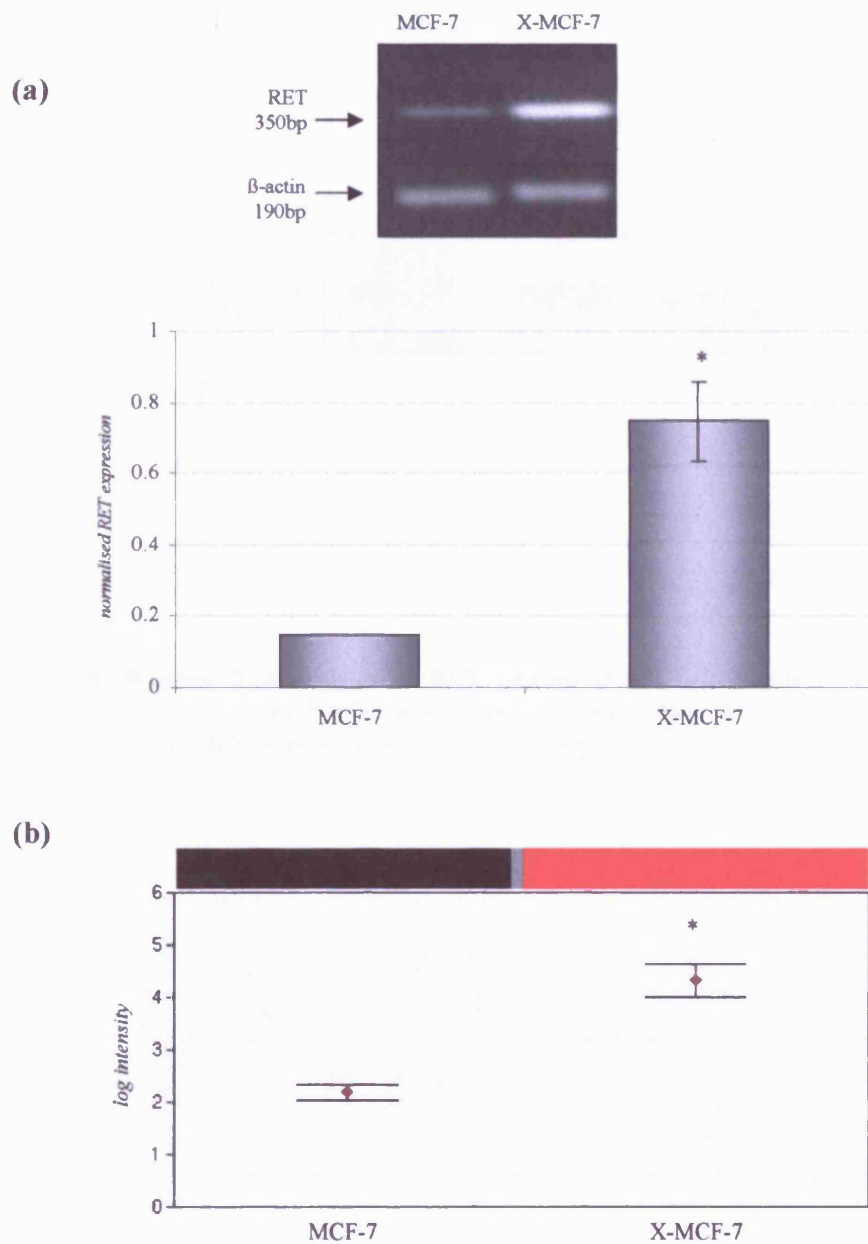
Figure 119. RET gene expression in the model of resistance to oestrogen-deprivation, X-MCF-7 cells. (a) PCR analysis was performed using primers for RET. β-actin was also amplified for the purpose of normalisation. PCR products were separated on an agarose gel, visualised by ethidium bromide staining, subject to densitometric analysis, and normalised prior to plotting. Representative signal is shown for triplicate experiment (plot shows standard errors), (*p=0.0328 relative to MCF-7 [students t-test]). (b) RET mRNA was increased in X-MCF-7 cells versus MCF-7 control using GeneSifter software applied to Affymetrix HG-U133A gene chip data. Log-intensity graphical output and heatmap are shown (plot shows mean intensity with standard errors) (*p=0.0037 relative to MCF-7 [Students t-test]).
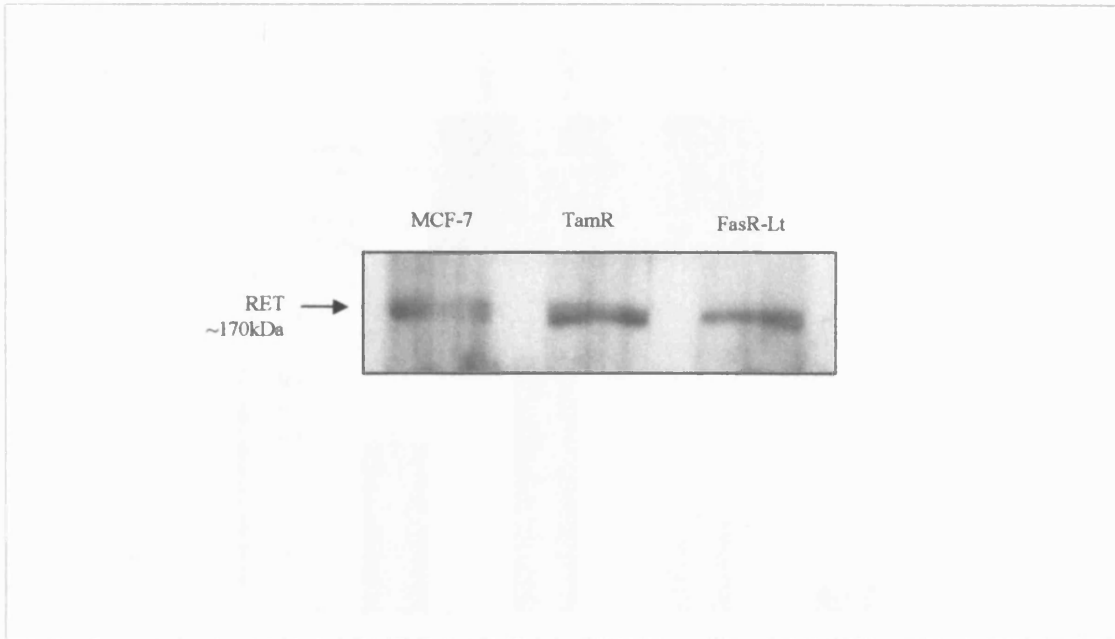
Figure 120. Western Blot analysis of RET protein in MCF-7, TamR & FasR-Lt cells. Fifty micrograms of protein from each cell line were subject to SDS PAGE/Western blotting and probed using monoclonal anti-human RET antibody with chemiluminescence detection.
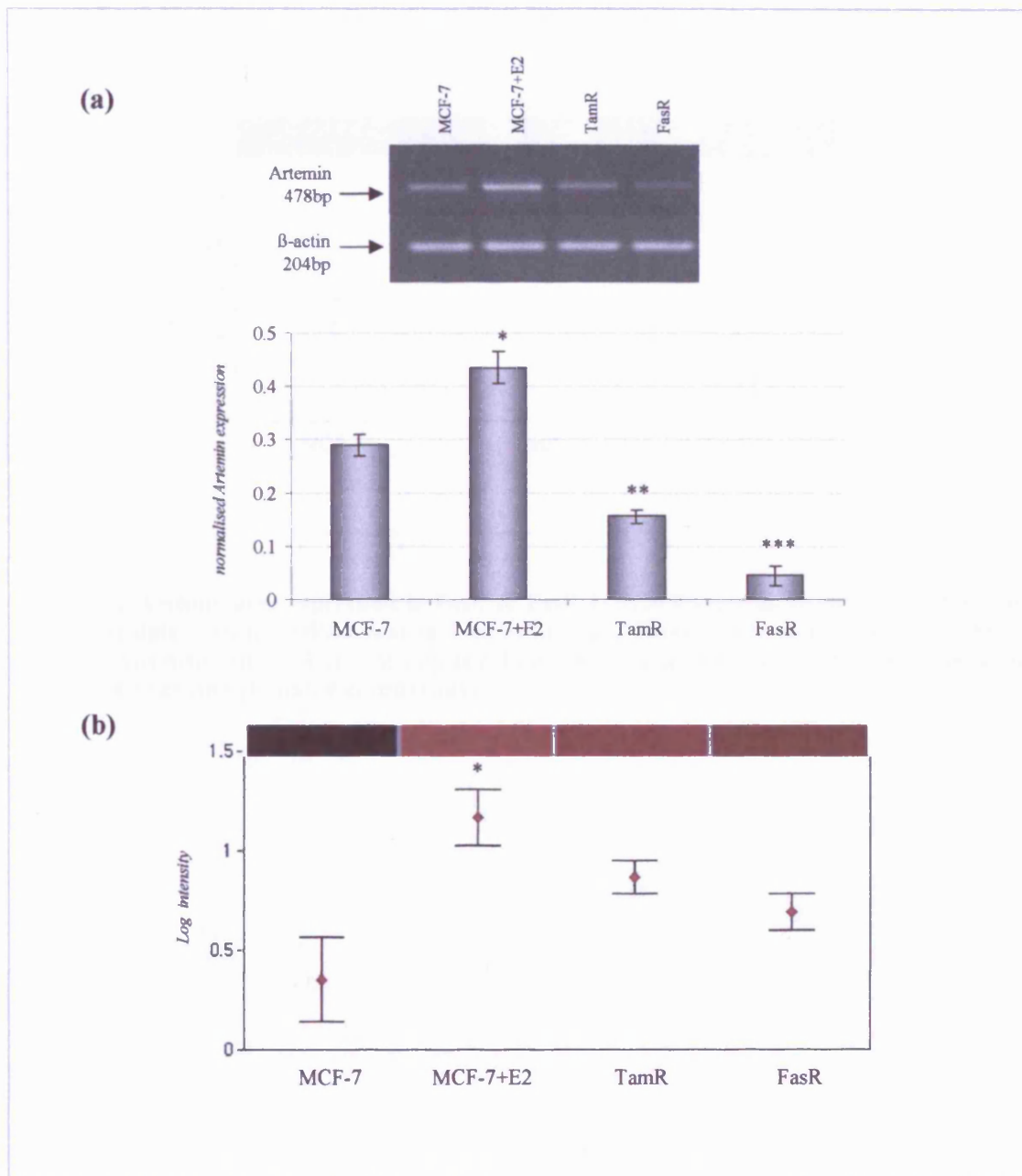
Figure 121. Artemin gene expression in TamR and FasR cells. (a) Gene profile was analysed by PCR using primers for Artemin. β-actin was also amplified for the purposes of normalisation. PCR products were separated on an agarose gel and was visualised by ethidium bromide staining. Representative PCR profile is shown from triplicate experiments. PCR profiles were then subject to densitometric analysis and plotted after normalisation (plot shows standard errors). (*p=0.004, **p=0.013 and ***p=0.0205 respectively for MCF-7+E2, TamR and FasR relative to MCF-7 [students t-test]). (b) Artemin mRNA was differentially expressed in TamR and FasR cells using GeneSifter software applied to Affymetrix HG-U133A gene chip data. RNA preparations used for Affymetrix genechips were identical to those used for Atlas Plastic arrays. Log-intensity graphical output and heatmap are shown (plot shows mean intensity with standard errors) (*p=0.0331 for MCF-7+E2 relative to MCF-7 [students t-test]).
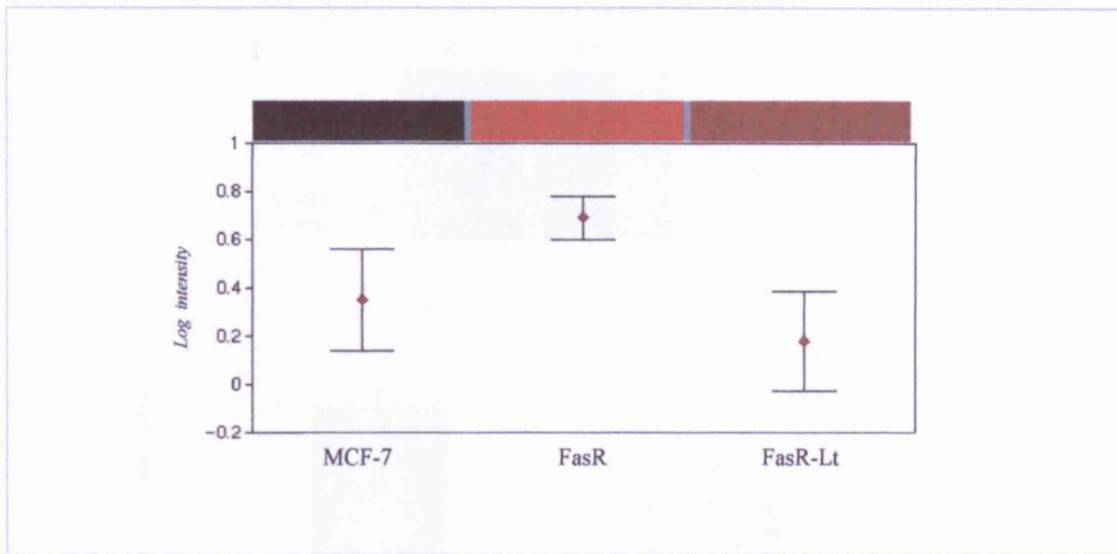
Figure 122. Artemin gene expression in FasR & FasR-Lt cells from a database constructed from Affymetrix data. Artemin mRNA was profiled in FasR and FasR-Lt cells using GeneSifter software applied to Affymetrix HG-U133A gene chip data. Log-intensity graphical output and heatmap are shown (plot shows mean intensity with standard errors).
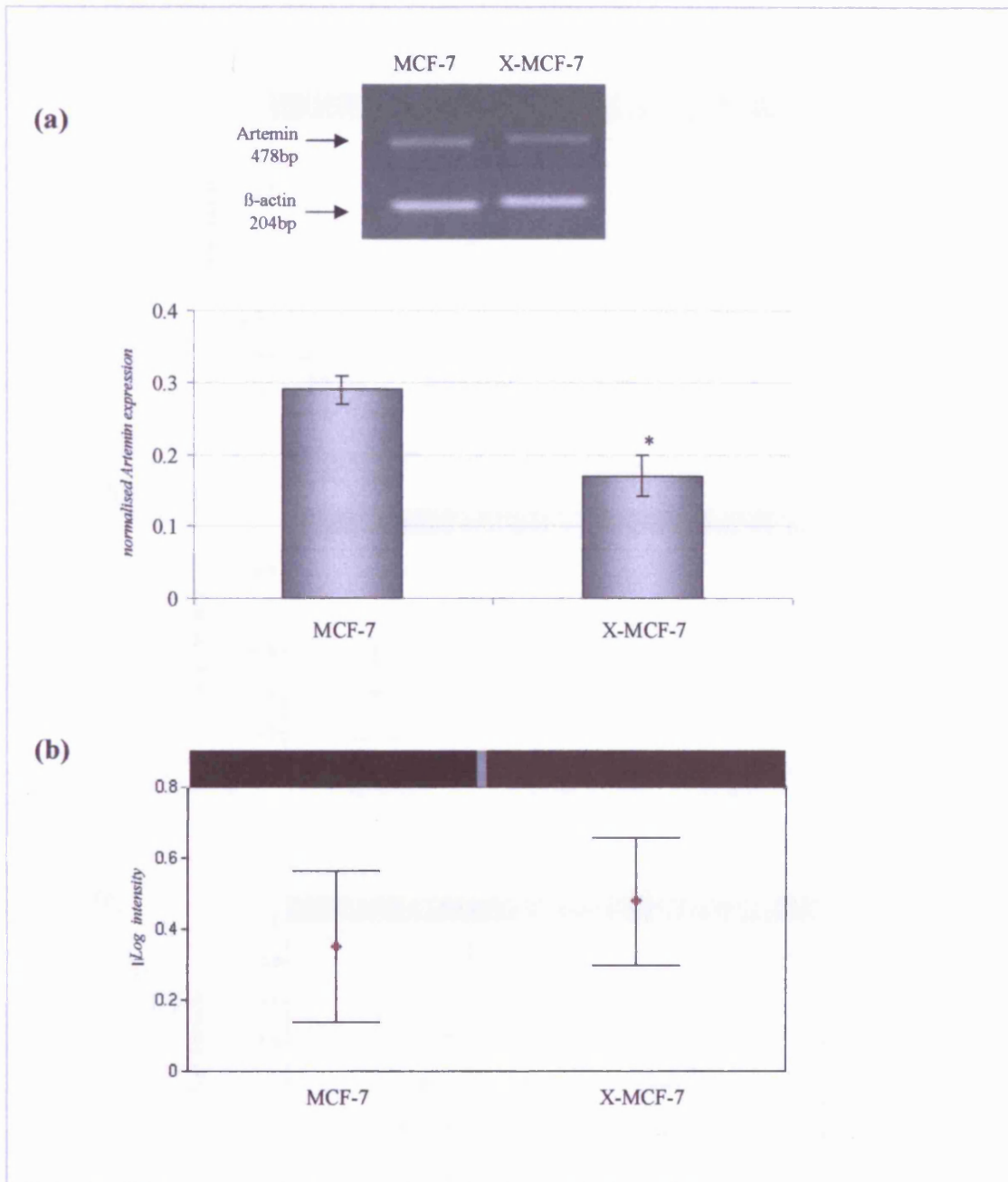
Figure 123. Artemin gene expression in the model resistant to oestrogen-deprivation, X-MCF-7 cells. PCR analysis was achieved using primers for Artemin. β-actin was also amplified for the purpose of normalisation. PCR products were separated on an agarose gel and visualised by ethidium bromide staining. A representative PCR profile is shown for triplicate experiments. PCR profiles were then subject to densitometric analysis and plotted after normalisation (plot shows standard errors). (*p=0.0204 relative to MCF-7 [students t-test]). (b) Artemin software applied to Affymetrix HG-U133A gene chip data. Log-intensity graphical output and heatmap are shown (plot shows mean intensity with standard errors).
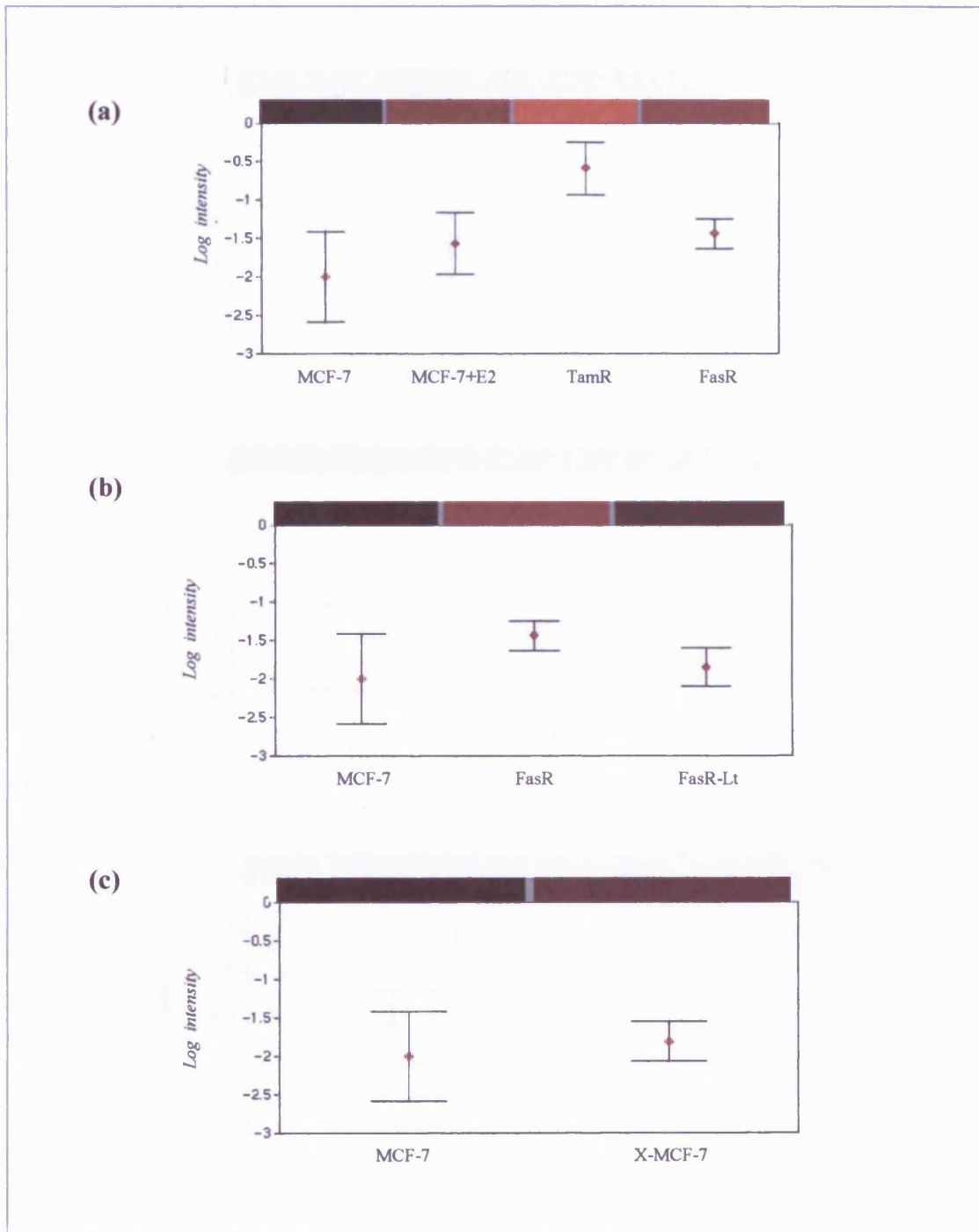
Figure 124. Persephin gene expression in (a) TamR and FasR cells, (b) FasR and FasR-Lt cells, and (c) X-MCF-7 cells from a database constructed from Affymetrix data. Persephin mRNA was profiled in TamR and FasR cells using GeneSifter software applied to Affymetrix HG-U133A gene chip data. RNA preparations used for Affymetrix genechip were identical to those used for Atlas Plastic arrays. Log-intensity graphical output and heatmap are shown (plot shows mean intensity with standard errors).
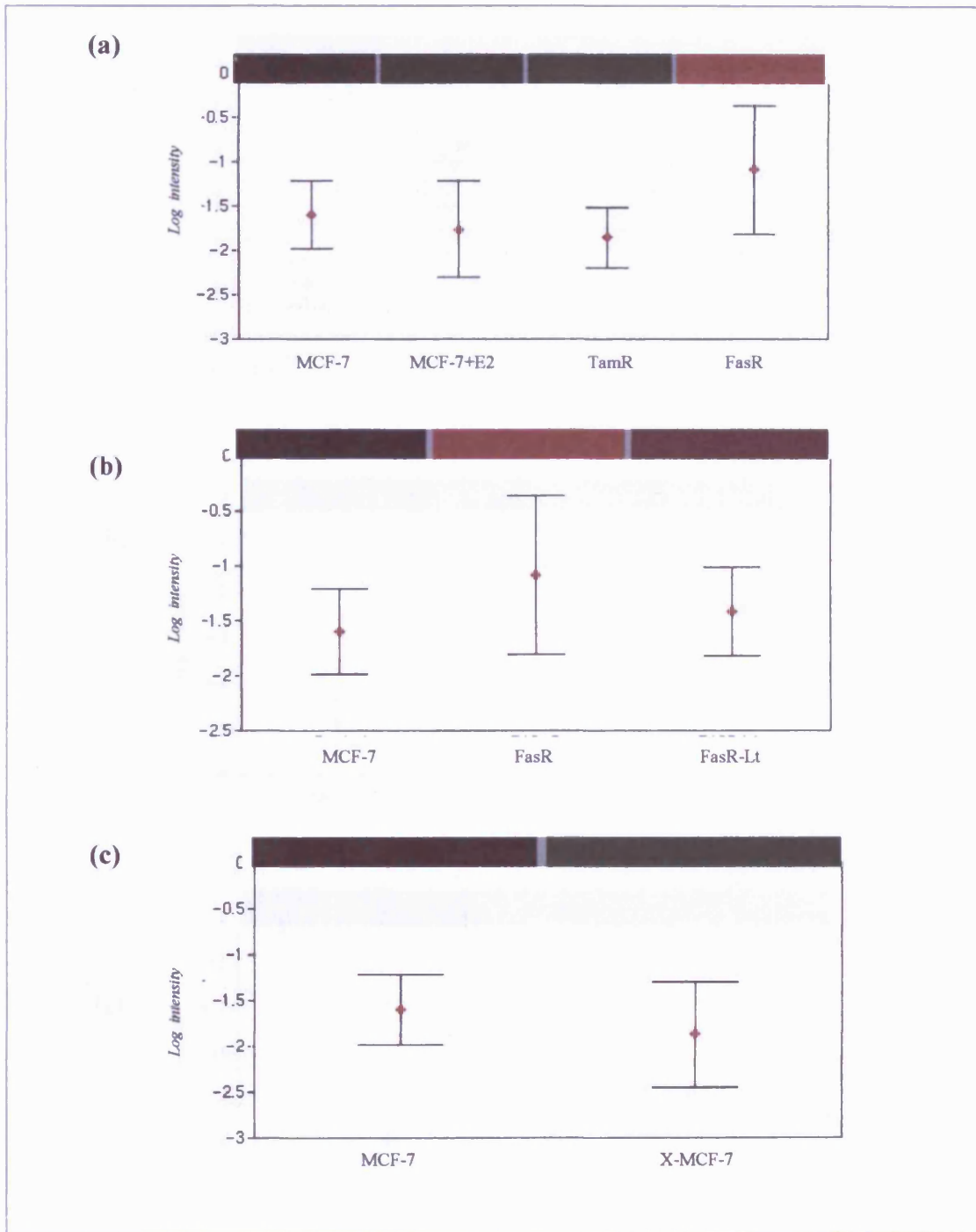
Figure 125. GDNF gene expression in (a) TamR and FasR cells, (b) FasR and FasR-Lt cells, and (c) X-MCF-7 cells from a database constructed from Affymetrix data. GDNF mRNA was profiled in TamR and FasR cells using GeneSifter software applied to Affymetrix HG-U133A gene chip data. RNA preparations used for Affymetrix genechip were identical to those used for Atlas Plastic arrays. Log-intensity graphical output and heatmap are shown (plot shows mean intensity with standard errors).
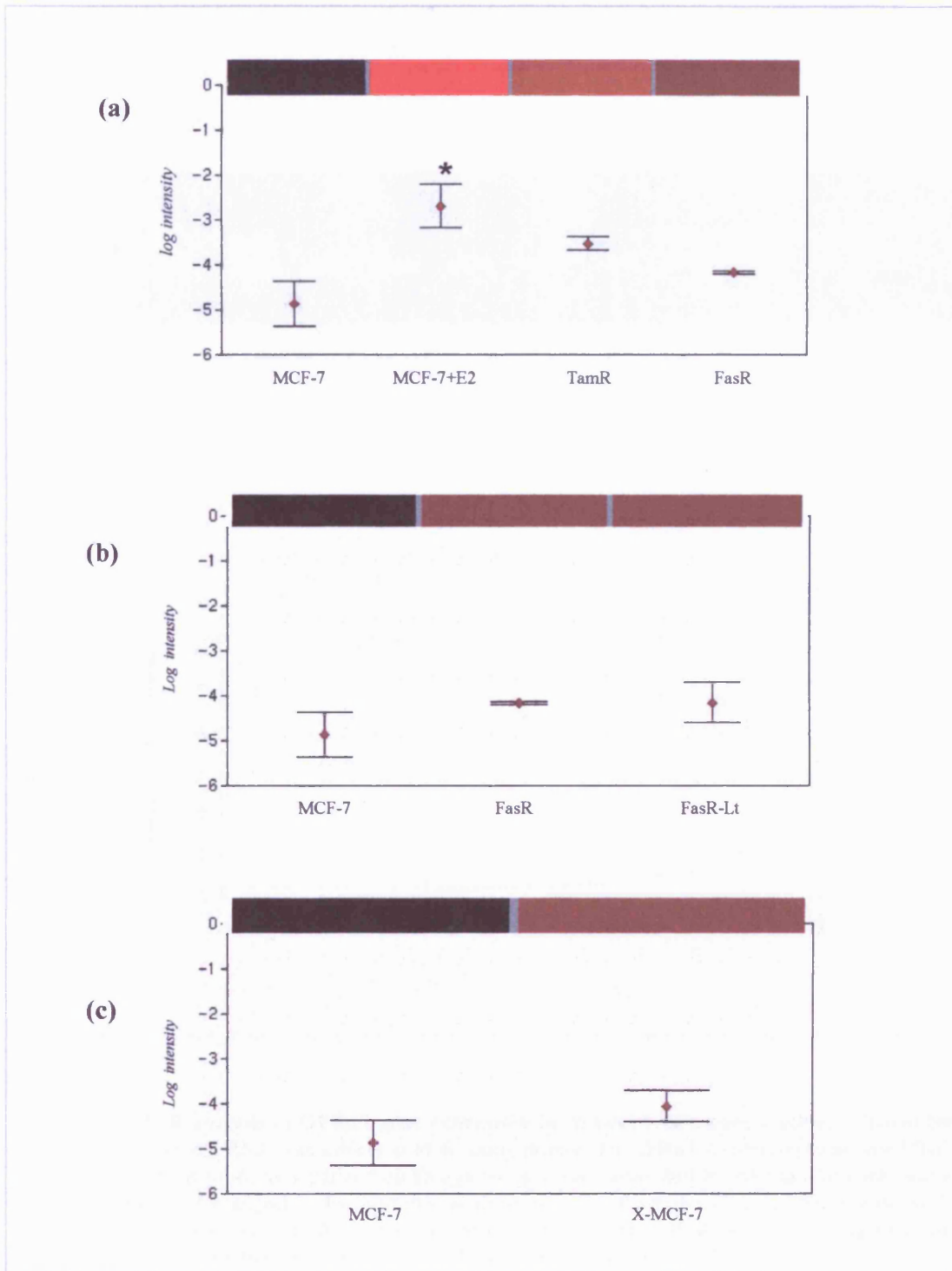
Figure 126. Neurturin gene expression in (a) TamR and FasR cells, (b) FasR and FasR-Lt cells, and (c) X-MCF-7 cells from a database constructed from Affymetrix data. GDNF mRNA was profiled in TamR and FasR cells using GeneSifter software applied to Affymetrix HG-U133A gene chip data. RNA preparations used for Affymetrix genechip were identical to those used for Atlas Plastic arrays. Log-intensity graphical output and heatmap are shown (plot shows mean intensity with standard errors). (*p=0.0356 for MCF-7+E2 relative to MCF-7 [students t-test]).
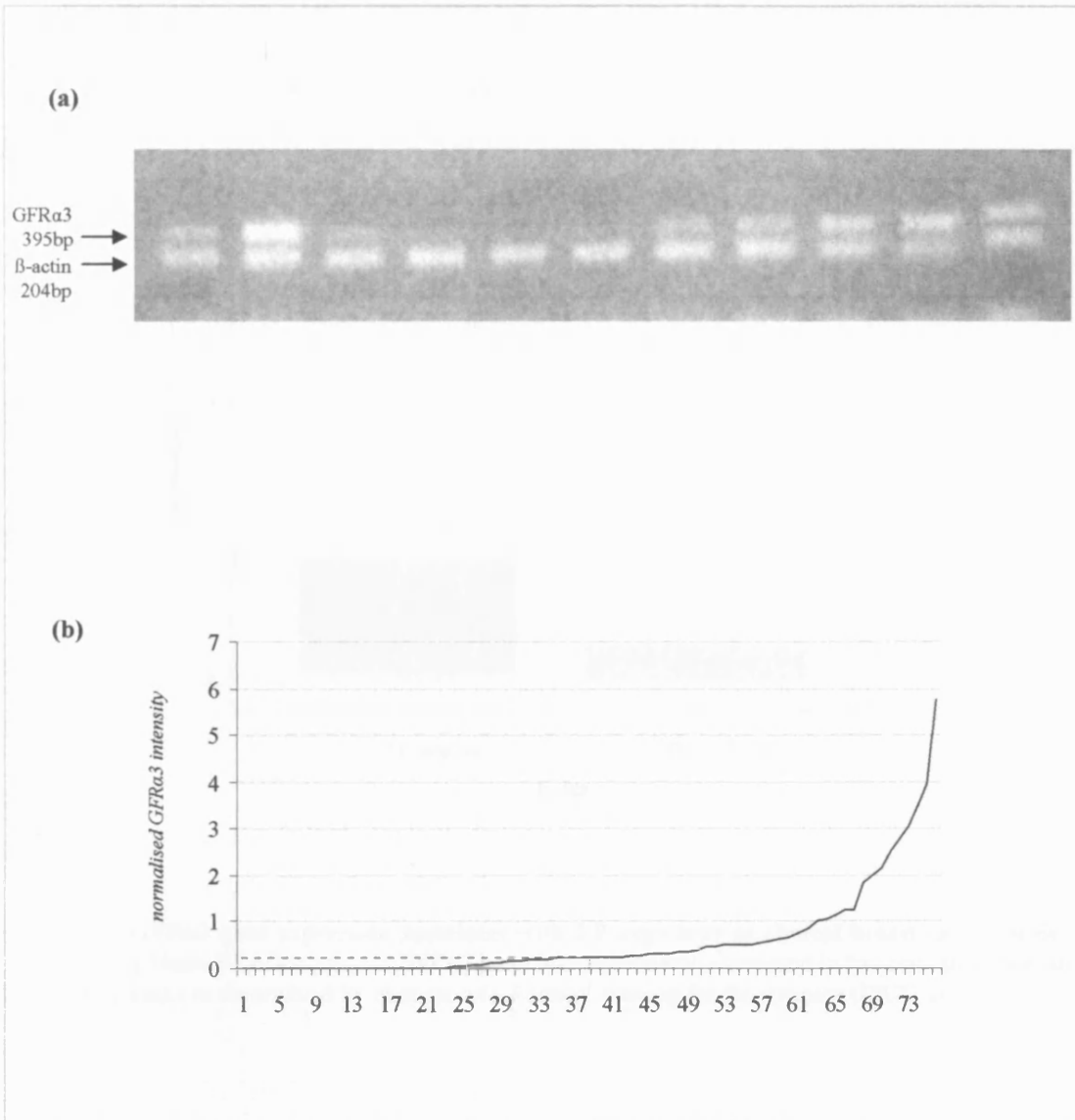
Figure 127. PCR analysis of GFRα3 gene expression in clinical breast cancer series. Clinical breast cancer (n=78) derived RNA was subject to PCR using primers for GFRα3. β-actin was also amplified for normalisation. PCR products separated on an agarose gel were visualised by ethidium bromide staining. (a) PCR profiles were subject to densitometric analysis and normalisation to β-actin. Representative PCR profiles for samples are shown. (b) Frequency distribution chart shows PCR densitometry signal intensity for n=78 samples encompassing a range 0 to 5.74, and median 0.227 (marked as dashed line).
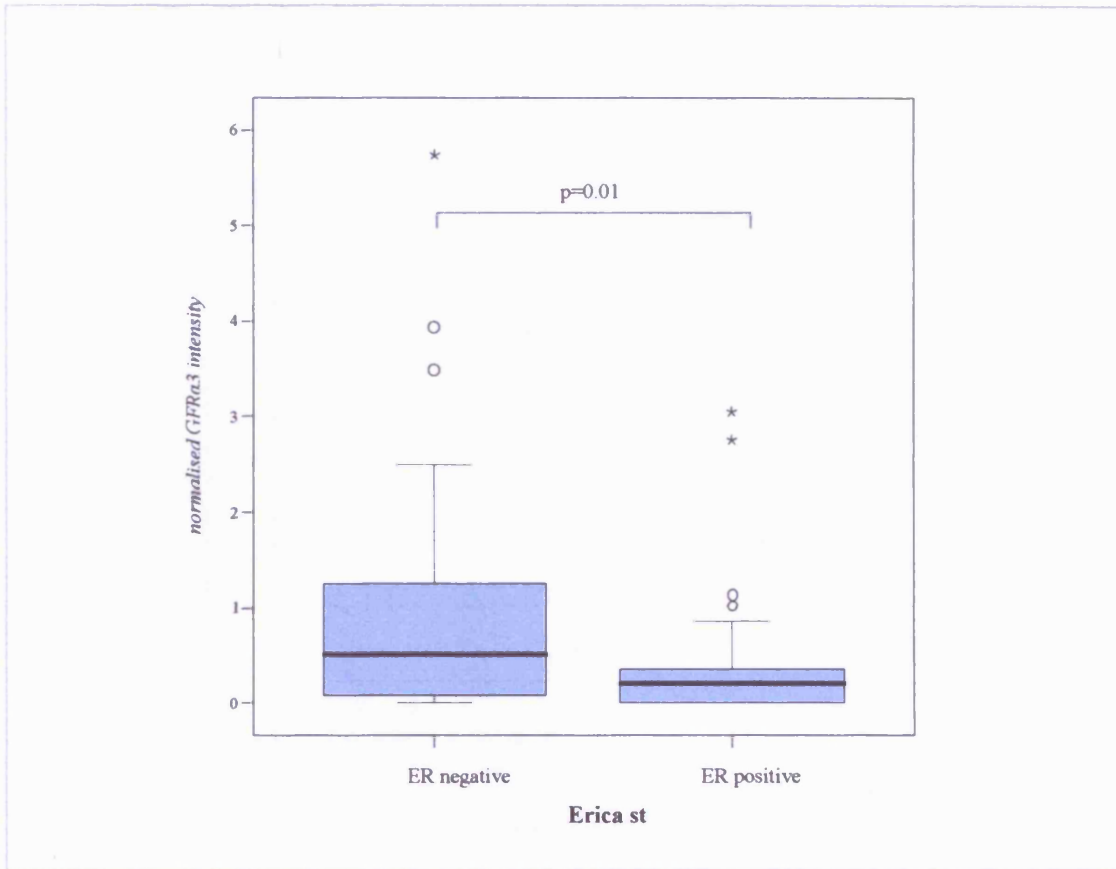
Figure 128. GFRα3 gene expression associates with ER negativity in clinical breast cancer series (n=78). Using Mann-Whitney analysis GFRα3 gene was significantly increased in tumours exhibiting an ER negative status as determined by immunocytochemical staining for the receptor (ERICA) .
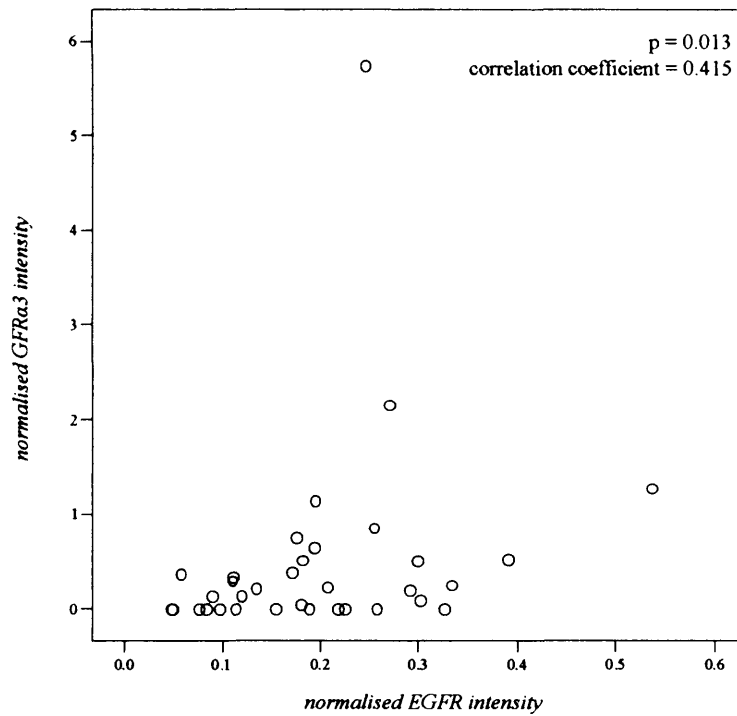
Figure 129. GFRα3 gene correlates with increased EGFR gene expression in clinical breast cancer series (n=78). Using Spearmann's analysis PTTG1 gene was significantly increased in tumours with increased EGFR gene expression.
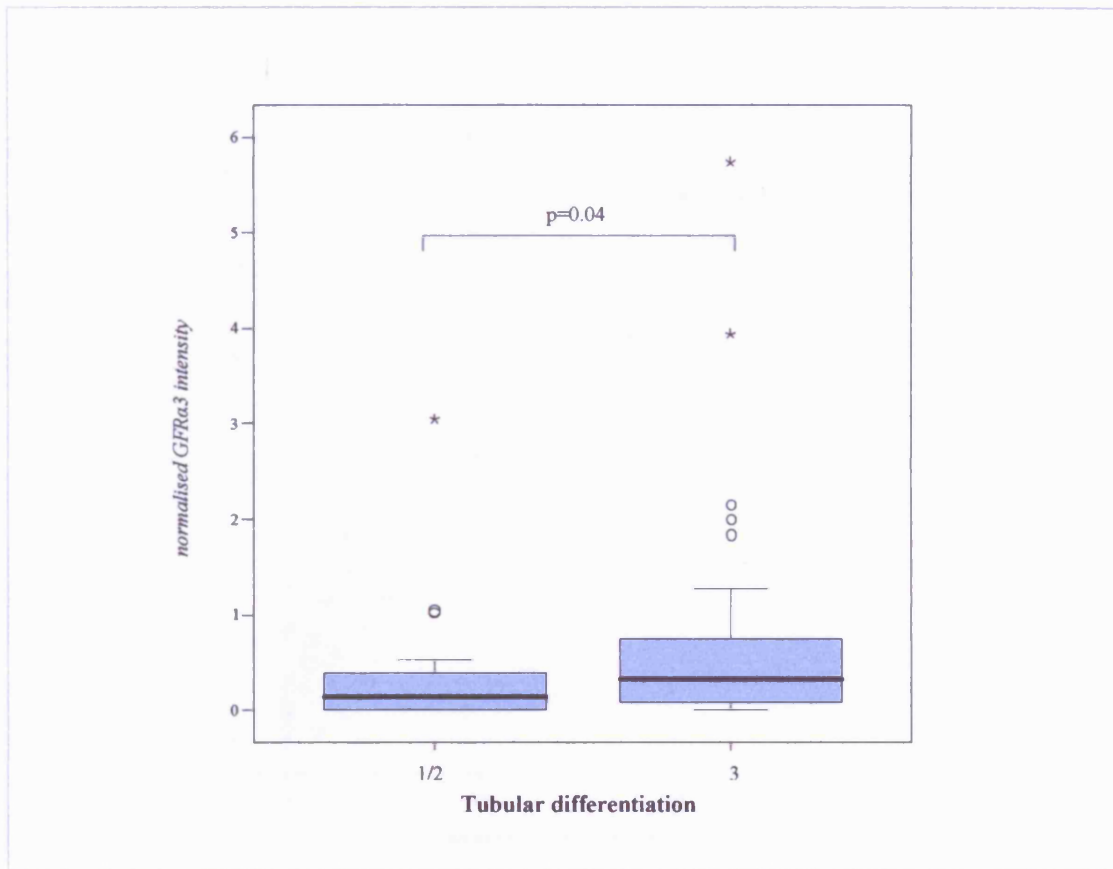
Figure 130. GFRα3 gene expression associates with tubular differentiation in clinical breast cancer series (n=78). Using Mann-Whitney U test GFRα3 gene was significantly increased in tumours with grade 3 tumours.

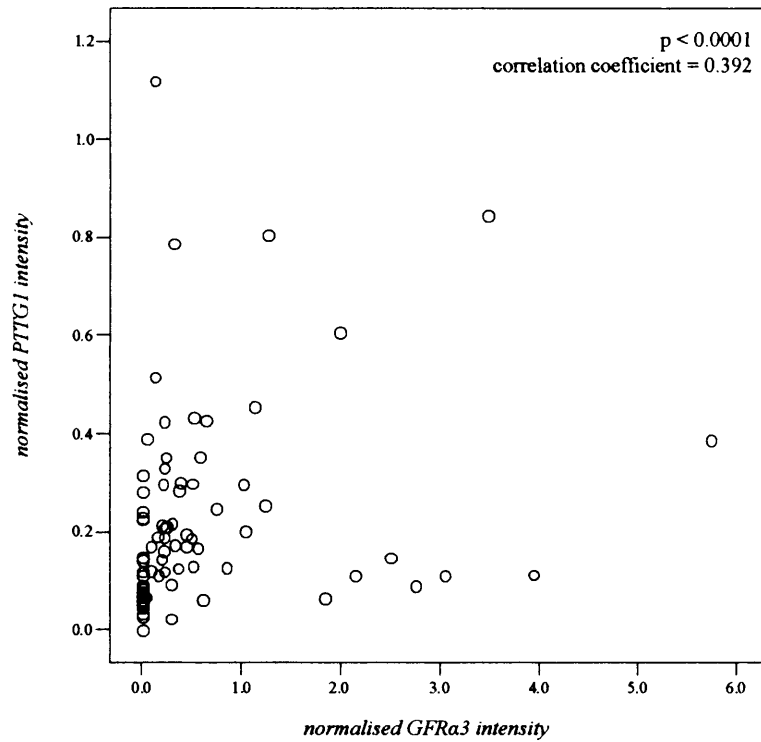**Figure 131. GFRα3 and PTTG1 gene expression correlation in clinical breast cancer series (n=78) using Spearmann's analysis.**
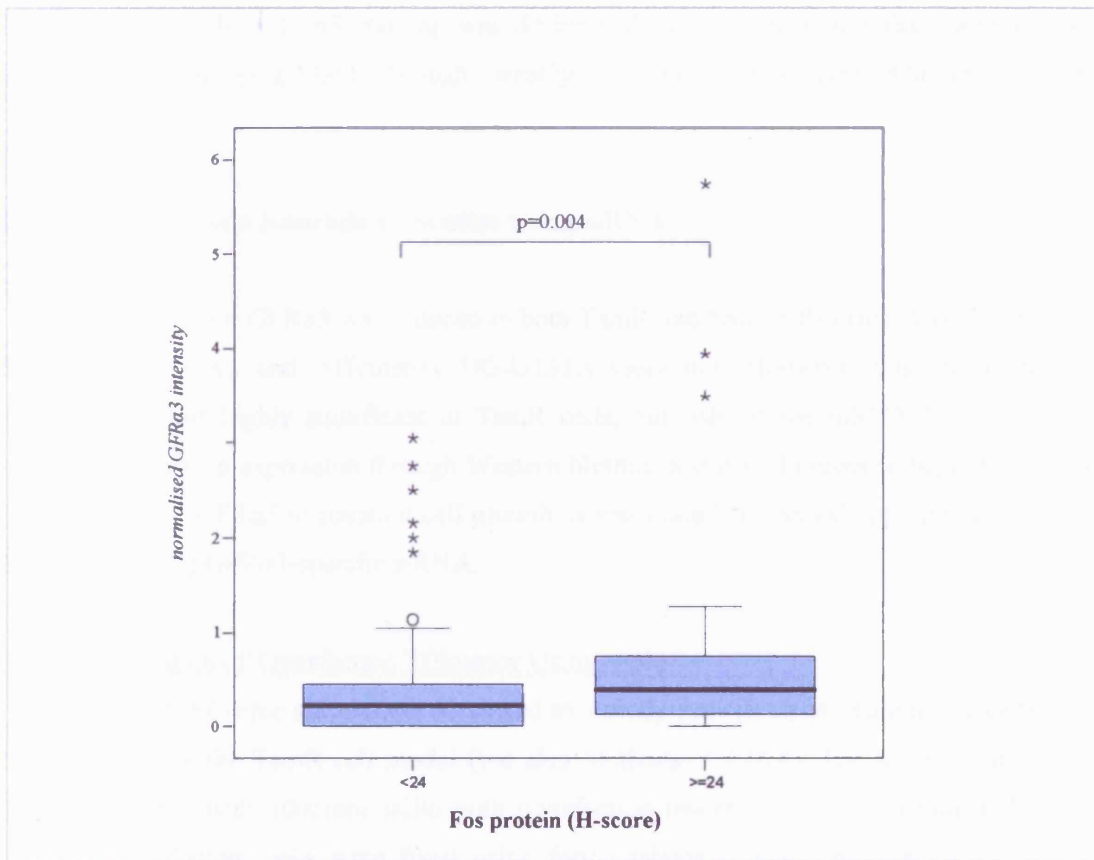
Figure 132. GFRα3 mRNA expression associates with Fos positivity (H-score status) in clinical breast cancer series (n=78).

DAB staining, as described previously. As with cell pellets, GFRα3 immunostaining was predominantly tumour epithelial in cytoplasm and membrane and with no nuclear staining (Fig.133a and 133b). GFRα3 staining was differential in the clinical samples, varying from intensely staining (Fig.133a) through weakly staining/negative (Fig.133b to Fig.133c respectively).

5.1.5 GFRα3 Gene Knockdown Studies Using siRNA

The gene for GFRα3 was induced in both TamR and FasR cells using Atlas Plastic 12k Human Microarrays and Affymetrix HG-U133A Genechip. However, this elevation was observed as most highly significant in TamR cells, not only at the mRNA level, but also according to protein expression through Western blotting and ICC. In order to begin to explore the relevance of GFRα3 to resistant cell growth, it was therefore deemed appropriate, to target TamR cells using GFRα3-specific siRNA.

5.1.5.1 Estimation of Transfection Efficiency Using siGlo

siGlo RISC-Free siRNA was employed to initially provide an estimation of transfection efficiency within the TamR cell model (see also Methods: 2.2.16.5). The seeded TamR cells were transfected with 100nmol siGlo with transfection reagent in DCCM media. Following overnight incubation, cells were fixed using formaldehyde solution, mounted using DAPI-containing Vectashield mountant and visualised as described previously. Transfection with siGlo reagent overnight yielded a transfection efficiency of 97% (Fig.134). Additionally, it was noted usually that overnight incubation with siGlo and DF transfection reagent showed only a slight reduction in cell number compared to non-transfected cells in this instance.

5.1.5.2 Estimation of Knockdown Efficiency Achievable in TamR Cells Using Lamin siRNA

Use of a positive silencing control siRNA directed against the gene for gene Lamin A/C in TamR cells provided some indication of gene knockdown achievable with this model. TamR cells were seeded at a confluency of 70-80% 24 hours prior to transfection. Using PCR analysis, RNA extracted 24 hours post transfection showed a 78% and 65% knockdown in Lamin mRNA with Lamin-specific gene knockdown compared to missense and DCCM control respectively (Fig.135). It is also worth noting that other controls used, media, siGlo, and irrelevant GFRα3 siRNA did not show any effect/ interference on Lamin A/C mRNA levels.

5.1.5.3 Effect of GFRα3 siRNA on mRNA and Protein

Following the acceptable mRNA knockdown of Lamin A/C in TamR cells using the Dharmacon method, siRNA directed towards the GFRα3 gene was evaluated in highly confluent

TamR cells. At 24 hours, GFRα3 mRNA was successfully reduced to undetectable levels as measured using PCR analysis compared to missense control or DCCM alone (Fig.136a). However, some degree of variability from one control (media, siGlo, Lamin) to the next was demonstrated in this, and subsequent (Fig.136b) experiments, where DF alone was included, effects could be significant.

As described previously, due to the 4-7 day timescale of subsequent siRNA experiments, TamR cells were also required to be seeded at an initial density of 250,000 cells/ well). Since only low yields of RNA can be extracted from 12 well plates, adequate recovery can be extremely difficult either under conditions of further reduced cell number or as a consequence of subsequent extraction procedures, and unfortunately, 4 day GFRα3 knockdown PCR analysis was thus unavailable. However, further PCR studies using GFRα3 siRNA in TamR cells were able to show a 78% and 86% reduction in mRNA at day 7 post-transfection versus missense and DCCM control respectively (Fig.136b). DF control produced unreliable results for analysis due to no actin band.

TamR cells seeded at a high initial density were also subject to GFRα3 knockdown and protein analysed using Western blotting analysis in the first instance at 48 hours post-transfection (Fig.137a). GFRα3 protein was only reduced by 14% and 25% relative to missense and DCCM control respectively. However, improved effects were observed over a 4-7 day timescale where TamR cells were seeded at an initial density of 250,000 cells/ well. Western blotting showed a reduction of GFRα3 protein of 13.8% and 41.9% at day 4 post-transfection compared to missense and DCCM control (Fig.137b). Following the re-application of GFRα3 siRNA at day 4, cells harvested at day 7 again showed a protein knockdown of 35% and 82% versus missense and DCCM controls. Loss of protein was also evident with the DF only control (Fig.137c); although in this instance there was too low a yield of protein from this sample for even actin protein detection.

5.1.5.4 GFRα3 siRNA Effects on Cell Growth

The growth viability effects of using siRNA directed to the GFRα3 gene can be seen from cells in culture (Fig.138). Microscopic evaluation at day 4 of GFRα3 siRNA treatment reveals an 81% (p=0.0042) and 88% (p<0.01) decrease in cell number compared to missense and DCCM control respectively (Fig.139). While in this experiment DF treatment alone in TamR cells promoted substantial loss of cell numbers this was not as severe when included with other controls (i.e. Lamin, missense controls), and of note, cell numbers within the GFRα3 siRNA-treated sample as remained significantly lower than both Lamin siRNA and missense control.
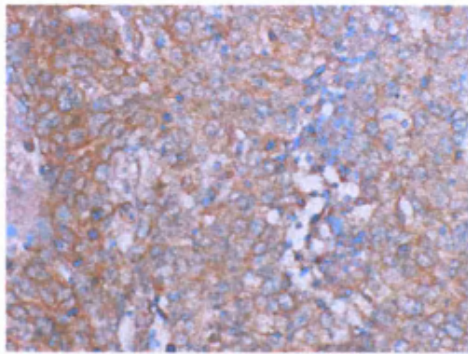
(a) i -Sample1 x20
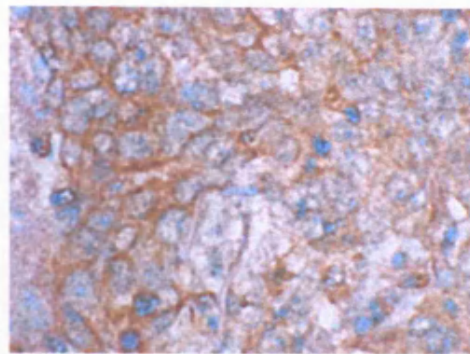
(a) ii -Sample1 x40
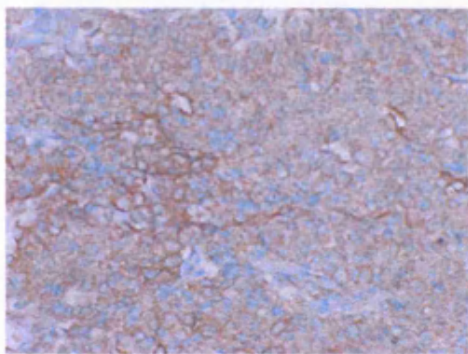
(b) i -Sample2 x20
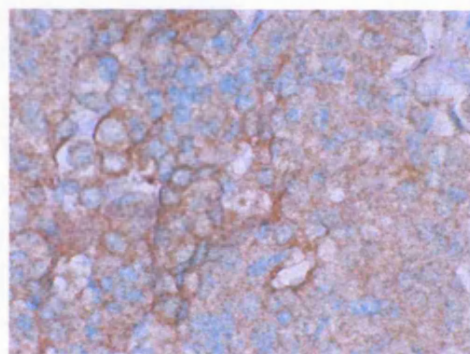
(b) ii -Sample 2 x40
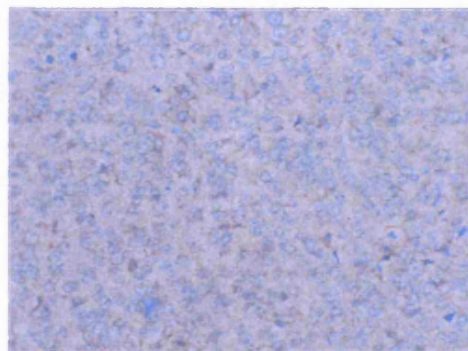
(c) -Sample3 x20

Figure 133. Immunocytochemical analysis of GFRα3 in paraffin embedded clinical breast cancer samples. Tissue was formalin fixed, and embedded in paraffin blocks. 5μm sections prepared from the blocks were stained using monoclonal anti-human GFRα3 antibody after (enzymatic) antigen retrieval and detected using DAKO Envision detection system with DAB staining. Fig. A and b show samples 1 and 2 demonstrating significant staining, whereas Fig. C shows sample 3 with low staining for GFRα3. Original magnification shown.

DAPI-stained
nuclei
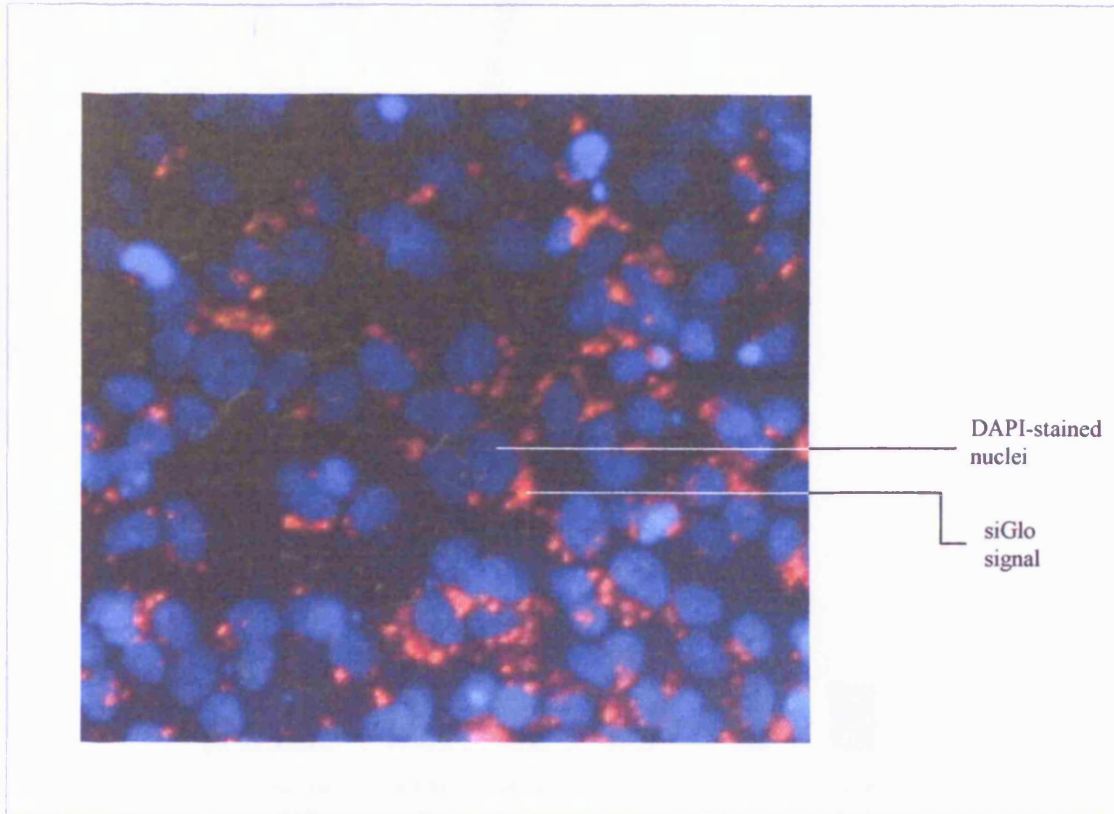
siGlo
signal

Figure 134. Estimation of siRNA Transfection Efficiency using siGlo in TamR cells. TamR cells transfected with 100nmol siGlo overnight (~12 hours) were fixed, mounted using Vectashield agent, and fluorescence microscopy performed. Magnification of x40 is shown with DAPI-stained nuclei with siGlo transfection fluorescent (red) marker.
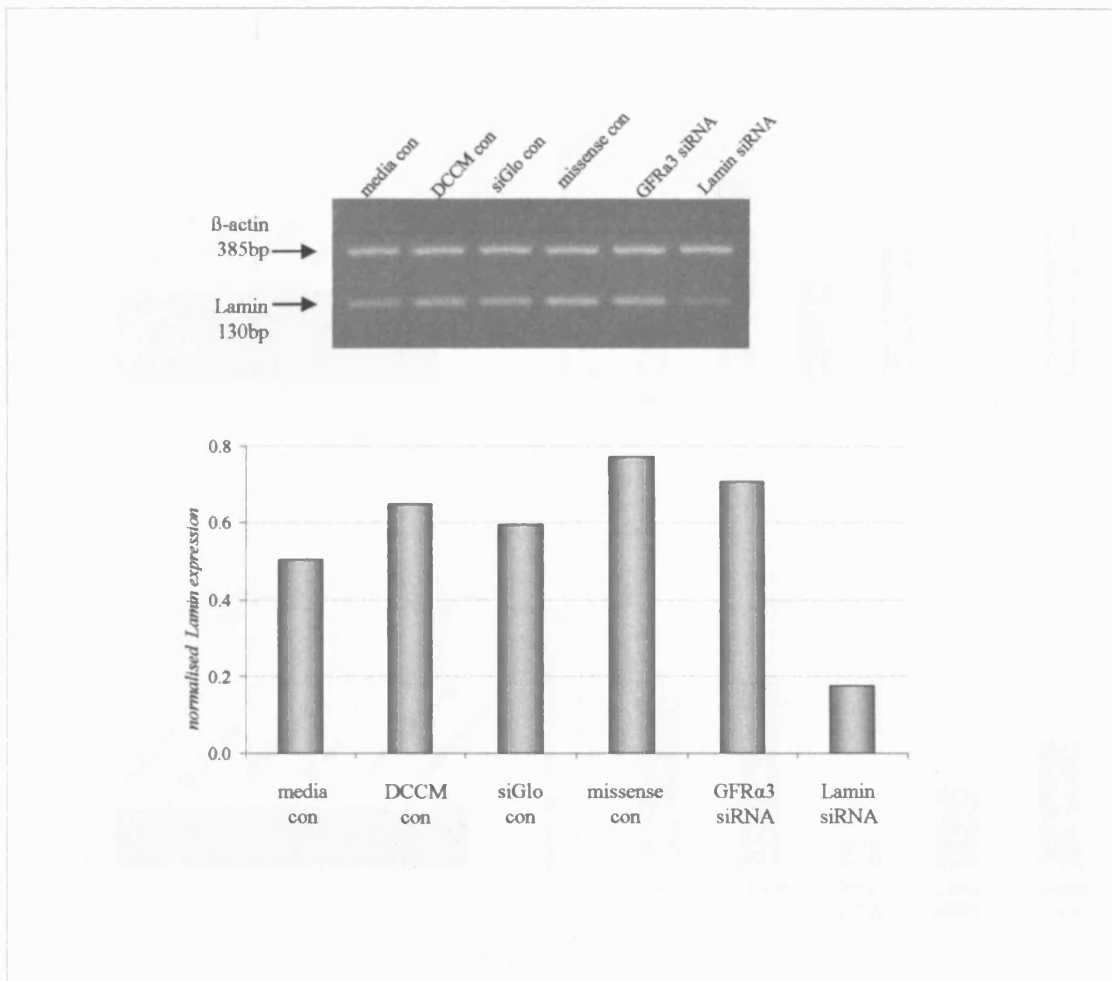
Figure 135. siRNA mediated Lamin gene knockdown in TamR cells to evaluate achievable gene knockdown. Lamin gene knockdown was achieved in TamR cells using 100nmol smartpool reagents according to the Dharmacon protocol. One microgram of RNA extracted from cells 24 hours post siRNA transfection was reverse transcribed and gene expression was determined using primers for Lamin (with β-actin co-amplification for normalisation). Controls included were irrelevant (GFRα3) siRNA, siGlo, Missense, DCCM media, and Media (phenol red-free RPMI/ 5% serum) control alongside the Lamin siRNA.
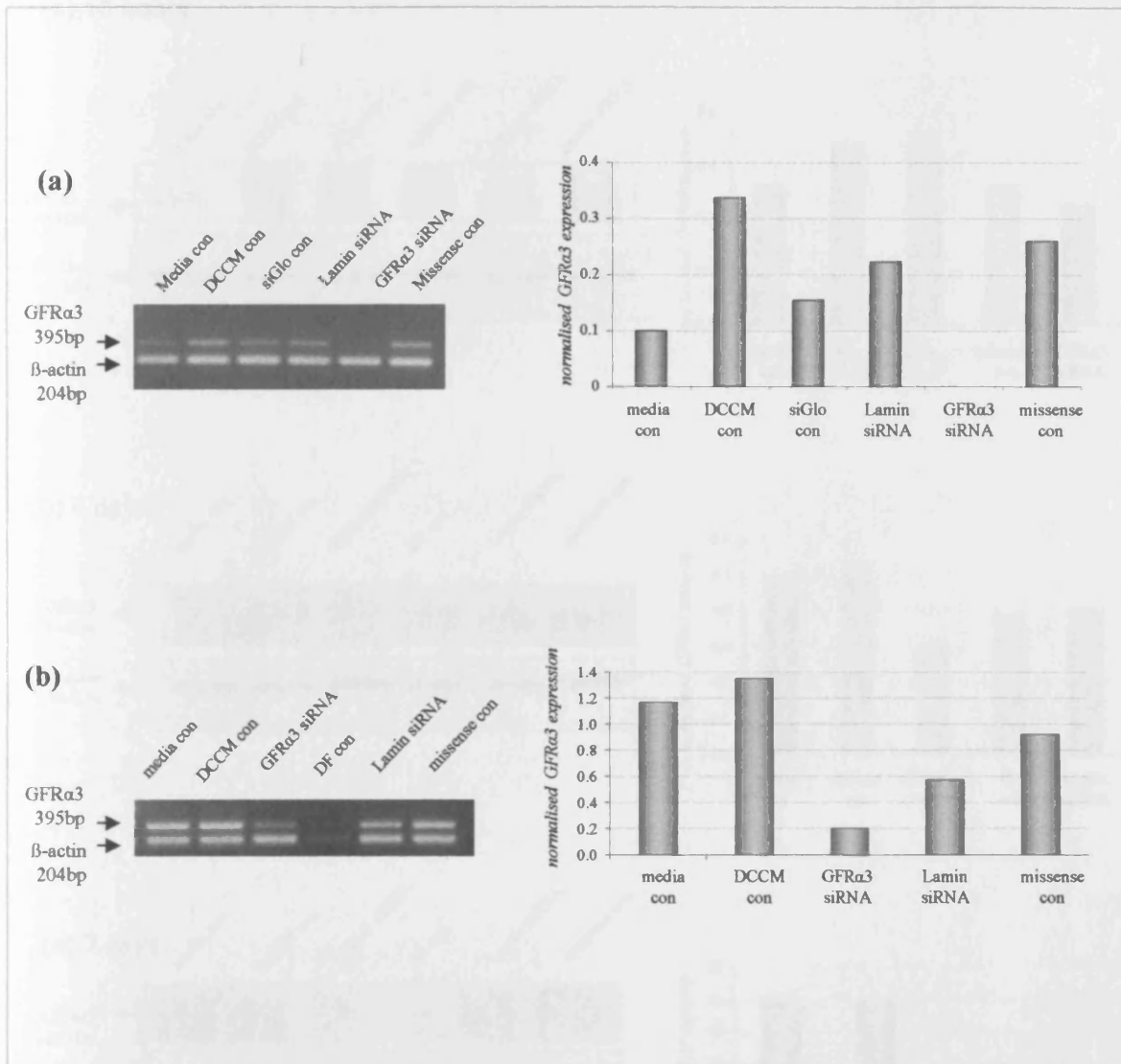
Figure 136. GFRα3 siRNA mediated gene knockdown in TamR cells. GFRa3 gene knockdown was achieved in TamR cells using 100nmol smartpool reagents according to the Dharmacon protocol. One microgram of RNA extracted from cells (a) 24 hours and (b) 7 days post siRNA transfection was reverse transcribed and gene expression was determined using primers for GFRα3 (with β-actin co-amplification for normalisation). Controls included were siGlo, missense 'scrambled', Lamin siRNA, DharmaFECT (DF) transfection reagent, DCCM media, and media (phenol red-free RPMI/ 5% serum) control.

(a) 48 hours
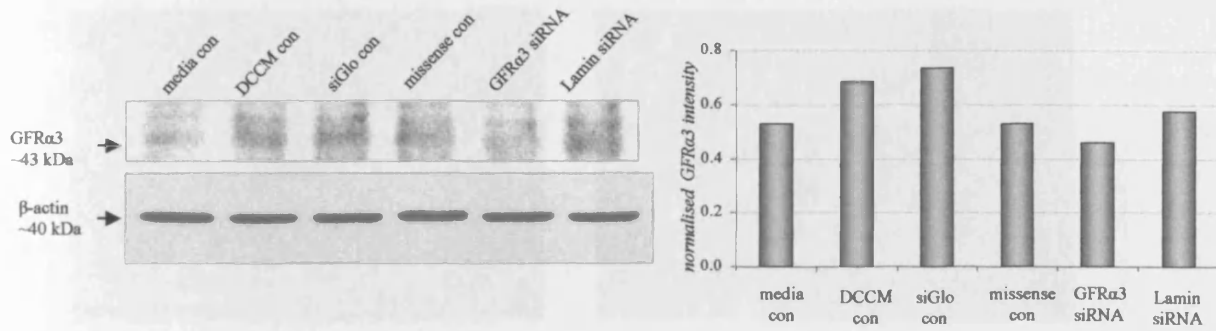
(b) 4 days
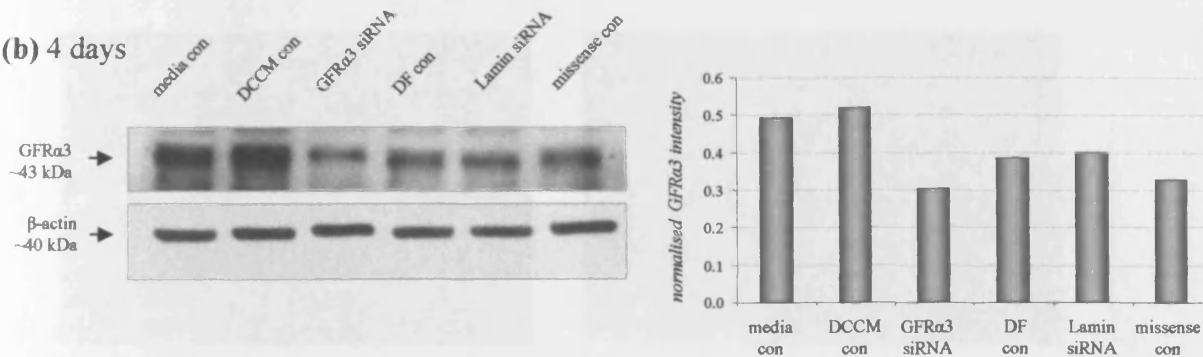
(c) 7 days
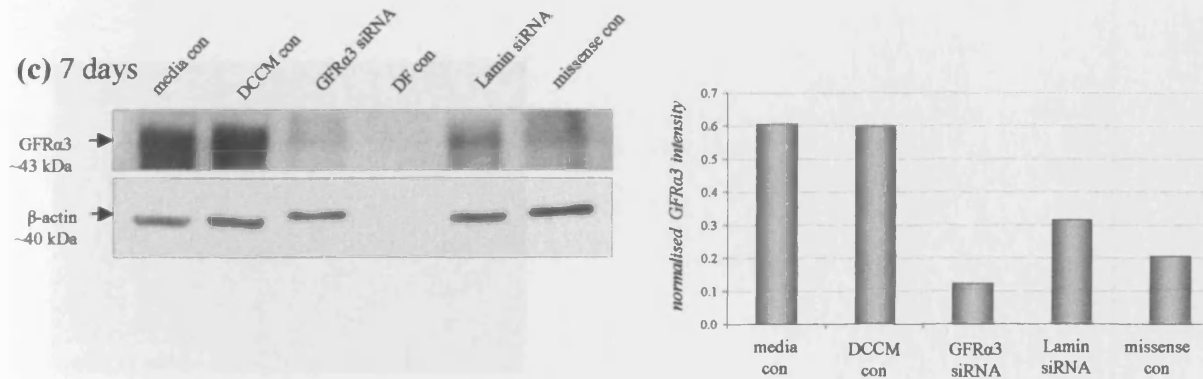
Figure 137. **GFRα3 siRNA mediated protein knockdown in TamR cells.** GFRα3 gene knockdown was achieved in TamR cells using 100nmol smartpool reagents according to the Dharmacon protocol. GFRα3 protein knockdown was determined by subjecting 50ug protein from cells (a) 48 hours, (b) 4 days, and (c) 7 days post siRNA transfection to 7.5% SDS PAGE and Western blotting. Proteins were probed with monoclonal anti-GFRα3 antibody with chemiluminescent detection. Equivalence of protein loading in Western blots was subsequently demonstrated by detection of β-actin on the same blot using monoclonal antibody to the protein. Controls included were siGlo, missense, Lamin siRNA, DharmaFECT (DF) transfection reagent, and media (phenol red-free RPMI/ 5% serum) control, and DCCM media control.
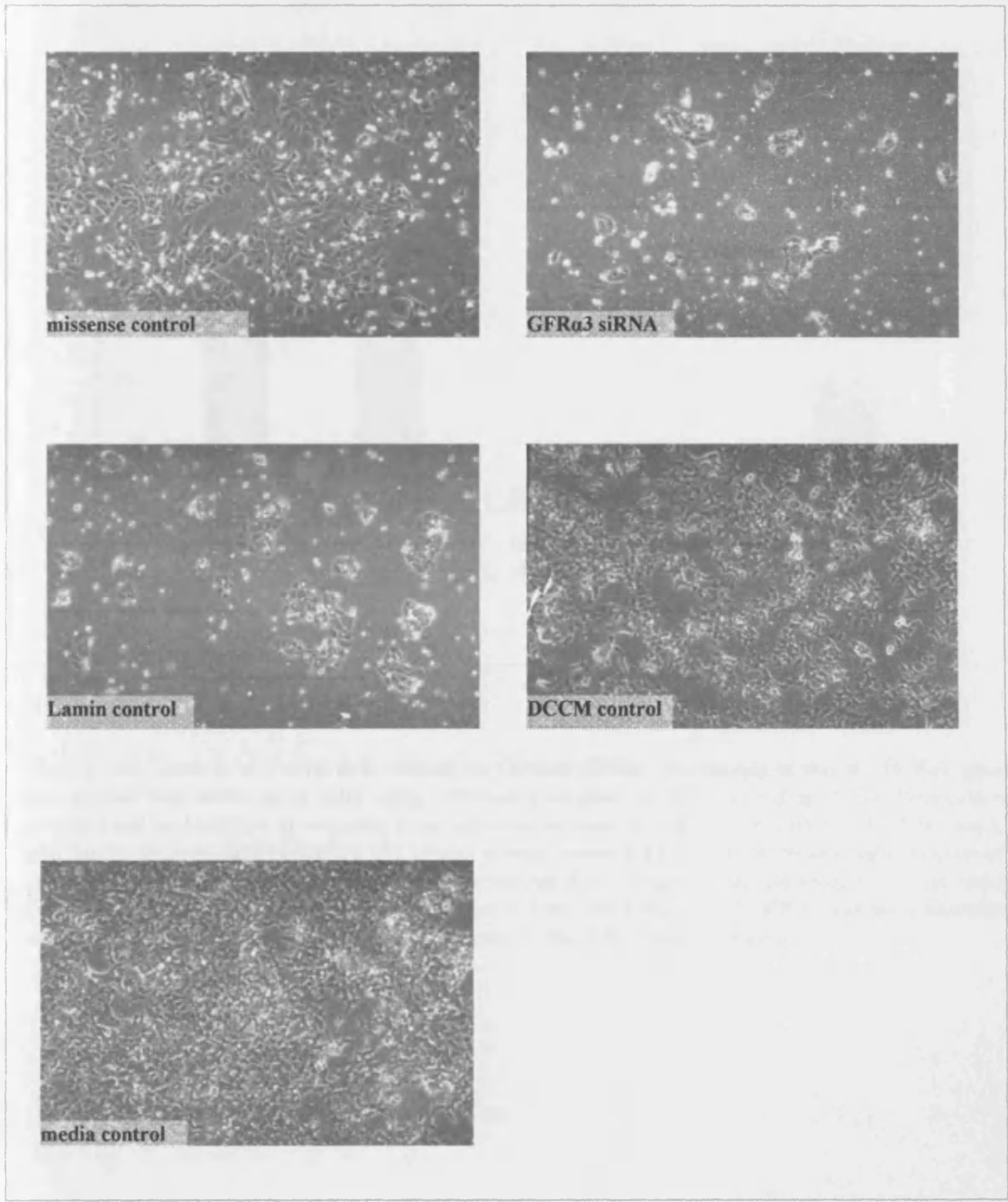
Figure 138. Growth of TamR cells subject to GFRα3 siRNA knockdown at day 4. GFRα3 gene knockdown was achieved in cells using 100nmol smartpool reagents according to the Dharmacon protocol. Control or test cells were counted from a total of four fields and photographed at 10x magnification using phase-contrast microscope. Controls included were missense, Lamin siRNA, DCCM media, and media (phenol red-free RPMI/ 5% serum) control, alongside GFRα3 test siRNA.
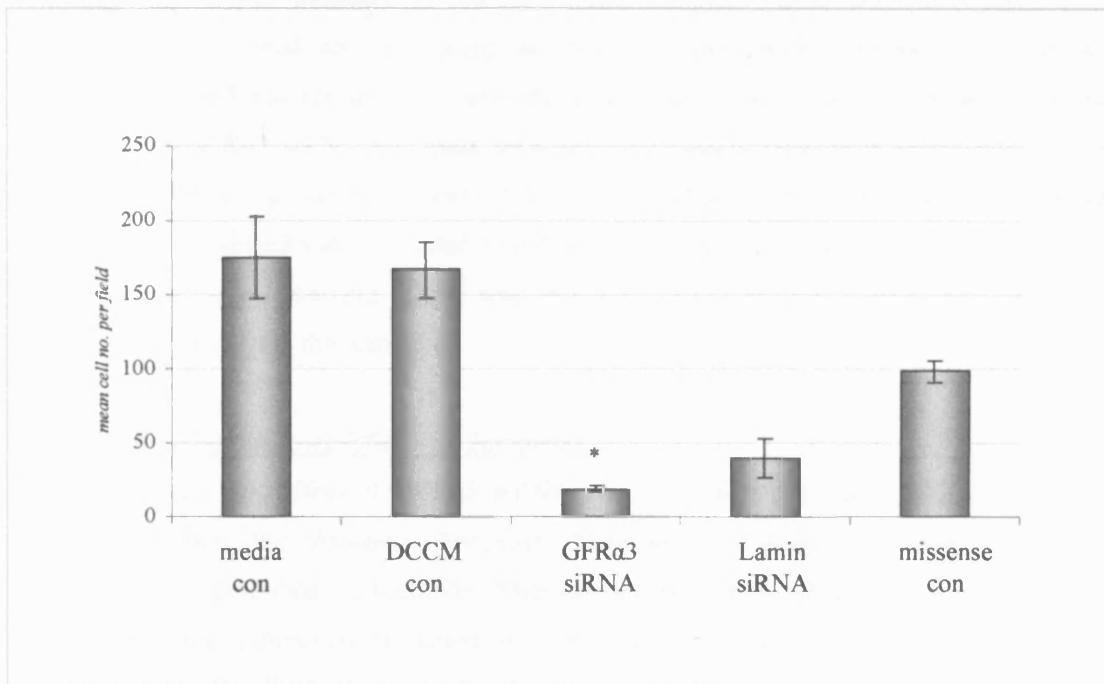
Figure 139. Growth of TamR cells subject to GFRα3 siRNA knockdown at day 4. GFRα3 gene knockdown was achieved in cells using 100nmol smartpool reagents according to the Dharmacon protocol and as described in Methods. Controls included were missense, Lamin siRNA, DCCM media, and Media (phenol red-free RPMI/ 5% serum) control versus GFRα3 siRNA. Microscopic evaluation of cells was performed using phase contrast microscopy at x10 magnification counting for a total and 4 fields per photographed. (standard errors are shown; *p=0.0042 for GFRα3 siRNA relative to missense control; p<0.01 for GFRα3 relative to DCCM control [Students t-test performed]).

5.1.5.5 GFRα3 Knockdown Effects on Cell Proliferation

Immunostaining using an antibody to the proliferation marker Ki67 (Mib1) was used to determine any anti-proliferative effects of GFRα3 siRNA. TamR cells at 4 days post-transfection were fixed and processed as described previously. Following microscopic evaluation of Ki67 nuclear immunoreactivity a significant reduction of 32% and 33% was observed with GFRα3 siRNA treatment compared to missense control (p<0.001) and DCCM control (p=0.0051) (Fig.140and Fig.141). A loss of overall cell number on these coverslips was also observed in GFRα3 siRNA-treated TamR cells with only occasional foci of cells with low percentage positivity remaining. There was only a small reduction in preparations from cells containing DF reagent in this instance.

5.1.5.6 GFRα3 Knockdown Effects on Apoptosis

The apoptotic effect of GFRα3 siRNA was determined in TamR cells 4 days post-transfection using the Apoalert Apoptosis Mitochondrial Membrane Sensor Kit (BD Biosciences) as described in methods. Microscopic evaluation of the slides again clearly demonstrated the substantial reduction in overall cell number following GFRα3 siRNA-treatment of TamR cells, to the extent that there were only approximately 10% cells present on the slide for evaluation. Although a small number of apoptotic cells were present in samples which contained DF reagent, an increased number was observed within the GFRα3 siRNA sample (Fig.142). Another indication of cell-kill with GFRα3-mediated siRNA was the substantial number of dead cells observed floating within this sample before performing the assay. The increase in dead cells was estimated at 103% (p=0.05) in cells subject to GFRα3 siRNA compared to missense control, and 578% relative to DCCM control (P<0.001) (Fig.143). In general, all samples showed slightly higher levels of live cells relative to media control, but again there was no substantial effect of DF alone.

5.1.6 Impact of EGFR Inhibitor Gefitinib and Faslodex on GFRα3 Gene and Protein Expression in Resistant Cells

In order to determine if there was any regulation of GFRα3 by EGFR or ER signalling, GFRα3 mRNA expression was determined using PCR and Western blotting analysis in TamR and FasR resistant cell lines which had been subjected to the inhibitory doses of EGFR-TK inhibitor Gefitinib (10^{-6}M) or Faslodex (10^{-7}M in TamR) for seven days. Treatment with the EGFR-TKI inhibitor resulted in a marked further induction of GFRα3 gene in both TamR and FasR cells (approximately 3.1-fold and 2.2-fold increase in TamR and FasR cells respectively; Fig.144). Western blotting also showed an increase in GFRα3 protein levels in response to Gefitinib in TamR cells (Fig.145). In contrast, GFRα3 protein levels remained relatively

unchanged with Gefitinib treatment in either MCF-7 or FasR cells, although higher levels of protein were still demonstrated in untreated TamR and, to some degree, FasR cells compared to parental MCF-7 cell line. Using PCR analysis, GFRα3 mRNA was also observed to be induced in TamR cells treated with $(10^{-7}M)$ Faslodex by approximately 1.8-fold (Fig.146), although this was not explored at the protein level.

5.1.7 GFRα3 Ligand Artemin Overcomes Gefitinib Inhibition in TamR Cells

TamR cells were grown in the presence of the GFRα3 ligand Artemin at concentrations of 1ng/ml- 50ng/ml for 7 days with or without EGFR-TKI $(10^{-6}M)$ treatment (Fig.147). The addition of the EGFR-TKI alone substantially reduced TamR cell number by 80% versus untreated cells (p<0001). Interestingly, although Artemin has little stimulatory effect on the already high basal, growth in TamR cells, its administration in the presence of the anti-EGFR agent was shown to significantly reduce the inhibition caused by the Gefitinib in a dose-dependent manner. Thus, the highest concentration of Artemin at 50ng/ml was capable of restoring TamR cell number to a value of 78% of the untreated cells (p=0.0025), thus substantially overcoming Gefitinib growth inhibition.

5.1.8 GFRα3 and Family Receptor/ Ligand Expression in the TamR/TKI-R Double Resistant Cell Line

Cells resistant to tamoxifen and gefitinib (TamR/TKI-R) were cultured for 7 days at around 70% confluency before being extracted for RNA, and PCR performed for GFRα3 coamplifed with β-actin. PCR results demonstrate these TamR/TKI-R cells have elevated levels of GFRα3 compared to TamR cells (Fig.148).
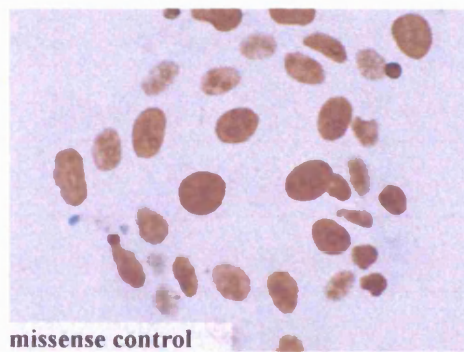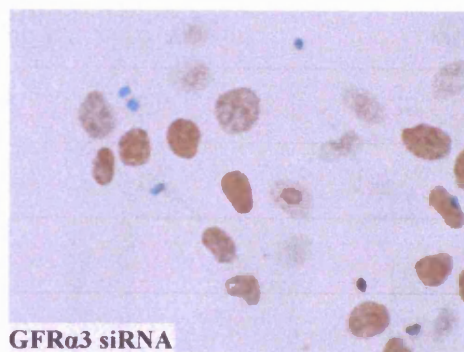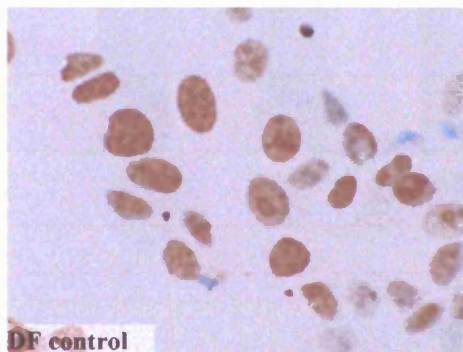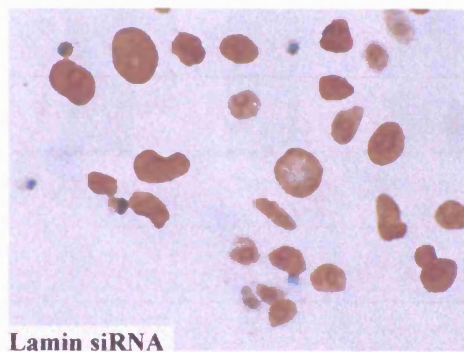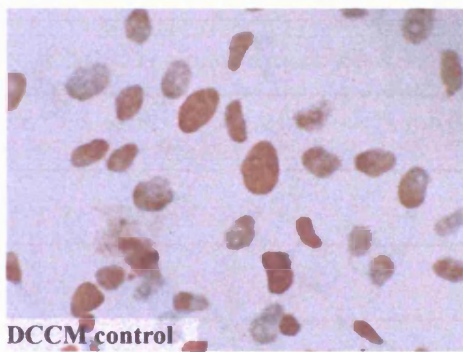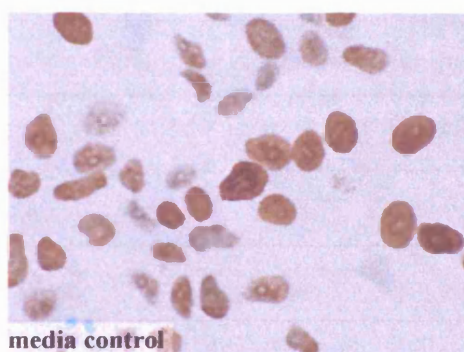
Figure 140. Anti-proliferative effects of GFRα3 siRNA knockdown at day 4 as measured by Ki67 mib1) immunostaining. GFRα3 gene knockdown was achieved in cells using 100nmol smartpool reagents according to the Dharmacon protocol. Control or test cells were fixed in formal saline solution 4 days post transfection, probed using monoclonal anti-human antibody to mib1 and detected using DAKO Envision detection system with DAB staining. Controls included were missense, DharmaFECT (DF) transfection reagent, Lamin siRNA, DCCM media, and media (phenol red-free RPMI/ 5% serum) control versus GFRα3 siRNA. Photographs shows immunostaining at x40 original magnification.
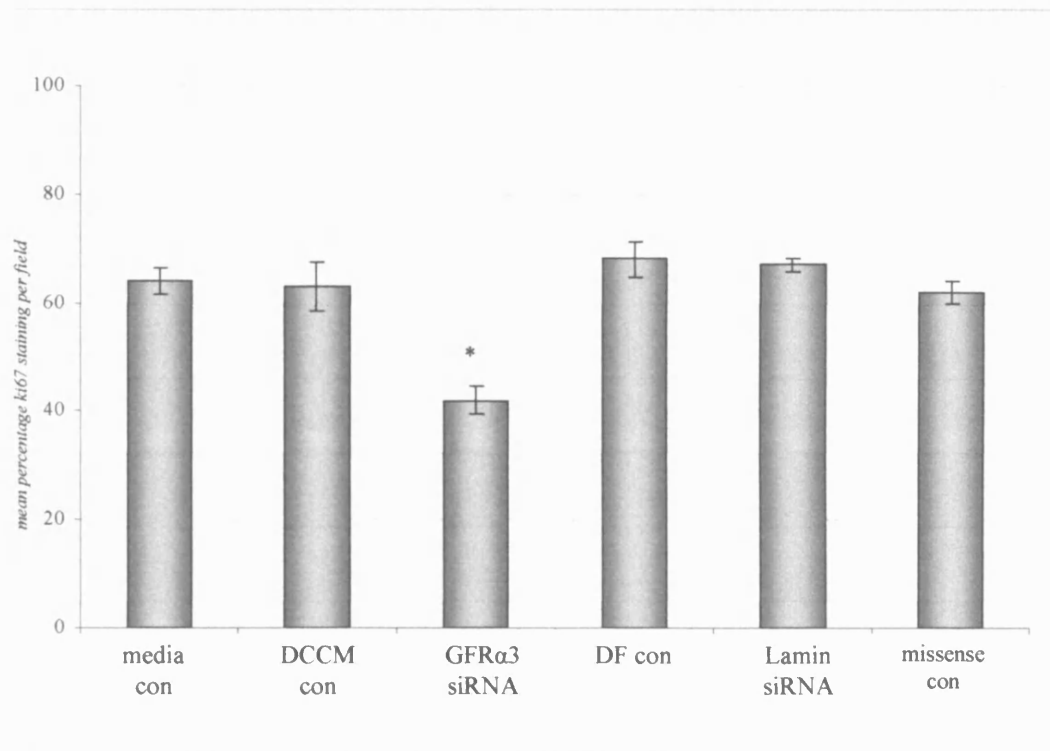
Figure 141. Microscopic evaluation of the anti-proliferative effects of GFRα3 siRNA knockout at day 4 as measured by ki67 (MIB1) immunostaining in TamR cells. Controls included were missense 'scrambled', DharmaFECT (DF) transfection reagent, Lamin siRNA, DCCM media, and media (phenol red-free RPMI/ 5% serum) control. Microscopic evaluation of mib1 immunoreactivity was graded as percentage positivity from six fields per test slide. (plot shows mean cell percentage staining per field with standard errors) (*p<0.001 p=0.0051 for GFRα3 siRNA relative to missense control and DCCM control respectively [students t-test]).
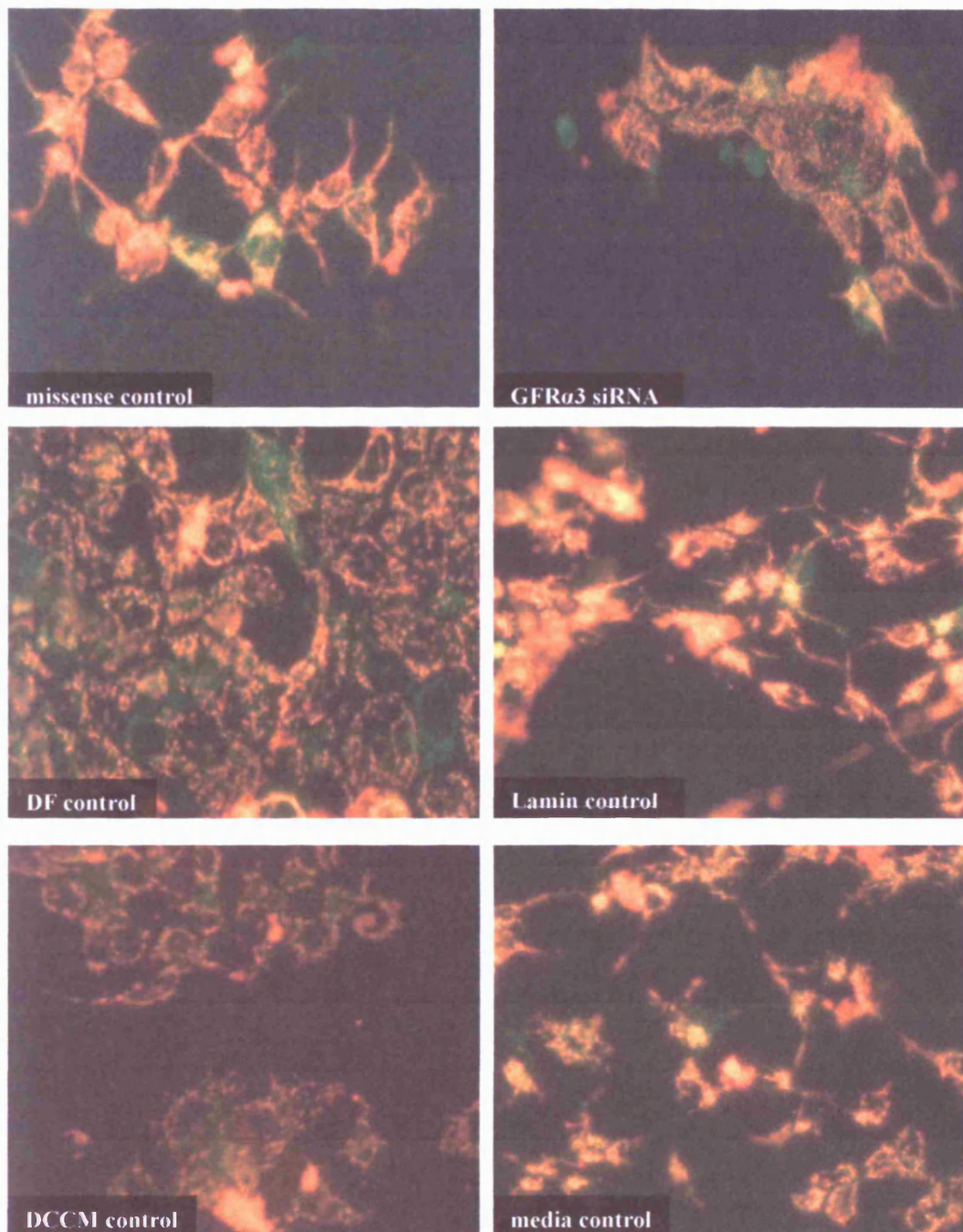
Figure 142. Apoptotic effects of GFRα3 siRNA knockout at day 4 as measured by the Apoalert Apoptosis Mitochondrial Membrane Sensor kit in TamR cells. GFRα3 gene knockdown was achieved in TamR cells using 100nmol smartpool reagents according to the Dharmacon protocol. Cells were processed for detection of apoptosis using the Apoalert Apoptosis Mitochondrial Membrane Sensor kit according to the manufacturers instructions. Controls included were missense, DharmaFECT (DF) transfection reagent, Lamin siRNA, DCCM media, and media (phenol red-free RPMI/ 5% serum) control versus test GFRα3 siRNA. Live and apoptotic cells are represented by red or green fluorescence respectively. Images show cells at x40 magnification.
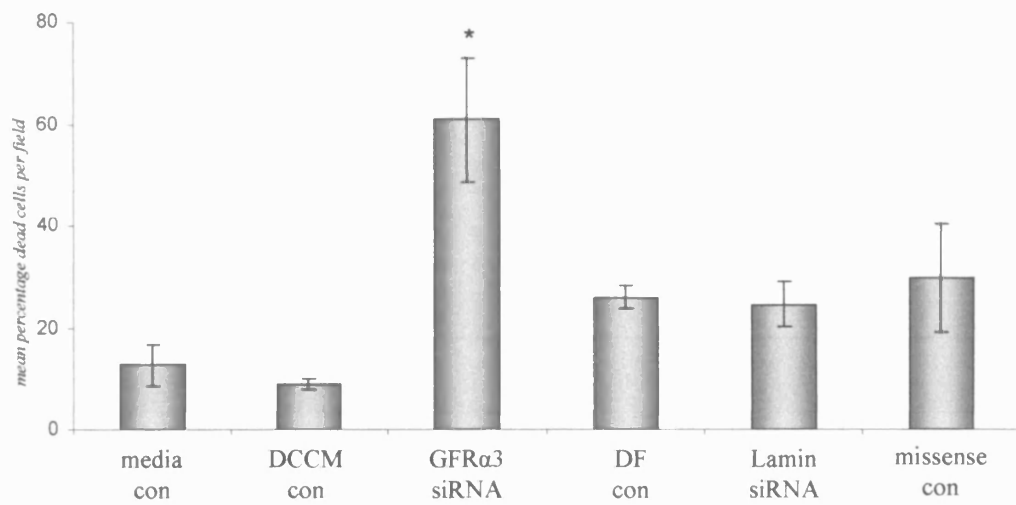
Figure 143. Microscopic Evaluation of the Apoptotic effects of GFRα3 siRNA knockdown at day 4 as measured by Apoalert Apoptosis Mitochondrial Membrane Sensor kit in TamR cells. Microscopic evaluation of apoptosis was performed at 40x magnification using fluorescence detection, counting red (live) or green (dead) cell numbers from six fields per test slide. Controls included were Missense, DharmaFECT (DF) transfection reagent, Lamin siRNA, DCCM media, and media (phenol red-free RPMI/ 5% serum) control versus test GFRα3 siRNA. (Plot shows mean percentage dead cells per field with standard errors). (*p=0.05 and *p<0.001 for GFRα3 siRNA relative to missense control and DCCM control respectively).
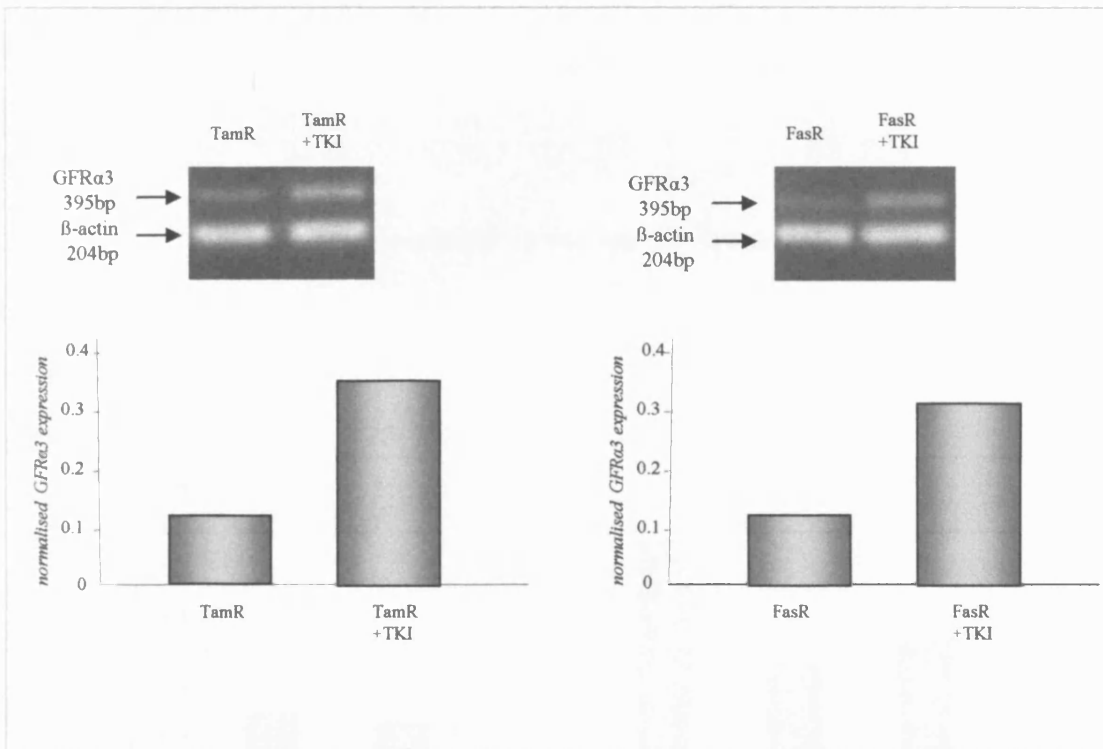
Figure 144. GFRα3 gene induction in TamR & FasR cells treated with EGFR-TK inhibitor Gefitinib (10^{-6}M). TamR and FasR cells were grown in 100mm dishes in the presence or absence of TKI (10^{-6}M) for 7 days before harvesting according to the TriReagent protocol as described in methods. One microgram of RNA extracted from cells was reverse transcribed and gene expression was determined using primers for GFRα3 (with β-actin co-amplification for normalisation). Representative PCR profiles are shown which were subject to densitometric analysis and normalisation to β-actin prior to graphical display.
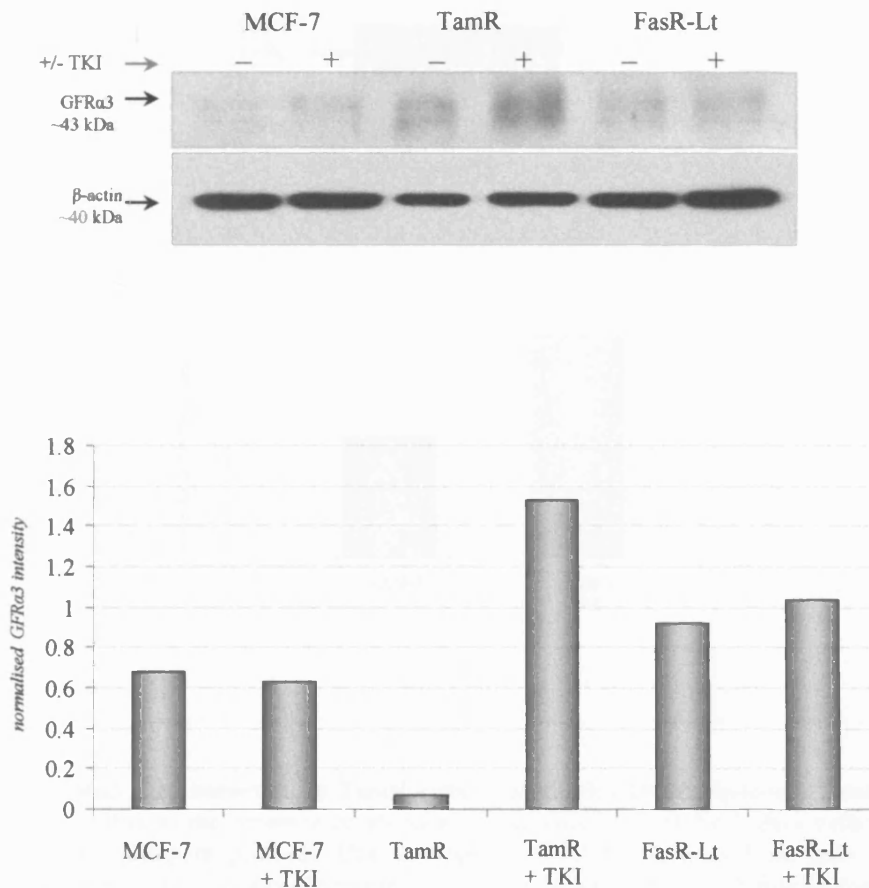
Figure 145. GFRα3 protein in TamR & FasR cells treated with EGFR-TK inhibitor Gefitinib.
MCF-7, TamR and FasR cells grown in 100mm dishes in the presence or absence of TKI (10^{-6}M) for 7 days before harvesting for protein as described in methods. GFRα3 protein was determined by subjecting 50µg protein from cells to 7.5% SDS PAGE and Western blotting. Proteins were probed with monoclonal anti-GFRα3 antibody with chemiluminescent detection with resultant blots subsequently subject to densitometric analysis. Equivalence of protein loading in Western blots was subsequently demonstrated by detection of β-actin on the same blot using monoclonal antibody to the protein. Normalised intensity subsequently plotted.
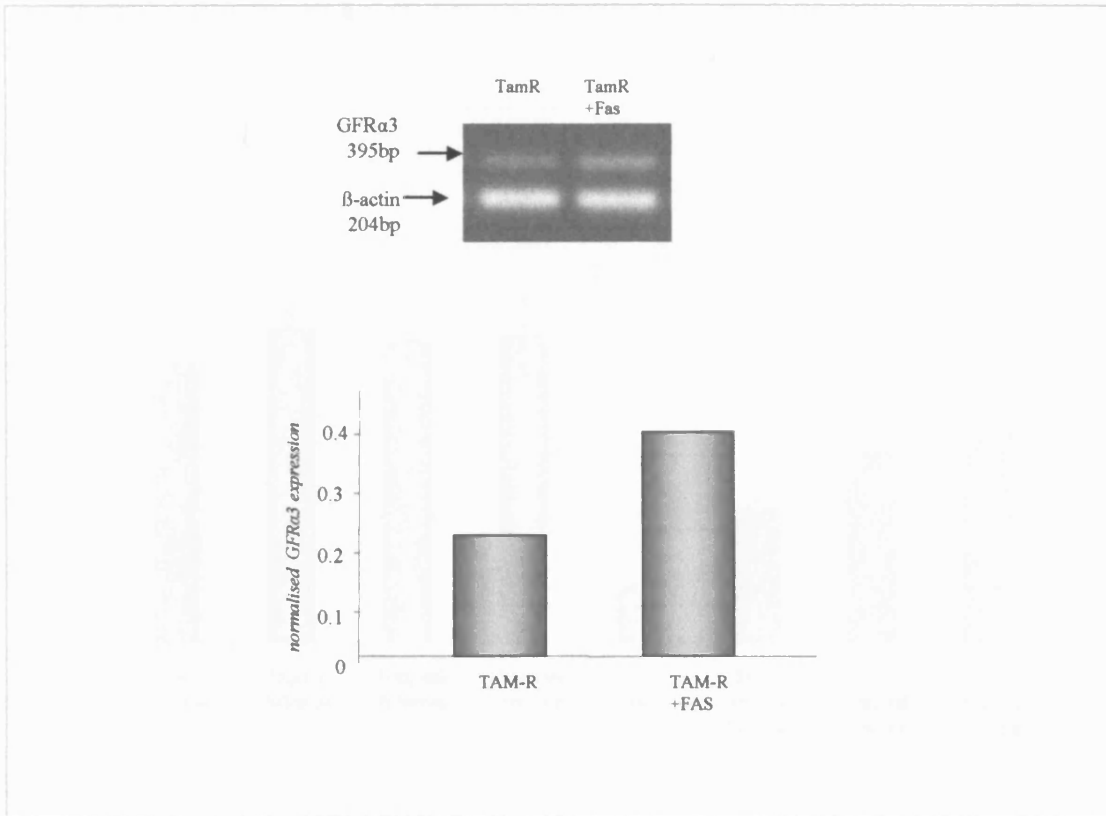
Figure 146. GFRα3 gene induction in TamR cells treated with 10^{-7}M Faslodex. TamR cells were grown in 100nn dishes in the presence or absence of Faslodex (10^{-7}M) for 7 days before harvesting according to the TriReagent protocol. One microgram of RNA extracted from cells was reverse transcribed and gene expression was determined using primers for GFRα3 (with β-actin coamplification for normalisation). Representative PCR profiles are shown which were subject to densitometric analysis and normalisation to β-actin.
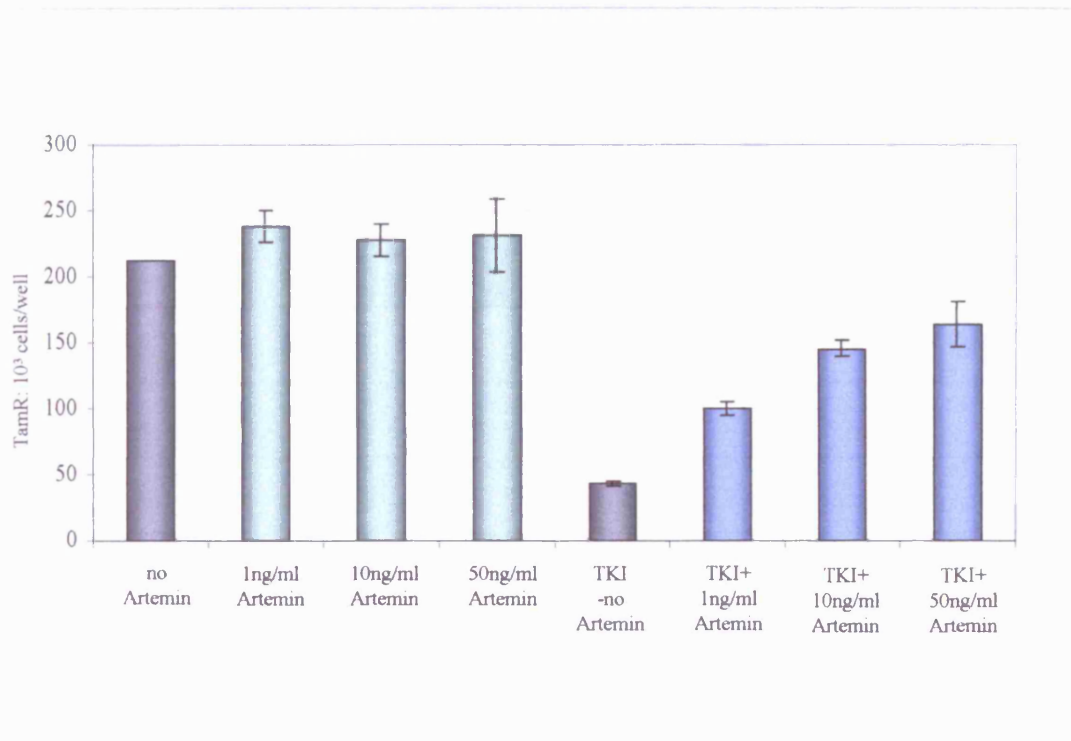
Figure 147. Growth of TamR cells in the presence of GFRα3-specific ligand Artemin alone (green) or in combination with (10⁻⁶M) TKI (blue). TamR cells were grown in triplicate in 100mm dishes with 1-50ng/ml artemin in the presence or absence of TKI (10^{-6}M) for 7 days before harvesting using trypsin/EDTA and counting using a Coulter Counter.
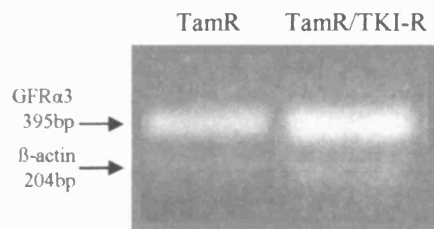
Figure 148. GFRα3 gene induction in TamR/TKI resistant cells. TamR/TKI resistant cells were grown in 100mm dishes for 7 days before harvesting. One microgram of RNA extracted from cells was reverse transcribed and gene expression was determined using primers for GFRα3 (with β-actin co-amplification for normalisation). Representative PCR profiles are shown

Chapter 6

DISCUSSION

DISCUSSION

RNA extraction optimisation and Microarray Hybridisation

The Atlas Plastic Human 12k microarray platform represented a relatively new introduction to the array market during the early phase of the project. The novelty of an innovative technology while potentially introducing advantages over older techniques also brought with it the necessity of an optimisation phase, particularly with regards to RNA preparation. To date only a limited number of publications using the 5k and 8k Atlas Plastic Array platform exist (Franscini et al., 2004, Sarkijarvi et al., 2006, Tasheva et al., 2004, Tsuchiya et al., 2005), and the RNA extraction procedures and precise methods of probe preparation used in these are furthermore often unclear. Of the limited reports, a number of the more recent ones have used 'Clontech Services', a facility set up by the manufacturer to aid probe preparation and array hybridisation (not available during the early stage of the project). Thus, the limited experience/ publications using Atlas Plastic 12k Arrays presented a challenge on initiation of this project.

The Tri Reagent method of RNA extraction proved to yield high levels of good quality total RNA starting material. Yields were comparable to those obtained previously within our own, and by other laboratories (Lenchik et al., 2005), and with relatively pure RNA obtained as demonstrated by 260/280nm ratio of 1.8 to 2. Additionally, intact 18S and 28S RNA bands post DNase clean-up with no genomic contamination provided the confidence to proceed in array probe preparation procedures using the RNA for subsequent hybridisation. Unfortunately, however, hybridisations using RNA extraction by this method produced results with unacceptably high background. A potential cause of this poor signal to noise ratio observed was considered to be excess non-specific adherence of unincorporated dNTPs within the hybridisation solution to the arrays and the failure of the post-hybridisation washing procedures to effectively remove these. Atlas Hybridisation boxes were subsequently used in an attempt to increase efficiency of array washing. The use of Hybridisation boxes was had potential to evenly facilitate fluid distribution during probe hybridisation and washing procedures. A slight improvement in background reduction was observed using this procedure, although there was no increase in signal intensity.

The RNA extraction protocols which were recommended by Clontech/ BD Biosciences resulted in sub-optimal yields and inadequate purity of RNA. Similarly, using the Clontech Nucleotrap mRNA purification kit, grossly low yields were produced which were variable between samples. Thus, despite around 2% of total RNA being reported to be extractable as poly A+RNA/mRNA (Sambrook et al., 1989) much lower, or no yield was obtained. Significantly, the Nucleotrap protocol utilises a suspension of Oligo(dT) latex beads on a

microfilter-contained spin column to bind polyA+RNA, and the procedure proved problematic in our laboratory. Resuspension of small volumes of beads proved a particularly difficult procedure as this involved repeated contact of beads and the Nucleotrap membrane, which was probably susceptible to damage, and may account for the retained and unwanted 28S and 18S RNA species within the mRNA post Nucleotrap procedure. According to the protocol, while 200μg of total RNA was regarded as sufficient for loading onto the column, the method may have proven more efficient using larger quantities of sample RNA to produce acceptable levels of mRNA yields. However, with the requirement for further processing of the RNA, this was impractical due to the associated large quantity of cell culture dishes required, and so the Nucleotrap method was abandoned.

Other polyadenylated RNA extraction methods were used as a possible alternative to those previously described or as an addition to the Tri Reagent method in an attempt to obtain satisfactory array signals with no background. Such protocols employ a high salt concentration in the binding buffer, permitting stabilisation of base-pair binding, followed by washing out all unwanted RNA species (Sambrook et al., 1989). Elution of the mRNA subsequently occurs through washing with a low salt buffer. However, these methods yielded undetectable levels of RNA. Due to the large amounts of washing steps required in such methods, a proportion of the product may have been lost. This would be particularly significant as stated above, mRNA species constitutes only around 2% of total RNA (Sambrook et al., 1989).

A further extraction and labelling protocol, the Atlas Pure Total RNA Labelling System was subsequently investigated and resulted in good yields and arrays with low background. However, there was still an absence of strong gene-specific signals. A number of factors are important in determining array signal strength. These include reagent quality, probe labelling efficiency, and the initial amount (and quality) of starting RNA used for probe labelling (Forster et al., 2003). RNA extractions using the denaturing solution as supplied with the Total RNA Labelling kit, consistently produced RNA with a high proportion of either low molecular weight RNA species, thought to consist of transfer RNA (tRNA), or of degraded RNA in addition to the strong 28S and 18S bands. As previously used RNA extraction protocols, namely Tri Reagent, had also undergone the same post extraction procedures, i.e. DNase-treatment and Qiagen clean-up, the only additional factor within the Atlas Total RNA Labelling System which may have contributed to selection for low molecular weight RNA, or degradation of RNA observed was the use of denaturing solution. The Tri Reagent method, as well as the Atlas Pure Total RNA Labelling System, are both based on guanidinium thiocyanate-phenol-chloroform extraction. The Atlas Pure Total system uses a denaturing solution (traditionally a guanidinium thiocyanate containing buffer also with components that allows the release of RNA, and with ribonuclease inhibitors in which the cell preparations are rigorously mixed. However, the Tri reagent protocol dispenses with these multiple steps in the protocol, including heavy vortexing,

with the use of a single and efficient step (Chomczynski and Sacchi, 1987), that may have better preserved RNA integrity, compared to the Atlas Pure Total RNA kit. Such high quantities of unwanted material in the sample using the Atlas Pure Total System may have caused the overestimation of RNA concentration, thus resulting in a lower amount of appropriate RNA employed for probe preparation or array hybridisation, and thus low array signal strength. However, a positive feature of this latter method remains the production of arrays with low background to signal ratio.

Ultimately then, the optimised protocol for RNA extraction and array hybridisation retained initial Tri Reagent RNA extraction procedure with its high yields and adequate quality, and subsequent DNase treatment and Qiagen clean-up. This replaces the RNA extraction step using the denaturing solution using the Atlas Total RNA Labelling System. The resultant RNA, after poly A+ enrichment from the Atlas Total System, was used for probe preparation and array hybridisation, with subsequent adequate array signal intensities and low background. RNA derived from the optimised method for extraction was validated for subsequent array work through the successful confirmation of profiling of the EGFR gene, which was found to be elevated in resistant cells, and also the gene for pS2, which was increased upon oestradiol-treatment, consistent with previous observations (Gee et al., 1995, Knowlden et al., 1997). Additionally, and in retrospect, the validity of using this protocol for RNA extraction was demonstrated by the subsequent successful selection of several genes relevant to antioestrogen resistant biology.

Gene Selection

With an ever-increasing size of microarrays platforms and associated data analysis software available it can be a daunting task to investigate even relatively simple biological questions. The current study used a 12k microarray and therefore potentially 12,000 data values, in quadruplicate were available. Several means of reducing the volume of information were thus examined. A data reduction of approximately 12,000 genes to around 300 genes was achieved by the careful application of a number of clustering/ statistical analysis methods, namely HCA and PAM, as well as t-test analysis. HCA and PAM analysis of the data showed distinct clusters which revealed the breadth of potential genes for further study. Both of these methods allowed the easy identification of specific profiles, such as those which were upregulated in both forms of antihormone resistance. Genes which displayed this "shared" profile following t-test analysis with a significance level $p \leq 0.05$ were given priority, although genes were also considered if a significant change was observed in one cell line, along with a trend in the other. Although these methods have not been previously used in the identification of determinants of endocrine resistance, some have nevertheless been used to classify breast tumours into pathological subsets, and good/bad prognostic groups (eg. (Perou et al., 1999, van 't Veer et al., 2002)).

Selection using t-test analysis for genes altered in TamR and FasR cells were used for the construction of the Excel-based database (CD-ROM included within this thesis).

Although, encouragingly, 60% of the genes selected were verified by Affymetrix and PCR analysis, other genes which have been classically associated with antihormone resistant growth, such as EGFR (Nicholson et al., 1994), were not identified by the methods used. Of course for EGFR, the mRNA increase may only be marginal and may not fully reflect the dramatically increased content of the protein and its activation status in the resistant cell lines (Knowlden et al., 2003). Importantly however, the Affymetrix system and PCR has permitted increased EGFR detection in TamR cells ~2-fold (Knowlden et al., 2003). Another explanation which may account for loss of signal detection for genes such as EGFR is that probe preparation for Atlas arrays from total RNA relies on the selection of polyadenylated (polyA+) RNA. Reports have shown that a small proportion of genes may have species of RNA which are not polyadenylated (Carninci, 2006). However, it is apparent that the main contributory factor for such a loss of gene detection with the Atlas Plastic arrays that may have led to an underperformance was a reduced sensitivity of these arrays, resulting in lowly expressed genes being undetected. As described previously, there was a high number of zero values observed with this dataset requiring processing (as advised by a number of independent sources) in order to upload into GeneSifter. Despite losing some genes owing to the low sensitivity of the arrays, data processing has nevertheless successfully yielded data which could be filtered for analysis to identify meaningful gene changes. Although there are numerous methods to identify the false discovery rate (FDR) for microarray data, such as the Bonferroni post-hoc test (which is available in GeneSifter) or Sequence Alignment and Modelling (SAM) (Qian and Huang, 2005, Tusher et al., 2001), such stringent data filtering procedures were deemed inappropriate as a markedly reduced number of genes was already achieved with the application of t-testing/HCA/PAM. To ensure that potentially relevant gene selection was made with regards to the biological significance of the gene, a thorough ontological examination of each selected gene from the ~300 genelist was performed to produce a final manageable set of genes for PCR verification.

It is also worth noting that using PAM or HCA analysis generated a fuller breadth of genes which appeared to be altered in both resistant cell lines. For example, our gene selection procedure including t-testing for both TamR and FasR cells resulted in 28 genes which were significantly altered. However, using PAM analysis, a four-fold increase in the number of elevated genes was achieved by placing genes within relevant clusters. Although not all genes reached significance, there is clearly future potential for studying the additional genes in these strong clusters, especially when taken together with comparable HCA results. However, for the purposes of data reduction and focussing in the remainder of this project, t-test analysis was applied to reduce gene number. Such significantly altered genes as selected in this project, were

subject to further verification, not only using PCR analysis, but also using Affymetrix genechip analysis. As stated above, using this alternative array platform, around 60% of altered gene profiles were verified, thus validating our array platform to a considerable extent and adding further confidence in the final gene choices made.

Ontological Examination

Cancer progression is hallmarked by the alteration of genes associated with the regulation of cell proliferation, survival, angiogenesis, invasion and immune surveillance (Hanahan and Weinberg, 2000) and some studies have used such ontological features as a means of gene selection and categorisation in microarray studies in breast cancer (Frasor et al., 2004). Moreover, a recent report investigated such gene expression using microarrays to decipher invasion mechanism of migratory cells *in-vivo* (Wang et al., 2004). Ontological examination of the genes altered in antihormone resistant cells in our study highlighted many that had an ontology related to the established cancer cell phenotype within these cell models, and this aided gene selection. Genes which were thus prioritised included those with a profile showing upregulation in both resistant cells lines, including PTTG1 and GFRα3, implicated in cell growth and proliferation, and in the case of PTTG1, also invasion and angiogenesis (Airaksinen and Saarma, 2002, Ramos-Morales et al., 2000, Solbach et al., 2004, Hamid and Kakar, 2003), and those genes induced in one resistant cell line only, such as PEA3 and Vitronectin., implicated in invasion (Bartsch et al., 2003, de Launoit et al., 2000).

Interestingly, although an ontological examination of genes detected between TamR and FasR cells revealed many similarities, nevertheless subtle differences were also observed. A larger proportion of proliferative genes, and fewer apoptotic genes were upregulated in FasR cells relative to TamR cells. This observation is further supported by the fewer numbers of cancer-associated genes being downregulated in FasR cells relative to TamR cells. Within this subset of genes, there are also fewer proliferative genes downregulated, and additional apoptotic genes downregulated. These figures are consistent with observation within our laboratory that shows FasR cells have a higher growth rate compared to TamR cells, in keeping with their markedly reduced ER content and their aggressive phenotype (Nicholson et al., 2005); and unpublished observations). It is also worth noting that our ontological examination of both TamR and FasR cell lines indicates increases in invasive and angiogenic genes, reflective of the invasive capacity and may herald angiogenic capacity (Hiscox et al., 2004).

PCR verification

The technique of RT-PCR was used as a method of validating the gene array expression data. This technique, which is in common laboratory use, is deemed to provide a relatively accurate means of quantifying gene expression. For the ~30 genes examined by RT-PCR, gene

primers used were either designed using primer3 software or were those already designed by Clontech. The analysis was performed initially on triplicate RNA samples originally used for array hybridisation, and then on further triplicate RNA preparations from an entirely different set of experiments adding further confidence to the verification.

The majority of genes analysed displayed profiles similar to those observed in the Atlas Plastic arrays. Thus for example, PTTG1 gene was robustly elevated in antihormone resistant cell lines by array and PCR. Following PCR validation a number of interesting induced genes were selected for further study, namely PEA3, Vitronectin, and also the PTTG1 and GFRα3 "shared genes". However, it is unclear why approximately 30% of gene profiles were not confirmed by PCR/Affymetrix in our study. It is believed that genes which are expressed at low levels may have poor reproducibility not only across sample sets, but in addition may produce spuriously high gene increases that do not reflect the actual changes (Butte, 2002), and it is likely that this may subsequently result in some genes not being verified. This may be exemplified by PCR results obtained for genes such as Legumain. An additional contributory factor may however be the primer design (although these were in general designed using Primer3 software (Rozen and Skaletsky, 2000) with a high level of stringency, and sequences subsequently being checked against other non-related gene sequences using Blast software). Primers may feasibly amplify a number of variants of the gene. Confounding issue of both wild-type and variant expression for some genes makes gene expression profiles difficult to interpret. Also an assumption is made that selected sequences will be highly homologous to the oligonucleotide sequences present on the Atlas Plastic arrays (or even Affymetrix arrays) but this may not always be the case. Reassuringly however, oligonucleotide arrays are likely to be highly specific due to the superior commercial sequence design for the gene, where the manufacturer of the Atlas Plastic arrays claims the oligonucleotide sequences are thoroughly pre-tested for specificity and minimal cross hybridisation (Clontech_BD-Biosciences:Atlas_pdf, 2006).

PEA3 is a member of the ets family of genes which encode transcription factors shown to be involved in tumourigenesis (Davidson et al., 2004). PEA3 mRNA was found to be elevated in TamR cells only using GeneSifter analysis on Atlas Plastic 12k arrays, a profile which was confirmed with PCR and Affymetrix. In addition, immunocytochemical and Western blotting analysis also confirmed PEA3 elevation at the protein level in TamR cells. Importantly, ets family members can be activated by MAPK signalling (O'Hagan et al., 1996), which itself is raised in the TamR cells (Knowlden et al., 2003). They are also known to interact with the Wnt signalling component β-catenin, which has been shown to have a role in mammary tumourigenesis (Howe and Brown, 2004). Significantly, β-catenin was demonstrated to be increased in our TamR cells with an elevated activation, and increased β-catenin associated genes, which may explain the migratory abilities of the cells (Hiscox et al., 2006a). PEA3, along with other invasive proteins such as MMPs were found elevated in breast cancer patients (Davidson et al., 2004), and it has also been shown to be able to directly activate MMPs (Higashino et al., 1995). Interestingly, PEA3 (and c-jun) were also demonstrated to upregulate HER2, a predominant feature of TamR cells (Knowlden et al., 2003).

In contrast to PEA3, Vitronectin mRNA was induced only in FasR cells, using Atlas Plastic and Affymetrix arrays. Significantly, Vitronectin belongs to a group of proteins which are chemotactic factors associated with cell adhesion and immune response and has been demonstrated to have a role in migration in breast cancer cells (Campo McKnight et al., 2006). Ovarian tumour cells stimulated by Vitronectin also were also demonstrated to have enhanced proliferation and motility (Hapke et al., 2003) (REF??). Moreover, these events, were associated with activation of MAPK, and by microarray analysis, altered EGFR expression was shown (Hapke et al., 2003). Such a role for Vitronectin in FasR cells would correspond to the observed increased invasive nature and their increased EGFR levels (Nicholson et al., 2005).

PTTG1 is a nuclear and cytoplasmic protein (Chien and Pei, 2000) found in a number of tissues including thymus colon and small intestine (Chen et al., 2000). With levels of the protein reported to be elevated in proliferating cells, it is thought to be regulated in a cell-cycle dependant manner (Ramos-Morales et al., 2000). As a securin protein, it functions to prevent sister chromatid separation during cell division in normal cells (Nasmyth, 2005). Two other PTTG1 gene homologues have also been reported, termed PTTG2 and PTTG3 which are 91% and 89% homologous to the PTTG1 amino acid sequence, and subsequently have showed differential expression in tumour tissues, suggesting their involvement in tumourigenesis alongside PTTG1 (Chen et al., 2000). PTTG1 has been documented to be overexpressed in a number of cancers including pituitary (McCabe et al., 2002), lung (Rehfeld et al., 2006), gastric (Wen et al., 2004), thyroid (Saez et al., 2006), ovary (Puri et al., 2001), and breast (Ogbagabriel *et al.*, 2005; Solbach *et al.*, 2004). The oncogenic features attributed to PTTG1 are thought to be a consequence of its overexpression, rather than its mutation (Hamid and Kakar, 2003). In addition to deregulating cell cycle and allowing increased proliferation, overexpression of PTTG1 also has the potential to impact on angiogenesis, invasion as it also functions as a nuclear transcription factor (Yu and Melmed, 2004)(refs). PTTG1 has also been demonstrated to stimulate fibroblast growth factor (FGF-2)- mediated angiogenesis and in pituitary tumours upregulated VEGF expression (McCabe et al., 2002). In thyroid cancer, this angiogenic capabilities of PTTG1 were demonstrated when it was reported to have regulated angiogenic and apoptotic-associated genes (Kim et al., 2006). Although a link of PTTG1 to breast cancer has been made (Ogbagabriel et al., 2005, Solbach et al., 2004, Thompson and Kakar, 2005), to date there is no reported literature of its association with endocrine resistant disease.

In our own models of resistance to antioestrogens, PTTG1 mRNA and protein was significantly elevated in TamR, FasR and X-MCF-7 cells. In addition to these observations, PTTG2 and PTTG3 also showed some increased mRNA levels in FasR and X-MCF-7 cells, but with no change in TamR cells. The preferential expression of one homologous protein form over the other has also been noted previously, with variable expression of PTTG1 to 3 in normal and cancerous samples (Hamid and Kakar, 2003). Interestingly, our studies show that PTTG1 mRNA is upregulated in MCF-7 cells in response to oestradiol-treatment. This is consistent with several *in-vitro* studies that have demonstrated PTTG1 gene to be oestrogen regulated (Heaney and Melmed, 1999) and *in-vivo* studies that have linked oestrogen-regulated PTTG1 with the oestrous cycle (Heaney et al., 2002).

As described previously, TamR and FasR cells have been shown to have elevated levels of growth factor signalling, notably EGFR, as well as enhanced signalling through MAPK (Gee et al., 2001, Hutcheson et al., 2003), and this pathway has also been reported to regulate PTTG1

mRNA and protein expression in astocytes (Tfelt-Hansen *et al.*, 2004) and pituitary cells (Vlotides et al., 2006). Interestingly, upregulation of PTTG1 in pituitary cells was via the MAPK pathway, and resulted in the activation of c-Fos, a transcription factor which we have also directly associated with PTTG1 (and GFRα3) mRNA in clinical samples. Additionally, other signalling mechanisms implicated in the development of resistance to antioestrogens in breast cancer cells, including our own (Knowlden et al., 2003), such as the insulin, IGF-1, and PI3K/AKT pathways, have also been shown to regulate PTTG1 mRNA and protein, demonstrated in both non-tumour and malignant cells (Chamaon et al., 2005, Thompson and Kakar, 2005). It is noteworthy that PTTG1 levels were elevated in our ER-negative FasR-Lt cells and that PTTG1 was also highest in the ER-negative MDA-MB-231 cells. Such cells, which are rapidly growing and highly invasive, also show increased expression of several growth factor receptors, notably including EGFR, as well as readily detectable IGF-1R (Nicholson et al., 2005).

Interestingly, although EGFR signalling has been linked to the regulation of PTTG1 in astrocytes and pituitary cells (Tfelt-Hansen et al., 2004, Vlotides et al., 2006), treatment of our FasR cells with gefitinib, an EGFR inhibitor, actually promoted a further increase in PTTG1 mRNA and protein. This result, may reflect the capacity of gefitinib to induce IGF-1R signalling in antihormone resistant breast cancer cells, that acts to limit the anti-tumour response (Jones et al., 2005, Knowlden et al., 2005), and the capacity of insulin and IGF-1 to upregulate PTTG1 in a PI3K and MAPK-dependant manner (Thompson and Kakar, 2005). The induction of PTTG1 mRNA in TamR cells with Faslodex treatment may equally be indicative of a compensatory cell growth mechanism to overcome maximal inhibitory effects of the agent. The cross-talk mechanisms as described above involving EGFR and IGF-1R may very well impinge on the PTTG1 gene induction, which is reported to confer cell proliferative effects (Hamid and Kakar, 2003, Pei, 2001).

Interestingly, although these data strongly indicate that the increased levels of PTTG1 found in our TamR and FasR cells result from their increased levels of EGFR and IGF-1R signalling, a consistently increased level of PTTG1 was also observed in X-MCF-7 cells, which do not depend on such classical growth factor signalling. These cells however, do show increased AKT-MAPK activity, elements equally capable of promoting PTTG1 expression (Chamaon et al., 2005, Tfelt-Hansen et al., 2004, Thompson and Kakar, 2005)

As stated above, PTTG1 protein has been reported to be localised within the nucleus, as well as cytoplasm (Chien and Pei, 2000), and this was also observed while performing ICC assays in our resistant cell lines. Interestingly, although nuclear localisation of PTTG1 is thought to be facilitated by the PTTG1 binding-factor (PBF) and that this enhances the activity of PTTG1 as a transactivation protein, targeting downstream elements such as c-myc (Pei, 2001), generally, there was no difference in PBF mRNA expression across MCF-7, TamR, or

FasR cells. The constant levels of PBF mRNA observed within TamR and FasR cells is consistent with recent findings which demonstrated PTTG1-driven cell growth promoted via MAPK/EGFR in pituitary cells also showed no alteration in PBF levels (Vlotides et al., 2006).

Clinical data

Any early assessment of the potential importance of a gene in breast cancer must involve evaluation of its clinical prevalence. Therefore we examined PTTG1 expression in a series of breast cancers of known clinico-pathological history. Levels of PTTG1 mRNA expression were associated with poorly differentiated tumours showing increased nuclear pleomorphism and lymph node involvement. These observations are of particular significance since such pathological and biological features often relate to poor patient survival (Elston and Ellis, 2002).

The results of our study linking PTTG1 with lymph node involvement are in agreement with a recent report by (Solbach et al., 2004) who proposed PTTG1 as a marker for tumour aggressiveness. Similarly, (Ramaswamy et al., 2003) identified PTTG1 as part of a gene expression signature that was associated with metastatic spread in breast cancer. The association of PTTG1 protein with highly pleomorphic breast tumours has also recently been reported, where such tumours showed increased invasiveness as well as proliferative capacity (Ogbagabriel et al., 2005). Significantly, the association of PTTG1 mRNA in breast tumours showing increased nuclear pleomorphism is consistent with PTTG1 acting as a securin during the cell cycle, and PTTG1 overexpression has been shown to induce aneuploidy within cells *in-vitro* (Yu et al., 2003, Yu et al., 2000a). Indeed, PTTG1 expression disrupts sister chromatid separation, a key element leading to aneuploidy (Yu et al., 2003, Christopoulou et al., 2003). The potential importance of these observations is emphasised by the knowledge that uneven sister chromatid separation can lead to chromosomal gain or loss (Kops et al., 2005) which in turn may be associated with a number of oncogenic events such as activation of proto-oncogenes or loss of heterozygosity of tumour-suppressor genes, ultimately leading to aberrant genetic mutations, conferring aggressive growth behaviour (Zou et al., 1999). Interestingly, the p53 tumour suppressor protein has been shown to directly bind to the promoter of PTTG1 to reduce its tumour-forming capabilities (Kho et al., 2004). However, where there is an absence of functional p53, PTTG1 has been shown to promote aneuploidy (Yu et al., 2000a).

Consistent with the report of Ogbagabriel et al., (2005), PTTG1 mRNA overexpression in our clinical series showed an association with increased mitotic activity and, in our preliminary immunohistochemical study (n=3) PTTG1 immunostaining was often seen strongly in mitotic cells. These data are reinforced in the current investigation by the direct correlation of PTTG1 levels with increased Ki67 immunostaining, where Ki67 is a reliable marker for cell proliferation (van Diest et al., 2004). In this context, it is noteworthy that Ramos-Morales et al.,

(2000) have shown PTTG1 is at increased levels in rapidly proliferating cells, and where its expression was regulated in a cell-cycle dependant manner, peaking in the G2/M phase. PTTG1, in its function as a transactivating protein, was also reported to function to target the c-myc promoter region, increasing c-myc expression to potentially activate cell cycle progression (Pei, 2001).

Consistent with our microarray/ PCR observations of PTTG1 being induced by oestradiol treatment in MCF-7 cells, an association of PTTG1 mRNA expression and ERα staining was observed, in our clinical series, albeit only in the ER-positive patient cohort. Within this cohort PTTG1 not only associated with ER-positivity but also with the oestrogen-regulated, PgR protein. These data are somewhat surprising since ER loss is frequently associated with poorly differentiated tumours displaying high grades of nuclear pleomorphism and elevated proliferative capacity (Nicholson et al., 2005). However, it is also worth noting that despite this association, PTTG1 expression could also be found at high levels in ER-negative patient samples, and more, recent immunocytochemical findings within our laboratory showed PTTG1 protein within a clinical series from patients with *de novo* resistant disease with particularly elevated levels, in this instance, more closely associating with ER-negativity (JM.Gee and MY.Cheong, *personal communication*). It is also noteworthy that highest PTTG1 protein expression was consistently found elevated in ER-negative MDA-MB-231 and FasR-Lt.

As stated above, elevated mRNA expression of PTTG1 was also associated, in clinical samples with staining for the transcription factor Fos. The Fos nuclear phosphoprotein can be found as a heterodimer with Jun, resulting in the formation of the AP-1 transcription factor, which is also the target for cross-talk with the ER, as well as growth factor signalling (Klinge, 2000). Previous studies from the TCCR have linked increased Fos expression with the loss of endocrine response in clinical breast cancer specimens (Gee et al., 1995, Gee et al., 1999), and it is tempting to speculate a causative role for PTTG1 in these events. With Fos and PTTG1 lying downstream of a common regulatory pathway. Indeed further exploration of the structure of the PTTG1 gene reveals that it does house AP1/ AP2 (Kakar and Jennes, 1999), SP1 and NF-Y binding sequences (Clem et al., 2003) suggesting transcriptional regulation by growth factor signalling, perhaps involving the Fos/ AP-1 complex.

siRNA gene knockdown studies

siRNA studies have recently come to the forefront of research since they allow effective and rapid gene knockdown, enabling detailed study of gene function and its impact on cellular events. In the current study, Dharmacon's siRNA reagents and protocols were used. A wide range of genes are available for study and the manufacturer provides a number of options when considering use of siRNA. Rather than selecting one sequence that targets a specific area of the

gene of interest, we opted for the Dharmacon Smartpool which is a combination of 4 sequences which guarantee at least a 70% gene knockdown. Focussing on FasR-Lt, that expressed highest levels of PTTG1, our study initially revealed, that effective transfection rates (~74% in FasR-Lt cells) were achievable, as determined by siGlo transfection, and that successful gene knockdown was to be attained in such cells, as demonstrated by the successful reduction in mRNA levels of Lamin A/C.

Using the Dharmacon's system to investigate the cellular importance of PTTG1 revealed that PTTG1 siRNA was able to reduce PTTG1 mRNA levels by 62% and protein by 95% at 4 days post-transfection, and that this was associated with a 72% reduction in cell numbers in FasR-Lt cells compared to the missense control. Encouragingly, the reduction in cell numbers was paralleled by a fall (23%) in Ki67 immunostaining, a marker of cell proliferation, and there was an induction of apoptosis (29%). In our study, DCCM media was used to minimise any interference of serum with the transfection procedure. Although some unwanted gene-inhibition effects of using this media were observed compared to RPMI media, these effects were inconstant and did not prevent effective knockdown effects with PTTG1 being detected. Our PTTG1 siRNA data are consistent with the proposed role of PTTG1 in cell cycle regulation (Ogbagabriel et al., 2005), and PTTG1 knockdown has also been shown to promote p53-dependant apoptosis in hepatoma and colorectal cell lines (Cho-Rok et al., 2006). Interestingly, although PTTG1 gene knockdown *in-vivo* similarly inhibits growth of hepatoma cell-derived xenografts (Cho-Rok et al., 2006), a much more complex interplay of PTTG1 and apoptosis/p53 has also been recognised, where PTTG1 not only regulates p53-dependant apoptosis (Hamid and Kakar, 2004), but where p53 in turn regulates PTTG1 (Kho et al., 2004). Additionally, in the absence/ failure of a functional p53, PTTG1 has also been suggested to support the survival of aneuploid cells and promote tumourigenesis (Yu et al., 2000b).

The GDNF family of four receptors (GFRαs) and their ligands are believed to promote the survival and maintenance of different neuronal cells. However, as well as in the nervous system, the ligands have several other roles including morphogenesis in kidney development and regulation of spermatogonial differentiation (Takahashi, 2001). GFRα receptors signal through a complex with a co-receptor, the tyrosine-kinase RET receptor (Sariola and Saarma, 2003, Baloh et al., 1998). It is thought that upon ligand binding, the dimeric or monomeric GFRα interacts with two RET molecules, inducing its autophosphorylation (Airaksinen and Saarma, 2002). GFRα3 generally complexes with its preferred ligand Artemin resulting in RET activation (Airaksinen and Saarma, 2002) and promotion of downstream kinase signalling. However, although the four GFRα ligands have been assigned preferential receptors, an added complexity is introduced as a number of these ligands can weakly cross activate other receptors within the family (Airaksinen and Saarma, 2002). Thus, GFRα3 can be triggered not only by Artemin, but also under certain conditions by GDNF. In turn, while GFRα1 is primarily activated by GDNF, it can also be activated by Artemin and Neurturin; GFRα2 is triggered by Neurturin but also GDNF; whereas GFRα4 is only activated by Persephin (Airaksinen and Saarma, 2002). Furthermore, GFRα signalling may also occur independently of RET (for example, involving recruitment and signalling through c-src (Kodama et al., 2005).

Interestingly, our study revealed increased GFRα3 mRNA in TamR and FasR cells, also with a slight induction in FasR-Lt cells. Western blotting and immunocytochemical analysis also again revealed an overall elevated level of GFRα3 staining particularly in TamR, followed by FasR-Lt cells where staining was still increased versus MCF-7 cells. Immunocytochemical studies again showed TamR cells with highest GFRα3 staining, but additionally revealed, there was slightly higher cytoplasmic than membrane staining, whereas in FasR-Lt cells higher membrane staining than cytoplasmic was observed. The principal GFRα3 ligand Artemin was detectable at the mRNA level in these resistant cells. Profiling further GFRα receptors and also their ligands by PCR revealed differential mRNA expression. For example, alongside GFRα3, some induction of the RET receptor was observed in TamR cells, as were the GFRα2/GFRα4 ligands Neurturin and Persephin respectively. In FasR cells (again alongside increased GFRα3 and detectable RET), it was both the GFRα2/GFRα4 receptors and their ligands Neurturin and Persephin that were increased. However, while X-MCF-7 cells showed highly elevated levels of mRNA for GFRα2, Neurturin and RET, there was only slight induction of GFRα4 and no increase in GFRα3 expression versus MCF-7 cells. A level of differential regulatory signalling

across the various resistant models is thus suggested, whereby different GFRα receptors and/or ligands may be recruited depending on the type of endocrine resistance. It is also worth noting that the GFRα1 mRNA was elevated in the hormone responsive MCF-7 parental cells only, and has more recently been noted to be oestrogen regulated in hormone responsive ZR-75-1 cells and associated with also ER-positivity in clinical array studies (Dorssers et al., 2005). Interestingly, GFRα1 is significantly downregulated in both TamR and FasR cells (whereas the other GFRα receptor family members show increases), suggesting a dichotomy of function for these receptor members between the hormone responsive and resistant phases.

As described above, the RET receptor mRNA was expressed in the MCF-7, TamR and FasR models but highly elevated in the X-MCF-7 cell line, as well as in MCF-7 cells treated with oestradiol. Western blotting using the monoclonal antibody against RET confirmed the protein was detectable in MCF-7, TamR and FasR cells. However, among these three models, the greatest level of expression was recorded in TamR cells. Alongside the prominent elevation of GFRα3 noted, this observation is highly suggestive that GFRα3/RET signalling has increased importance to TamR cells. The RET protein isoforms at 150kDa and 170kDa were most often detected in our cells, and interestingly a published study showed the 150kDa form had the highest signalling activity while the 170kDa protein represented a mature glycosylated form (Miyazaki et al., 1993). However, we have also detected other RET bands in Western blotting, where a 120kDa RET protein has been suggested to be the single polypeptide pre-glycosylated version of the protein in neuroblastoma cells, while a 190kDa band additionally marks a mature glycosylated form (Miyazaki et al., 1993).

Importantly, the RET receptor has been implicated in a number of pathological conditions. In papillary thyroid cancer (Asai et al., 2006), this cell surface receptor tyrosine kinase transduces signals for cell growth and differentiation via its oncogenic activation *in-vivo* and *in-vitro* by cytogenetic rearrangement (Grieco et al., 1990). Furthermore, mutations in the RET gene have been associated with several disorders including multiple endocrine neoplasia (MEN 2A and MEN2B), Hirschsprung disease (HSCR), and familial medullary thyroid carcinoma (FMTC) (Asai et al., 2006). Although we have established that RET protein is present in our endocrine responsive and resistant cells, an equivalent study remains to be performed in clinical material. Such a study should reveal whether the predominant form of RET in breast cancer cells is always the wild-type protein, or if a mutant form can be present. PCR studies using various primers for the RET gene applied to the same clinical series as used with GFRα3 are ongoing in our group.

While there is limited association reported between GFRα3 (or other family members) and the candidate growth factor receptors (e.g. EGFR, IGF1R) which have been associated with development of resistance to endocrine therapies in breast cancer, the subsequently activated RET receptor may feasibly contribute to the stimulation of a number of signalling events

(Arighi et al., 2005, Kodama et al., 2005) which have been demonstrated to be significant mechanisms in driving resistance in our resistant cell lines. These include the activation of AKT, MAPK and c-src signalling (Hiscox et al., 2006b, Jordan et al., 2004, Knowlden et al., 2003, McClelland et al., 2001). Additionally, the RET receptor is also capable of interacting with IRS1 and 2 which are key mediators in IGF-1R signalling again demonstrated to be an important mechanism in TamR cells, in particular as an alternative cell survival pathway during their response to gefitinib treatment (Jones et al., 2005, Knowlden et al., 2005). Significantly, in this study we have found further increases in GFRα3 mRNA and protein in both TamR and FasR cells in response to gefitinib. These data are complimented by our findings that GFRα3 is also elevated in cells that have acquired full resistance to tamoxifen and gefitinib (TamR/TKI-R) which have been shown to exhibit increased IGF-1R and AKT activation (Jones et al., 2004).

These observations indicate further increases in GFRα3/RET signalling could comprise a key mechanism recruited by TamR cells to limit their maximal response to gefitinib, perhaps interplaying with the gefitinib-induced IGF-1R signalling that is implicated in this event. In this regard, the GFRα3 ligand Artemin can indeed override the growth inhibitory effects of gefitinib, suggesting an active role for GFRα3 in resistance to this anti-EGFR agent. Interestingly, although this most likely occurs through Artemin/GFRα3/RET interactions, other GFRα3 ligands, such as GDNF have been reported to be able to signal independently of RET (Arighi, 2005). For example, in RET deficient cell lines, GDNF can trigger src-family kinases, PLC-γ, CREB, and induce Fos (Arighi et al., 2005). This latter relationship is perhaps significant as we have also noted increased GFRα3 mRNA associating with increased Fos staining in clinical breast cancer material, where increased Fos has in turn been demonstrated to be a feature of highly proliferative cells and clinical tamoxifen resistance (Gee et al., 1999). The further induction of GFRα3 mRNA in TamR cells with Faslodex treatment may similarly be indicative of a compensatory mechanism recruited to overcome maximal inhibition by this agent that depletes ER signalling.

The association in this study implied between GFRα/RET receptor signalling and breast cancer represents a largely unexplored research avenue in this disease (and is unique in the context of therapeutic resistance). A relatively-recent report identified RET expression in a number of breast cancer cell lines including MCF-7, BT474, and MDA-MB-453/468 cells (Meric et al., 2002). Significantly, the oncogenic potential of RET in the mouse mammary gland in-vivo has also been demonstrated, where interestingly RET overexpression was associated with a parallel increased level of the insulin receptor (IR). IR is a further member of the type II family of growth factor receptors which include the IGF-1R, and which is found increased in breast tumours (Frittitta et al., 1997, Papa et al., 1990), and alongside the observations that both IGF-1R signalling and GFRα3 equate with resistance to antioestrogens or gefitinib in our

models (Jones et al., 2005, Knowlden et al., 2005) provides further evidence of RET/type II receptor interplay.

A frequently observed chimeric gene RET/PTC (papillary thyroid cancer) is formed from the fusion of the tyrosine kinase domain of the RET and the gene H4, though other fusion proteins may be formed with other genes (Arighi et al., 2005). Although overexpression of RET/PTC is associated with human papillary thyroid carcinomas (Asai et al., 2006), a study which produced transgenic mice harbouring the RET/PTC gene also revealed that tumours were additionally formed in the mammary gland. The oestradiol induction of RET observed in our study correlates with reports that suggest that other RET-fusion proteins have been shown to be elevated by oestradiol treatment (in prostate cells) (Tekur et al., 2001), suggesting some link between RET and oestrogen signalling. This may perhaps also explain that the most substantial induction of RET was in X-MCF-7 cells, which retain a functional ER and exhibit markedly elevated oestrogen regulated gene expression (Nicholson et al., 2004, Staka et al., 2005). These various findings certainly suggest further investigation of RET and RET fusion products in the context of both endocrine resistance and during endocrine response is warranted.

Clinical data

GFRα3 was heterogeneously detected in clinical disease, and interestingly correlated with EGFR positivity and also an ER- tumour status, as well as being increased in poorly differentiated tumours. These are prominent features of *de novo* endocrine resistance or poor prognosis in the clinic (REFS), supportive of the links we have made between this gene and endocrine resistance when this is acquired by the MCF-7 model system *in-vitro*. The link with ER negativity is particularly interesting, given the inherent gefitinib resistance commonly exhibited by many ER-/EGFR+ cancers in the clinic (Agrawal et al., 2005). The clinical finding of elevated GFRα3 in ER- tumours may thus reinforce the concept that increased GFRα3 signalling may limit the anti-tumour effect of this anti-EGFR agent as based on our experimental findings. Preliminary GFRα3 immunostaining was also achieved within a small series of clinical samples (n=3), further reinforcing that GFRα3 is relevant to clinical breast cancer.

Interestingly a close association was found between the levels of GFRα3 and PTTG mRNA expression in the clinical material. A common feature relating to overexpression of both GFRα3 and PTTG1 in these samples was increased Fos expression, which as described earlier, drives transcription of genes via the AP-1 transcription site which can be regulated by growth factor signalling as well as by cross-talk with ER (DeNardo et al., 2005). Fos has also been associated resistance to antioestrogens in clinical breast cancer material (Gee et al., 1995, Gee et al., 1999), and so their correlation with this element may suggest an equivalent clinical

relationship for PTTG1 and GFRα3 and furthermore a mechanistic/transcriptional link between these genes/proteins; further studies are needed to clarify the nature of this association.

siRNA gene knockdown studies

Our studies exploring the role for GFRα3 further in endocrine resistant cells focussed around TamR cells since these exhibited the most prominent GFRα3 increases in our models. Interestingly, the TamR cells were in general less amenable to siRNA treatment, possibly reflecting the higher toxicity of the DharmaFect reagents in such cells. However, despite this, GFRα3 knockdown of at least 78% and 35% was achieved with GFRα3 siRNA relative to all controls at both the mRNA and protein level respectively, and this action promoted reduced cell growth and proliferative capacity (decreased Ki67 immunostaining), together with an increased level of apoptosis. These data are consistent with GFRα3 playing an active role in promoting cellular growth (Airaksinen and Saarma, 2002) of TamR cells, clearly acting as a cell growth and survival factor. Since EGFR or IGF1R blockade is also growth inhibitory in such cells (Knowlden et al., 2005, Knowlden et al., 2003), these observations suggest that GFRa3 interplays with these candidate pathways to drive TamR growth, providing a previously-unrecognised dimension of endocrine resistance.

Our experimental studies demonstrate the importance for further exploration of both PTTG1 and GFRα3 (and/or its family receptors/ligands) as a growth contributor in endocrine resistant breast cancer. Importantly, the genes are also clinically represented, where they cumulatively relate to diverse phenotypic features that have again been associated with endocrine resistance and poor prognosis. These findings are further reinforced by the published ontology for these genes, by the potential links with growth factor receptor /kinase signalling (many aspects of which are also elevated in endocrine resistant cells), and for the previous PTTG1 observations made in clinical breast cancer (notably increased expression associated with breast cancer invasiveness (Solbach et al., 2004)). As such, these genes may both prove useful markers for adverse clinical behaviour, although this remains to be fully addressed at a protein level in clinical samples with parallel endocrine response/survival data. This will be possible since this project has shown that immunohistochemistry is viable for detecting the PTTG1 or GFRα3 proteins in paraffin-embedded clinical breast cancer samples.

We have shown that PTTG1 is likely to be a key player in endocrine resistance, limiting anti-EGFR response, and promoting adverse clinical features. Its targeting may thus improve outlook, if achievable, in multiple settings. With regards to future value as a therapeutic target, our siRNA results, as well as other reports (Kakar and Malik, 2006, Solbach et al., 2005) have confirmed the considerable potential of targeting PTTG1 to reduce cell proliferation or induce apoptosis. Our experimental results are unique in this regard in the context of treating endocrine resistance. Owing to the ubiquitous nature of the protein, targeting specificity may be a hurdle. However, as for other cell-cycle regulatory elements (Swanton, 2004), small molecule inhibitors could perhaps be designed to facilitate the degradation of PTTG1 within the cancer cell. Alternatively, increased knowledge of the signalling mechanism involving PTTG1 may reveal ways to target the key regulators or effectors of PTTG1. PTTG1 inhibition may be relevant to improve response and subvert resistance either alone or alongside currently used therapies which fail to show complete inhibition of breast cancer in the clinic, notably endocrine agents in ER+ cells. In addition, gefitinib has given mixed responses (Agrawal et al., 2005), and since use of this *in-vitro* appears to induce PTTG1, may have an improved anti-tumour effect if used in conjunction with PTTG1 inhibitors.

We have also shown that GFRα3 is a new contributor in tamoxifen resistance, is clinically-represented, and its role may extend to limiting anti-EGFR response, while other GFRαs seem relevant to further endocrine responsive/resistant states *in-vitro*. As such, inhibitors for these family of ligands and the GFRα receptors, notably GFRα3 in endocrine resistance and ER negative disease, or the coreceptor RET, may provide interesting new

therapeutic avenues for breast cancer. Membrane bound receptors are deemed an amenable target in terms of accessibility and because their subsequent signalling activation may be targetable. However, GFRα ligands have neuronal generative properties, where the GFRα1 ligand, GDNF has already been established in the context of Parkinsons disease (Hurelbrink and Barker, 2004) where the ligand was administered. This suggests an essential requirement for development of any GFRα inhibitory strategy would be breast cancer selectivity (assuming such agents were able to cross the blood-brain barrier), if we are to avoid a profound adverse impact on neuronal cells. There are currently a number of RET inhibitors entering the cancer armoury including Zactima (ZD6474; Astra Zeneca) and AMG706 (Amgen). Since these also target other factors such as the EGFR or VEGF family of receptors that contribute to breast cancer growth and progression, they may be of particular benefit if a responsive cohort of patients can be identified (potentially GFRα3/RET+, endocrine resistant disease).

In addition, the differential expression of PTTG1 isoforms, and especially the range of GFRα receptor/ligands may have further potential clinical prognostic/therapeutic potential. GFRα1 was recently found to be increased in the hormone sensitive ZR-75-1 cell line (Dorssers et al., 2005), but was downregulated in our resistant models, with GFRα3 being upregulated in our resistant cells. Such variance of expression across key phenotypes suggests potential usefulness of these markers as differential indicators of responsive/ resistant states, as well as potentially diverse targets.

For GFRα3, it will be worthwhile in the future to fully explore its signalling mechanism, including any interplay with RET and cross-talk with the candidate EGFR and IGF1R pathways considering the potential relevance revealed from this project for GFRα3/RET/Artemin in the context of driving endocrine resistant disease. As interaction has also been implicated between PTTG1 and GFRα3 expression, it may be advantageous to fully dissect the regulation of this interaction. Such studies could reveal whether PTTG1 or GFRα3 is upregulated by, or enters into further interaction with, classical growth factor signalling associated with endocrine resistance or indeed with other novel elements. Although this study has been able to draw some associations for additional GFRα family members/ligands (as well as PTTG2 and 3), clearly the precise contribution for these now needs uncovering, especially bearing in mind that we have shown that many of these are at differential levels of expression across the various cell models of resistance to tamoxifen, Faslodex and oestrogen-deprivation, as well as in the endocrine responsive parental cells in the case of GFRα1. These investigations would, in the first instance be performed at the mRNA and protein level, with further studies to knockdown the gene for each GFRα receptor or PTTG member to show relevance. Study of GFRα3 and the GFRα family, as well as PTTGs, in further breast cancer models of response/resistance (e.g. T47D derivatives) would also be valuable, as would extension of the studies to *de novo* tamoxifen resistant cell lines (e.g. BT474). Also, contribution to other endpoints such as migration, which were not included in this Thesis, could be evaluated as a consequence of gene knockdown. This may be of particular relevance for GFRα3 since it has previously been linked with invasive capacity in pancreatic tumour cells (Ceyhan et al., 2006) and our antioestrogen resistant cells do exhibit aggressive behaviour. Furthermore, the role of PTTG1 and GFRα3/RET/Artemin warrants further study in the context of the signalling underlying anti-EGFR failure (notably interplay with IGF1R), since these new elements may contribute to resistance to such additional therapies.

At a clinical level, increased access to archival primary breast cancer material with parallel response/resistance and prognostic data with various endocrine strategies (for example, the NCRI Adjuvant Breast Cancer [ABC] Trial in early breast cancer for tamoxifen response), as well as access to breast cancer samples (i) obtained from sequential biopsies before, during and on relapse with particular endocrine therapies or (ii) during anti-EGFR response/failure, will be essential to confirm that the PTTG1 and GFRα3 proteins are of clinical relevance to multiple *de novo*/acquired resistant states.

Finally, this project has revealed many potentially valuable avenues for future research in endocrine resistance through the generation of an extensive gene database. It may be worth

re-evaluating the dataset (and indeed PTTG1 and the GFRα family members) through open-access public cancer databases such as Oncomine (www.oncomine.org) to reveal potential correlations in large clinical datasets with key associated phenotypic/ prognostic data. Indeed, it may be possible to implement this procedure as a future prerequisite for gene verification by PCR, to ensure clinical relevance of any selected gene and to evaluate early its potential as a viable target for therapy.

REFERENCES

(1998) Tamoxifen for early breast cancer: an overview of the randomised trials. Early Breast Cancer Trialists' Collaborative Group. Lancet, 351, 1451-1467.

Agrawal, A., Gutteridge, E., Gee, J.M., Nicholson, R.I. and Robertson, J.F. (2005) Overview of tyrosine kinase inhibitors in clinical breast cancer. Endocr Relat Cancer, 12 Suppl 1, S135-144.

Airaksinen, M.S. and Saarma, M. (2002) The GDNF family: signalling, biological functions and therapeutic value. Nat Rev Neurosci, 3, 383-394.

Ali, S. and Coombes, R.C. (2002) Endocrine-responsive breast cancer and strategies for combating resistance. Nat Rev Cancer, 2, 101-112.

Amadori, D., Bertoni, L., Flamigni, A., Savini, S., De Giovanni, C., Casanova, S., De Paola, F., Amadori, A., Giulotto, E. and Zoli, W. (1993) Establishment and characterization of a new cell line from primary human breast carcinoma. Breast Cancer Res Treat, 28, 251-260.

Anolik, J.H., Klinge, C.M., Hilf, R. and Bambara, R.A. (1995) Cooperative binding of estrogen receptor to DNA depends on spacing of binding sites, flanking sequence, and ligand. Biochemistry, 34, 2511-2520.

Anzick, S.L., Kononen, J., Walker, R.L., Azorsa, D.O., Tanner, M.M., Guan, X.Y., Sauter, G., Kallioniemi, O.P., Trent, J.M. and Meltzer, P.S. (1997) AIB1, a steroid receptor coactivator amplified in breast and ovarian cancer. Science, 277, 965-968.

Arighi, E., Borrello, M.G. and Sariola, H. (2005) RET tyrosine kinase signaling in development and cancer. Cytokine Growth Factor Rev, 16, 441-467.

Arnold, S.F., Melamed, M., Vorojeikina, D.P., Notides, A.C. and Sasson, S. (1997) Estradiol-binding mechanism and binding capacity of the human estrogen receptor is regulated by tyrosine phosphorylation. Mol Endocrinol, 11, 48-53.

Arnold, S.F., Obourn, J.D., Jaffe, H. and Notides, A.C. (1995a) Phosphorylation of the human estrogen receptor by mitogen-activated protein kinase and casein kinase II: consequence on DNA binding. J Steroid Biochem Mol Biol, 55, 163-172.

Arnold, S.F., Obourn, J.D., Jaffe, H. and Notides, A.C. (1995b) Phosphorylation of the human estrogen receptor on tyrosine 537 in vivo and by src family tyrosine kinases in vitro. Mol Endocrinol, 9, 24-33.

Arnold, S.F., Vorojeikina, D.P. and Notides, A.C. (1995c) Phosphorylation of tyrosine 537 on the human estrogen receptor is required for binding to an estrogen response element. J Biol Chem, 270, 30205-30212.

Asai, N., Jijiwa, M., Enomoto, A., Kawai, K., Maeda, K., Ichiahara, M., Murakumo, Y. and

Takahashi, M. (2006) RET receptor signaling: dysfunction in thyroid cancer and Hirschsprung's disease. Pathol Int, 56, 164-172.

Auchus, R.J. and Fuqua, S.A. (1994) Hormone-nuclear receptor interactions in health and disease. The oestrogen receptor. Baillieres Clin Endocrinol Metab, 8, 433-449.

Aviram, M., Kaplan, M., Rosenblat, M. and Fuhrman, B. (2005) Dietary antioxidants and paraoxonases against LDL oxidation and atherosclerosis development. Handb Exp Pharmacol, 263-300.

Aviv, H. and Leder, P. (1972) Purification of biologically active globin messenger RNA by chromatography on oligothymidylic acid-cellulose. Proc Natl Acad Sci U S A, 69, 1408-1412.

Bach, I. (2000) The LIM domain: regulation by association. Mech Dev, 91, 5-17.

Baloh, R.H., Gorodinsky, A., Golden, J.P., Tansey, M.G., Keck, C.L., Popescu, N.C., Johnson, E.M., Jr. and Milbrandt, J. (1998a) GFRalpha3 is an orphan member of the GDNF/neurturin/persephin receptor family. Proc Natl Acad Sci U S A, 95, 5801-5806.

Baloh, R.H., Tansey, M.G., Lampe, P.A., Fahrner, T.J., Enomoto, H., Simburger, K.S., Leitner, M.L., Araki, T., Johnson, E.M., Jr. and Milbrandt, J. (1998b) Artemin, a novel member of the GDNF ligand family, supports peripheral and central neurons and signals through the GFRalpha3-RET receptor complex. Neuron, 21, 1291-1302.

Banerjee, S., Saxena, N., Sengupta, K., Tawfik, O., Mayo, M.S. and Banerjee, S.K. (2003) WISP-2 gene in human breast cancer: estrogen and progesterone inducible expression and regulation of tumor cell proliferation. Neoplasia, 5, 63-73.

Barrett, J.C. and Kawasaki, E.S. (2003) Microarrays: the use of oligonucleotides and cDNA for the analysis of gene expression. Drug Discov Today, 8, 134-141.

Bartsch, J.E., Staren, E.D. and Appert, H.E. (2003) Adhesion and migration of extracellular matrix-stimulated breast cancer. J Surg Res, 110, 287-294.

Beatson, G. (1896) On the treatment of inoperable cases of carcinoma of the mamma: suggestions for a new method of treatment with illustrative cases. . Lancet, 2, 104-107.

Beral, V. (2003) Breast cancer and hormone-replacement therapy in the Million Women Study. Lancet, 362, 419-427.

Berry, J. (2005) Are all aromatase inhibitors the same? A review of controlled clinical trials in breast cancer. Clin Ther, 27, 1671-1684.

Berry, M., Metzger, D. and Chambon, P. (1990) Role of the two activating domains of the oestrogen receptor in the cell-type and promoter-context dependent agonistic activity of the anti-oestrogen 4-hydroxytamoxifen. Embo J, 9, 2811-2818.

Boenisch, T. (2006) Basic Immunochemistry (DAKO online publication): http://www.dakousa.com/ishbbasicimm.pdf.

Bohen, S.P., Kralli, A. and Yamamoto, K.R. (1995) Hold 'em and fold 'em: chaperones and

signal transduction. Science, 268, 1303-1304.

Borrello, M.G., Mercalli, E., Perego, C., Degl'Innocenti, D., Ghizzoni, S., Arighi, E., Eroini, B., Rizzetti, M.G. and Pierotti, M.A. (2002) Differential interaction of Enigma protein with the two RET isoforms. Biochem Biophys Res Commun, 296, 515-522.

Bouker, K.B., Skaar, T.C., Fernandez, D.R., O'Brien, K.A., Riggins, R.B., Cao, D. and Clarke, R. (2004) interferon regulatory factor-1 mediates the proapoptotic but not cell cycle arrest effects of the steroidal antiestrogen ICI 182,780 (faslodex, fulvestrant). Cancer Res, 64, 4030-4039.

Brand, F.X., Ravanel, N., Gauchez, A.S., Pasquier, D., Payan, R., Fagret, D. and Mousseau, M. (2006) Prospect for anti-HER2 receptor therapy in breast cancer. Anticancer Res, 26, 463-470.

Briand, P. and Lykkesfeldt, A.E. (1984) Effect of estrogen and antiestrogen on the human breast cancer cell line MCF-7 adapted to growth at low serum concentration. Cancer Res, 44, 1114-1119.

Brigstock, D.R. (2003) The CCN family: a new stimulus package. J Endocrinol, 178, 169-175.

Britton, D.J., Hutcheson, I.R., Knowlden, J.M., Barrow, D., Giles, M., McClelland, R.A., Gee, J.M. and Nicholson, R.I. (2006) Bidirectional cross talk between ERalpha and EGFR signalling pathways regulates tamoxifen-resistant growth. Breast Cancer Res Treat, 96, 131-146.

Brunner, N., Frandsen, T.L., Holst-Hansen, C., Bei, M., Thompson, E.W., Wakeling, A.E., Lippman, M.E. and Clarke, R. (1993) MCF7/LCC2: a 4-hydroxytamoxifen resistant human breast cancer variant that retains sensitivity to the steroidal antiestrogen ICI 182,780. Cancer Res, 53, 3229-3232.

Brzozowski, A.M., Pike, A.C., Dauter, Z., Hubbard, R.E., Bonn, T., Engstrom, O., Ohman, L., Greene, G.L., Gustafsson, J.A. and Carlquist, M. (1997) Molecular basis of agonism and antagonism in the oestrogen receptor. Nature, 389, 753-758.

Bucci, C., Chiariello, M., Lattero, D., Maiorano, M. and Bruni, C.B. (1999) Interaction cloning and characterization of the cDNA encoding the human prenylated rab acceptor (PRA1). Biochem Biophys Res Commun, 258, 657-662.

Burdall, S.E., Hanby, A.M., Lansdown, M.R. and Speirs, V. (2003) Breast cancer cell lines: friend or foe? Breast Cancer Res, 5, 89-95.

Butt, A.J., McNeil, C.M., Musgrove, E.A. and Sutherland, R.L. (2005) Downstream targets of growth factor and oestrogen signalling and endocrine resistance: the potential roles of c-Myc, cyclin D1 and cyclin E. Endocr Relat Cancer, 12 Suppl 1, S47-59.

Butte, A. (2002) The use and analysis of microarray data. Nat Rev Drug Discov, 1, 951-960.

Buzdar, A.U. (2001) Endocrine therapy in the treatment of metastatic breast cancer. Semin Oncol, 28, 291-304.

Camirand, A., Zakikhani, M., Young, F. and Pollak, M. (2005) Inhibition of insulin-like growth factor-1 receptor signaling enhances growth-inhibitory and proapoptotic effects of gefitinib (Iressa) in human breast cancer cells. Breast Cancer Res, 7, R570-579.

Campbell, R.A., Bhat-Nakshatri, P., Patel, N.M., Constantinidou, D., Ali, S. and Nakshatri, H. (2001) Phosphatidylinositol 3-kinase/AKT-mediated activation of estrogen receptor alpha: a new model for anti-estrogen resistance. J Biol Chem, 276, 9817-9824.

Campo, L., Turley, H., Han, C., Pezzella, F., Gatter, K.C., Harris, A.L. and Fox, S.B. (2005) Angiogenin is up-regulated in the nucleus and cytoplasm in human primary breast carcinoma and is associated with markers of hypoxia but not survival. J Pathol, 205, 585-591.

Campo McKnight, D.A., Sosnoski, D.M., Koblinski, J.E. and Gay, C.V. (2006) Roles of osteonectin in the migration of breast cancer cells into bone. J Cell Biochem, 97, 288-302.

Cancela, L., Hsieh, C.L., Francke, U. and Price, P.A. (1990) Molecular structure, chromosome assignment, and promoter organization of the human matrix Gla protein gene. J Biol Chem, 265, 15040-15048.

Cancer.Research.UK (2004) CancerStats Monograph 2004, Cancer Research UK, London.

Carninci, P. (2006) Tagging mammalian transcription complexity. Trends Genet, 22, 501-510.

Casey, G. (1997) The BRCA1 and BRCA2 breast cancer genes. Curr Opin Oncol, 9, 88-93.

Castagnetta, L.A., Lo Casto, M., Granata, O.M., Polito, L., Calabro, M., Lo Bue, A., Bellavia, V. and Carruba, G. (1996) Estrogen content and metabolism in human breast tumor tissues and cells. Ann N Y Acad Sci, 784, 314-324.

Castoria, G., Migliaccio, A., Bilancio, A., Di Domenico, M., de Falco, A., Lombardi, M., Fiorentino, R., Varricchio, L., Barone, M.V. and Auricchio, F. (2001) PI3-kinase in concert with Src promotes the S-phase entry of oestradiol-stimulated MCF-7 cells. Embo J, 20, 6050-6059.

Ceresa, B.P. (2006) Regulation of EGFR endocytic trafficking by rab proteins. Histol Histopathol, 21, 987-993.

Ceyhan, G.O., Giese, N.A., Erkan, M., Kerscher, A.G., Wente, M.N., Giese, T., Buchler, M.W. and Friess, H. (2006) The neurotrophic factor artemin promotes pancreatic cancer invasion. Ann Surg, 244, 274-281.

Chadderton, T., Wilson, C., Bewick, M. and Gluck, S. (1997) Evaluation of three rapid RNA extraction reagents: relevance for use in RT-PCR's and measurement of low level gene expression in clinical samples. Cell Mol Biol (Noisy-le-grand), 43, 1227-1234.

Chamaon, K., Kirches, E., Kanakis, D., Braeuninger, S., Dietzmann, K. and Mawrin, C. (2005) Regulation of the pituitary tumor transforming gene by insulin-like-growth factor-I and insulin differs between malignant and non-neoplastic astrocytes. Biochem Biophys Res Commun, 331, 86-92.

Chan, C.M., Martin, L.A., Johnston, S.R., Ali, S. and Dowsett, M. (2002) Molecular changes associated with the acquisition of oestrogen hypersensitivity in MCF-7 breast cancer cells on long-term oestrogen deprivation. J Steroid Biochem Mol Biol, 81, 333-341.

Chavrier, P. and Goud, B. (1999) The role of ARF and Rab GTPases in membrane transport. Curr Opin Cell Biol, 11, 466-475.

Cheer, S.M., Plosker, G.L., Simpson, D. and Wagstaff, A.J. (2005) Goserelin: a review of its use in the treatment of early breast cancer in premenopausal and perimenopausal women. Drugs, 65, 2639-2655.

Chen, D., Pace, P.E., Coombes, R.C. and Ali, S. (1999) Phosphorylation of human estrogen receptor alpha by protein kinase A regulates dimerization. Mol Cell Biol, 19, 1002-1015.

Chen, J.M., Dando, P.M., Rawlings, N.D., Brown, M.A., Young, N.E., Stevens, R.A., Hewitt, E., Watts, C. and Barrett, A.J. (1997) Cloning, isolation, and characterization of mammalian legumain, an asparaginyl endopeptidase. J Biol Chem, 272, 8090-8098.

Chen, L., O'Bryan, J.P., Smith, H.S. and Liu, E. (1990) Overexpression of matrix Gla protein mRNA in malignant human breast cells: isolation by differential cDNA hybridization. Oncogene, 5, 1391-1395.

Chen, L., Puri, R., Lefkowitz, E.J. and Kakar, S.S. (2000) Identification of the human pituitary tumor transforming gene (hPTTG) family: molecular structure, expression, and chromosomal localization. Gene, 248, 41-50.

Cheung, K.L., Willsher, P.C., Pinder, S.E., Ellis, I.O., Elston, C.W., Nicholson, R.I., Blamey, R.W. and Robertson, J.F. (1997) Predictors of response to second-line endocrine therapy for breast cancer. Breast Cancer Res Treat, 45, 219-224.

Chien, W. and Pei, L. (2000) A novel binding factor facilitates nuclear translocation and transcriptional activation function of the pituitary tumor-transforming gene product. J Biol Chem, 275, 19422-19427.

Chirgwin, J.M., Przybyla, A.E., MacDonald, R.J. and Rutter, W.J. (1979) Isolation of biologically active ribonucleic acid from sources enriched in ribonuclease. Biochemistry, 18, 5294-5299.

Cho-Rok, J., Yoo, J., Jang, Y.J., Kim, S., Chu, I.S., Yeom, Y.I., Choi, J.Y. and Im, D.S. (2006) Adenovirus-mediated transfer of siRNA against PTTG1 inhibits liver cancer cell growth in vitro and in vivo. Hepatology, 43, 1042-1052.

Chomczynski, P. and Sacchi, N. (1987) Single-step method of RNA isolation by acid guanidinium thiocyanate-phenol-chloroform extraction. Anal Biochem, 162, 156-159.

Christopoulou, L., Moore, J.D. and Tyler-Smith, C. (2003) Over-expression of wild-type Securin leads to aneuploidy in human cells. Cancer Lett, 202, 213-218.

Cichy, J. and Pure, E. (2003) The liberation of CD44. J Cell Biol, 161, 839-843.

Clarke, R., Leonessa, F., Welch, J.N. and Skaar, T.C. (2001a) Cellular and molecular pharmacology of antiestrogen action and resistance. Pharmacol Rev, 53, 25-71.

Clarke, R., Skaar, T.C., Bouker, K.B., Davis, N., Lee, Y.R., Welch, J.N. and Leonessa, F. (2001b) Molecular and pharmacological aspects of antiestrogen resistance. J Steroid Biochem Mol Biol, 76, 71-84.

Clem, A.L., Hamid, T. and Kakar, S.S. (2003) Characterization of the role of Sp1 and NF-Y in differential regulation of PTTG/securin expression in tumor cells. Gene, 322, 113-121.

Clemmons, D.R. (1998) Role of insulin-like growth factor binding proteins in controlling IGF actions. Mol Cell Endocrinol, 140, 19-24.

Clontech_BD-Biosciences:Atlas_pdf. (2006) BD Atlas Plastic Human 12K Microarray: http://www.clontech.com/clontech/archive/OCT02UPD/pdf/Atlas_Plastic.pdf.

Clontech_Nucleotrap.(2006) http://www.clontech.com/clontech/archive/APR99UPD/nucleospin.shtml.

Cole, M.P., Jones, C.T. and Todd, I.D. (1971) A new anti-oestrogenic agent in late breast cancer. An early clinical appraisal of ICI46474. Br J Cancer, 25, 270-275.

Cooper, C.S. (2001) Applications of microarray technology in breast cancer research. Breast Cancer Res, 3, 158-175.

Coopman, P., Garcia, M., Brunner, N., Derocq, D., Clarke, R. and Rochefort, H. (1994) Anti-proliferative and anti-estrogenic effects of ICI 164,384 and ICI 182,780 in 4-OH-tamoxifen-resistant human breast-cancer cells. Int J Cancer, 56, 295-300.

Cristofanilli, M. (2006) Circulating tumor cells, disease progression, and survival in metastatic breast cancer. Semin Oncol, 33, S9-14.

Davidson, B., Konstantinovsky, S., Nielsen, S., Dong, H.P., Berner, A., Vyberg, M. and Reich, R. (2004) Altered expression of metastasis-associated and regulatory molecules in effusions from breast cancer patients: a novel model for tumor progression. Clin Cancer Res, 10, 7335-7346.

de Launoit, Y., Chotteau-Lelievre, A., Beaudoin, C., Coutte, L., Netzer, S., Brenner, C., Huvent, I. and Baert, J.L. (2000) The PEA3 group of ETS-related transcription factors. Role in breast cancer metastasis. Adv Exp Med Biol, 480, 107-116.

Demetri, G.D., Fletcher, C.D., Mueller, E., Sarraf, P., Naujoks, R., Campbell, N., Spiegelman, B.M. and Singer, S. (1999) Induction of solid tumor differentiation by the

peroxisome proliferator-activated receptor-gamma ligand troglitazone in patients with liposarcoma. Proc Natl Acad Sci U S A, 96, 3951-3956.

DeNardo, D.G., Kim, H.T., Hilsenbeck, S., Cuba, V., Tsimelzon, A. and Brown, P.H. (2005) Global gene expression analysis of estrogen receptor transcription factor cross talk in breast cancer: identification of estrogen-induced/activator protein-1-dependent genes. Mol Endocrinol, 19, 362-378.

Desai, K.V., Kavanaugh, C.J., Calvo, A. and Green, J.E. (2002) Chipping away at breast cancer: insights from microarray studies of human and mouse mammary cancer. Endocr Relat Cancer, 9, 207-220.

Desvergne, B. and Wahli, W. (1999) Peroxisome proliferator-activated receptors: nuclear control of metabolism. Endocr Rev, 20, 649-688.

Dey, B.R., Spence, S.L., Nissley, P. and Furlanetto, R.W. (1998) Interaction of human suppressor of cytokine signaling (SOCS)-2 with the insulin-like growth factor-I receptor. J Biol Chem, 273, 24095-24101.

Dharmacon.smartpool.url. http://www.dharmacon.com/tech/faqanswer.aspx?faqid=12.

Dixon, J.M. (2004) Exemestane and aromatase inhibitors in the management of advanced breast cancer. Expert Opin Pharmacother, 5, 307-316.

Dominguez, A., Ramos-Morales, F., Romero, F., Rios, R.M., Dreyfus, F., Tortolero, M. and Pintor-Toro, J.A. (1998) hpttg, a human homologue of rat pttg, is overexpressed in hematopoietic neoplasms. Evidence for a transcriptional activation function of hPTTG. Oncogene, 17, 2187-2193.

Dorssers, L.C., van Agthoven, T., Brinkman, A., Veldscholte, J., Smid, M. and Dechering, K.J. (2005) Breast cancer oestrogen independence mediated by BCAR1 or BCAR3 genes is transmitted through mechanisms distinct from the oestrogen receptor signalling pathway or the epidermal growth factor receptor signalling pathway. Breast Cancer Res, 7, R82-92.

Dowsett, M., Martin, L.A., Smith, I. and Johnston, S. (2005) Mechanisms of resistance to aromatase inhibitors. J Steroid Biochem Mol Biol, 95, 167-172.

Draghici, S., Khatri, P., Eklund, A.C. and Szallasi, Z. (2006) Reliability and reproducibility issues in DNA microarray measurements. Trends Genet, 22, 101-109.

Duan, R., Xie, W., Li, X., McDougal, A. and Safe, S. (2002) Estrogen regulation of c-fos gene expression through phosphatidylinositol-3-kinase-dependent activation of serum response factor in MCF-7 breast cancer cells. Biochem Biophys Res Commun, 294, 384-394.

Dukes, M., Waterton, J.C. and Wakeling, A.E. (1993) Antiuterotrophic effects of the pure antioestrogen ICI 182,780 in adult female monkeys (Macaca nemestrina): quantitative magnetic resonance imaging. J Endocrinol, 138, 203-210.

Earp, H.S., Dawson, T.L., Li, X. and Yu, H. (1995) Heterodimerization and functional interaction between EGF receptor family members: a new signaling paradigm with implications for breast cancer research. Breast Cancer Res Treat, 35, 115-132.

Easton, D.F. (1999) How many more breast cancer predisposition genes are there? Breast Cancer Res, 1, 14-17.

Eddy, S.F., Guo, S., Demicco, E.G., Romieu-Mourez, R., Landesman-Bollag, E., Seldin, D.C. and Sonenshein, G.E. (2005) Inducible IkappaB kinase/IkappaB kinase epsilon expression is induced by CK2 and promotes aberrant nuclear factor-kappaB activation in breast cancer cells. Cancer Res, 65, 11375-11383.

Eisen, M.B., Spellman, P.T., Brown, P.O. and Botstein, D. (1998) Cluster analysis and display of genome-wide expression patterns. Proc Natl Acad Sci U S A, 95, 14863-14868.

Eisen, M.B. and Brown, P.O. (1999) DNA arrays for analysis of gene expression. Methods Enzymol, 303, 179-205.

El-Tanani, M., Platt-Higgins, A., Rudland, P.S. and Campbell, F.C. (2004) Ets gene PEA3 cooperates with beta-catenin-Lef-1 and c-Jun in regulation of osteopontin transcription. J Biol Chem, 279, 20794-20806.

Elston, C.W. and Ellis, I.O. (2002) Pathological prognostic factors in breast cancer. I. The value of histological grade in breast cancer: experience from a large study with long-term follow-up. C. W. Elston & I. O. Ellis. Histopathology 1991; 19; 403-410. Histopathology, 41, 151.

Endoh, H., Maruyama, K., Masuhiro, Y., Kobayashi, Y., Goto, M., Tai, H., Yanagisawa, J., Metzger, D., Hashimoto, S. and Kato, S. (1999) Purification and identification of p68 RNA helicase acting as a transcriptional coactivator specific for the activation function 1 of human estrogen receptor alpha. Mol Cell Biol, 19, 5363-5372.

Engel, L.W. and Young, N.A. (1978) Human breast carcinoma cells in continuous culture: a review. Cancer Res, 38, 4327-4339.

Enmark, E., Pelto-Huikko, M., Grandien, K., Lagercrantz, S., Lagercrantz, J., Fried, G., Nordenskjold, M. and Gustafsson, J.A. (1997) Human estrogen receptor beta-gene structure, chromosomal localization, and expression pattern. J Clin Endocrinol Metab, 82, 4258-4265.

Farabegoli, F., Ceccarelli, C., Santini, D. and Taffurelli, M. (2005) Suppressor of cytokine signalling 2 (SOCS-2) expression in breast carcinoma. J Clin Pathol, 58, 1046-1050.

Fawell, S.E., Lees, J.A., White, R. and Parker, M.G. (1990) Characterization and colocalization of steroid binding and dimerization activities in the mouse estrogen receptor. Cell, 60, 953-962.

Fenner, M.H. and Elstner, E. (2005) Peroxisome proliferator-activated receptor-gamma

ligands for the treatment of breast cancer. Expert Opin Investig Drugs, 14, 557-568.

Fisher, B., Costantino, J.P., Wickerham, D.L., Redmond, C.K., Kavanah, M., Cronin, W.M., Vogel, V., Robidoux, A., Dimitrov, N., Atkins, J., Daly, M., Wieand, S., Tan-Chiu, E., Ford, L. and Wolmark, N. (1998) Tamoxifen for prevention of breast cancer: report of the National Surgical Adjuvant Breast and Bowel Project P-1 Study. J Natl Cancer Inst, 90, 1371-1388.

Fodor, S.P., Rava, R.P., Huang, X.C., Pease, A.C., Holmes, C.P. and Adams, C.L. (1993) Multiplexed biochemical assays with biological chips. Nature, 364, 555-556.

Forster, T., Roy, D. and Ghazal, P. (2003) Experiments using microarray technology: limitations and standard operating procedures. J Endocrinol, 178, 195-204.

Foster, J.S., Henley, D.C., Ahamed, S. and Wimalasena, J. (2001) Estrogens and cell-cycle regulation in breast cancer. Trends Endocrinol Metab, 12, 320-327.

Franscini, N., Bachli, E.B., Blau, N., Leikauf, M.S., Schaffner, A. and Schoedon, G. (2004) Gene expression profiling of inflamed human endothelial cells and influence of activated protein C. Circulation, 110, 2903-2909.

Frasor, J., Chang, E.C., Komm, B., Lin, C.Y., Vega, V.B., Liu, E.T., Miller, L.D., Smeds, J., Bergh, J. and Katzenellenbogen, B.S. (2006) Gene expression preferentially regulated by tamoxifen in breast cancer cells and correlations with clinical outcome. Cancer Res, 66, 7334-7340.

Frasor, J., Stossi, F., Danes, J.M., Komm, B., Lyttle, C.R. and Katzenellenbogen, B.S. (2004) Selective estrogen receptor modulators: discrimination of agonistic versus antagonistic activities by gene expression profiling in breast cancer cells. Cancer Res, 64, 1522-1533.

Frittitta, L., Cerrato, A., Sacco, M.G., Weidner, N., Goldfine, I.D. and Vigneri, R. (1997) The insulin receptor content is increased in breast cancers initiated by three different oncogenes in transgenic mice. Breast Cancer Res Treat, 45, 141-147.

Frogne, T., Jepsen, J.S., Larsen, S.S., Fog, C.K., Brockdorff, B.L. and Lykkesfeldt, A.E. (2005) Antiestrogen-resistant human breast cancer cells require activated protein kinase B/Akt for growth. Endocr Relat Cancer, 12, 599-614.

Fultz, K.E. and Gerner, E.W. (2002) APC-dependent regulation of ornithine decarboxylase in human colon tumor cells. Mol Carcinog, 34, 10-18.

Galat, A. (1993) Peptidylproline cis-trans-isomerases: immunophilins. Eur J Biochem, 216, 689-707.

Gazdar, A.F., Kurvari, V., Virmani, A., Gollahon, L., Sakaguchi, M., Westerfield, M., Kodagoda, D., Stasny, V., Cunningham, H.T., Wistuba, II, Tomlinson, G., Tonk, V., Ashfaq, R., Leitch, A.M., Minna, J.D. and Shay, J.W. (1998) Characterization of paired tumor and non-tumor cell lines established from patients with breast cancer. Int J

Cancer, 78, 766-774.

Gee, J.M., Ellis, I.O., Robertson, J.F., Willsher, P., McClelland, R.A., Hewitt, K.N., Blamey, R.W. and Nicholson, R.I. (1995) Immunocytochemical localization of Fos protein in human breast cancers and its relationship to a series of prognostic markers and response to endocrine therapy. Int J Cancer, 64, 269-273.

Gee, J.M., Willsher, P.C., Kenny, F.S., Robertson, J.F., Pinder, S.E., Ellis, I.O. and Nicholson, R.I. (1999) Endocrine response and resistance in breast cancer: a role for the transcription factor Fos. Int J Cancer, 84, 54-61.

Gee, J.M., Robertson, J.F., Ellis, I.O. and Nicholson, R.I. (2001) Phosphorylation of ERK1/2 mitogen-activated protein kinase is associated with poor response to anti-hormonal therapy and decreased patient survival in clinical breast cancer. Int J Cancer, 95, 247-254.

Gee, J.M., Harper, M.E., Hutcheson, I.R., Madden, T.A., Barrow, D., Knowlden, J.M., McClelland, R.A., Jordan, N., Wakeling, A.E. and Nicholson, R.I. (2003) The antiepidermal growth factor receptor agent gefitinib (ZD1839/Iressa) improves antihormone response and prevents development of resistance in breast cancer in vitro. Endocrinology, 144, 5105-5117.

Gee, J.M., Robertson, J.F., Gutteridge, E., Ellis, I.O., Pinder, S.E., Rubini, M. and Nicholson, R.I. (2005) Epidermal growth factor receptor/HER2/insulin-like growth factor receptor signalling and oestrogen receptor activity in clinical breast cancer. Endocr Relat Cancer, 12 Suppl 1, S99-S111.

Genecards.url. (2006) http://bioinfo.weizmann.ac.il/cards/index.shtml.

GeneSifter.url. (2006) http://help.GeneSifter.net/help/workflow/workflow.htm.

Gershon, D. (2002) Microarray technology: an array of opportunities. Nature, 416, 885-891.

Gilham, P.T. and Rosenberg, M. (1971) The isolation of 3'-terminal polynucleotides from RNA molecules. Biochim Biophys Acta, 246, 337-340.

Goss, P.E. (1999) Risks versus benefits in the clinical application of aromatase inhibitors. Endocr Relat Cancer, 6, 325-332.

Green, D.R. and Reed, J.C. (1998) Mitochondria and apoptosis. Science, 281, 1309-1312.

Green, S., Walter, P., Kumar, V., Krust, A., Bornert, J.M., Argos, P. and Chambon, P. (1986) Human oestrogen receptor cDNA: sequence, expression and homology to v-erb-A. Nature, 320, 134-139.

Grieco, M., Santoro, M., Berlingieri, M.T., Melillo, R.M., Donghi, R., Bongarzone, I., Pierotti, M.A., Della Porta, G., Fusco, A. and Vecchio, G. (1990) PTC is a novel rearranged form of the ret proto-oncogene and is frequently detected in vivo in human thyroid papillary carcinomas. Cell, 60, 557-563.

Guiochon-Mantel, A., Delabre, K., Lescop, P. and Milgrom, E. (1996) The Ernst Schering Poster Award. Intracellular traffic of steroid hormone receptors. J Steroid Biochem Mol Biol, 56, 3-9.

Guo, Y., Harris, R.B., Rosson, D., Boorman, D. and O'Brien, T.G. (2000) Functional analysis of human ornithine decarboxylase alleles. Cancer Res, 60, 6314-6317.

Gutierrez, M.C., Detre, S., Johnston, S., Mohsin, S.K., Shou, J., Allred, D.C., Schiff, R., Osborne, C.K. and Dowsett, M. (2005) Molecular changes in tamoxifen-resistant breast cancer: relationship between estrogen receptor, HER-2, and p38 mitogen-activated protein kinase. J Clin Oncol, 23, 2469-2476.

Hall, J.M. and McDonnell, D.P. (1999) The estrogen receptor beta-isoform (ERbeta) of the human estrogen receptor modulates ERalpha transcriptional activity and is a key regulator of the cellular response to estrogens and antiestrogens. Endocrinology, 140, 5566-5578.

Hall, J.M., Couse, J.F. and Korach, K.S. (2001) The multifaceted mechanisms of estradiol and estrogen receptor signaling. J Biol Chem, 276, 36869-36872.

Hamelers, I.H. and Steenbergh, P.H. (2003) Interactions between estrogen and insulin-like growth factor signaling pathways in human breast tumor cells. Endocr Relat Cancer, 10, 331-345.

Hamid, T. and Kakar, S.S. (2003) PTTG and cancer. Histol Histopathol, 18, 245-251.

Hamid, T. and Kakar, S.S. (2004) PTTG/securin activates expression of p53 and modulates its function. Mol Cancer, 3, 18.

Hanahan, D. and Weinberg, R.A. (2000) The hallmarks of cancer. Cell, 100, 57-70.

Hapke, S., Kessler, H., Luber, B., Benge, A., Hutzler, P., Hofler, H., Schmitt, M. and Reuning, U. (2003) Ovarian cancer cell proliferation and motility is induced by engagement of integrin alpha(v)beta3/Vitronectin interaction. Biol Chem, 384, 1073-1083.

Happerfield, L.C., Miles, D.W., Barnes, D.M., Thomsen, L.L., Smith, P. and Hanby, A. (1997) The localization of the insulin-like growth factor receptor 1 (IGFR-1) in benign and malignant breast tissue. J Pathol, 183, 412-417.

He, T.C., Chan, T.A., Vogelstein, B. and Kinzler, K.W. (1999) PPARdelta is an APC-regulated target of nonsteroidal anti-inflammatory drugs. Cell, 99, 335-345.

Heaney, A.P. and Melmed, S. (1999) Pituitary tumour transforming gene: a novel factor in pituitary tumour formation. Baillieres Best Pract Res Clin Endocrinol Metab, 13, 367-380.

Heaney, A.P., Singson, R., McCabe, C.J., Nelson, V., Nakashima, M. and Melmed, S. (2000) Expression of pituitary-tumour transforming gene in colorectal tumours. Lancet, 355, 716-719.

Heaney, A.P., Nelson, V., Fernando, M. and Horwitz, G. (2001) Transforming events in thyroid tumorigenesis and their association with follicular lesions. J Clin Endocrinol Metab, 86, 5025-5032.

Heaney, A.P., Fernando, M. and Melmed, S. (2002) Functional role of estrogen in pituitary tumor pathogenesis. J Clin Invest, 109, 277-283.

Higashino, F., Yoshida, K., Noumi, T., Seiki, M. and Fujinaga, K. (1995) Ets-related protein E1A-F can activate three different matrix metalloproteinase gene promoters. Oncogene, 10, 1461-1463.

Hirota, S., Ito, A., Nagoshi, J., Takeda, M., Kurata, A., Takatsuka, Y., Kohri, K., Nomura, S. and Kitamura, Y. (1995) Expression of bone matrix protein messenger ribonucleic acids in human breast cancers. Possible involvement of osteopontin in development of calcifying foci. Lab Invest, 72, 64-69.

Hiscox, S., Morgan, L., Barrow, D., Dutkowskil, C., Wakeling, A. and Nicholson, R.I. (2004) Tamoxifen resistance in breast cancer cells is accompanied by an enhanced motile and invasive phenotype: inhibition by gefitinib ('Iressa', ZD1839). Clin Exp Metastasis, 21, 201-212.

Hiscox, S., Jiang, W.G., Obermeier, K., Taylor, K., Morgan, L., Burmi, R., Barrow, D. and Nicholson, R.I. (2006a) Tamoxifen resistance in MCF7 cells promotes EMT-like behaviour and involves modulation of beta-catenin phosphorylation. Int J Cancer, 118, 290-301.

Hiscox, S., Morgan, L., Green, T.P., Barrow, D., Gee, J. and Nicholson, R.I. (2006b) Elevated Src activity promotes cellular invasion and motility in tamoxifen resistant breast cancer cells. Breast Cancer Res Treat, 97, 263-274.

Hodges, L.C., Cook, J.D., Lobenhofer, E.K., Li, L., Bennett, L., Bushel, P.R., Aldaz, C.M., Afshari, C.A. and Walker, C.L. (2003) Tamoxifen functions as a molecular agonist inducing cell cycle-associated genes in breast cancer cells. Mol Cancer Res, 1, 300-311.

Howe, L.R. and Brown, A.M. (2004) Wnt signaling and breast cancer. Cancer Biol Ther, 3, 36-41.

Howell, A., Osborne, C.K., Morris, C. and Wakeling, A.E. (2000) ICI 182,780 (Faslodex): development of a novel, "pure" antiestrogen. Cancer, 89, 817-825.

Howell, A., Robertson, J.F., Quaresma Albano, J., Aschermannova, A., Mauriac, L., Kleeberg, U.R., Vergote, I., Erikstein, B., Webster, A. and Morris, C. (2002) Fulvestrant, formerly ICI 182,780, is as effective as anastrozole in postmenopausal women with advanced breast cancer progressing after prior endocrine treatment. J Clin Oncol, 20, 3396-3403.

Howell, S.J., Johnston, S.R. and Howell, A. (2004) The use of selective estrogen receptor modulators and selective estrogen receptor down-regulators in breast cancer. Best Pract

Res Clin Endocrinol Metab, 18, 47-66.

Howell, A. (2005) The future of fulvestrant ("Faslodex"). Cancer Treat Rev, 31 Suppl 2, S26-33.

Howell, A. (2006) Fulvestrant ('Faslodex'): current and future role in breast cancer management. Crit Rev Oncol Hematol, 57, 265-273.

Hu, X.F., Veroni, M., De Luise, M., Wakeling, A., Sutherland, R., Watts, C.K. and Zalcberg, J.R. (1993) Circumvention of tamoxifen resistance by the pure anti-estrogen ICI 182,780. Int J Cancer, 55, 873-876.

Hughes, T.R., Mao, M., Jones, A.R., Burchard, J., Marton, M.J., Shannon, K.W., Lefkowitz, S.M., Ziman, M., Schelter, J.M., Meyer, M.R., Kobayashi, S., Davis, C., Dai, H., He, Y.D., Stephaniants, S.B., Cavet, G., Walker, W.L., West, A., Coffey, E., Shoemaker, D.D., Stoughton, R., Blanchard, A.P., Friend, S.H. and Linsley, P.S. (2001) Expression profiling using microarrays fabricated by an ink-jet oligonucleotide synthesizer. Nat Biotechnol, 19, 342-347.

Hurelbrink, C.B. and Barker, R.A. (2004) The potential of GDNF as a treatment for Parkinson's disease. Exp Neurol, 185, 1-6.

Hutcheson, I.R., Knowlden, J.M., Madden, T.A., Barrow, D., Gee, J.M., Wakeling, A.E. and Nicholson, R.I. (2003) Oestrogen receptor-mediated modulation of the EGFR/MAPK pathway in tamoxifen-resistant MCF-7 cells. Breast Cancer Res Treat, 81, 81-93.

Ibrahim, Y.H. and Yee, D. (2005) Insulin-like growth factor-I and breast cancer therapy. Clin Cancer Res, 11, 944s-950s.

Inoue, A., Yoshida, N., Omoto, Y., Oguchi, S., Yamori, T., Kiyama, R. and Hayashi, S. (2002) Development of cDNA microarray for expression profiling of estrogen-responsive genes. J Mol Endocrinol, 29, 175-192.

Ito, Y., Okada, Y., Sato, M., Sawai, H., Funahashi, H., Murase, T., Hayakawa, T. and Manabe, T. (2005) Expression of glial cell line-derived neurotrophic factor family members and their receptors in pancreatic cancers. Surgery, 138, 788-794.

Itoh, T., Karlsberg, K., Kijima, I., Yuan, Y.C., Smith, D., Ye, J. and Chen, S. (2005) Letrozole-, anastrozole-, and tamoxifen-responsive genes in MCF-7aro cells: a microarray approach. Mol Cancer Res, 3, 203-218.

Jansen, M.P., Foekens, J.A., van Staveren, I.L., Dirkzwager-Kiel, M.M., Ritstier, K., Look, M.P., Meijer-van Gelder, M.E., Sieuwerts, A.M., Portengen, H., Dorssers, L.C., Klijn, J.G. and Berns, E.M. (2005) Molecular classification of tamoxifen-resistant breast carcinomas by gene expression profiling. J Clin Oncol, 23, 732-740.

Jarrous, N., Eder, P.S., Wesolowski, D. and Altman, S. (1999) Rpp14 and Rpp29, two protein subunits of human ribonuclease P. Rna, 5, 153-157.

Jeltsch, J.M., Roberts, M., Schatz, C., Garnier, J.M., Brown, A.M. and Chambon, P. (1987) Structure of the human oestrogen-responsive gene pS2. Nucleic Acids Res, 15, 1401-1414.

Jensen, E. and Jacobson, H. (1962) Basic guides to the mechanism of estrogen action. Recent Prog Horm Res, 18, 387-414.

Jensen, E.V., Block, G.E., Smith, S., Kyser, K. and DeSombre, E.R. (1971) Estrogen receptors and breast cancer response to adrenalectomy. Natl Cancer Inst Monogr, 34, 55-70.

Joel, P.B., Traish, A.M. and Lannigan, D.A. (1995) Estradiol and phorbol ester cause phosphorylation of serine 118 in the human estrogen receptor. Mol Endocrinol, 9, 1041-1052.

Joel, P.B., Traish, A.M. and Lannigan, D.A. (1998) Estradiol-induced phosphorylation of serine 118 in the estrogen receptor is independent of p42/p44 mitogen-activated protein kinase. J Biol Chem, 273, 13317-13323.

Johnson, A.C., Murphy, B.A., Matelis, C.M., Rubinstein, Y., Piebenga, E.C., Akers, L.M., Neta, G., Vinson, C. and Birrer, M. (2000) Activator protein-1 mediates induced but not basal epidermal growth factor receptor gene expression. Mol Med, 6, 17-27.

Johnston, S.R. and Dowsett, M. (2003) Aromatase inhibitors for breast cancer: lessons from the laboratory. Nat Rev Cancer, 3, 821-831.

Johnston, S.R. (2005) Combinations of endocrine and biological agents: present status of therapeutic and presurgical investigations. Clin Cancer Res, 11, 889s-899s.

Johnston, S.R. (2006) Clinical efforts to combine endocrine agents with targeted therapies against epidermal growth factor receptor/human epidermal growth factor receptor 2 and mammalian target of rapamycin in breast cancer. Clin Cancer Res, 12, 1061s-1068s.

Johnstone, R.W., Wang, J., Tommerup, N., Vissing, H., Roberts, T. and Shi, Y. (1998) Ciao 1 is a novel WD40 protein that interacts with the tumor suppressor protein WT1. J Biol Chem, 273, 10880-10887.

Jones, H.E., Goddard, L., Gee, J.M., Hiscox, S., Rubini, M., Barrow, D., Knowlden, J.M., Williams, S., Wakeling, A.E. and Nicholson, R.I. (2004) Insulin-like growth factor-I receptor signalling and acquired resistance to gefitinib (ZD1839; Iressa) in human breast and prostate cancer cells. Endocr Relat Cancer, 11, 793-814.

Jones, H.E., Gee, J.M., Taylor, K.M., Barrow, D., Williams, H.D., Rubini, M. and Nicholson, R.I. (2005) Development of strategies for the use of anti-growth factor treatments. Endocr Relat Cancer, 12 Suppl 1, S173-182.

Jordan, N.J., Gee, J.M., Barrow, D., Wakeling, A.E. and Nicholson, R.I. (2004) Increased constitutive activity of PKB/Akt in tamoxifen resistant breast cancer MCF-7 cells. Breast Cancer Res Treat, 87, 167-180.

Kakar, S.S. (1998) Assignment of the human tumor transforming gene TUTR1 to chromosome band 5q35.1 by fluorescence in situ hybridization. Cytogenet Cell Genet, 83, 93-95.

Kakar, S.S. and Jennes, L. (1999) Molecular cloning and characterization of the tumor transforming gene (TUTR1): a novel gene in human tumorigenesis. Cytogenet Cell Genet, 84, 211-216.

Kakar, S.S. and Malik, M.T. (2006) Suppression of lung cancer with siRNA targeting PTTG. Int J Oncol, 29, 387-395.

Karnik, P.S., Kulkarni, S., Liu, X.P., Budd, G.T. and Bukowski, R.M. (1994) Estrogen receptor mutations in tamoxifen-resistant breast cancer. Cancer Res, 54, 349-353.

Kato, S., Endoh, H., Masuhiro, Y., Kitamoto, T., Uchiyama, S., Sasaki, H., Masushige, S., Gotoh, Y., Nishida, E., Kawashima, H. and et al. (1995) Activation of the estrogen receptor through phosphorylation by mitogen-activated protein kinase. Science, 270, 1491-1494.

Kaufman, P. and Rousseeuw, P. (2005) Finding Groups in Data: An Introduction to Cluster Analysis. John WIley and Sons.

Kelsey, J.L. and Berkowitz, G.S. (1988) Breast cancer epidemiology. Cancer Res, 48, 5615-5623.

Kelsey, J.L., Gammon, M.D. and John, E.M. (1993) Reproductive factors and breast cancer. Epidemiol Rev, 15, 36-47.

Key, M. (2006) Antigen Retrieval (DAKO online publication): http://www.dakousa.com/ishbantigenretr.pdf.

Key, T.J. and Pike, M.C. (1988) The role of oestrogens and progestagens in the epidemiology and prevention of breast cancer. Eur J Cancer Clin Oncol, 24, 29-43.

Key, T.J., Verkasalo, P.K. and Banks, E. (2001) Epidemiology of breast cancer. Lancet Oncol, 2, 133-140.

Kho, P.S., Wang, Z., Zhuang, L., Li, Y., Chew, J.L., Ng, H.H., Liu, E.T. and Yu, Q. (2004) p53-regulated transcriptional program associated with genotoxic stress-induced apoptosis. J Biol Chem, 279, 21183-21192.

Kim, D.S., Franklyn, J.A., Stratford, A.L., Boelaert, K., Watkinson, J.C., Eggo, M.C. and McCabe, C.J. (2006) Pituitary tumor-transforming gene regulates multiple downstream angiogenic genes in thyroid cancer. J Clin Endocrinol Metab, 91, 1119-1128.

King, H.C. and Sinha, A.A. (2001) Gene expression profile analysis by DNA microarrays: promise and pitfalls. Jama, 286, 2280-2288.

Kirkby, K.A. and Adin, C.A. (2006) Products of heme oxygenase and their potential therapeutic applications. Am J Physiol Renal Physiol, 290, F563-571.

Kirkegaard, T., Witton, C.J., McGlynn, L.M., Tovey, S.M., Dunne, B., Lyon, A. and

Bartlett, J.M. (2005) AKT activation predicts outcome in breast cancer patients treated with tamoxifen. J Pathol, 207, 139-146.

Klinge, C.M. (2000) Estrogen receptor interaction with co-activators and co-repressors. Steroids, 65, 227-251.

Knowlden, J.M., Gee, J.M., Bryant, S., McClelland, R.A., Manning, D.L., Mansel, R., Ellis, I.O., Blamey, R.W., Robertson, J.F. and Nicholson, R.I. (1997) Use of reverse transcription-polymerase chain reaction methodology to detect estrogen-regulated gene expression in small breast cancer specimens. Clin Cancer Res, 3, 2165-2172.

Knowlden, J.M., Hutcheson, I.R., Jones, H.E., Madden, T., Gee, J.M., Harper, M.E., Barrow, D., Wakeling, A.E. and Nicholson, R.I. (2003) Elevated levels of epidermal growth factor receptor/c-erbB2 heterodimers mediate an autocrine growth regulatory pathway in tamoxifen-resistant MCF-7 cells. Endocrinology, 144, 1032-1044.

Knowlden, J.M., Hutcheson, I.R., Barrow, D., Gee, J.M. and Nicholson, R.I. (2005) Insulin-like growth factor-I receptor signaling in tamoxifen-resistant breast cancer: a supporting role to the epidermal growth factor receptor. Endocrinology, 146, 4609-4618.

Knudsen, S. (2002) A Biologists Guide to Analysis of Microarray Data. John Wiley and Sons.

Kodama, Y., Asai, N., Kawai, K., Jijiwa, M., Murakumo, Y., Ichihara, M. and Takahashi, M. (2005) The RET proto-oncogene: a molecular therapeutic target in thyroid cancer. Cancer Sci, 96, 143-148.

Kops, G.J., Weaver, B.A. and Cleveland, D.W. (2005) On the road to cancer: aneuploidy and the mitotic checkpoint. Nat Rev Cancer, 5, 773-785.

Kousteni, S., Bellido, T., Plotkin, L.I., O'Brien, C.A., Bodenner, D.L., Han, L., Han, K., DiGregorio, G.B., Katzenellenbogen, J.A., Katzenellenbogen, B.S., Roberson, P.K., Weinstein, R.S., Jilka, R.L. and Manolagas, S.C. (2001) Nongenotropic, sex-nonspecific signaling through the estrogen or androgen receptors: dissociation from transcriptional activity. Cell, 104, 719-730.

Kousteni, S., Han, L., Chen, J.R., Almeida, M., Plotkin, L.I., Bellido, T. and Manolagas, S.C. (2003) Kinase-mediated regulation of common transcription factors accounts for the bone-protective effects of sex steroids. J Clin Invest, 111, 1651-1664.

Kraus, W.L., Montano, M.M. and Katzenellenbogen, B.S. (1994) Identification of multiple, widely spaced estrogen-responsive regions in the rat progesterone receptor gene. Mol Endocrinol, 8, 952-969.

Kristensen, V.N., Sorlie, T., Geisler, J., Yoshimura, N., Linegjaerde, O.C., Glad, I., Frigessi, A., Harada, N., Lonning, P.E. and Borresen-Dale, A.L. (2005) Effects of anastrozole on the intratumoral gene expression in locally advanced breast cancer. J

Steroid Biochem Mol Biol, 95, 105-111.

Kuiper, G.G., Enmark, E., Pelto-Huikko, M., Nilsson, S. and Gustafsson, J.A. (1996) Cloning of a novel receptor expressed in rat prostate and ovary. Proc Natl Acad Sci U S A, 93, 5925-5930.

Kumar, V., Green, S., Stack, G., Berry, M., Jin, J.R. and Chambon, P. (1987) Functional domains of the human estrogen receptor. Cell, 51, 941-951.

Kuroda, S., Tokunaga, C., Kiyohara, Y., Higuchi, O., Konishi, H., Mizuno, K., Gill, G.N. and Kikkawa, U. (1996) Protein-protein interaction of zinc finger LIM domains with protein kinase C. J Biol Chem, 271, 31029-31032.

Kurokawa, H., Lenferink, A.E., Simpson, J.F., Pisacane, P.I., Sliwkowski, M.X., Forbes, J.T. and Arteaga, C.L. (2000) Inhibition of HER2/neu (erbB-2) and mitogen-activated protein kinases enhances tamoxifen action against HER2-overexpressing, tamoxifen-resistant breast cancer cells. Cancer Res, 60, 5887-5894.

Kurokawa, K., Kawai, K., Hashimoto, M., Ito, Y. and Takahashi, M. (2003) Cell signalling and gene expression mediated by RET tyrosine kinase. J Intern Med, 253, 627-633.

Lacroix, M. and Leclercq, G. (2004) Relevance of breast cancer cell lines as models for breast tumours: an update. Breast Cancer Res Treat, 83, 249-289.

Laemmli, U.K. (1970) Cleavage of structural proteins during the assembly of the head of bacteriophage T4. Nature, 227, 680-685.

Land, H., Parada, L.F. and Weinberg, R.A. (1983) Tumorigenic conversion of primary embryo fibroblasts requires at least two cooperating oncogenes. Nature, 304, 596-602.

Lannigan, D.A. (2003) Estrogen receptor phosphorylation. Steroids, 68, 1-9.

Lasfargues, E.Y. and Ozzello, L. (1958) Cultivation of human breast carcinomas. J Natl Cancer Inst, 21, 1131-1147.

Le Goff, P., Montano, M.M., Schodin, D.J. and Katzenellenbogen, B.S. (1994) Phosphorylation of the human estrogen receptor. Identification of hormone-regulated sites and examination of their influence on transcriptional activity. J Biol Chem, 269, 4458-4466.

Leevers, S.J., Vanhaesebroeck, B. and Waterfield, M.D. (1999) Signalling through phosphoinositide 3-kinases: the lipids take centre stage. Curr Opin Cell Biol, 11, 219-225.

Lenchik, N.I., Desiderio, D.M. and Gerling, I.C. (2005) Two-dimensional gel electrophoresis characterization of the mouse leukocyte proteome, using a tri-reagent for protein extraction. Proteomics, 5, 2202-2209.

Lerner, L.J., Holthaus, F.J., Jr. and Thompson, C.R. (1958) A non-steroidal estrogen antiagonist 1-(p-2-diethylaminoethoxyphenyl)-1-phenyl-2-p-methoxyphenyl ethanol. Endocrinology, 63, 295-318.

Leung, Y.F. and Cavalieri, D. (2003) Fundamentals of cDNA microarray data analysis. Trends Genet, 19, 649-659.

Levenson, A.S. and Jordan, V.C. (1999) Selective oestrogen receptor modulation: molecular pharmacology for the millennium. Eur J Cancer, 35, 1974-1985.

Li, X., Zhang, S. and Safe, S. (2006) Activation of kinase pathways in MCF-7 cells by 17beta-estradiol and structurally diverse estrogenic compounds. J Steroid Biochem Mol Biol, 98, 122-132.

Lin, Y.Z., Li, S.W. and Clinton, G.M. (1990) Insulin and epidermal growth factor stimulate phosphorylation of p185HER-2 in the breast carcinoma cell line, BT474. Mol Cell Endocrinol, 69, 111-119.

Liu, C., Sun, C., Huang, H., Janda, K. and Edgington, T. (2003) Overexpression of legumain in tumors is significant for invasion/metastasis and a candidate enzymatic target for prodrug therapy. Cancer Res, 63, 2957-2964.

Lonard, D.M. and O'Malley, B.W. (2005) Expanding functional diversity of the coactivators. Trends Biochem Sci, 30, 126-132.

Loose-Mitchell, D.S., Chiappetta, C. and Stancel, G.M. (1988) Estrogen regulation of c-fos messenger ribonucleic acid. Mol Endocrinol, 2, 946-951.

Love, R.R., Astrow, S.H., Cheeks, A.M. and Havighurst, T.C. (2003) Ornithine decarboxylase (ODC) as a prognostic factor in operable breast cancer. Breast Cancer Res Treat, 79, 329-334.

Lowry, O.H., Rosebrough, N.J., Farr, A.L. and Randall, R.J. (1951) Protein measurement with the Folin phenol reagent. J Biol Chem, 193, 265-275.

Lynch, C.C., Crawford, H.C., Matrisian, L.M. and McDonnell, S. (2004) Epidermal growth factor upregulates matrix metalloproteinase-7 expression through activation of PEA3 transcription factors. Int J Oncol, 24, 1565-1572.

MacGregor, J.I. and Jordan, V.C. (1998) Basic guide to the mechanisms of antiestrogen action. Pharmacol Rev, 50, 151-196.

Madden, S.L., Cook, D.M., Morris, J.F., Gashler, A., Sukhatme, V.P. and Rauscher, F.J., III. (1991) Transcriptional repression mediated by the WT1 Wilms tumor gene product. Science, 253, 1550-1553.

Maines, M.D., Mayer, R.D., Erturk, E., Huang, T.J. and Disantagnese, A. (1999) The oxidoreductase, biliverdin reductase, is induced in human renal carcinoma--pH and cofactor-specific increase in activity. J Urol, 162, 1467-1472.

Maines, M.D. (2005) New insights into biliverdin reductase functions: linking heme metabolism to cell signaling. Physiology (Bethesda), 20, 382-389.

Manni, A., Washington, S., Griffith, J.W., Verderame, M.F., Mauger, D., Demers, L.M., Samant, R.S. and Welch, D.R. (2002) Influence of polyamines on in vitro and in vivo

features of aggressive and metastatic behavior by human breast cancer cells. Clin Exp Metastasis, 19, 95-105.

Marhaba, R. and Zoller, M. (2004) CD44 in cancer progression: adhesion, migration and growth regulation. J Mol Histol, 35, 211-231.

Marini, A., Mirmohammadsadegh, A., Nambiar, S., Gustrau, A., Ruzicka, T. and Hengge, U.R. (2006) Epigenetic inactivation of tumor suppressor genes in serum of patients with cutaneous melanoma. J Invest Dermatol, 126, 422-431.

Martin, L.A., Farmer, I., Johnston, S.R., Ali, S., Marshall, C. and Dowsett, M. (2003) Enhanced estrogen receptor (ER) alpha, ERBB2, and MAPK signal transduction pathways operate during the adaptation of MCF-7 cells to long term estrogen deprivation. J Biol Chem, 278, 30458-30468.

Martin, L.A., Pancholi, S., Chan, C.M., Farmer, I., Kimberley, C., Dowsett, M. and Johnston, S.R. (2005) The anti-oestrogen ICI 182,780, but not tamoxifen, inhibits the growth of MCF-7 breast cancer cells refractory to long-term oestrogen deprivation through down-regulation of oestrogen receptor and IGF signalling. Endocr Relat Cancer, 12, 1017-1036.

Masamura, S., Santner, S.J., Heitjan, D.F. and Santen, R.J. (1995) Estrogen deprivation causes estradiol hypersensitivity in human breast cancer cells. J Clin Endocrinol Metab, 80, 2918-2925.

Masure, S., Cik, M., Pangalos, M.N., Bonaventure, P., Verhasselt, P., Lesage, A.S., Leysen, J.E. and Gordon, R.D. (1998) Molecular cloning, expression and tissue distribution of glial-cell-line-derived neurotrophic factor family receptor alpha-3 (GFRalpha-3). Eur J Biochem, 251, 622-630.

Matsui, K., Sugimori, K., Motomura, H., Ejiri, N., Tsukada, K. and Kitajima, I. (2006) PEA3 cooperates with c-Jun in regulation of HER2/neu transcription. Oncol Rep, 16, 153-158.

May, F.E. and Westley, B.R. (1995) Estrogen regulated messenger RNAs in human breast cancer cells. Biomed Pharmacother, 49, 400-414.

McCabe, C.J., Boelaert, K., Tannahill, L.A., Heaney, A.P., Stratford, A.L., Khaira, J.S., Hussain, S., Sheppard, M.C., Franklyn, J.A. and Gittoes, N.J. (2002) Vascular endothelial growth factor, its receptor KDR/Flk-1, and pituitary tumor transforming gene in pituitary tumors. J Clin Endocrinol Metab, 87, 4238-4244.

McClelland, R.A., Manning, D.L., Gee, J.M., Anderson, E., Clarke, R., Howell, A., Dowsett, M., Robertson, J.F., Blamey, R.W., Wakeling, A.E. and Nicholson, R.I. (1996) Effects of short-term antiestrogen treatment of primary breast cancer on estrogen receptor mRNA and protein expression and on estrogen-regulated genes. Breast Cancer Res Treat, 41, 31-41.

McClelland, R.A., Barrow, D., Madden, T.A., Dutkowski, C.M., Pamment, J., Knowlden, J.M., Gee, J.M. and Nicholson, R.I. (2001) Enhanced epidermal growth factor receptor signaling in MCF7 breast cancer cells after long-term culture in the presence of the pure antiestrogen ICI 182,780 (Faslodex). Endocrinology, 142, 2776-2788.

McGuire, W.L. (1975) Current status of estrogen receptors in human breast cancer. Cancer, 36, 638-644.

McInerney, E.M. and Katzenellenbogen, B.S. (1996) Different regions in activation function-1 of the human estrogen receptor required for antiestrogen- and estradiol-dependent transcription activation. J Biol Chem, 271, 24172-24178.

McPherson, K., Steel, C.M. and Dixon, J.M. (2000) ABC of breast diseases. Breast cancer-epidemiology, risk factors, and genetics. Bmj, 321, 624-628.

Meijer, D., van Agthoven, T., Bosma, P.T., Nooter, K. and Dorssers, L.C. (2006) Functional screen for genes responsible for tamoxifen resistance in human breast cancer cells. Mol Cancer Res, 4, 379-386.

Menard, S., Tagliabue, E., Campiglio, M. and Pupa, S.M. (2000) Role of HER2 gene overexpression in breast carcinoma. J Cell Physiol, 182, 150-162.

Meric, F., Lee, W.P., Sahin, A., Zhang, H., Kung, H.J. and Hung, M.C. (2002) Expression profile of tyrosine kinases in breast cancer. Clin Cancer Res, 8, 361-367.

Miyazaki, K., Asai, N., Iwashita, T., Taniguchi, M., Isomura, T., Funahashi, H., Takagi, H., Matsuyama, M. and Takahashi, M. (1993) Tyrosine kinase activity of the ret proto-oncogene products in vitro. Biochem Biophys Res Commun, 193, 565-570.

Montano, M.M., Muller, V., Trobaugh, A. and Katzenellenbogen, B.S. (1995) The carboxy-terminal F domain of the human estrogen receptor: role in the transcriptional activity of the receptor and the effectiveness of antiestrogens as estrogen antagonists. Mol Endocrinol, 9, 814-825.

Mosesson, Y. and Yarden, Y. (2004) Oncogenic growth factor receptors: implications for signal transduction therapy. Semin Cancer Biol, 14, 262-270.

Moshier, J.A., Malecka-Panas, E., Geng, H., Dosescu, J., Tureaud, J., Skunca, M. and Majumdar, A.P. (1995) Ornithine decarboxylase transformation of NIH/3T3 cells is mediated by altered epidermal growth factor receptor activity. Cancer Res, 55, 5358-5365.

Munroe, P.B., Olgunturk, R.O., Fryns, J.P., Van Maldergem, L., Ziereisen, F., Yuksel, B., Gardiner, R.M. and Chung, E. (1999) Mutations in the gene encoding the human matrix Gla protein cause Keutel syndrome. Nat Genet, 21, 142-144.

Murphy, L.C. and Watson, P.H. (2006) Is oestrogen receptor-beta a predictor of endocrine therapy responsiveness in human breast cancer? Endocr Relat Cancer, 13, 327-334.

Murthy, R.V., Arbman, G., Gao, J., Roodman, G.D. and Sun, X.F. (2005) Legumain

expression in relation to clinicopathologic and biological variables in colorectal cancer. Clin Cancer Res, 11, 2293-2299.

Nasmyth, K. (2005) How do so few control so many? Cell, 120, 739-746.

Neer, E.J., Schmidt, C.J., Nambudripad, R. and Smith, T.F. (1994) The ancient regulatory-protein family of WD-repeat proteins. Nature, 371, 297-300.

Nicholson, R.I., McClelland, R.A., Finlay, P., Eaton, C.L., Gullick, W.J., Dixon, A.R., Robertson, J.F., Ellis, I.O. and Blamey, R.W. (1993) Relationship between EGF-R, c-erbB-2 protein expression and Ki67 immunostaining in breast cancer and hormone sensitivity. Eur J Cancer, 29A, 1018-1023.

Nicholson, R.I., McClelland, R.A., Gee, J.M., Manning, D.L., Cannon, P., Robertson, J.F., Ellis, I.O. and Blamey, R.W. (1994a) Epidermal growth factor receptor expression in breast cancer: association with response to endocrine therapy. Breast Cancer Res Treat, 29, 117-125.

Nicholson, R.I., McClelland, R.A., Gee, J.M., Manning, D.L., Cannon, P., Robertson, J.F., Ellis, I.O. and Blamey, R.W. (1994b) Transforming growth factor-alpha and endocrine sensitivity in breast cancer. Cancer Res, 54, 1684-1689.

Nicholson, R.I., McClelland, R.A., Robertson, J.F. and Gee, J.M. (1999) Involvement of steroid hormone and growth factor cross-talk in endocrine response in breast cancer. Endocr Relat Cancer, 6, 373-387.

Nicholson, R., Madden, T.A., Bryant, S. and Gee, J.M. (2002) Cellular and molecular actions of estrogens and antiestrogens in breast cancer- In: Endocrine Therapy of Breast Cancer. Martin Dunitz Ltd, London, UK.

Nicholson, R.I., Hutcheson, I.R., Knowlden, J.M., Jones, H.E., Harper, M.E., Jordan, N., Hiscox, S.E., Barrow, D. and Gee, J.M. (2004a) Nonendocrine pathways and endocrine resistance: observations with antiestrogens and signal transduction inhibitors in combination. Clin Cancer Res, 10, 346S-354S.

Nicholson, R.I., Staka, C., Boyns, F., Hutcheson, I.R. and Gee, J.M. (2004b) Growth factor-driven mechanisms associated with resistance to estrogen deprivation in breast cancer: new opportunities for therapy. Endocr Relat Cancer, 11, 623-641.

Nicholson, R.I., Hutcheson, I.R., Hiscox, S.E., Knowlden, J.M., Giles, M., Barrow, D. and Gee, J.M. (2005) Growth factor signalling and resistance to selective oestrogen receptor modulators and pure anti-oestrogens: the use of anti-growth factor therapies to treat or delay endocrine resistance in breast cancer. Endocr Relat Cancer, 12 Suppl 1, S29-36.

Normanno, N., Ciardiello, F., Brandt, R. and Salomon, D.S. (1994) Epidermal growth factor-related peptides in the pathogenesis of human breast cancer. Breast Cancer Res Treat, 29, 11-27.

O'Brien, K.A., Lemke, S.J., Cocke, K.S., Rao, R.N. and Beckmann, R.P. (1999) Casein

kinase 2 binds to and phosphorylates BRCA1. Biochem Biophys Res Commun, 260, 658-664.

O'Hagan, R.C., Tozer, R.G., Symons, M., McCormick, F. and Hassell, J.A. (1996) The activity of the Ets transcription factor PEA3 is regulated by two distinct MAPK cascades. Oncogene, 13, 1323-1333.

Ogbagabriel, S., Fernando, M., Waldman, F.M., Bose, S. and Heaney, A.P. (2005) Securin is overexpressed in breast cancer. Mod Pathol, 18, 985-990.

Osborne, C.K. (1998) Tamoxifen in the treatment of breast cancer. N Engl J Med, 339, 1609-1618.

Osborne, C.K., Coronado-Heinsohn, E.B., Hilsenbeck, S.G., McCue, B.L., Wakeling, A.E., McClelland, R.A., Manning, D.L. and Nicholson, R.I. (1995) Comparison of the effects of a pure steroidal antiestrogen with those of tamoxifen in a model of human breast cancer. J Natl Cancer Inst, 87, 746-750.

Osborne, C.K., Yochmowitz, M.G., Knight, W.A., 3rd and McGuire, W.L. (1980) The value of estrogen and progesterone receptors in the treatment of breast cancer. Cancer, 46, 2884-2888.

Osborne, C.K. and Fuqua, S.A. (1994) Mechanisms of tamoxifen resistance. Breast Cancer Res Treat, 32, 49-55.

Osborne, C.K., Zhao, H. and Fuqua, S.A. (2000) Selective estrogen receptor modulators: structure, function, and clinical use. J Clin Oncol, 18, 3172-3186.

Osborne, C.K., Pippen, J., Jones, S.E., Parker, L.M., Ellis, M., Come, S., Gertler, S.Z., May, J.T., Burton, G., Dimery, I., Webster, A., Morris, C., Elledge, R. and Buzdar, A. (2002) Double-blind, randomized trial comparing the efficacy and tolerability of fulvestrant versus anastrozole in postmenopausal women with advanced breast cancer progressing on prior endocrine therapy: results of a North American trial. J Clin Oncol, 20, 3386-3395.

Ottaviano, Y.L., Issa, J.P., Parl, F.F., Smith, H.S., Baylin, S.B. and Davidson, N.E. (1994) Methylation of the estrogen receptor gene CpG island marks loss of estrogen receptor expression in human breast cancer cells. Cancer Res, 54, 2552-2555.

Palmieri, C., Saji, S., Sakaguchi, H., Cheng, G., Sunters, A., O'Hare, M.J., Warner, M., Gustafsson, J.A., Coombes, R.C. and Lam, E.W. (2004) The expression of oestrogen receptor (ER)-beta and its variants, but not ERalpha, in adult human mammary fibroblasts. J Mol Endocrinol, 33, 35-50.

Papa, V., Pezzino, V., Costantino, A., Belfiore, A., Giuffrida, D., Frittitta, L., Vannelli, G.B., Brand, R., Goldfine, I.D. and Vigneri, R. (1990) Elevated insulin receptor content in human breast cancer. J Clin Invest, 86, 1503-1510.

Park, B.H., Vogelstein, B. and Kinzler, K.W. (2001) Genetic disruption of PPARdelta

decreases the tumorigenicity of human colon cancer cells. Proc Natl Acad Sci U S A, 98, 2598-2603.

Peck, R., Olsen, C. and Devore, J. (2000) Introduction To Statistics and Data Analysis. Duxbury Resource Center

Pedram, A., Razandi, M. and Levin, E.R. (2006) Nature of functional estrogen receptors at the plasma membrane. Mol Endocrinol, 20, 1996-2009.

Pei, L. and Melmed, S. (1997) Isolation and characterization of a pituitary tumor-transforming gene (PTTG). Mol Endocrinol, 11, 433-441.

Pei, L. (2000) Activation of mitogen-activated protein kinase cascade regulates pituitary tumor-transforming gene transactivation function. J Biol Chem, 275, 31191-31198.

Pei, L. (2001) Identification of c-myc as a down-stream target for pituitary tumor-transforming gene. J Biol Chem, 276, 8484-8491.

Pennica, D., Swanson, T.A., Welsh, J.W., Roy, M.A., Lawrence, D.A., Lee, J., Brush, J., Taneyhill, L.A., Deuel, B., Lew, M., Watanabe, C., Cohen, R.L., Melhem, M.F., Finley, G.G., Quirke, P., Goddard, A.D., Hillan, K.J., Gurney, A.L., Botstein, D. and Levine, A.J. (1998) WISP genes are members of the connective tissue growth factor family that are up-regulated in wnt-1-transformed cells and aberrantly expressed in human colon tumors. Proc Natl Acad Sci U S A, 95, 14717-14722.

Perou, C.M., Jeffrey, S.S., van de Rijn, M., Rees, C.A., Eisen, M.B., Ross, D.T., Pergamenschikov, A., Williams, C.F., Zhu, S.X., Lee, J.C., Lashkari, D., Shalon, D., Brown, P.O. and Botstein, D. (1999) Distinctive gene expression patterns in human mammary epithelial cells and breast cancers. Proc Natl Acad Sci U S A, 96, 9212-9217.

Perou, C.M., Sorlie, T., Eisen, M.B., van de Rijn, M., Jeffrey, S.S., Rees, C.A., Pollack, J.R., Ross, D.T., Johnsen, H., Akslen, L.A., Fluge, O., Pergamenschikov, A., Williams, C., Zhu, S.X., Lonning, P.E., Borresen-Dale, A.L., Brown, P.O. and Botstein, D. (2000) Molecular portraits of human breast tumours. Nature, 406, 747-752.

Picard, D., Kumar, V., Chambon, P. and Yamamoto, K.R. (1990) Signal transduction by steroid hormones: nuclear localization is differentially regulated in estrogen and glucocorticoid receptors. Cell Regul, 1, 291-299.

Ponglikitmongkol, M., Green, S. and Chambon, P. (1988) Genomic organization of the human oestrogen receptor gene. Embo J, 7, 3385-3388.

Portella, G., Salvatore, D., Botti, G., Cerrato, A., Zhang, L., Mineo, A., Chiappetta, G., Santelli, G., Pozzi, L., Vecchio, G., Fusco, A. and Santoro, M. (1996) Development of mammary and cutaneous gland tumors in transgenic mice carrying the RET/PTC1 oncogene. Oncogene, 13, 2021-2026.

Pratt, W.B. and Toft, D.O. (1997) Steroid receptor interactions with heat shock protein and immunophilin chaperones. Endocr Rev, 18, 306-360.

Puri, R., Tousson, A., Chen, L. and Kakar, S.S. (2001) Molecular cloning of pituitary tumor transforming gene 1 from ovarian tumors and its expression in tumors. Cancer Lett, 163, 131-139.

Pyronnet, S. (2000) Phosphorylation of the cap-binding protein eIF4E by the MAPK-activated protein kinase Mnk1. Biochem Pharmacol, 60, 1237-1243.

Qian, H.R. and Huang, S. (2005) Comparison of false discovery rate methods in identifying genes with differential expression. Genomics, 86, 495-503.

Qin, C., Nguyen, T., Stewart, J., Samudio, I., Burghardt, R. and Safe, S. (2002) Estrogen up-regulation of p53 gene expression in MCF-7 breast cancer cells is mediated by calmodulin kinase IV-dependent activation of a nuclear factor kappaB/CCAAT-binding transcription factor-1 complex. Mol Endocrinol, 16, 1793-1809.

Ramakrishnan, R., Dorris, D., Lublinsky, A., Nguyen, A., Domanus, M., Prokhorova, A., Gieser, L., Touma, E., Lockner, R., Tata, M., Zhu, X., Patterson, M., Shippy, R., Sendera, T.J. and Mazumder, A. (2002) An assessment of Motorola CodeLink microarray performance for gene expression profiling applications. Nucleic Acids Res, 30, e30.

Ramaswamy, S., Ross, K.N., Lander, E.S. and Golub, T.R. (2003) A molecular signature of metastasis in primary solid tumors. Nat Genet, 33, 49-54.

Ramos-Morales, F., Dominguez, A., Romero, F., Luna, R., Multon, M.C., Pintor-Toro, J.A. and Tortolero, M. (2000) Cell cycle regulated expression and phosphorylation of hpttg proto-oncogene product. Oncogene, 19, 403-409.

Riggins, R.B., Zwart, A., Nehra, R. and Clarke, R. (2005) The nuclear factor kappa B inhibitor parthenolide restores ICI 182,780 (Faslodex; fulvestrant)-induced apoptosis in antiestrogen-resistant breast cancer cells. Mol Cancer Ther, 4, 33-41.

Rocha, R.L., Hilsenbeck, S.G., Jackson, J.G., VanDenBerg, C.L., Weng, C., Lee, A.V. and Yee, D. (1997) Insulin-like growth factor binding protein-3 and insulin receptor substrate-1 in breast cancer: correlation with clinical parameters and disease-free survival. Clin Cancer Res, 3, 103-109.

Rogatsky, I., Trowbridge, J.M. and Garabedian, M.J. (1999) Potentiation of human estrogen receptor alpha transcriptional activation through phosphorylation of serines 104 and 106 by the cyclin A-CDK2 complex. J Biol Chem, 274, 22296-22302.

Rozen, S. and Skaletsky, H. (2000) Primer3 on the WWW for general users and for biologist programmers. Methods Mol Biol, 132, 365-386.

Sabnis, G.J., Jelovac, D., Long, B. and Brodie, A. (2005) The role of growth factor receptor pathways in human breast cancer cells adapted to long-term estrogen deprivation. Cancer Res, 65, 3903-3910.

Sachdev, D. and Yee, D. (2001) The IGF system and breast cancer. Endocr Relat Cancer,

8, 197-209.

Sainsbury, R. (2004) Aromatase inhibition in the treatment of advanced breast cancer: is there a relationship between potency and clinical efficacy? Br J Cancer, 90, 1733-1739.

Sambrook, J., Fritsch, E. and Maniatis, T. (1989) Molecular Cloning: A Laboratory Manual. Cold Spring Harbour Press.

Santen, R.J., Song, R.X., Zhang, Z., Kumar, R., Jeng, M.H., Masamura, S., Lawrence, J., Jr., MacMahon, L.P., Yue, W. and Berstein, L. (2005) Adaptive hypersensitivity to estrogen: mechanisms and clinical relevance to aromatase inhibitor therapy in breast cancer treatment. J Steroid Biochem Mol Biol, 95, 155-165.

Sariola, H. and Saarma, M. (2003) Novel functions and signalling pathways for GDNF. J Cell Sci, 116, 3855-3862.

Sarkijarvi, S., Kuusisto, H., Paalavuo, R., Levula, M., Airla, N., Lehtimaki, T., Kaprio, J., Koskenvuo, M. and Elovaara, I. (2006) Gene expression profiles in Finnish twins with multiple sclerosis. BMC Med Genet, 7, 11.

Schratt, G.M., Nigh, E.A., Chen, W.G., Hu, L. and Greenberg, M.E. (2004) BDNF regulates the translation of a select group of mRNAs by a mammalian target of rapamycin-phosphatidylinositol 3-kinase-dependent pathway during neuronal development. J Neurosci, 24, 7366-7377.

Schwab, M., Varmus, H.E. and Bishop, J.M. (1985) Human N-myc gene contributes to neoplastic transformation of mammalian cells in culture. Nature, 316, 160-162.

Sedehizade, F., von Klot, C., Hanck, T. and Reiser, G. (2005) p42(IP4)/centaurin alpha1, a brain-specific PtdIns(3,4,5)P3/Ins(1,3,4,5)P4-binding protein: membrane trafficking induced by epidermal growth factor is inhibited by stimulation of phospholipase C-coupled thrombin receptor. Neurochem Res, 30, 1319-1330.

Seldin, D.C., Landesman-Bollag, E., Farago, M., Currier, N., Lou, D. and Dominguez, I. (2005) CK2 as a positive regulator of Wnt signalling and tumourigenesis. Mol Cell Biochem, 274, 63-67.

Shiau, A.K., Barstad, D., Loria, P.M., Cheng, L., Kushner, P.J., Agard, D.A. and Greene, G.L. (1998) The structural basis of estrogen receptor/coactivator recognition and the antagonism of this interaction by tamoxifen. Cell, 95, 927-937.

Shibata, Y., Haruki, N., Kuwabara, Y., Nishiwaki, T., Kato, J., Shinoda, N., Sato, A., Kimura, M., Koyama, H., Toyama, T., Ishiguro, H., Kudo, J., Terashita, Y., Konishi, S. and Fujii, Y. (2002) Expression of PTTG (pituitary tumor transforming gene) in esophageal cancer. Jpn J Clin Oncol, 32, 233-237.

Shou, J., Massarweh, S., Osborne, C.K., Wakeling, A.E., Ali, S., Weiss, H. and Schiff, R. (2004) Mechanisms of tamoxifen resistance: increased estrogen receptor-HER2/neu cross-talk in ER/HER2-positive breast cancer. J Natl Cancer Inst, 96, 926-935.

Simpson, E.R. and Davis, S.R. (2001) Minireview: aromatase and the regulation of estrogen biosynthesis--some new perspectives. Endocrinology, 142, 4589-4594.

Sivaraman, V.S., Wang, H., Nuovo, G.J. and Malbon, C.C. (1997) Hyperexpression of mitogen-activated protein kinase in human breast cancer. J Clin Invest, 99, 1478-1483.

Sivars, U., Aivazian, D. and Pfeffer, S.R. (2003) Yip3 catalyses the dissociation of endosomal Rab-GDI complexes. Nature, 425, 856-859.

Sledge, G.W., Jr. and Miller, K.D. (2003) Exploiting the hallmarks of cancer: the future conquest of breast cancer. Eur J Cancer, 39, 1668-1675.

Solbach, C., Roller, M., Fellbaum, C., Nicoletti, M. and Kaufmann, M. (2004) PTTG mRNA expression in primary breast cancer: a prognostic marker for lymph node invasion and tumor recurrence. Breast, 13, 80-81.

Solbach, C., Roller, M., Peters, S., Nicoletti, M., Kaufmann, M. and Knecht, R. (2005) Pituitary tumor-transforming gene (PTTG): a novel target for anti-tumor therapy. Anticancer Res, 25, 121-125.

Sommer, A., Hoffmann, J., Lichtner, R.B., Schneider, M.R. and Parczyk, K. (2003) Studies on the development of resistance to the pure antiestrogen Faslodex in three human breast cancer cell lines. J Steroid Biochem Mol Biol, 85, 33-47.

Song, D.H., Dominguez, I., Mizuno, J., Kaut, M., Mohr, S.C. and Seldin, D.C. (2003) CK2 phosphorylation of the armadillo repeat region of beta-catenin potentiates Wnt signaling. J Biol Chem, 278, 24018-24025.

Song, R.X., Zhang, Z. and Santen, R.J. (2005) Estrogen rapid action via protein complex formation involving ERalpha and Src. Trends Endocrinol Metab, 16, 347-353.

Soule, H.D., Vazguez, J., Long, A., Albert, S. and Brennan, M. (1973) A human cell line from a pleural effusion derived from a breast carcinoma. J Natl Cancer Inst, 51, 1409-1416.

Speirs, V., Carder, P.J., Lane, S., Dodwell, D., Lansdown, M.R. and Hanby, A.M. (2004) Oestrogen receptor beta: what it means for patients with breast cancer. Lancet Oncol, 5, 174-181.

Staka, C.M., Nicholson, R.I. and Gee, J.M. (2005) Acquired resistance to oestrogen deprivation: role for growth factor signalling kinases/oestrogen receptor cross-talk revealed in new MCF-7X model. Endocr Relat Cancer, 12 Suppl 1, S85-97.

Swanton, C. (2004) Cell-cycle targeted therapies. Lancet Oncol, 5, 27-36.

Tacchini, L., De Ponti, C., Matteucci, E., Follis, R. and Desiderio, M.A. (2004) Hepatocyte growth factor-activated NF-kappaB regulates HIF-1 activity and ODC expression, implicated in survival, differently in different carcinoma cell lines. Carcinogenesis, 25, 2089-2100.

Takahashi, M. (2001) The GDNF/RET signaling pathway and human diseases. Cytokine

Growth Factor Rev, 12, 361-373.

Tanaka, T., Inazawa, J. and Nakamura, Y. (1996) Molecular cloning of a human cDNA encoding putative cysteine protease (PRSC1) and its chromosome assignment to 14q32.1. Cytogenet Cell Genet, 74, 120-123.

Tasheva, E.S., Ke, A., Deng, Y., Jun, C., Takemoto, L.J., Koester, A. and Conrad, G.W. (2004) Differentially expressed genes in the lens of mimecan-null mice. Mol Vis, 10, 403-416.

Tekur, S., Lau, K.M., Long, J., Burnstein, K. and Ho, S.M. (2001) Expression of RFG/ELE1alpha/ARA70 in normal and malignant prostatic epithelial cell cultures and lines: regulation by methylation and sex steroids. Mol Carcinog, 30, 1-13.

Tfelt-Hansen, J., Yano, S., Bandyopadhyay, S., Carroll, R., Brown, E.M. and Chattopadhyay, N. (2004) Expression of pituitary tumor transforming gene (PTTG) and its binding protein in human astrocytes and astrocytoma cells: function and regulation of PTTG in U87 astrocytoma cells. Endocrinology, 145, 4222-4231.

Thompson, A.D., 3rd and Kakar, S.S. (2005) Insulin and IGF-1 regulate the expression of the pituitary tumor transforming gene (PTTG) in breast tumor cells. FEBS Lett, 579, 3195-3200.

Toft, D. and Gorski, J. (1966) A receptor molecule for estrogens: isolation from the rat uterus and preliminary characterization. Proc Natl Acad Sci U S A, 55, 1574-1581.

Tsuchiya, M.I., Okuda, H., Takaki, Y., Baba, M., Hirai, S., Ohno, S. and Shuin, T. (2005) Renal cell carcinoma- and pheochromocytoma-specific altered gene expression profiles in VHL mutant clones. Oncol Rep, 13, 1033-1041.

Tusher, V.G., Tibshirani, R. and Chu, G. (2001) Significance analysis of microarrays applied to the ionizing radiation response. Proc Natl Acad Sci U S A, 98, 5116-5121.

Umesono, K. and Evans, R.M. (1989) Determinants of target gene specificity for steroid/thyroid hormone receptors. Cell, 57, 1139-1146.

van 't Veer, L.J., Dai, H., van de Vijver, M.J., He, Y.D., Hart, A.A., Mao, M., Peterse, H.L., van der Kooy, K., Marton, M.J., Witteveen, A.T., Schreiber, G.J., Kerkhoven, R.M., Roberts, C., Linsley, P.S., Bernards, R. and Friend, S.H. (2002) Gene expression profiling predicts clinical outcome of breast cancer. Nature, 415, 530-536.

van de Vijver, M.J. (2005) Biological variables and prognosis of DCIS. Breast, 14, 509-519.

van Diest, P.J., van der Wall, E. and Baak, J.P. (2004) Prognostic value of proliferation in invasive breast cancer: a review. J Clin Pathol, 57, 675-681.

Vasilcanu, D., Weng, W.H., Girnita, A., Lui, W.O., Vasilcanu, R., Axelson, M., Larsson, O., Larsson, C. and Girnita, L. (2006) The insulin-like growth factor-1 receptor inhibitor PPP produces only very limited resistance in tumor cells exposed to long-term

selection. Oncogene, 25, 3186-3195.

Vlotides, G., Cruz-Soto, M., Rubinek, T., Eigler, T., Auernhammer, C.J. and Melmed, S. (2006) Mechanisms for growth factor-induced Pituitary Tumor Transforming Gene-1 (PTTG1) expression in pituitary folliculostellate TtT/GF cells. Mol Endocrinol.

Wakeling, A.E., Dukes, M. and Bowler, J. (1991) A potent specific pure antiestrogen with clinical potential. Cancer Res, 51, 3867-3873.

Wakeling, A.E. and Bowler, J. (1992) ICI 182,780, a new antioestrogen with clinical potential. J Steroid Biochem Mol Biol, 43, 173-177.

Wang, W., Goswami, S., Lapidus, K., Wells, A.L., Wyckoff, J.B., Sahai, E., Singer, R.H., Segall, J.E. and Condeelis, J.S. (2004) Identification and testing of a gene expression signature of invasive carcinoma cells within primary mammary tumors. Cancer Res, 64, 8585-8594.

Wang, Z., Yu, R. and Melmed, S. (2001) Mice lacking pituitary tumor transforming gene show testicular and splenic hypoplasia, thymic hyperplasia, thrombocytopenia, aberrant cell cycle progression, and premature centromere division. Mol Endocrinol, 15, 1870-1879.

Webb, P., Nguyen, P., Shinsako, J., Anderson, C., Feng, W., Nguyen, M.P., Chen, D., Huang, S.M., Subramanian, S., McKinerney, E., Katzenellenbogen, B.S., Stallcup, M.R. and Kushner, P.J. (1998) Estrogen receptor activation function 1 works by binding p160 coactivator proteins. Mol Endocrinol, 12, 1605-1618.

Weigel, N.L. and Zhang, Y. (1998) Ligand-independent activation of steroid hormone receptors. J Mol Med, 76, 469-479.

Weisz, A. and Bresciani, F. (1993) Estrogen regulation of proto-oncogenes coding for nuclear proteins. Crit Rev Oncog, 4, 361-388.

Whitehead, J.P., Clark, S.F., Urso, B. and James, D.E. (2000) Signalling through the insulin receptor. Curr Opin Cell Biol, 12, 222-228.

Wright, P.S., Cooper, J.R., Cross-Doersen, D.E., Miller, J.A., Chmielewski, P.A., Wagner, R.L., Streng, K.A. and Flanagan, M.A. (1995) Regulation of ornithine decarboxylase mRNA levels in human breast cancer cells: pattern of expression and involvement of core enhancer promoter element. Cell Growth Differ, 6, 1097-1102.

Wu, R.Y. and Gill, G.N. (1994) LIM domain recognition of a tyrosine-containing tight turn. J Biol Chem, 269, 25085-25090.

Yasmeen, A., Berdel, W.E., Serve, H. and Muller-Tidow, C. (2003) E- and A-type cyclins as markers for cancer diagnosis and prognosis. Expert Rev Mol Diagn, 3, 617-633.

Yee, D. (2006) Targeting insulin-like growth factor pathways. Br J Cancer, 94, 465-468.

Yu, R., Heaney, A.P., Lu, W., Chen, J. and Melmed, S. (2000a) Pituitary tumor transforming gene causes aneuploidy and p53-dependent and p53-independent

apoptosis. J Biol Chem, 275, 36502-36505.

Yu, R., Ren, S.G., Horwitz, G.A., Wang, Z. and Melmed, S. (2000b) Pituitary tumor transforming gene (PTTG) regulates placental JEG-3 cell division and survival: evidence from live cell imaging. Mol Endocrinol, 14, 1137-1146.

Yu, R., Lu, W., Chen, J., McCabe, C.J. and Melmed, S. (2003) Overexpressed pituitary tumor-transforming gene causes aneuploidy in live human cells. Endocrinology, 144, 4991-4998.

Yu, R. and Melmed, S. (2004) Pituitary tumor transforming gene: an update. Front Horm Res, 32, 175-185.

Yue, W., Wang, J.P., Conaway, M.R., Li, Y. and Santen, R.J. (2003) Adaptive hypersensitivity following long-term estrogen deprivation: involvement of multiple signal pathways. J Steroid Biochem Mol Biol, 86, 265-274.

Zahraoui, A., Touchot, N., Chardin, P. and Tavitian, A. (1989) The human Rab genes encode a family of GTP-binding proteins related to yeast YPT1 and SEC4 products involved in secretion. J Biol Chem, 264, 12394-12401.

Zemlickova, E., Dubois, T., Kerai, P., Clokie, S., Cronshaw, A.D., Wakefield, R.I., Johannes, F.J. and Aitken, A. (2003) Centaurin-alpha(1) associates with and is phosphorylated by isoforms of protein kinase C. Biochem Biophys Res Commun, 307, 459-465.

Zhang, X., Horwitz, G.A., Prezant, T.R., Valentini, A., Nakashima, M., Bronstein, M.D. and Melmed, S. (1999) Structure, expression, and function of human pituitary tumor-transforming gene (PTTG). Mol Endocrinol, 13, 156-166.

Zhu, B., Ping, G., Shinohara, Y., Zhang, Y. and Baba, Y. (2005) Comparison of gene expression measurements from cDNA and 60-mer oligonucleotide microarrays. Genomics, 85, 657-665.

Zou, H., McGarry, T.J., Bernal, T. and Kirschner, M.W. (1999) Identification of a vertebrate sister-chromatid separation inhibitor involved in transformation and tumorigenesis. Science, 285, 418-422.

APPENDICES

Appendix I: Preparation of Tissue Culture Reagents

Preparation of charcoal-stripped FCS (csFCS), phenol red-free media: csFCS was prepared by adjusting the pH of 100ml of FCS to 4.2, after which the solution was equilibrated for 30 minutes at 4°C. A solution of charcoal/ dextran was prepared by the addition of 11% activated charcoal (norit) and 0.06% dextran C to 18ml of distilled water, which was subsequently mixed vigorously for 1 hour. A volume of 5ml of the charcoal solution was added to 100ml of FCS and incubated at 4°C for 16 hours with gentle agitation. After removal of the charcoal by centrifugation at 12,000g for 40 minutes, the solution was filtered several times through a Whatman No.4 (grade 3) filter paper. The pH of the filtered solution was adjusted to 7.2, and sterilised filtering through a 0.2μM filter. Media was then prepared using a 5% csFCS in phenol red-free RPMI for tissue culture work.

Tissue culture stock solutions: Stock solutions were prepared at the following concentrations in ethanol: oestradiol (10^{-5}M), tamoxifen (10^{-3}M), Faslodex (10^{-3}M), and gefitinib (10^{-2}M), which were all stored at -20°C. For experimental work, stock solution was further diluted to a final concentration of oestradiol (10^{-9}M), tamoxifen (10^{-7}M), Faslodex (10^{-7}M), and gefitinib (10^{-6}M) in above csFCS/ phenol red-free media.

X-medium preparation: X-medium for maintenance of X-MCF-7 cells was prepared by subjecting FCS to charcoal-stripping as described above. The csFCS was subsequently heat-inactivated by heating at 65°C for 30 minutes. A volume of 5% was then added to phenol red-free RPMI, also supplemented with 4mM L-glutamine.

Constituents of Coulter Counter isoton solution for cell counting: Isoton II azide-free balanced electrolyte solution Coulter counter solution was purchased from Beckman Coulter Ltd (UK) and consisted of 7.9g/l NaCl, 1.9g/l disodium hydrogen orthophosphate, 0.4g/l EDTA disodium salt, 0.2g/l dihydrogen orthophosphate, and 0.3g/l sodium fluoride.

Appendix II: PCR Solutions

<u>10x TNE Buffer</u>:

(100mM Tris; 2.0M NaCl; 10mM EDTA; pH 7.4).

12.1g Trizma Base, 3.7g EDTA, 116.8g NaCl was added To 800ml distilled water and pH set to 7.4 with concentrated HCl. The volume was made up to 1litre with distilled water, and autoclaved.

<u>50x TAE buffer</u>:

For a 50x TAE solution the following were prepared in distilled water: 242g Tris base, 57.1 ml glacial acetic acid, 18.72g EDTA (or 100ml of stock 0.5M). The pH was adjusted to 8.3 and solution was made up to 1litre.

<u>Agarose Gel Loading Buffer</u>

A 6x sucrose-based agarose gel loading buffer was prepared with: bromophenol blue (0.25%) and sucrose (w/v) 40%

Appendix III: Microarray Solutions/ Methods

<u>20x SSC</u>

(3M NaCl, 0.3M sodium citrate; pH7)

175.3g of NaCl and 88.2g of sodium citrate were dissolved in 800ml of distilled water. The pH was adjusted to 7.0 using 1M HCl, and the volume subsequently made up to a litre with distilled water. The solution was sterilised by autoclaving.

<u>Clontech/ BD Biosciences Stripping protocol for Atlas Plastic Arrays</u>

The Plastic Microarray stripping protocol was as described in the Atlas Plastic Microarray handbook. Briefly, the hybridised microarray (face-up) was incubated with 45ml of prewarmed stripping solution (0.1M Na_2CO_3 aq) at 80°C for 5 minutes in a rocking oven. The array was removed, immediately rinsed in a bath of room temperature deionised water, and air dried. The efficiency of stripping was determined by exposing the array to an autoradiograph film at least 7 days prior to reapeating as appropriate (up to 3 times).

Appendix IV: Protein Detection

Gel composition for SDS-PAGE

Reagent	Resolving Gel (10ml)		Stacking Gel (5ml)
	7.5% (ml)	15% (ml)	5% (ml)
distilled water	4.8	2.3	6.1
0.5M Tris-HCl; pH8.8	—	—	2.5
1.5M Tris-HCl	2.5	2.5	—
Acrylamide/ bisacrylamide (30%)	2.5	5	1.25
10% APS	0.1	0.1	0.1
10% SDS	0.1	0.1	0.05
TEMED	0.006	0.006	0.01

Additional Retrieval Methods Used in the optimisation of PTTG1 and GRFα3 Antibodies

0.01M citric acid; pH6, heat (microwave; 30min) retrieval

Sections housed within a plastic slide-holder within a Saran wrap-covered plastic beaker containing 1L of 0.01M (2.1g/1L) citric acid buffer (Sigma, Doeset, UK) (pH6) were heated in a Proline; 950 watt microwave at 560W (power level 6) for 30 minutes. The slides were subsequently cooled in running tap water for 10 minutes and then immersed in PBS for 5 minutes. Sections were then outlined on the slide using a waterproof PAP pen. Subsequent steps were as 2.17.2.

0.01 M EDTA; pH8, heat (pressure cooker; 2min) retrieval

Sections housed within a metal slide-holder in 2L of 0.01 M (7.44g/2L) EDTA (Sigma, Dorset, UK) (pH8) were pressure cooked for 2 minutes at full pressure. After heat treatment, sections were cooled in running tap water within the open pressure cooker for 10 minutes and then immersed in PBS for 5 minutes. Sections were then outlined on the slide using a waterproof PAP pen. Subsequent steps were as 2.17.2.

0.01 M EDTA; pH8, heat (microwave) retrieval

Sections housed within a plastic slide-holder within a covered plastic beaker containing 1L of 0.01M (3.72g/1L) EDTA (pH8) were heated in a Proline; 950 watt microwave at full power for 1 minute, then at 560W (power level 6) for 9minutes. The beaker containing the sections remained within the heated buffer for a further 20 minutes, after which the slides were immediately transferred into distilled water for 5 minutes, then immersed in PBS for 5 minutes. Sections were then outlined on the slide using a waterproof PAP pen. Subsequent steps were as 2.17.2.

Cell Pellet Paraffin Block Protocol

The following protocol were performed by M.James in TCCR with the pellets then made available for the project.

Materials and Equipmant

Formaldehyde (37%) was supplied by Fisher Scientific (Loughborough, UK). Noble Agar and Tissue embedding medium (Paraplast/ Paraffin wax) was from Sigma (Dorset, UK). All other materials were as listed in 2.1 and 2.17. The Rotary Shandon Finesse Microtome was supplied by Thermo Electron Corporation (Berkshire, UK). The cell pellet arrays were prepared using a Beecher Systems manual microarrayer (MTA-1). (All other equipment were as listed in 2.16.

Methods

Cell lines were grown in 150mm dishes up to 70% confluency/ log-phase of growth in their appropriate experimental media as described in 2.1. After removing the media, cells were collected using a cell scraper and resuspended in fresh phenol red-free medium supplemented with 5%csFCS. The cell suspension was then centrifuged at 950rpm for 5 minutes at room temperature and immediately fixed by immersion of the cell aggregate in a 4% formaldehyde PBS solution for 70 minutes. Cells suspended within the formaldehyde solution were then allowed to settle for a further 50minutes within a 1.5ml tube. After removing the supernatant, a mixture of cell/ agar (equal volume 12% noble agar solution) was produced within a syringe, and the mixture left overnight to solidify. A cell plug was then extruded from the syringe and sectioned using a scalpal into 5mm pellets which were subsequently re-fixed in 4% formaldehyde solution for a further 2 hours. After dehydrating/ clearing , the pellets (3-6 pellets per cell line block) were then embedded in Paraplast for the formation of a paraffin block. Each block was then sectioned at 5µm onto slides for initial assessment of cell integrity and validity using haematoxylin and eosin (H&E) staining, as well as other biomarkers

specific to each resistant cell line, notably, including ER and pS2, prior to cutting test slides onto Superfrost coated slides. For the production of cell pellet arrays bearing multiple cell lines, Validated donor pellet blocks from the various cell lines are core-punched (0.6mm) and arrayed into a recipient block using a manual microarrayer.

TESPA coating of coverslips

Slides were treated with aminopropyl-triethoxysilane (TESPA, Sigma, Dorset, UK) as follows. Slides were racked in a holder and soaked in Decon (10% aq. dilution) overnight. After 2 hours of rinsing under tap water slides were dried in the oven, and then left to cool at room temperature. Slaides were immersed in a bath of 2% TESPA in acetone for 5 seconds, followed by placing in a bath of acetone for 2x 1 minute and then finally in a bath of distilled water for 2x 1 minute. Slides were then air dried.